Shusheng Zhang · Sai Bi · Xinyue Song
Editors

Nucleic Acid Amplification Strategies for Biosensing, Bioimaging and Biomedicine

Springer

Nucleic Acid Amplification Strategies for Biosensing, Bioimaging and Biomedicine

Shusheng Zhang · Sai Bi ·
Xinyue Song
Editors

Nucleic Acid Amplification Strategies for Biosensing, Bioimaging and Biomedicine

Springer

Editors
Shusheng Zhang
Shandong Provincial Key Laboratory of Detection Technology for Tumour Markers
Linyi University
Linyi, Shandong, China

Sai Bi
College of Chemistry and Chemical Engineering
Qingdao University
Qingdao, Shandong, China

Xinyue Song
Shandong Provincial Key Laboratory of Detection Technology for Tumour Markers,
College of Chemistry and Chemical Engineering
Linyi University
Linyi, Shandong, China

ISBN 978-981-13-7043-4 ISBN 978-981-13-7044-1 (eBook)
https://doi.org/10.1007/978-981-13-7044-1

Library of Congress Control Number: 2019935994

This Springer imprint is published by the registered company Springer Nature Singapore Pte Ltd.
The registered company address is: 152 Beach Road, #21-01/04 Gateway East, Singapore 189721, Singapore

Nucleic acid amplification strategies are a new class of strategies including multiple isothermal and thermocycling amplification techniques. This book mainly introduces the typical nucleic acid amplification strategies, experimental research methods, their applications and future development trends in the construction of optical and electrochemical biosensors, in vitro and in vivo bioimaging systems and biomedical platforms. This book can be used as a reference for scientific researchers in related disciplines. It can also be used as a teaching reference book for undergraduate or postgraduate students in chemistry, materials, medicine and environment.

Foreword

Nucleic acid amplification strategies have been rapidly developed over the past years to enable highly sensitive and specific detection of a wide range of biomolecules, an essential process in biochemical analysis and early clinical test of tumor markers for cancer diagnosis. Understanding the theory, methodology, characteristic and dynamic of amplification strategies is of great importance to in-depth study and application. However, the development of accurate and robust methods based on nucleic acid amplification is still in urgent need for the analysis of practical samples.

Professor Shusheng Zhang, Dr. Sai Bi and Dr. Xinyue Song kindly provide this book that focuses on nucleic acid amplification strategies. The overall aim of the book is to bring to readers a complete scope of nucleic acid amplification strategies, ranging from fundamental theory and experimental techniques to major applications and future development trends. Hence, the content of the book covers basic concepts, knowledge and research methods of nucleic acid amplification strategies and a variety of optical and electrochemical detection techniques that are widely applicable in many fields, especially in biosensing, bioimaging and biomedicine. More specifically, this book is divided into four parts with 15 chapters. Part I (Chap. 1) is the introduction that gives an overview of the theoretical basis for nucleic acid amplification strategies, as well as typical examples. Part II (Chaps. 2–10) summarizes the applications of nucleic acid amplification strategies for the construction of biosensors: The first half, from Chaps. 2 to 6, goes through five major types of nucleic acid amplification strategy-based optical biosensors, including fluorescence, chemiluminescence, electrochemiluminescence, colorimetric and surface plasmon resonance biosensors; and the second half, from Chaps. 7 to 10, discusses electrochemical-related biosensors, including electrochemical DNA sensors, photoelectrochemical biosensors, nanopore sensors and quartz crystal microbalance. Part III (Chaps. 11 and 12) introduces nucleic acid amplification strategy-based bioimaging, within which Chap. 11 is to summarize nucleic acid amplification strategy-based fluorescence imaging, including applications of isothermal and thermal cycling amplification techniques, and Chap. 12 is to describe nucleic acid amplification strategy-based surface-enhanced Raman spectroscopy for bioimaging,

such as nucleic acid-induced distance change and aggregation. Finally, Part IV (Chaps. 13–15) gives an overview of the current state-of-the-art development and future perspectives of applying nucleic acid amplification strategies for biomedicine: Chap. 13 focuses on applications of nucleic acid amplification strategies for in vitro and in vivo detection of metal ions; Chap. 14 highlights applications of various nucleic acid amplification strategies in theranostics; and Chap. 15 summarizes and prospects the use of miniaturized devices for nucleic acid amplification strategies.

Since nucleic acid amplification strategies are at the stage of development, many theoretical models and experimental methods are still being developed and improved. Relying on the deep understanding and fruitful research achievements of Prof. Shusheng Zhang, the authors present to readers a comprehensive overview of the emerging nucleic acid amplification strategies and their application and prospects in the fields of biosensing, bioimaging and biomedicine. It is for sure that many readers will be able to learn systematically the theoretical and practical knowledge, and gain thinking and enlightenment from this book. Readers are also encouraged to explore and contribute to the growing literature of this evolving field. We earnestly hope that this book will promote the scientific excitement and contribute to the advance of biosensing, bioimaging and biomedicine.

Nanjing, China

Yi-Tao Long, Ph.D.
Professor of Chemistry, School of Chemistry
and Chemical Engineering, Nanjing University

Preface

The writing and publishing of *Nucleic Acid Amplification Strategies for Biosensing, Bioimaging and Biomedicine* are a matter of course with the vigorous development of nucleic acid amplification techniques. This book contains the following two aspects of significance.

Firstly, nucleic acid amplification is an emerging technology and closely related to life science. Since the invention of polymerase chain reaction (PCR) in 1980s, PCR-based methods have been widely used in clinical diagnosis and treatment because trace DNA can be exponentially amplified with high efficiency. In consideration of the complicated temperature control of the thermocycling amplification technique, isothermal amplification techniques based on both tool enzyme and enzymes-free strategy have been developed for signal amplification. With the specific properties of tool enzymes, such as polymerase, exonuclease and endonuclease, various tool enzyme-based isothermal amplification techniques such as rolling circle amplification (RCA) and recombinase polymerase amplification (RPA) have been developed. Based on complementary base pairing, isothermal amplification techniques such as hybridization chain reaction (HCR) and catalytic hairpin assembly (CHA) have realized the non-enzymatic amplification with high efficiency, which further extends the nucleic acid amplification strategies. On the one hand, the amplification techniques meet the needs of sensitive detection of a wide range of biomolecules. On the other hand, the diverse requirements of nucleic acid amplification strategies pose new challenges to the existing methods such as higher specificity and portability. Novel amplification techniques are needed, and the development direction of the amplification strategies is also reflected in the topic of this book.

Secondly, nucleic acid amplification is closely integrated with real applications. Through combining with optical and electrochemical detection techniques, nucleic acid amplification strategies have been widely used in biosensing, bioimaging and biomedicine and become more and more important in disease diagnosis, especially in cancers. Over the past decades, the development of the nucleic acid amplification strategies is unprecedented. Under this great situation, how to expand the applications of nucleic acid amplification strategies in more aspects should be addressed.

In this book, we cover this topic in the presentation and discussion of the nucleic acid amplification strategies, such as features, advantages, disadvantages and challenges.

The compilation and distribution of *Nucleic Acid Amplification Strategies for Biosensing, Bioimaging and Biomedicine* also reflect the prosperous development of biochemical analysis. Each chapter of the book is written by scientists in the field, which not only summarizes the framework and development of nucleic acid amplification strategies at a high level, but also provides a systematic introduction for readers to understand their achievements in biosensing, bioimaging and biomedicine.

Linyi, China Shusheng Zhang
Qingdao, China Sai Bi
Linyi, China Xinyue Song

Acknowledgements

It is a special privilege to express our heartfelt gratitude and respect for all the people who helped us with this book. First and foremost, we would like to give our deepest gratitude to the Fund Committee. Our work has been financially supported by the National Natural Science Foundation of China and Nature Science Foundation of Shandong Province. Secondly, we are greatly indebted to all the professors in our institute who have achieved interesting and meaningful research work. Last but not least, we would like to show our thanks to teachers and students in the Linyi University. With their help and cooperation, we can finish the book successfully.

Contents

Contributors

Sai Bi College of Chemistry and Chemical Engineering, Qingdao University, Qingdao, Shandong, People's Republic of China

Zhongfeng Gao Shandong Provincial Key Laboratory of Detection Technology for Tumour Markers, College of Chemistry and Chemical Engineering, Linyi University, Linyi, People's Republic of China

Shanwen Hu Shandong Provincial Key Laboratory of Detection Technology for Tumour Markers, College of Chemistry and Chemical Engineering, Linyi University, Linyi, People's Republic of China

Yanxialei Jiang Shandong Provincial Key Laboratory of Detection Technology for Tumour Markers, College of Chemistry and Chemical Engineering, Linyi University, Linyi, People's Republic of China

Yao Jiang Shandong Provincial Key Laboratory of Detection Technology for Tumour Markers, College of Chemistry and Chemical Engineering, Linyi University, Linyi, People's Republic of China

Qiong Li Shandong Provincial Key Laboratory of Detection Technology for Tumour Markers, College of Chemistry and Chemical Engineering, Linyi University, Linyi, Shandong, People's Republic of China

Xueming Li Shandong Provincial Key Laboratory of Detection Technology for Tumour Markers, College of Chemistry and Chemical Engineering, Linyi University, Linyi, People's Republic of China

Lishang Liu Shandong Provincial Key Laboratory of Detection Technology for Tumour Markers, College of Chemistry and Chemical Engineering, Linyi University, Linyi, People's Republic of China

Min Liu Shandong Provincial Key Laboratory of Detection Technology for Tumour Markers, College of Chemistry and Chemical Engineering, Linyi University, Linyi, Shandong, People's Republic of China

Pengfei Shi Shandong Provincial Key Laboratory of Detection Technology for Tumour Markers, College of Chemistry and Chemical Engineering, Linyi University, Linyi, People's Republic of China

Xinyue Song Shandong Provincial Key Laboratory of Detection Technology for Tumour Markers, College of Chemistry and Chemical Engineering, Linyi University, Linyi, People's Republic of China

Yingnan Sun Shandong Provincial Key Laboratory of Detection Technology for Tumour Markers, College of Chemistry and Chemical Engineering, Linyi University, Linyi, People's Republic of China

Dongmei Xi Shandong Provincial Key Laboratory of Detection Technology for Tumour Markers, College of Chemistry and Chemical Engineering, Linyi University, Linyi, Shandong, People's Republic of China

Beibei Xie Shandong Provincial Key Laboratory of Detection Technology for Tumour Markers, College of Chemistry and Chemical Engineering, Linyi University, Linyi, People's Republic of China

Yongcun Yan College of Chemistry and Chemical Engineering, Qingdao University, Qingdao, Shandong, People's Republic of China

Huairong Zhang Shandong Provincial Key Laboratory of Detection Technology for Tumour Markers, College of Chemistry and Chemical Engineering, Linyi University, Linyi, People's Republic of China

Xiaoru Zhang Shandong Key Laboratory of Biochemical Analysis, College of Chemistry and Molecular Engineering, Qingdao University of Science and Technology, Qingdao, Shandong, People's Republic of China

Xiangjiang Zheng Shandong Provincial Key Laboratory of Detection Technology for Tumour Markers, College of Chemistry and Chemical Engineering, Linyi University, Linyi, People's Republic of China

Hong Zhou Shandong Provincial Key Laboratory of Detection Technology for Tumour Markers, College of Chemistry and Chemical Engineering, Linyi University, Linyi, Shandong, People's Republic of China

Abbreviations

2D	Two-dimensional
3WJ	Three-way junction
5-FU	5-fluorouracil
5-FUdR	5-fluoro-2'-deoxyuridine
AA	Ascorbic acid
AAO	Anodized aluminum oxide
AAP	L-ascorbic acid 2-phosphate trisodium salt
ABA	Acetamiprid-binding aptamer
ABEI	N-(aminobutyl)-N-(ethylisoluminol)
ABTS	2,2'-azino-bis(3-ethylbenzothiazoline)-6-sulfonate disodium salt
ADM	Aspirating–depositing–moving
AFP	α-fetoprotein
AgNC	Silver nanoclusters
AGR2	Anterior gradient homolog 2
AMP	Adenosine monophosphate
Apt-NPs	Aptamer-conjugated nanoparticles
aptNTr	Aptamer-tethered DNA nanotrain
ATP	Adenosine triphosphate
AuNPs	Gold nanoparticles
bbc-DL-DNA	Bio-barcode dendrimer-like DNA
bbcDNA	Bio-barcode DNA
BCP	Biocatalytic precipitation
BER	Base excision repair
BHQ2	Black hole quencher 2
BiGDM	Beads-in-gel droplet microarray
BIP	Backward inner primer
BLM	Bleomycin
BN	Boron nitride
BPB	Bromophenol blue

BRCA	Branched rolling circle amplification
CA 125	Carcinoma antigen 125
CAH	Contact angle hysteresis
CCD	Charge-coupled device
CCPs	Cationic conjugated polymers
CEA	Carcinoembryonic antigen
CHA	Catalyzed hairpin assembly
CHEF	Chelation-induced enhanced fluorescence
CiE	Cross-interface emulsification
CL	Chemiluminescence
CLIA	CL immunoassay
ClyA	Cytolysin A
CNTs	Carbon nanotubes
CNVs	Copy number variations
CP	Capture probe
CRET	Chemiluminescence resonance energy transfer
DA	Dopamine
DBCO	Dibenzocyclooctyne
DDA	Discrete dipole approximation
ddPCR	Digital droplet polymerase chain reaction
DDS	Drug delivery system
dLAMP	Digital loop-mediated isothermal amplification
DMSO	Dimethyl sulfoxide
DNA	Deoxyribonucleic acid
DNA-4WJ	DNA four-way junction
DNAzyme	G-quadruplex deoxyribozyme
dNTPs	Deoxyribonucleotide triphosphates
DOX	Doxorubicin
dsDNA	Double-stranded DNA
DSN	Duplex-specific nuclease
DSNSA	Duplex-specific nuclease signal amplification
DTTC	Diethylthiatricarbocyanine
EAA	Exonuclease-assisted amplification
ECL	Electrochemiluminescence
E-DNA	Electrochemical DNA
EF	Electromagnetic field
ELISAs	Enzyme-linked immunoassays
ESA	Excited-state absorption
ESIPT	Excited-state intramolecular proton transfer
ETU	Energy transfer upconversion
Exo I	Exonuclease I
Exo III	Exonuclease III
FAM	Carboxyfluorescein
FI-CL	Flow injection-chemiluminescence
FIP	Forward inner primer

FRET	Fluorescence resonance energy transfer
FTD	Fast-track diagnostics
GO	Graphene oxide
GOD	Glucose oxidase
GOxNPs	Graphene oxide nanoparticles
HCR	Hybridization chain reaction
HDA	Helicase-dependent amplification
HfO_2	Hafnium oxide
HRCA	Hyperbranching rolling circle amplification
HRP	Horseradish peroxidase
ICT	Intramolecular charge transfer
KD	Dissociation constant
LAMP	Loop-mediated isothermal amplification
LCR	Ligase chain reaction
LOD	Limit of detection
L-RCA	Ligation-rolling circle amplification
LSPR	Localized surface plasmon resonance
LSPs	Localized surface plasmons
MB	Magnetic beads
MC-DIP	Multichannel dynamic interfacial printing
MCH	Mercaptohexanol
mGO	Magnetic graphene oxide
miRNA	Microribonucleic acid
MMPs	Magnetic microparticles
MnPP	Manganese porphyrin
MNPs	Magnetic nanoparticles
MoS_2	Molybdenum disulfide
MPs	Magnetic particles
mRNAs	messenger RNAs
MSNs	Mesoporous silica nanoparticles
MspA	Mycobacterium smegmatis porin A
MV digital PCR	Multivolume digital PCR
NASBA	Nucleic acid sequence-based amplification
NC	Nanocrystal
NCI	National Cancer Institute
NCs	Nanoclusters
NEANA	Nicking endonuclease-assisted nanoparticle amplification
NEase	Nicking endonuclease
NESA	Nicking enzyme signaling amplification
NIPT	Noninvasive prenatal testing
NIR	Near-infrared ranges
NPs	Nanoparticles
NTPs	Nucleoside triphosphate
OmpG	Outer membrane protein G
PA	Photon avalanche

PAHs	Polycyclic aromatic hydrocarbons
PCR	Polymerase chain reaction
PDGF-BB	Platelet-derived growth factor BB
PDMA	Planar monolayer droplet array
PDMS	Polydimethylsiloxane
pDNA	Probe DNA
PEB	3-[4-(phenylethynyl)benzylthio]propanoic acid
PEC	Photoelectrochemical
PET	Polyethylene terephthalate
PGD	Preimplantation genetic diagnosis
PLGA	Poly lactic-co-glycolic acid
POC	Point of care
PSA	Prostate-specific antigen
PSPs	Propagating surface plasmons
PTK7	Protein tyrosine kinase-7
PVA	Poly(vinyl alcohol)
QCM	Quartz crystal microbalance
QCM-D	Quartz crystal microbalance with dissipation
QDs	Quantum dots
RCA	Rolling circle amplification
RCPs	Rolling circle amplification products
RCT	Rolling circle transcription
RET	Resonance energy transfer
RI	Refractive index
RNA	Ribonucleic acid
RT-PCR	Reverse transcription polymerase chain reaction
SCLC	Small-cell lung cancer
SDA	Strand displacement amplification
SECL	Synergistic enhanced chemiluminescence
SELEX	System evolution of ligands by exponential enrichment
SERS	Surface-enhanced Raman scattering
SH	Superhydrophobic
SiNx	Silicon nitride
SiO_2	Silica oxide
SL	Superhydrophilic
SMRT	Single-molecule real-time sequencing
SNP	Single-nucleotide polymorphism
SODA	Sequential operation droplet array
SP	Sessile probe
SPO-SP	Superamphiphobic-superamphiphilic
SPR	Surface plasmon resonance
SPRi	Surface plasmon resonance imaging
SPs	Surface plasmons
ssDNA	Single-stranded DNA
SWCNTs	Single-walled carbon nanotubes

TBM	Truncated-barrel mutant
TBR	Tris(2,2'-bipyridyl)ruthenium
TdT	Deoxynucleotidyl transferase
TDT	Targeted drug transport
TEHP	Template enhanced hybridization processes
T-EXPAR	Target-triggered isothermal exponential amplification reaction
TMB	3,3',5,5'-Tetramethylbenzidine
TMPyP4	5,10,15,20-Tetra-(n-methyl-4-pyridyl) porphyrin
T-NESA	Target-triggering nicking enzyme signaling amplification
UCL	Upconversion luminescence
UCNCs	Upconverting rare-earth nanocrystals
UCNPs	Upconversion nanoparticles
UDG	Uracil-DNA glycosylase
ULQ	Upper limit of quantification
α-HL	α-hemolysin
β-hCG	Human chorionic gonadotrophin-β
γ-CD-P-MB	γ-CD-mediated dual-pyrene-labeled stemless molecular beacon
λ-Exo	λ-exonuclease

Part I
Introduction of Nucleic Acid Amplification Strategies

Chapter 1
Nucleic Acid Amplification Strategies for Biosensing, Bioimaging, and Biomedicine

Hong Zhou

Abstract Nucleic acid amplification methods are nucleic acid-assistant signal amplification strategies, which have been widely studied and applied for fundamental laboratory research, pharmacogenomics, gene diagnosis, and protein detection for many kinds of infectious diseases or cancers. Up to now, smart design and efficient applications of various nucleic acid molecule-based recycling amplification techniques have emerged as most promising tools, providing greatly enhanced sensitivity and selectivity for the targets in complicated biological samples, including blood, urine, saliva, tissues, and even living cells. Understanding the principles, characteristics, and dynamics of these amplification strategies is of great importance to their applications and research.

1.1 General

Nucleic acid amplification strategies have already become one of powerful tools for efficient and smart signal amplified detection of a wide range of biomolecule, which have been widely applied in many fields, especially in biosensing, bioimaging, and biomedicine. Generally, based on the temperature requirements, nucleic acid-assistant amplification techniques could be divided into two categories: thermocycling amplification techniques and isothermal amplification techniques. Polymerase chain reaction (PCR) (Mullis and Faloona 1987) and ligase chain reaction (LCR) (Barany 1991) are served as traditional thermocycling amplification techniques. Since the first report of PCR in 1985, much attention has been aroused for the studies of PCR or LCR to obtain cost-effective, simple, and robust genotyping assays with high sensitivity, specificity, and multiplexing ability (Shen et al. 2012; Monis and Giglio 2006; Shin et al. 2014). Even showing many advantages, one big problem is that both PCR and LCR strategies requires thermostable DNA polymerases or

H. Zhou (✉)
Shandong Provincial Key Laboratory of Detection Technology for Tumour Markers, College of Chemistry and Chemical Engineering, Linyi University, Linyi 276005, Shandong, People's Republic of China
e-mail: zhouhong830215@126.com

S. Zhang et al. (eds.), *Nucleic Acid Amplification Strategies for Biosensing, Bioimaging and Biomedicine*, https://doi.org/10.1007/978-981-13-7044-1_1

DNA ligases as well as thermal machines, such as a thermal cycler. With the development of nucleic acid technologies, isothermal nucleic acid-assistant amplification strategies gradually come into researches' sight as a promising alternative to PCR for amplified assay of biomarkers.

In comparison to PCR and LCR, isothermal nucleic acid-assistant amplification strategies exhibit many advantages such as simple conditions, instrument-free, time-saving, and high sensitivity. Isothermal nucleic acid-assistant amplification techniques have been widely expanded and are quite qualified for sensitive and accurate assay of a series of targets, such as DNA/RNA, proteins, metal ions, other small molecules, and cells (Zhao et al. 2015). The combination between these efficient amplification strategies and nanotechnology has also aroused widespread attention by taking both advantages from unique properties of nanomaterials and nucleic acid-assistant amplification strategies (Zhou et al. 2018). Recently, many kinds of isothermal amplification strategies have been proposed with different reaction mechanisms, for example, rolling circle amplification (RCA), strand displacement amplification (SDA), helicase-dependent amplification (HDA), loop-mediated isothermal amplification, nucleic acid-cleaving enzymes or DNAzyme-assisted amplification strategies, and enzyme-free DNA strand displacement-assisted isothermal amplification strategies, etc. And above strategies have been widely and smartly designed and reported for constructing many sensing methods with signal amplification, including electrochemistry, electrogenerated chemiluminescence, photoelectrochemistry, chemiluminescence, surface plasmon resonance, fluorescence or Raman spectra technologies, etc. Insights into the functionality and structure of nucleic acids bring the opportunities for better understanding of biological events involved with target binding, signal transfer, signal output at molecules, or even atom level. Moreover, advances in nucleic acid-based amplification technologies are expected to provide greatly enhanced biosensing performance and wide applications in the fields of bioimaging, single-molecule detection, diseases diagnostics, and drug delivery.

1.2 The Typical Nucleic Acid Amplification Strategies

1.2.1 Thermocycling Amplification Techniques

1.2.1.1 Polymerase Chain Reaction (PCR)

PCR is a most commonly used signal amplification technique due to its high sensitivity and good reproducibility (Mullis and Faloona 1987; Saiki et al. 1988), operating polymerase enzymes-assistant strand separation and annealing under a cyclic heating and cooling process. In the presence of primer pair, a large amount of specific DNA products were produced known as the amplification capability of PCR (Erlich et al. 1991; Gibbs 1991; Saiki et al. 1985). As a powerful technology, PCR-based technologies have been well studied and widely employed for molecular diagno-

sis, biomedical, and life science research. However, there are still some drawback and challenges. For example, the required large instrument and extreme reaction conditions for thermal cycling reaction, largely limit further applications of PCR in point-of-care (POC) analysis, which needs rapid response without precision instruments. Moreover, the smallest amount of contaminating DNA could also be amplified which interfere with the final testing results severely. Finally, miRNAs cannot be directly detected using PCR technologies because miRNA is too short to act as a PCR template.

1.2.1.2 Ligase Chain Reaction (LCR)

LCR is another common DNA-dependent strategy for signal amplification in which four oligonucleotides as primers as well as two template strands are required (Marshall et al. 1994). After annealing reaction, the generated nick between adjacent oligonucleotides could be covalently sealed by DNA ligase through a phosphodiester bond, resulting in perfectly target-matched primer bases at the junction and thus one fragment for each template strand (Marshall et al. 1994). The formed ligated products could serve as templates for subsequent cycling reactions similar as that in PCR, obtaining exponential amplification for the desired fragments (Andras et al. 2001). While facing with a single-base change at the junction site, primers will not hybridize perfectly, and thus, no further amplification could be obtained. Which is crucial for this method is to use DNA ligase lacking bluntend ligation activity in order to prevent target-induced ligation. Ligation occurs under the conditions of NADH or ATP-activated enzyme (Cao 2004), substrate adenylation, and nick-closure. LCR is more sensitive and specific than previous PCR technique with the reported data showing that the specificity and sensitivity for LCR are 100 and 97.6%, respectively, while for PCR only 90 and 99.5%, respectively (Davis et al. 1998). Despite this positive report results, target independent ligation especially in the absence of template DNA remains one of the biggest problems bringing in-creased in background signal and thus annoying false-positive results during the detections.

1.2.2 Isothermal Amplification Techniques

1.2.2.1 Rolling Circle Amplification (RCA)

The first isothermal enzymatic process we mentioned here is RCA reaction during which a short DNA or RNA sequence could form a long ssDNA or RNA strand with tens to hundreds of repeated complementary sequences to the previously added circular DNA templates, including plasmids, bacteriophage, and circular RNA of viroids. Different from above-mentioned thermocycling amplification techniques, which require thermostable DNA polymerase, the whole RCA process is carried out at a constant temperature (30–65 °C) without expensive thermal cyclers. There-

fore, RCA has been widely employed in biosensors, showing great potential as a popular nucleic acid-assistant isothermal amplification strategy (Fire and Xu 1995; Blanco et al. 1989). During RCA process, nucleic acid replication starts after primer sequence has annealed to the circular template and continuously added nucleotides by polymerase on the primer stand until it reaches the other end of the primer, forming a complete loop. Then, the following strand displacement activity further kicks in and displaces the previously prepared strand and initiating the synthesis of the next loop. The same replication process proceeds loop after loop until no nucleotides or active polymerase is available in solution. The produced ultra-long ssDNA strand with a large number of repeated bases with lengths up to 10^5 bases makes (Banér et al. 1998) RCA to be widely utilized in signal amplified diagnosis field for various DNA, RNA, or protein detection via electrochemical or optical sensing techniques.

1.2.2.2 Nucleic Acid-Cleaving Enzymes Assisted Isothermal Amplification Strategies

Traditional nucleic acid-cleaving enzymes showing cleave effect to the phosphodiester bonds of nucleic acids could be divided into endonuclease and exonucleases (Exos) on the basis of cleaving mechanism. Endonuclease contains of restriction endonuclease which shows catalysis effect for the cleavage of specific dinucleotide sequences at restriction sites and nicking endonuclease (NEase) which catalyzes the hydrolytic action of single strand in a duplex at a corresponding recognition site, providing another complete ssDNA for further target nucleic acid recycling (Zhou et al. 2013). Different from endonuclease, exonucleases (Exos) exhibit catalysis effect on ssDNA or dsDNA and stepwise remove mononucleotides from 3′-end or 5′-end (Wu et al. 2009).

1.2.2.3 Enzyme-Assisted Strand Displacement Amplification (E-SDA)

E-SDA isothermal amplification process involved a DNA polymerase for strand-displacing and a nicking endonuclease (Walker et al. 1992a, b). It generally begins with a polymerase extension reaction forming a new complementary strand with a special nicking site, which would be cleaved by a NEase. Under further assistance of DNA polymerase, the 3′-end of the nick could be further extended, generating a displaced downstream strand and regenerating the nicking site. Therefore, thousands of target copies could be accumulated after the unidirectional amplification process of SDA (Walker et al. 1992a, b). Furthermore, due to the unique characters of NEase which showed specific catalysis effect to one strand in a duplex at a specific recognition site, this technologies could be integrated in other amplification methods to obtain enhanced detection signals. For example, employing a circular strand displacement polymerization reaction and target-specific hairpin structured fluorescent probes, a low detection limit of 6.4 pM target ssDNA could be achieved within 1000 s (Guo et al. 2009).

1.2.2.4 DNAzyme-Assisted Isothermal Amplification Strategies

DNAzymes are a kind of nucleic acids with specific catalytic ability of cleaving specific substrates with the help of cofactors, for instance metal ions (Liu et al. 2009). Benefited from their nucleic acid structure and excellent biocompatibility, DNAzymes have become a promising material which could be employed for the recognization of a series of analytes through in vitro or even in vivo sensing or imaging. The preparation of DNAzymes is relatively inexpensive with excellent batch-to-batch stability and consistency. Moreover, they are easy to functionalized for further design of versatile signal amplification and readout purposes. The first DNAzyme, which was discovered in 1994 by Breaker and Joyce through a process called in vitro selection, shows ability of a catalyzing transesterification reaction with the help of Pb^{2+} (Breaker and Joyce 1994). This Pb^{2+}-dependent DNAzyme demonstrated that single-stranded DNA served as a catalyst similar to ribozymes and proteins. After that discovery, more DNAzymes structures have been developed to catalyze various biological reactions such as RNA/DNA cleavage, ligation, and phosphorylation reactions (Breaker and Joyce 1995). Up to now, the most currently available DNAzyme are still RNA-cleaving DNAzymes that cleave a single RNA linkage embedded in a DNA sequence. This kind of DNAzyme consists of a substrate strand as well as an enzyme strand. The substrate strand includes a single RNA linkage (rA) known as a cleaving site, and the enzyme strand is composed of one catalytic core and two arms. The motifs of the enzyme strand hold distinct primary/secondary structures, corresponding cofactors, pH dependencies, and specific substrates. The substrate strand will be cleaved by the active enzyme strand into two parts upon catalytic cofactors, such as different metal ions and amino acids. This unique property provides opportunities for constructing DNAzyme-based biosensors dependent on different kinds of cofactor. From the cleaving mechanism of DNAzyme, we can see that the cleaving activity showed high specificity in substrate recognition and multiple enzymatic turnover properties, making it not only versatile recognition elements but also outstanding signal amplifiers for biosensing (Gong et al. 2015).

Besides cleaving DNAzyme, G-quadruplex DNAzyme is another type of DNAzyme in which G-rich sequences could fold into a parallel or an antiparallel G-quadruplex in the presence of K^+, Pb^{2+}, or NH_4^+ (Willner et al. 2008). For example, G-quadruplex DNAzyme could showed peroxidase-mimic activity in the presence of hemin to selectively catalyze luminol/H_2O_2, generating chemiluminescence (CL) signal, or to oxidize 2,2-azino-bis-(3-ethylben-zthiazoline-6-sulfonic acid) (ABTS), leading to color changes. As the studies progressed, high recognition function and catalytic activity of DNAzyme were found and developed, providing DNAzymes as excellent functional molecular probes for signal amplification during the construction of biosensing, bioimaging, and biomedicine systems.

1.2.2.5 Helicase-Dependent Isothermal Amplification (HDA)

The amplification mechanism of HDA is very similar to that of PCR (Vincent et al. 2004). However, during this isothermal amplification, different from employing a DNA denaturation step under a condition of high temperature as that in PCR, HDA simply utilizes a helicase to realize DNA strand separation and ssDNA-binding proteins to prevent the separated DNA strands from rehybridising. After introducing helicase, it is very easy to avoid the requirement of a thermal cycler, and thus, all exponential amplification experiments could be carried out at room temperature. While many other kinds of isothermal amplification methods, an initial heating step is required to denature the dsDNA target before operating amplification process at a lower temperature (Vincent et al. 2004). Generally, dsDNA target is first unwound by the helicase, followed by primer annealing and polymerase (e.g., exo-Klenow fragment)-assistant amplification. The simplicity and good compatibility of HDA procedure make it to be a powerful alternative tool to PCR tool for the detection of various nucleic acids and other analytes. Since HDA amplification reaction was first reported by Vincent and co-workers in 2004, a large number of studies have been reported for developing HDA-based smart assays of various samples in the fields of chemical biosensing (Chow et al. 2008; Goldmeyer et al. 2007; Tong et al. 2011). Moreover, benefited from its isothermal experiments conditions and comparative simple protocols, further development of HDA-based microfluidics and microfabrication could realize for very practical point-of-care applications (Mahalanabis et al. 2010; Zhang et al. 2011; Ramalingam et al. 2009).

One great problem we cannot avoid for HDA is that before HDA optimization experiments for following experimental conditions are needed including buffer composition and primer sets. The unfortunate thing is these kinds of optimization process are usually conducted through PCR experiments, thus bringing a large amount of extra cost and inconvenience to HDA method. In addition, optimizations are involved in the identification of the rate-limiting steps in HDA, for instance the interaction between ssDNA-binding proteins and target DNA strands as this interaction effectively prevents rehybridisation of the helicase-separated DNA strands. Another possible rate-limiting step is the efficiency of the helicase-catalyzed unwinding of the target dsDNA since tests on several polymerases did not show any appreciable difference among them (Vincent et al. 2004). Therefore, further research efforts are urgently needed to find better helicases and ssDNA-binding proteins, obtaining enhanced efficiencies compared to that of current helicases and ssDNA-binding proteins.

1.2.2.6 Loop-Mediated Isothermal Amplification (LAMP)

In order to obtain better amplification systems with enhanced specificity and simplify, Notomi and co-workers developed LAMP strategy in 2000 (Notomi et al. 2000). The LAMP-based one-step reaction shows excellent specificity by employing a set of four target-specific primers, covering a forward inner primer (FIP), a backward inner primer (BIP), and two outer primers (F3 and B3), which demonstrate recog-

nition activity for six distinct sites in the amplified DNA sequence (Tomita et al. 2008). During LAMP process, FIP and BIP play most important roles, containing one functional sequences for priming extension in the first stage while the other functional sequences for self-priming in the second stage, which are related to the sense and antisense sequences of the target dsDNA. DNA polymerase-mediated LAMP reaction coupled with strand displacement process consists of two steps: One is starting structure-producing step and the subsequent cycling amplification step. Among them, four primers are required in the first starting structure-producing stage, while only two inner primers are needed for the second cycling amplification step. Detailed speaking, strand displacement DNA synthesis triggered by an outer primer (F3) could release a ssDNA, which then serves as a template for DNA synthesis primed by both BIP and B3 to form a stem-loop DNA structure. After initiation by one inner primer complementary to the loop on the product, the cycling amplification process is repeated by each inner primer alternately, leading to the geometric accumulation of 10^9 copies of the target sequence within an hour (Zhang et al. 2014). The final products are stem-loop DNAs with different inverted target repeats and cauliflower-like structures with multiple loops, which can be sensitively detected by using various analytical technologies. As we can see that, the developed LAMP method with high specificity and efficiency exhibits promising applications in pathogens, SNPs, and RNAs detection (Mori and Notomi 2009). Additionally, due to the gentle experimental conditions and simple but efficient signal amplification effect, LAMP-assistant commercial test kits have been successfully developed and currently could be purchased from many suppliers currently (e.g., Eiken Chemical Corporation).

1.2.2.7 Enzyme-Free DNA Strand Displacement-Assisted Isothermal Amplification Strategies

Three types of classical enzyme-free strand displacement reactions contain hybridization chain reaction (HCR), catalyzed hairpin assembly (CHA), and entropy-driven toehold-mediated DNA strand displacement reaction, which have attracted much attention to obtain much improved performances during enzyme-free optical biosensors for amplified detection of various targets.

HCR was first reported in 2004 by Dirks and Pierce, which was an enzyme-free target-induced signal amplification strategy with high simplicity and versatility (Dirks and Pierce 2004). Generally, two partially complementary monomer DNAs were employed with a long-stem and short-loop hairpin structure (H1 and H2). Without the addition of target DNA strand, this two DNA hairpins' mixture is stable and concomitant at room temperature. While, the target ssDNA could break the energy balance in long stems protected loops and then serve as a HCR initiator to trigger an alternating HCR and generate a long nicked dsDNA. The repeated units of HCR product can be further employed as templates for the assembly of various nanospecies, generating complicated DNA superstructures. DNA self-assembly formed as nanostructures in this approach makes DNA to be an efficient tool for recognition, trans-

ducer, and signal amplification, simultaneously. Since its discovery, HCR has been regarded as one of most attractive techniques for DNA nanotechnology, biosensing, bioimaging, and biomedicine, which has been utilized to develop promising biosensors for the detection of various small molecules, nucleic acids, proteins, and cells (Bi et al. 2017).

Catalyzed hairpin assembly (CHA) is another enzyme-free signal amplification method achieved by DNA hybridization (self-assembling and disassembling) rather than HCR. Since it was first proposed by Pierce and co-workers in 2008, CHA has become an important irreplaceable DNA molecular engineering tool in recent years due to its unique advantages such as isothermal experimental conditions, enzyme-free, highly predictable and precisely designed or controlled (Yin et al. 2008). CHA strategy can be integrated into a variety of analytical applications, including multiple assays, the spatial organization of biomolecules, and exponential signal amplification. Due to the features of gentle and enzyme-free experiment conditions, the CHA signal amplification technology demonstrates competitive advantages to the classical PCR or enzyme-assistant amplification strategies, thus providing an appealing tool for clinical diagnosis, environmental monitoring, bacterial virus detection, etc.

The last important type of amplification strategy is based on entropy-driven toehold-mediated DNA strand displacement introduced by Zhang and co-workers in their seminal work in 2007 (Zhang et al. 2007). In contrast to above-mentioned HCR and CHA, which are driven by the negative free energy change of base pair formation, this entropy-driven catalytic reaction employ a series of single-stranded linear DNA molecules to play multiple roles in the catalytic circuit via toehold-assisted branch migration (Zhang and Winfree 2009). This kind of toehold-mediated strand displacement is much simpler, faster, and more stable than hairpin-based designs and easy to operate without complicated secondary structures of pseudoknots or kissing loops in DNA molecules, or high background leakage from undesired interactions between metastable hairpin structures.

During the toehold-mediated DNA strand displacement isothermal amplification reaction, the previously hybridized DNA strand could be displaced by another perfectly complementary DNA strand and drop off from the DNA duplex containing a "toehold" overhang. Here, the toehold is known as a single-stranded domain with 5–8 bases where strand displacement could initiate through branched chain migration. The kinetics of the strand displacement process is influenced and regulated by bases species and number in the toehold domain. Theoretically, toehold-mediated DNA strand displacement strategy could obtain 10^6-fold faster rate than that of traditional strand displacement (Srinivas et al. 2013). Up to now, the toehold-mediated strand displacement reaction has been vastly employed in designing various smart DNA-assistant biosensing platforms, including molecular devices, autonomous walkers, logic robot, molecular automata for sensitive and selective detection or diagnostics of many targets and diseases.

1.3 Overview of This Book

Many kinds of nucleic acid amplification reactions provide powerful tools for various targets employing a variety of detection methods, including fluorescence, surface-enhanced Raman scattering, chemiluminescence, colorimetric assays, surface plasmon resonance (SPR), and electrochemiluminescence (ECL), for highly sensitive biosensing with wide dynamic range. Benefited from rapid development in nanotechnology, chemistry, and biotechnology, these nucleic acid amplification-based methods have been expanded to detect targets ranging from RNA and DNA to cells, small molecules, proteins, and even ions via molecules' recognition events. Following the development of applications of these methods in sequencing and intracellular bioimaging has also been successfully demonstrated. Further combination with nanomaterials with unique optical and electronic properties realizes significantly improved assay performances, providing excellent including specificity and robustness.

Despite excellent performances of these nucleic acid-based amplification strategies for constructing ultrasensitive biosensing systems, there are still several challenging problems needed to be addressed. The first problem is unsatisfied accuracy with many interference factors and insufficient procedures for the prevention and control of nucleic acid contamination. For example, the signal of interferons from chemical reagents, laboratory disposables, equipment, or the environment could result in annoying false-positive results in the assay even in optimized conditions. Besides, well-controlled experiments conditions are required, for instance, strict buffer systems, thus showing much limited practical applications. For example, different optimal buffer systems are required for polymerase or nucleic acid-cleaving enzymes. That means when the sensing system was carried out in biological samples, including blood, urine, or saliva, most of these sensors perform poorly with low sensitivity and selectivity. The second problem is the limited types of analytes. Besides nucleic acid, only a few proteins or cells with corresponding well-selected aptamer structures could be successfully detected employing these nucleic acid-based signal amplification strategies, for example, thrombin, human IgE, PDGF-BB, K562 cells, and Romas cells. A large majority of clinical protein cancer biomarkers or cancer cells could not be detected through these powerful amplification strategies because no corresponding aptamer related to these biomarkers or cancer cells. Therefore, more broadly suitable molecular machine or translators deserved to explore for general clinical cancer relevant protein biomarkers. At the same time, SELEX techniques (system evolution of ligands by exponential enrichment) have been developed rapidly to provide more suitable aptamers structures for most protein targets.

That means although isothermal nucleic acid amplification strategies have already moved a big step to solve an essential problem in precise and effective clinical cancer diagnosis, breaking the rules of programed heating, the limiting factors from buffer still exist. Also, intracellular detection of important disease-related gene or RNA still needs more studies and development due to the complicated environment inside cells which could greatly influence the effect of nuclease. Good news is recent reports

have proved that nanomaterial-assistant nucleic acid amplification strategies could greatly enhance the ability of cell transfection, stability, and sensitivity of optical biosensors, thus providing promising opportunities for in vivo imaging, diagnosis, or therapy of tumor cells. For example, noble nanoparticles (Au or Ag), which hold excellent biocompatibility and stability, could bring various enhanced specific SERS or LSPR signal for nucleic acid amplification strategy-based multiple detection of clinic targets. More importantly, these kinds of nanoparticles also show protection effect for nucleic acids from enzymatic degradation in complex biofluids that is very essential for real clinic samples detection or in vivo assay.

In addition to above-mentioned two problems, another challenge is how to provide rapid, low-cost, and multiplex clinical diagnostics platforms on the basis of these nucleic acid amplification strategies. Recently, nucleic acid amplification strategy-assistant-efficient multimode microchip detection and in vivo 3D imaging have been reported as promising tends. Furthermore, increasing types of portable devices for point-of-care (POC) diagnosis have attracted researchers' attention for the development integrated and digital devices. For example, some portable and disposable paper-based or microchip-based platforms have been designed with the combination of both advantages between smart portable devices and efficient nucleic acid-based amplification strategies. Under the development of engineering and the physical and biological sciences, these promising rapid-response devices are expected to come out to be commercial available in near future. After overcoming the stability problem of probes in enzyme resistance inside of cells, nucleic acid amplification strategy-assisted modern detection method could be a strong tool to understand the life process, providing accurate information for diagnosis of early-stage cancers and following efficient treatment. Benefited from the advances of nanomaterial and new-emerging analytical methodology, it is expected that simple handled biosensing systems based on gentle amplification strategies could be developed brilliantly which can satisfy clinic sensitive detection, drug delivery, and disease therapeutics of many malignant diseases with low-cost, time-solving, and high stability in complex bio-samples.

In this book, we introduce concepts and mechanisms of various nucleic acid-assistant amplification strategies and also discuss recent representative works about the constructions of these strategy-based optical and electrochemical biosensing for various analytes including DNA/RNA, ions, other small molecules, proteins inside or outside cells, or even cancer cells. Most commonly used biosensing methods involved are reviewed as separate chapters in this book including chemiluminescence, electrogenerated chemiluminescence, photoelectrochemistry, electrochemistry, surface plasmon resonance, fluorescence, quartz crystal microbalance and Raman spectra technologies. The introduced and summarized development in nucleic acid amplification strategy-assistant biosensing platforms as well as the facing challenges and outlook of these strategies for real-time clinical detections are expected to bring new horizons to further design and construction of biosensor, environmental detection, theranostics, imaging in vitro and in vivo with the help of advances of various kinds of novel nanomaterials, smart micro-devices and POC sensing systems.

References

Andras SC, Power JB, Cocking EC (2001) Strategies for signal amplification in nucleic acid detection. Mol Biotechnol 1:29–44

Banér J, Nilsson M, Mendel-Hartvig M et al (1998) Signal amplification of padlock probes by rolling circle replication. Nucleic Acids Res 26:5073–5078

Barany F (1991) Genetic disease detection and DNA amplification using cloned thermostable ligase. Proc Natl Acad Sci U S A 88:189–193

Bi S, Yue S, Zhang SS (2017) Hybridization chain reaction: a versatile molecular tool for biosensing, bioimaging, and biomedicine. Chem Soc Rev 46:4281–4298

Blanco L, Bernad A, Lázaro JM et al (1989) Highly efficient DNA synthesis by the phage phi 29 DNA polymerase. Symmetrical mode of DNA replication. J Biol Chem 264:8935–8940

Breaker RR, Joyce GF (1994) A DNA enzyme that cleaves RNA. Chem Bio 4:223–229

Breaker RR, Joyce GF (1995) A DNA enzyme with Mg^{2+}-dependent RNA phosphoesterase activity. Chem Bio 2:655–660

Cao W (2004) Recent developments in ligase-mediated amplification and detection. Trends Biotechnol 1:38–44

Chow WHA, McCloskey C, Tong YH et al (2008) Application of isothermal helicase-dependent amplification with a disposable detection device in a simple sensitive stool test for toxigenic Clostridium difficile. J Mol Diagn 10:452–458

Davis JD, Riley PK, Peters CW et al (1998) A comparison of ligase chain reaction to polymerase chain reaction in the detection of *Chlamydia trachomatis* endocervical infections. Infect Dis Obstet Gynecol 2:257–260

Dirks RM, Pierce NA (2004) Triggered amplification by hybridization chain reaction. Proc Natl Acad Sci U S A 101:15275–15278

Erlich HA, Gelfand D, Sninsky JJ (1991) Recent advances in the polymerase chain reaction. Science 252:1643–1651

Fire A, Xu SQ (1995) Biological sciences rolling replication of short DNA circles. Proc Natl Acad Sci U S A 92:4641–4645

Gibbs RA (1991) Polymerase chain reaction techniques. Curr Opin Biotechnol 2:69–75

Goldmeyer J, Kong HM, Tang W (2007) Development of a novel one-tube isothermal reverse transcription thermophilic helicase-dependent amplification platform for rapid RNA detection. J Mol Diagn 5:9639–9644

Gong L, Zhao Z, Lv YF et al (2015) DNAzyme-based biosensors and nanodevices. Chem Commun 51:979–995

Guo Q, Yang X, Wang K, Tan W et al (2009) Sensitive fluorescence detection of nucleic acids based on isothermal circular strand-displacement polymerization reaction. Nucleic Acids Res 37:e20

Liu JW, Cao ZH, Lu Y (2009) Functional nucleic acid sensors. Chem Rev 109:1948–1998

Mahalanabis M, Do J, ALmuayad H (2010) An integrated disposable device for DNA extraction and helicase dependent amplification. Biomed Microdevices 12:353–359

Marshall RL, Laffler TG, Cerney MB et al (1994) Detection of HCV RNA by the asymmetric gap ligase chain reaction. PCR Methods Appl 2:80–84

Monis PT, Giglio S (2006) Nucleic acid amplification-based techniques for pathogen detection and identification. Infect Genet Evol 1:2–12

Mori Y, Notomi T (2009) Loop-mediated isothermal amplification (LAMP): a rapid, accurate, and cost-effective diagnostic method for infectious diseases. J Infect Chemother 15:62–69

Mullis KB, Faloona FA (1987) Specific synthesis of DNA in vitro via a polymerasecatalyzed chain reaction. Methods Enzymol 155:335–350

Notomi T, Okayama H, Masubuchi H et al (2000) Loop-mediated isothermal amplification of DNA. Nucleic Acids Res 28:e63

Ramalingam N, San TC, Kai TJ et al (2009) Microfluidic devices harboring unsealed reactors for real-time isothermal helicase-dependent amplification. Microfluid Nanofluidics 7:325–336

Saiki RK, Scharf S, Faloona F et al (1985) Enzymatic amplification of beta-globin genomic sequences and restriction site analysis for diagnosis of sickle cell anemia. Science 230:1350–1354
Saiki RK, Gelfand DH, Stoffel S et al (1988) Primer-directed enzymatic amplification of DNA with a thermostable DNA polymerase. Science 239:487–491
Shen W, Deng H, Gao Z (2012) Gold nanoparticle-enabled real-time ligation chain reaction for ultrasensitive detection of DNA. J Am Chem Soc 36:14678–14681
Shin GW, Chung B, Jung GY (2014) Multiplex ligase-based genotyping methods combined with CE. Electrophoresis 7:1004–1016
Srinivas N, Ouldridge TE, Šulc P et al (2013) On the biophysics and kinetics of toehold-mediated DNA strand displacement. Nucleic Acids Res 44:10641–10658
Tomita N, Mori Y, Kanda H et al (2008) Loop-mediated isothermal amplification (LAMP) of gene sequences and simple visual detection of products. Nat Protoc 3:877–882
Tong YH, Lemieux B, Kong HM (2011) Multiple strategies to improve sensitivity, speed and robustness of isothermal nucleic acid amplification for rapid pathogen detection. BMC Biotechnol 11:50
Vincent M, Xu Y, Kong H (2004) Helicase-dependent isothermal DNA amplification. EMBO Rep 5:795–800
Walker GT, Little MC, Nadeau JG et al (1992a) Isothermal in vitro amplification of DNA by a restriction enzyme/DNA polymerase system. Proc Natl Acad Sci U S A 89:392–396
Walker GT, Fraiser MS, Schram JL et al (1992b) Strand displacement amplification—an isothermal, in vitro DNA amplification technique. Nucleic Acids Res 20:1691–1696
Willner I, Shlyahovsky B, Zayats M et al (2008) DNAzymes for sensing, nanobiotechnology and logic gate applications. Chem Soc Rev 37:1153–1165
Wu Z, Zhen Z, Jiang JH (2009) Terminal protection of small-molecule-linked DNA for sensitive electrochemical detection of protein binding via selective carbon nanotube assembly. J Am Chem Soc 131:12325–12332
Yin P, Choi HM, Calvert CR et al (2008) Programming bio-molecular self-assembly pathways. Nature 451:318–322
Zhang DY, Winfree E (2009) Control of DNA strand dis-placement kinetics using toehold exchange. J Am Chem Soc 131:17303–17314
Zhang DY, Turberfield AJ, Yurke B et al (2007) Engineering entropy-driven reactions and networks catalyzed by DNA. Science 318:1121–1125
Zhang Y, Park S, Liu K et al (2011) A surface topography assisted droplet manipulation platform for biomarker detection and pathogen identification. Lab Chip 11:398–406
Zhang X, Lowe SB, Gooding JJ (2014) Brief review of monitoring methods for loop-mediated isothermal amplification (LAMP). Biosens Bioelectron 61:491–499
Zhao YX, Chen F, Li Q et al (2015) Isothermal amplification of nucleic acids. Chem Rev 115:12491–12545
Zhou H, Zhang YY, Liu J et al (2013) Efficient quenching of electrochemiluminescence from K-doped graphene-CdS: Eu NCs by G-quadruplex-hemin and target recycling-assisted amplification for ultrasensitive DNA biosensing. Chem Commun 49:2246–2248
Zhou H, Liu J, Xu JJ et al (2018) Optical nano-biosensing interface via nucleic acid amplification strategy: construction and application. Chem Soc Rev 47:1996–2019

Part II
Nucleic Acid Amplification Strategies for Biosensing

Chapter 2
Fluorescence Techniques Based on Nucleic Acid Amplification Strategies: Rational Design and Application

Xinyue Song and Yao Jiang

Abstract Modern fluorescence detection technology plays an important role in the current bioanalysis and clinical detection with merits of the high sensitivity and accuracy. The technology of nucleic acids amplification opens up avenues to establish sensitive fluorescence detection technology. In this chapter, we described the construction of the newly developed fluorescent nano-biosensors based on nucleic acid amplification strategy and provided insightful views on: (1) fluorescence dyes and nanomaterials to develop sensitive and feasible nucleic acid amplification-based fluorescence detection methods; (2) the rational design and application of fluorescence biosensor based on nucleic acid amplification strategies; (3) fluorescence collection and commercial instruments based on nucleic acid amplification strategies.

2.1 Introduction

The fluorescence analysis system has been widely applied in detecting biomolecules with advantages of simplicity, convenience, and sensitivity. Recently, fluorescence detection methods have been integrated with various nucleic acids amplification reactions to construct a series of analysis interfaces and novel analysis strategies, which have developed remarkably sensitive and selective detection methods in bioanalysis.

2.2 Fluorescent Dyes and Nanomaterials

Commercially available organic dyes and fluorescent nanomaterials such as quantum dots (QDs), metal nanoclusters, and upconversion nanoparticles (UCNPs) have been widely used as fluorescent probes. Usually, fluorescence changes induced by

X. Song (✉) · Y. Jiang
Shandong Provincial Key Laboratory of Detection Technology for Tumour Markers, College of Chemistry and Chemical Engineering, Linyi University, Linyi 276005, People's Republic of China
e-mail: songxinyue428@163.com

Y. Jiang
e-mail: tz_jiangyao@163.com

S. Zhang et al. (eds.), *Nucleic Acid Amplification Strategies for Biosensing, Bioimaging and Biomedicine*, https://doi.org/10.1007/978-981-13-7044-1_2

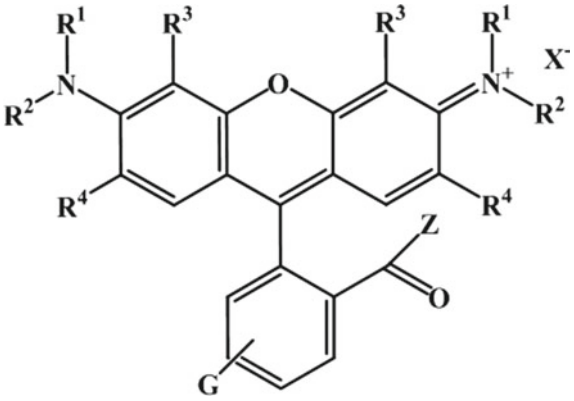

Fig. 2.1 Molecular structures of rhodamine dyes. Reproduced from Beija et al. (2009) by permission of The Royal Society of Chemistry

intramolecular charge transfer (ICT), photoinduced electron transfer, Förster resonance energy transfer (FRET), excited-state intramolecular proton transfer (ESIPT), and chelation-induced enhanced fluorescence (CHEF) have been used advantageously in the design of fluorescent probes.

2.2.1 Organic Fluorescent Dyes

Many organic fluorophores have been widely used as the labels for nucleic acid fluorescent probes. The organic fluorophores may form covalent or noncovalent linkages with the analyzed sample.

2.2.1.1 Rhodamine Dyes

Rhodamine dyes, a family of fluorophores, own the basic molecular structure of xanthenes which are shown in Fig. 2.1 (Beija et al. 2009).

Owing to their high absorption coefficient, high fluorescence quantum yield (QY), and good photostability, rhodamines are used as laser dyes (Drexhage 1976; Amat-Guerri et al. 1993), fluorescence standards for QY and polarization (Prazeres et al. 2008), as well as fluorescent probes for single-molecule imaging (Bossi et al. 2008; Li et al. 2008) and living cells imaging (Huang et al. 2008; Liu et al. 2008). Their absorption and emission properties are strongly influenced by substituents in the xanthene structure.

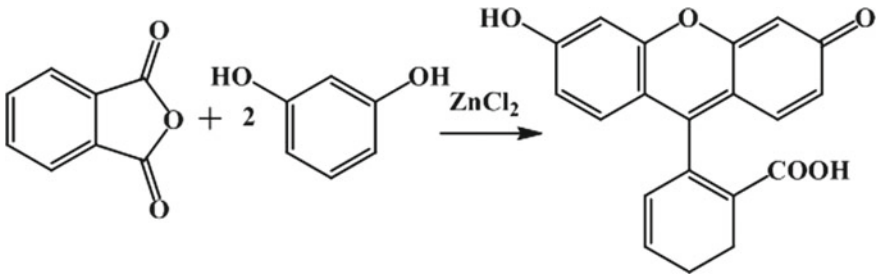

Fig. 2.2 Synthesis of fluorescein. Reprinted with the permissions from Sameiro and Goncalves (2009). Copyright 2009 American Chemical Society

2.2.1.2 Fluorescein

Fluorescein belongs to polycyclic fluorophores and is one of the most common labels used in biological applications. It may be synthesized from phthalic anhydride and 1,3-dihydroxy-benzene (resorcinol) in the presence of zinc chloride via the Friedel–Crafts reaction (Fig. 2.2) (Sameiro and Goncalves 2009; Sun et al. 1997; Ueno et al. 2004). Alternatively, methanesulfonic acid may be used as the catalyst (Sun et al. 1997; Gašperšič et al. 2010). Its maximum absorption and fluorescence wavelengths locate in the visible region of the electromagnetic spectra ($\lambda_{abs} = 490$ nm and $\lambda_{em} = 512$ nm, in water). They can switch between spiral- and open-ring structural forms in different pH because of their special spironolactone structure. The former structure is nonfluorescence, but the latter has excellent optical and chemical properties, such as a large molar extinction coefficient and high fluorescence QY due to its conjugate rigid plane system (Sjöback et al. 1995). Due to these excellent photophysical properties including non-toxicity and low cost, fluorescein dyes have been widely used in bioimaging.

However, fluorophores derived from fluorescein and their macromolecular conjugates do have some disadvantages, namely (i) a relatively high rate of photobleaching (Udenfriend et al. 1972; Talhavini and Atvars 1999); (ii) pH-sensitive fluorescence (Weigele et al. 1973; Martin 1975); (iii) a relatively broad fluorescence emission spectrum, limiting their efficiency in multicolor applications (Martin 1975); (iv) a tendency to self-quenching on conjugation to biopolymers, particularly at high degrees of substitution (Bridges et al. 1986).

2.2.1.3 BODIPY Dyes

BODIPY dyes were first discovered in 1968 by Treibs and Kreuzer (Treibs and Kreuzer 1968). Their basic structure was 4,4-difluoro-4-bora-3a,4a-diaza-s-indacene (Fig. 2.3). Valuable alternatives to other heterocycle skeleton fluorophores were provided which fluoresced at wavelengths beyond 500 nm (Gonçalves 2010). BODIPY fluorophores have attracted much attention in the design of fluorescent labels and

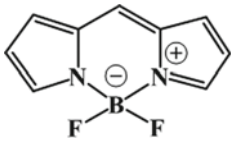

Fig. 2.3 Basic structure of BODIPY fluorophores, 4,4-difluoro-4-bora-3a,4a-diaza-s-indacene. Reproduced from (Printed with the permission from Sameiro and Goncalves (2009). Copyright 2009 American Chemical Society)

biomolecule sensors, because they present many excellent spectral properties, such as high extinction coefficients, high fluorescence QY, and good photostability. This kind of dyes is relatively easy to be oxidized and reduced, which could be used to design photoswitches based on the theory of electron or charge transfer. Moreover, they are relatively insensitive to the environmental polarity and pH (Loudet and Burgess 2007). Consequently, BODIPY fluorophores are widely used to label proteins and DNA.

The fluorescence characteristics of the widely used fluorophores were shown in Table 2.1.

2.2.2 Quantum Dots (QDs)

During the past few decades, the synthesis and biofunctionalization of colloidal semiconductor nanocrystals have attracted much interest to researchers in the areas of biology and medicine. These nanometer-sized crystalline particles, also called QDs, consist of periodic groups of II-VI (e.g., CdSe) or III-V (e.g., InP) materials (Alivisatos et al. 2005).

QDs with small size (1–10 nm) are usually composed of a core and a capping shell which largely affect their photophysical and optical properties. The shell additionally makes the surface defects of the core insensitive, preventing it from environmental damage (Yin and Alivisatos 2005). The molar extinction coefficients of QDs are 10–100 times higher than those of common fluorophores. QDs have another incomparable characteristic, size-dependent optical and electronic properties caused by the quantum confinement (Adams and Barbante 2013). Thus, the emission range of QDs could be tuned by the regulation of the core size during the synthesis process. Furthermore, the broad excitation spectra and narrowly defined emission peak allow multicolor QDs to be excited from one source without emission signal overlap (Alivisatos et al. 2005).

Due to the extreme brightness and resistance to photobleaching, QDs only need very low laser intensities to excite, making them especially useful for the live-cell imaging, especially three-dimensional (3-D) reconstructions and four-dimensional (4-D) bioimaging. The intense brightness is also particularly helpful for single-particle detection and biomedical assays. Furthermore, the synthesis methods of

Table 2.1 Spectral properties of labeled dyes

Fluorescent Labels	λex (nm)	λem (nm)	ε(e)
Pyrene	345	378	44,000
AMCA	353	442	19,000
Acridine	362	462	11,000
BODIPY 493/503	500	506	89,000
ATTO 488	501	523	90,000
6-FAM	494	518	83,000
Alexa Fluor 488	495	518	71,000
FITC	492	520	78,000
Rhodamine Green	504	533	78,000
TET	521	536	99,000
JOE	520	548	75,000
HEX	533	559	98,000
Rhodamine B	543	565	106,000
Cy3	550	570	150,000
TAMRA	560	582	89,000
Texas Red	595	613	107,000
ROX	587	607	82,000
Cy5	643	667	250,000
NAP	603	670	49,200
Cy5.5	675	694	250,000
DyLight 680	682	715	140,000
DyLight 755	752	778	210,000
DyLight 800	770	794	270,000

QDs have been updating and optimizing, making QDs applicable in biological environments. Thus, the biological application of QDs has been expanded, such as fluorescent labels for cellular structures and organelles, tracing cell lineage, monitoring physiological events in live cells, measuring cell motility, and tracking cells in vivo.

Even QDs have been widely used to develop sensitive fluorescence biosensors; they also faced many disadvantages and were optimized based on developed strategies. First, they suffered from luminescence intermittency known as blinking, which could be overcome by shell engineering and/or decreasing the excitation intensity (Li et al. 2013). Then, their inorganic nature and insolubility have been successfully mitigated by different coating and capping agents. Furthermore, their synthesis costs and the toxicity of the precursors are usually stated. Thus, "green synthesis" or biosynthesis are newly developed (Ahmed et al. 2014; Beri and Khanna 2011; Bao et al. 2010).

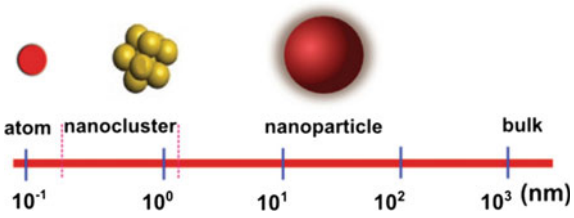

Fig. 2.4 Hierarchy of materials from atoms to bulk. The size of metal nanoclusters falls in between individual atoms and plasmonic NPs. Reproduced from Yu et al. (2015) by permission of The Royal Society of Chemistry

2.2.3 Metal Nanoclusters (MNCs)

Recently, noble MNCs have attracted great attention due to their specific physicochemical properties (Gao et al. 2017). Noble metal nanoclusters are emerging nanoparticle fluorophores with long-lived emission (10^{-8}–10^{-5} s), and their fluorescence could be tuned in the visible and near-infrared (NIR) spectrum. The clusters comprise approximately 18–100 gold and/or silver atoms. Compared to traditional fluorescent dyes and QDs, MNCs have several remarkable advantages: First, MNCs display excellent biocompatibility due to the negligible toxicity of their composition elements. Second, MNCs have extraordinary chemical and photophysical stability. Third, their ultrasmall sizes make them suitable for biolabeling with negligible disturbance of the functions of to-be-labeled bioentities and excellent in vivo clearance. Fourth, the size and composition of MNCs could be changed to tune the fluorescent emissions from visible to NIR. Owing to the above excellent characteristics, MNCs have shown great potential in numerous bioanalysis. However, most noble MNCs show relatively low fluorescence QY compared with organic dyes and QDs (Higaki et al. 2016). To overcome this limitation, the introduction of the protection ligand has attracted great attention (Yao et al. 2015; Yu et al. 2015). Additionally, the fluorescence of MNCs is mainly depended on its structure, metal composition, hydrophilic property, surface charge, and environment. Thus, the effect factors should be optimized to improve the fluorescence QY of MNCs (Fig. 2.4).

2.2.4 Upconversion Nanomaterials

Based on multiple photon absorptions or energy transfers, upconversion is a process which converts low energy light (i.e. NIR) to higher energy light (UV-vis) (Auzel 2004). Rare-earth nanoparticles are widely used upconversion materials which exhibit luminescence properties arising from 4f transitions since their higher lying 5 s and 5p orbitals could effectively shield the 4f orbitals from the effect of the outer ligand field. Therefore, rare earths doped into suitable matrices can generate

upconversion luminescence (UCL) from the UV to NIR region under the excitation of continuous-wave laser. The mechanisms of the upconversion process could be roughly divided into three classes: excited-state absorption (ESA) or multistep (or sequential) absorption, energy transfer upconversion (ETU), and photon avalanche (PA). Other details have been summarized in previous reviews (Auzel 2004; Joubert 1999).

Upconversion nanoparticles (UCNPs) generally comprise inorganic host, sensitizer, and activator. The low lattice phonon energy of host materials is a prerequisite to minimize non-radiative losses and maximize the radiative emission. Due to the low photon energies (~350 cm^{-1}) and high chemical stability, fluorides have been widely used as host materials. To date, $NaYF_4$, $NaYbF_4$, $NaGdF_4$, $NaLaF_4$, LaF_3, GdF_3, GdOF, La_2O_3, Lu_2O_3, Y_2O_3, Y_2O_2S, and others have been reported as host materials for UCL process. Ytterbium ions (Yb^{3+}) have larger absorption cross section at around 980 nm than other lanthanide ions and are often used as sensitizers. The rare-earth ions, Er^{3+}, Tm^{3+}, and Ho^{3+}, are frequently used as activators to generate UCL under NIR excitation due to their ladder-like arrangement energy levels. Usually, the content of activators is limited to less than 2 mol% to minimize the cross-relaxation energy loss (Fig. 2.5).

Under the excitation of single-wavelength laser, multicolor UCNPs could be obtained with emission ranging from UV to NIR regions by the precise control of dopant combinations and concentrations (Fig. 2.6, Wang and Liu 2008). Furthermore, the change of particles size, crystallinity, and capping ligands of UCNPs could tune their UCL. For example, Niu et al. reported the UCNPs crystallinity played a vital role in their UCL which can be easily tuned when subjected to different reaction temperatures and times (Niu et al. 2011). Schietinger and coworkers reported the UCL of $NaYF_4$:Yb/Er NPs is size-dependent (Schietinger et al. 2009).

Compared with downconversion fluorescent materials, UCNPs have unique luminescence properties and have attracted much attention in biological applications, including the noninvasive and deep penetration of NIR radiation, negligible biological autofluorescence, long lifetime, and feasibility of multiple labeling. Thus, UCNPs have widely used as fluorescence marker and energy donors for fluorescence resonance energy transfer (FRET) assays in complex biological samples (Zhang et al. 2006).

2.2.5 Cationic Conjugated Polymers

With the delocalized electronic structure, conjugated polymers (CPs) could transfer the excitation energy along the polymer backbone to acceptors through electron transfer or FRET, leading to their fluorescence quenching or the enhancement of the fluorescence signal of the acceptor (Feng et al. 2008; Ho et al. 2008). Cationic conjugated polymers (CCPs) easily react with the negatively charged DNA probes due to the electrostatic interaction. Cationic polyfluorenes and polythiophene derivatives reported by the Bazan group and the Leclerc group have been widely used in

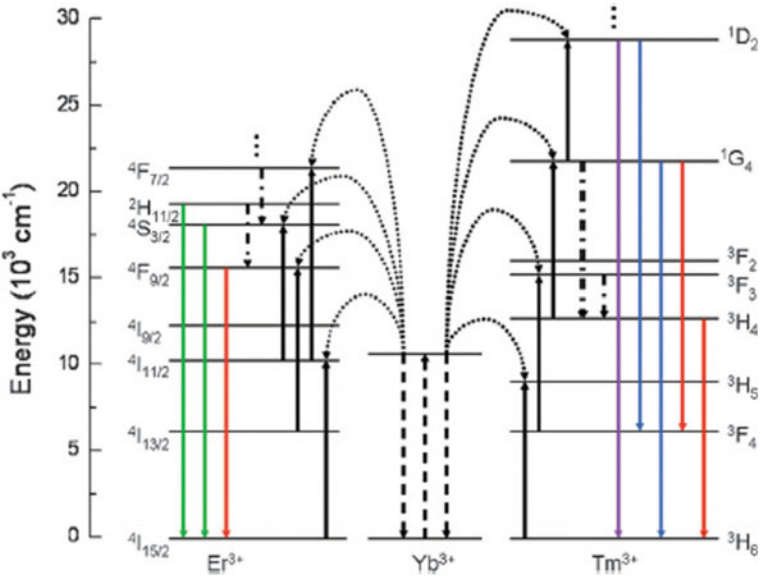

Fig. 2.5 Upconversion mechanism of the Yb, Er/Tm co-doped UCNPs. Under excitation at 980 nm, an electron of Yb^{3+} is excited from the $^2F_{7/2}$ to the $^2F_{5/2}$ level. The energy may be transferred to Er^{3+}/Tm^{3+} nonradiatively to excite it to the corresponding excited level. For Yb, Er co-doped UCNPs, the emission bands at 520, 540, and 654 nm may be assigned to $^2H_{11/2}$ – $^4I_{15/2}$, $^4S_{3/2}$ – $^4I_{15/2}$, and $^4F_{9/2}$ –$^4I_{15/2}$ transitions of Er^{3+}. For Yb, Tm co-doped UCNPs, the emission bands at 365, 451, 481, 646, and 800 nm may be assigned to $^1D_2$ –$^3H_6$, $^1D_2$–$^3F_4$, $^1G_4$–$^3H_6$, $^1G_4$–$^3F_4$, and $^3H_4$–$^3H_6$, respectively (Reproduced from Zhou et al. 2012 by permission of The Royal Society of Chemistry)

DNA sensing (see their typical chemical structures in Fig. 2.7) (Liu and Bazan 2004; Ho et al. 2002, 2008; Gaylord et al. 2002; Baker et al. 2006). Cationic polyfluorenes have feasible structures with facile substitutions at the fluorene C9 position, good chemical and thermal stability, and high fluorescence QYs. Their conformations could be changed when bound to DNA, leading to significantly fluorescence changes. Based on this theory, cationic polyfluorenes could be successfully utilized as optical transducers for simple, rapid, sensitive, and homogeneous detections of single nucleotide polymorphism (SNP) genotyping (Duan et al. 2007), DNA methylation (Feng et al. 2010), and DNA damage (Feng et al. 2009). The use of CCPs as FRET donors has several advantages: (i) The assays are performed in homogeneous solution, and cumbersome procedures are avoided to simplify operations and increase reproducibility; (ii) a common spectrofluorometer or UV viewing cabinet could collect the fluorescence information; (iii) trace amounts of analyte DNA are needed due to the amplificated fluorescence signal and the improved detection sensitivity; (iv) electrostatic interactions could assist CCPs to form complex with the oppositely charged DNA instead of covalent linkage. What's more, primers do not require fluorescent labels. Therefore, the CCPs-based nucleic acid assays are quite

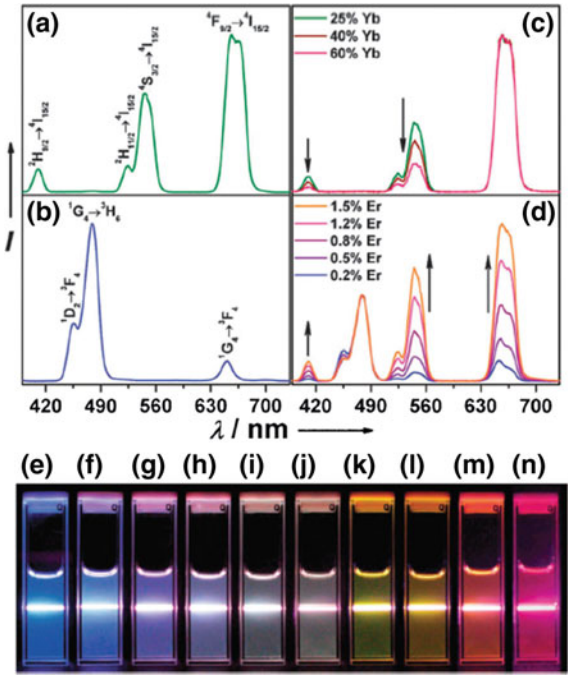

Fig. 2.6 UC multicolor tuning in Ln^{3+}-doped cubic $NaYF_4$ NPs. UC emission spectra of **a** $NaYF_4$:Yb/Er (18:2 mol%), **b** $NaYF_4$:Yb/Tm (20/0.2 mol%), **c** $NaYF_4$:Yb/Er (25–60:2 mol%), and **d** $NaYF_4$:Yb/Tm/Er (20:0.2:0.2-1.5 mol%) particles in ethanol solutions (10 mM). The spectra in **c** and **d** were normalized to Er^{3+} 650 nm and Tm^{3+} 480 nm emissions, respectively. Compiled PL photographs show corresponding colloidal solutions of **e** $NaYF_4$:Yb/Tm (20:0.2 mol%), **f**–**j** $NaYF_4$:Yb/Tm/Er (20:0.2:0.2-1.5 mol%), and **k**–**n** $NaYF_4$:Yb/Er (18-60:2 mol%) upon excitation at 980 nm with a 600 mW diode laser. Reprinted with the permission from ref. Wang and Liu (2008). Copyright 2008 American Chemical Society

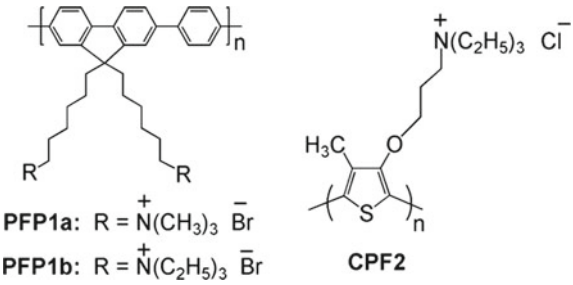

Fig. 2.7 Chemical structures of cationic polyfluorene and polythiophene derivatives. Reprinted with the permission from Liu and Bazan (2004). Copyright 2004 American Chemical Society; printed with the permission from Ho et al. (2008). Copyright 2008 American Chemical Society

suitable to identify susceptibility genes, early stage cancer diagnosis, mutagenesis, or aging assays. However, CCPs still face several disadvantages including weak biocompatibility, aggregation-induced self-quenching, and easy photobleaching. Novel designs for polymer chemical structures are desired to circumvent these limitations. Recently, the newly developed conjugated polymer-based microarrays make multiplexed target detection promising (Liu and Bazan 2005; Zheng and He 2009).

2.3 Fluorescence Reporter Based on Nucleic Acid Amplification Strategies

2.3.1 Fluorescent Dyes Aggression

During the nucleic acid amplification, the introduced fluorescent dyes got closer to emit enhanced fluorescence. Take pyrene for an example. During the process of nucleic acid amplification, the pyrene moieties tagged on the hairpins are brought into close proximity with the others. Since pyrene is a spatially sensitive fluorescent dye, the pyrene molecule at excited state could form an excimer when it was close to the one at excited state. Thus, numerous pyrene excimers along the nucleic acid amplification products were produced; the improved fluorescence could be used to detect target biomolecule s with high selectivity (Huang et al. 2011).

2.3.2 Fluorescence Resonance Energy Transfer (FRET)

The 3′ end of one DNA is labeled with a fluorescent donor, while the 5′ end of its complementary dsDNA is labeled with the corresponding fluorescent acceptor. Their distance is adjusted to guarantee that efficient FRET can take place when they are hybridized. In the non-radiative process, a photon from the energy donor excites an electron in energy acceptor to the excited singlet state with higher vibrational levels. As a result, the energy level of the donor molecule returns to the ground state without emitting fluorescence and the acceptor fluorophore will emit fluorescence in its own specific color. The energy transfer is owing to the dipole orientations of the molecules, and its efficiency is highly dependent on the donor to distance. Effective energy transfer usually occurs within a distance of 10–100 Å range which is roughly the distance between 3 and 30 nucleotides in the dsDNA (Haugland et al. 1969). Thus, therefore, no energy transfer should occur when the two probes are apart from each other and free in solution. Another prerequisite is the spectra match between the fluorescence emission spectrum of the donor and the absorption spectrum of the acceptor. The transferred energy could excite a fluorophore as energy acceptor to emit fluorescence or lose in the form of heat if the acceptor molecule is not a fluorophore. Therefore, the energy transfer efficiency could be evaluated by the decrease in donor

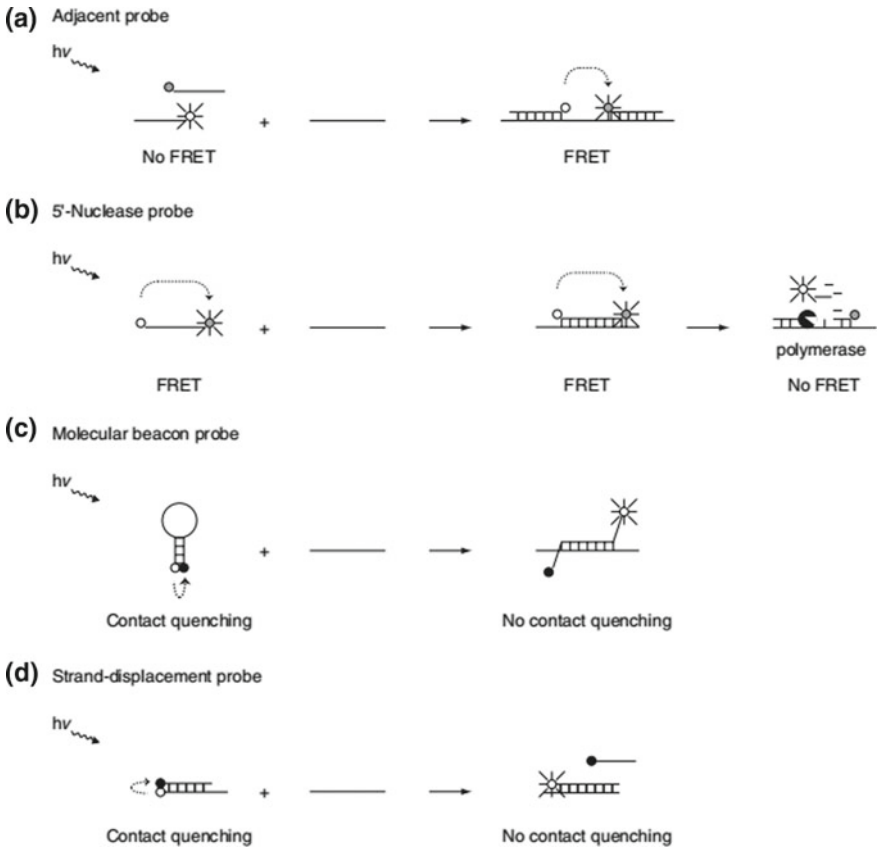

Fig. 2.8 Schematic overview of energy transfer and fluorescence signal generation in fluorescent hybridization probes. Reprinted from Marras (2006), with kind permission from Springer Science + Business Media

fluorescence or the increase in acceptor fluorescence. Marras et al. concluded the guidelines in choosing the appropriate fluorophore–quencher combinations for the establishment of fluorescent hybridization probes (Fig. 2.8, Marras 2006).

The frequently used fluorophore and quencher labels were listed in Table 2.2 and 2.3.

Besides those, the newly developed fluorescent nanomaterials like QDs, GO, and UCNPs could also be used to establish the FRET-based fluorescence biosensor. In 1998, Chen et al. (1998) developed FRET strategy to detect the ligase chain reaction (LCR) products. The acceptor dye fluoresces when gets in close proximity with the donor dye. However, LCR is difficult to use the common homogenous detection techniques such as Taqman probe (Bardea et al. 2011), molecular beacon (Zheng et al. 2011), and specific fluorescent dye of DNA (Cheng et al. 2008) since LCR is based on the amplification of the ligated probes instead of the primer extension such

Table 2.2 Fluorophore labels for fluorescent hybridization probes. Reprinted from Marras (2006), with kind permission from Springer Science + Business Media

Fluorophore	Alternative fluorophore	Excitation (nm)	Emission (nm)
Coumarin	Biosearch Blue, LC Cyan 500	430	475
FAM	–	495	515
TET	CAL Fluor Gold 540	525	540
HEX	ATTO 532, CAL Fluor Orange 560, JOE, VIC	535	555
Cy3	NED, Oyster 556, Quasar 570	550	570
TMR	Alexa 546, CAL Fluor Red 590	555	575
ROX	Alexa 568, CAL Fluor Red 610, LC Red 610	575	605
Texas Red	Alexa 594, CAL Fluor Red 610, LC Red 610	585	605
LC Red 640	CAL Fluor Red 635	625	640
Cy5	ATTO 647 N, LC Red 670, Oyster 645, Quasar 670	650	670
LC Red 705	Cy5.5, Quasar 705	800	710

Table 2.3 Quenchers labels for fluorescent hybridization probes. Reprinted from Marras (2006), with kind permission from Springer Science + Business Media

Quencher	Absorption maximum (nm)
Deep Dark Quencher I	430
Dabcy 1	475
Eclipse	530
FQ	532
Black Hole Quencher I	534
Qsy-7	571
Black Hole Quencher 2	580
Deep Dark Quencher II	630
RQ	645
Blackberry Quencher 650	650
QSY-21	660
Black Hole Quencher 3	670

as PCR, SDA, RCA, and so on. Therefore, it is desirable to develop feasible, highly sensitive, and specific methods for homogeneous LCR products. Nowadays, FRET and real-time fluorescence assay for homogeneous detection of LCR products have been developed. Cheng et al. (2012) used CCPs as an indicator to develop a novel homogeneous LCR assay for the detection of SNP. For LCR, two pairs of unique target-complement probes were designed. After the LCR, the two adjacent probes are ligated to form one DNA strand with a fluorescein label at its 5′ end and phos-

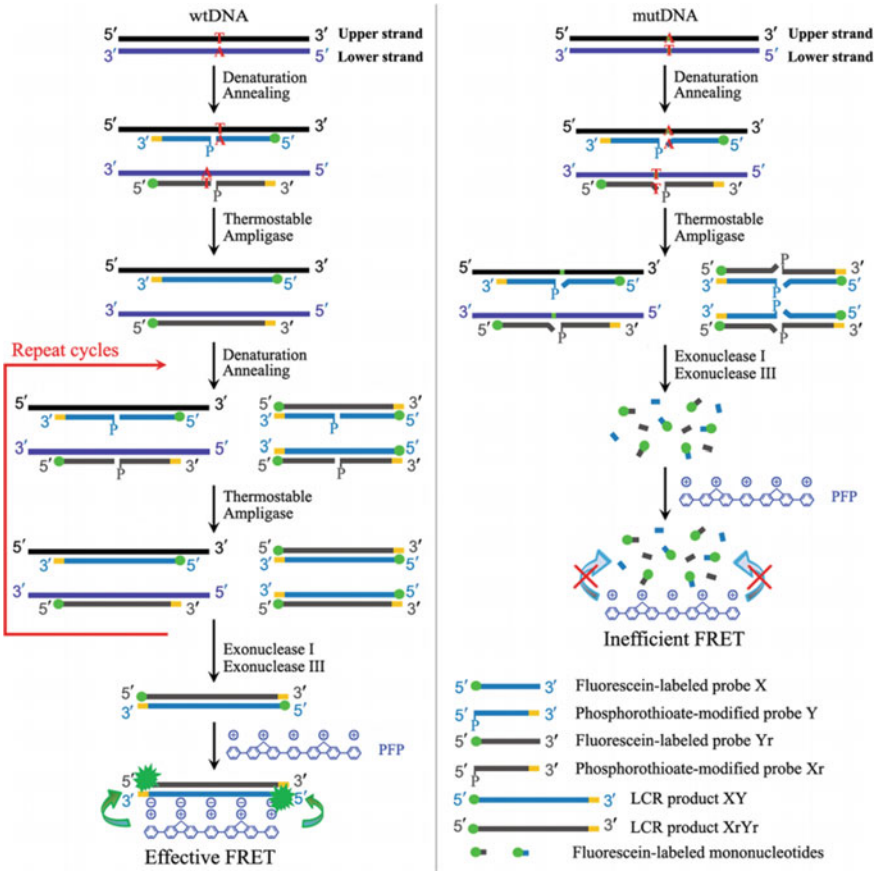

Fig. 2.9 Principle of homogeneous LCR detection based on FRET of SNP. Reprinted with the permission from Cheng et al. (2012). Copyright 2012 American Chemical Society

phorothioate modification at its 3′ end, which is resistant to the exonuclease I and exonuclease III degradation. Based on the strong electrostatic interactions, effective FRET from the CCP to the fluorescein-labeled DNA can occur. This proposed assay strategy extends the application of LCR and provides a new platform for homogeneous detection of SNP (Fig. 2.9).

The exonuclease-assisted CCP biosensor integrated with LCR could also be used for miRNA genotyping (Yuan et al. 2014). However, CCPs can detect all dsDNA without any sequence specificity; thus, unspecific amplification could also generate fluorescence, which makes the discrimination of single-base difficult. To resolve this problem, Sun et al. (2015) labeled a pair of LCR probes with a fluorophore and a quencher, respectively. When the pair of LCR probes was ligated in LCR, the quencher would specifically quench the fluorescence generated from the fluorophore

based on the efficient FRET. Thus, the decrease of fluorescence intensity can be real-time monitored with LCR to realize the one-step detection of SNPs.

Recently developed nanomaterials could be served as the energy acceptor to develop FRET sensing platform. Li's group developed the HCR-AuNPs to detect the anterior gradient protein 2 homolog (AGR-2) (Li et al. 2017). In the absence of AGR-2, the free aptamer acted as an initiator and activated the fluorescently labeled hairpins to trigger HCR. The produced HCR dsDNA product generated intense fluorescence without the quenching by the AuNPs due to their weak interaction. However, when the aptamer bound to the AGR-2, the HCR process would be inhibited. Thus, the fluorescently labeled hairpins were adsorbed on AuNPs, quenching the overall fluorescence of the system. Based on this strategy, AGR-2 was detected with high sensitivity.

Besides AuNPs as the fluorescence quencher, polydopamine nanotubes could also be used to establish the FRET system with the fluorescent dye. Ge et al. combined cycled SDA, fluorescently labeled DNA probe, and polydopamine nanotubes to develop a quantitation fluorometric assay of nucleic acids. In the absence of target DNA, polydopamine nanotubes could quench the fluorescence of the absorbed fluorescence molecules. The addition of analyte (target DNA) and polymerase would open the stem of the molecular beacon to bind with the primer, further triggered the target strand displacement polymerization, and synthesized dsDNA. Due to the strand displacement activity of the polymerase, the hybridized target was displaced and further hybridized with another molecular beacon to trigger the next round of polymerization. Finally, a large amount of dsDNA with loaded fluorescence molecules would be produced. The developed fluorescent sensing strategy showed good analytical performances toward DNA detection with a wide linear range and low LOD (Ge et al. 2018) (Fig. 2.10).

Luo et al. described a fluorometric ATP assay that made use of carbon dots and GO along with toehold-mediated strand displacement reaction. In the absence of target, the fluorescence of carbon dots is strong and in the "on" state, because the signal probe hybridized with the aptamer strand and could not combine with GO. In the presence of ATP, it would bind to the aptamer and induced a strand displacement reaction. Consequently, the signal probe was released, the sensing strategy would change into the "off" state with the addition of GO (Fig. 2.11). This aptasensor exhibited selective and sensitive response to ATP and had a 3.3 nM detection limit (Luo et al. 2018).

2.3.3 Photoinduced Electron Transfer Strategy

Photoinduced electron transfer occurs when an excited-state electron transferred from an electron-rich species (a donor) to an electron-deficient species (an acceptor). Based on this strategy, novel fluorescence biosensing systems have been designed (Aigner et al. 2014; Liu et al. 2015; Su et al. 2012; Tao et al. 2015). Via the photoinduced electron transfer, guanine can efficiently quench the fluorescence of many

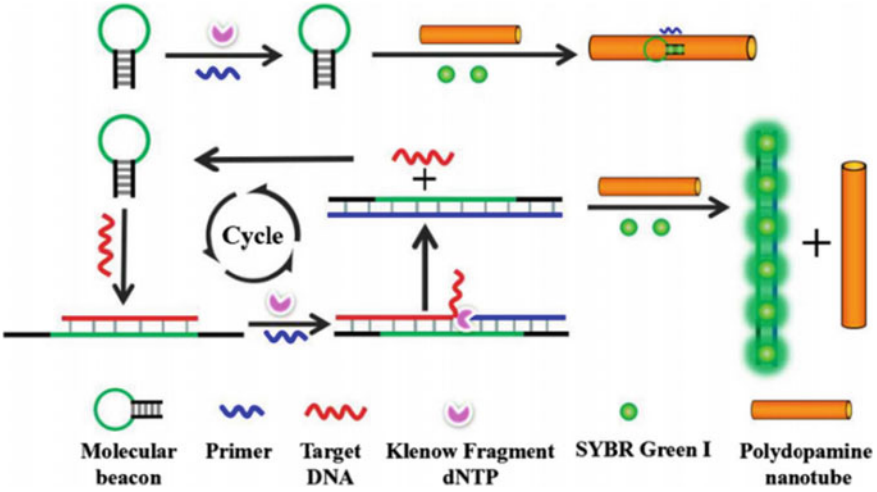

Fig. 2.10 Schematic of the label-free sensor for sensitive nucleic acids detection by combining cycled strand displacement amplification and the polydopamine nanotube strategy. Reprinted from Ge et al. (2018), with kind permission from Springer Science + Business Media

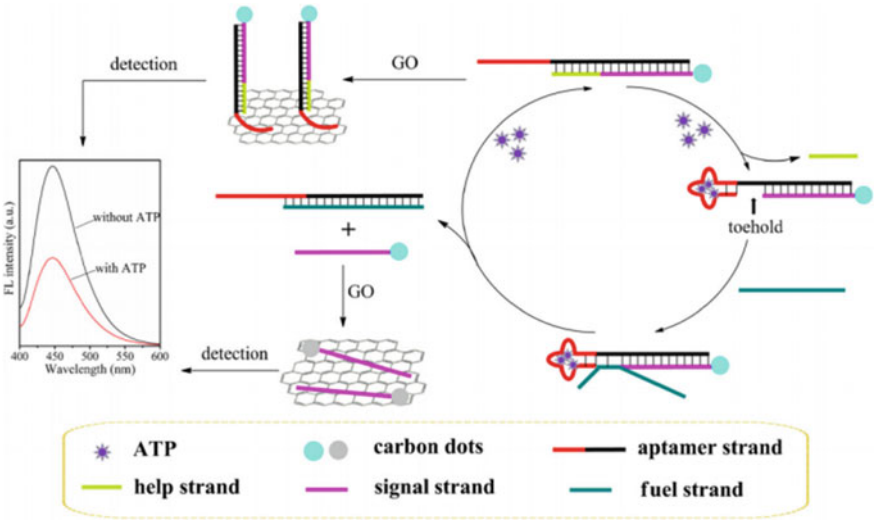

Fig. 2.11 Schematic illustration of CD-based signal amplification fluorescence sensor for detection of ATP. Reprinted from Luo et al. (2018) with kind permission from Springer Science + Business Media

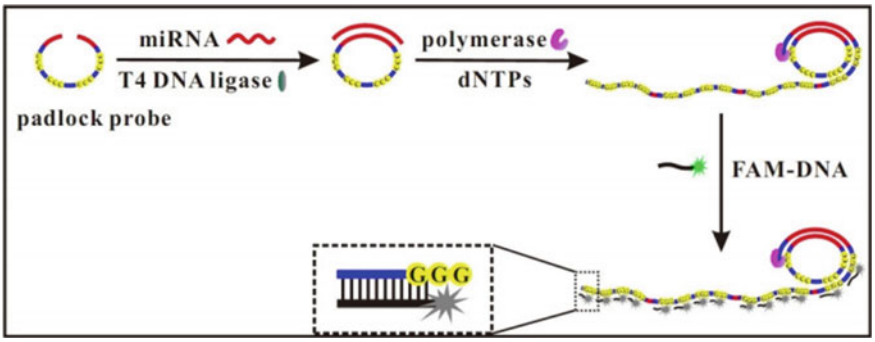

Fig. 2.12 Schematic of the strategy for photoinduced electron transfer-based RCA fluorescence detection of miRNA with linear DNA as signal probe. Reproduced from Zhou et al. (2016) by permission of John Wiley & Sons Ltd

fluorophores (Zhang et al. 2012; Tao et al. 2015). Zhou et al. first integrated RCA and photoinduced electron transfer into one detection process. A circular DNA as the recognition probe was used to hybridize with the target miRNA and further primed a RCA reaction. The generated RCA products could be hybridized with thousands of FAM-labeled linear DNA probes, leading to FAM to be close to—GGG—base of RCA product. Due to the photoinduced electron transfer between FAM and guanine, the fluorescence of FMA was significantly quenched. This method provided a simple, isothermal, and low-cost approach for sensitive detection of miRNA and held a great potential for early diagnosis in gene-related diseases (Fig. 2.12). Furthermore, the target-dependent circularization of the padlock probe and the ligation reaction could obtain higher specificity, leading to discrimination between miRNA family members (Zhou et al. 2016).

2.4 Rational Design of Fluorescence Biosensor Based on Nucleic Acid Amplification Strategies

2.4.1 Fluorophores Chemically Conjugated to DNA

Fluorescent molecules described in the section "*Fluorescent Dyes and Nanomaterials*" could be chemically conjugated to DNA to establish the fluorescently labeled oligonucleotides. Molecular beacons with chemically conjugated fluorophores and quencher are widely used. Iovannisci and Winn-Deen utilized fluorescent dye-labeled oligonucleotides to generate fluorescently labeled LCR products. With a fluorescent sequencer, as little as 0.5 fmol of fluorescently labeled products could be detected (Iovannisci and Winn-Deen 1993). Meng et al. developed a fluorescent detection of ligated products on microbeads (Meng et al. 2010). In this method, three primers

were used and two allele-specific primers were labeled with two different fluorescent dyes at their 5′ end. The ligation products were then captured by streptavidin-coated microbeads, and then, fluorescence signals were collected by a fluorescent microscope and used for genotyping. Many of the existing molecular beacon probes still have presented disadvantages such as the complex synthesis process, costliness of materials, toxicity of the heavy metal ion, and supersubtle optimization. Therefore, it is still highly important and desirable to develop low-cost, efficient, and universal molecular beacon for biochemical sensing. Recently, a novel γ-CD-mediated dual-pyrene-labeled stemless molecular beacon (γ-CD-P-MB) was designed by bounding the two pyrene molecule-labeled DNA probe in the γ-CD hydrophobic cavity (Zheng et al. 2011). Via the γ-CD amplification, the loaded pyrene molecules could trigger remarkable excimer fluorescence enhancement. In addition, the stable and strong binding interaction between γ-CD and pyrene could tune the stem stability of the probes, obtaining higher target-binding selectivity and sensitivity than conventional DNA probes (Meng et al. 2012). The pyrene excimer with large MegaStokes shifting (~130 nm) and long fluorescence lifetime (~ 40 ns) could effectively avoid background interference; thus, it could achieve the sensitive detection in complex biological media (Huang et al. 2011). Based on this strategy, Zou and his coworkers developed a ligation-rolling circle amplification (L-RCA)-based fluorescent method for the detection of SNP. With the low LOD (40 fM), this developed method was recognized to provide a great genotyping platform for pathogenic diagnosis and genetic analysis (Zou et al. 2014). Besides conditional fluorescent dyes, near-infrared fluorescent dyes could also be used to label DNA and combined RCA to detect nucleic acid molecules (Xu et al. 2017). Yang et al. established a HCR/GO fluorescent signaling platform for miRNA detection. Briefly, the target miRNA initiated the HCR between fluorophore-labeled hairpins. The fluorescence of excess hairpins would be completely quenched by GO due to their close distance, while the HCR product would retain fluorescence due to the separation of the fluorophores from GO (Yang et al. 2012). The improved sensitivity higher than those of other GO-based fluorescent nucleic acid assays (Dong et al. 2010). The simple operation, low cost, and enhanced fluorescent signal make the HCR/GO platform a very interesting candidate for in situ fluorescence imaging of miRNAs and possibly other biomolecules. Besides miRNA, HCR/GO platform could be used to detect biothiols (Ge et al. 2014).

2.4.2 A Label-Free Fluorescent Strategy

The chemical conjugation between fluorescent molecules and DNA probe usually need complex chemical reaction. Recently, a label-free fluorescent strategy has been developed which the fluorescent dyes intercalate into the grooves of dsDNA (Xu and Zheng 2016). However, the fluorescent ligands of dsDNA, such as SYBR Green, exhibit strong fluorescence, resulting in a relatively high background signal. Hence, it is still a great challenge to develop feasible fluorescent methods based on nucleic acid amplification to detect biomarkers sensitively and selectively. Based on the HCR

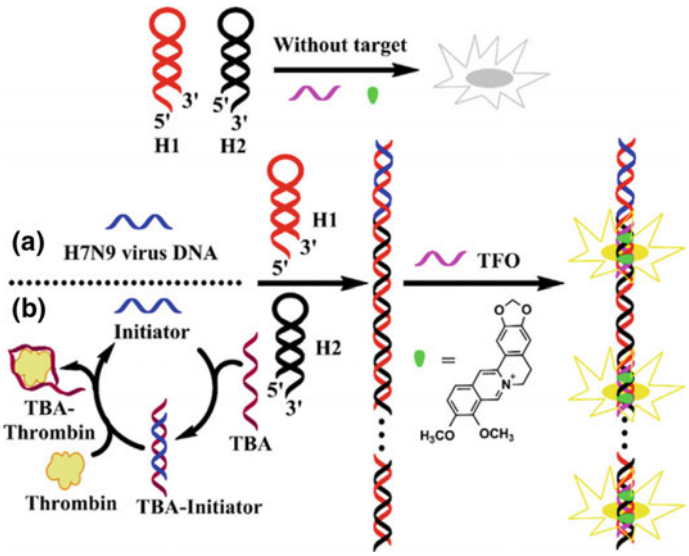

Fig. 2.13 Chematic illustration of label-free fluorescent detection of H7N9 virus DNA (**a**) and thrombin (**b**) using HCR amplification and DNA triplex assembly with berberine as the triplex indicator. Reprinted from Zou et al. (2018). Copyright 2018, with permission from Elsevier

amplification and DNA triplex assembly, Zou's group constructed a label-free light-up fluorescent sensing platform for the detection of avian influenza A (H7N9) virus DNA and thrombin which used berberine as the triplex indicator and fluorophore. In the presence of targets, the HCR can occur between H1 and H2, and then, DNA triplex assembly forms between HCR products and triplex-forming oligonucleotide. The triplex structures are easily recognized by berberine, resulting in a dramatic increase in the fluorescence intensity at 530 nm. In the absence of targets, the HCR process could not be triggered and the triplex structures could form, which resulted in a relatively low background signal (Fig. 2.13, Zou et al. 2018). To improve the performance of the HCR-based fluorescent nucleic acid assays significantly, Niu et al. designed an enzyme-coupled HCR to achieve the fluorescence detection of target DNA. Fluorescent molecules generated by the HRP-catalyzed oxidation reaction showed a linear increase in fluorescence intensity with the target DNA concentration (Niu et al. 2010).

In comparison with other isothermal nucleic acid amplification approaches, HDA has significant advantages of simple reaction scheme and time-saving procedure. Especially, HDA can achieve over a million-fold amplification within a short reaction time (less than 1 h) and has been widely applied for the detection of DNA (Crannell et al. 2014), telomerase (Chen et al. 2016), transcription factor (Cao and Zhang 2013), and pathogens (Andresen et al. 2009).

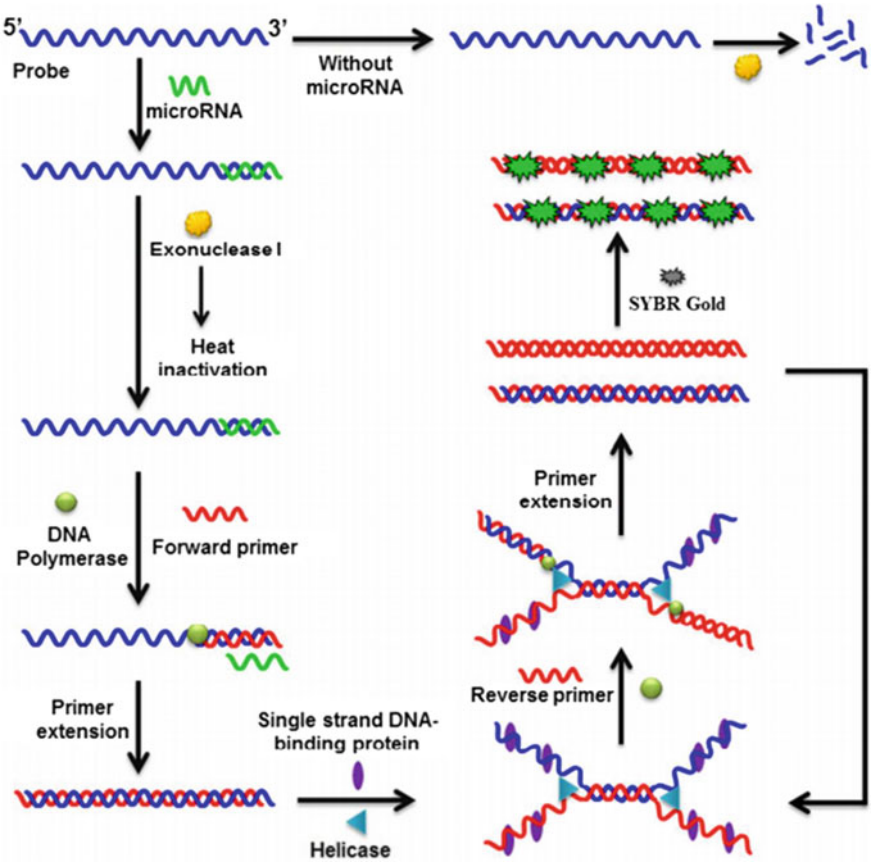

Fig. 2.14 A simple, rapid, and sensitive fluorescent method for label-free detection of microRNAs based on HDA. Reprinted with the permission from Ma et al. (2017). Copyright 2017 American Chemical Society

Ma et al. developed a label-free fluorescent method to achieve the simple, rapid, and sensitive detection of microRNAs based on HDA. A linear probe with specific binding to target microRNAs escaped from exonuclease I (Exo I) digestion and then was amplified by HDA to generate a distinct fluorescence signal with SYBR as the indicator (Fig. 2.14). This assay could be finished within 30 min amplification time and exhibited a high sensitivity and a large concentration range (around five orders of magnitude) (Ma et al. 2017).

Zhao and his coworkers developed a dual-color fluorescence platform for the detection of complementary dsDNA. Firstly, Ru complex, $Ru(bpy)_2(dppx)^{2+}$ (bpy = 2.2'-bipyridine, dppx = 7,8-dimethyldipyrido[3.2-a:2′,3′-c]-phenanthroline), was served as an effective fluorescence quencher for QDs via photoinduced electron transfer process. Then, complementary dsDNA could compete with the QDs and

captured the Ru complex due to the stronger binding affinity. Therefore, Ru complex intercalated DNA complex and free QDs were obtained, leading to the new emergence of red fluorescence of Ru complex and restoration of QDs fluorescence. Based on this process, they developed a simple, fast, and sensitive detection of dsDNA (Zhao et al. 2009). Inspired by this design, Liu et al. developed a highly selective detection for specific ssDNA sequences. The magnetic microparticles (MMPs) were served as solid reaction carriers. Specific ssDNA including target DNA, capture DNA, and auxiliary DNA was designed to induce hybridization and form HCR products. As followed, a large amount of Ru complex could intercalate into the HCR products and restored the QDs fluorescence. As compared, in the absence of the target DNA, the HCR products could not be conjugated to the MMPs and the QDs fluorescence was quenched by the Ru complex. The developed method could be used to recognize the ssDNA with high selectivity against single- and two-base mismatched sequences. Thus, the developed HCR-based fluorescence method had great potential for the application of DNA diagnostics and clinical analysis (Liu et al. 2013).

2.5 Fluorescence Collection and Commercial Instrument

2.5.1 Real-Time or Quantitative Nucleic Acid Amplification Strategies

Higuchi et al. developed an real-time PCR strategy (also called quantitative PCR, qPCR). Fluorescence molecules, ethidium bromide, were intercalated into each amplification reaction; thus, nucleic acid amplification products with increased amounts of fluorescence molecules were produced. The fluorescence was further excited and collected with a computer-controlled cooled CCD camera (Higuchi et al. 1992, 1993). By plotting this fluorescence increment versus the cycle number, the real-time PCR provided a more complete picture of the PCR process than electrophoresis. The developed dPCR introduced fluorescent reporter molecules into the PCR process and owned the merits of excellent sensitivity, high specificity, reproducible data, low contamination risk, and reduced operation time. Thus, qPCR has been widely used in various research areas like bioanalysis and biomedicine (Navarro et al. 2015). With outstanding merits, the developed qPCR matured into a competitive market, and the first commercial instrumentation was made available by Applied Biosystems in 1996. Nowadays, Applied Biosystems and other companies produced various qPCR instruments (Didenko 2006; Valasek and Repa 2005). Based on these commercial instruments, a large number of qPCR techniques have been developed for the DNA detection. Besides DNA, zhang et al. developed a ligation-mediated PCR with SYBR Green I as the fluorescent indicator to real-time detect small biological molecules in a high-throughput format. This method is extremely sensitive with a detection limit of as low as 18.8 fM for ATP and 17.3 fM for NAD^+, and it could also discriminate target molecules from their analogues (Zhang et al. 2015).

Recently, a real-time accelerated reverse transcription loop-mediated isothermal amplification (RT-LAMP) assay was proposed. The RT-LAMP assay is a specific, effective, and rapid gene amplification method, and the whole procedure could be finished with one hour. The RT-LAMP assay was successfully used for virus isolation, surveillance, and differentiation (Parida et al. 2004, 2005).

FRET strategy was also used to design the qPCR (Kongklieng et al. 2015). Besides commercially available dark quenchers (BHQ-1, BHQ-2, BBQ-650), unsymmetrical dialkylamino-substituted zinc azaphthalocyanine with a wide absorption spectra (300–700 nm), unique spectral and photophysical properties could be used as effective fluorescence quenchers in DNA hybridization probes (Demuth et al. 2018).

2.5.2 Multiplex Nucleic Acid Amplification Strategies

Chamberlain et al. developed multiplex PCR in 1988 (Chamberlain et al. 1988). Since then, much effort has been devoted to optimize multiplex PCR to achieve the distinction of several amplification products by fluorophores with different wavelengths (Lee et al. 1993; Henegariu et al. 1997; Rachlin et al. 2005). Now, multiplex PCR has widely used in the detection of viruses, bacteria, and genetic modifications (Schuler et al. 2016). Real-time multiplex PCR assays offer automated analysis in a closed tube system, but limited by the low throughput. To overcome this bottleneck, greater multiplexing PCR assays were proposed and achieved by the application of different fluorescent-labeled probes (Lee et al. 1993), hydrolysis probes (Holland et al. 1991), molecular beacons (Tyagi and Kramer 1996), and mediator probes (Faltin et al. 2012).

2.5.3 Digital Nucleic Acid Amplification Strategies

The calibration curves are necessary to obtain quantitative results of the fluorescence data which could be obtained by performing several amplification experiments using variable and known concentrations of DNA. However, the calibration curves bring several disadvantages to the real-time nucleic acid amplification strategies such as the time-consuming process and unavailable standards. Thus, the digital droplet polymerase chain reaction (ddPCR) was designed to enable a direct quantification of nucleic acids without a calibration curve (Baker 2012; Heredia et al. 2013; Hindson et al. 2011; Whale et al. 2012). Compared to RT-PCR, the ddPCR method has greater tolerance to inhibitors and better repeatability at low concentrations (Morisset et al. 2013). It is based on partitioning the sample into small droplets. The size of the droplets should be controlled to let only some of them carry DNA template before amplification which would fluoresce after PCR. Accurate results are obtained when the average number of templates per droplet is similar. The average template number

per droplet before PCR, λ, is determined from the ratio of fluorescent droplets to total droplets, p, making use of the poisson distribution, according to the following equation:

$$\lambda = -\ln(1 - p)$$

In the ddPCR, only droplet counting is needed instead of a calibration curve for quantification. Several dPCR methods have been developed for the quantification of miRNA, gene (Hui et al. 2018; Menschikowski et al. 2015), and genetically modified organisms (Dobnik et al. 2015; Niu et al. 2018).

Although, the microfluidic device-based droplet-generating technique is quite popular. However, the multistep procedure would inevitably cause "rain effect" that some targets are missing, and others are present in high concentrations, leading to false results and inaccurate screening detection standard (Dobnik et al. 2016). Therefore, new approaches for dPCR should meet the requirement of simplicity, reproducibility, and commercialization. Printing technology, especially inkjet printing, could precisely control small volumes and produce monodisperse microdroplet for use in digital PCR assays (Chen et al. 2012, 2013; Yang et al. 2016; Zeng et al. 2015; Zhang et al. 2016). This technique is recognized as one of the most promising methods for efficient microarray fabrication since it could be precisely manipulated, dispersed with spatial control, and widely used in many areas (Zhang et al. 2016). This system is composed of three parts: an inkjet of generating the droplets, a coiled fused-silica capillary for thermal cycling and a laser-induced fluorescence detector for positive droplet counting. In addition, droplet volume can also be controlled via adjusting the driving voltage and applied pulse waveform on the piezo actuator of the inkjet system. Based on inkjet printing technology, the absolute quantification of the HPV sequence has been achieved in Caski cells (Zhang et al. 2018). The commercial and miniaturized instruments based on nucleic acid amplification were detailedly described in Chap. 15.

2.6 Perspectives

In this chapter, we have summarized remarkable advances in the development of fluorescence biosensor based on nucleic acid amplification strategies. Traditional and commercial fluorescent dyes, novel near-infrared fluorescent dyes, aggression-induced emission molecules, nanomaterials like quantum dots, metal nanoclusters and upconversion nanoprobes, cationic conjugated polymer could be used to label molecular beacons, or intercalate into the dsDNA, or establish fluorescence resonance energy transfer probes. These fluorescent molecules could be combined with nucleic acid amplification strategies to develop "turn-on" and "turn-off" biosensor. Owing to their versatile functions, feasibility, and low cost, nucleic acid amplification strategies have been used to establish and develop broadly applicable fluorescent biosensors

in various biological areas. In addition, novel fluorophores with high quantum yield, bright fluorescence in the near-infrared region, and negligible perturbation to the normal biological process need to be further explored. In addition to intensity-based measurement, other fluorescence signaling techniques, such as lifetime, polarization, and localization, showed various advantages in developing specific fluorescent biosensors. These feasible signaling techniques combined with novel probe design would obtain great developments in the further. Finally, the integration of nucleic acid fluorescent probes with high-throughput platforms such as microfluidic chips or microarray chips will be a rapidly expanding field. These new methodologies will make significant new contributions to real-time monitoring of biochemical events, rapid identification, and characterization of a large number of enzymes in a complex system, drug screening, and disease diagnosis at the early stages.

References

Adams FC, Barbante C (2013) Nanoscience, nanotechnology and spectrometry. Spectrochim Acta B 86:3–13

Ahmed M, Guleria A, Rath MC et al (2014) Facile and green synthesis of CdSe quantum dots in protein matrix: tuning of morphology and optical properties. J Nanosci Nanotechnol 14:5730–5742

Aigner D, Freunberger SA, Wilkening M et al (2014) Enhancing photoinduced electron transfer efficiency of fluorescent pH-probes with halogenated phenols. Anal Chem 86:9293–9300

Alivisatos AP, Gu W, Larabell C (2005) Quantum dots as cellular probes. Annu Rev Biomed Eng 7:55–76

Amat-Guerri F, Costela A, Figuera JM et al (1993) Laser action from rhodamine 6G-doped poly (2-hydroxyethyl methacrylate) matrices with different crosslinking degrees. Chem Phys Lett 209:352–356

Andresen D, Von NR, Bier FF (2009) Helicase dependent OnChip-amplification and its use in multiplex pathogen detection. Clin Chim Acta 403:244–248

Auzel F (2004) Upconversion and anti-Stokes processes with f and d ions in solids. Cheminform 35:139–173

Baker ES, Hong JW, Gaylord BS et al (2006) PNA/dsDNA complexes: site specific binding and dsDNA biosensor applications. J Am Chem Soc 128:8484–8492

Baker M (2012) Digital PCR hits its stride. Nat Methods 9:541–544

Bao H, Hao N, Yang Y et al (2010) Biosynthesis of biocompatible cadmium telluride quantum dots using yeast cells. Nano Res 3:481–489

Bardea A, Burshtein N, Rudich Y et al (2011) Sensitive detection and identification of DNA and RNA using a patterned capillary tube. Anal Chem 83:9418–9423

Beija M, Afonso CA, Martinho JM (2009) Synthesis and applications of Rhodamine derivatives as fluorescent probes. Chem Soc Rev 38:2410–2433

Beri RK, Khanna PK (2011) Green synthesis of cadmium selenide nanocrystals: the scope of 1, 2, 3-selendiazoles in the synthesis of magic-size nanocrystals and quantum dots. J Nanosci Nanotechnol 11:5137–5142

Bossi M, Fölling J, Belov VN et al (2008) Multicolor far-field fluorescence nanoscopy through isolated detection of distinct molecular species. Nano Lett 8:2463–2468

Bridges MA, Mcerlane KM, Kwong E et al (1986) Fluorometric determination of nanogram quantities of protein in small samples: application to calcium-transport adenosine triphosphatase. Clin Chim Acta 157:73–79

Cao A, Zhang CY (2013) Real-time detection of transcription factors using target-converted helicase-dependent amplification assay with zero-background signal. Anal Chem 85:2543–2547
Chamberlain JS, Gibbs RA, Ranier JE et al (1988) Deletion screening of the duchenne muscular dystrophy locus via multiplex DNA amplification. Nucleic Acids Res 16:11141–11156
Chen F, Lin Z, Zheng Y et al (2012) Development of an automatic multi-channel ink-jet ejection chemiluminescence system and its application to the determination of horseradish peroxidase. Anal Chim Acta 739:77–82
Chen F, Mao S, Zeng H et al (2013) Inkjet nanoinjection for high-thoughput chemiluminescence immunoassay on multicapillary glass plate. Anal Chem 85:7413–7418
Chen F, Zhang D, Zhang Q et al (2016) Zero-background helicase-dependent amplification and its application to reliable assay of telomerase activity in cancer cell by eliminating primer-dimer artifacts. Chem Bio Chem 17:1171–1176
Chen XN, Livak KJ, Kwok PY (1998) A homogeneous, ligase-mediated DNA diagnostic test. Genome Res 8:549–556
Cheng Y, Du Q, Wang L et al (2012) Fluorescently cationic conjugated polymer as an indicator of ligase chain reaction for sensitive and homogeneous detection of single nucleotide polymorphism. Anal Chem 84:3739–3744
Cheng Y, Li Z, Zhang X et al (2008) Homogeneous and label-free fluorescence detection of single-nucleotide polymorphism using target-primed branched rolling circle amplification. Anal Biochem 378:123–126
Crannell ZA, Rohrman B, Richardskortum R (2014) Quantification of HIV-1 DNA using real-time recombinase polymerase amplification. Anal Chem 86:5615–5619
Demuth C, Spindler KLG, Johansen JS et al (2018) Measuring KRAS mutations in circulating tumor DNA by droplet digital PCR and next-generation sequencing. Transl Oncol 11:1220–1224
Didenko VV (2006) Fluorescent energy transfer nucleic acid probes. Methods in Molecular Biology™
Dobnik D, Stebih D, Blejec A et al (2016) Multiplex quantification of four DNA targets in one reaction with Bio-Rad droplet digital PCR system for GMO detection. Sci Rep 6:35451
Dobnik D, Spilsberg B, Bogožalec KA et al (2015) Multiplex quantification of 12 European Union authorized genetically modified maize lines with droplet digital polymerase chain reaction. Anal Chem 87:8218–8226
Dong H, Gao W, Yan F et al (2010) Fluorescence resonance energy transfer between quantum dots and graphene oxide for sensing biomolecules. Anal Chem 82:5511–5517
Drexhage KH (1976) Fluorescence efficiency of laser dyes. J Res Nat Bur Stand 80A:421
Duan X, Li Z, He F et al (2007) A sensitive and homogeneous SNP detection using cationic conjugated polymers. J Am Chem Soc 129:4154
Faltin B, Wadle S, Roth G et al (2012) Mediator probe PCR: a novel approach for detection of real-time PCR based on label-free primary probes and standardized secondary universal fluorogenic reporters. Clin Chem 58:1546–1556
Feng F, Duan X, Wang S (2009) Fluorescence-amplifying assay for irradiated DNA lesions using water-soluble conjugated polymers. Macromol Rapid Comm 30:147–151
Feng F, He F, An L et al (2008) Fluorescent conjugated polyelectrolytes for biomacromolecule detection. Adv Mater 20:2959–2964
Feng F, Tang Y, He F et al (2010) Cationic conjugated polymer/DNA complexes for amplified fluorescence assays of nucleases and methyltransferases. Adv Mater 19:3490–3495
Gao G, Zhang M, Gong D et al (2017) The size-effect of gold nanoparticles and nanoclusters in the inhibition of amyloid-β fibrillation. Nanoscale 9:4107–4113
Gašperšič J, Hafner-Bratkovič I, Stephan M et al (2010) Tetracysteine-tagged prion protein allows discrimination between the native and converted forms. FEBS J 277:2038–2050
Gaylord BS, Heeger AJ, Bazan GC (2002) DNA detection using water-soluble conjugated polymers and peptide nucleic acid probes. Proc Natl Acad Sci 99:10954–10957

Ge J, Bai DM, Geng X et al (2018) Fluorometric determination of nucleic acids based on the use of polydopamine nanotubes and target-induced strand displacement amplification. Microchim Acta 185:105

Ge J, Huang ZM, Xi Q et al (2014) A novel graphene oxide based fluorescent nanosensing strategy with hybridization chain reaction signal amplification for highly sensitive biothiol detection. Chem Commun 50:11879–11882

Gonçalves MST (2010) Fluorescent labeling of biomolecules with organic probes. Cheminform 40:190–212

Haugland RP, Yguerabide J, Stryer L (1969) Dependence of the kinetics of singlet-singlet energy transfer on spectral overlap. PNAS 63:23–30

Henegariu O, Heerema NA, Dlouhy SR et al (1997) Multiplex PCR: critical parameters and step-by-step protocol. Biotechniques 23:504–511

Heredia NJ, Belgrader P, Wang S et al (2013) Droplet Digital™ PCR quantitation of HER2 expression in FFPE breast cancer samples. Methods 59:S20–S23

Higaki T, Liu C, Zeng C et al (2016) Controlling the atomic structure of Au30 nanoclusters by a ligand-based strategy. Angew Chem Int Ed 55:6694–6697

Higuchi R, Dollinger G, Walsh PS et al (1992) Simultaneous amplification and detection of specific DNA sequences. Nat Biotechnol 10:413–417

Higuchi R, Fockler C, Dollinger G et al (1993) Kinetic PCR analysis: real-time monitoring of DNA amplification reactions. Biotechnology 11:1026–1030

Hindson BJ, Ness KD, Masquelier DA et al (2011) High-throughput droplet digital PCR system for absolute quantitation of DNA copy number. Anal Chem 83:8604–8610

Ho HA, Boissinot M, Bergeron MG et al (2002) Colorimetric and fluorometric detection of nucleic acids using cationic polythiophene derivatives. Angew Chem Int Ed 41:1548–1551

Ho HA, Najari A, Leclerc M (2008) Optical detection of DNA and proteins with cationic polythiophenes. Acc Chem Res 39:168–178

Holland PM, Abramson RD, Watson R et al (1991) Detection of specific polymerase chain reaction product by utilizing the 5′-3′ exonuclease activity of thermus aquaticus DNA polymerase. Proc Natl Acad Sci USA 88:7276–7280

Huang J, Wu Y, Chen Y et al (2011) Pyrene-excimer probes based on the hybridization chain reaction for the detection of nucleic acids in complex biological fluids. Angew Chem Int Ed 123:421–424

Huang K, Yang H, Zhou Z et al (2008) Multisignal chemosensor for Cr^{3+} and its application in bioimaging. Org Lett 10:2557–2560

Hui Y, Wu Z, Qin Z et al (2018) Micro-droplet digital polymerase chain reaction and real-time quantitative polymerase chain reaction technologies provide highly sensitive and accurate detection of Zika Virus. Virol Sin 33:270–277

Iovannisci DW, Winn-Deen ES (1993) Ligation amplification and fluorescence detection of Mycobacterium tuberculosis DNA. Mol Cell Probe 7:35–43

Joubert MF (1999) Photon avalanche upconversion in rare earth laser materials. Opt Mater 11:181–223

Kongklieng A, Intapan PM, Boonmars T et al (2015) Detection of Babesia canis vogeli and Hepatozoon canis in canine blood by a single-tube real-time fluorescence resonance energy transfer polymerase chain reaction assay and melting curve analysis. J Vet Diagn Invest 27:191–195

Lee LG, Connell CR, Bloch W (1993) Allelic discrimination by nick-translation PCR with fluorgenic probes. Nucleic Acids Res 21:3761–3766

Li L, Tian G J. Luo Y et al (2013) Blinking, flickering, and correlation in fluorescence of single colloidal CdSe quantum dots with different shells under different excitations. J Phys Chem C 117:4844–4851

Li L, Tian X, Zou G et al (2008) Quantitative counting of single fluorescent molecules by combined electrochemical adsorption accumulation and total internal reflection fluorescence microscopy. Anal Chem 80:3999–4006

Li Z, Miao X, Cheng Z et al (2017) Hybridization chain reaction coupled with the fluorescence quenching of gold nanoparticles for sensitive cancer protein detection. Sens Actuators B Chem 243:731–737
Liu B, Bazan GC (2004) Homogeneous fluorescence-based DNA detection with water soluble conjugated polymers. Chem Mater 16:4467–4476
Liu B, Bazan GC (2005) Methods for strand-specific DNA detection with cationic conjugated polymers suitable for incorporation into DNA chips and microarrays. PNAS 102:589–593
Liu WH, Howarth M, Greytak AB et al (2008) Compact biocompatible quantum dots functionalized for cellular imaging. J Am Chem Soc 130:1274–1284
Liu Y, Luo M, Yan J et al (2013) An ultrasensitive biosensor for DNA detection based on hybridization chain reaction coupled with the efficient quenching of a ruthenium complex to CdTe quantum dots. Chem Commun 49:7424–7426
Liu ZZ, Wang BL, Ma Z et al (2015) Fluorogenic probe for the human ether-a-Go-Go-related gene potassium channel imaging. Anal Chem 87:2550–2554
Loudet A, Burgess K (2007) BODIPY®dyes and their derivatives: syntheses and spectroscopic properties. Chem Rev 39:4891–4932
Luo J, Shen X, Li B et al (2018) Signal amplification by strand displacement in a carbon dot based fluorometric assay for ATP. Microchim Acta 185:392–400
Ma F, Liu M, Tang B et al (2017) Rapid and sensitive quantification of MicroRNAs by isothermal Helicase-dependent amplification. Anal Chem 89:6182–6197
Marras SAE (2006) Selection of fluorophore and quencher pairs for fluorescent nucleic acid hybridization probes. Methods Mol Biol 335:3
Martin MM (1975) Hydrogen bond effects on radiationless electronic transitions in xanthene dyes. Chem Phys Lett 35:105–111
Meng HM, Fu T, Zhang XB et al (2012) Efficient fluorescence turn-on probe for zirconium via a target-triggered DNA molecular beacon strategy. Anal Chem 84:2124–2128
Meng X, Yang X, Wang K et al (2010) Direct fluorescence detection of point mutations in human genomic DNA using microbead-based ligase chain reaction. Talanta 80:1725–1729
Menschikowski M, Jandeck C, Friedemann M et al (2015) Identification and quantification of heterogeneously-methylated DNA fragments using epiallele-sensitive droplet digital polymerase chain reaction (EAST-ddPCR). Epigenetics 10:803–809
Morisset D, Štebih D, Milavec M et al (2013) Quantitative analysis of food and feed samples with droplet digital PCR. PLoS ONE 8:e62583
Navarro E, Serrano-Heras G, CastaãO MJ et al (2015) Real-time PCR detection chemistry. Clin Chim Acta 439:231–250
Niu C, Xu Y, Zhang C et al (2018) Ultrasensitive single fluorescence-labeled probe-mediated single universal primer-multiplex-droplet digital polymerase chain reaction for high-throughput genetically modified organism screening. Anal Chem 90:5586–5593
Niu S, Jiang Y, Zhang S (2010) Fluorescence detection for DNA using hybridization chain reaction with enzyme-amplification. Chem Commun 46:3089–3091
Niu WB, Wu SL, Zhang SF et al (2011) Multicolor output and shape controlled synthesis of lanthanide-ion doped fluorides upconversion nanoparticles. Dalton Trans 40:3305–3314
Parida M, Posadas G, Inoue S et al (2004) Real-time reverse transcription loop-mediated isothermal amplification for rapid detection of west nile virus. J Clin Microbiol 42:257–263
Parida M, Horioke K, Ishida H et al (2005) Rapid detection and differentiation of dengue virus serotypes by a real-time reverse transcription-loop-mediated isothermal amplification assay. J Clin Microbiol 43:2895–2903
Prazeres TJV, Fedorov A, Barbosa SP et al (2008) Accurate determination of the limiting anisotropy of rhodamine 101 implications for its use as a fluorescence polarization standard. J Phys Chem A 112:5034
Rachlin J, Ding C, Cantor C et al (2005) MuPlex: multi-objective multiplex PCR assay design. Nucleic Acids Res 33:W544

Sameiro T, Goncalves T (2009) Fluorescent labeling of biomolecules with organic probes. Chem Rev 109:190–212
Schietinger S, Menezes LS, Lauritzen B et al (2009) Observation of size dependence in multicolor upconversion in single Yb^{3+}, Er^{3+} codoped $NaYF_4$ nanocrystals. Nano Lett 9:2477–2481
Schuler F, Trotter M, Zengerle R et al (2016) Monochrome multiplexing in PCR by photobleaching of fluorogenic hydrolysis probes. Anal Chem 88:2590–2595
Sjöback R, Nygren J, Kubista M (1995) Absorption and fluorescence properties of fluorescein. Spectrochim Acta A 51:L7–L21
Su X, Zhu X, Zhang C et al (2012) In situ, real-time monitoring of the 3' to 5' exonucleases secreted by living cells. Anal Chem 84:5059–5068
Sun WC, Gee KR, Klaubert DH et al (1997) Synthesis of fluorinated fluoresceins. J Org Chem 62:6469–6475
Sun Y, Lu X, Su F et al (2015) Real-time fluorescence ligase chain reaction for sensitive detection of single nucleotide polymorphism based on fluorescence resonance energy transfer. Biosens Bioelectron 74:705–710
Talhavini M, Atvars TDZ (1999) Photostability of xanthene molecules trapped in poly(vinyl alcohol) (PVA) matrices. J Photochem Photobiol A 120:141–149
Tao M, Shi Z, Cheng R et al (2015) Highly specific fluorescence detection of T4 polynucleotide kinase activity via photo-induced electron transfer. Anal Biochem 485:18–24
Treibs A, Kreuzer FH (1968) Difluorboryl-komplexe von di-und tri-pyrrylmethenen. Justus Liebigs Ann Chem 718:208–223
Tyagi S, Kramer FR (1996) Molecular beacons: probes that fluoresce upon hybridization. Nat Biotechnol 14:303–308
Ueno Y, Jiao GS, Burgess K (2004) Preparation of 5- and 6-carboxyfluorescein. Synth-Stuttg 15:2591–2593
Udenfriend S, Stein S, Böhlen P et al (1972) Fluorescamine: a reagent for assay of amino acids, peptides, proteins, and primary amines in the picomole range. Science 178:871–872
Valasek MA, Repa JJ (2005) The power of real-time PCR. Adv Physiol Educ 29:151–159
Wang F, Liu XG (2008) Upconversion multicolor fine-tuning: visible to near-infrared emission from lanthanide-doped $NaYF_4$ nanoparticles. J Am Chem Soc 130:5642–5643
Weigele M, Debernardo S Leimgruber W (1973) Fluorometric assay of secondary amino acids. Biochem Biophys Res Commun 50:352–356
Whale AS, Huggett JF, Cowen S et al (2012) Comparison of microfluidic digital PCR and conventional quantitative PCR for measuring copy number variation. Nucleic Acids Res 40:e82
Xu X, Zhang B, Gan P et al (2017) On-nylon membrane detection of nucleic acid molecules by rolling circle amplification. Anal Biochem 533:26–33
Xu Y, Zheng Z (2016) Direct RNA detection without nucleic acid purification and PCR: Combining sandwich hybridization with signal amplification based on branched hybridization chain reaction. Biosens Bioelectron 79:593–599
Yang L, Liu C, Ren W et al (2012) Graphene surface-anchored fluorescence sensor for sensitive detection of microRNA coupled with enzyme-free signal amplification of hybridization chain reaction. ACS Appl Mater Interfaces 4:6450–6453
Yang J, Katagiri D, Mao S et al (2016) Inkjet printing based assembly of thermoresponsive core-shell polymer microcapsules for controlled drug release. J Mater Chem B 4:4156–4163
Yao C, Tian S, Liao L et al (2015) Synthesis of fluorescent phenylethanethiolated gold nanoclusters via pseudo-AGR method. Nanoscale 7:16200–16203
Yin Y, Alivisatos AP (2005) Colloidal nanocrystal synthesis and the organic-inorganic interface. Nature 437:664–670
Yu P, Wen X, Toh YR et al (2015) Fluorescent metallic nanoclusters: electron dynamics, structure, and applications. Part Part Syst Char 32:142–163
Yuan Z, Zhou Y, Gao S et al (2014) Homogeneous and sensitive detection of microRNA with ligase chain reaction and lambda exonuclease-assisted cationic conjugated polymer biosensing. ACS Appl Mater Interfaces 6:6181–6185

Zeng H, Yang J, Katagiri D et al (2015) Investigation of monodisperse droplet generation in liquids by inkjet. Sens Actuators B Chem 220:958–961

Zhang JS, Qin WP, Zhao D (2006) Energy transfer processes on both Er^{3+} ion concentration and excitation densities in Yb^{3+}-Er^{3+} codoped LaF_3 matrix. J Lumin 119:341–345

Zhang W, Li N, Koga D et al (2018) Inkjet printing based droplet generation for integrated online digital polymerase chain reaction. Anal Chem 90:5329–5334

Zhang W, Mao S, Yang J et al (2016) The use of an inkjet injection technique in immunoassays by quantitative on-line electrophoretically mediated microanalysis. J Chromatogr A 1477:127–131

Zhang Y, Liu J, Zhang CY (2015) Real-time monitoring of small biological molecules by ligation-mediated polymerase chain reaction. Chem Commun 51:12270–12273

Zhao D, Chan WH, He ZK et al (2009) Quantum dot-ruthenium complex dyads: recognition of double-strand DNA through dual-color fluorescence detection. Anal Chem 81:3537–3543

Zheng J, Li J, Jiang Y et al (2011) Design of aptamer-based sensing platform using triple-helix molecular switch. Anal Chem 83:6586–6592

Zheng W, He L (2009) Label-free, real-time multiplexed DNA detection using fluorescent conjugated polymers. J Am Chem Soc 131:3432–3433

Zhou F, Meng R, Liu Q et al (2016) Photoinduced electron transfer-based fluorescence quenching combined with rolling circle amplification for sensitive detection of microRNA. Chemistryselect 1:6422–6428

Zhou J, Liu Z, Liu FY (2012) Upconversion nanophosphors for small-animal imaging. Chem Soc Rev 41:1323–1349

Zou L, Li T, Shen R et al (2018) A label-free light-up fluorescent sensing platform based upon hybridization chain reaction amplification and DNA triplex assembly. Talanta 189:137–142

Zou Z, Qing Z, He X et al (2014) Ligation-rolling circle amplification combined with $\hat{I}^3$-cyclodextrin mediated stemless molecular beacon for sensitive and specific genotyping of single-nucleotide polymorphism. Talanta 125:306–312

Chapter 3
Nucleic Acid Amplification Strategies-Based Chemiluminescence Biosensors

Sai Bi and Yongcun Yan

Abstract Chemiluminescence (CL) has become one of the most attractive techniques to construct biosensors with the advantages of high sensitivity, low cost, simple manipulation, and high throughput. In CL reactions, the luminescent substrate is excited by chemical reactions, during which a light emission is generated. So far, diverse CL biosensing platforms have been developed for sensitive and selective detection of a wide range of analytes, such as nucleic acids, small molecules, proteins, and even cells. In particular, to improve the detection sensitivity, nucleic acid amplification strategy-based CL biosensors have been developed, including the fabrication of novel signal amplification probes, the development of new CL systems, the construction of tool enzyme-based biosensing platforms and the strand displacement reaction-based enzyme-free signal amplification strategies.

3.1 Nucleic Acid-Based CL Nanoprobes for Signal Amplification

Nanoprobes are powerful ways to improve the detection sensitivity and selectivity (Chen et al. 2013; He et al. 2015; Li et al. 2016a, b, c; Liu et al. 2018). So far, a series of novel biofunctional nanoprobes have been developed for signal amplification, which have been successfully applied to the construction of biosensors. For example, many efforts have been made using magnetic particles (MPs), gold nanoparticles (AuNPs), and carbon materials to improve the sensitivity. MPs demonstrate the advantages of large surface area for molecular immobilization and purification, easy separation, and simple manipulation (Chen et al. 2017; Xianyu et al. 2018; Yang et al. 2016; Zheng et al. 2016). AuNPs, as a class of nanomaterials with unique optical and electrochemical properties, have been successfully applied in biochemical analysis

S. Bi (✉) · Y. Yan
College of Chemistry and Chemical Engineering, Qingdao University, Qingdao 266071, Shandong, People's Republic of China
e-mail: bisai11@126.com

Y. Yan
e-mail: yanyongcun0@163.com

S. Zhang et al. (eds.), *Nucleic Acid Amplification Strategies for Biosensing, Bioimaging and Biomedicine*, https://doi.org/10.1007/978-981-13-7044-1_3

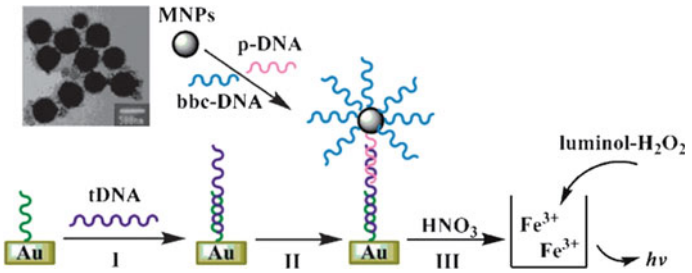

Fig. 3.1 FL-CL detection of DNA hybridization based on biobarcode functionalized magnetic nanoparticle labels (bbcMNPs). Reproduced from Bi et al. (2009a, b, c) by permission of The Royal Society of Chemistry

(Bi et al. 2015a, b, c, d, e; Medeghini et al. 2018; Zhang et al. 2018a, b, c, d, e; Zhou et al. 2018a, b). AuNPs have the advantages of easy synthesis in a wide range of sizes (from ~1 to more than 100 nm). Further, as excellent biolabels, AuNPs can easily conjugate with biomolecules (e.g., proteins and DNAs) retaining the bioactivity (Li et al. 2018a, b, c; Sun et al. 2014; Zhang et al. 2018a, b, c, d, e). Carbon materials, such as carbon nanotubes (CNTs) and graphene, have attracted more and more interest in biosensing because of the excellent electrical, optical, and mechanical properties and good chemical stability (Cao et al. 2018; Geim 2009; He et al. 2018; Kong et al. 2016; Li et al. 2018a, b, c; Pan et al. 2018). In addition, due to the large surface area-to-weight ratio, easy preparation, and low cost, carbon materials have been versatilely applied to the development of signal amplification platforms, achieving sensitive detection of a wide range of analytes (Bi et al. 2014a, b).

To avoid the cross reaction and improve the detection sensitivity, the concept of biobarcode nanoprobes has been proposed (Chen et al. 2014; Dong et al. 2015; Wang et al. 2015a, b; Zhang et al. 2018a, b, c, d, e). For example, a flow injection-chemiluminescence (FI-CL) system has been developed for the detection of target DNA using biobarcode magnetic nanoparticles (MNPs) (Fig. 3.1) (Bi et al. 2009a, b, c). In this assay, biobarcode MNPs were fabricated via labeling biobarcode DNA (bbcDNA) and probe DNA (pDNA) with the ratios of approximately $1:1.22 \times 10^6:1.69 \times 10^5$. The target DNA was analyzed in a sandwich-type detection protocol. The sensitivity was improved by one order of magnitude over that only using single DNA as probe.

It has been reported that hemin/G-quadruplex DNAzyme has the same catalytic activity as HRP molecules (Chen et al. 2018a, b, c; Qiu et al. 2017; Wang et al. 2017). DNAzyme with thermostability is also easy to synthesize and modify (Abu-Ghazalah et al. 2010; Zhou et al. 2015). Using multilayer hemin/G-quadruplex-wrapped AuNPs as tags, disposable protein array for multiplex CL imaging of α-fetoprotein (AFP), human chorionic gonadotrophin-β (β-hCG), carcinoma antigen 125 (CA 125), and carcinoembryonic antigen (CEA) was realized (Zong et al. 2013). In this work, biotinylated DNA and alkylthiol-capped ssDNA were assembled on AuNPs with high ratio. Then hemin and K^+ were added to form multilayer HRP-mimicking DNAzyme

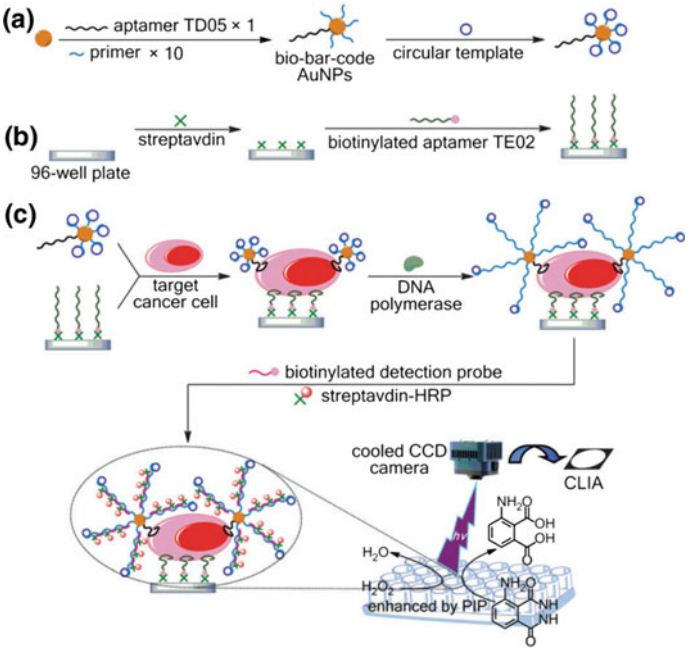

Fig. 3.2 CL imaging of cancer cells through biobarcode nanoprobe-based RCA. Reproduced from Bi et al. (2013a, b, c, d) by permission of The Royal Society of Chemistry

on the surface of AuNPs. After CL immunoassay (CLIA), the DNAzyme/AuNP tag was linked to sandwich immunocomplexes by biotin-streptavidin conjugation. The CL signal was amplified markedly using the multilayer DNAzyme/AuNP labels.

Moreover, a biobarcode AuNPs-based CL imaging array has been developed for high-throughput and sensitive detection of Ramos cells (Fig. 3.2) (Bi et al. 2013a, b, c, d). Dual aptamers were used in this strategy to improve the specificity. Firstly, biobarcode AuNPs were constructed through functionalizing aptamer TD05 and primers with a ratio of 1:10 to specifically recognize cells and initiate rolling circle amplification (RCA), respectively. At the same time, aptamer TE02 was immobilized on the microplate well to capture Ramos cells. Upon introduction of the synthesized biobarcode AuNP probes, a sandwich complex of AuNP-aptamer TD05-cell-aptamer TE02 was formed. In the presence of DNA polymerase/dNTPs, RCA was triggered on the AuNPs to assemble a large amount of horseradish peroxidase (HRP) molecules to catalyze the PIP-enhanced luminol-H_2O_2 CL system. The CL images were recorded on a cooled charge-coupled device (CCD), achieving ultrasensitive detection of Ramos cells as low as 163 cells. Similarly, RCA-based biobarcode strategy was proposed for thrombin detection on microchip via in situ formation of multi-G-quadruplex/hemin DNAzyme (Wang et al. 2018a, b).

Mesoporous silica nanoparticles (MSNs) as novel controlled release materials have been used to deliver drugs and biomolecules. Based on MSN-controlled release

system, an analyte-triggered CL system was prepared for sensitive detection of cocaine, in which a large number of glucose molecules were loaded into the pores of MSNs. Then flexible linear aptamer of cocaine was added to wrap the MSN-glucose compounds via electrostatic interaction. In the presence of cocaine, the aptamer on MSNs specifically bound with cocaine, leading to the open of MSN pores and the release of glucose. The glucose oxidase in solution catalyzed the oxidation of glucose to produce H_2O_2, which further enhanced the CL emission of luminol. The CL signals were positively related to the concentrations of cocaine. Cocaine could be detected by this sensitive MSN-based CL biosensor with the LOD of 1.43 μM (Chen et al. 2016).

3.2 Development of CL Systems for Signal Amplification

In CL assays, the development of detection systems is of great significance to improve the sensitivity. The enzyme molecules are important in CL systems to determine the H_2O_2 and other compounds through coupling enzyme-catalyzed reactions. For example, the HRP-catalyzed oxidation of luminol has been applied to enhance the sensitivity of the CL system (Landi-Librandi et al. 2011; Liu and Zhang 2015; Roda and Guardigli 2012). In addition, a variety of phenol derivatives have been developed as enhancers for luminol-based CL systems, which can greatly increase the emission intensity (Clough et al. 2016; Liu et al. 2015). Certain chemical indicators, such as phenol red, cresolphthalein, phenolphthalein, and bromophenol blue (BPB), have also been found as efficient enhancers for HRP-catalyzed luminol-H_2O_2 CL reaction (Luedeke et al. 2016; Nie et al. 2015; Yang et al. 2015; Zhang et al. 2018a, b, c, d, e). Recently, through combining with the biofunctionalized nanoprobes for signal amplification, the luminol-H_2O_2-HRP-BPB CL system has been successfully applied in immunoassays (Bi et al. 2009a, b, c).

In addition, the development of metal ion-catalyzed CL systems also holds promise in improving the detection sensitivity. For example, the luminol-H_2O_2-Fe^{3+} CL system has been extensively studied and readily applied to ultrasensitive detection of target DNA using biobarcode magnetic nanoparticles (MNPs) as labeling probes, achieving a detection limit as low as 0.32 fM (Bi et al. 2009a, b, c). Moreover, through using biobarcode dendrimer-like DNA (bbc-DL-DNA) as probes for signal amplification, a new CL system of luminol-H_2O_2-Ru^{3+} was developed for sensitive and selective detection of cancer cells based on aptamer recognition (Bi et al. 2010a, b, c, d).

Besides single-metal-ion catalysis, the development of synergistic enhanced chemiluminescence (SECL) systems also attracts intensive research interest. For example, a SECL system of luminol-H_2O_2-Cu^{2+}-Fe^{3+} was proposed, which significantly intensified the CL signals in comparison to monometallic catalyst Cu^{2+} or Fe^{3+} (Bi et al. 2010a, b, c, d). Through fabricating a kind of multiplex nanoprobes (CuS/DNA/Au/DNA/MNP) and using MNPs as both DNA molecular carriers and reporter labels, this SECL system was applied in amplified biosensing of target DNA

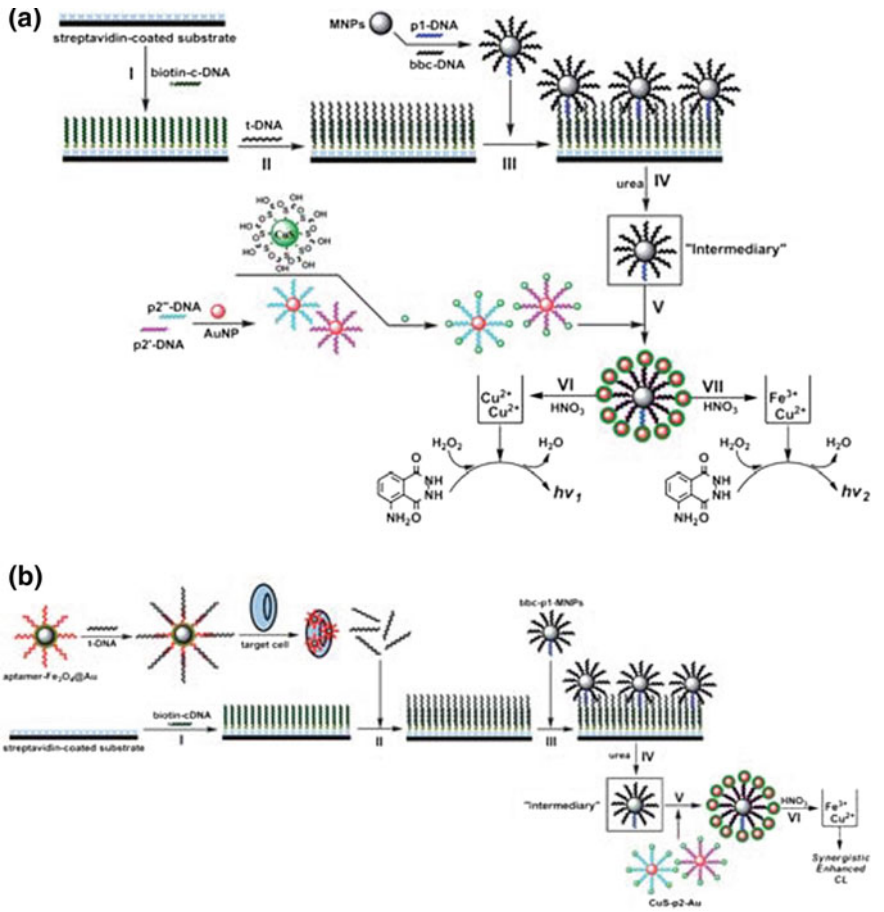

Fig. 3.3 SECL detection of DNA hybridization and Ramos cells based on a dual-amplification strategy. Reproduced from Bi et al. (2010a, b, c, d) by permission of The Royal Society of Chemistry

and Ramos cells with excellent specificity, achieving the detection limits down to 6.8 aM and 56 cells/mL, respectively, which was one of the most sensitive bioanalysis methods (Fig. 3.3).

Chemiluminescence resonance energy transfer (CRET) system has become more and more popular in bioanalysis. In a typical CRET system, a nonradiative dipole–dipole energy transfer occurs from a CL donor to a certain acceptor via the specific oxidation of a luminescent substrate during CL reaction (Cai et al. 2018; Freeman et al. 2011; Shuhendler et al. 2014; Zhen et al. 2016; Zhou et al. 2018a, b). In contrast to fluorescence resonance energy transfer (FRET), CRET occurs through oxidizing a luminescent substrate with no requirement of an excitation source, which thus can minimize nonspecific signals and avoid photobleaching caused by external light excitation to improve the detection sensitivity. For example, in the CRET system

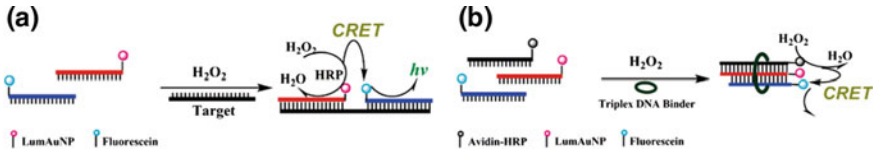

Fig. 3.4 Binary and triplex DNA molecular beacons based on CRET system for ATP detection. Reprinted with the permission from Zhang et al. 2009. Copyright 2009 American Chemical Society

of luminol-H_2O_2-HRP-fluorescein, the CL energy transfers from luminol donor to fluorescein acceptor because fluorescein can absorb part of the excited-state energy of luminol (~425 nm) and re-emit the light at longer wavelengths (~510 nm). Enlightened by this phenomenon, Zhang et al. designed binary and triplex CRET molecular beacons as signaling probes, achieving sensitive detection of ATP in cancer cells based on structure-switching aptamer recognition (Fig. 3.4) (Zhang et al. 2009).

Based on the luminol-H_2O_2-HRP-fluorescein CRET system, an enzyme-free amplified CL imaging platform was also proposed for microRNA detection based on target-catalyzed DNA four-way junction (DNA-4WJ) (Bi et al. 2015a, b, c, d, e). In this method, target microRNA-let-7a triggered a cascade of toehold-mediated strand displacement reactions among four DNA hairpins to form the DNA-4WJ, during which the target microRNA was displaced to catalyze the additional self-assembly process. In the DNA-4WJ structure, fluorophore fluorescein amidite (FAM) and G-quadruplex sequences were encoded in a close proximity. In the presence of hemin/K^+, the HRP-mimicking DNAzymes were formed to catalyze the luminol-H_2O_2 CL system and further transfer to FAM. Importantly, in this system, the background signal was efficiently reduced using magnetic graphene oxide (MGO) to remove excess hairpins and hemin via magnetic separation. Thus, the detection sensitivity was significantly improved with a detection limit of 6.9 fM. Similarly, another CRET amplification platform was developed based on self-assembly of DNA network on magnetic microparticles (MMPs), achieving ultrasensitive CRET imaging of miRNA-122 (Bi et al. 2016a, b, c, d).

Through theoretical calculations, it has been found that graphene or graphene oxide (GO) with the long-range nanoscale energy transfer property has excellent quenching efficiency (Li et al. 2017b; Luong and Vashist 2017; Yang et al. 2017a, b). Accordingly, a GO-based luminol-H_2O_2-HRP-fluorescein cascade CRET system was proposed, in which luminol serves as the CL substrate and donor, fluorescein as enhancer and acceptor, and GO as further energy acceptor of fluorescein. Based on the high adsorption of single-stranded DNA (ssDNA) on GO via π–π interaction, a cascade CRET system-based biosensing platform was constructed for sensitive detection of nucleic acids via base-pairing hybridization and protein via aptamer recognition (Fig. 3.5) (Bi et al. 2012a, b). Briefly, a FAM-labeled ssDNA probe was absorbed on GO noncovalently, resulting in a quenched CRET signal. Upon the introduction of target DNA or thrombin, the probe DNA was released from GO through the formation of DNA duplex or DNA/thrombin complex. The increased distance between the probe DNA and GO make the CRET restored from luminol-

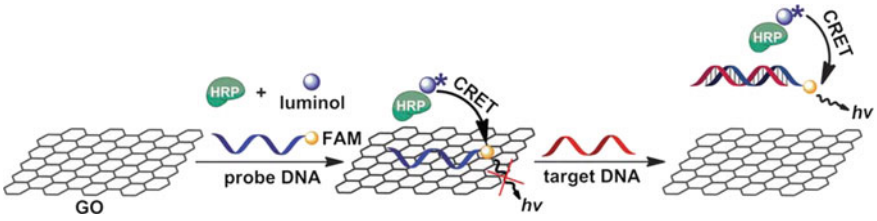

Fig. 3.5 Cascade CRET system based on DNA-GO complex. Reproduced from Bi et al. (2012a, b) by permission of The Royal Society of Chemistry

H_2O_2-HRP to FAM, and the recovered CL intensity was proportional to the target concentration.

Moreover, this cascaded CRET process was applied to microRNA detection through using HRP-mimicking DNAzyme as catalyst. In this assay, three modes of cascaded CRET hot-spot-active substrates were constructed by covalently attaching HRP-mimicking DNAzyme/fluorescein-labeled DNA hairpins on MGO, which results in an "off" signal due to the quenching effect of GO on the luminol/H_2O_2/HRP-mimicking DNAzyme/fluorescein CRET system (Bi et al. 2015a, b, c, d, e). Once addition of target microRNA, it opened the loop domain of hairpin probe, resulting in a recovered CRET signal for sensitive and selective detection of microRNA. More importantly, this CRET substrate demonstrated excellent controllability, reproducibility, and reversibility through strand displacement reaction, which thus held great promise in the development of versatile optical platforms for bioanalysis.

The aggregated AuNPs can not only induce color change of solution but also catalyze the generation of CL signal, for example, in luminol-H_2O_2 system. Accordingly, a label-free CL system based on the aggregation of AuNPs has been developed for the detection of DNA hybridization (Qi et al. 2009). In this strategy, the presence of target DNA led to the hybridization between probe DNA and target DNA after annealing in buffered salt. After hybridization, the as-prepared AuNPs with the average diameter of 13 nm were added and the salt in hybridization solution screened the repulsion between negatively charged AuNPs ((-)AuNPs) and therefore led to the aggregation of AuNPs. Then, the aggregated AuNPs produced strong CL emission after adding luminol and H_2O_2. In contrast, in the absence of target DNA, probe DNA would adsorb on the surface of AuNPs in 0.5 M NaCl and therefore prevented the aggregation of AuNPs. The dispersed AuNPs had weak catalytic activity and led to a weak CL intensity. Compared to AuNP-based colorimetric methods for target DNA detection, the sensitivity was increased more than six orders. Further, single-based mismatched DNA strands were well distinguished from perfectly complementary targets using this CL assay. Similarly, aggregated AuNPs-amplified CL was further used in aptasensor for acetamiprid detection (Qi et al. 2016). In the presence of acetamiprid, the strong interaction between acetamiprid and acetamiprid-binding aptamer (ABA) occurred and the dispersed AuNPs were aggregated at 0.5 M NaCl, leading to a significant enhancement of AuNPs catalytic properties. This CL

aptasensor did not need aptamer labeling or modifying, which can be finished within 0.5-1 h. However, the (-)AuNPs-based label-free CL system with high-salt medium would influence the hybridization between aptamer and target. Alternatively, positively charged AuNPs ((+)AuNPs) were used to construct CL aptasensor without high salt (Qi et al. 2017). In addition to the above AuNP-catalyzed CL system, another AuNPs triggered luminol-$AgNO_3$ CL system was proposed to detect Hg^{2+} based on interstrand cooperative coordination (Cai et al. 2011). Briefly, the capture probe was firstly immobilized on the microwell surface via amino anchor. Then Hg^{2+} was added into microwell and capture probe cooperatively coordinated with Hg^{2+} to form T-Hg-T complex. After washing off residual Hg^{2+}, $NH_2OH/HAuCl_4$ was added. The captured Hg^{2+} catalyzed the formation of AuNPs on T-Hg-T complex. Finally, luminol and $AgNO_3$ were added, and the CL signal was read out with the catalysis of AuNPs. In contrast, the absence of Hg^{2+} would not accelerate the synthesis of AuNPs as well as the emission of CL.

3.3 Tool Enzyme Amplification-Based CL Biosensors

In traditional sensing mode, the target-to-signal ratio is usually 1: 1. Thus, the detection sensitivity is often not low enough to satisfactorily determine trace amounts of analytes in complex samples. To improve the sensitivity, many target recycling-based strategies have been developed, in which the target acts as the "catalyst" to initiate the reaction, resulting in a target-to-signal ratio of 1: n and significantly amplified signals (Min et al. 2017; Qi et al. 2018a, b, c). Up to now, diverse tool enzyme-based CL biosensors have been proposed for target recycling amplification, which have demonstrated versatile applications in sensing of diverse biomolecules, from small molecules and nucleic acids to proteins and even cancer cells (Li et al. 2016a, b, c, 2018a, b, c; Wang et al. 2018a, b; Xu et al. 2012, Zhang et al. 2018a, b, c, d, e).

Rolling circle amplification (RCA) is an isothermal enzymatic amplification reaction, which is carried out with a circular DNA template and a primer in the presence of polymerase. The RCA process can lead to the production of long DNA or RNA strands that are the tandem repeating sequences complementary to circular template. Thus, RCA has demonstrated as a powerful tool for signal amplification (Bi et al. 2013a, b, c, d; Cheng et al. 2009; Wang et al. 2015a, b; Zhao et al. 2008). For example, a triggered polycatenated DNA scaffold was proposed to construct ultrasensitive CL biosensors through combining RCA and DNAzyme amplification (Fig. 3.6) (Bi et al. 2010a, b, c, d). In comparison to traditional RCA methods, in which one target only initiates the formation of one circular template for RCA, mechanically interlocked polycatenated nanostructures were self-assembled upon the introduction of target DNA. The resulting polycatenated DNA nanostructures were further used for RCA reaction to synthesize hemin/G-quadruplex HRP-mimicking DNAzyme chains to catalyze the luminol-H_2O_2 CL system. In particular, the high background induced by excess hemin itself was overcome by attaching the RCA products on MNPs through biotin–streptavidin interaction. This assay was further applied to thrombin detection

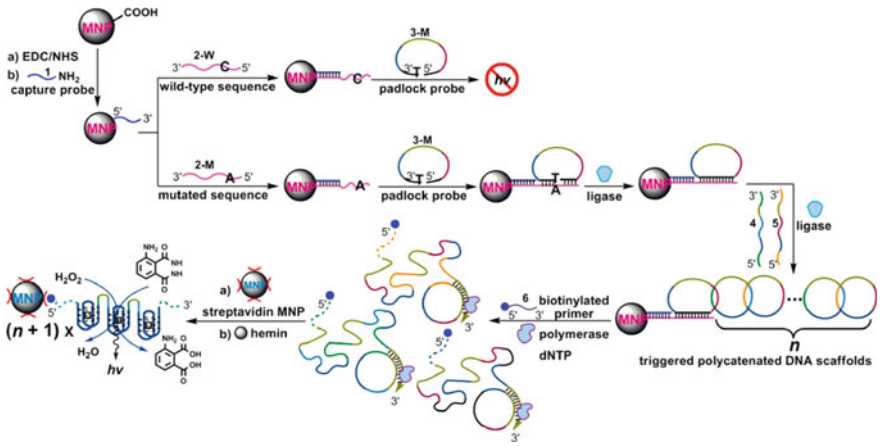

Fig. 3.6 Polycatenated DNA scaffold-mediated RCA reaction and DNAzyme amplification for CL detection of single-nucleotide polymorphisms (SNPs). Reprinted with the permission from Bi et al. (2010a, b, c, d). Copyright 2010 American Chemical Society

based on specific recognition of aptamers. This CL biosensor demonstrated ultra-high sensitivity that was comparable to PCR methods. Moreover, a branched rolling circle amplification (BRCA) protocol based on hybridization chain reaction (HCR) was developed for CL analysis of MTase activity and DNA methylation. Compared to traditional BRCA, the proposed assay demonstrated high amplification in well-controlled manner (Bi et al. 2013a, b, c, d).

In addition to polymerase, nicking-enzyme-based CL amplification methods were also developed, in which nicking enzyme could recognize specific sequences of double-stranded DNA (dsDNA) and cleave one of the two DNA strands. As shown in Fig. 3.7, the ssDNA included a linker DNA and two HRP mimicking DNAzyme sequences, which was blocked by a short ssDNA to form a quasi-circular structure I. Once addition of target DNA, the components were self-assembled into the supramolecular structure II. Then, nicking enzyme Nt.AlwI was introduced to cleave the linker strand, resulting in the dissociation of target DNA to initiate another strand-scission cycle. In the presence of hemin, the cleaved DNAs were assembled into HRP-mimicking DNAzymes, which thus catalyzed the oxidation of luminol by H_2O_2 to generate CL signals. In addition, Fe_3O_4@Au complexes were used to reduce background for sensitivity improvement. This nicking-enzyme-based target recycling amplification achieved a detection limit as low as 8.6 aM (Bi et al. 2010a, b, c, d).

Combined with proximity hybridization, another nicking-enzyme-assisted in situ recycling strategy was presented for CL detection of target DNA, CEA, and thrombin (Zong et al. 2014). The molecular beacon was designed with cleavage site for nicking enzyme Nt. BbvCI. Luminophore Cy5 on stem was quenched by nearby black hole quencher2 (BHQ2). Two help ssDNA could hybridize with the stem of the molecular beacon, the target-related sequence, and part of each other. In the presence of target

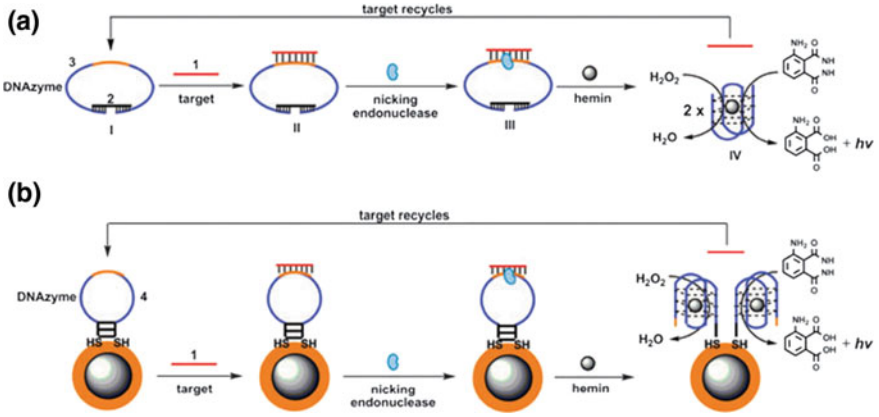

Fig. 3.7 **a** Nicking-enzyme-assisted strand circular amplification for CL detection of target DNA and **b** the use of Fe_3O_4@Au to reduce background. Reproduced from Bi et al. (2010a, b, c, d) by permission of The Royal Society of Chemistry

DNA, molecular beacon was opened through the formation of proximity complex. Then CL signal was generated in peroxalate-H_2O_2 CL system in which the oxidation product 1,2-dioxetanedione transferred its energy to Cy5. The nicking enzyme Nt. BbvCI could cleave the unfolded molecular beacon and release proximity complex, leading to a recycling process to generate strong CL emission. Similarly, CEA and thrombin were detected using this nicking-enzyme-assisted target recycling strategy.

Moreover, a target-triggered polymerase-nicking-enzyme-based cascade amplification reaction was developed for label-free CL detection of microRNA (Bi et al. 2016a, b, c, d). As shown in Fig. 3.8, upon recognition of target microRNA, the conformational changes of DNA hairpins occurred, resulting in the cascaded recycling amplification processes and the generation of a large number of HRP-mimicking DNAzymes to produce significantly enhanced CL signals. Since a feedback function was integrated in the system, this strategy achieved high sensitivity for microRNA detection with a detection limit of 0.82 fM. Moreover, a series of two-input logic gates were constructed using two microRNAs as inputs to generate controllable CL outputs.

Another polymerase-nicking-enzyme-based cascade amplification CL protocol was developed through combing hemin/G-quadruplex HRP-mimicking DNAzyme with DNA machine for ultrasensitive imaging of BCR/ABL fusion gene (Xu et al. 2016a, b). In the presence of BCR/ABL, three tailored DNA probes formed a bis-three-way junction. Then, the DNA machine was initiated with the assistant of DNA polymerase and nicking enzyme, leading to the autonomous generation of DNA products which further triggered another DNA machine. As a result, a large number of DNA products containing G-quadruplex sequences were generated to catalyze the CL signal. With the amplification of cyclic self-assembly, as low as 23 fM BCR/ABL fusion gene can be detected by this assay. Further, microRNA was also detected using

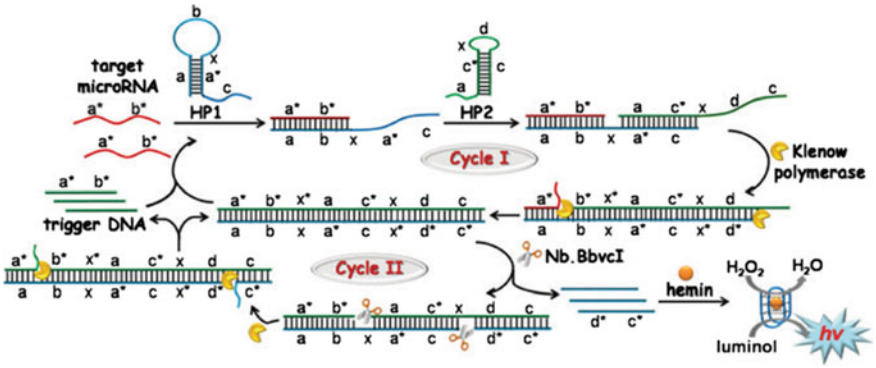

Fig. 3.8 Target-triggered cascade recycling amplification for CL detection of microRNA. Reproduced from Bi et al. (2016a, b, c, d) by permission of The Royal Society of Chemistry

CL exponential isothermal amplification reaction, achieving a detection limit of 2.91 fM and excellent selectivity to distinguish single-base mismatched microRNA-21 (Xu et al. 2016a, b).

A novel ligation chain reaction (LCR) method using ampligase has been developed for SNP detection based on luminol-H_2O_2-HRP-mimicking DNAzyme-fluorescein CRET system (Fig. 3.9) (Bi et al. 2015a, b, c, d, e). In this system, four target-complement probes were designed for the amplification of K-ras (G12C). After LCR, the products with biotin modification were captured on streptavidin-magnetic particles, which facilitated the CRET reaction from HRP DNAzyme-catalyzed luminol-H_2O_2 CL system to fluorescein. Through using a cooled low-light CCD to collect the signals, the SNP-induced CL images were recorded with a detection limit as low as 0.86 fM. In this assay, the high sensitivity can be attributed to not only the exponential amplification efficiency of LCR but also the employment of streptavidin-coated magnetic particles to separate the excess hemin to reduce the background, which provided a new way to genetic diagnosis.

Exonuclease III (Exo III), which does not require specific recognition sequence, has become an ideal candidate for the development of universal biosensing platforms (Bi et al. 2012a, b; Hu et al. 2014; Li et al. 2017a, b; Wang et al. 2014). Recently, an Exo III-based target recycling amplification strategy has been developed for label-free CL detection of target DNA (Fig. 3.10) (Gao and Li 2014). Firstly, the loop region of P2 hybridized with G-quadruplex-forming DNA probe (P1). P1 and P2 were designed with protruding 3′-termini so the P1/P2 hybrid would avoid the digestion. Then target DNA hybridized P2 to form a blunt 3′-terminus of P2, leading to the initiation of Exo III-assisted target recycling amplification (Cycle I) and the release of P1, target DNA, and secondary target DNA. Importantly, the secondary target DNA could hybridize P1/P2 hybrid probe and trigger another cycle to release P1. After the addition of hemin and K^+, a large number of P1 yield G-quadruplex HRP-mimicking DNAzyme to catalyze the CL emission in the presence of luminol and H_2O_2. In addition, the same group employed single-walled carbon nanotubes (SWCNTs) in

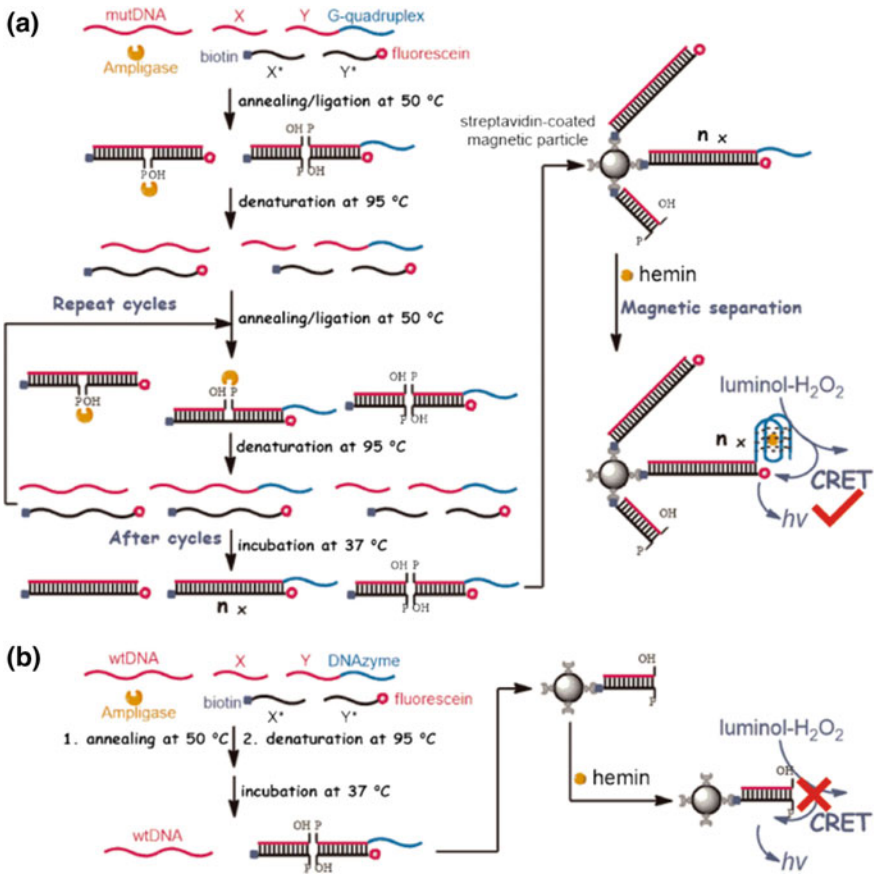

Fig. 3.9 CRET imaging of SNP based on LCR amplification. Reprinted from Bi et al. (2015a, b, c, d, e), Copyright 2015, with permission from Elsevier

the Exo III-assisted target recycling amplification strategy to improve the detection sensitivity by virtue of the high intrinsic surface area and various functional groups of SWCNTs (Gao and Li 2013). In this assay, free hemin was strongly adsorbed on the surface of SWCNTs due to the strong affinity of SWCNTs with hemin, while the formed DNAzyme cannot be adsorbed. After ultracentrifugation, superfluous hemin would be removed and the background was therefore reduced. Further, GO was also used in the Exo III-assisted luminol-H_2O_2-FAM CRET system for site-specific detection of DNA methylation owing to its strong affinity to ssDNA (Chen and Li 2014). The FAM-labeled probe DNA was adsorbed onto GO by noncovalent binding. The target-methylated DNA was unchanged after treated with bisulfite and could hybridize with FAM-labeled probe DNA, which triggered the Exo III-assisted recycling release of FAM. The CL emission of luminol-H_2O_2-HRP was transferred to FAM via CRET, leading to the decrease CL at 420 nm and enhanced CL at ca.

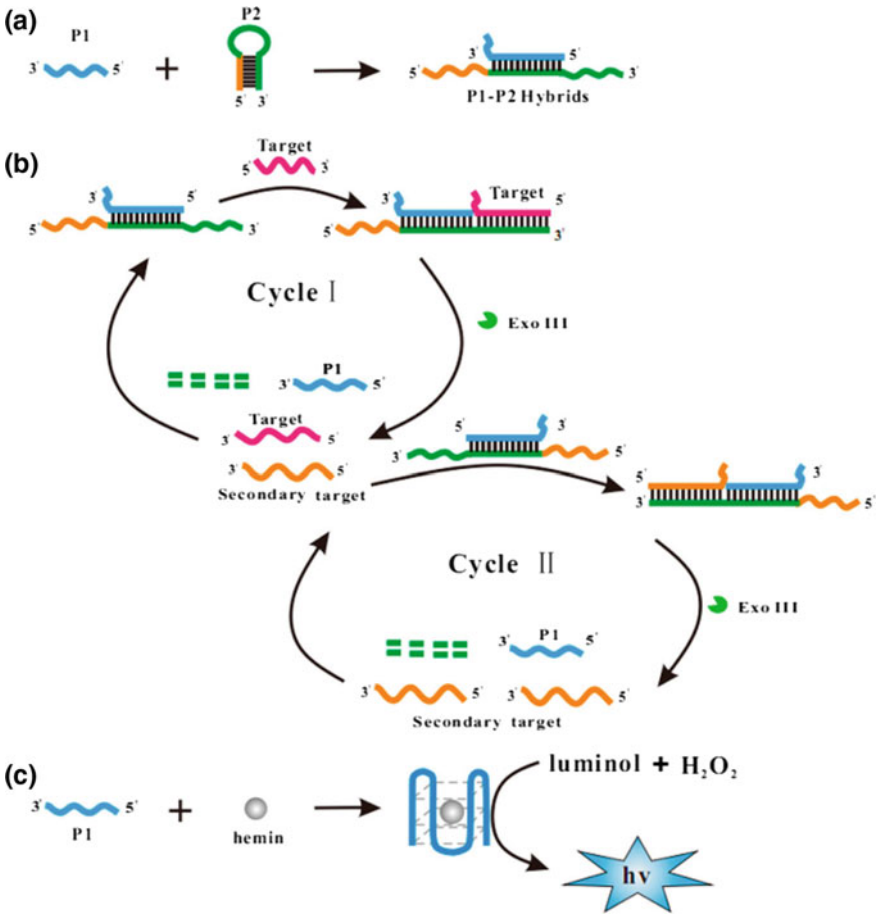

Fig. 3.10 Exo III-assisted recycling amplification for target DNA detection using HRP-mimicking DNAzyme to catalyze the CL signals. Reprinted with the permission from Gao and Li (2014). Copyright 2014 American Chemical Society

510 nm. Whereas unmethylated DNA (5′-CG-3′) would change to 5′-UG-3′ after treated with bisulfite so the probe DNA was still on the surface of GO. Because of the quenching of GO, there was no CL signal at ca. 510 nm. DNA methyltransferase activity was also detected using this Exo III-assisted target recycling amplification system.

The Exo III-assisted cascade amplification target recycling strategy was further applied for CL detection of platelet-derived growth factor BB (PDGF-BB) by taking advantage of recognition property of aptamer and cleavage function of Exo III (Bi et al. 2014a, b). Upon the introduction of PDGF-BB, the aptamer occurred conformational change, which initiated the Exo III-based target recycling amplification reaction, resulting in the release of numerous G-quadruplex sequences. In the pres-

ence of hemin, HRP-mimicking DNAzymes were formed to catalyze the oxidation of luminol by H_2O_2 to generate an amplified CL signal for PDGF-BB detection. Similarly, another versatile Exo III-based target recycling amplification strategy has been proposed for label-free CL detection of target DNA, which further applied to establish a series of "signal-on" and "signal-off" two-input molecular logic gates (Yan et al. 2017). These exonuclease-based strategies demonstrated the advantages of isothermal performance, simple design in sequences, homogeneous reaction, effective-cost without labeling, and high amplification efficiency, which thus can be considered as universal platforms in biosensing, biocomputation, and nanotechnology.

More recently, HCR was integrated into Exo III-assisted target recycling amplification for construction of a versatile cascade amplification biosensor for label-free CL detection of target DNA and protein. In this system, the initiator triggered the Exo III-assisted target recycling reaction. At the same time, the released ssDNA further initiated the HCR, resulting in the formation of HRP-mimicking DNAzyme chains for signal amplification. As low as 5.7 fM target DNA can be detected using this amplified label-free CL biosensor, which also had good performance in real sample assays. Moreover, based on specific aptamer recognition, this method was versatilely applied to sensitive and selective detection of lysozyme, which demonstrated broad application prospects in bioanalysis and clinical diagnosis (Qi et al. 2018a, b, c).

3.4 Enzyme-Free Signal Amplification CL Biosensors

On the basis of toehold-mediated DNA strand displacement reaction, diverse enzyme-free signal amplification strategies have been developed (Bi et al. 2015a, b, c, d, e, 2016a, b, c, d; Qi et al. 2018a, b, c; Wang et al. 2012; You et al. 2015; Yu et al. 2018). HCR is a powerful nonenzymic amplification strategy based on toehold-mediated strand displacement reaction triggered by initiators (Bi et al. 2017; Chen et al. 2018a, b, c; Dirks and Pierce 2004). Based on HCR, a sandwich-type instantaneous derivatization technology was developed for CL detection of DNA target with high selectivity and sensitivity (Wang et al. 2013). To further improve the sensitivity of HCR-based CL method, streptavidin-modified polystyrene microspheres were introduced into the system to facilitate the dual-amplification strategy (Zhou et al. 2017). Catalytic hairpin assembly (CHA) is another typical enzyme-free isothermal amplification reaction based on toehold-mediated strand displacement reaction. The process of CHA does not require enzymatic catalysis and the output signals can be designed to be diverse. For example, based on CHA and proximity-dependent DNAzyme formation, a DNA nanotweezer was designed for CL detection of microRNAs (Li et al. 2016a, b, c). As shown in Fig. 3.11, the double-crossover DNA nanotweezer was constructed by self-assembly, which contained an arched structure and two split G-rich DNAs. In the both presence of miRNA-21 and miRNA-155, the released miRNA-21-miRNA-155-set strand was attacked by assistant strand, resulting in the release of miRNA-21 and miRNA-155. The released two miRNAs triggered the CHA and turned the opened tweezer to closed state. Therefore, the split

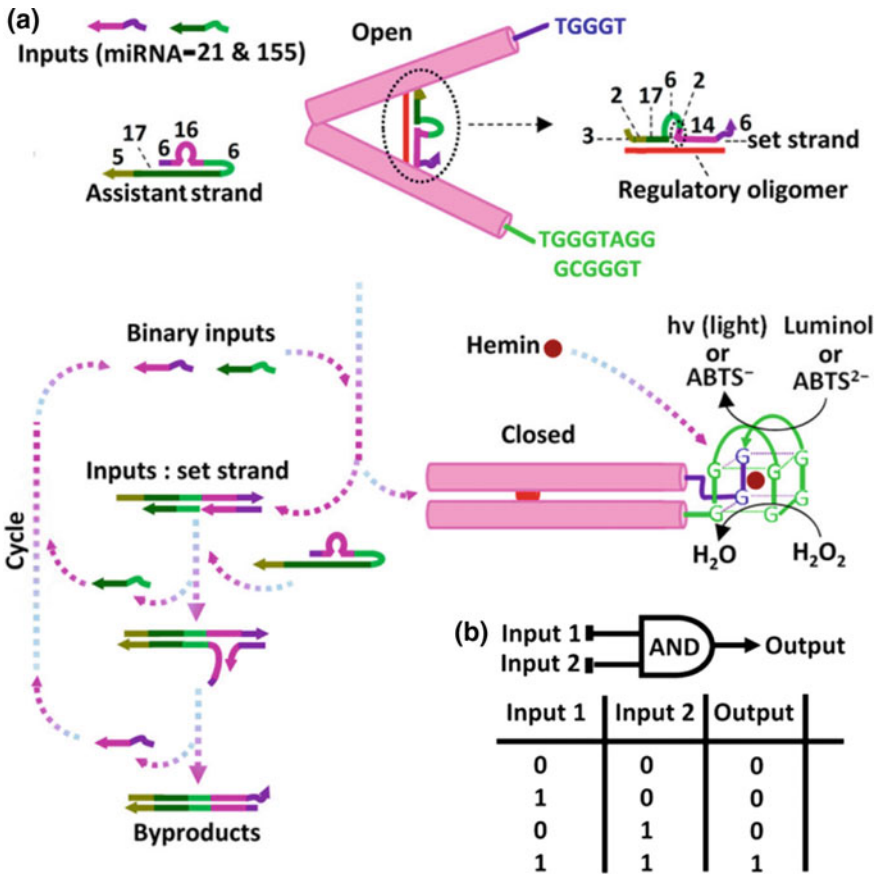

Input 1	Input 2	Output
0	0	0
1	0	0
0	1	0
1	1	1

Fig. 3.11 **a** CHA-based DNA nanotweezer for microRNA detection and logic gate operation; **b** truth table of "AND" logic gate. Reprinted with the permission from Li et al. (2016a, b, c). Copyright 2016 American Chemical Society

G-rich strands at the termini of two arms bound to hemin to form DNAzyme, which catalyzed the CL reaction of luminol-H_2O_2. The amplified CL signal can only be observed at the simultaneous presence of miRNA-21 and miRNA-155, so an AND logic gate operation was build based on the binary target inputs. In addition, Bi's group developed a cross-catalytic hairpin assembly (CHA)-based exponential signal amplification strategy for CRET detection of target DNA (Yue et al. 2017a, b).

The recent work reported a strategy to integrate CHA with HCR to self-assemble hyperbranched DNA structures as enzyme-free amplifier for homogeneous CRET detection of microRNA (Bi et al. 2016a, b, c, d). Upon introduction of target DNA, a single-stranded region was produced to initiate the CHA-HCR cascade amplification circuits, resulting in the formation of hemin/G-quadruplex nanowires to catalyze the oxidation of luminol by H_2O_2 to generate a CL signal. Due to the close proximity of

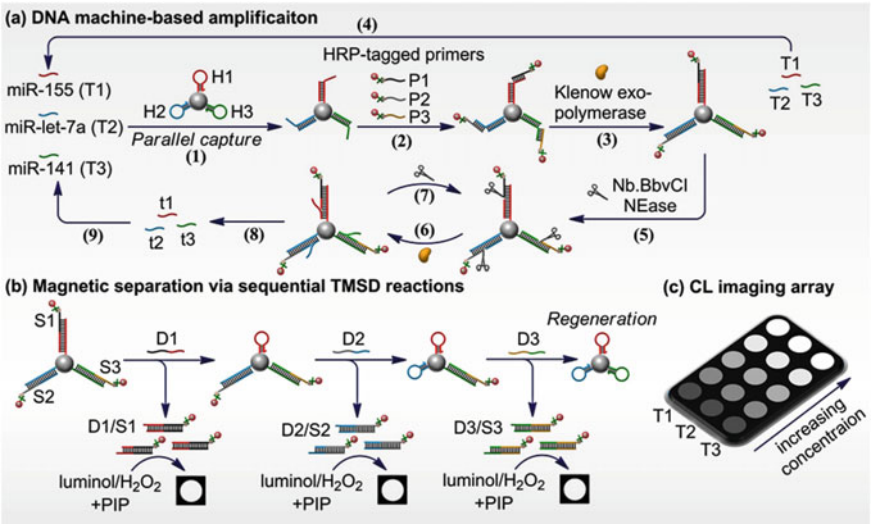

Fig. 3.12 CLIA for simultaneous detection of multiple miRNAs based on **a** polymerase/nicking-enzyme-assisted DNA machine and **b** programmable strand displacement-mediated magnetic separation. Reprinted from Bi et al. 2017. Copyright 2015, with permission from Elsevier

hemin/G-quadruplex HRP-mimicking DNAzymes to FAM in the nanowires, the CL energy further transferred to FAM to stimulate a CRET process, realizing sensitive detection of a general DNA target.

High-throughput assay is of great significance to bioanalytical and clinical applications. Recently, a CL imaging array (CLIA) was reported for simultaneous analysis of three microRNAs through integrating polymerase/nicking-enzyme-assisted DNA machine and toehold-mediated strand displacement reaction (Fig. 3.12) (Yue et al. 2017a, b). In this assay, three kinds of hairpins were parallelly immobilized on the MPs, which were designed to specially recognize corresponding microRNAs (microRNA-155, microRNA-let-7a, and microRNA-141). Upon recognition of target miRNAs, the DNA machine was initiated with the assistance of DNA polymerase and nicking enzyme Nb.BbvCI for exponential amplification of targets. Subsequently, the toehold-mediated strand displacement reactions were performed with the displacement probes, resulting in the release of HRP-tagged DNA hybrids for CL imaging. In addition to the achievement of a widely linear range covering five orders of magnitude, an ultrahigh sensitivity as low as fM level, and excellent selectivity to differentiate single-base mismatched microRNA, this CLIA assay also demonstrated the advantages of easy operation, high throughput and good reproducibility and recyclability, which thus can be widely applied in biosensing, biomedical research, disease screening, and so on.

References

Abu-Ghazalah RM, Irizar J, Helmy AS et al (2010) A study of the interactions that stabilize DNA frayed wires. Biophys Chem 147:123–129

Bi S, Chen M, Jia XQ et al (2015a) Hyperbranched hybridization chain reaction for triggered signal amplification and concatenated logic circuits. Angew Chem Int Ed 54:8144–8148

Bi S, Chen M, Jia XQ, Dong Y (2015b) A hot-spot-active magnetic graphene oxide substrate for microRNA detection based on cascaded chemiluminescence resonance energy transfer. Nanoscale 7:3745–3753

Bi S, Cui YY, Li L (2013a) Ultrasensitive detection of mRNA extracted from cancerous cells achieved by DNA rotaxane-based cross-rolling circle amplification. Analyst 138:197–203

Bi S, Hao SY, Li L et al (2010a) Bio-bar-code dendrimer-like DNA as signal amplifier for cancerous cells assay using ruthenium nanoparticle-based ultrasensitive chemiluminescence detection. Chem Commun 46:6093–6095

Bi S, Ji B, Zhang ZP et al (2013b) A chemiluminescence imaging array for the detection of cancer cells by dual-aptamer recognition and bio-bar-code nanoprobe-based rolling circle amplification. Chem Commun 49:3452–3454

Bi S, Ji B, Zhang ZP, Zhu JJ (2013c) Metal ions triggered ligase activity for rolling circle amplification and its application in molecular logic gate operations. Chem Sci 4:1858–1863

Bi S, Jia XQ, Ye JY et al (2015c) Linear light-scattering of gold nanostars for versatile biosensing of nucleic acids and proteins using exonuclease III as biocatalyst to signal amplification. Biosens Bioelectron 71:427–433

Bi S, Li L, Cui YY (2012a) Exonuclease-assisted cascaded recycling amplification for label-free detection of DNA. Chem Commun 48:1018–1020

Bi S, Li L, Zhang SS (2010b) Triggered polycatenated DNA scaffolds for DNA sensors and aptasensors by a combination of rolling circle amplification and DNAzyme amplification. Anal Chem 82:9447–9454

Bi S, Luo BY, Ye JY et al (2014a) Label-free chemiluminescent aptasensor for platelet-derived growth factor detection based on exonuclease-assisted cascade autocatalytic recycling amplification. Biosens Bioelectron 62:208–213

Bi S, Xiu B, Ye JY et al (2015d) Target-catalyzed DNA four-way junctions for CRET imaging of microRNA, concatenated logic operations, and self-assembly of DNA nanohydrogels for targeted drug delivery. ACS Appl Mater Interfaces 7:23310–23319

Bi S, Yan YM, Yang XY et al (2009a) Gold nanolabels for new enhanced chemiluminescence immunoassay of alpha-fetoprotein based on magnetic beads. Chem-Eur J 15:4704–4709

Bi S, Ye JY, Dong Y et al (2016a) Target-triggered cascade recycling amplification for label-free detection of microRNA and molecular logic operations. Chem Commun 52:402–405

Bi S, Yue SZ, Song WL et al (2016b) A target-initiated DNA network caged on magnetic particles for amplified chemiluminescence resonance energy transfer imaging of microRNA and targeted drug delivery. Chem Commun 52:12841–12844

Bi S, Yue SZ, Wu Q et al (2016c) Initiator-catalyzed self-assembly of duplex-looped DNA hairpin motif based on strand displacement reaction for logic operations and amplified biosensing. Biosens Bioelectron 83:281–286

Bi S, Yue SZ, Wu Q et al (2016d) Triggered and catalyzed self-assembly of hyperbranched DNA structures for logic operations and homogeneous CRET biosensing of microRNA. Chem Commun 52:5455–5458

Bi S, Yue SZ, Zhang SS (2017) Hybridization chain reaction: a versatile molecular tool for biosensing, bioimaging, and biomedicine. Chem Soc Rev 46:4281–4298

Bi S, Zhang JL, Zhang SS (2010c) Ultrasensitive and selective DNA detection based on nicking endonuclease assisted signal amplification and its application in cancer cell detection. Chem Commun 46:5509–5511

Bi S, Zhang ZP, Dong Y et al (2015e) Chemiluminescence resonance energy transfer imaging on magnetic particles for single-nucleotide polymorphism detection based on ligation chain reaction. Biosens Bioelectron 65:139–144

Bi S, Zhao TT, Jia XQ et al (2014b) Magnetic graphene oxide-supported hemin as peroxidase probe for sensitive detection of thiols in extracts of cancer cells. Biosens Bioelectron 57:110–116

Bi S, Zhao TT, Luo BY (2012b) A graphene oxide platform for the assay of biomolecules based on chemiluminescence resonance energy transfer. Chem Commun 48:106–108

Bi S, Zhao TT, Luo BY et al (2013d) Hybridization chain reaction-based branched rolling circle amplification for chemiluminescence detection of DNA methylation. Chem Commun 49:6906–6908

Bi S, Zhou H, Zhang SS (2009b) Bio-bar-code functionalized magnetic nanoparticle label for ultrasensitive flow injection chemiluminescence detection of DNA hybridization. Chem Commun 7:5567–5569

Bi S, Zhou H, Zhang SS (2009c) Multilayers enzyme-coated carbon nanotubes as biolabel for ultrasensitive chemiluminescence immunoassay of cancer biomarker. Biosens Bioelectron 24:2961–2966

Bi S, Zhou H, Zhang SS (2010d) A novel synergistic enhanced chemiluminescence achieved by a multiplex nanoprobe for biological applications combined with dual-amplification of magnetic nanoparticles. Chem Sci 1:681–687

Cai LP, Deng LY, Huang XY et al (2018) Catalytic chemiluminescence polymer dots for ultrasensitive in vivo imaging of intrinsic reactive oxygen species in mice. Anal Chem 90:6929–6935

Cai S, Lao K, Lau C et al (2011) "Turn-on" chemiluminescence sensor for the highly selective and ultrasensitive detection of Hg^{2+} ions based on interstrand cooperative coordination and catalytic formation of gold nanoparticles. Anal Chem 83:9702–9708

Cao Y, Fatemi V, Fang S et al (2018) Unconventional superconductivity in magic-angle graphene superlattices. Nature 556:43

Chen C, Li B (2014) Chemiluminescence resonance energy transfer biosensing platform for site-specific determination of DNA methylation and assay of DNA methyltransferase activity using exonuclease III-assisted target recycling amplification. Biosens Bioelectron 54:48–54

Chen J, Huang Z, Luo Z et al (2018a) Multichannel-structured three-dimensional chip for highly sensitive pathogenic bacteria detection based on fast DNA-programmed signal polymerization. Anal Chem 90:12019–12026

Chen M, Bi S, Jia XQ et al (2014) Aptamer-conjugated bio-bar-code Au-Fe_3O_4 nanoparticles as amplification station for electrochemiluminescence detection of tumor cells. Anal Chim Acta 837:44–51

Chen S, Liu P, Su KW et al (2018b) Electrochemical aptasensor for thrombin using co-catalysis of hemin/G-quadruplex DNAzyme and octahedral Cu_2O-Au nanocomposites for signal amplification. Biosens Bioelectron 99:338–345

Chen YT, Kolhatkar AG, Zenasni O et al (2017) Biosensing using magnetic particle detection techniques. Sensors 17:36

Chen Z, Tan Y, Xu K et al (2016) Stimulus-response mesoporous silica nanoparticle-based chemiluminescence biosensor for cocaine determination. Biosens Bioelectron 75:8–14

Chen ZH, Liu Y, Wang YZ et al (2013) Dynamic evaluation of cell surface N-Glycan expression via an electrogenerated chemiluminescence biosensor based on concanavalin A-integrating gold-nanoparticle-modified $Ru(bpy)_3^{2+}$-doped silica nanoprobe. Anal Chem 85:4431–4438

Chen ZQ, Liu Y, Xin C et al (2018c) A cascade autocatalytic strand displacement amplification and hybridization chain reaction event for label-free and ultrasensitive electrochemical nucleic acid biosensing. Biosens Bioelectron 113:1–8

Cheng YQ, Zhang X, Li ZP et al (2009) Highly sensitive determination of microRNA using target-primed and branched rolling-circle amplification. Angew Chem Int Ed 48:3268–3272

Clough JM, Balan A, van Daal TJ et al (2016) Probing force with mechanobase-induced chemiluminescence. Angew Chem Int Ed 55:1445–1449

Dirks RM, Pierce NA (2004) Triggered amplification by hybridization chain reaction. Proc Nat Acad Sci USA 101:15275–15278

Dong HF, Meng XD, Dai WH et al (2015) Highly sensitive and selective microRNA detection based on DNA-bio-bar-code and enzyme-assisted strand cycle exponential signal amplification. Anal Chem 87:4334–4340

Freeman R, Liu XQ, Willner I (2011) Chemiluminescent and chemiluminescence resonance energy transfer (CRET) detection of DNA, metal ions, and aptamer-substrate complexes using hemin/G-quadruplexes and CdSe/ZnS quantum dots. J Am Chem Soc 133:11597–11604

Gao Y, Li B (2013) G-quadruplex DNAzyme-based chemiluminescence biosensing strategy for ultrasensitive DNA detection: combination of exonuclease III-assisted signal amplification and carbon nanotubes-assisted background reducing. Anal Chem 85:11494–11500

Gao Y, Li B (2014) Exonuclease III-assisted cascade signal amplification strategy for label-free and ultrasensitive chemiluminescence detection of DNA. Anal Chem 86:8881–8887

Geim AK (2009) Graphene: status and prospects. Science 324:1530–1534

He Y, Li JH, Liu Y (2015) Reusable and dual-potential responses electrogenerated chemiluminescence biosensor for synchronously cytosensing and dynamic cell surface N-Glycan evaluation. Anal Chem 87:9777–9785

He YX, Yang S, Liu H et al (2018) Reinforced carbon fiber laminates with oriented carbon nanotube epoxy nanocomposites: Magnetic field assisted alignment and cryogenic temperature mechanical properties. J Colloid Interface Sci 517:40–51

Hu R, Liu T, Zhang XB et al (2014) Multicolor fluorescent biosensor for multiplexed detection of DNA. Anal Chem 86:5009–5016

Kong DQ, Bi S, Wang ZH et al (2016) In situ growth of three-dimensional graphene films for signal-on electrochemical biosensing of various analytes. Anal Chem 88:10667–10674

Landi-Librandi AP, de Oliveira CA, Azzolini A et al (2011) In vitro evaluation of the antioxidant activity of liposomal flavonols by the HRP-H_2O_2-luminol system. J Microencapsul 28:258–267

Li C, Chen XJ, Zhang Z et al (2018a) Gold nanoparticle-DNA conjugates enhanced determination of dopamine by aptamer-based microcantilever array sensor. Sens Actuators, B 275:25–30

Li CC, Zhang Y, Liu WJ et al (2018b) A triple-amplification strategy for sensitive detection of telomerase at the single-cell level. Chem Commun 54:9317–9320

Li D, Cheng W, Li Y et al (2016a) Catalytic hairpin assembly actuated DNA nanotweezer for logic gate building and sensitive enzyme-free biosensing of microRNAs. Anal Chem 88:7500–7506

Li DD, Lai WY, Zhang et al. (2018) Printable transparent conductive films for flexible electronics. Adv Mater 30:24

Li P, Liu L, Xiao HB, Zhang W et al (2016b) A new polymer nanoprobe based on chemiluminescence resonance energy transfer for ultrasensitive imaging of intrinsic superoxide anion in mice. J Am Chem Soc 138:2893–2896

Li Q, Lu ZC, Tan XC et al (2017a) Ultrasensitive detection of aflatoxin B-1 by SERS aptasensor based on exonuclease-assisted recycling amplification. Biosens Bioelectron 97:59–64

Li X, Xie ZP, Wang W et al (2016c) Rapid detection of Dam methyltransferase activity based on the exonuclease III-assisted isothermal amplification cycle. Anal Methods 8:2771–2777

Li XJ, Wang YG, Shi L et al (2017b) A novel ECL biosensor for the detection of concanavalin A based on glucose functionalized $NiCo_2S_4$ nanoparticles-grown on carboxylic graphene as quenching probe. Biosens Bioelectron 96:113–120

Liu F, Zhang C (2015) A novel paper-based microfluidic enhanced chemiluminescence biosensor for facile, reliable and highly-sensitive gene detection of Listeria monocytogenes. Sens Actuators, B 209:399–406

Liu J, Zhang LL, Fu CY et al (2015) Employment of 4-(1,2,4-triazol-1-yl)phenol as a signal enhancer of the chemiluminescent luminol-H_2O_2-horseradish peroxidase reaction for detection of hepatitis C virus in real samples. Luminescence 30:1297–1302

Liu X, Fan N, Wu L et al (2018) Lighting up alkaline phosphatase in drug-induced liver injury using a new chemiluminescence resonance energy transfer nanoprobe. Chem Commun 54:12479–12482

Luedeke M, Miller E, Sprague JE (2016) Technical note: the effects of Bluestar (R) and luminol when used in conjunction with tetramethylbenzidine or phenolphthalein. Forensic Sci Int 262:156–159
Luong JHT, Vashist SK (2017) Immunosensing procedures for carcinoembryonic antigen using graphene and nanocomposites. Biosens Bioelectron 89:293–304
Medeghini F, Hettich M, Rouxel R et al (2018) High-pressure effect on the optical extinction of a single gold nanoparticle. ACS Nano 12:10310–10316
Min XH, Xia L, Zhuang Y et al (2017) An AIEgens and exonuclease III aided quadratic amplification assay for detecting and cellular imaging of telomerase activity. Sci Bull 62:997–1003
Nie F, Luo K, Zheng XH et al (2015) Novel preparation and electrochemiluminescence application of luminol functional-Au nanoclusters for ALP determination. Sens Actuators, B 218:152–159
Pan Y, Sun KA, Liu SJ et al (2018) Core-shell ZIF-8@ZIF-67-derived CoP nanoparticle-embedded N-doped carbon nanotube hollow polyhedron for efficient overall water splitting. J Am Chem Soc 140:2610–2618
Qi HJ, Yue SZ, Bi S et al (2018a) A versatile homogeneous chemiluminescence biosensing platform based on exonuclease-assisted hybridization chain reaction. Sens Actuators, B 273:1525–1531
Qi HJ, Yue SZ, Bi S et al (2018b) DNA logic assembly powered by a triplex-helix molecular switch for extracellular pH imaging. Chem Commun 54:8498–8501
Qi HJ, Yue SZ, Bi S et al (2018c) Isothermal exponential amplification techniques: from basic principles to applications in electrochemical biosensors. Biosens Bioelectron 110:207–217
Qi Y, Li B, Zhang Z (2009) Label-free and homogeneous DNA hybridization detection using gold nanoparticles-based chemiluminescence system. Biosens Bioelectron 24:3581–3586
Qi Y, Xiu FR, Yu G et al (2017) Simple and rapid chemiluminescence aptasensor for Hg^{2+} in contaminated samples: A new signal amplification mechanism. Biosens Bioelectron 87:439–446
Qi Y, Xiu FR, Zheng M et al (2016) A simple and rapid chemiluminescence aptasensor for acetamiprid in contaminated samples: Sensitivity, selectivity and mechanism. Biosens Bioelectron 83:243–249
Qiu ZL, Shu J, He Y et al (2017) CdTe/CdSe quantum dot-based fluorescent aptasensor with hemin/G-quadruplex DNzyme for sensitive detection of lysozyme using rolling circle amplification and strand hybridization. Biosens Bioelectron 87:18–24
Roda A, Guardigli M (2012) Analytical chemiluminescence and bioluminescence: latest achievements and new horizons. Anal Bioanal Chem 402:69–76
Shuhendler AJ, Pu KY, Cui L et al (2014) Real-time imaging of oxidative and nitrosative stress in the liver of live animals for drug-toxicity testing. Nat Biotechnol 32:373
Sun JS, Xianyu YL, Jiang XY (2014) Point-of-care biochemical assays using gold nanoparticle-implemented microfluidics. Chem Soc Rev 43:6239–6253
Wang DZ, Tang W, Wu XJ et al (2012) Highly selective detection of single-nucleotide polymorphisms using a quartz crystal microbalance biosensor based on the toehold-mediated strand displacement reaction. Anal Chem 84:7008–7014
Wang GL, Liu KL, Shu JX et al (2015a) A novel photoelectrochemical sensor based on photocathode of PbS quantum dots utilizing catalase mimetics of bio-bar-coded platinum nanoparticles/G-quadruplex/hemin for signal amplification. Biosens Bioelectron 69:106–112
Wang HH, Li MJ, Zheng YN et al (2018a) An ultrasensitive photoelectrochemical biosensor based on [Ru(dcbpy)2d ppz]2 +/Rose Bengal dyes co-sensitized fullerene for DNA detection. Biosens Bioelectron 120:71–76
Wang J, Mao S, Li HF et al (2018b) Multi-DNAzymes-functionalized gold nanoparticles for ultrasensitive chemiluminescence detection of thrombin on microchip. Anal Chim Acta 1027:76–82
Wang M, Fu ZL, Li BC et al (2014) One-step, ultrasensitive, and electrochemical assay of microRNAs based on T7 exonuclease assisted cyclic enzymatic amplification. Anal Chem 86:5606–5610
Wang S, Bi S, Wang ZH et al (2015b) A plasmonic aptasensor for ultrasensitive detection of thrombin via arrested rolling circle amplification. Chem Commun 51:7927–7930
Wang S, Cazelles R, Liao WC et al (2017) Mimicking horseradish peroxidase and NADH peroxidase by heterogeneous Cu^{2+}-modified graphene oxide nanoparticles. Nano Lett 17:2043–2048

Wang X, Lau C, Kai M et al (2013) Hybridization chain reaction-based instantaneous derivatization technology for chemiluminescence detection of specific DNA sequences. Analyst 138:2691–2697
Xianyu YL, Wang QL, Chen YP (2018) Magnetic particles-enabled biosensors for point-of-care testing. Trends Anal Chem 106:213–224
Xu QF, Cao AP, Zhang LF et al (2012) Rapid and label-free monitoring of exonuclease III-assisted target recycling amplification. Anal Chem 84:10845–10851
Xu Y, Bian X, Sang Y et al (2016a) Bis-three-way junction nanostructure and DNA machineries for ultrasensitive and specific detection of BCR/ABL fusion gene by chemiluminescence imaging. Sci Rep 6:32370
Xu Y, Li D, Cheng W, Hu R et al (2016b) Chemiluminescence imaging for microRNA detection based on cascade exponential isothermal amplification machinery. Anal Chim Acta 936:229–235
Yan YC, Yue SZ, Zhao T et al (2017) Exonuclease-assisted target recycling amplification for label-free chemiluminescence assay and molecular logic operations. Chem Commun 53:12201–12204
Yang JJ, Cao JT, Wang H et al (2017a) Ferrocene-graphene sheets for high-efficiency quenching of electrochemiluminescence from Au nanoparticles functionalized cadmium sulfide flower-like three dimensional assemblies and sensitive detection of prostate specific antigen. Talanta 167:325–332
Yang JJ, Cao JT, Wang YL et al (2017b) Sandwich-like electrochemiluminescence aptasensor based on dual quenching effect from hemin-graphene nanosheet and enzymatic biocatalytic precipitation for sensitive detection of carcinoembryonic antigen. J Electroanal Chem 787:88–94
Yang LH, Jin MJ, Du PF et al (2015) Study on enhancement principle and stabilization for the luminol-H_2O_2-HRP chemiluminescence system. PLoS ONE 10:14
Yang Y, Liu JJ, Liang C et al (2016) Nanoscale metal-organic particles with rapid clearance for magnetic resonance imaging-guided photothermal therapy. ACS Nano 10:2774–2781
You MX, Zhu GZ, Chen T et al (2015) Programmable and multiparameter DNA-based logic platform for cancer recognition and targeted therapy. J Am Chem Soc 137:667–674
Yu S, Wang Y, Jiang LP et al (2018) Cascade amplification-mediated in situ hot-spot assembly for microRNA detection and molecular logic gate operations. Anal Chem 90:4544–4551
Yue SZ, Zhao TT, Bi S et al (2017a) Programmable strand displacement-based magnetic separation for simultaneous amplified detection of multiplex microRNAs by chemiluminescence imaging array. Biosens Bioelectron 98:234–239
Yue SZ, Zhao TT, Qi HJ et al (2017b) Cross-catalytic hairpin assembly-based exponential signal amplification for CRET assay with low background noise. Biosens Bioelectron 94:671–676
Zhang KY, Lv SZ, Lin ZZ et al (2018a) Bio-bar-code-based photoelectrochemical immunoassay for sensitive detection of prostate-specific antigen using rolling circle amplification and enzymatic biocatalytic precipitation. Biosens Bioelectron 101:159–166
Zhang N, Shi XM, Guo HQ et al (2018b) Gold nanoparticle couples with entropy-driven toehold-mediated DNA strand displacement reaction on magnetic beads: toward ultrasensitive energy-transfer-based photoelectrochemical detection of miRNA-141 in real blood sample. Anal Chem 90:11892–11898
Zhang Q, Gong Y, Guo XJ et al (2018c) Multifunctional gold nanoparticle-based fluorescence resonance energy-transfer probe for target drug delivery and cell fluorescence imaging. ACS Appl Mater Interfaces 10:34840–34848
Zhang SS, Yan YM, Bi S (2009) Design of molecular beacons as signaling probes for adenosine triphosphate detection in cancer cells based on chemiluminescence resonance energy transfer. Anal Chem 81:8695–8701
Zhang Y, Huang XC, Luo F et al (2018d) Highly sensitive electrochemical immunosensor for golgi protein 73 based on proximity ligation assay and enzyme-powered recycling amplification. Anal Chim Acta 1040:150–157
Zhang Z, Zhu NF, Zou YM et al (2018e) A novel and sensitive chemiluminescence immunoassay based on AuNCs@pepsin@luminol for simultaneous detection of tetrabromobisphenol A bis(2-hydroxyethyl) ether and tetrabromobisphenol A mono(hydroxyethyl) ether. Anal Chim Acta 1035:168–174

Zhao WA, Ali MM, Brook MA et al (2008) Rolling circle amplification: applications in nanotechnology and biodetection with functional nucleic acids. Angew Chem Int Ed 47:6330–6337

Zhen X, Zhang CW, Xie C et al (2016) Intraparticle energy level alignment of semiconducting polymer nanoparticles to amplify chemiluminescence for ultrasensitive in vivo imaging of reactive oxygen species. ACS Nano 10:6400–6409

Zheng B, von See MP, Yu E et al (2016) Quantitative magnetic particle imaging monitors the transplantation, biodistribution, and clearance of stem cells in vivo. Theranostics 6:291–301

Zhou J, Duan J, Zhang XE et al (2018a) A chiral responsive carbon dots-gold nanoparticle complex mediated by hydrogen peroxide independent of surface modification with chiral ligands. Nanoscale 10:18606–18612

Zhou J, Fleming AM, Averill AM et al (2015) The NEIL glycosylases remove oxidized guanine lesions from telomeric and promoter quadruplex DNA structures. Nucleic Acids Res 43:4039–4054

Zhou Y, Wang Y, Wang X et al (2017) Polystyrene microspheres coupled with hybridization chain reaction for dual-amplified chemiluminescence detection of specific DNA sequences. Journal of Analysis and Testing 1:306–314

Zhou Z, Liu X, Yue L et al (2018b) Controlling the catalytic and optical properties of aggregated nanoparticles or semiconductor quantum dots using DNA-based constitutional dynamic networks. ACS nano 12:10725

Zong C, Wu J, Liu M et al (2014) Proximity hybridization-triggered signal switch for homogeneous chemiluminescent bioanalysis. Anal Chem 86:5573–5578

Zong C, Wu J, Xu J et al (2013) Multilayer hemin/G-quadruplex wrapped gold nanoparticles as tag for ultrasensitive multiplex immunoassay by chemiluminescence imaging. Biosens Bioelectron 43:372–378

Chapter 4
Nucleic Acid Amplification Strategy-Based Electrochemiluminescence Research

Huairong Zhang

Abstract Electrochemiluminescence (electrogenerated chemiluminescence, ECL) has been widely used in analytical chemistry due to its excellent properties. However, low-level detection of targets still remains a challenge in the modern biochemical and biomedical research. Thus, nucleic acid amplification strategies combined with ECL technology have already become a powerful tool for efficient and smart signal-amplified detection.

4.1 General

4.1.1 Electrochemiluminescence (ECL) Assays

ECL is a technology to convert electrochemical energy into optical energy, and the process was induced by the electrochemical oxidation or reduction on ECL-active molecular through applying potential at the working electrode (Richter et al. 2004; Zhou et al. 2016; Zhang et al. 2017a; Yetisen et al. 2013). As shown in Fig. 4.1 (Wu et al. 2014), the electron-transfer reactions at the electrode surface formed the excited states of ECL-active molecular which could produce the light when decays to the ground state. ECL technique integrates the advantages of both electrochemistry and spectroscopy, such as stability, sensitivity, simplicity, facility, and wide dynamic range. Moreover, background signals could be ignored, as it does not require a light source, which finally leads to high sensitivity. Besides, high specificity was obtained due to the emitter–coreactant relationship and the excited states can be regulated by alternating the applying potential (Zhang et al. 2013a, 2016; Serena et al. 2017; Li et al. 2017a). ECL has become a powerful analytical technique since detailed studies by Bard and Hercules and et al. in the mid-1960s. By employing ECL-active molecules as signal tags, ECL technology in the sensor or materials field was summarized in plenty review articles (Guo et al. 2011b; Liu et al. 2015; Miao et al.

H. Zhang (✉)
Shandong Provincial Key Laboratory of Detection Technology for Tumour Markers, College of Chemistry and Chemical Engineering, Linyi University, Linyi, People's Republic of China
e-mail: zhanghuairong999@126.com

S. Zhang et al. (eds.), *Nucleic Acid Amplification Strategies for Biosensing, Bioimaging and Biomedicine*, https://doi.org/10.1007/978-981-13-7044-1_4

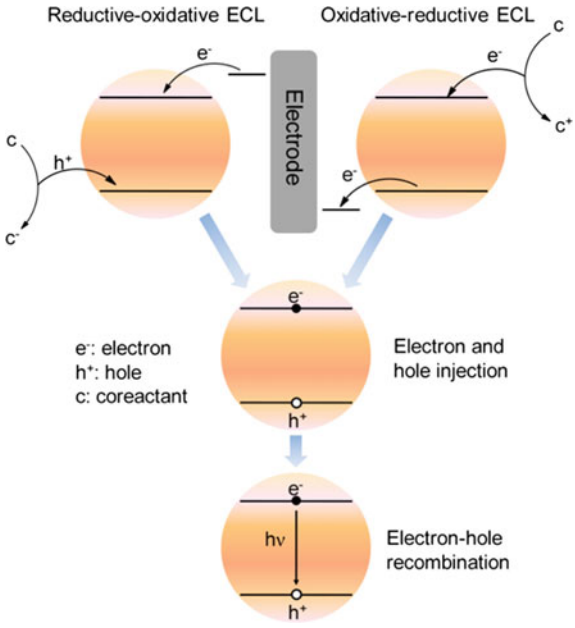

Fig. 4.1 Schematic mechanisms of reductive–oxidative (R–O) and oxidative–reductive (O–R). Reprinted with the permission from Richter (2004). Copyright 2004 American Chemical Society

2008). The combination of isothermal amplification and biosensor based on ECL technology has also attracted intense attention and led to more simple and sensitive biomolecule analysis (Zhao et al. 2015; Craw et al. 2012; Reid et al. 2018). Herein, a general overview about the latest developments and applications of nucleic acid amplification strategies-based ECL techniques was given in the sensitive and selective detection of nucleic acids, enzyme, proteins, tumor cells, and small molecules.

4.2 Nucleic-Acid-Amplification-Assisted ECL Assays

4.2.1 Nucleic Acid-ECL Biosensors Assisted by Nucleic Acid Amplification Strategies

Sensitive and specific nucleic acids targets biosensor is an important tool for early genetic disease diagnosis and treatment. Some specific nucleic acids were studied due to the hybridization to its complementary DNA with high specificity (Wang et al. 2018a; Zhang et al. 2015b). The principle was used to develop ECL biosensor assisted by signal amplification for nucleic acid detections. In recent years, rolling circle amplification (RCA) and hyperbranching RCA (HRCA) are widely used in DNA biosensor as it can extend the strength of DNA by synthesizing many repeating DNA sequences (Zhang et al. 2015a; Jiang et al. 2014a, b; Ali et al. 2014).

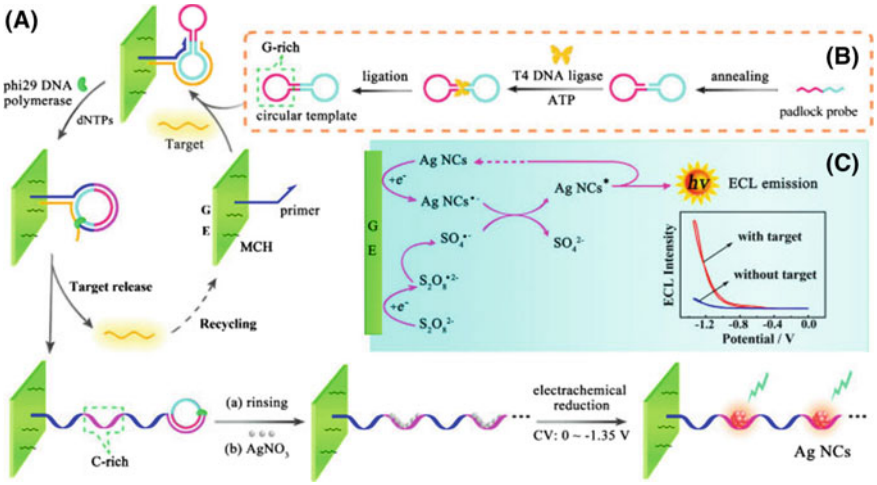

Fig. 4.2 Schematic illustration of **a** the principle of target-cycling synchronized RCA and in situ electrochemical generation of AgNCs, **b** preparation of the circular template, and **c** ECL mechanism of AgNCs/$S_2O_8^{2-}$-based ECL system. Reprinted with the permission from Chen et al. (2016). Copyright 2016 American Chemical Society

Based on enzyme-free target recycling amplification and 2D DNA nanoprobe (DNP), Chai's group built an electrochemical biosensor for micro-RNA detection (Zhang et al. 2018). A large amount of ferrocene-labeled DNA strands were released from working electrode after the liberated target opened hairpin *H* for triggering another TSDR, which results in a dramatic decrease of the electrochemical response. As a result, one input of the target can induce 2 N ferrocene-labeled DNA strands released from the electrode surface. Thus, this strategy provided a novel method for detecting various nucleic acids in nascent stages of cancer. Yuan et al. built a sensitive micro-RNA (miRNA) biosensor based on RCA amplification and Pb^{2+}-induced DNAzyme-assisted target recycling (Fig. 4.2). Due to the RCA amplification and in situ electrochemically generated silver nanoclusters (AgNCs), the detection limit of miRNA could be down to 0.3 fM (Chen et al. 2016). *Listeria monocytogenes* (*L. monocytogenes*) is a highly infectious type of pathogens that can be passed through the food chain. Thus, a highly sensitive and specific assay using HRCA combined with magnetic bead method for *L. monocytogenes* detection was built to ensure food safety (Long et al. 2011). The method can detect 10 aM synthetic gene targets and as low as 0.0002 ng/μl of genomic DNA from *L. monocytogenes*. This method offered a highly sensitive, isothermal, and selective ECL assay for *L. monocytogenes* detection due to the powerful amplification of HRCA.

Nucleic acid amplification strategies were usually used combined with nanoparticles or DNA walkers to enhance the sensitivity. Lin and coworkers designed an ultrasensitive ECL biosensor for sensitive p53 gene (0.02 fM) detection assisted by MagneSphere Paramagnetic Particles, HRCA and NEase-assisted target recycling

amplification (Yang et al. 2016). Zhang's group also developed a highly selective and sensitive ECL biosensing approach for Kras mutant gene detection (Zhang et al. 2017b). ECL biosensor was proposed based on the high discrimination capability of LNA and dual signal amplification approaches including DNA walkers and HRCA. The assay has large potential to application in diagnostics and individualized patients' therapeutic strategies for cancer.

DNA strands can assemble into two or three dimensions with different structures after properly designed. Self-assembled DNA nanostructure is an effective and simple tool for signal amplification via target or signal probe hybridization. Based on self-assembled DNA nanostructures as carriers, Liu et al. fabricated an ultrasensitive and label-free ECL signal amplification biosensor, which was used for detection of micro-RNA-21 (Liu et al. 2014). HCR is another DNA amplification method, briefly; an initiator (target) triggered the process of this method and finally led to the polymerization of oligonucleotides into a long nicked double-stranded DNA (dsDNA) polymers. As shown in Fig. 4.3, a highly sensitive DNA sequence detection based on HCR signal amplification and ECL technology was proposed (Chen et al. 2012). Target DNA was triggered and led to the formation of long-range double-stranded DNA molecule through in situ HCR. As the grooves of dsDNA polymers could be used as carriers of numerous $Ru(phen)_3^{2+}$ ions, the intensity of ECL signal could be largely amplified. ECL strategy assisted by HCR not only shows high selectivity against single-base mismatch sequences, but also enables low femtomolar detection of nucleic acid.

Furthermore, some kinds of nanoparticles could be applied in signal amplification method due to their catalysis or assembly abilities. Jiang and coworkers found that a novel magnetic nanoparticle $CoFe_2O_4$ has the peroxidase-like activity which could enhance the ECL intensity of N-(aminobutyl)-N-(ethylisoluminol) (ABEI)-H_2O_2 system. Based on this theory, a sensitive and selective ECL biosensor was built for MUC1 detection with a detection limit at fM level (Jiang et al. 2017). DNA damage mainly includes alkylation of bases, bulky adduct formation, oxidation of bases, mismatch of bases, and hydrolysis of bases. As we all know, the damage of DNA may cause less effective DNA repair than normal cells. Besides, damaged DNA will transfer to daughter cells by asexual reproduction and finally lead to cancer (Zhou et al. 2012a). Therefore, analysis of DNA damage is significant for the diagnosis of early stages of cancer and other diseases. An ECL biosensor by using CdTe@SiO_2 as nanoprobes for signal amplification was fabricated for specific sequence DNA detection (Wei et al. 2013). The "sandwich-type" DNA complexes were fabricated by self-assembly of capture DNA on working electrode. Capture DNA could hybridized with one end of target DNA, and the other end of target DNA was recognized by CdTe@SiO_2-modified DNA. The different concentrations of target DNA were identified by ECL intensity of the CdTe@SiO_2-labeled DNA probe. This method could recognize single-base-mismatched DNA from complementary DNA by different ECL intensities. Finally, a sensitive ECL biosensor based on CdTe@SiO_2 labeled probe was developed for the sequence-specific DNA detection. Another ultrasensitive DNA biosensor was fabricated by utilizing the resonance energy transfer (RET) between $Ru(dcbpy)_3^{2+}$ and QDs. The nanostructure

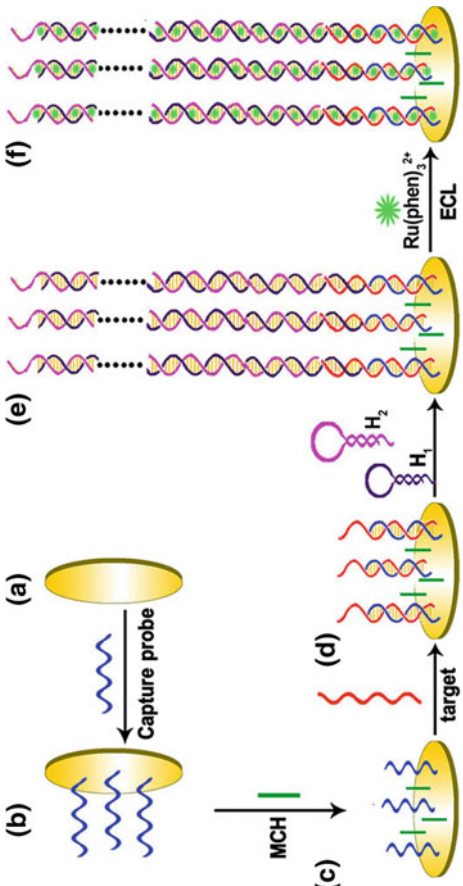

Fig. 4.3 Illustration of the universal and highly sensitive HCR-based strategy for ECL detection of DNA. Reprinted with the permission from Chen et al. (2012). Copyright 2012 American Chemical Society

(QDs-Ru(dcbpy)$_3^{2+}$) used as an ECL-RET model contains both the donor and the acceptor, which efficiently reduced the energy loss and improved the ECL efficiency of the QDs. By employing target recycling CHA, this ECL biosensor could detect miRNA-141 of human prostate cancer cells with an estimated detection limit of 33 aM, which showed potential applications in early cancer diagnosis and therapeutic monitoring. Most importantly, the ECL technology could be applied to study the DNA damage caused by several genotoxic chemicals with great potential (Li et al. 2017b).

For the past few years, isothermal amplifications in designing sensitive and selective analysis of DNA damage and single-nucleotide polymorphism (SNPs) assisted by DNA machines attracted much attention due to their simple operation and autonomous and circular amplification (Chen et al. 2013; Zhou et al. 2011a, b). The isothermal amplification reactions mostly used scission reactions or enzyme-assisted replication as the DNA machines. Chen's group developed a sensitive ECL assay for mRNA detection by employing DNA biogate and DSN-assisted target recycling. Wang et al. first encapsulated a mass of Ru(bpy)$_3^{2+}$ into the MSNs, and the negatively charged ssDNA could be electrostatically adsorbed onto the MSNs to seal the mesopores as a DNA biogate. After mRNA hybridization with ssDNA, the entrapped Ru(bpy)$_3^{2+}$ molecules were released and the ECL signals with co-reactant TPA were available. This facile method enables the accurate quantification of survivin mRNA detection in cancer cells with a low detection limit of 0.1 fM (Wang et al. 2015). Besides, other ECL approaches for detection of SNPs based on an isothermal cycle-assisted, triple-stem probes were fabricated with simplicity, selectivity, and sensitivity. Those methods have great promise for SNP analysis, and it will be extensively applied in diagnostics and therapeutics (Zhao et al. 2018; Chen et al. 2015).

4.2.2 Proteins-ECL Biosensors Assisted by Nucleic Acid Amplification Strategies

In the recent years, employment of nucleic acid as amplified indicators in sensitive detection of proteins attracted great attention (Wang et al. 2011b; Zhang et al. 2012a; Xu et al. 2013a). Excellent improvements in the performance of the biosensors were realized due to amplification strategies. For example, Jie etc. developed a new amplified ECL strategy for selective and sensitive detection of thrombin based on HCR amplification and resonance energy transfer (RET) between composite QDs and AuNPs (Jie and Yuan 2012). Composite QDs display intense ECL signal and provide promising advantages for ECL biosensing. This approach provides a conveniently and rapidly performing, impressive LODs and a comparable low background signal. The reason should be the HCR is an enzyme-free, initiator-triggered reaction and the magnetic property of the composite QDs. Other simple, highly sensitive ECL biosensors were also developed based on the amplification capability of HCR.

Wei's group (Wu et al. 2015) reported one example of a single-stranded DNA specific exonuclease-based ECL aptasensor. In this work, the presence of thrombin could combine with aptamer DNA that induces the dissociation of dsDNA due to the stronger interaction between thrombin and aptamer DNA. Then, a type of exon nuclease named RecJf catalyzed the removal of deoxynucleotide monophosphates from the 50-end to the 30-end of DNA with a target recycling amplification. Subsequently, two-hairpin DNA in solution reacted with the capture probe and formed an extended dsDNA through HCR, which efficiently introduced numerous Eu-MWCNTs as ECL indicators through an amidation reaction. Thus, a detection limit as low as 0.23 pmol L^{-1} for thrombin was realized. The proposed ECL biosensors for protein detection based on HCR exhibited a sensitive, selective, stable response for detection of proteins and showed great potential in cancer or other disease diagnosis (Xiao et al. 2013; Tang et al. 2011).

In conventional enzyme-linked immunoassays (ELISAs), bioactive enzyme was mostly used as the label of secondary antibody. However, the conjugated sites' availability was always limited for enzyme on each antibody. Therefore, artificial mimic enzymes, such as catalytic nucleic acids (DNAzymes), attracted extensive study interest. This should be due to the advantages of low cost, being easy to label, having more stability against heat treatment, and hydrolysis. Hemin/G-quadruplex as a new amplification tool, possessing the horseradish peroxidase (HRP)-mimicking activities, is an interesting DNAzyme which has surprising potential in biosensing events (Chinnapen and Sen 2002; Willner et al. 2008; Cai et al. 2013; Travascio et al. 2001; Wang et al. 2011a). DNAzymes provide biocatalytic detection of hybridization process in the presence of hemin (Xiao et al. 2004). The detection of proteins is underway by extension of the concept to design the DNAzyme linked to aptamers. A ECL biosensor based on graphene-oxide NPs (GOxNPs) and hemin/G-quadruplex DNAzyme which shows bi-enzyme cascade amplification effect was designed for ultrasensitive detection of thrombin (Xiao et al. 2014). The details were shown in Fig. 4.4, Pt nanoparticles and glucose oxidase nanoparticles (GOxNPs) were carried by hollow were Au nanoparticles (HAuNPs). The GOxNPs and hemin/G-quadruplex -DNAzyme both have mimicked horseradish peroxidase (HRP) activity. Herein, Pt NPs, GOxNPs and hemin/G-quadruplex could form mimicking bi-enzyme cascade catalysis system to catalyze H_2O_2 to generate high-concentration dissolved oxygen which results in a great enhanced ECL signal. Besides, a novel ECL immunosensor was designed for ultrasensitive detection of alpha-1-fetoprotein (AFP) based on the in situ bi-enzymatic reaction to generate coreactant of peroxydisulfate for signal amplification (Wang et al. 2012b). After a certain amounts of glucose were added into detection solution, glucose oxidase (GOD) catalyzed the oxidation of glucose and at the same time H_2O_2 was generated, which could be further catalyzed by horseradish peroxidase (HRP) to generate O_2 for the signal amplification. As low as detection limit of 3.3×10^{-4} ng mL^{-1} of AFP was obtained by this novel strategy with due to the advantages of good selectivity, sensitivity, reproducibility, and simplicity which might has a new promise employment in clinical detection.

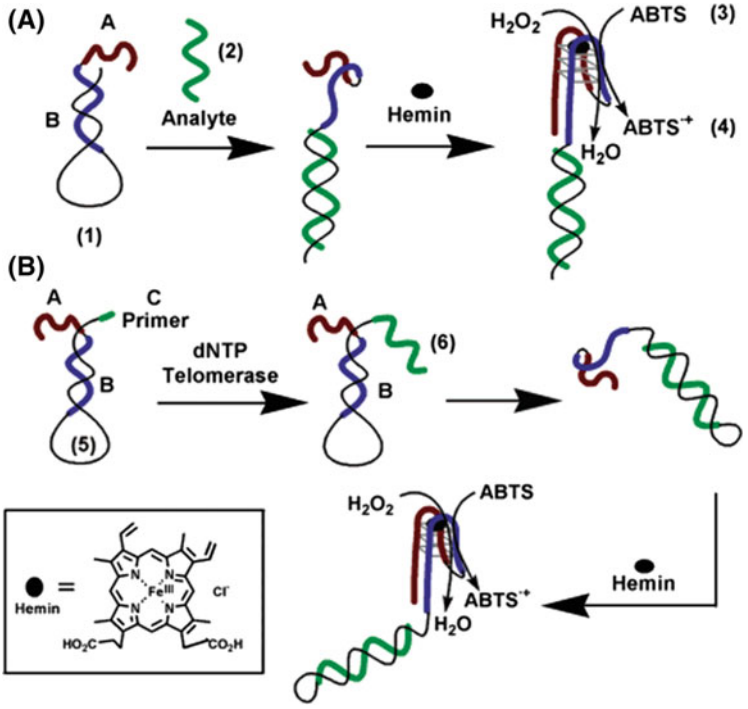

Fig. 4.4 **a** Analysis of DNA by opening of a Beacon Nucleic Acid and the generation of a DNAzyme. **b** Analyzing telomerase activity by a functional DNA Beacon that self-generates a DNAzyme. Reprinted with the permission from Xiao et al. (2004). Copyright 2004 American Chemical Society

Due to the catalysis ability, excellent electron-transfer ability, and biocompatible performance, employing nanomaterials as signal amplifier is a popular strategy used for the development of ultrasensitive biosensor methods. Nanomaterials often employed as carriers to load large amounts of biomolecules and ECL signal labels in order to amplify the signal due to the good biocompatibility, large surface area, fascinating electrocatalytic activity, excellent conductivity, and outstanding optical properties. Rapid evolution in nanoparticles promotes development of high-performance ECL immunosensors; they can used as a promoter to enrich signal tags, improve the electron-transfer velocity at the interface of electrode, and increase the surface area. Therefore, ECL biosensor design by using nanomaterials as signal amplifiers is of great interest (Duan et al. 2010; Pinijsuwan et al. 2008; Jie et al. 2008, 2010; Wu et al. 2010). The study focused on designing nanocomposites or nanomaterials as nanocarriers loaded on the working electrode, which increased the specific surface area to capture a large amount of targets or tags and improved the electronic transmission rate (Zhang et al. 2012c, 2013b, c; Liu et al. 2012, 2013). Xu reported an ECL sandwich immunosensor by using enzyme antibody-conjugated gold nanorods (AuNRs)

and functionalized graphene as the sensor platform (Xu et al. 2013b). The synthesized Au NRs were used as carriers to immobilize glucose oxidase and secondary antibodies, which were applied as signal tags. The surface of working electrode was modified with chitosan-functionalized graphene in order to immobilize more primary antibodies. Finally, a low LOD, stable, and strong ECL method was obtained to detect cancer biomarkers based on the multiple signal amplification of chitosan-functionalized graphene and Au NRs. Yuan's group focused on study coreactant of common ECL regents, synergistic catalyzer and utilizing novel catalyzer to develop nanomaterial-based ECL immunoassay (Mao et al. 2011; Wang et al. 2012a; Liao et al. 2013; Xiao et al. 2014; Zhao et al. 2013). As shown in Fig. 4.5, an ultrasensitive ECL immunosensor to achieve quantitative detection of HIgG in serum and aqueous buffers samples with low LOD, high sensitivity, good stability, and wide dynamic response was prepared (Wang et al. 2012c). The designed Fe_3O_4-NP-modified GO nanosheets ($Ru(bpy)_3^{2+}$/Fe_3O_4@GO) were utilized as signal reporters because the numbers of $Ru(bpy)_3^{2+}$ molecules were modified on the surface of the magnetic Fe_3O_4-loaded graphene nanosheet (GN). An ultrasensitive NIR ECL immunosensor was designed for protein detection by utilizing SiO_2 nanospheres and AuNP-GN hybrids for dual amplification. Xu's group developed a novel dual-potential ECL approach for the activity of telomerase detection in cancer cell (Zhang et al. 2014b). In this approach, luminol molecules aggregated by Au NPs could produce an ECL signal in the presence of coreactant H_2O_2 after added proper voltage; besides, L-Au NPs could also enhance the ECL intensity of CdS NCs due to the surface plasmon resonance (SPR) of Au NPs. By detecting two ECL signals, this approach can be utilized to detect the activity of telomerase extracted from 100 to 9000 cancer cells. This ECL strategy with dual-potential signals could avoid false positive or negative results in bioanalysis and showed great promise in clinical research. Using nanoparticles as amplifying tools could encourage researchers to take great interest in the development of ECL biosensors and open new avenues on the design of nanoparticles-based ECL sensors. For example, a sensitive strategy combined DNA cycle device with magnetic micro-beads (MB) was developed and applied to thrombin detection. The graphene oxide (GO) was employed to amplify the signal and enhance electrochemiluminescence (ECL) intensity (Guo et al. 2011a). Besides, a novel visual electrochemiluminescence (ECL) analysis on a micro-array chip was reported for detection of telomerase activity. Luminol molecules and DNAzyme-modified Au nanoparticles (NPs) were used as amplification labels with double-catalytic ability (Zhang et al. 2014a). The luminescence signal could be enhanced by DNAzyme-L-Au NP bioconjugates effectively. This strategy provides a sensitive and simple visual means for detecting telomerase.

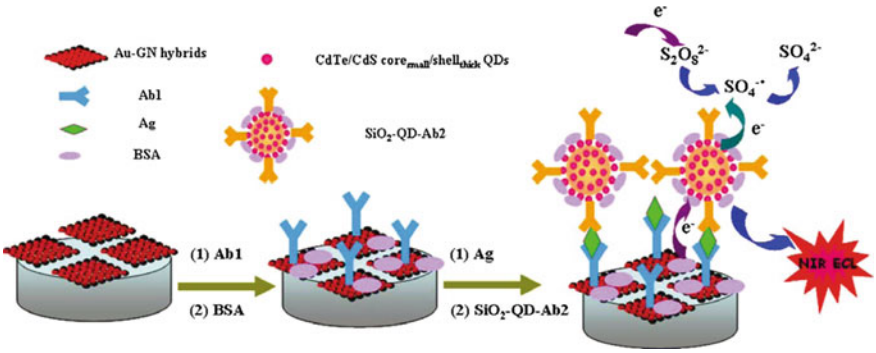

Fig. 4.5 NIR-ECL immunoassay of HIgG with dual amplification strategy. Reprinted with the permission from Wang et al. (2012a, b, c). Copyright 2012 American Chemical Society

4.2.3 Cancer Cells-ECL Biosensors Assisted by Nucleic Acid Amplification Strategies

Cancer cells, which could be unlimitedly reproduced in the body, are the major causes of morbidity and mortality worldwide. As the tumor is of great cause of death in human beings, early detection and therapy play essential roles in modern medicine. Tumor cells originate from genetic abnormalities and usually behave differently at the molecular level. For decades, clinical tumor diagnosis primarily utilizes the morphology of cancer cells or tissues which cannot realize tumor early diagnosis. As a result, the optimal time for early tumor therapy was missed. Thus, more sensitive and selective technologies should be developed for cancer cell detection (Xi et al. 2014; He et al. 2014; Chen et al. 2014). For example, aptamers, composed by a specific part of DNA or RNA, possess the properties of high specificity, low molecular weight, easy discovery, versatility in application, and manipulation. Aptamer was selected to use in tumor diagnostic assays due to their ability to distinguish different cancer cell types with an equilibrium dissociation constant (Kd) in the nanomolar to picomolar range. ECL, as a useful technology, was used for cancer cell detection assisted by nucleic acid amplification strategies. In the cytosensors, the proposed methods possess highly selective and sensitive by employing signal amplification technology and high-affinity aptamers. For example, as the ECL intensity of CdS NCs film could be enhanced by Au nanoparticles (NPs), a sensitive ECL approach was built for HL-60 cancer cell detection (Zhang et al. 2012b). This method could test cancer cells with a sensitive and selective range from 20 to 1.0×10^6 cells/mL by making use of the amplification ability of Au NPs. In addition, the designed proposal has potential in study diagnosis of tumor due to its simplicity, high sensitivity, and low cost. An original dendrimer/CdSe-ZnS QDs nanocluster was designed for sensitive assay of cancer cells (Jie et al. 2011). As shown in Fig. 4.6, magnetic beads (MBs) were immobilized with aptamers, which then combined with dendrimer/CdSe-ZnS QDs nanocluster for cancer cells detection. Large numbers of CdSe-ZnS QDs were labeled on

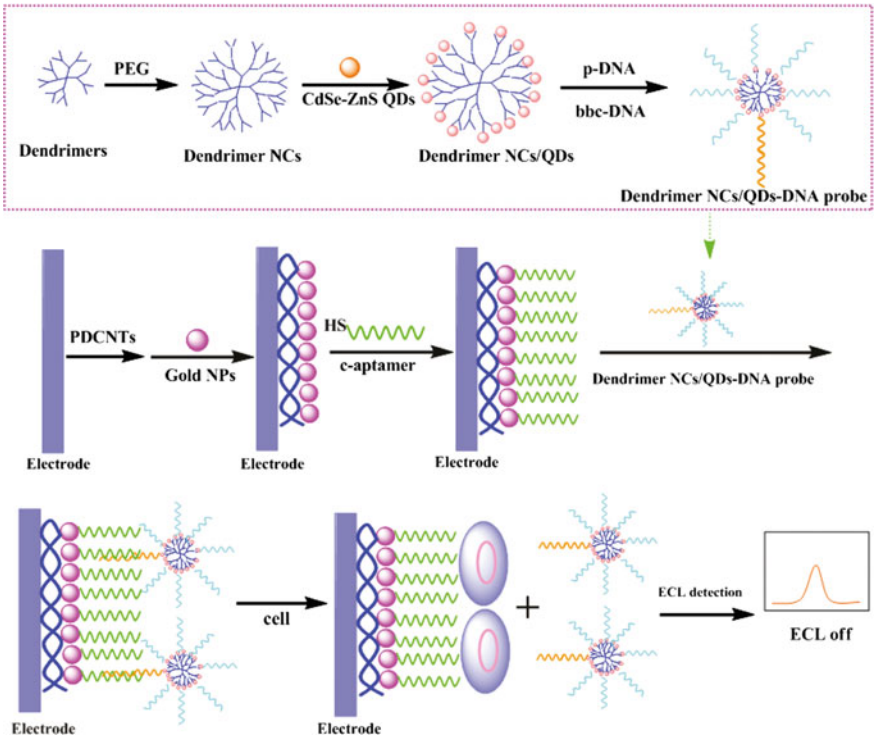

Fig. 4.6 Fabrication steps of the dendrimer NCs/QDs-DNA probe and ECL biosensor for signal-off detection of cells. Reprinted with the permission from Jie et al. (2011). Copyright 2011 American Chemical Society

the nanocluster, which could amplify the ECL signal significantly. Moreover, the MBs could greatly simplify the separation procedures. Excellent difference between target cells and control cells indicates that this assay has excellent potential to offer a convenient, selective, sensitive, and cost-effective method for accurate and early tumor cell detection. Another simple ECL assay based on a proximity hybridization-regulated strategy was designed for highly specific and sensitive detection of overexpressing surface protein on cancer cell surface (Wang et al. 2018b). This work reports a proximity hybridization-regulated ECL cytosensors for detection of proteins on living cell surface with good specificity and sensitivity. This simple, specific, and sensitive strategy has greatly potential for detection of proteins and specific cells on clinical application.

In addition, a high-sensitivity ECL approach using nanoprobe and aptamer for cancer cells detection was reported (Ding et al. 2012). The nanoprobe was combined with linker DNA, tris (2, 2′-bipyridyl) ruthenium (TBR)-labeled signal DNA and gold nanoparticles (AuNPs). Nanoprobe was dropped from the biocomplexes as aptamer DNA conjugated with tumor cells with higher affinity, subsequently

nanoprobe hybridized with the capture DNA modified on another magnetic bead (MB2) and form magnetic nanocomposite. This method can detect as low as 5 cells/ml Romas cell with great selectivity. Besides, ECL detection was also performed to detect Ramos cells by functionalized signal DNA, which was partly complementary to the aptamer DNA (Ding et al. 2010). As the target cells from the ECL probes could replace the signal DNA, the ECL intensity could directly express the number of the tumor cells. As low as 89 Ramos cells per mL could be detected based on the developed ECL probe. The proposed methods for tumor cell detection with ECL technology shows wide applications in clinical diagnosis of tumor due to the low cost, simplicity, and high sensitivity.

4.2.4 Small Molecules-ECL Biosensors Assisted by Nucleic Acid Amplification Strategies

Basic biosensing platforms were built to evaluate small bioactive molecules related to different disease states. ECL biosensors based on signal amplification were developed for small bioactive molecules detection in recent years (Yuan et al. 2014; Zhou et al. 2012b). A unique ECL method using cycle amplification technique, magnetic separation, and dendrimer QD hybrid superstructure was designed for ATP detection (Jie et al. 2012). A large amount of QDs were modified on the surface of magnetic nanoparticles by dendrimer nanoclusters, and the built superstructure exhibited outstanding enhanced ECL intensity. This approach can detect ATP with highly selective and sensitive due to the magnetic property of the nanocomposites, and it has great potential to detect ATP in tumor cells. Jiang and coworkers combined their previous discovery that Hg^{2+} has an efficient quenching effect on the ECL signal of N-(aminobutyl)-N-(ethylisoluminol) (ABEI), and the theory was used to develop an exonuclease-assisted aptamer-based ECL sensor. Exo I was employed on a GCE electrode to digest the aptamer in the protein-aptamer complex, leading to the release of Hg^{2+}, and induce a strong detectable ECL readout, as well as mucin 1 for target recycling (Jiang et al. 2016). Ju's group constructed an Mg^{2+}-dependent DNAzyme-triggered ratiometric ECL biosensor to detect Mg^{2+} extracted from HeLa cell. The analysis method was built using DNAzyme-strand-functionalized QDs acting as capture probe; luminol-reduced Au NPs (Au@luminol) as an oxidative–reductive ECL signal probe and Cy5 modified Mg^{2+} substrate strand as quencher (Cheng et al. 2014).

4.3 Conclusions and Perspectives

A deeper analysis and discussion about the recent development of nucleic acid amplification strategies on ECL technology was summarized above. The need of ultrasensitive diagnosis and early therapy for cancer or other diseases was one of the hottest

fields now. Wide varieties of ECL assays combined with nucleic acid amplification strategies with the properties of wide dynamic range, multiplexing capabilities, high selectivity, and sensitivity have offered an opportunity for this study. ECL biosensing technology provide a high-effective strategy for quantitative analysis of genes, proteins, cells, and other small molecules, which provide valuable information for early diagnosis of cancer or other diseases and early clinical treatment. In order to meet the demand of early disease diagnosis and clinical application, visible ECL imaging of single cancer cells or single particles was developed for high-throughput analysis and highly selective single-molecule detection in biological systems with signal amplification (Zhu et al. 2018; Pana et al. 2018). Due to the amplification of nanoparticles and nucleic acid amplification strategies, ECL microscopy could provide promising potential as an optical readout to investigate the electrochemical activity of single nanoparticles and study the information of single cell in a high-throughput way. To sum up, ECL bioassay assisted by nucleic acid amplification strategies could lead as a good biosensor for diagnosis of tumor or other diseases.

References

Ali MM, Li F, Zhang ZQ (2014) Rolling circle amplification: a versatile tool for chemical biology, materials science and medicine. Chem Soc Rev 43:3324–3341

Cai Y, Li N, Kong DM et al (2013) Fluorogenic substrate screening for G-quadruplex DNAzyme-based sensors. Biosens Bioelectron 49:312–317

Chen AY, Gui GF, Zhuo Y (2015) Signal-off electrochemiluminescence biosensor based on Phi29 DNA polymerase mediated strand displacement amplification for MicroRNA detection. Anal Chim 87:6328–6334

Chen AY, Ma SY, Zhuo Y et al (2016) In situ electrochemical generation of electrochemiluminescent silver naonoclusters on target-cycling synchronized rolling circle amplification platform for microRNA detection. Anal Chem 88:3203

Chen M, Bi S, Jia XQ et al (2014) Aptamer-conjugated bio-bar-code Au-Fe_3O_4 nanoparticles as amplification station for electrochemiluminescence detection of tumor cells. Anal Chim Acta 837:44

Cheng Y, Huang Y, Lei JP et al (2014) Design and biosensing of Mg^{2+}-dependent DNAzyme-triggered ratiometric electrochemiluminescence. Anal Chem 86:5158

Chen Y, Xu J, Su J et al (2012) In situ hybridization chain reaction amplification for universal and highly sensitive electrochemiluminescent detection of DNA. Anal Chem 84:7750–7755

Chen Y, Yang ML, Xiang Y et al (2013) Ligase chain reaction amplification for sensitive electrochemiluminescent detection of single nucleotide, polymorphisms. Anal Chim Acta 796:1–6

Chinnapen DJF, Sen D (2002) Hemin-stimulated docking of cytochrome C to a hemin-DNA aptamer complex. Biochemistry 41:5202–5212

Craw P, Balachandran W (2012) Isothermal nucleic acid amplification technologies for point-of-care diagnostics: a critical review. Lab Chip 12(14):2469–2486

Ding CF, Ge Y, Zhang SS (2010) Electrochemical and electrochemiluminescence determination of cancer cells based on aptamers and magnetic beads. Chem Eur J 16:10707–10714

Ding CF, Wei S, Liu HT (2012) Electrochemiluminescent determination of cancer cells based on aptamers, nanoparticles, and magnetic beads. Chem Eur J 18:263–7268

Duan R, Zhou X, Xing D (2010) Electrochemiluminescence biobarcode method based on cysteamine-gold nanoparticle conjugates. Anal Chem 82:3099–3103

Guo YS, Jia XP, Zhang SS (2011a) DNA cycle amplification device on magnetic microbeads for determination of thrombin based on graphene oxide enhancing signal-on electrochemiluminescence. Chem Commun 2:725–727

Guo YS, Sun YS, Zhang SS (2011b) Electrochemiluminescence induced photoelectrochemistry for sensing of the DNA based on DNA-linked CdS NPs superstructure with intercalator molecules. Chem Commun 47:1595–1597

He P, Qiao WP, Liu LJ et al (2014) A highly sensitive surface plasmon resonance sensor for the detection of DNA and cancer cells by a target-triggered multiple signal amplification strategy. Chem Commun 50:10718–10721

Jiang DN, Liu F, Liu C et al (2014a) Induction of an electrochemiluminescence sensor for DNA detection of Clostridium perfringens based on rolling circle amplification. Anal Methods 6:1558–1562

Jiang XY, Wang HJ, Yuan R et al (2014b) Design and biosensing of Mg^{2+}-dependent DNAzyme-triggered ratiometric electrochemiluminescence. Anal Chem 86:5158–5163

Jiang XY, Wang HJ, Yuan R et al (2016) Signal-switchable electrochemiluminescence system coupled with target recycling amplification strategy for sensitive mercury ion and Mucin 1 assay. Anal Chem 88:9243

Jiang XY, Wang HJ, Yuan R et al (2017) Functional three-dimensional porous conductive polymer hydrogels for sensitive electrochemiluminescence in situ detection of H_2O_2 released from live cells. Anal Chem 89:4280

Jie G, Zhang J, Wang D et al (2008) Electrochemiluminescence immunosensor based on CdSe nanocomposites. Anal Chem 80:4033–4039

Jie GF, Liu P, Wang L et al (2010) Electrochemiluminescence immunosensor based on nanocomposite film of CdS quantum dots-carbon nanotubes combined with gold nanoparticles-chitosan. Electrochem Commun 12:22–26

Jie GF, Wang L, Yuan JX et al (2011) Versatile electrochemiluminescence assays for cancer cells based on dendrimer/CdSe-ZnS-quantum dot nanoclusters. Anal Chem 83:3873–3880

Jie GF, Yuan GX (2012) Novel Magnetic Fe_3O_4@CdSe composite quantum dot-based electrochemiluminescence detection of thrombin by a multiple DNA cycle amplification strategy. Anal Chem 84:2811–2817

Jie GF, Yuan JX, Zhang J (2012) Quantum dots-based multifunctional dendritic superstructure for amplified electrochemiluminescence detection of ATP. Biosens Bioelectron 31:69–76

Li LL, Chen Y, Zhu JJ (2017a) Recent advances in electrochemiluminescence Analysis. Anal Chem 89:358–371

Li ZY, Lin ZF, Wu XY et al (2017b) Highly efficient electrochemiluminescence resonance energy transfer system in one nanostructure: its application for ultrasensitive detection of MicroRNA in cancer cells. Anal Chem 89:6029

Liao N, Zhuo Y, Chai YQ et al (2013) Reagentless electrochemiluminescent detection of protein biomarker using graphene-based magnetic nanoprobes and poly-l-lysine as co-reactant. Biosens Bioelectron 45:189–194

Liu F, Zhang Y, Ge SG et al (2012) Magnetic graphene nanosheets based electrochemiluminescence immunoassay of cancer biomarker using CdTe quantum dots coated silica nanospheres as labels. Talanta 99:512–519

Liu T, Chen X, Hong CY et al (2014) Label-free and ultrasensitive electrochemiluminescence detection of microRNA based on long-range self-assembled DNA nanostructures. Microchim Acta 181:7–8

Liu WY, Zhang Y, Ge SG et al (2013) Core-shell Fe_3O_4-Au magnetic nanoparticles based nonenzymatic ultrasensitive electrochemiluminescence immunosensor using quantum dots functionalized graphene sheet as labels. Anal Chim Acta 770:132–139

Liu ZY, Qi WJ, Xu GB (2015) Recent advances in electrochemiluminescence. Chem Soc Rev 44:3117–3142

Long Y, Zhou XM, Xing D (2011) Electrochemiluminescence gene-sensing of Listeria monocytogenes with hyperbranching rolling circle amplification technology. Biosens Bioelectron 26:2897–2904

Mao L, Yuan R, Chai YQ et al (2011) Potential controlling highly-efficient catalysis of wheat-like silver particles for electrochemiluminescence immunosensor labeled by nano-Pt@Ru and multi-sites biotin/streptavidin affinity. Analyst 136:1450–1455

Miao WJ (2008) Electrogenerated chemiluminescence and its biorelated applications. Chem Rev 108(7):2506–2553

Pana R, Xua MC, Burgess JD et al (2018) Direct electrochemical observation of glucosidase activity in isolated single lysosomes from a living cell. PNAS 115:4087–4092

Pinijsuwan S, Rijiravanich P, Somasundrum M et al (2008) Sub-femtomolar electrochemical detection of DNA hybridization based on latex/gold nanoparticle-assisted signal amplification. Anal Chem 80:6779–6784

Reid MS, Le XC, Zhang HQ (2018) Exponential isothermal amplification of nucleic acids and assays for proteins, cells, small molecules, and enzyme activities: an EXPAR example. Angew Chem Int Ed 57(37):11856–11866

Richter MM (2004) Electrochemiluminescence (ECL). Chem Rev 104:3003–3036

Serena C, Alessandro A, Conor F et al (2017) Aggregation-induced electrochemiluminescence of platinum(II) complexes. J Am Chem Soc 139:1460–14610

Tang J, Tang DP, Li QF et al (2011) Sensitive electrochemical immunoassay of carcinoembryonic antigen with signal dual-amplification using glucose oxidase and an artificial catalase. Anal Chim Acta 697:16–22

Travascio P, Witting PK, Mauk AG et al (2001) The peroxidase activity of a hemin-DNA oligonucleotide complex: free radical damage to specific guanine bases of the DNA. J Am Chem Soc 123:1337–1348

Wang FA, Elbaz J, Orbach R et al (2011a) Amplified analysis of DNA by the autonomous assembly of polymers consisting of DNAzyme. J Am Chem Soc 133:17149–17151

Wang GF, Huang H, Wang BJ et al (2011b) A supersandwich multienzyme DNA label based electrochemical immunosensor. Chem Commun 48:720–722

Wang GJ, Jin F, Dai N et al (2012a) Signal-enhanced electrochemiluminescence immunosensor based on synergistic catalysis of nicotinamide adenine dinucleotide hydride and silver nanoparticles. Anal Biochem 422:7–13

Wang HM, Li CX, Liu XQ (2018a) Construction of an enzyme-free concatenated DNA circuit for signal amplification and intracellular imaging. Chem Sci 9:5842–5849

Wang HJ, Yuan R, Chai YQ et al (2012b) Bi-enzyme synergetic catalysis to in situ generate coreactant of peroxydisulfate solution for ultrasensitive electrochemiluminescence immunoassay. Biosens Bioelectron 37:6–10

Wang J, Han HY, Jiang XC et al (2012c) Signal-on dual-potential electrochemiluminescence based on luminol-gold bifunctional nanoparticles for telomerase detection. Anal Chem 84:4893–4899

Wang J, Li XL, Zhang JD et al (2015) Integration of DNA bio-gates and duplex-specific nuclease signal amplification: towards electrochemiluminescence detection of survivin mRNA. Chem Commun 51:11673

Wang XF, Gao HF, Qi HL et al (2018b) Proximity hybridization-regulated immunoassay for cell surface protein and protein-overexpressing cancer cells via electrochemiluminescence. Anal Chem 90:3013–3018

Wei W, Zhou J, Li H et al (2013) Fabrication of CdTe@SiO_2 nanoprobes for sensitive electrogenerated chemiluminescence detection of DNA damage. Analyst 138:3253–3258

Willner I, Shlyahovsky B, Zayats M et al (2008) DNAzymes for sensing, nanobiotechnology and logic gate applications. Chem Soc Rev 37:1153–1165

Wu D, Xin X, Pang XH et al (2015) Dual signal amplification strategy for the fabrication of an ultrasensitive electrochemiluminescent aptasensor. ACS Appl Mater Inter 7:12663

Wu P, Hou XD, Xu JJ (2014) Electrochemically generated versus photoexcited luminescence from semiconductor nanomaterials: bridging the valley between two worlds. Chem Rev 114:11027–11059

Wu YF, Shi HY, Yuan LA et al (2010) A novel electrochemiluminescence immunosensor via polymerization-assisted amplification. Chem Commun 46:7763–7765

Xi DM, Wang XD, Ai SY et al (2014) Detection of cancer cells using triplex DNA molecular beacons based on expression of enhanced green fluorescent protein (eGFP). Chem Commun 50:9547–9549

Xiao LJ, Chai YQ, Yuan R et al (2013) Amplified electrochemiluminescence of luminal based on hybridization chain reaction and in situ generate co-reactant for highly sensitive immunoassay. Talanta 115:577–582

Xiao LJ, Chai YQ, Yuan R et al (2014) Highly enhanced electrochemiluminescence based on pseudo triple-enzyme cascade catalysis and generation of co-reactant for thrombin detection. Analyst 139:1030–1036

Xiao Y, Pavlov V, Niazov T et al (2004) Atalytic beacons for the detection of DNA and telomerase activity. J Am Chem Soc 126:7430–7431

Xu J, Wu J, Zong C et al (2013a) Manganese porphyrin-dsDNA complex: a mimicking enzyme for highly efficient bioanalysis. Anal Chem 85:3374–3379

Xu SJ, Liu Y, Wang TH et al (2013b) Positive potential operation of a cathodic electrogenerated chemiluminescence immunosensor based on luminol and graphene for cancer biomarker detection. Anal Chem 83:3817–3823

Yang LL, Tao YZ, Yue GY et al (2016) Highly selective and sensitive electrochemiluminescence biosensor for p53 DNA sequence based on nicking endonuclease assisted target recycling and hyperbranched rolling circle amplification. Anal Chem 88:5097

Yetisen AK, Akram MS, Lowe CR (2013) Paper-based microfluidic point-of-care diagnostic devices. Lab Chip 13(12):2210–2251

Yuan YL, Wei SQ, Liu GP et al (2014) Ultrasensitive electrochemiluminescent aptasensor for ochratoxin A detection with the loop-mediated isothermal amplification. Anal Chim Acta 811:70–75

Zhang B, Liu BQ, Tang DP et al (2012a) DNA-based hybridization chain reaction for amplified bioelectronic signal and ultrasensitive detection of proteins. Anal Chem 84:5392–5399

Zhang HR, Li BX, Sun ZM et al (2017a) Integration of intracellular telomerase monitoring by electrochemiluminescence technology and targeted cancer therapy by reactive oxygen species. Chem Sci 8(12):8025–8029

Zhang HR, Wang YZ, Wu MS (2014a) Visual electrochemiluminescence detection of telomerase activity based on multifunctional Au nanoparticles modified with G-quadruplex deoxyribozyme and luminol. Chem Commun 50:12575–12577

Zhang HR, Wang YZ, Wei Zhao (2016) Visual color-switch electrochemiluminescence biosensing of cancer cell based on multichannel bipolar electrode chip. Anal Chem 88:2884–2890

Zhang HR, Wu MS, Xu JJ (2014b) Signal-on dual-potential electrochemiluminescence based on luminol-gold bifunctional nanoparticles for telomerase detection. Anal Chem 86:3834–3840

Zhang HR, Xia XH, Xu JJ et al (2012b) Sensitive cancer cell detection based on Au nanoparticles enhanced electrochemiluminescence of CdS nanocrystalfilm supplemented by magnetic separation. Electrochem Commun 25:112–115

Zhang HR, Xu JJ, Chen HY (2013a) Electrochemiluminescence ratiometry: a new approach to DNA biosensing. Anal Chem 85:5321–5325

Zhang P, Wu XY, Yuan R (2015a) An "off On" electrochemiluminescent biosensor based on DNAzyme-assisted target recycling and rolling circle amplifications for ultrasensitive detection of microRNA. Anal Chem 87:3202–3207

Zhang XL, Yang ZH, Chang YY et al (2018) Novel 2D-DNA-nanoprobe-mediated enzyme-free-target-recycling amplification for the ultrasensitive electrochemical detection of microRNA. Anal Chem 90:9538–9544

Zhang Y, Dai WJ, Liu F et al (2013b) Ultrasensitive electrochemiluminescent immunosensor based on dual signal amplification strategy of gold nanoparticles-dotted graphene composites and CdTe quantum dots coated silica nanoparticles. Anal Bioanal Chem 405:4921–4929

Zhang Y, Ge SG, Wang SW et al (2012c) Magnetic beads-based electrochemiluminescence immunosensor for determination of cancer markers using quantum dot functionalized PtRu alloys as labels. Analyst 137:2176–2182

Zhang Y, Li L, Yang HM et al (2013c) Gold–silver nanocomposite-functionalized graphene sensing platform for an electrochemiluminescent immunoassay of a tumor marker. RSC Adv 3:14701–14709

Zhang Y, Wang LX, Luo F et al (2017b) An electrochemiluminescence biosensor for Kras mutations based on locked nucleic acid functionalized DNA walkers and hyperbranched rolling circle amplification. Chem Commun 53:2910

Zhang Y, Zheng B, Zhu CF (2015b) Single-layer transition metal dichalcogenide nanosheet based nanosensors for rapid, sensitive, and multiplexed detection of DNA. Adv Mater 27:935–939

Zhao M, Chen AY, Huang D (2018) MoS_2 quantum dots as new electrochemiluminescence emitters for ultrasensitive bioanalysis of lipopolysaccharide. Anal Chim 89:8335–8342

Zhao M, Zhuo Y, Chai YQ et al (2013) Quantum dot-based near-infrared electrochemiluminescent immunosensor with gold nanoparticle-graphene nanosheet hybrids and silica nanospheres double-assisted signal amplification. Analyst 138:6639–6644

Zhao YC, Chen F, Li Q (2015) Isothermal amplification of nucleic acids. Chem Rev 115:12491–12545

Zhou H, Han TQ, Wei Q et al (2016) Efficient enhancement of electrochemiluminescence from cadmium sulfide quantum dots by glucose oxidase mimicking gold nanoparticles for highly sensitive assay of methyltransferase activity. Anal Chem 88(5):2976–2983

Zhou H, Liu J, Xu JJ et al (2011a) Ultrasensitive DNA detection based on Au nanoparticles and isothermal circular double-assisted electrochemiluminescence signal amplification. Chem Commun 47:8358–8360

Zhou H, Liu J, Xu JJ et al (2011b) Highly sensitive electrochemiluminescence detection of single-nucleotide polymorphisms based on isothermal cycle-assisted triple-stem probe with dual-nanoparticle label. Anal Chem 83:8320–8328

Zhou J, Lu Q, Tong YW et al (2012a) Detection of DNA damage by using hairpin molecular beacon probes and graphene oxide. Talanta 99:625–630

Zhou XM, Su Q, Xing D (2012b) An electrochemiluminescent assay for high sensitive detection of mercury (II) based on isothermal rolling circular amplification. Anal Chim Acta 713:45–49

Zhu MJ, Pan JB, Wu ZQ et al (2018) Electrogenerated chemiluminescence imaging of electrocatalysis at a single Au-Pt Janus nanoparticle. Angew Chem Int Ed 57:4010–4014

Chapter 5
Nucleic Acid Amplification Strategy-Based Colorimetric Assays

Pengfei Shi and Xiangjiang Zheng

Abstract Colorimetric assays, using colored substances in solution to determine the concentration without the aid of advanced instrumentation, are a convenient, cost-effective, and rapid method for ions, small molecules, oligonucleotides, miRNA, and protein detections. Nucleic acid amplification strategies play an important role in highly sensitive detection. Based on nucleic acid amplification, colorimetric assays detections would be more sensitive, proved by many detections, such as DNA, miRNA, and tumor cells. In this chapter, we introduce the nucleic acid amplification strategy-based colorimetric assays, including various amplification methods and colored substances. Au nanoparticles and Ag nanoparticles are usually employed as the colored substances by aggregation. HRP-catalyzed conversion of ABTS and TMB is also used as colored substances, which can be oxidized by hydrogen peroxide with color change, widely applied in electrochemical analysis and detection. The nucleic acid amplification strategies contain enzyme-assisted (PCR, RCA, NEANA, EASA, LAMP, DSN, NASBA, ESPAR, HDA) and enzyme-free (HCR, SDA). Additionally, the future perspectives and advantages of adoption nucleic acid amplification techniques in colorimetric assays are also discussed.

5.1 Introduction

In the development of analysis and detection, targeting recognition with a simple measurable signal is worth drawing attention. Many detection methods have been used, such as fluorescence, electrochemistry, surface plasmon resonance, colorimetry, atomic force microscope, and so on. Among them, the colorimetric method has attracted interest because of its rapidness, simplicity, and no need to use expensive analytical instruments (Chen et al. 2018a, b). In the reported documents, the

P. Shi (✉) · X. Zheng
Shandong Provincial Key Laboratory of Detection Technology for Tumour Markers, College of Chemistry and Chemical Engineering, Linyi University, Linyi 276005, People's Republic of China
e-mail: shipengfei913@163.com

X. Zheng
e-mail: zxj4408@126.com

S. Zhang et al. (eds.), *Nucleic Acid Amplification Strategies for Biosensing, Bioimaging and Biomedicine*, https://doi.org/10.1007/978-981-13-7044-1_5

colored substances usually employ Au nanoparticles, Ag nanoparticles, and fluoresceins. HRP-catalyzed conversion of 3, 3′, 5, 5′-tetramethylbenzidine (TMB) or 2, 2′-azino-bis (3-ethylbenzothiazoline)-6-sulfonate disodium salt (ABTS) to the colored product is also widely applied in colorimetry (Chen et al. 2018a, b; Geng et al. 2014; Gong et al. 2014; Huang et al. 2013; Ke et al. 2011). Nucleic acid amplification strategies play an important role in highly sensitive detections. Up to now, many colorimetric assays based on nucleic acid amplification have been developed, such as rolling circle amplification (RCA), helicase-dependent amplification (HDA), polymerase chain reaction (PCR), duplex-specific nuclease signal amplification (DSNSA), ligase chain reaction (LCR), hybridization chain reaction (HCR), exonuclease-assisted amplification (EAA), nicking endonuclease-assisted nanoparticle amplification (NEANA), loop-mediated isothermal amplification (LAMP), nucleic acid sequence-based amplification (NASBA), strand displacement amplification (SDA), and hairpin catalytic assembly (HCA) reaction. Based on this principle, detection of proteins, DNA, metal ions, viruses, amino acids, small molecules, and cancerous cells has been developed.

5.2 Colorimetric Assays Based on Au Nanoparticles

Gold nanoparticles (AuNPs) present a promising platform for colorimetric assays due to their high photostability and unique size-dependent optical properties. The aggregation of AuNPs leads to a color change from red to blue, ascribing to their distance dependent and size-dependent optical properties. AuNPs can aggregate when they are cross-linked to targets or at a high ionic strength. The absorption peak of the aggregated AuNPs broadens and red-shifts (Fu et al. 2013; Kumvongpin et al. 2016; Liu et al. 2016a, b; Ma et al. 2012; Niazi et al. 2013). The large color change can be easily read out with naked eyes as an end-point detection method, and thus, no expensive instrument is required. With these characteristics, AuNPs-based colorimetric strategies are suitable to create a fast, specific, and low-cost analysis platform for point-of-care diagnostics (Wang et al. 2015a, b, c).

5.2.1 Colorimetric Assays Detection Based on Enzyme-Assisted Strategy Amplification and AuNPs

Most enzymes are proteins, which present specific catalytic functions and control the efficiency of organic transformations. The catalytic power that may increase the rate of chemical reaction by factors of a million is the remarkable characteristic of enzymes. Among many types of enzymes, the enzymes involved in the actions of nucleic acids and peptides are powerful biological tools.

5.2.1.1 Colorimetric Assays Detection Based on PCR and AuNPs

PCR assay played a powerful tool in detecting biological targets such as nucleic acids and proteins in the entire sample. Although the first PCR coupling with colorimetric method was developed in 1995 (Armstrong et al. 1995), currently reported bio-barcode probe strategies still require many experimental steps, which also include microarrayer-based immobilization of oligonucleotides on a glass chip and light-scattering measurement. As shown in Fig. 5.1, Nam reported a colorimetric PCR that minimizes the above requirements while detecting 30 aM concentrations of cytokines (Nam et al. 2005). Compared with other detection methods, this strategy is fast and simple. Based on PCR and colorimetric assay, herpes simplex virus and genes were also reported (Tan et al. 2007).

5.2.1.2 Colorimetric Assays Detection Based on RCA and AuNPs

RCA is a polymerase-based isothermal DNA amplification technique, which can generate long single-stranded DNA (ssDNA) molecules with tandem repeats that are complementary to a circular template. Unlike PCR, it is an isothermal amplification process. It does not require thermal cycling or the use of sophisticated instruments. And, RCA usually can provide 10^3 to 10^4-fold increase in the intensity of the signal (Wang et al. 2014). The colorimetric assay detection based on RCA has been used for the novel, ultrasensitive detection of DNA, proteins, and bacteria. As shown in Fig. 5.2, Xing developed a new highly sensitive colorimetric method for the detection of target H1N1 DNA. The method is based on the signal enhancement of RCA and the capability of ssDNA to stabilize unmodified AuNPs. The assay requires only 3 h from start to finish and achieves a detection limit as low as 1 pM (Xing et al. 2013). Similarly, based on AuNPs and RCA, Hu presented miRNA detections with a detection limit of 0.13 pM (Hu et al. 2017).

Wang, Chen, and Liang developed highly sensitive and novel colorimetric RCA immunoassays for detecting proteins CRP, AFP, and CEA, respectively. With the addition of CRP, a sandwich structure was formed. The RCA product was obtained by magnetic separation, and long tandem repeated sequences mediated the aggregation of AuNPs. The signal was observed by the naked eye and quantified using absorption spectra with a detection limit of 30 fg mL^{-1}. Based on similar methods, Chen presented high sensitivity for the detection of AFP with the detection limit 33.45 pg mL^{-1} (Chen et al. 2015) and Liang reported detection of CEA with the detection limit as low as 2 pM (Liang et al. 2014). High affinity between CEA aptamer and its target (CEA) would lead to form a complex; however, the introduced CDNA cannot hybridize with the aptamer. Based on RCA strategy, a large number of single-stranded DNA (ssDNA) can be generated by CDNA as primer. ssDNA can be easily adsorbed onto AuNPs and prevent salt-induced AuNPs aggregation, resulting in the color change.

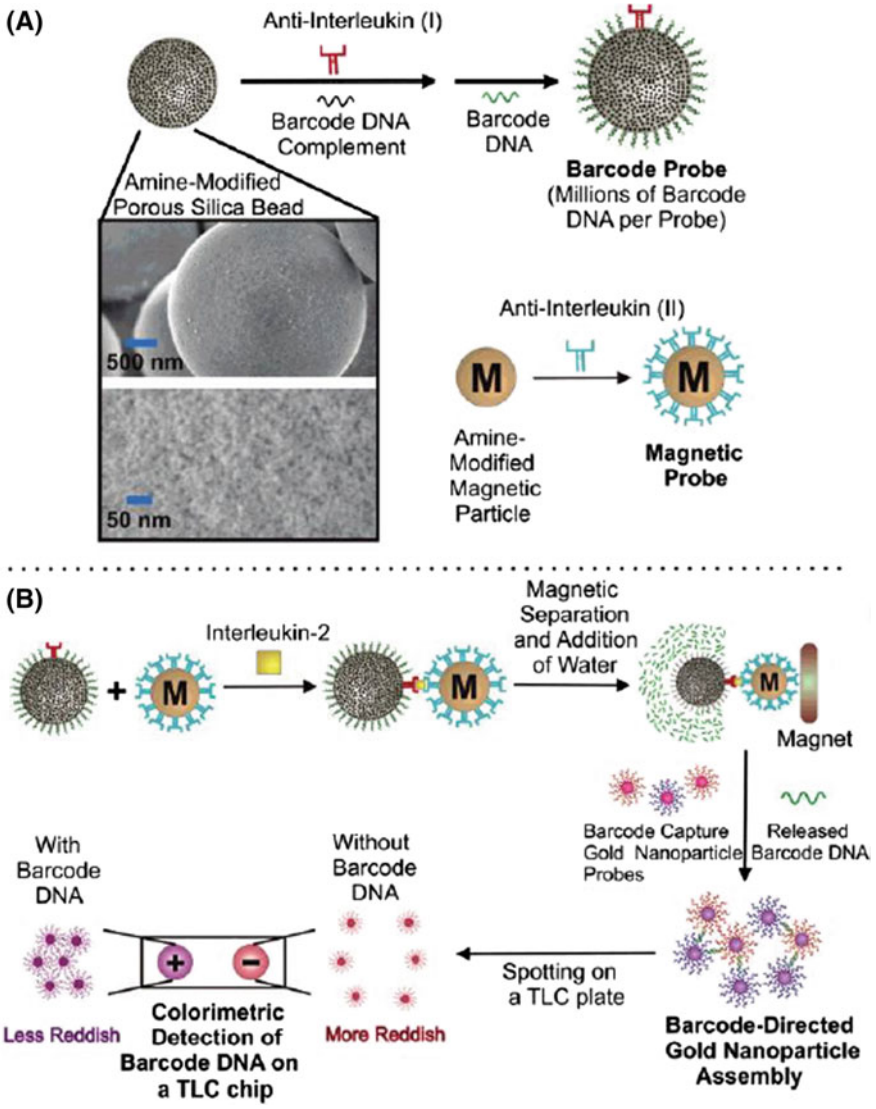

Fig. 5.1 Colorimetric biobarcode assay. **a** Probe preparation and electron micrograph images of amine-modified porous silica beads (inset). **b** Interleukin-2 detection scheme. Reprinted with the permission from Nam et al. (2005). Copyright 2005 American Chemical Society

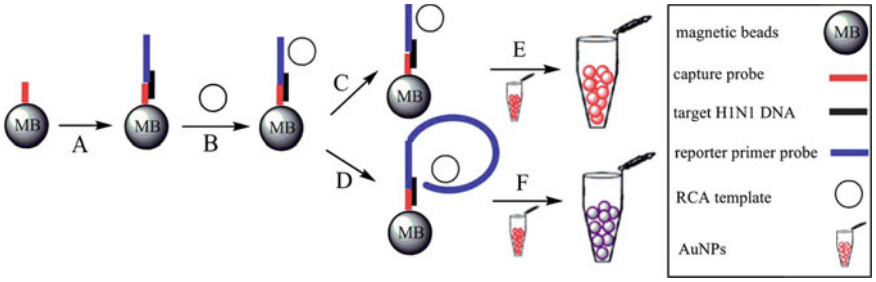

Fig. 5.2 Scheme of the RCA-based assay for H1N1 DNA detection. (A) Target H1N1 DNA and reporter probe are added to the capture probe-labeled beads; (B) the circular RCA template is added; (C) the RCA components are added and stored at 20 °C for 120 min (negative control); (D) the RCA components are added and incubated at 37 °C for 120 min; and (E) colorimetric or UV-vis spectra analysis of the RCA products. Reproduced from Xing et al. (2013) by permission of The Royal Society of Chemistry

5.2.1.3 Nicking Endonuclease Strategies Amplification and AuNPs

In the case of colorimetric detection based on DNA–AuNP conjugates, Liu and co-workers developed a nicking endonuclease-assisted nanoparticle amplification (NEANA) system that offered 10^3-fold improvement in detection sensitivity (10 pM). It is worth noting that this method transcended traditional sandwich hybridization methods. And, a single-base mismatch selectivity with simple naked eye colorimetric detection was also realized (Xu et al. 2009). Using NEANA, Li developed a simple method for highly sensitive detection of proteins (human thrombin) and small molecules (ATP). Using this method, ATP was detected with a detection limit of 100 nM and the human thrombin was detected with a detection limit of 50 pM by the naked eye (Li et al. 2012). To further improve detection, Xu demonstrated the combination of RCA and NEANA for rapid colorimetric DNA detection. This dual-amplification technology eliminates the need for costly and time-consuming target fluorescence labeling, which relies upon high specificity ligation and rolling circle replication of a padlock probe. As shown in Fig. 5.3, the coupling two amplification methods (RCA and NEANA) present high sensitivity. Based on the fixed of linker, particle probes, and modifiable padlock probe, random target sequences were detected with great detection capacity (Xu et al. 2012). Although this improvement allows NEANA to detect any target sequence, target-specific padlock probes are required. Thus, this might result in a high cost when detecting different targets. By coupling invasive reaction with NEANA (termed as IR-NEANA for brief), Zou proposed a colorimetric DNA detection with the detection limit of IR-NEANA as low as 1 pM. In a large amount of wild-type DNA backgrounds, the specificity of the method can reach as low as 1% (Zou et al. 2015). Many miRNA is a marker of many human tumors; thus, it is necessary to detect it, contributing to early tumor diagnosis, which was also proved in reported articles. Persano reported a naked-eye colorimetric detection of miRNA (miRNA-10b) based on the NEANA. The assay

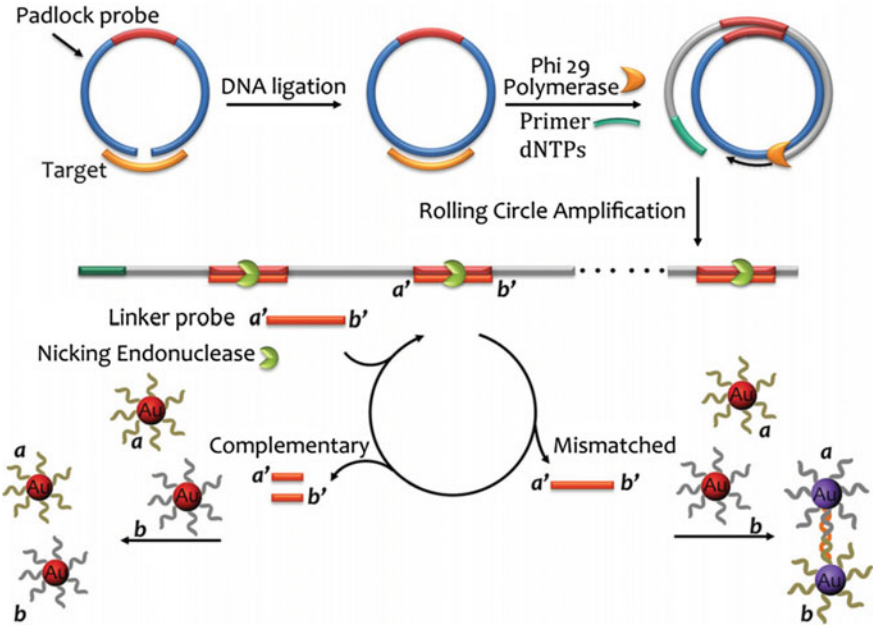

Fig. 5.3 Colorimetric DNA detection through rolling circle amplification and nicking endonuclease-assisted nanoparticle amplification. Reproduced from Xu et al. (2012) by permission of John Wiley & Sons Ltd.

was also validated in cancer cells (Persano et al. 2016). Similar works were also reported by other groups (Xia et al. 2017; Luo et al. 2012; Yu et al. 2016; Xie et al. 2012).

In cancer diagnostics, how to detect cancer cells rapidly and effectively at their earliest stages is a challenge. Based on cell-triggered cyclic enzymatic signal amplification (CTCESA), Zhang developed a rare cancer cells detections based on colorimetric method. In the presence of target cells, hairpin aptamer probes can bind to the target cells and result in linker DNA hybridization and cleavage by NESNA. The target CCRF-CEM cells could be detected by the naked eye with a detection limit of 40 cells (Zhang et al. 2014). Dual-signal amplification method has potential application in point-of-care cancer diagnosis. As shown in Fig. 5.4, based on combining multi-DNA with cyclic enzymatic amplification, Yu dominated a colorimetric strategy for cancer cell detection. The mDNAs bond to the linker DNA to form double-stranded structures, and the nicking enzyme would cleave the linker DNA, leading to the release of the cleaved linker DNA and free mDNAs. Meanwhile, the released mDNAs could be reused. After magnetic separation again, the supernatant was added into AuNPs solution. These ssDNAs were adsorbed on the Au NPs to prevent particle aggregation and result in the red color of AuNPs. With the increased number of target HL-60 cells, the more dispersive AuNPs were present. The HL-60

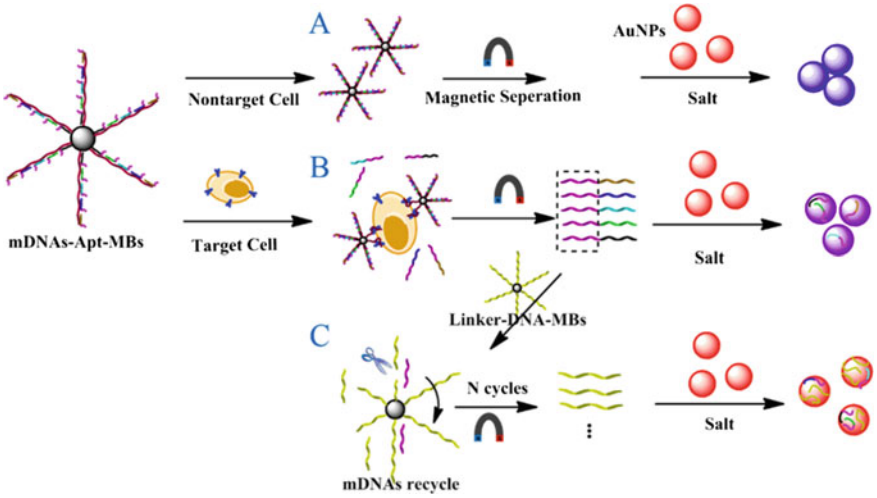

Fig. 5.4 Schematic representation of the visual detection of HL-60 cells based on aptamer DNA conformational switch and non-crosslinking AuNPs aggregation. Reprinted with the permission from Yu et al. (2016). Copyright 2016 American Chemical Society

cells were detected with a detection limit of four cells in buffer solution (Yu et al. 2016).

5.2.1.4 DNA Enzyme Strategies Amplification and AuNPs

DNA enzyme, a kind of catalytic DNA molecules, depends on specific metal ions (e.g., Hg^{2+}, Pb^{2+}, Cu^{2+}, and Zn^{2+}) as cofactors and accounts for specific cleavage sites of the substrate strand of DNA enzyme. DNA enzymes have been reported for a variety of applications, including usual assays to detect metal ions in environmental contaminants, DNA computing, nanowire production, and drugs in preclinical models of cancer. Liu reported a label-free colorimetric Pb^{2+} sensor based on molecular beacon (MB) and DNA enzyme by recycling using enzyme strand for signal amplification. In his work, Pb^{2+} was detected with detection limit of 20 pM (Liu et al. 2018a, b). Chen developed another cascade signal amplification method for Hg^{2+} detection based on target-guided recycling assembly of the active DNA enzyme, enabling the visual detection of Hg^{2+} down to 10 pM without instrumentation (Chen et al. 2017). Detection of vascular endothelial growth factor (VEGF) is achieved by target-catalyzed branched DNA cascade amplification with a low detection limit of 185 pM (Chang et al. 2016).

Based on the ion-dependent DNA enzymes, our group designed a complete set of two-input logic gates, shown in Fig. 5.5. The logic gates are functional components and the respective cofactor ions as inputs. Using AuNP-based homogeneous colorimetric detection, the outputs of the cleaved active sites of the gates perform

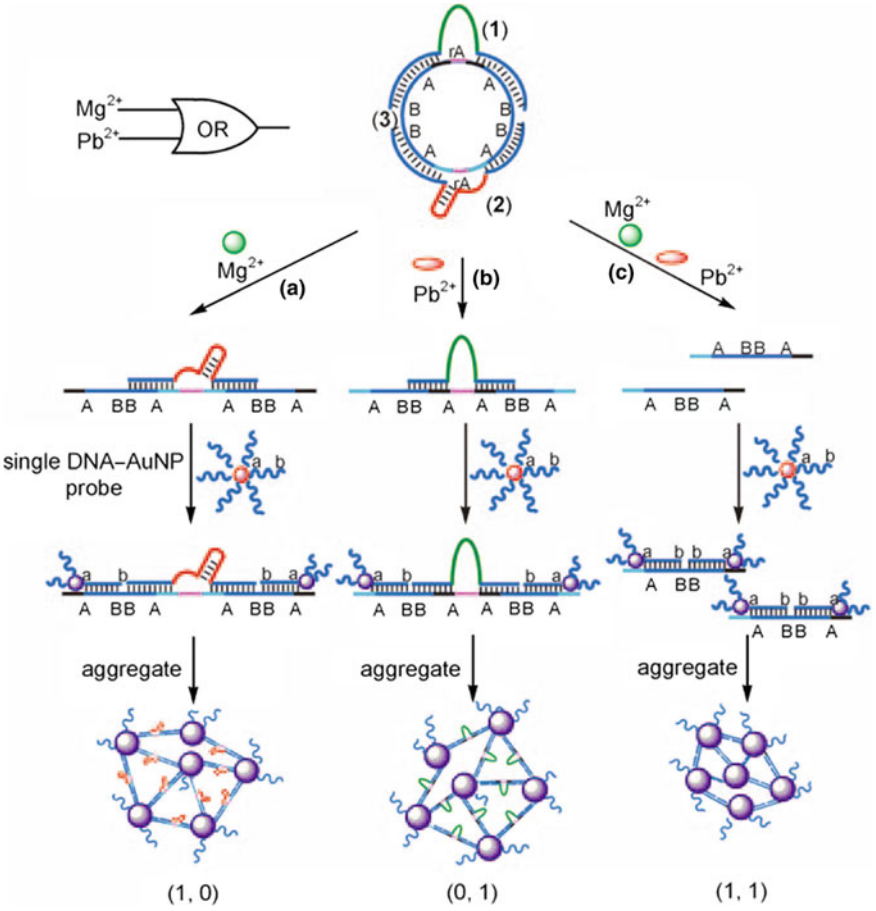

Fig. 5.5 OR logic gate system that is activated by Mg^{2+} and Pb^{2+} ions as inputs and connected to single $DNA_{a\text{-}b}$-AuNP probes as colorimetric outputs. Reproduced from Bi et al. (2010) by permission of John Wiley & Sons Ltd.

the gate functions (Bi et al. 2010). This strategy would become a general method for any metal ion with a specific DNAzyme and other targets.

5.2.1.5 EASA Strategies Amplification and AuNPs

Exonuclease III catalyzes the stepwise removal of mononucleotides from blunt or recessed 30-hydroxyl termini of duplex DNAs. Compared with other nucleases such as nicking endonuclease and DNA enzyme, exonuclease III does not require a specific recognition site, which may offer a universally adaptable system. As shown in Fig. 5.6, Zhou reported a rapid AuNP-based colorimetric DNA biosensor. Based on

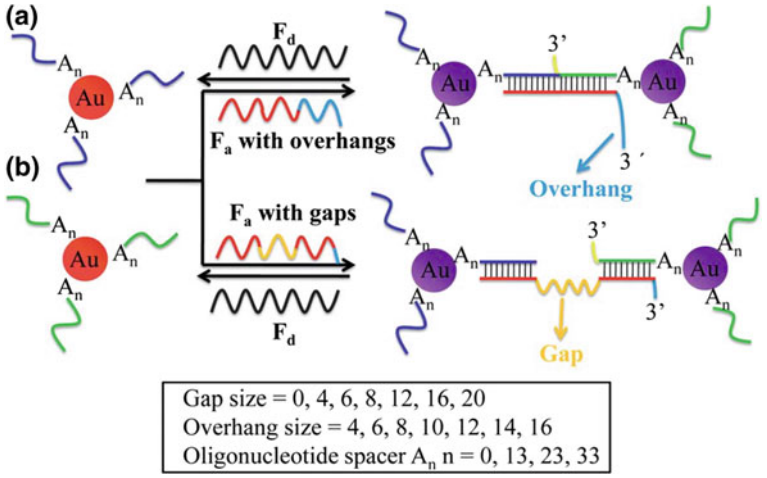

Fig. 5.6 Scheme of DNA-directed assembly and disassembly of DNA-functionalized AuNPs. Oligomer Fa contains overhangs (**a**) and gaps (**b**). Reproduced from Zhou et al. (2013a, b) by permission of The Royal Society of Chemistry

EASA, the sensor was successfully prepared with the detection limit as low as 2 nM (Zhou et al. 2013a, b).

Using Exo III, a linker DNA, and two DNA-modified AuNPs, Cui developed a simple, low-cost, sensitive, and selective colorimetric DNA detection method with the detection limit of 15 pM (Cui et al. 2011). Using EASA, AuNPs, and combining terminal protection of small molecule-capped DNA probes, Yang developed a label-free colorimetric assay for highly sensitive folate receptor detection with a detection limit of 10 pM by the naked eye (Yang and Gao 2014).

5.2.1.6 Colorimetric Assays Detection Based on LAMP and AuNPs

Loop-mediated isothermal amplification (LAMP) has been developed as an alternative method capable of detecting only a few copies of target nucleic acid under isothermal conditions. This technique can be achieved simply by using a water bath or an inexpensive heating block. Suebsing proposed a new LAMP-AuNPs assay for molecular detection of E. hepatopenaei in shrimp without sacrificing sensitivity or specificity (Suebsing et al. 2013a). This method significantly reduced the time, ease, and cost. Additionally, Suebsing first reported *Penaeus vannamei* nodavirus (*Pv*NV) detection using the LAMP assay combined with colorimetric AuNPs, which offers a simple, rapid, and sensitive technique (Suebsing et al. 2013b). Based on LAMP and AuNP hybridization probe, Watthanapanpituck reported a human DNA in forensic evidence. The detection limit was 718 fg of genomic DNA (Watthanapanpituck et al. 2014). Similar work was documented by Zhou groups (Zhou et al. 2013a, b). Hepati-

tis E virus (HEV) infection is a communicable disease in the third world countries. HEV detection was realized by Chen group with 10^1 copies of HEV RNA detected visually (Chen et al. 2014). Similar work was developed by Wong group, and the detection limit was 17 aM (Wong et al. 2014).

5.2.1.7 Duplex-Specific Nuclease and AuNPs

Duplex-specific nuclease (DSN) can cleave DNA in double-stranded DNA or DNA–RNA heteroduplexes (Shi et al. 2016). Significantly, DSN can clearly discriminate among mismatched duplexes. By coupling the DSN amplification and AuNPs, DSN-assisted colorimetric assay can be generated with improved sensitivity and specificity. Based on this method, Wang group (Wang et al. 2015b) reported the miR-122 detection with detection limit of 16 pM. In Shi's work, the DNA probe was labeled with ferrocene (Fc) and immobilized on the electrode surface, which triggered the assembly of positively charged AuNPs through electrostatic interaction. The electrochemical signal can be obtained by recording the oxidation current of Fc (Shi et al. 2016).

5.2.1.8 Colorimetric Assays Detection Based on EXPAR and AuNPs

As is mentioned previously, ultrasensitive miRNA detection is very important. Based on isothermal exponential amplification reaction (EXPAR) amplification and AuNPs, Li reported a miRNA detection method with the detection limit of 46 fM (Li et al. 2016a, b, c). Tan's group have developed a method for detecting short oligonucleotides that combines EXPAR through aggregation of DNA-functionalized AuNPs with the detection limit of 100 fM in under 10 min (Tan et al. 2005). Similarly, based on EXPAR and AuNPs, Zhang developed a sensitive detection method for transcription factor NF-κB p50. In his work, NF-κB p50 was converted to the oligonucleotides through protein–DNA interaction, exonuclease III digestion, and EXPAR, resulting in the detection of NF-κB p50 visually (Zhang et al. 2012).

5.2.1.9 Colorimetric Assays Detection Based on HDA and AuNPs

Except for the most common isothermal amplifications, the combination of helicase-dependent isothermal amplification (tHDA)-ELISA and AuNPs detections for molecular identifying of pathogen was also reported. This technique did not require thermocycler machine because of tHDA of DNA targets coupled with ELISA to allow simple analysis of several samples simultaneously. Gill describes a colorimetric method using tHDA and AuNPs probes for more simple, rapid, and cost-effective diagnosis of bacterium in gastrointestinal biopsies. In addition, using this assay, they detected as little as 10 CFU mL^{-1} of *H. pylori* within less than 1 h (Gill et al. 2008).

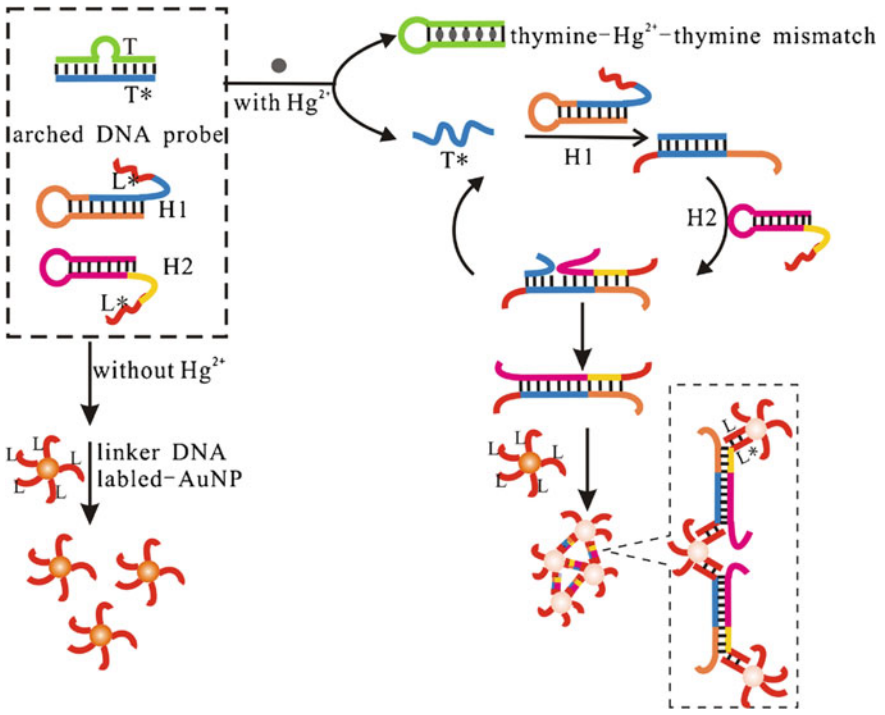

Fig. 5.7 Illustration of the enzyme-free colorimetric assay for mercury (II) using DNA conjugated to gold nanoparticle along with strand displacement amplification. Reproduced from Liu et al. (2018b) with kind permission from Springer Science + Business Media

5.2.2 Colorimetric Assays Detection Based on Enzymes-Free Strategies Amplification and AuNPs

5.2.2.1 Colorimetric Assays Detection Based on SDA and AuNPs

SDA refers to the displacement of one or more pre-hybridized strands from partial or full complementary dsDNAs, which is initiated at the complementary single-stranded domains. SDA is enzyme-free, however, SDA was only applied in DNA nanotechnology in the past decade.

Liu firstly developed an enzyme-free detection approach for Hg^{2+} by using the color change of DNA–AuNP and SDA strategy. As shown in Fig. 5.7, the first example of gold sandwich assay based on nucleic acid amplification is to detect Hg^{2+} concentration. The assay has a detection range over four orders of magnitude and a 3.4 nM detection limit. The biomarker DNA methylation in tumor and cancer plays an important role in many biological processes. Li presented a novel colorimetric method for assaying M.SssI activity-based AuNPs and SDA assay with a detection limit of 0.08 U mL^{-1} (Li et al. 2017a, b). Zhang developed a sensitive colorimetric

sensor to detect PDGF-BB with a detection limit of 1.1 nM (Zhang et al. 2015). In addition to the conventional merits of AuNPs colorimetric, this detection system also offered several advantages in that this method could convert the detection of trace PDGF-BB to the detection of a large amount of the amplification product; it offered ultrahigh detection specificity, which was capable of detecting PDGF-BB in complicated biological sample such as human breast cancer tissue sample extract without any interference; it provided an obvious color change when the concentration of PDGF-BB was as low as 4.0 nM. Importantly, this method provides a simple and direct visualization detection strategy with no need any complicated instrumentation.

5.2.2.2 Colorimetric Assays Detection Based on HCR and AuNPs

Compared with other competing amplification assays, the prominent merit of HCR is that it allows for specific self-assembly and extension with enzyme-free at room temperature. Based on HCR and AuNPs, Liu presented a highly sensitive and specific DNA assay. In his work, the strategy was not only nonchemical modifications but also has no need to eliminate the enzymatic reactions and separation processes. Importantly, this method offers high selectivity for the determination between perfectly matched target oligonucleotides (Liu et al. 2014). Based on HCR and AuNPs, Wang presented a novel method for sensitive mercury ion (Hg^{2+}) detection with the detection limit of 30 nM (Wang et al. 2015a). Similarly, $UO_2{}^{2+}$ was detected based on this strategy. As shown in Fig. 5.8, in the presence of $UO_2{}^{2+}$, rigid DNA triangles was formed by the HCA reaction, which resulted in the aggregation of AuNPs with a "turn-on" fluorescent signal and a color change. The detection limit was 0.1 pM (Yun et al. 2018). With the elegant amplification effect of HCR and AuNPs, Wang presented a low detection limit (15 nM for Hg^{2+} and 1 μM for adenosine) (Wang et al. 2015a). Using this enzyme-free and isothermal signal amplification method, Ma detected target DNA at concentrations as low as 0.5 nM with the naked eye (Ma et al. 2014). Similar work was also reported by Liu group (Liu et al. 2013). Using gold nanorods (AuNRs), Xu developed a novel and simple colorimetric biosensor by combining the unique optical properties of unmodified AuNRs with the amplification strategy of HCR, which was capable of detecting DNA sensitively and selectively. The detection mechanism is based on the dispersion/aggregation of AuNRs under the high concentration of salt. The approach is able to detect target DNA in a range of 0–60 nM with a detection limit of 1.47 nM and exhibits high selectivity to distinguish fully matched and single-base mismatched DNA (Xu et al. 2018a, b). Colorimetric methods for protein detection based on nucleic acid amplification have been developed. Lin's group constructed a new method for detection of acetylcholinesterase (AChE) activity based on signal amplification of DNA enzyme and HCR with the assembly of AuNPs. The detection limits of AChE and donepezil are as low as 5 μU mL^{-1} and 0.5 nM, respectively (Zou et al. 2018).

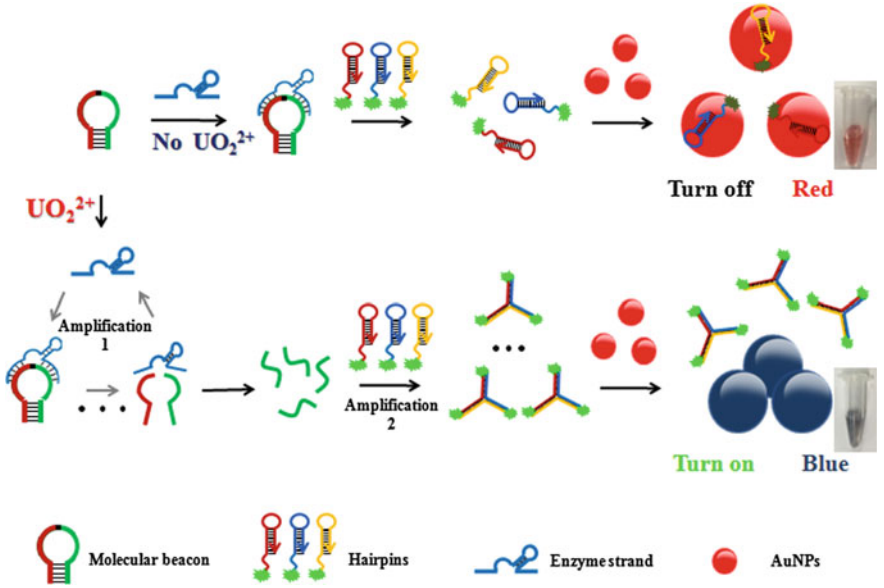

Fig. 5.8 Schematic illustration of enzyme-free dual-amplification strategy based on enzyme-strand recycle and HCR reaction for ultrasensitive fluorescent and colorimetric detection of uranyl. Reprinted from Yun et al. (2018). Copyright 2018, with permission from Elsevier

5.3 Colorimetric Assay Based on Catalyzation

The enzyme horseradish peroxidase (HRP) is used extensively in biochemistry applications (Goto et al. 2009; Tang et al. 2012). It can catalyze the oxidation of various organic substrates by hydrogen peroxide (Aktas et al. 2015; Chen et al. 2015; Du et al. 2011; Gao et al. 2013, 2015). The common HRP chromogenic substrates are presented in Fig. 5.9 (Liu et al. 2016a, b; Shao et al. 2017).

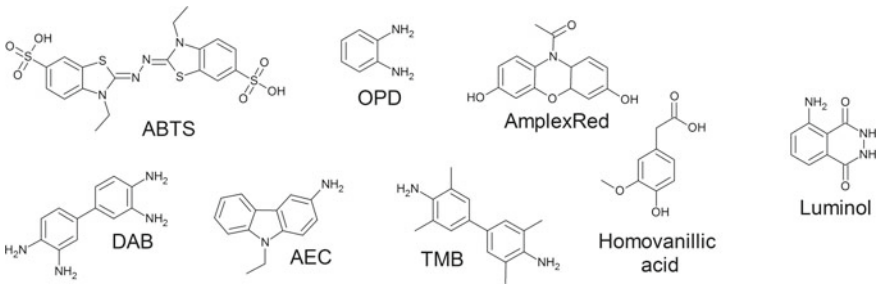

Fig. 5.9 Most common HRP chromogenic substrates. Reproduced from LHcheM (2015) by permission of Wikipedia Commons

5.3.1 Colorimetric Assay Based on HRP Catalyst

2,2′-Azino-bis(3-ethylbenzothiazoline-6-sulfonic acid) (ABTS) is a peroxidase substrate, which can be oxidized by hydrogen peroxide from colorless to the green-colored product $ABTS^{-}$ (Li et al. 2013, 2016a, b, c; Liu et al. 2014). Similarly, 3,3′,5,5′-Tetramethylbenzidine (TMB) is another important chromogenic substrate in colorimetric assay (Lai et al. 2017; Li et al. 2017a, b; Liang et al. 2015). TMB can be oxidized by peroxidase from colorless to the blue-colored product diamine. And, this color change can be read on a spectrophotometer at the wavelengths of 370 and 650 nm. Thus, ABTS and TMB were widely used in colorimetric detection of nucleic acid and protein (Luan et al. 2017a, b; Miao et al. 2015a, b; Nie et al. 2014; Paniel and Baudart 2013; Persano et al. 2013; Sang et al. 2017; Shen et al. 2018a, b).

Based on exonuclease-assisted target recycling and magnetic aptamer–HRP–platinum composite probes, Miao presented an ultrasensitive chloramphenicol (CAP) detection with the detection limit of 0.0003 ng mL^{-1}, shown in Fig. 5.10 (Miao et al. 2015a, b). Based on HRP-assisted HCR and colorimetric assay, miR-155 was detected visually with a detection limit of 31.8 fM by Ying (Ying et al. 2017). Similarly, nucleic acid detection has also been realized based on HCR signal amplification and HRP–$ABTS^{2-}$ chromogenic system. The colorimetric assay system exhibits excellent sensitivity, and the detection limits have been calculated to be 5.2 fM (Lu et al. 2017).

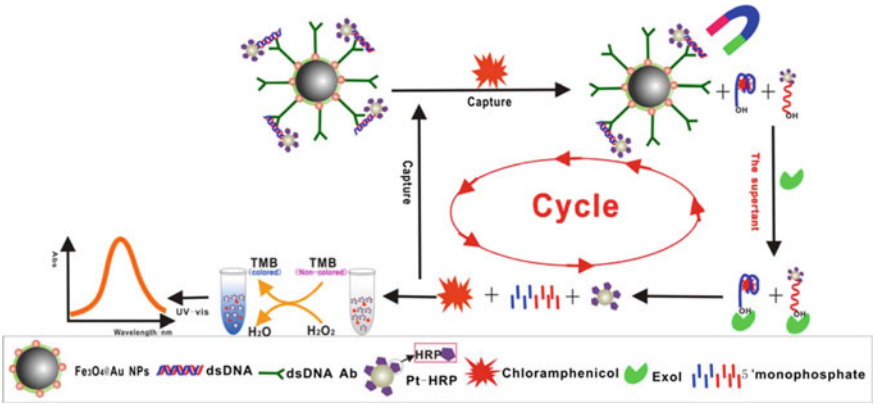

Fig. 5.10 Detection procedures and color development for chloramphenicol. Reproduced from Miao et al. (2015a, b) by permission of The Royal Society of Chemistry

5.3.2 Colorimetric Assay Based on Mimic HRP Catalyst

In recent years, many materials were explored to mimic natural HRP, such as hemin-containing complexes, iron oxide nanoparticles, and platinum nanoparticles. These HRP-like artificial enzymes have been widely used in tumor immunostaining and biomarker detection (Wei et al. 2017). G-quadruplex sequences bind hemin to form numerous peroxidase mimicking DNA enzymes, which could catalyze TMB or ABTS to reduce H_2O_2, causing substantially intensified color change of the probe solution.

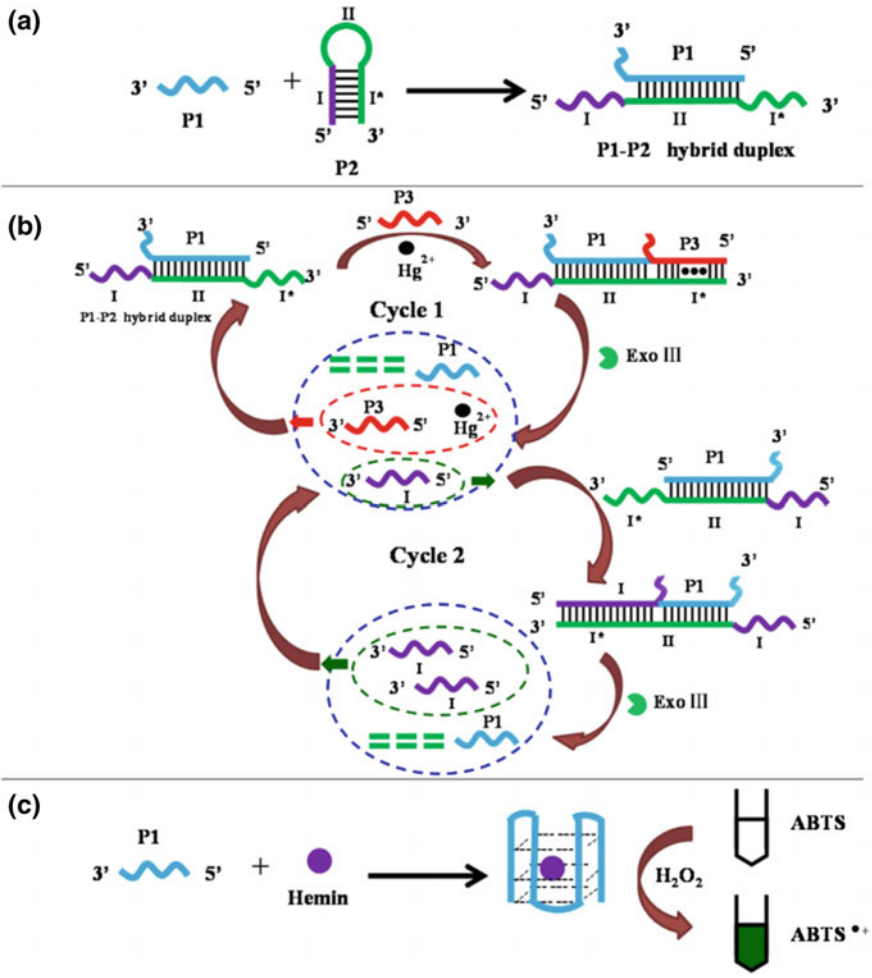

Fig. 5.11 Detection of Hg^{2+} based on dual-cycle target recycling strategy. Reprinted from Zhang et al. (2017). Copyright 2017, with permission from Elsevier

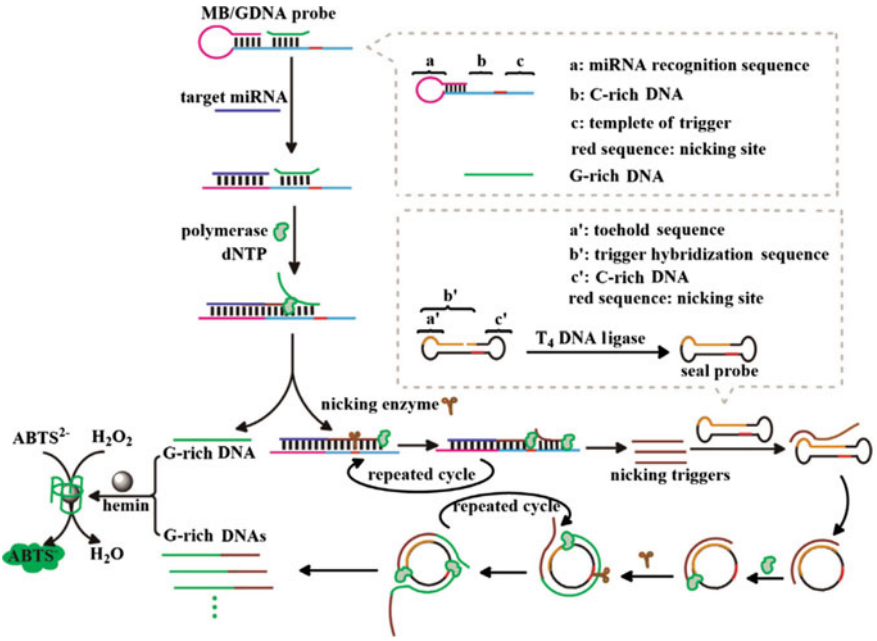

Fig. 5.12 Detection of miRNA based on nucleic acid amplification machine. Reprinted from Li et al. (2016a, b, c). Copyright 2016, with permission from Elsevier

As shown in Fig. 5.11, detection of Hg^{2+} is proposed based on recycling amplification strategy and hemin/G-quadruplex mimic HRP (Zhang et al. 2017), and similar work was also reported by Ren group (Ren et al. 2015), with the detection limit as low as pM. Based on dual-nicking enzyme signal amplification (NESA) coupled with target-activated split peroxidase, DNA enzyme detection of antibiotic was developed by Cui (Cui et al. 2018). This method exhibited excellent specificity and sensitivity toward kanamycin with a detection limit as low as 14.7 pM.

As mentioned previously, cancer-related miRNAs have been regarded as special biomarkers for tumor detections. As shown in Fig. 5.12, Li designed a colorimetric biosensing for miRNA (Li et al. 2016a, b, c). The amplification machine was composed of C-rich DNA-modified molecular beacon (MB), trigger template, polymerase and nicking enzyme, G-rich DNA (GDNA) probe, and a dumbbell-shaped amplification template. This strategy showed a high sensitivity in the range from 10 aM to 1.0 nM, which enabled successful visual analysis of trace amount of miRNA.

Based on mimic HRP system, Zhang described an isothermal colorimetric method for amplified detection of the CaMV 35S promoter sequence. It is based on target DNA-triggered unlabeled molecular beacon (UMB) termini binding, exonuclease III (Exo III)-assisted target recycling, and hemin/G-quadruplex (DNA enzyme) signal amplification (Zhang et al. 2018), shown in Fig. 5.13. DNA detection based on the target-induced formation of a three-way junction has been achieved. It has a 0.8 pM

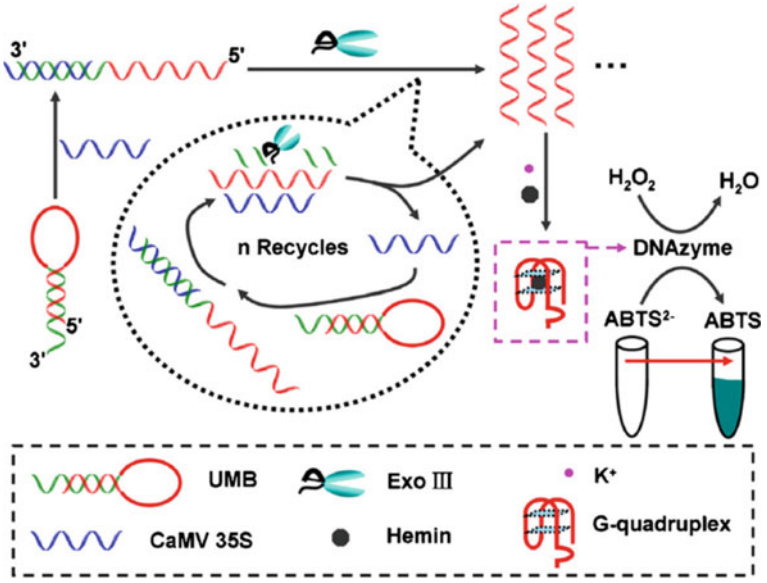

Fig. 5.13 Sensitive detection of DNA based on dual-signal amplification. Reprinted from Zhang et al. (2018), with kind permission from Springer Science + Business Media

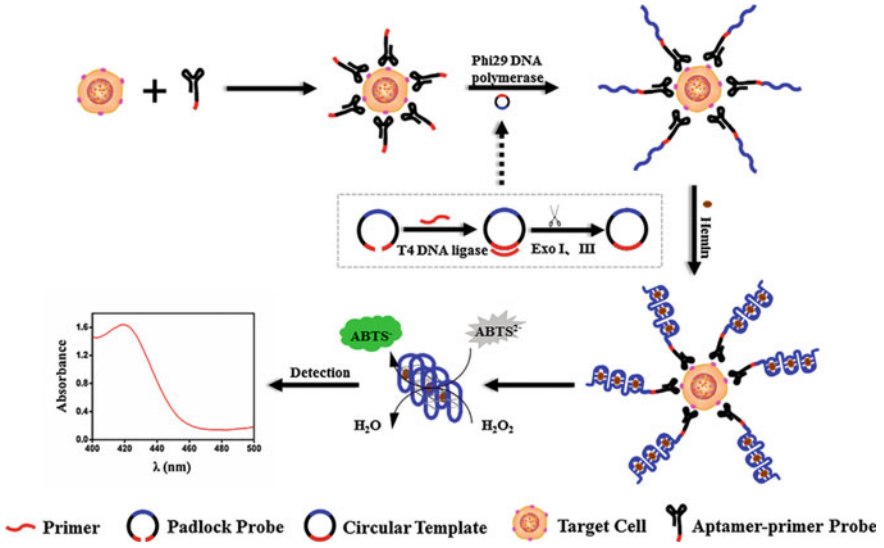

Fig. 5.14 Colorimetric assay of tumor cells by aptamer-induced RCA on cell surface. Reprinted from Xu et al. (2018a, b). Copyright 2018, with permission from Elsevier

detection limit and applied to the isothermal determination of target DNA with high selectivity (Wang et al. 2017).

Cell detection has also been detected based on aptamer-induced RCA on cell surface. As shown in Fig. 5.14, the designed colorimetric assay could distinguish as low as ten cancer cells in 10,000 times of benign cells mixture, showing very high sensitivity and selectivity (Xu et al. 2018a, b).

5.4 Colorimetric Assays Based on Other Indicators

Similar to AuNPs, silver nanoparticles are also used as color substrate in colorimetric assays (Chen et al. 2010). As shown in Fig. 5.15, high sensitively and selectively for the detection of Hg^{2+} were developed based on the silver ion catalysis to form colored $KMnO_4$, HCR and silver nanowire for signal amplification (Tang et al. 2015).

As shown in Fig. 5.16, a colorimetric aptasensor is presented for the determination of zearalenone (ZEN) based on the nontarget-induced aptamer walker, catalytic reaction of AuNPs, exonuclease III (Exo III) as a signal amplifier, and 4-nitrophenol as a colorimetric agent. The presented aptasensor was capable to detect ZEN in a

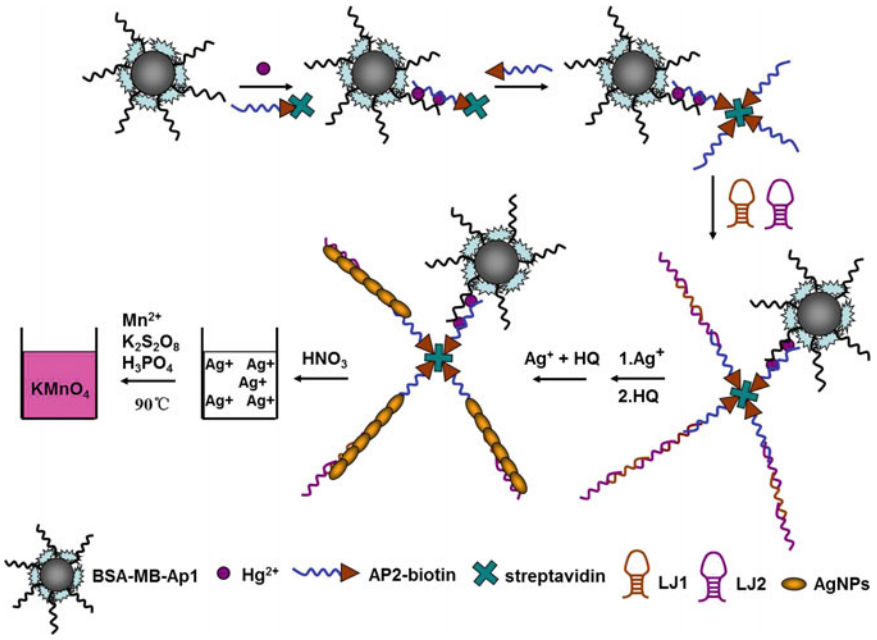

Fig. 5.15 Colorimetric sensor for Hg^{2+} based on HCR reaction and silver nanowire amplification. Reproduced from Tang et al. (2015) by permission of The Royal Society of Chemistry

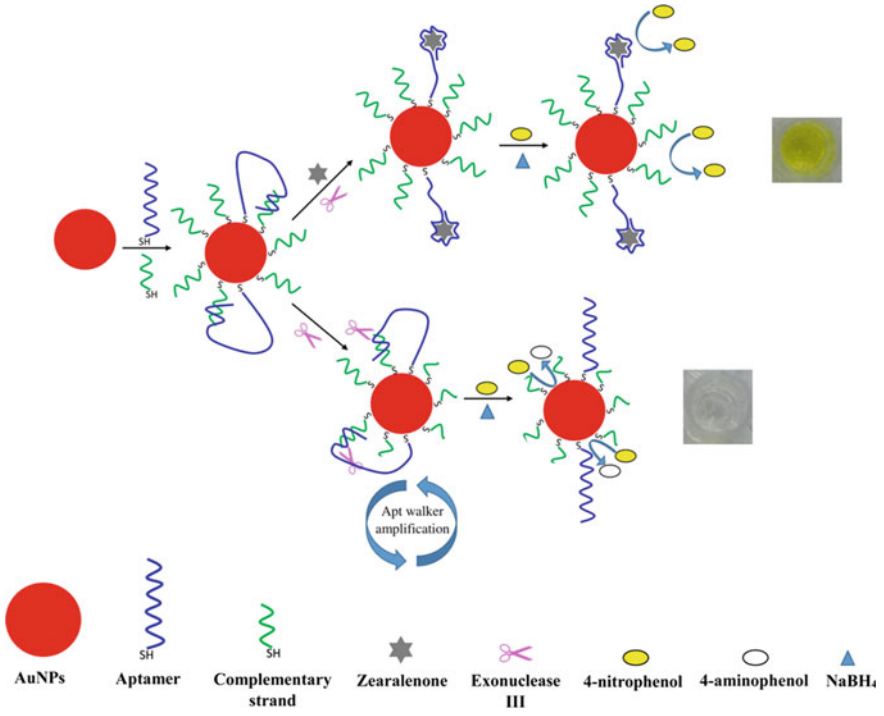

Fig. 5.16 Representation of the colorimetric aptasensor for the detection of ZEN based on the Exo III-assisted aptamer walker and catalytic reaction of AuNPs. Reprinted with the permission from Taghdisi et al. (2018). Copyright 2018 American Chemical Society

wide linear dynamic range, 20–80,000 ng L^{-1}, with a detection limit of 10 ng L^{-1} (Taghdisi et al. 2018).

By introducing acetylcholinesterase (AChE)-catalyzed hydrolysis of acetylcholine with the change solution (pH and phenol red as an indicator), Guo developed a pH-responsive colorimetric strategy. As shown in Fig. 5.17, this strategy showed a linear range from 50 pM to 50 nM with a detection limit of 38 pM (Guo et al. 2017). Additionally, Chen reported an upconversion fluorescent and colorimetric dual-readout assay for H_2O_2 as well as choline and acetylcholine chloride via enzyme-controlled cyclic signal amplification strategy. Based on the rapid H_2O_2/Fe^{2+}/OPD reaction, this method is flexible and time-saving, and the sensing assay can present fluorescent and colorimetric dual-readout signal, convincing the experimental results (Chen et al. 2018a, b). Based on RCA, Hamidi reported colorimetric method for monitoring of H5N1 and hydroxy naphthol blue (HNB) as a metal indicator. Pyrophosphate is produced via DNA polymerization and chelates the Mg^{2+} in the buffer solution based on RCA. This causes the solution color change. Based on this assay, H5N1 was linear in the concentration range from 0.16 to 1.20 pM with a detection limit of 28 fM (Hamidi and Ghourchian 2015).

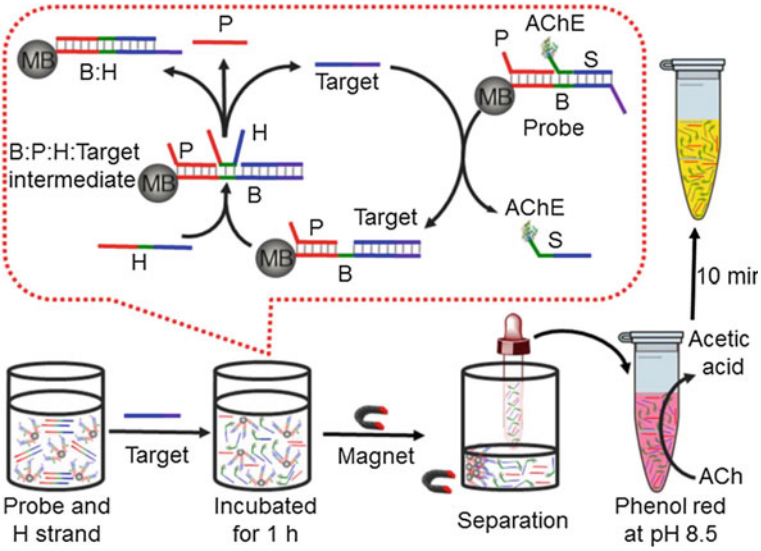

Fig. 5.17 Schematic diagram of the proposed pH-responsive colorimetric strategy for DNA detection sensitized with nonenzymatic cascade amplification. Reprinted from Guo et al. (2017). Copyright 2017, with permission from Elsevier

5.5 Conclusion

In this chapter, a series of colorimetric detections based on nucleic acid amplification methods are summarized and introduced during recent years. Given the significant merits of ultrahigh detection sensitivity, nucleic acid amplification has demonstrated as a powerful protocol for colorimetric assays. The chapter highlighted the colorimetric assays based on nucleotides amplification, which mainly included EAA, NEANA, LAMP, NASBA, PCR, RCA, SDA, and HCR. The colored substances usually employ Au nanoparticles, Ag nanoparticles, dyes, fluoresceins, ABTS, and TMB. The nucleic acid amplification strategy techniques in colorimetric assays and their future perspectives are also discussed. Additionally, colorimetric assays based on nucleic acid amplification techniques have been expanded to detect a wide range of targets, such as nucleic acids, proteins, and biological small molecules. With the development of ultrahigh detections, colorimetric assays based on dual and multi-amplifications would become promising in future.

References

Aktas GB, Skouridou V, Masip L (2015) Novel signal amplification approach for HRP-based colorimetric genosensors using DNA binding protein tags. Biosens Bioelectron 74:1005–1010

Armstrong P, Borovsky D, Shope RE et al (1995) Sensitive and specific colorimetric dot assay to detect eastern equine encephalomyelitis viral RNA in mosquitoes (diptera: culicidae) after polymerase chain reaction amplification. J Med Entomol 32:42–52

Bi S, Yan YM, Hao SY (2010) Colorimetric logic gates based on supramolecular DNAzyme structures. Angew Chem Int Ed 122:4540–4544

Chang CC, Chen CY, Chuang TL et al (2016) Aptamer-based colorimetric detection of proteins using a branched DNA cascade amplification strategy and unmodified gold nanoparticles. Biosens Bioelectron 78:200–205

Chen C, Luo M, Ye T et al (2015) Sensitive colorimetric detection of protein by gold nanoparticles and rolling circle amplification. Analyst 140:4515–4520

Chen J, Pan J, Chen S (2017) A naked-eye colorimetric sensor for Hg^{2+} monitoring with cascade signal amplification based on target-induced conjunction of split DNAzyme fragments. Chem Commun 53:10224–10227

Chen QH, Lu Y, Wan J, Wan J et al (2014) Colorimetric detection of hepatitis E virus based on reverse transcription loop mediated isothermal amplification (RT-LAMP) assay. J Virol Methods 197:29–33

Chen H, Lu Q, He K et al (2018a) A cyclic signal amplification strategy to fluorescence and colorimetric dual-readout assay for the detection of H_2O_2-related analytes and application to colorimetric logic gate. Sensor Actuat B-Chem 260:908–917

Chen YX, Huang KJ, Niu KX (2018b) Recent advances in signal amplification strategy based on oligonucleotide and nanomaterials for microRNA detection-a review. Biosens Bioelectron 99:612–624

Chen Z, He Y, Luo S et al (2010) Label-free colorimetric assay for biological thiols based on ssDNA/silver nanoparticle system by salt amplification. Analyst 135:1066–1069

Cui L, Ke G, Zhang WY et al (2011) A universal platform for sensitive and selective colorimetric DNA detection based on Exo III assisted signal amplification. Biosens Bioelectron 26:2796–2800

Cui X, Li R, Liu X et al (2018) Low-background and visual detection of antibiotic based on target-activated colorimetric split peroxidase DNAzyme coupled with dual nicking enzyme signal amplification. Anal Chim Acta 997:1–8

Du Y, Li B, Guo S et al (2011) G-Quadruplex-based DNAzyme for colorimetric detection of cocaine: using magnetic nanoparticles as the separation and amplification element. Analyst 136:493–497

Fu Z, Zhou X, Xing D (2013) Sensitive colorimetric detection of Listeria monocytogenes based on isothermal gene amplification and unmodified gold nanoparticles. Methods 64:260–266

Gao H, Gan N, Pan D et al (2015) A sensitive colorimetric aptasensor for chloramphenicol detection in fish and pork based on the amplification of a nano-peroxidase-polymer. Anal Methods 7:6528–6536

Gao XX, Jia YH, Yang JF et al (2013) Design of DNAzyme catalytic amplification-based biosensing platform for colorimetric detection of Lead (II). Chinese J Anal Chem 41:670–674

Geng Y, Wu J, Shao L et al (2014) Sensitive colorimetric biosensing for methylation analysis of p16/CDKN2 promoter with hyperbranched rolling circle amplification. Biosens Bioelectron 61:593–597

Gill P, Alvandi AH, Abdul-Tehrani H et al (2008) Colorimetric detection of Helicobacter pylori DNA using isothermal helicase-dependent amplification and gold nanoparticle probes. Diagn Microbiol Infect Dis 62:119–124

Gong X, Li J, Zhou W et al (2014) Target recycling amplification for label-free and sensitive colorimetric detection of adenosine triphosphate based on un-modified aptamers and DNAzymes. Anal Chim Acta 828:80–84

Goto M, Honda E, Ogura A et al (2009) Colorimetric detection of loop-mediated isothermal amplification reaction by using hydroxy naphthol blue. Biotechniques 46:167–172

Guo Y, Yang K, Sun J et al (2017) A pH-responsive colorimetric strategy for DNA detection by acetylcholinesterase catalyzed hydrolysis and cascade amplification. Biosens Bioelectron 94:651–656

Hamidi SV, Ghourchian H (2015) Colorimetric monitoring of rolling circle amplification for detection of H5N1 influenza virus using metal indicator. Biosens Bioelectron 72:121–126

Hu B, Guo J, Xu Y et al (2017) A sensitive colorimetric assay system for nucleic acid detection based on isothermal signal amplification technology. Anal Bioanal Chem 409:4819–4825

Huang Y, Chen J, Zhao S et al (2013) Label-free colorimetric aptasensor based on nicking enzyme assisted signal amplification and DNAzyme amplification for highly sensitive detection of protein. Anal Chem 85:4423–4430

Ke R, Zorzet A, Goransson J et al (2011) Colorimetric nucleic acid testing assay for RNA virus detection based on circle-to-circle amplification of padlock probes. J Clin Microbiol 49:4279–4285

Kumvongpin R, Jearanaikool P, Wilailuckana C et al (2016) High sensitivity, loop-mediated isothermal amplification combined with colorimetric gold-nanoparticle probes for visual detection of high risk human papillomavirus genotypes 16 and 18. J Virol Methods 234:90–95

Lai W, Wei Q, Xu M et al (2017) Enzyme-controlled dissolution of MnO_2 nanoflakes with enzyme cascade amplification for colorimetric immunoassay. Biosens Bioelectron 89:645–651

Li J, Fu HE, Wu LJ et al (2012) General colorimetric detection of proteins and small molecules based on cyclic enzymatic signal amplification and hairpin aptamer probe. Anal Chem 84:5309–5315

Li J, Gao Z, Ye H et al (2017a) A non-enzyme cascade amplification strategy for colorimetric assay of disease biomarkers. Chem Commun 53:9055–9058

Li J, Jia Y, Zheng J et al (2013) Aptamer degradation inhibition combined with DNAzyme cascade-based signal amplification for colorimetric detection of proteins. Chem Commun 49:6137–6139

Li D, Cheng W, Yan Y et al (2016a) A colorimetric biosensor for detection of attomolar microRNA with a functional nucleic acid-based amplification machine. Talanta 146:470–476

Li RD, Yin BC, Ye BC (2016b) Ultrasensitive, colorimetric detection of microRNAs based on isothermal exponential amplification reaction-assisted gold nanoparticle amplification. Biosens Bioelectron 86:1011–1016

Li S, Lai J, Qi L et al (2016c) Sensitive and selective colorimetric detection of Hg^{2+} by a Hg^{2+} induced dual signal amplification strategy based on cascade-type catalytic reactions. Analyst 141:2362–2366

Li ZM, Zhong ZH, Liang RP et al (2017b) The colorimetric assay of DNA methyltransferase activity based on strand displacement amplification. Sensor Actuat B-Chem 238:626–632

Liang D, You W, Yu Y et al (2015) A cascade signal amplification strategy for ultrasensitive colorimetric detection of BRCA1 gene. RSC Adv 5:27571–27575

Liang K, Zhai S, Zhang Z et al (2014) Ultrasensitive colorimetric carcinoembryonic antigen biosensor based on hyperbranched rolling circle amplification. Analyst 139:4330–4334

Liu H, Chen Y, Song C et al (2018a) Novel and label-free colorimetric detection of radon using AuNPs and lead(II)-induced GR5 DNAzyme-based amplification strategy. Anal Bioanal Chem 410:4227–4234

Liu P, Yang X, Sun S et al (2013) Enzyme-free colorimetric detection of DNA by using gold nanoparticles and hybridization chain reaction amplification. Anal Chem 85:7689–7695

Liu S, Leng X, Wang X et al (2018b) Enzyme-free colorimetric assay for mercury(II) using DNA conjugated to gold nanoparticles and strand displacement amplification. Microchim Acta 184:1969–1976

Liu X, Chen M, Hou T et al (2014) Label-free colorimetric assay for base excision repair enzyme activity based on nicking enzyme assisted signal amplification. Biosens Bioelectron 54:598–602

Liu Y, Xie J, Zhang Z et al (2016a) An ultrasensitive colorimetric strategy for protein O-GlcNAcylation detection via copper deposition-enabled nonenzymatic signal amplification. RSC Adv 6:89484–89491

Liu Z, Xia X, Yang C et al (2016b) Colorimetric detection of Maize chlorotic mottle virus by reverse transcription loop-mediated isothermal amplification (RT-LAMP) with hydroxynapthol blue dye. RSC Adv 6:73–78

LHcheM (2015) Structures of HRP substrates. Wikimedia Commons, Chemical Structures
Lu S, Hu T, Wang S et al (2017) Ultra-sensitive colorimetric assay system based on the hybridization chain reaction-triggered enzyme cascade amplification. ACS Appl Mater Interfaces 9:167–175
Luan Q, Gan N, Cao Y et al (2017a) Mimicking an enzyme-based colorimetric aptasensor for antibiotic residue detection in milk combining magnetic loop-DNA probes and CHA-assisted target recycling amplification. J Agric Food Chem 65:5731–5740
Luan Q, Miao Y, Gan N et al (2017b) A POCT colorimetric aptasensor for streptomycin detection using porous silica beads-enzyme linked polymer aptamer probes and exonuclease-assisted target recycling for signal amplification. Sensor Actuat B-Chem 251:349–358
Luo Y, Zhang Y, Xu L et al (2012) Colorimetric sensing of trace UO_2^{2+} by using nanogold-seeded nucleation amplification and label-free DNAzyme cleavage reaction. Analyst 137:1866–1871
Ma C, Wang W, Li Z et al (2012) Simple colorimetric DNA detection based on hairpin assembly reaction and target-catalytic circuits for signal amplification. Anal Biochem 429:99–102
Ma C, Wang W, Mulchandani A et al (2014) A simple colorimetric DNA detection by target-induced hybridization chain reaction for isothermal signal amplification. Anal Biochem 457:19–23
Miao Y, Gan N, Li T et al (2015a) A colorimetric aptasensor for chloramphenicol in fish based on double-stranded DNA antibody labeled enzyme-linked polymer nanotracers for signal amplification. Sensor Actuat B-Chem 220:679–687
Miao Y, Gan N, Ren HX et al (2015b) A triple-amplification colorimetric assay for antibiotics based on magnetic aptamer-enzyme co-immobilized platinum nanoprobes and exonuclease-assisted target recycling. Analyst 140:7663–7671
Nam JM, Wise AR, Groves JT (2005) Colorimetric bio-barcode amplification assay for cytokines. Anal Chem 77:6985–6988
Niazi A, Jorjani ON, Nikbakht H et al (2013) A nanodiagnostic colorimetric assay for 18S rRNA of Leishmania pathogens using nucleic acid sequence-based amplification and gold nanorods. Mol Diagn Ther 17:363–370
Nie J, Zhang DW, Tie C et al (2014) G-quadruplex based two-stage isothermal exponential amplification reaction for label-free DNA colorimetric detection. Biosens Bioelectron 56:237–242
Paniel N, Baudart J (2013) Colorimetric and electrochemical genosensors for the detection of Escherichia coli DNA without amplification in seawater. Talanta 115:133–142
Persano S, Guevara ML, Wolfram J et al (2016) Label-free isothermal amplification assay for specific and highly sensitive colorimetric miRNA detection. ACS Omega 1:448–455
Persano S, Valentini P, Kim JH et al (2013) Colorimetric detection of human papilloma virus by double isothermal amplification. Chem Commun 49:10605–10607
Ren W, Zhang Y, Huang WT et al (2015) Label-free colorimetric detection of Hg^{2+} based on Hg^{2+}-triggered exonuclease III-assisted target recycling and DNAzyme amplification. Biosens Bioelectron 68:266–271
Sang Y, Xu Y, Xu L et al (2017) Colorimetric and visual determination of microRNA via cycling signal amplification using T7 exonuclease. Microchim Acta 184:2465–2471
Shao F, Jiao L, Miao L et al (2017) A pH Indicator-linked Immunosorbent assay following direct amplification strategy for colorimetric detection of protein biomarkers. Biosens Bioelectron 90:1–5
Shen C, Shen B, Mo F et al (2018a) High-sensitive colorimetric biosensing of PIK3CA gene mutation based on mismatched ligation-triggered cascade strand displacement amplification. Sensor Actuat B-Chem 273:377–383
Shen ZF, Li F, Jiang YF et al (2018b) Palindromic Molecule Beacon-Based Cascade Amplification for Colorimetric Detection of Cancer Genes. Anal Chem 90:3335–3340
Shi HY, Yang L, Zhou XY et al (2016) A gold nanoparticle-based colorimetric strategy coupled to duplex-specific nuclease signal amplification for the determination of microRNA. Microchim Acta 184:525–531
Suebsing R, Prombun P, Srisala J et al (2013a) Loop-mediated isothermal amplification combined with colorimetric nanogold for detection of the microsporidian Enterocytozoon hepatopenaei in penaeid shrimp. J Appl Microbiol 114:1254–1263

Suebsing R, Prombun P, Kiatpathomchai W (2013b) Reverse transcription loop-mediated isothermal amplification (RT-LAMP) combined with colorimetric gold nanoparticle (AuNP) probe assay for visual detection of Penaeus vannamei nodavirus (PvNV). Lett Appl Microbiol 56:428–435

Taghdisi SM, Danesh NM, Ramezani M et al (2018) Novel colorimetric aptasensor for zearalenone detection based on nontarget-induced aptamer walker, gold nanoparticles, and exonuclease-assisted recycling amplification. ACS Appl Mater Interfaces 10:12504–12509

Tan E, Erwin B, Dames S, Voelkerding K et al (2007) Isothermal DNA amplification with gold nanosphere-based visual colorimetric readout for herpes simplex vrus detection. Clin Chem 53:2017–2020

Tan E, Wong J, Nguyen D et al (2005) Isothermal DNA amplification coupled with DNA nanosphere-based colorimetric detection. Anal Chem 77:7984–7992

Tang L, Liu Y, Ali MM et al (2012) Colorimetric and ultrasensitive bioassay based on a dual-amplification system using aptamer and DNAzyme. Anal Chem 84:4711–4717

Tang S, Tong P, Wang M et al (2015) A novel colorimetric sensor for Hg^{2+} based on hybridization chain reaction and silver nanowire amplification. Chem Commun 51:15043–15046

Wang P, Jin B, Xing Y et al (2014) Rolling circle amplification immunoassay combined with gold nanoparticle aggregates for colorimetric detection of protein. J Nanosci Nanotechno 14:5662–5668

Wang Q, Yang XH, Yang XH et al (2015a) Colorimetric detection of mercury ion based on unmodified gold nanoparticles and target-triggered hybridization chain reaction amplification. Spectrochim Acta A: Mol Biomol Spectrosc 136:283–287

Wang Q, Yang X, Yang X et al (2015b) An enzyme-free colorimetric assay using hybridization chain reaction amplification and split aptamers. Analyst 140:7657–7662

Wang Q, Li RD, Yin BC et al (2015c) Colorimetric detection of sequence-specific microRNA based on duplex-specific nuclease-assisted nanoparticle amplification. Analyst 140:6306–6312

Wang X, Liu W, Yin B et al (2017) An isothermal strand displacement amplification strategy for nucleic acids using junction forming probes and colorimetric detection. Microchim Acta 184:1603–1610

Watthanapanpituck K, Kiatpathomchai W, Chu E et al (2014) Identification of human DNA in forensic evidence by loop-mediated isothermal amplification combined with a colorimetric gold nanoparticle hybridization probe. Int J Legal Med 128:923–931

Wei X, Xu H, Li W et al (2017) Colorimetric visualization of Cu^{2+} based on Cu^{2+} -catalyzed reaction and the signal amplification induced by K^{+}-aptamer-Cu^{2+} complex. Sensor Actuat B-Chem 241:498–503

Wong JK, Yip SP, Lee TM (2014) Ultrasensitive and closed-tube colorimetric loop-mediated isothermal amplification assay using carboxyl-modified gold nanoparticles. Small 10:1495–1499

Xia N, Liu K, Zhou Y et al (2017) Sensitive detection of microRNAs based on the conversion of colorimetric assay into electrochemical analysis with duplex-specific nuclease-assisted signal amplification. Int J Nanomedicine 12:5013–5022

Xie XJ, Xu W, Liu XG (2012) Improving colorimetric assays through protein enzyme-assisted gold nanoparticle amplification. Accounts Chem Res 45:1511–1520

Xing Y, Wang P, Zang Y et al (2013) A colorimetric method for H1N1 DNA detection using rolling circle amplification. Analyst 138:3457–3462

Xu C, Lan L, Yao Y et al (2018a) An unmodified gold nanorods-based DNA colorimetric biosensor with enzyme-free hybridization chain reaction amplification. Sensor Actuat B-Chem 273:642–648

Xu L, Jiang Z, Mu Y et al (2018b) Colorimetric assay of rare disseminated tumor cells in real sample by aptamer-induced rolling circle amplification on cell surface. Sensor Actuat B-Chem 259:596–603

Xu W, Xie X, Li D et al (2012) Ultrasensitive colorimetric DNA detection using a combination of rolling circle amplification and nicking endonuclease-assisted nanoparticle amplification (NEANA). Small 8:1846–1850

Xu W, Xue X, Li T et al (2009) Ultrasensitive and selective colorimetric DNA detection by nicking endonuclease assisted nanoparticle amplification. Angew Chem Int Ed 48:6849–6852
Yang X, Gao Z (2014) Gold nanoparticle-based exonuclease III signal amplification for highly sensitive colorimetric detection of folate receptor. Nanoscale 6:3055–3058
Ying N, Sun T, Chen Z et al (2017) Colorimetric detection of microRNA based hybridization chain reaction for signal amplification and enzyme for visualization. Anal Biochem 528:7–12
Yu T, Dai PP, Xu JJ et al (2016) Highly Sensitive Colorimetric Cancer Cell Detection Based on Dual Signal Amplification. ACS Appl Mater Interfaces 8:4434–4441
Yun W, Wu H, Liu X et al (2018) Ultra-sensitive fluorescent and colorimetric detection of $UO2^{2+}$ based on dual enzyme-free amplification strategies. Sensor Actuat B-Chem 255:1920–1926
Zhang H, Li F, Chen H et al (2015) AuNPs colorimetric sensor for detecting platelet-derived growth factor-BB based on isothermal target-triggering strand displacement amplification. Sensor Actuat B-Chem 207:748–755
Zhang H, Wang K, Bu S et al (2018) Colorimetric detection of microRNA based on DNAzyme and nuclease-assisted catalytic hairpin assembly signal amplification. Mol Cell Probes 38:13–18
Zhang X, Xiao K, Cheng L et al (2014) Visual and highly sensitive detection of cancer cells by a colorimetric aptasensor based on cell-triggered cyclic enzymatic signal amplification. Anal Chem 86:5567–5572
Zhang Y, Hu J, Zhang CY (2012) Sensitive detection of transcription factors by isothermal exponential amplification-based colorimetric assay. Anal Chem 84:9544–9549
Zhang Z, Xie J, Yu J et al (2017) A novel colorimetric immunoassay strategy using iron(iii) oxide magnetic nanoparticles as a label for signal generation and amplification. J Mater Chem B 51454-1460
Zhou C, Mu Y, M-c Yang et al (2013a) Gold nanoparticles based colorimetric detection of target DNA after loop-mediated isothermal amplification. Chem Res Chin Univ 29:424–428
Zhou Z, Wei W, Zhang Y et al (2013b) DNA-responsive disassembly of AuNP aggregates: influence of nonbase-paired regions and colorimetric DNA detection by exonuclease III aided amplification. J Mater Chem B 1:2851–2858
Zou B, Cao X, Wu H et al (2015) Sensitive and specific colorimetric DNA detection by invasive reaction coupled with nicking endonuclease-assisted nanoparticles amplification. Biosens Bioelectron 66:50–54
Zou L, Li X, Li T et al (2018) Hybridization chain reaction and DNAzyme-based dual signal amplification strategy for sensitive colorimetric sensing of acetylcholinesterase activity and inhibitor screening in rat blood. Sensor Actuat B-Chem 267:272–278

Chapter 6
Nucleic Acid Amplification Strategies in Surface Plasmon Resonance Technologies

Xueming Li

Abstract Surface plasmon resonance (SPR) is a real-time and label-free technology for molecular interactions, chemical detection, and immunoassays. In this chapter, the application of nucleic acid amplification strategies, such as PCR, HCR, RCA, and SDA, in SPR technologies was summarized, providing an insight into the nucleic acid amplification strategies in SPR technologies.

6.1 Introduction

SPR-based biosensors are very powerful tools for real-time and label-free study of interactions between various biological and chemical analytes and have been widely applied in therapeutics, pharmacy, food safety, environmental monitoring, and homeland security (Wijaya et al. 2011; Homola 2008). The surface plasmons were first observed by R. W. Wood in 1902, when anomalous narrow dark bands were discovered in the diffraction spectrum of a metal grating illuminated with polychromatic light (Wood 1902). This anomaly was completely explained in 1968, when Otto (Otto 1968) and the same year Kretschmann (Kretschmann and Raether 1968), reported the optical excitation of surface plasmons by attenuated total reflection. In 1983, Liedberg et al. demonstrated the application of SPR-based sensors in gas detection and biosensing (Fig. 6.1) (Liedberg et al. 1983). Since then, the enormous potential of SPR sensor technology for detecting chemical and biological substances has received increasing attention from the scientific community. Today, SPR-based biosensors are used more and more not only in gas sensing, but in many other important applications, such as food safety, biology, and medical diagnostics. And numerous research papers have been published about the exploitation of SPR biosensors.

Biosensor is an analytical device, which composed of biological elements such as tissues, microorganisms, organelles, cell receptors, enzymes, antibodies, and physicochemical sensors. A physicochemical change, which can be detected by the trans-

X. Li (✉)
Shandong Provincial Key Laboratory of Detection Technology for Tumour Markers, College of Chemistry and Chemical Engineering, Linyi University, Linyi 276005, People's Republic of China
e-mail: lixueming1988@163.com

S. Zhang et al. (eds.), *Nucleic Acid Amplification Strategies for Biosensing, Bioimaging and Biomedicine*, https://doi.org/10.1007/978-981-13-7044-1_6

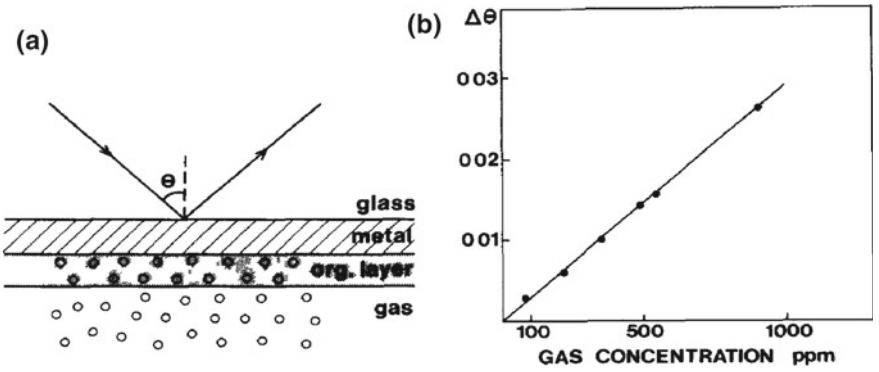

Fig. 6.1 **a** Schematic view of the layer system used in the gas sensing application. **b** Measured response to halothane gas exposure in the ppm range. Reprinted from Liedberg et al. (1983) Copyright (1983), with permission from Elsevier

ducer, is produced by the biological element when it specifically interacts with the target analyte. The transducer transforms the physicochemical change to an analog electronic signal which is relevant to the amount or concentration of the specific analyte (Tudos and Schasfoort 2008; Saha et al. 2012). The biosensor based on SPR technology is a type of optical refractometer, by which the change of the refractive index of the medium resulting from the binding and dissociation of the analyte molecules on the SPR sensor surface can be measured (Zeng et al. 2014).

6.2 Type of Surface Plasmon resonance

Surface plasmons (SPs) are coherent oscillations of free electrons at the boundaries between metal and dielectric which are often categorized into two classes: propagating surface plasmons (PSPs) and localized surface plasmons (LSPs). PSPs can be excited on the metallic films which have several approaches as the Kretschman and Otto prism coupler, optical waveguides coupler, diffraction gratings, and optical fiber coupler, whereas LSPs can be excited on metallic nanoparticles, which both can induce a strong enhancement of electromagnetic filed in the near-field region (resonance amplification), leading to an extensive application in surface enhanced raman scattering (SERS), fluorescence enhancement, refractive index (RI) measurement, biomolecular interaction detection, and so on (Chen and Ming 2012).

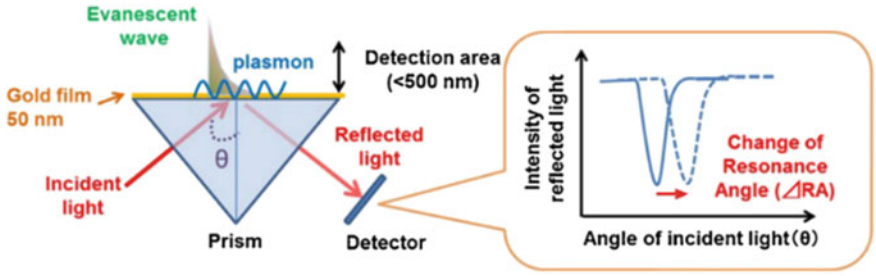

Fig. 6.2 Schematic description of conventional SPR sensor (Yanase et al. 2014)

6.2.1 Conventional SPR

In a conventional prism based SPR, a flat gold film is illuminated at a steep angle in total internal reflection mode, whereas the gold films can initiate SPR directly via polarized light. As shown in Fig. 6.2, the incident light is introduced to and reflected by the gold film through a prism. The intensity of the reflected light will change with the angle of the incident light and monitored by the detector. At a certain angle of the incident light, the intensity of the reflected light has a maximum loss, at which the light will excite surface plasmon resonance. The angle is called resonance angle or SPR angle. The adsorption of the accumulated mass, such as proteins or nucleic acids, will result in the changing of the refractive index of the media near the metal surface which will lead to the shift of the SPR angle (Yanase et al. 2014). The methodology based on SPR technology requires no labels for detection preventing the disruptive chemistry modification for labeling (Linman and Cheng 2009). For a more comprehensive description of SPR theory, there are a number of reviews available (Hinman et al. 2018; Linman et al. 2010; Singh 2016).

6.2.2 SPR Imaging

Generally, the standard SPR biosensor instrument has 1–4 flow cells or channels on a single sensor chip which limits its application in high-throughput screening and multiplex analysis. To overcome this limitation, an excellent alternative method is the combination of SPR biosensor with arrays. SPR imaging (SPRi), a modified version of SPR design, has been developed, which can measure hundreds or thousands of samples simultaneously. An array is prepared on the SPR sensor chip, and the whole of the chip can be visualized via a video CCD camera through a label-free approach (Scarano et al. 2010). Interacting with the specific analyte, each active site (spot) of the array on the chip provides SPR signal information simultaneously, where the data can be collected in a fixed angle/angle scanning/wavelength scanning format. Detailed information of the biomolecular interactions in the array, such as the affinity

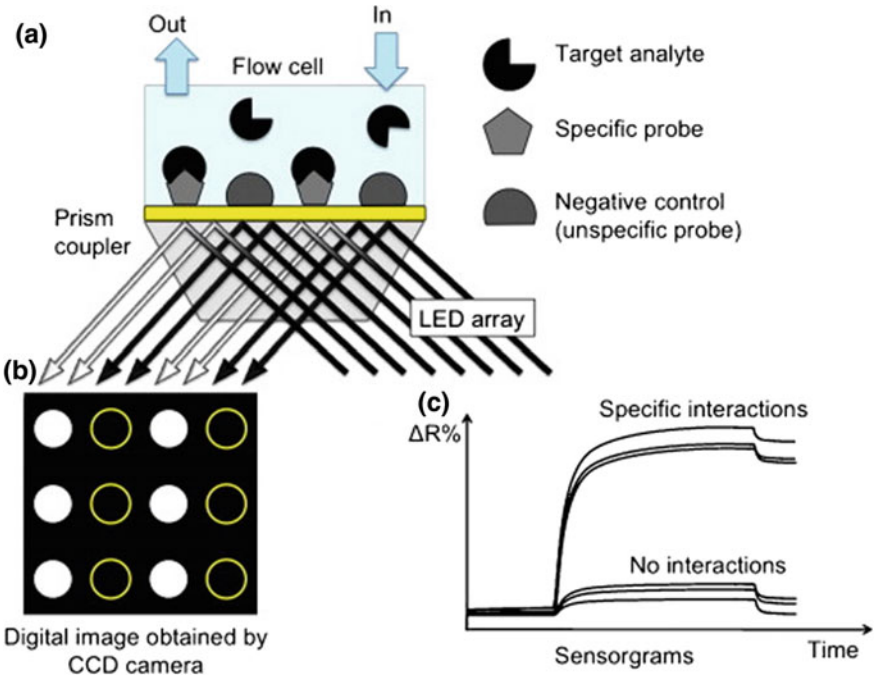

Fig. 6.3 General principle of SPRi. Reprinted from Scarano et al. (2010) Copyright (2010), with permission from Elsevier

and kinetic data, can be provided simultaneously. SPRi is faster and consumes lesser reagent than conventional techniques, providing a robust and sensitive manner for high-throughput screening of biomolecular interactions (Nguyen et al. 2015; Scarano et al. 2010) (Fig. 6.3).

6.2.3 Localized Surface Plasmon Resonance (LSPR)

Localized surface plasmon resonance (LSPR) is another optical phenomenon type of surface plasmon resonance. Without the metal film and the prism, the LSPR is generated by light near the conductive nanoparticles (NPs) or nanowires, the size of the which are smaller than the wavelength of the incident light. The interaction between the incident light and the surface electrons of the metal nanostructure produces the resonance of the localized plasmon. During the interaction, a portion of the incident light was absorbed and another portion was scattered in different directions. When the LSPR excited, the intensity of the absorption and scattering is dramatically enhanced and correlated with the composition, size, and shape of the

NPs as well as on the refractive index of the surrounding dielectric medium (Willets and Van Duyne 2007). Typically, the materials used for plasmonic applications are noble metals, such as gold or silver, which exhibit LSPR during the visible range of the spectrum. Among them, gold is preferred for biological applications due to its inert nature and biocompatibility, and thiol–gold association for immobilization of biomolecules (Mayer and Hafner 2011).

6.3 Nucleic Acid Amplification Strategies in SPR Technologies

Generally, the low signal intensity of the SPR assays severely impedes their widespread applications in disease diagnostics, especially in the high-sensitive and high-selective detection of the trace amount of targets in complex biological samples. To enhance the signal intensity and obtain efficient SPR-based assays, the development of amplification strategies is a straightforward and efficient way. Most of the present strategies are based on the nanomaterials, such as Au, Ag, SiO_2, magnetic or carbon-based nanoparticle, nanorod, nanoflower, or nanosheet. There are a number of publications about the nanomaterial-enhanced SPR sensors (Lou et al. 2017). Among these nanomaterials, Au NPs are one of the mostly and extensively used for the enhancement of SPR signals through the electronic coupling interaction between the localized surface plasmon of the Au NPs and the surface plasmon wave associated with the SPR gold film (Springer et al. 2014). For example, the amplification strategies for SPR assays using secondary antibodies labeled with Au NPs (Huang et al. 2005) aggregation of a network of Au NPs, Au NPs–polymer growth, and DNA-functionalized Au NPs amplification all have demonstrated the enhancement of the SPR signal.

Nevertheless, the signal enhancement can be further improved by combining the novel and powerful nucleic acid amplification strategies, such as PCR, HCR, RCA, and SDA amplification (Zhao et al. 2008; Bi et al. 2017; Zhou et al. 2018). There have been some reviews summarized the nanomaterial-based amplification strategies for SPR assays (Zhang et al. 2017; Fong and Yung 2013; Šípová and Homola 2013). However, a systematical and comprehensive review of the nucleic acid amplification strategies for SPR assays is needed. In this chapter, the application of nucleic acid amplification strategies in SPR technologies was summarized, providing an insight into the nucleic acid amplification strategies in surface plasmon resonance technologies.

6.3.1 Rolling Circle Amplification (RCA)

RCA, with unique characteristics, such as mild reaction conditions, ease of operation, high efficiency, excellent sensitivity, and specificity, has been attracting much attention as an advanced molecular amplification technique. In RCA reaction, the primer can be amplified isothermally by a circular template in the presence of certain DNA polymerases, producing a long single-stranded DNA. The thousands of tandem repeats of the RCA product, as the detection sites, can hybridize with a great deal of complementary DNA labeled with signal molecules to enhance the signals. The RCA strategies have been widely applied to the detection of various target molecules by coupling with electrochemistry, chemiluminescence, fluorescence, surface-enhanced Raman spectroscopy, colorimetry, and SPR (Ali et al. 2014).

Recently, Shusheng Zhang et al. combined with RCA and bio-bar-coded Au NP enhancement for ultrasensitive detection of the human thrombin using a SPR aptasensor. The sensor platform exhibited a broad dynamic range, excellent selectivity, and ultrahigh sensitivity. The assay platform is represented in Fig. 6.4, where the sensor surface was initially modified with the hairpin aptamer probe and mercaptohexanol (MCH) through an Au–S affinity binding. A hairpin structure was used to partially cage the primary sequence of the thrombin aptamer to reduce the nonspecific binding. When the thrombin was introduced to the sensor surface, the interaction of the thrombin and the aptamer opened the hairpin structure and a stable thrombin–aptamer complex was formed. The aptamer–primer complex, in which the secondary aptamer for thrombin was linked with a RCA primer, was extended through the RCA reaction producing a linear sequence with thousands of tandem repeats. Then the RCA products were introduced onto the SPR sensor surface and bound to the immobilized thrombin through the interaction of the secondary aptamer and the thrombin, in a classic sandwich assay format. Finally, a large amount of bio-bar-coded Au NPs were introduced onto sensor surface and assembled on the linear RCA products for the enhancement of the SPR signals by the increase of the surface mass and the refractive index of clustered Au NP conjugates. The detection limit was as low as 0.78 aM, which was almost 9 orders of magnitude lower compared with the direct SPR detection. Furthermore, the SPR sensor surface could be regenerated by 1 M HCl for the reusability of the sensor chip (He et al. 2014a).

6.3.2 Polymerase Chain Reaction (PCR)

PCR amplification is useful technology in molecular biology to amplify DNA across several orders of magnitude, generating thousands to millions of copies of a particular DNA sequence. This strategy is very useful for the detection of diseases caused by genetic factors. Generally, the detection of the PCR product is carried out using electrophoresis, in which a carcinogenic chemical such as an ethidium bromide is used as the developing agent (Fakruddin et al. 2013). Although this method is simple

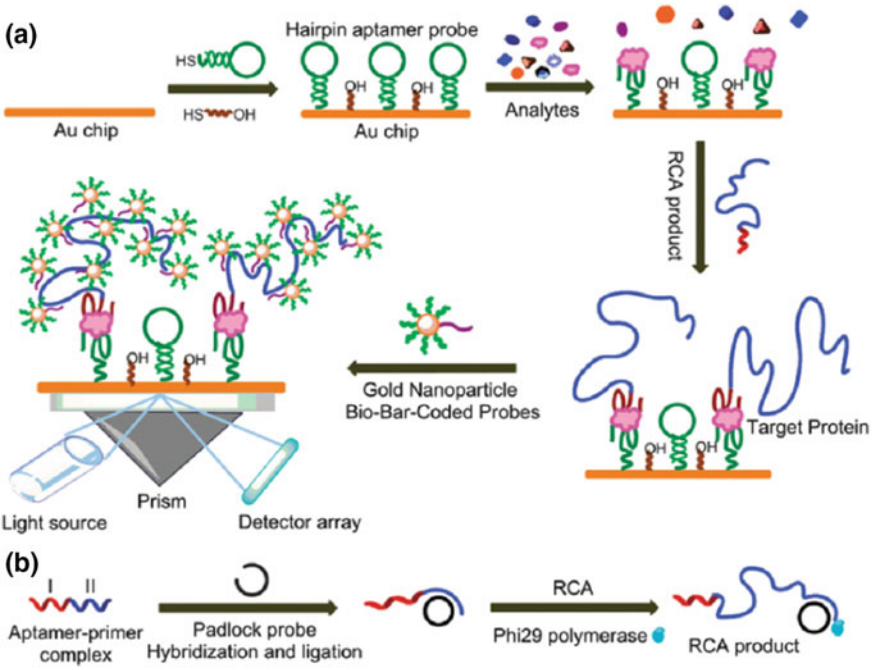

Fig. 6.4 Illustration of the SPR assay for protein detection using signal amplification by aptamer-based RCA and bio-bar-coded aunp enhancement. Reproduced from He et al. (2014a) with permission from The Royal Society of Chemistry

and effective to detect the PCR products, it cannot determine the sequence of the product DNA is the same as expected. Be aimed at hereat, Isao Karube demonstrated an asymmetric PCR strategy for DNA detection using SPR sensor. The target DNA sequence was amplified through asymmetric PCR, producing the PCR product with a single-stranded probe binding site, located in the 3′-terminus. A flow injection SPR sensor was used for the detection of the PCR product, by which the formation of intra- and intermolecular complexes was avoided (Kai et al. 1999). Although PCR can provide high sensitivity of detection, the highly precise temperature cycling, complex sample preparation, and strict laboratory conditions impede its widespread use for various analysis.

6.3.3 Hybridization Chain Reaction (HCR)

HCR is another type of nucleic acid amplification reaction triggered by a target DNA fragment, in which two stable species of DNA hairpins, as the monomers, self-assemble into complex structures through a cascade of hybridization events.

The HCR product, which is a type of nicked double helices analogous to alternating copolymers, can be functionalized act as an amplifying transducer for biosensing applications. Without the participation of enzymes, this strategy avoids the limitation of the thermostability of enzymes and the specific recognition sites for nicking endonucleases (Bi et al. 2017).

Normally, the detection of low molecular weight chemical and biological analytes under extremely dilute conditions is one of the main challenges for all electrical, mechanical, and optical sensors. SPR sensors have the unique ability for real-time detection of the molecular binding events. However, the sensitivities of SPR sensors are insufficient to detect trace amounts of small molecular weight molecules due to the extremely low signal intensity of small molecules. Therefore, signal amplification strategies are necessary for more sensitive detection of them. Adenosine triphosphate (ATP, 507 Da) plays fundamental roles in the regulation and integration of cellular processes and has also been used as substrate for cell viability and cell injury. Xuemei Li et al. developed a SPR detection system coupled with HCR for amplified detection of DNA and ATP with high sensitivity. Figure 6.5 represents the HCR-based SPR assay for ATP detections. The magnetic beads (MB) were modified with the ATP aptamer S_1, which partly hybridized with the trigger DNA S_2. In the presence of ATP, the trigger DNA was released from the MB due to the formation of the complex structure between ATP and the aptamer. After magnetic separation, the released trigger DNA S_2 was introduced onto the SPR sensor chip surface and hybridized with the capture DNA. The unpaired fragment of the trigger DNA worked as a trigger to initiate the linear assembly of Fc-modified hairpin H_1 and H_2 through HCR onto the SPR sensor surface. The assemblies of the large amount of Fc-modified H_1 and H_2 significantly enhance the SPR signals by increasing the refractive index of the surface. For DNA detection, the trigger DNA S_2 would work as the analyte, capture by the capture DNA S_3, and trigger the HCR event. The detection limit was 0.3 fM for DNA detection, which is 6 orders lower than a LSPR amplified with gold nanoparticles (Spadavecchia et al. 2013) and 0.48 nM for ATP detection. The authors also applied the HCR-based SPR system, with high sensitivity and selectivity, to ATP analysis in complicated biological samples, including human serum and lysates of HeLa cells and K562 leukemia cells. In addition, the biosensor surface can be reused through the regeneration step by the injection of 1 M HCl to remove the hybridized double-stranded DNA, which would make the assay more cost-effective and efficient (Li et al. 2014).

Different from the traditional HCR, in which the hairpin DNA is sequentially opened and assembled into a linear structure, nonlinear HCR is a hairpin-free and dendritically assembled system. In the nonlinear HCR amplification system, double-stranded DNA monomers are activated by a trigger sequence and dendritically assembled into highly branched nanostructure. Since the hairpin-free strands have few secondary structures, the reaction could be completed faster, and dendritic DNA nanostructures with high molecular weights can be formed (Xuan and Hsing 2014). Therefore, the nonlinear HCR could dramatically improve the sensitivity of SPR assays than traditional HCR. By employing the nonlinear HCR amplification, Shijia Ding et al. developed a label-free SPR biosensor for DNA and ATP detection. As

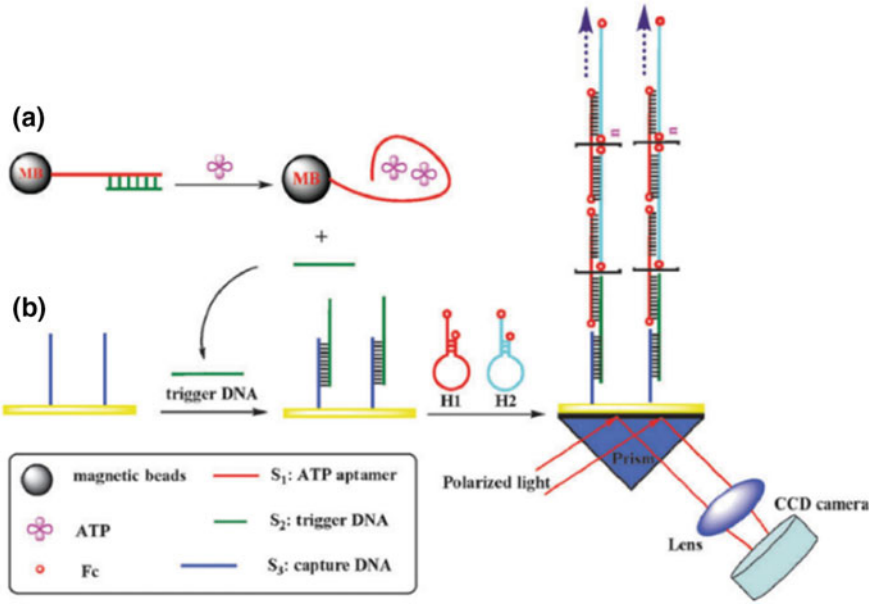

Fig. 6.5 Illustration of the SPR assay for ATP detection with the DNA-based HCR. Reproduced from Li et al. (2014) with permission from The Royal Society of Chemistry

shown in Fig. 6.6, the capture probe is immobilized on the SPR sensor surface for capturing the target DNA. The target DNA had two sections: One terminal of the target DNA hybridizes with the capture probe and the other terminal works as the trigger of the nonlinear HCR. When the double-stranded DNA monomers are introduced onto the sensor surface, the nonlinear HCR is initiated and a dendritic growth of DNA dendrimer is self-assembled on the sensor surface causing the greatly amplified SPR signal. This biosensing strategy, with a detection limit down to 0.85 pM, showed good reproducibility and precision and had been successfully applied for detection of target DNA in complex sample matrices (Ding et al. 2017).

6.3.4 Strand Displacement Amplification (SDA)

Strand displacement amplification (SDA), which can provide exponential amplification of a trace of DNA or RNA, has attracted more and more attention due to its fast, efficient, and no special equipment requirement (Walker et al. 1992). Therefore, the SDA technology is believed to be a suitable strategy to implement simply determination of miRNA combined with SPR technology to produce high sensitivity. Combining with a SDA strategy and Au NP enhancement for improving the sensitivity of the SPR sensor, Yinyin Peng et al. developed a simple and sensitive

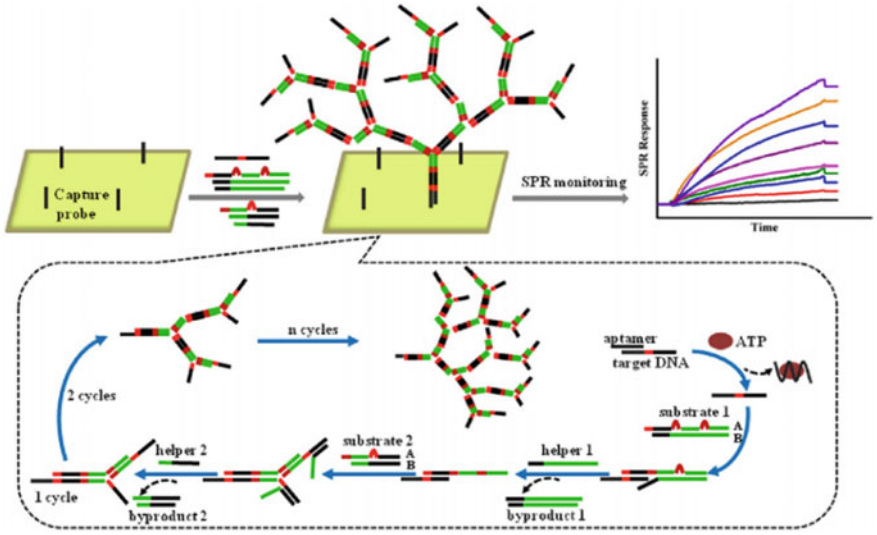

Fig. 6.6 Schematic representation of SPR biosensing srategy for DNA and ATP detection. Reprinted from Ding et al. (2017). Copyright (2016), with permission from Elsevier

SPRi biosensor for the detection of miRNA-155. As shown in Fig. 6.7, initiated by the miRNA, a large number of the DNA triggers are produced for further analysis through a SDA and enzymatic amplification cycle. The DNA triggers are captured onto the gold sensor chip surface by the capture probe. Then the DNA–Au NP is introduced onto the sensor surface through the hybridization with the unpaired fragment of the DNA trigger. The sandwich assembly of the DNA–Au NP results in a large increase in the SPR signal. The detection limit of this method for miRNA-155 detection is down to 45 pM (Zeng et al. 2017).

6.3.5 DNAzyme Signal Amplification

Recently, catalytic nucleic acids (DNAzymes) have been the focus of growing interest as amplifying units for the detection of DNA or aptamer–substrate complexes (Pelossof et al. 2011). Due to the good stability, low costs, and easy preparation, DNAzymes have been widely employed in various biosensor based assays. Among them, the horseradish peroxidase- (HRP-) mimicking DNAzyme, consisting of G-quadruplex and hemin, is one of the most frequently applied DNAzymes. The HRP-mimicking DNAzyme has been widely applied in electrochemical, chemiluminescent, and colorimetric assays due to its excellent properties. Utilizing the efficient catalytic activity of HRP-mimicking DNAzyme on the oxidative polymerization of aniline to polyaniline, Li et al. reported a ultrasensitive SPR biosensor for detection

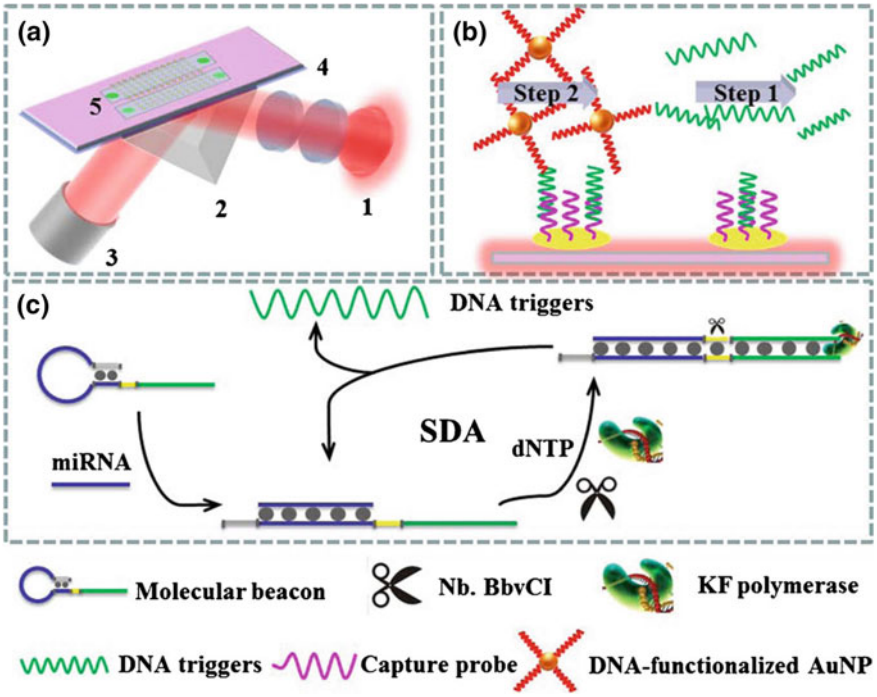

Fig. 6.7 Schematic of SPRi system combined with a SDA strategy and AuNP enhancement for improving the sensitivity of the SPR sensor for miRNA-155 detection. Reprinted from Zeng et al. (2017) with kind permission from Springer Science + Business Media

of bleomycin (BLM). As shown in Fig. 6.8, in the present of BLM, the DNA probe P1 on the sensor surface is cleaved and switches off the hybridization of the G-rich DNA probe P2 onto the sensor surface. As a result, less HRP-mimicking DNAzymes are formed, and less amount of polyaniline is deposited on the sensor surface (Li et al. 2017). Because of the high refractive index of the polyaniline, the SPR response is significantly enhanced (Gong et al. 2015) and the detection limit of BLM was down to 0.35 pM.

In addition, the hemin, with high extinction coefficient, can form the hemin/G-quadruplex on the gold surface of SPR sensor, would dramatically alter the dielectric properties of the surface. Thus, the hemin/G-quadruplex can be used as an amplifying label for SPR detection of different sensing events. Itamar Willner et al. developed a sensitive SPR sensor for Pb^{2+} detection employing the hemin/G-quadruplex nanostructure and the Pb^{2+}-dependent DNAzyme. As shown in Fig. 6.9, the sensor surface was coated with AuNPs to enhance the sensitivity of the SPR sensor. A G-rich DNA, containing the substrate of the Pb^{2+}-dependent DNAzyme, was assembled onto the Au NPs in which the G-rich domain was caged by the Pb^{2+}-dependent DNAzyme. In the presence of Pb^{2+}, the substrate was cleaved, leading to the release of the complex. The uncaged G-rich DNA self-assembled into the hemin/G-quadruplex

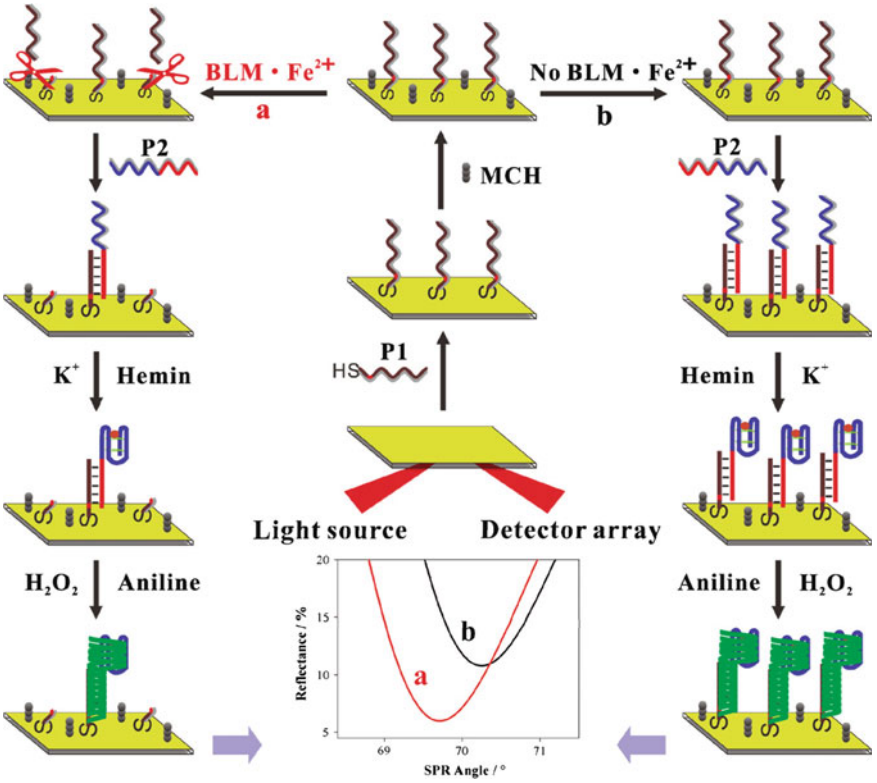

Fig. 6.8 Schematic of the SPR biosensor based on the HRP-mimicking DNAzyme catalyzed deposition of polyaniline. Reprinted with the permission from Li et al. (2017). Copyright 2016 American Chemical Society

structure resulting in the dielectric changes at the sensor surface detected by the SPR sensor. This sensing platform enabled the detection of Pb^{2+} down to 5 fM and revealed an impressive sensitivity and selectivity (Pelossof et al. 2012).

6.3.6 Multiple Signal Amplification Strategy

Although various amplification strategies have been devoted to SPR technology for sensitively detecting target analytes to meet the requirements of clinical diagnosis and medical treatment of diseases, the signal enhancement efficiency of single amplification strategy is insufficient. The signal enhancement can be further improved by combining multiple signal amplification strategies. For example, by combining the target-triggered isothermal exponential amplification with the magnetic nanoparticle-

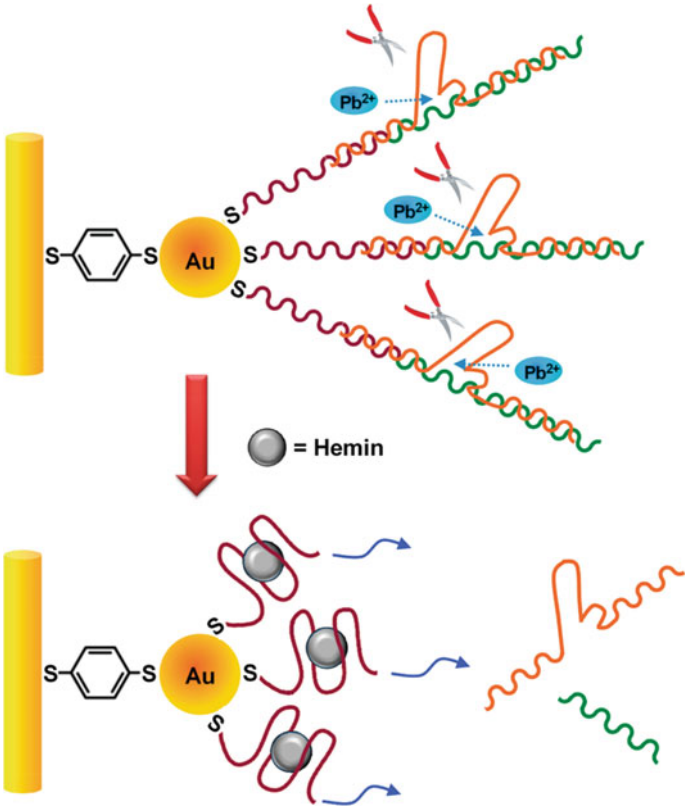

Fig. 6.9 Schematic presentation for the nucleic acid 1/2-functionalized Au NP monolayer-modified surface for the SPR detection of Pb^{2+} ions by the Pb^{2+}-dependent DNAzyme and the Hemin/G-quadruplex label. Reprinted with permission from Pelossof et al. (2012). Copyright 2012 American Chemical Society

based RCA, Shusheng Zhang et al. proposed a sensitive and versatile SPR sensor for the detection of DNA and Ramos cells. Although this methodology is relatively complex, the integration of multiple signal amplification strategy exactly produces a remarkable amplification efficiency. As shown in Fig. 6.10, the strategy includes the following three steps: (1) target-triggered isothermal exponential amplification reaction (T-EXPAR), (2) magnetic nanoparticle-based RCA reaction, and (3) AuNPs-enhanced SPR assay. The LOD for the multiple amplification strategy is 9.3 aM for DNA detection and 10 cells for Ramos cells (He et al. 2014b).

Jian-Ding Qiu et al. reported an ultrasensitive strategy for SPR detection of adenosine, in which an aptamer-based target-triggering cascade multiple cycle amplification strategy combined with Au NPs enhancement was designed to enhance the SPR signals. The amplification strategy was composed of the aptamer-based target-triggering nicking enzyme signaling amplification (T-NESA), the nicking enzyme

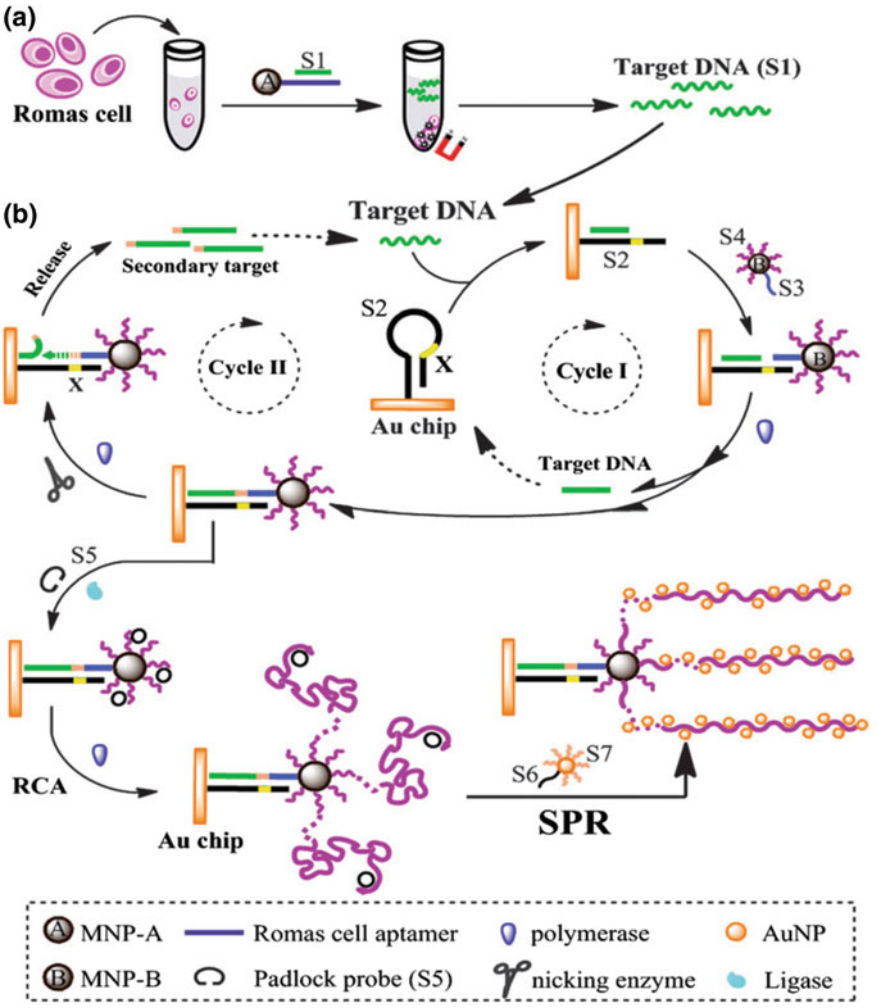

Fig. 6.10 Schematic representation of the multiple signal amplification SPR assay for DNA and cancer cells. Reproduced from He et al. (2014b) with permission from The Royal Society of Chemistry

signaling amplification (NESA) and HCR, which was triggered by the adenosine. The multiple cycle amplification strategy significantly enhanced the SPR signals and exhibited a detection limit of 4 fM for adenosine (Yao et al. 2015) (Fig. 6.11).

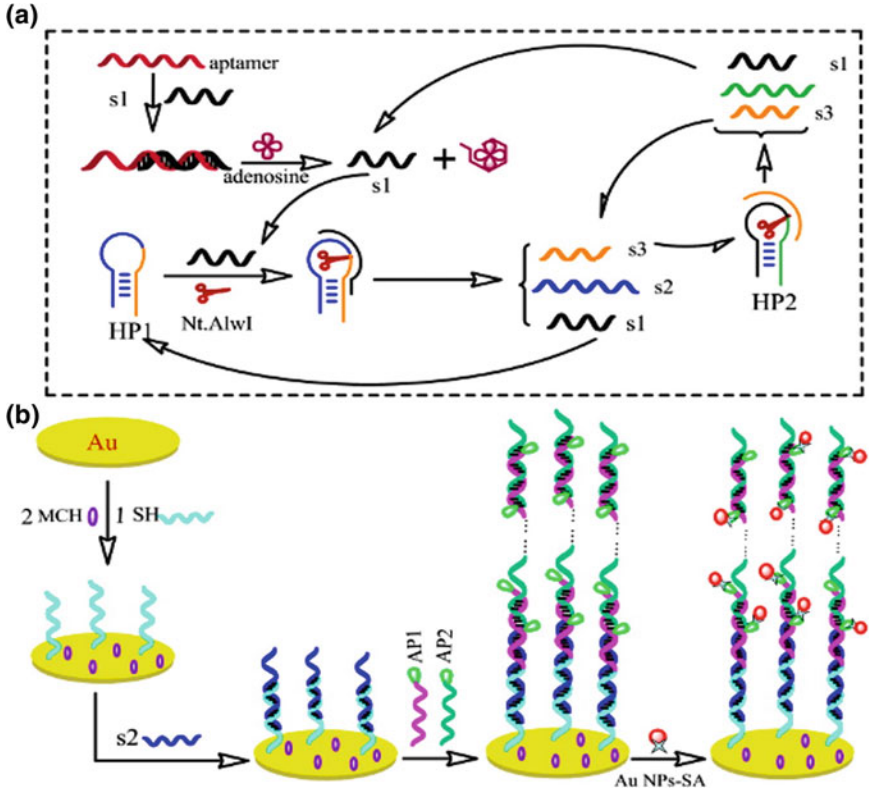

Fig. 6.11 Schematic illustration of (A) dual NESA and (B) HCR and Au NPs signal amplification-based SPR assay for the detection of adenosine. Reprinted with permission from Yao et al. (2015). Copyright 2015 American Chemical Society

6.4 Conclusions and Perspectives

In this chapter, we have summarized the remarkable advances in the development of nucleic acid amplification strategies for novel ultrasensitive SPR biosensors. Further construction of nucleic acid amplification reactions on smartly designed modern SPR biosensor interfaces will be widely applied in the recent biosensing field due to their excellent designability and stability, and demonstrates great promise for clinical application. Since the limited signal enhancement efficiency of single amplification strategy, the development of multiple signal amplification strategies, in which the nucleic acid amplification strategies, nanomaterials, enzyme amplification, and so on is combined, would be a trend in the future. In addition, the combination of SPR sensors with other sensor techniques, such as electrochemical analysis techniques, fluorescence spectroscopy or SERS, to achieve more sensitive and specific detection would also be a trend of SPR techniques.

Reference

Ali MM, Li F, Zhang ZQ et al (2014) Rolling circle amplification: a versatile tool for chemical biology, materials science and medicine. Chem Soc Rev 43(10):3324–3341

Bi S, Yue S, Zhang S (2017) Hybridization chain reaction: a versatile molecular tool for biosensing, bioimaging, and biomedicine. Chem Soc Rev 46(14):4281–4298

Chen Y, Ming H (2012) Review of surface plasmon resonance and localized surface plasmon resonance sensor. Photonic Sens 2(1):37–49

Ding X, Cheng W, Li Y et al (2017) An enzyme-free surface plasmon resonance biosensing strategy for detection of DNA and small molecule based on nonlinear hybridization chain reaction. Biosens Bioelectron 87:345–351

Fakruddin M, Mannan KSB, Chowdhury A et al (2013) Nucleic acid amplification: alternative methods of polymerase chain reaction. J Pharm Bioallied Sci 5(4):245–252

Fong KE, Yung LYL (2013) Localized surface plasmon resonance: A unique property of plasmonic nanoparticles for nucleic acid detection. Nanoscale 5(24):12043–12071

Gong L, Zhao ZL, Lv YF et al (2015) DNAzyme-based biosensors and nanodevices. Chem Commun 51(6):979–995

He P, Liu L, Qiao W et al (2014a) Ultrasensitive detection of thrombin using surface plasmon resonance and quartz crystal microbalance sensors by aptamer-based rolling circle amplification and nanoparticle signal enhancement. Chem Commun 50(12):1481–1484

He P, Qiao W, Liu L et al (2014b) A highly sensitive surface plasmon resonance sensor for the detection of DNA and cancer cells by a target-triggered multiple signal amplification strategy. Chem Commun 50(73):10718–10721

Hinman SS, McKeating KS, Cheng Q (2018) Surface plasmon resonance: material and interface design for universal accessibility. Anal Chem 90(1):19–39

Homola J (2008) Surface plasmon resonance sensors for detection of chemical and biological species. Chem Rev 108(2):462–493

Huang L, Reekmans G, Saerens D et al (2005) Prostate-specific antigen immunosensing based on mixed self-assembled monolayers, camel antibodies and colloidal gold enhanced sandwich assays. Biosens Bioelectron 21(3):483–490

Kai E, Sawata S, Ikebukuro K et al (1999) Detection of PCR products in solution using surface plasmon resonance. Anal Chem 71(4):796–800

Kretschmann E, Raether H (1968) Notizen: radiative decay of non radiative surface plasmons excited by light. Z Naturforsch, A: Phys Sci 23(12):2135–2136

Li H, Chang J, Hou T et al (2017) HRP-mimicking DNAzyme-catalyzed in situ generation of polyaniline to assist signal amplification for ultrasensitive surface plasmon resonance biosensing. Anal Chem 89(1):673–680

Li X, Wang Y, Wang L et al (2014) A surface plasmon resonance assay coupled with a hybridization chain reaction for amplified detection of DNA and small molecules. Chem Commun 50(39):5049–5052

Liedberg B, Nylander C, Lunström I (1983) Surface plasmon resonance for gas detection and biosensing. Sens Actuators 4:299–304

Linman MJ, Abbas A, Cheng Q (2010) Interface design and multiplexed analysis with surface plasmon resonance (SPR) spectroscopy and spr imaging. Analyst 135(11):2759–2767

Linman MJ, Cheng QJ (2009) Surface plasmon resonance: new biointerface designs and high-throughput affinity screening. In: Zourob M, Lakhtakia A (eds) Optical guided-wave chemical and biosensors i. Springer, Berlin Heidelberg, Berlin, Heidelberg, pp 133–153

Lou Z, Han H, Zhou M et al (2017) Fabrication of magnetic conjugation clusters via intermolecular assembling for ultrasensitive surface plasmon resonance (SPR) detection in a wide range of concentrations. Anal Chem 89(24):13472–13479

Mayer KM, Hafner JH (2011) Localized surface plasmon resonance sensors. Chem Rev 111(6):3828–3857

Nguyen HH, Park J, Kang S et al (2015) Surface plasmon resonance: a versatile technique for biosensor applications. Sensors 15(5):10481–10510

Otto A (1968) Excitation of nonradiative surface plasma waves in silver by the method of frustrated total reflection. Z Phys A: Hadrons Nucl 216(4):398–410

Pelossof G, Tel-Vered R, Liu XQ et al (2011) Amplified surface plasmon resonance based DNA biosensors, aptasensors, and Hg^{2+} sensors using hemin/G-quadruplexes and Au nanoparticles. Chem Eur J 17(32):8904–8912

Pelossof G, Tel-Vered R, Willner I (2012) Amplified surface plasmon resonance and electrochemical detection of Pb^{2+} ions using the Pb^{2+}-dependent DNAzyme and hemin/G-quadruplex as a label. Anal Chem 84(8):3703–3709

Saha K, Agasti SS, Kim C et al (2012) Gold nanoparticles in chemical and biological sensing. Chem Rev 112(5):2739–2779

Scarano S, Mascini M, Turner APF et al (2010) Surface plasmon resonance imaging for affinity-based biosensors. Biosens Bioelectron 25(5):957–966

Singh P (2016) Spr biosensors: historical perspectives and current challenges. Sens Actuators B Chem 229:110–130

Šípová H, Homola J (2013) Surface plasmon resonance sensing of nucleic acids: A review. Anal Chim Acta 773:9–23

Spadavecchia J, Burras A, Lyskawa J et al (2013) Approach for plasmonic based DNA sensing: Amplification of the wavelength shift and simultaneous detection of the plasmon modes of gold nanostructures. Anal Chem 85(6):3288–3296

Springer T, Ermini ML, Spackova B et al (2014) Enhancing sensitivity of surface plasmon resonance biosensors by functionalized gold nanoparticles: size matters. Anal Chem 86(20):10350–10356

Tudos A J, Schasfoort R B M (2008) Chapter 1 Introduction to surface plasmon resonance. In: Handbook of surface plasmon resonance. The Royal Society of Chemistry, pp 1–14.

Walker GT, Fraiser MS, Schram JL et al (1992) Strand displacement amplification—an isothermal, invitro DNA amplification technique. Nucleic Acids Res 20(7):1691–1696

Wijaya E, Lenaerts C, Maricot S et al (2011) Surface plasmon resonance-based biosensors: from the development of different spr structures to novel surface functionalization strategies. Curr Opin Solid State Mater Sci 15(5):208–224

Willets KA, Van Duyne RP (2007) Localized surface plasmon resonance spectroscopy and sensing. Annu Rev Phys Chem 58:267–297

Wood RW (1902) On a remarkable case of uneven distribution of light in a diffraction grating spectrum. The London, Edinburgh, and Dublin Philosophical Magazine and Journal of Science 4(21):396–402

Xuan F, Hsing IM (2014) Triggering hairpin-free chain-branching growth of fluorescent DNA dendrimers for nonlinear hybridization chain reaction. J Am Chem Soc 136(28):9810–9813

Yanase Y, Hiragun T, Ishii K et al (2014) Surface plasmon resonance for cell-based clinical diagnosis. Sensors 14(3):4948–4959

Yao GH, Liang RP, Yu XD et al (2015) Target-triggering multiple-cycle amplification strategy for ultrasensitive detection of adenosine based on surface plasma resonance techniques. Anal Chem 87(2):929–936

Zeng K, Li H, Peng Y (2017) Gold nanoparticle enhanced surface plasmon resonance imaging of microrna-155 using a functional nucleic acid-based amplification machine. Microchimica Acta 184(8):2637–2644

Zeng S, Baillargeat D, Ho HP et al (2014) Nanomaterials enhanced surface plasmon resonance for biological and chemical sensing applications. Chem Soc Rev 43(10):3426–3452

Zhang D, Zhang Q, Lu Y et al (2017) Nanoplasmonic biosensor using localized surface plasmon resonance spectroscopy for biochemical detection. In: Rasooly A, Prickril B (eds) Biosensors and biodetection: methods and protocols, vol 1. Optical-based detectors. Springer, New York, New York, NY, pp 89–107

Zhao WA, Ali MM, Brook MA et al (2008) Rolling circle amplification: applications in nanotechnology and biodetection with functional nucleic acids. Angew Chem Int Ed 47(34):6330–6337

Zhou H, Liu J, Xu JJ et al (2018) Optical nano-biosensing interface via nucleic acid amplification strategy: construction and application. Chem Soc Rev 47(6):1996–2019

Chapter 7
Application of Nucleic Acid Amplification Strategies in Electrochemical DNA Sensors

Zhongfeng Gao

Abstract In recent decades, electrochemical DNA sensor has been demonstrated as up-and-coming alternative clinical diagnostic equipment through studying biological recognition matters and transforming them into a sensitive electrochemical output signals. This is because the conventional diagnostic strategies, for example, optical methods, have certain limitations including expensive, laborious, time-consuming, low sensitivity, and selectivity. Nucleic acid amplification strategies and principle of electrochemical signaling are two the most important aspects that should be considered before constructing highly sensitive and selective electrochemical sensor. In this chapter, we show how we are able to construct and investigate biosensing systems that utilize electrochemical signaling. Representative assays demonstrating the performance and merits of each nucleic acid amplification strategies are showed along with discussions on the limits of each strategy. Starting off from their sensing principles and significant characters, the adoption of nucleic acid amplification strategies in biosensing and their future outlooks are also provided.

7.1 Introduction

For sensitive biosensing, optical signals, such as fluorescence and colorimetry, are often used to quantitative detection of the target concentration. Conventional optical-based nucleic acid amplification methods not only demand accurate and cost equipment but also require sophisticated numerical algorithms to interpret the experimental data. In recent years, massive creative designs of electrochemical DNA sensors based on nucleic acid amplification techniques have been reported for trace target detection. These types of devices combine nucleic acid amplification methods with electrochemical transducers to produce an amplified signal, and thus offer a precise,

Z. Gao (✉)
Shandong Provincial Key Laboratory of Detection Technology for Tumour Markers, College of Chemistry and Chemical Engineering, Linyi University, Linyi 276005, Shandong, People's Republic of China
e-mail: gaozhongfeng@lyu.edu.cn

S. Zhang et al. (eds.), *Nucleic Acid Amplification Strategies for Biosensing, Bioimaging and Biomedicine*, https://doi.org/10.1007/978-981-13-7044-1_7

inexpensive, and user-friendly platform for various practical applications, including environmental monitoring and clinical diagnosis.

A classic electrochemical DNA sensor studies the variation of electrical current that generated by redox reactions on the sensor surface. This method possesses several merits, including rapidity, simplicity, high sensitivity, and inexpensive. In particular, an electronic signal is directly yielded from electrochemical reactions; thus, costly equipment for signal transduction can be avoided. On account of the immobilization of functional DNA probes on electrode surfaces, miniaturized, portable, and sensitive biosensing systems can be created accordingly.

7.2 Preparation of Electrochemical DNA Sensor and Its Redox Labeling Methods

7.2.1 Preparation of Electrochemical DNA Sensor

For a classical electrochemical DNA sensor, gold electrode is one of the most frequently used working electrodes, and the thiolated DNA probes can be readily attached on the surface by stable gold–sulfur bonds (Gorodetsky et al. 2008). By phosphoramidite chemistry, the modification of terminal thiolated DNA can be simply realized when chemical synthesizes the probe. When the clean gold surface is immersed in a thiolated DNA solution, the immobilization of DNA can be realized readily on gold electrode surface, producing a self-assembled monolayer (SAM). The gold surface that immobilized with mixed SAM from alkanethiol alcohols and thiolated DNA generate a significantly better quality (less nonspecific adsorption and uniform packing) than that immobilized purely of thiolated DNA. The alkanethiol (e.g., 6-Mercaptohexanol)-DNA mixed SAM is traditionally used (White et al. 2008). Long alkanethiols, such as 11-mercaptoundecanol, are also found to passivate gold electrode surfaces. And the stability has been demonstrated after long-term dry storage (Lai et al. 2006).

In recent years, researchers devoted many efforts to explore new immobilization methods and supporting materials for the fabrication of DNA biosensors. In 2008, a DNA electrochemical biosensor based on covalent immobilization of ssDNA by coupling of sol-gel and self-assembled methods was fabricated (Fig. 7.1a). 3-Glycidoxypropyltrimethoxysiloxane (GPTMS) and 3-mercaptopropyltrimethoxysiloxane (MPTMS) were employed to prepare functional sol-gel film, which could assemble on the gold electrode surface by the sulfur-Au chemistry (Li et al. 2008b). Through co-condensation between silanols, GPTMS sol-gel interconnected into MPTMS sol-gel and offered epoxide groups for covalent immobilization of aminated ssDNA by epoxide/amine coupling reaction. The as-prepared biosensor showed promising performance, including good selectivity, high sensitivity, and regeneration ability. Furthermore, covalent immobilization of aminated ssDNA by diazotization coupling on self-assembled 4-ATP monolayer was

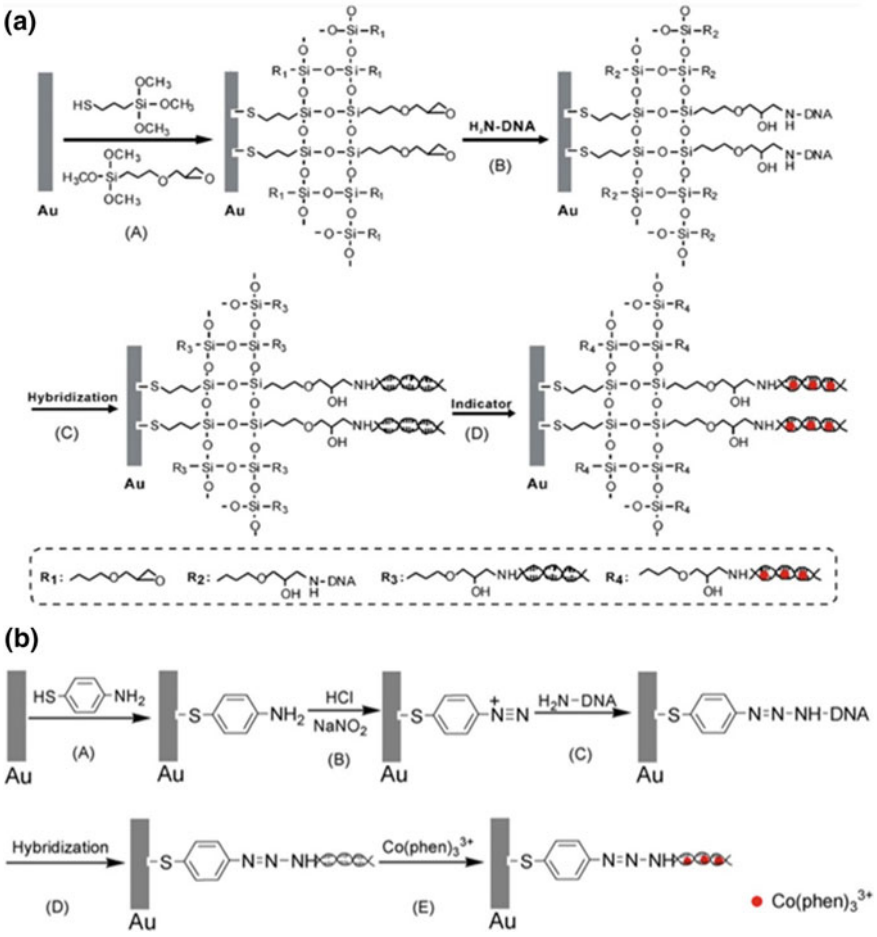

Fig. 7.1 **a** Schematic representation for the construction of electrochemical DNA biosensor based on covalent attachment of DNA on self-assembled MPTMS-GPTMS sol-gel-modified gold electrode. Reprinted from Li et al. (2008b). Copyright 2008, with permission from Elsevier. **b** Fabrication of electrochemical DNA biosensor based on covalent immobilization of DNA on self-assembled diazo-ATP-modified gold electrode using diazotization coupling. Reprinted from Li et al. (2009a). Copyright 2009, with permission from Elsevier

developed (Fig. 7.1b) (Li et al. 2009a). The 4-ATP could stably assemble on the gold surface by sulfur–gold interaction. Through diazotization interaction, diazo-ATP for covalent immobilization of ssDNA was achieved, providing remarkable conductibility for electron transfer. Other materials, such as conducting polymers (Li et al. 2008c; Nie et al. 2009), also have been demonstrated to prepare functional DNA sensor with significant sensitivity and selectivity, which could be used for the detection of DNA hybridization events.

7.2.2 *Redox Labeling Methods for Electrochemical DNA Sensor*

On the basis of the redox reactions of electroactive probes that confined to the gold electrode surface, sensitive electrochemical signaling is readily accomplished (Wang et al. 2008). In the past two decades, various redox labeling strategies have been reported for electrochemical DNA sensors. Redox reporter can be used to label DNA probe by an intercalation or covalent linker. To indirectly investigate the electrochemical performance of DNA SAM, the solution-diffused redox reporters are frequently employed. Therefore, the variations in the electrochemical response reflect the target concentration in the system.

7.2.2.1 Intercalation-Based Methods

Intercalation is the insertion of a reporter between the adjacent base pairs of a DNA duplex through a noncovalent interaction. The reporters, named intercalators, are mostly aromatic, planar, and polycyclic. Intensively investigated DNA intercalators include methylene blue (MB), Meldola's blue (MDB), and some transition metal complexes. Typically, thiolated dsDNA with mismatched or matched sequences are first attached on gold electrode and then incubated with redox-active intercalator at micromolar concentration. In this case, the electrochemical reporter can be easily addressable, producing electrochemical signals.

MB, an organic molecule that belongs to the phenothiazine family, is a widely used redox indicator in electrochemical DNA sensors (Liu et al. 2012). It generates different voltammetric signals in the presence of ssDNA or dsDNA. As an indicator of the extent of DNA sensor, the widespread use of MB is owing to the relatively low potential value of its electrochemical reaction. For example, the oxidation potential is around −0.20 V versus Ag/AgCl depending on the experimental conditions used (Loaiza et al. 2007). Thus, it allows minimization of potential electroactive interferences. In comparison with the electrochemical signals obtained in the presence of ssDNA probes, MB exhibits higher electrochemical signals after the hybridization process. These enhanced signals might be attributed to the interaction of MB with G bases, as well as to its intercalation in the dsDNA, if there are at least two G-C base pairs (Bang et al. 2005). To investigate DNA-mediated charge transport, intercalated redox reporters are extensively employed. By using the intercalator, the density or amount of self-assembled DNA on the electrode surface can be accurately examined and ssDNA and dsDNA can be accurately differentiated. In addition, the DNA-mediated electron transfer at long range can be greatly influenced by coupling of intercalators into the p-stack of DNA. The electrochemical signals generated from redox reporters have been proved sensitive to subtle perturbations in the base stacking and DNA sequences. Meanwhile, the mismatches, protein binding, and structural damages all lead to less efficient charge flow within DNA.

Another classic electrochemical indicator, MDB, can intercalate into the dsDNA by the planar phenoxazine ring in its structure (Reid et al. 2002). The electrochemical active center of MDB is not fully enveloped by the bulky DNA when the aromatic ring of MDB intercalates into dsDNA. Thus, it is still available for redox activity, and it can be employed as a hybridization indicator for electrochemical biosensing assays (Pedrero et al. 2011; Radoi and Compagnone 2009).

Transition metal complexes exhibit significant potential and have been demonstrated as the mostly used electroactive indicators for bimolecular analysis. We developed a complex diaquabis [*N*-(2-pyridinylmethyl) benzamide-2-*N*, O]-cadmium(II) dinitrate {$[CdL_2(H_2O)_2](NO_3)_2$, where L = *N*-(2-pyridinylmethyl) benzamide}(Zhang et al 2007). The proposed $[CdL_2]^{2+}$ had excellent electrochemical activity and could intercalate into the double helix of dsDNA. Using $[CdL_2]^{2+}$ as an electroactive indicator, the detection of human hepatitis B virus DNA was investigated by differential pulse voltammetry (DPV). The copper (II) complex of Luteolin $C_{30}H_{18}CuO_{12}$ (CuL_2) was demonstrated to intercalate into double helices of the dsDNA (Niu et al. 2009). Using CuL_2 as an electroactive indicator, ssDNA fragment of human hepatitis B virus could be selectively detected. A complex of rutin(R) $C_{54}H_{58}MnO_{32}$ (abbreviated by MnR_2) was reported and also used as the electrochemical indicator for the detection of DNA hybridization event (Niu et al. 2008). We summarized the classic transition metal complexes and their interaction to DNA in a review, which is helpful for the reader to understand (Li et al. 2008a).

7.2.2.2 Covalently Tethered Redox-Active Methods

Using flexible alkyl linkages, various reporters, including MB and ferrocene (Fc), have been tethered covalently to the distal terminus of DNA. By varying the surface density or orientation of DNA SAM, the position of redox reporters can be easily regulated due to the highly restricted mobility of the redox reporters. When the length of alkyl linkages is limited, the only surface-controlled process is the redox reaction of reporters without the consideration of diffusive processes. In this case, the interpretation of obtained results is simplified. It should be noted that only one redox reporter is present on each DNA construct. Thus, it is a powerful tool to examine DNA density on the electrode surface in a 1:1 ratio with the reporter.

The reaction protocol has been successfully developed for covalent tethering of MB and Fc (Willner and Zayats 2007; Gao et al. 2014). The preparation of amino-labeled DNA probes and subsequent immobilization of the redox reporter by the amino functionality to the terminal phosphodiester are often involved. For MB, the NHS-ester of *N*-(carboxypropyl)methylene blue has been the gold-standard route. For Fc, *N*-hydroxysuccinimide (NHS) ester of ferrocenecarboxylic acid is typically used. It should be prepared freshly right before tethering to the amino-labeled DNA probe because the activated ester is unstable.

7.2.2.3 Solution-Diffused Methods

Owing to the strong electrostatic interactions, the common negatively charged redox reporters, which are freely diffusing in aqueous solution, cannot reach the DNA-immobilized electrode surface. For instance, the electronegative DNA phosphate backbone can electrostatically repel the negatively charged $[Fe(CN)_6]^{3-/4-}$ ions. Thus, the redox reporters cannot get into close proximity with the electrode surface (Gao et al. 2015). This results in a high electron transfer resistance, which can be monitored through recording electrochemical impedance spectroscopy (EIS). However, the diffusion of $[Fe(CN)_6]^{3-/4-}$ ions toward the sensor surface can be improved upon treatment or binding to positively charged proteins, which leads to a decrease in the electron transfer resistance (Zhou et al. 2012).

$[Ru(NH_3)_6]^{3+/2+}$ is another solution-based redox system and often employed as a stable and accurate reporter to determine the DNA density on the electrode surface (Gao et al. 2013). The $[Ru(NH_3)_6]^{3+}$ ions diffuse to the sensor surface and electrostatically bind to the electronegative DNA backbone. Their characteristic surface redox reaction can be adapted to discriminate the contribution of solution-diffused redox centers: DNA dehybridization is detected by a reduced signal from the electrostatically bound $[Ru(NH_3)_6]^{3+}$. Besides, the surface densities of both double- and single-stranded DNA can be detected by integration of the reduction peak of $[Ru(NH_3)_6]^{3+}$ to $[Ru(NH_3)_6]^{2+}$. Following the treatment of $[Ru(NH_3)_6]^{3+}$ with a concentration of 5.0 mM or lower ionic strength, the surface concentration of $[Ru(NH_3)_6]^{3+}$, Γ_{Ru}, can be calculated by the following equation (Steel et al. 1998):

$$\Gamma_{Ru} = \frac{Q}{nFA} \tag{7.1}$$

where Q represents the charge obtained by integrating the reduction peak area of surface-bound $[Ru(NH_3)_6]^{3+}$, n is the number of electrons involved in the redox reaction (which is 1), F represents Faraday's constant, and A is the electrode area. This equation assumes as follows: (1) The interaction between $[Ru(NH_3)_6]^{3+}$ is purely electrostatic; (2) full saturation of the DNA-modified surface with $[Ru(NH_3)_6]^{3+}$ occurs; (3) there is complete exchange of $[Ru(NH_3)_6]^{3+}$ with compensation by Na^+ ions; (4) every phosphate molecule is accessible for electrostatic binding to the redox cations.

Under saturation conditions (i.e., where the highest possible concentration of surface-bound $[Ru(NH_3)_6]^{3+}$, Γ_{Ru}, was achieved), the measured Γ_{Ru} value can be converted to the surface density of DNA (Cheng et al. 2007), Γ_{DNA}, using the following equation:

$$\Gamma_{DNA} = \Gamma_{Ru}\left(\frac{z}{m}\right)N_A \tag{7.2}$$

where z represents the valence of the redox cation and m is the number of nucleotides in the DNA.

7.3 Electrochemical Sensors Based on Nucleic Acid Amplification

The signal amplification methods can be divided into two groups based on whether the temperature changes during reactions (Patterson et al. 2013). One category is thermocycling amplification methods. For example, polymerase chain reaction (PCR), which is recognized as a traditional signal amplification strategy for sensitive and selective detection of nucleic acids at extremely low concentrations. The other group called isothermal amplification method that has been established since the early 1990s.

7.3.1 Electrochemical Sensors Based on Thermocycling PCR Amplification Systems

The electrochemical real-time method is first reported by Hsing and co-workers using solid-phase PCR with a simple experimental setup (Yeung et al. 2006) (Fig. 7.2a). To extend electrode-bound primers, a reaction mix containing ferrocene-modified dUTP is employed. Thus, any amplification is measurable as an increase in ferrocene redox current. They further implemented this strategy within an integrated PCR chip with microfabricated electrodes and realized a detection limit as low as 3×10^3 copies and a 1000-fold dynamic range (Yeung et al. 2008). Although pioneering, this method still has several disadvantages relative to standard optical approaches. For example, compared to standard optical approaches which can realize low detection limits of three DNA copies, its sensitivity and dynamic range are poorly presented (Bustin et al. 2009). This discrepancy presumably arises because of the inefficiency of solid-phase polymerization (Pemov et al. 2005). The degradation or loss of primers during electrochemical measurement indicates a second limitation. In this case, they were only able to measure at between four and six amplification cycles, thus reduces the precision of detection.

The development of second-generation techniques which are more analogous to current optical methods is motivated by the limited sensitivity and precision of the above generation electrochemical PCR. The first-generation techniques are reported to monitor amplifications by testing either the loss of electroactive intercalating reporters or the consumption of electroactive nucleobases upon binding or incorporating into dsDNA.

Defever and co-workers, the first group to explore solution-phase electrochemical PCR, used electrochemical method to directly monitor the concentration of free nucleotides in solution as they are consumed during amplification (Defever et al. 2009) (Fig. 7.2b). They first developed the electrochemical approach capable of monitoring PCR at each cycle, significantly improving the system accuracy. The redox reactivity of 7-deaza-dGTP, the guanidine analogue, was also investigated. They indicated that when its base incorporates into a dsDNA, it can be effectively reduced. The

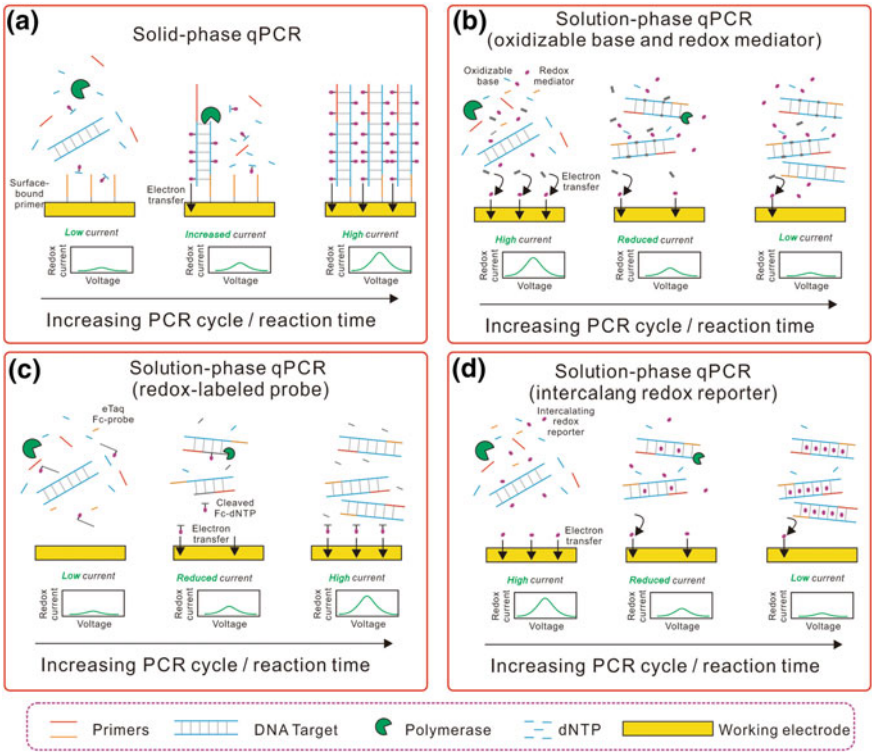

Fig. 7.2 **a** The electrochemical real-time PCR system using surface-bound primers that are elongated by amplification. Reprinted with the permission from Yeung et al. (2006). Copyright 2006 American Chemical Society. **b** A direct method for the electrochemical detection of PCR products measures electroactive nucleotides using redox mediators. Reprinted with the permission from Defever et al. (2009). Copyright 2009 American Chemical Society. **c** The electrochemical eTaq PCR platform uses a redox label-modified probe. Reprinted from Luo et al. (2011). Copyright 2011, with permission from Elsevier. **d** The use of electroactive redox reporters that intercalate in dsDNA is a direct electrochemical method for monitoring PCR in real time. Reprinted from Patterson et al. (2013). Copyright 2013, with permission from Elsevier

detection limits as low as 283 bp sequence from human cytomegalovirus (HCMV) and 2300 bp sequence from the bacterial genome of *Achromobacter xylosoxidans* were obtained with a wide dynamic range over eight orders of magnitude.

Inspired by the TaqMan method, an electrochemical analog, which named 'eTaq' and supported sequence-specific, electrochemical qPCR, was reported by Luo and coworkers (Luo et al. 2011) (Fig. 7.2c). In this method, eTaq probe is modified with an electroactive reporter, such as MB or Fc. The diffusion of the reporter to a negatively charged indium tin oxide electrode was decreased due to the high molecular weight and negative charge. Upon hydrolysis into less highly charged, lower-molecular-weight mononucleotides diffusion of the reporter to the electrode surface is increased, improving the observed electrochemical signal. In consequence, they employed this

method to detect a 137 bp segment of human genomic DNA with low background and excellent signal-to-noise ratio. However, the authors stated that the precision, dynamic range, and detection limit of the strategy have not been well investigated. For example, the detection of a single, relatively high target concentration about 1.6×10^6 copies is presented. And, this method has not yet been investigated in the context of a fully integrated truly continuous system, which is the second concern. Manual pipetting was used to transfer the amplicons from the solution onto the electrode chip at specific cycles, although their preliminary results showed feasibility.

To conduct optical qPCR, DNA-intercalating fluorescent dyes are usually employed. Thus, in electrochemical qPCR systems, the employment of electroactive intercalators has not surprisingly been discovered (Fig. 7.2d) (Patterson et al. 2013; Wilhelm and Pingoud 2003). When a low-molecular-weight redox reporter attaches to a high-molecular-weight amplicon, the diffusivity is reduced, which is commonly explored and demonstrated. The reduced diffusivity decreases the efficiency with which the reporter approaches the electrode surface and transfers an electron. Several intercalating reporters have been well exploited, to further improve this strategy, by Defever and co-workers. And, they showed that $Os[(bpy)_2DPPZ]^{2+}$ (DPPZ is dipyrido[3,2-a:2′,3′-c]phena-zine) displayed the critical attributes of good thermal stability, strong binding efficiency to double-stranded amplicons, low inhibition efficiency for PCR, and high sensitivity. To examine PCR at each cycle by using this reporter, quantitative detection of the same target from HCMV was processed. They finally achieved a low detection limit of 10^3 copies with a wide dynamic range over six orders of magnitude (Defever et al. 2011). An intercalation-based microfluidic qPCR system has been developed by Won and co-workers. They realized accurate detection of initial copy numbers of Chlamydia trachomatis DNA by a homemade microelectrode-patterned glass chip using MB as an intercalating reporter (Won et al. 2011). A low detection limit of 10^3 copies target DNA was obtained with a dynamic range spanning four orders of magnitude. In support of the proposed signaling principle, Won et al. have demonstrated that the transport of MB to the electrode decreases by more than an order of magnitude upon intercalation into a 612 bp dsDNA.

7.3.2 Electrochemical Sensor Based on Isothermal Amplification

Although PCR presents significant biosensing performance and is by far the most well-established approach to amplify nucleic acids, it still has many limitations, including high cost, easy contamination, and time-consuming (Pedrero et al. 2011). In addition, the requirement of a sophisticated thermal cycler greatly restricts the applications of PCR in the point-of-care measurements and resource-limited settings. Alternatively, isothermal amplification that combines with electrochemical methods indicates an extensive attraction and great opportunity for biosensing applications.

7.3.2.1 Quantitative Electrochemical Methods Using Helicase-Dependent Amplification

The mechanism of helicase-dependent amplification (HDA) is similar to that of PCR, accelerating adaptation in current biosensing approaches. Generally, three steps are included in HAD reaction that are template separation, primer hybridization, and primer extension (Qi et al. 2018). The first step is template separation. DNA helicase is used to separate dsDNAs, and each of them is covered by ssDNA-binding proteins. For the second step, two specific primers attach to each ssDNA, respectively, and finally extend their sequence to form the corresponding dsDNAs in the presence of DNA polymerase. By taking the newly generated dsDNAs as the substrates, the next cycle of HDA reaction starts with the use of DNA helicase. As a result, the continuous cycle processes lead to an exponential amplification of the target. To dissociate the two DNA strands, instead of using high temperatures, a thermostable DNA helicase is employed in this method, which processes this step enzymatically (Deng and Gao 2015; Barreda-Garcia et al. 2015; Vincent et al. 2004).

Taking advantage of the similarities between HDA and PCR, Kivlehan et al. proposed $Os[(bpy)_2DPPZ]^{2+}$ as an intercalating redox reporter to establish the first isothermal real-time electrochemical system (Kivlehan et al. 2011). Using a disposable microplate with embedded electrodes, continuous measurements were conducted every 38 s throughout the reaction, achieving excellent temporal resolution. However, they mention that HAD is inhibited by the proposed electrochemical reporter, and thus almost twice the time is needed for the determination of the same initial targets number as their optical method (e.g., ~28 min for fluorescence versus ~45 min for electrochemistry at 105 copies).

In addition to homogeneous detection, Lobo-Castanon et al. proposed an HDA-based heterogenous-phase strategy by determining the unpurified HDA amplicons to electrochemical detect transgene extracted from the Cauliflower Mosaic Virus 35 S Promoter (CaMV35S) (Moura-Melo et al. 2015) (Fig. 7.3). The HDA products attached to the signaling probes that were modified with fluorescein isothiocyanate (FITC) and further bound to the thiolated P35S-capture probes. To combine with the FITC, the anti-FITC-peroxidase (POD) fragments were added. By catalyzing the oxidation of 3,3′,5,5′-tetramethylbenzidine (TMB) under the condition of H_2O_2, the electrochemical signal was detected, which performed highly sensitive and selective detection of target CaMV35S with a low detection limit down to 30 copies.

Despite the merits of HDA, optimization of experimental conditions including primer sets and buffer composition, to ensure the HDA reaction can be conducted effectively, is often ineluctable. However, PCR experiments are often used for the optimization. As a result, more investigations should be carried out to achieve the whole potential of HDA. Moreover, the development of helicases and ssDNA-binding proteins should be focused in future researches. Finally, the improvement of the efficiency of the existing helicases and ssDNA-binding proteins should not be ignored, which are important to the identification of the rate-limiting step in HDA.

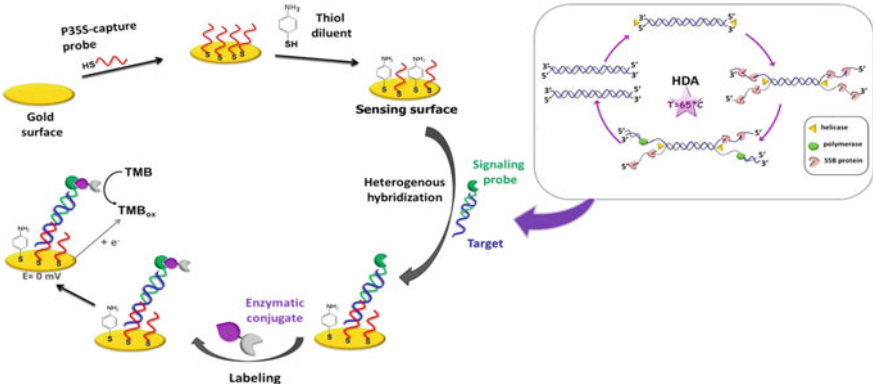

Fig. 7.3 HDA-based heterogenous-phase electrochemical biosensor for transgene detection. Reprinted with the permission from Moura-Melo et al. (2015). Copyright 2015 American Chemical Society

7.3.2.2 Quantitative Electrochemical Sensor Using Loop-Mediated Isothermal Amplification

Loop-mediated isothermal amplification (LAMP) is another widely used isothermal strategy to be integrated into an electrochemical platform and employs strand displacing polymerase and a loop-forming primers to produce large, concatemeric amplicons comprising multiple copies of the amplification analytes (Notomi et al. 2000). LAMP has demonstrated to be an effective and alternative protocol to PCR because of its significant amplification yields and specificity. For instance, a high amplicon yield can be obtained by LAMP method (>500 ng/ml, even ~100 times greater than PCR) (Nagamine et al. 2002b). Similarly, the specificity of LAMP is remarkable greater than that of PCR, because it needs that four to six distinct primer probes simultaneously recognize six to eight different regions within the target (Nagamine et al. 2002a). Despite the complexity, commercially available master mixes and readily accessible primer design software have greatly decreased the overheads and cost of LAMP, contributing to its increasing popularity (Mori and Notomi 2009). Given these strengths, it is reasonable that, in recent years, LAMP has been integrated with electrochemical method to develop a real-time biosensing platform combining the very real benefits of both.

LAMP has recently been used to combine with electrochemical method for the detection of various analytes. The electrochemical detection is conducted by detecting redox molecules in the absence or presence of amplicons or by immobilizing redox-labeled LAMP amplicons on the surface of electrode. The LAMP amplicons can be measured after the amplification reactions or be detected in real time. The expected electrochemical signals can be monitored by square wave voltammetry (SWV), linear sweep voltammetry (LSV), differential pulse voltammetry (DPV), and the change of conductivity.

Nagatani and co-workers first presented a semi-real-time electrochemical monitoring approach based on the reverse transcription LAMP using a screen-printed electrode for the detection of influenza virus RNA (Nagatani et al. 2011). They used MB as an electroactive DNA intercalator to combine with amplified DNA, and SWV was used as the electrochemical signal in the RT-LAMP biosensing system. Based on the RT-LAMP, amplification process of DNA was successfully monitored by recording and analyzing the MB electrochemical signal with only one screen-printed working electrode. The obtained electrochemical current was greatly related to the concentration of target RNA and the extent of DNA amplification. This approach avoids potential cross-contamination because both the amplification and the detection processes are possible in a single tube, and laborious probe immobilization is not needed. Moreover, this approach offers a novel aspect to fabricate sensitive electrochemical handheld biosensors.

Recently, Marchal and co-workers reported a sensitive and selective electrochemical LAMP approach to determinate single DNA copies by using one nonintercalating reporter ($Ru(NH_3)_6^{3+}$) and three intercalating redox reporters (MB, $[Os(bpy)_2dppz]^{2+}$, and PhP), respectively. Compared with the traditional PCR and fluorescence LAMP assays, they carefully studied the sensing performance that monitored by each of the four electrochemical reporters (Martin et al. 2016). More intercalating redox reporters were used, with the progress of the reaction, to combine with the LAMP amplicons. Besides, in the presence of $Ru(NH_3)_6^{3+}$, it prefers to bind with the by-product pyrophosphate anion, which can be released significantly in the reaction. The two distinct combination assays between nonintercalating and intercalating probes with LAMP products lead to a reduced current along with the amplification. Thus, the proposed approach provided an accurate and reliable merit for real-time electrochemical LAMP.

Taking a different approach, a microfluidic multiplex electrochemical LAMP (named μME-LAMP) system was developed by Kong and colleagues for the sensitive and real-time detection of multiple bacteria (Luo et al. 2014) (Fig. 7.4a). Multiplex assay was achieved with the addition of different samples into the isolated electrochemical microchambers. A lower electrochemical current was generated after performing the LAMP reaction than that generated before LAMP, owing to the intercalation of MB into the DNA duplex and the slow diffusion of MB to the electrode surface. The proposed μME-LAMP chip realized the detection limits as low as 17, 28, and 16 copies/μL for *Haemophilus influenza*, *Mycobacterium tuberculosis*, and *Klebsiella pneumonia*, respectively.

Taken advantages of LAMP, a microfluidic electrochemical quantitative (MEQ)-LAMP platform is developed for simple, sensitive, rapid, and quantitative determination of Salmonella genomic DNA at the point of care by Hsieh and co-workers. DNA amplification was electrochemically processed in real time utilizing MB to record measurements at 1-min intervals within a monolithic microfluidic device. By a single-step process, they realized a low detection limit as few as 16 copies of target sequence in less than an hour (Hsieh et al. 2012) (Fig. 7.4b). Compared with most other electrochemical detection systems, this method exhibits better sensitivity and faster response speed. As the sensor surface can be simply modified to contain

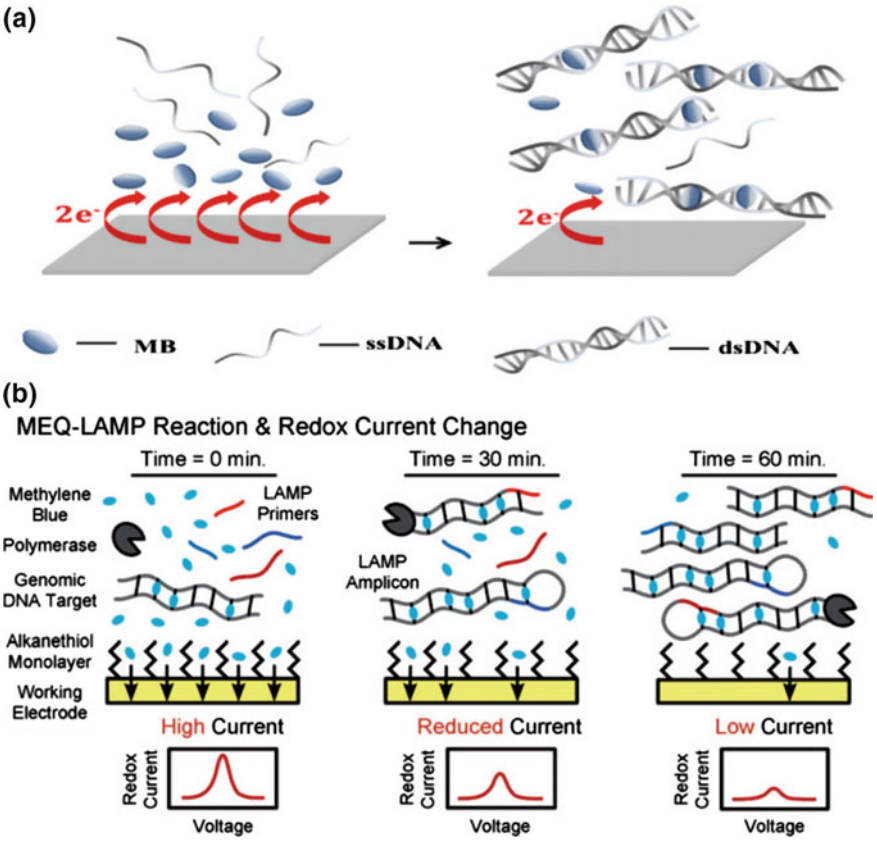

Fig. 7.4 **a** Schematic of the principle of the microfluidic multiplex electrochemical LAMP (named μME-LAMP) system for real-time quantitative multiple bacteria. Reprinted from Luo et al. (2014). Copyright 2014, with permission from Elsevier. **b** MEQ-LAMP system for pathogenic DNA detection. Reproduced from Hsieh et al. (2012) by permission of John Wiley & Sons Ltd.

multiple chambers for parallel determination of multiple targets, the proposed MEQ-LAMP strategy is readily compatible with multiplexing. The significant potential and the performance for expanded capability might inspire researchers to envision the MEQ-LAMP platform as a viable protocol for biosensing at the point of care.

Accurate calibration and control of temperature are demanded for quantitative detection because the activity of polymerase in LAMP is greatly influent by temperature. Therefore, create stable LAMP enzymes and other LAMP biochemical components is in great demand. In addition, nonenzymatic LAMP biosensing methods might also be achieved that could be practical and potential for remote settings. LAMP, as a powerful tool, has significant promise in the establishment of practical approaches in future.

7.3.2.3 Quantitative Electrochemical Sensor Using Rolling Circle Amplification

Rolling circle amplification (RCA), a sensitive and selective isothermal amplification technique, has been broadly employed in various domains owing to its high efficiency and simplicity (Gao et al. 2018). Various electrochemical RCA (ERCA) strategies have been reported to achieve ultrahigh sensitivity, such as hyperbranched rolling circle amplification (HRCA) and padlock exponential rolling circle amplification (P-ERCA). Lizardi and co-workers first proposed HRCA for the determination of single base mismatch in a small quantity of human genomic DNA (Lizardi 1998). In addition, HRCA is simplicity, less time-consuming, ultrahigh sensitivity, and cost-effective performance. Compared with conventional PCR assay, HRCA has the advantage that it can be carried out at constant temperature without the need of complex thermal cyclers. During the past decades, HRCA has been extensively used for the detection of viral RNA, DNA, metal ions, small molecules, and proteins.

In 2013, Lin et al. developed a label-free electrochemical aptasensor for the determination of platelet-derived growth factor B-chain (PDGF-BB) based on HRCA with high specificity and sensitivity (Wang et al. 2013) (Fig. 7.5a). First, cDNA was attached on the gold electrode surface by Au–S bond and it could partially hybridize with aptamer probe to form the DNA duplex. When PDGF-BB was added, it prefers to hybridize with the aptamer probe, removing the aptamer probe from the electrode surface. In this case, the cDNA presented free state and able to hybridize with a padlock probe. The padlock probe contains a small gap, and it could generate a circular padlock probe in the presence of *E. coli* DNA ligase. Primer 1 was hybridized with the circular padlock probe, leading to the RCA reaction by polymerase to generate long ssDNA with repeated region, providing as the templates to hybridize with primer 2. Therefore, primer 2 extended immediately forward with the addition of DNA polymerase. In this case, a number of dsDNA were produced on the electrode surface. Finally, the electrochemical indicator, MB, was used to insert into the dsDNA, generating significant electrochemical signals that were proportional to the amount of target. Thus, a label-free electrochemical aptasensor based on HRCA amplification was established, realizing a detection limit as low as 1.6 fM of PDGF-BB and high selectivity against other interferents, such as thrombin, lysozyme, and human serum albumin (HSA).

Yi and colleagues created an electrochemical biosensor for sensitive determination of DNA fragments by integrating HRCA with hairpin-mediated circular strand displacement polymerization (CSD) (Li et al. 2016) (Fig. 7.5b). The hairpin probe that immobilized on the gold electrode surface can be opened to form the dsDNA, when target DNA was added. Then, the unfolded stem binds with biotin-labeled primer probe, resulting in the DNA strand polymerization with the aid of dNTPs and DNA polymerase. Therefore, the target DNA was released to trigger the next cycle of hybridization process with hairpin probes, resulting in the accumulation of biotin-labeled DNAs. Given the specific and strong streptavidin–biotin interaction, massive streptavidin molecules were attached on gold surface. With the addition of HRCA primers and circular templates, the HRCA reaction was occurred. Consequently,

Fig. 7.5 **a** HRCA-based electrochemical biosensor for PDGF-BB detection. Reproduced from Wang et al. (2013) by permission of The Royal Society of Chemistry. **b** Electrochemical DNA biosensor based on the cascade signal amplification of hairpin-mediated CSD and HRCA. Reprinted from Li et al. (2016). Copyright 2016, with permission from Elsevier. **c** Schematic illustration of P-ERCA assay and $CoFe_2O_4$ MNPs assisted no substrate nanoelectrocatalysis for miR-21 detection. Reprinted from Yu et al. (2017). Copyright 2017, with permission from Elsevier

massive dsDNA with various lengths were generated. Finally, the biotin-labeled probes are selectively attached to the dsDNA, which further linked to the streptavidin–alkaline phosphatase (ST-AP). The recorded electrochemical signal that catalyzed by alkaline phosphatase (AP) was produced from the irreversible conversion of α-naphthyl phosphate (α-NP) to electroactive products, which was measured by DPV. The proposed strategy realized an ultrahigh sensitivity for DNA detection with a low detection limit down to 8.9 aM.

Taking a different approach, P-ERCA has been recently established. Yu and colleagues developed a P-ERCA method for electrochemical determination of microRNA-21 (miR-21) using magnetic nanoparticles (MNPs) for nonsubstrate nanoelectrocatalysis (Yu et al. 2017) (Fig. 7.5c). The exponential growth of P-ERCA triggers was demonstrated during the continuous process of polymerization and cleavage. Meanwhile, the electrode surface was modified with capture probe I (CP I), which could hybridize with triggers and further produce the immobilization of CP II/Au@$CoFe_2O_4$/Tb-Gra composites on the surface. Finally, the expected signal was electrochemically measured from the MNPs-aided nonsubstrate nanoelectrocatalysis. The proposed method showed an excellent sensitivity, realizing a low detection

limit of 0.3 fM for miR-21 detection. Taken together, the electrochemical P-ERCA approaches are universal and suitable for the detection of various targets, such as proteins and nucleic acids. The method has the advantages of low cost, rapid response, high sensitivity, simplicity, and specificity, which holds significant promise in the development of clinical diagnostics, environmental monitoring, and food safety.

Despite its significant performance, RCA-based electrochemical devices, or diagnostic protocols have yet to reach the commercial market. To date, the RCA amplification kit has been created only for research use, such as the Illustra TempliPhi DNA amplification kits from GE HealthCare (Buckinghamshire, UK). Developing RCA-based electrochemical sensors is of importance for point-of-care testing and holds great business opportunities in future.

7.3.2.4 Quantitative Electrochemical Sensor Using Nanomaterial-Assisted Amplification

To meet the growing requirements for ultrasensitive biosensing, scientists have established various strategies to improve the response of the electrochemical DNA sensor by modifying with functional nanomaterials. With the development of nanotechnology, significant attention has been paid to various nanomaterials, such as MNPs, quantum dots (QDs), metal nanoparticles, carbon-based nanomaterials, and polymeric NPs. Owing to the remarkable biological compatibility, chemical stability, nontoxicity, high surface area, remarkable conductivity, and catalytic activity, the introduction of nanomaterials has significantly enhanced the biosensing performance to obtain the amplified electrochemical signal and the stabilized recognition probes.

In recent years, many reviews on functional nanomaterials and their biosensing applications have been published. Herein, we simply concentrate on the recent development of nanomaterial-based signal amplification strategies, especially gold nanoparticle (AuNPs), in ultrasensitive DNA-based electrochemical biosensing. In 2008, Zhang and co-workers fabricated an electrochemical sensor based on a structure-switching aptamer and reporter DNA loaded on AuNPs for the detection of adenosine (Fig. 7.6a) (Zhang et al. 2008). The electroactive complex, $[Ru(NH_3)_6]^{3+}$, acts as a signaling transducer. As a single AuNP can be loaded with hundreds of reporter DNA strands, this provides a great amplification of electrochemical signal for the detection of adenosine. Based on this method, the adenosine could be determined with a detection limit as low as 0.18 nM. Next, Hu et al. developed a sensitive electrochemical DNA sensor based on multifunctional encoded AuNPs and nanoporous gold (NPG) electrode (Fig. 7.6b) (Hu et al. 2008). Different from the above-mentioned AuNPs with one kind of DNA probe, the AuNPs we used here labeled with two kinds of DNA biobarcode. One is complementary to the target DNA, while the other is not, decreasing the cross-reaction of targets on the same AuNPs. Given the multifunctional encoded AuNPs and dual-amplification effects of the electrode, the proposed biosensor achieved a low detection limit of 28 aM DNA.

Taken the advantages of high loading capacity, programmable ability, and signal amplification ability, AuNPs were widely used for the fabrication of electrochemical

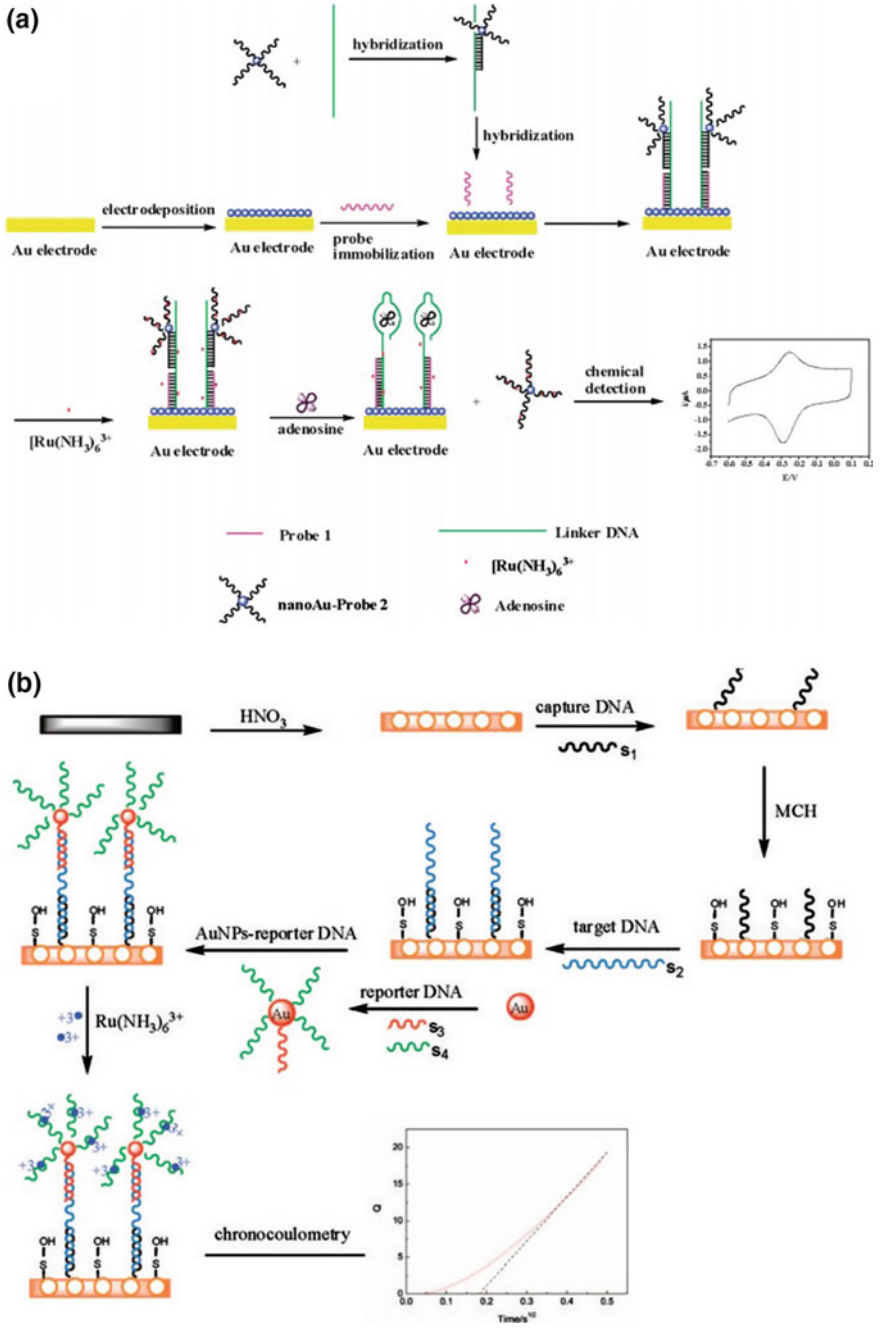

Fig. 7.6 **a** Schematic representation of the adenosine detection based on AuNPs. Reprinted with the permission from Zhang et al. (2008). Copyright 2008 American Chemical Society. **b** Chronocoulometry detection of DNA hybridization by two steps of amplification. Reprinted with the permission from Hu et al. (2008). Copyright 2008 American Chemical Society

sensors to detect various targets, such as DNA (Zhong et al. 2009; Hu et al. 2009; Li et al. 2009b), miRNA (Song et al. 2016), thrombin (Zhang et al. 2009a), human α-fetoprotein (Ding et al. 2009), and cancer cell (Ding et al. 2010). As multiple DNA can be attached to the gold surface to construct biobarcode AuNPs, amplified electrical biobarcode assay for one-pot detection of multiple targets was realized (Li et al. 2010a, b; Zhang et al. 2009b, 2011). In addition, other nanomaterials, such as functionalized metal–organic framework, also show significant sensing performance and promising for the detection of a wide range of targets (Shi et al. 2017).

7.3.2.5 Quantitative Electrochemical Sensor Using Enzyme-Free Nucleic Acid Amplification

Toehold-mediated strand displacement (TMSD) has proved to be a useful strategy for the design of enzyme-free isothermal amplification systems to selectively and sensitively detect a broad range of targets (Zhang and Seelig 2011). Firstly, a long ssDNA, in a typical TMSD, hybridizes to the toehold area of dsDNA, initiating the strand displacement rapidly and producing a new dsDNA with all complementary base pairs (Genot et al. 2011; Yurke et al. 2000). Hybridization chain reaction (HCR) is a prominent example of TMSD. A cascade of hybridization events, in a typical HCR, was occurred between alternating two hairpin probes induced by an initiator, producing a long-nicked dsDNA (Dirks and Pierce 2004). Not only linear HCR, branched HCR strategies for exponential amplification have also been constructed (Bi et al. 2017). For example, a TMSD-based nonlinear HCR designs that usually occur in an exponential manner are reported by Hsing and colleagues (Xuan and Hsing 2014) (Fig. 7.7a). Firstly, they added trigger into the system, which was used to hybridize with the toehold of Substrate-A and triggering the first TMSD reaction. In this case, the black probe could be displaced to open the first functional loop. A new toehold of the displaced strand was exposed, hybridizing with the Assistant-A and extending forward to open the second loop. Thus, By-product-A was released. Substrate-A has two exposed sequences, and it could further hybridize with the toehold of Substrate-B. Consequently, the dissociation of By-product-B and the hybridization of Assistant-B were proceeded. In this case, the product, consisting two ssDNA that are the same as the trigger DNA, is exposed and continually triggers TMSD reactions, which therefore leading to the exponentially growth of the branched DNA nanostructure.

An enzyme-free and immobilization-free electrochemical biosensing method based on nonlinear HCR system has been established for nucleic acid detection (Xuan et al. 2015) (Fig. 7.7b). The PNA probes labeled with ferrocene (Fc-PNAs) freely dispersed in solution in the absence of target, which can attach to the surface of negatively charged indium tin oxide (ITO) electrode and generate a significant electrochemical current. In the presence of the target, the nonlinear HCR was triggered and the branched DNA/PNA nanostructures were exponentially generated, and it hardly in close to the ITO electrode surface. Therefore, the reduction of the electrochemical signal was significantly amplified. It is worth noting that Fc-PNA was used to hybridize onto the dendritic DNA nanostructures with strong binding strength and

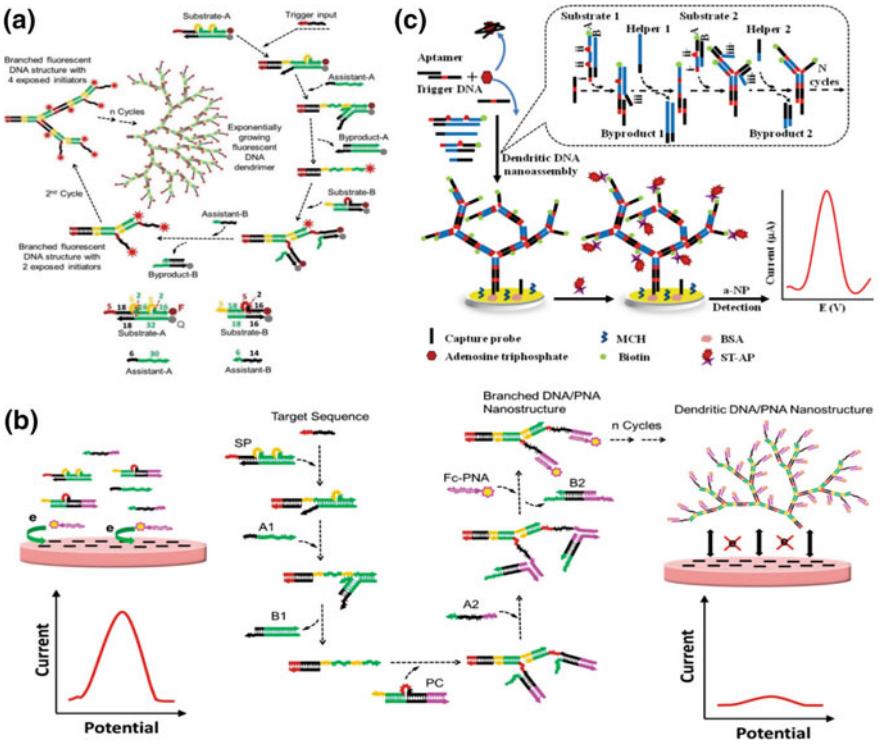

Fig. 7.7 **a** Enzyme-free exponential amplification method on the basis of TMSD-mediated nonlinear HCR. Reprinted with the permission from Xuan and Hsing (2014). Copyright 2014 American Chemical Society. **b** Principle of enzyme-free and immobilization-free exponential amplification assay based on nonlinear HCR for electrochemical detection of nucleic acids. Reprinted with the permission from Xuan et al. (2015). Copyright 2015 American Chemical Society. **c** A enzyme-free and solid-phase exponential amplification system based on nonlinear HCR for the detection of ATP. Reprinted from Ding et al. (2017), with kind permission from Springer Science + Business Media

high hybridization kinetics efficiency between DNA and PNA. The proposed method demonstrated a high sensitivity with a low detection limit of 100 fM.

Ding et al. designed an electrochemical biosensor, unlike the immobilization-free strategy that stated above, by attaching the capture probe onto the surface of gold electrode to detect ATP (Ding et al. 2017) (Fig. 7.7c). With the addition of ATP, it preferable to attach with its aptamer, resulting in the release of trigger DNA which could hybridize with the toehold of Substrate 1. Thus, the first TMSD reaction was triggered. Helper 1 was designed to hybridize with the region iii of Substrate 1-B and extended forward to generate the By-product-1. Substrate 1-A strand was designed with two identical sequences and combined with the two toeholds of Substrates 2, respectively. Then, By-product 2 was dissociated with the assistant of Helper 2. Finally, the product, consisting two target regions, was produced. Another cycle of reaction could be triggered, leading to the exponentially growth of DNA nanostruc-

tures. The resultant electrode surface was immobilized with DNA dendrimers that modified with terminal biotin by capture probe, which linked to ST-AP to produce significant electrochemical signal by the irreversible conversion of α-NP to electroactive products catalyzed by AP. This assay realized a detection limit as low as 5.8 nM of ATP.

Enzyme-free methods, compared with enzyme-assisted isothermal amplification methods, have the merit of simple and rapid response because of the inherent nonenzyme property (Gao et al. 2016). Moreover, enzyme-free strategies have excellent structural versatility, amplification efficiency, and controllable kinetics, which thus have significant promise in the application areas of biosensing, bioimaging, and biomedicine.

7.4 Conclusion

In this chapter, a series of nucleic acid amplification methods have been summarized and their electrochemical applications in fabrication of sensitive and selective biosensors during the recent years have been introduced. Given the significant merits of high amplification efficiency and biosensing sensitivity, nucleic acid amplification has been proved as a powerful protocol for electrochemical bioassays. With the development of bioanalytical chemistry, including DNAzymes and aptamers, electrochemical biosensors based on nucleic acid amplification techniques have been expanded to detect a wide range of targets, such as proteins, nucleic acids, ions, and small biomolecules. Furthermore, the combination of nucleic acid amplification with portable devices or microsystems has facilitated the development of clinical diagnosis with ultrahigh selectivity and sensitivity. In this research field, initial research was concentrated on the preparation of biosensing platforms that can perform concurrent and real-time electrochemical detection during the amplification process. In recent years, scientists have already developed promising electrochemical systems that deliver quantification capabilities and sensitivity that potentially rival bench-top optical systems. To date, the approach of integrating nucleic acid amplification with intercalating electroactive molecules within microfluidic electrochemical devices holds great potential and promising for practical applications. With the development of detection mechanisms and amplification techniques, coupled with straight-forward sample preparation and multiplexed assays, electrochemical strategies might bring new power for real-time detection to the clinical diagnostic at point-of-care in future (Patterson et al. 2013).

References

Bang GS, Cho S, Kim BG (2005) A novel electrochemical detection method for aptamer biosensors. Biosens Bioelectron 21:863–870

Barreda-Garcia S, Gonzalez-Alvarez MJ, de-Los-Santos-Alvarez N et al (2015) Attomolar quantitation of *Mycobacterium tuberculosis* by asymmetric helicase-dependent isothermal DNA-amplification and electrochemical detection. Biosens Bioelectron 68:122–128

Bi S, Yue S, Zhang S (2017) Hybridization chain reaction: a versatile molecular tool for biosensing, bioimaging, and biomedicine. Chem Soc Rev 46:4281–4298

Bustin SA, Benes V, Garson JA et al (2009) The MIQE guidelines: minimum information for publication of quantitative real-time PCR experiments. Clin Chem 55:611–622

Cheng AK, Ge B, Yu HZ (2007) Aptamer-based biosensors for label-free voltammetric detection of lysozyme. Anal Chem 79:5158–5164

Defever T, Druet M, Rochelet-Dequaire M et al (2009) Real-time electrochemical monitoring of the polymerase chain reaction by mediated redox catalysis. J Am Chem Soc 131:11433–11441

Defever T, Druet M, Evrard D et al (2011) Real-time electrochemical PCR with a DNA intercalating redox probe. Anal Chem 83:1815–1821

Deng H, Gao Z (2015) Bioanalytical applications of isothermal nucleic acid amplification techniques. Anal Chim Acta 853:30–45

Ding C, Zhang Q, Zhang S (2009) An electrochemical immunoassay for protein based on bio bar code method. Biosens Bioelectron 24:2434–2440

Ding C, Ge Y, Zhang S (2010) Electrochemical and electrochemiluminescence determination of cancer cells based on aptamers and magnetic beads. Chem Eur J 16:10707–10714

Ding X, Wang Y, Cheng W et al (2017) Aptamer based electrochemical adenosine triphosphate assay based on a target-induced dendritic DNA nanoassembly. Microchim Acta 184:431–438

Dirks RM, Pierce NA (2004) Triggered amplification by hybridization chain reaction. Proc Natl Acad Sci USA 101:15275–15278

Gao ZF, Gao JB, Zhou LY et al (2013) Rapid assembly of ssDNA on gold electrode surfaces at low pH and high salt concentration conditions. RSC Adv 3:12334–12340

Gao ZF, Ling Y, Lu L et al (2014) Detection of single-nucleotide polymorphisms using an ON-OFF switching of regenerated biosensor based on a locked nucleic acid-integrated and toehold-mediated strand displacement reaction. Anal Chem 86:2543–2548

Gao ZF, Chen DM, Lei JL et al (2015) A regenerated electrochemical biosensor for label-free detection of glucose and urea based on conformational switch of i-motif oligonucleotide probe. Anal Chim Acta 897:10–16

Gao ZF, Huang YL, Ren W et al (2016) Guanine nanowire based amplification strategy: enzyme-free biosensing of nucleic acids and proteins. Biosens Bioelectron 78:351–357

Gao ZF, Liu R, Wang J et al (2018) Controlling droplet motion on an organogel surface by tuning the chain length of DNA and its biosensing application. Chem 4(12):2929–2943

Genot AJ, Zhang DY, Bath J et al (2011) Remote toehold: a mechanism for flexible control of DNA hybridization kinetics. J Am Chem Soc 133:2177–2182

Gorodetsky AA, Buzzeo MC, Barton JK (2008) DNA-mediated electrochemistry. Bioconjug Chem 19:2285–2296

Hsieh K, Patterson AS, Ferguson BS et al (2012) Rapid, sensitive, and quantitative detection of pathogenic DNA at the point of care through microfluidic electrochemical quantitative loop-mediated isothermal amplification. Angew Chem Int Ed 51:4896–4900

Hu K, Lan D, Li X et al (2008) Electrochemical DNA biosensor based on nanoporous gold electrode and multifunctional encoded DNA-Au bio-bar codes. Anal Chem 80:9124–9130

Hu K, Liu P, Ye S et al (2009) Ultrasensitive electrochemical detection of DNA based on PbS nanoparticle tags and nanoporous gold electrode. Biosens Bioelectron 24:3113–3119

Kivlehan F, Mavre F, Talini L et al (2011) Real-time electrochemical monitoring of isothermal helicase-dependent amplification of nucleic acids. Analyst 136:3635–3642

Lai RY, Seferos DS, Heeger AJ et al (2006) Comparison of the signaling and stability of electrochemical DNA sensors fabricated from 6- or 11-carbon self-assembled monolayers. Langmuir 22:10796–10800

Li F, Chen W, Tang C et al (2008a) Recent development of interaction of transition metal complexes with DNA based on biosensor and its applications. Talanta 77:1–8

Li F, Chen W, Zhang S (2008b) Development of DNA electrochemical biosensor based on covalent immobilization of probe DNA by direct coupling of sol-gel and self-assembly technologies. Biosens Bioelectron 24:787–792

Li X, Xia J, Zhang S (2008c) Label-free detection of DNA hybridization based on poly(indole-5-carboxylic acid) conducting polymer. Anal Chim Acta 622:104–110

Li F, Chen W, Dong P et al (2009a) A simple strategy of probe DNA immobilization by diazotization-coupling on self-assembled 4-aminothiophenol for DNA electrochemical biosensor. Biosens Bioelectron 24:2160–2164

Li G, Li X, Wan J et al (2009b) Dendrimers-based DNA biosensors for highly sensitive electrochemical detection of DNA hybridization using reporter probe DNA modified with Au nanoparticles. Biosens Bioelectron 24:3281–3287

Li X, Liu J, Zhang S (2010a) Electrochemical analysis of two analytes based on a dual-functional aptamer DNA sequence. Chem Commun 46:595–597

Li X, Xia J, Li W et al (2010b) Multianalyte electrochemical biosensor based on aptamer- and nanoparticle-integrated bio-barcode amplification. Chem Asian J 5:294–300

Li X, Guo J, Zhai Q et al (2016) Ultrasensitive electrochemical biosensor for specific detection of DNA based on molecular beacon mediated circular strand displacement polymerization and hyperbranched rolling circle amplification. Anal Chim Acta 934:52–58

Liu A, Wang K, Weng S et al (2012) Development of electrochemical DNA biosensors. Trends Anal Chem 37:101–111

Liu J, Cui M, Niu L et al (2016) Enhanced peroxidase-like properties of graphene-hemin-composite decorated with Au nanoflowers as electrochemical aptamer biosensor for the detection of K562 leukemia cancer cells. Chem Eur J 22:18001–18008

Lizardi PM, Huang X, Zhu Z et al (1998) Mutation detection and single-molecule counting using isothermal rolling-circle amplification. Nat Genet 19:225–232

Loaiza OA, Campuzano S, Pedrero M et al (2007) DNA sensor based on an *Escherichia coli* lac Z gene probe immobilization at self-assembled monolayers-modified gold electrodes. Talanta 73:838–844

Luo X, Xuan F, Hsing IM (2011) Real time electrochemical monitoring of PCR amplicons using electroactive hydrolysis probe. Electrochem Commun 13:742–745

Luo J, Fang X, Ye D et al (2014) A real-time microfluidic multiplex electrochemical loop-mediated isothermal amplification chip for differentiating bacteria. Biosens Bioelectron 60:84–91

Martin A, Grant KB, Stressmann F et al (2016) Ultimate single-copy DNA detection using real-time electrochemical LAMP. ACS Sens 1:904–912

Mori Y, Notomi T (2009) Loop-mediated isothermal amplification (LAMP): a rapid, accurate, and cost-effective diagnostic method for infectious diseases. J Infect Chemother 15:62–69

Moura-Melo S, Miranda-Castro R, De-Los-Santos-Alvarez N et al (2015) Targeting helicase-dependent amplification products with an electrochemical genosensor for reliable and sensitive screening of genetically modified organisms. Anal Chem 87:8547–8554

Nagamine K, Hase T, Notomi T (2002a) Accelerated reaction by loop-mediated isothermal amplification using loop primers. Mol Cell Probes 16:223–229

Nagamine K, Kuzuhara Y, Notomi T (2002b) Isolation of single-stranded DNA from loop-mediated isothermal amplification products. Biochem Biophys Res Commun 290:1195–1198

Nagatani N, Yamanaka K, Saito M et al (2011) Semi-real time electrochemical monitoring for influenza virus RNA by reverse transcription loop-mediated isothermal amplification using a USB powered portable potentiostat. Analyst 136:5143–5150

Nie G, Zhang Y, Guo Q et al (2009) Label-free DNA detection based on a novel nanostructured conducting poly(indole-6-carboxylic acid) films. Sensors Actuat B-Chem 139:592–597

Niu S, Zhao M, Hu L et al (2008) Carbon nanotube-enhanced DNA biosensor for DNA hybridization detection using rutin-Mn as electrochemical indicator. Sensors Actuat B-Chem 135:200–205
Niu S, Han B, Cao W et al (2009) Sensitive DNA biosensor improved by Luteolin copper(II) as indicator based on silver nanoparticles and carbon nanotubes modified electrode. Anal Chim Acta 651:42–47
Notomi T, Okayama H, Masubuchi H et al (2000) Loop-mediated isothermal amplification of DNA. Nucleic Acids Res 28:e63
Patterson AS, Hsieh K, Soh HT et al (2013) Electrochemical real-time nucleic acid amplification: towards point-of-care quantification of pathogens. Trends Biotechnol 31:704–712
Pedrero M, Campuzano S, Pingarrón JM (2011) Electrochemical genosensors based on PCR strategies for microorganisms detection and quantification. Anal Methods 3:780–789
Pemov A, Modi H, Chandler DP et al (2005) DNA analysis with multiplex microarray-enhanced PCR. Nucleic Acids Res 33:e11
Qi et al (2018) Isothermal exponential amplification techniques: from basic principles to applications in electrochemical biosensors. Biosens Bioelectron 110:207–217
Radoi A, Compagnone D (2009) Recent advances in NADH electrochemical sensing design. Bioelectrochemistry 76:126–134
Reid GD, Whittaker DJ, Day MA et al (2002) Femtosecond electron-transfer reactions in mono- and polynucleotides and in DNA. J Am Chem Soc 124:5518–5527
Shi P, Zhang Y, Yu Z et al (2017) Label-free electrochemical detection of ATP based on amino-functionalized metal-organic framework. Sci Rep 7:6500
Song T, Guo X, Li X et al (2016) Label-free electrochemical detection of RNA based on "Y" junction structure and restriction endonuclease-aided target recycling strategy. J Electroanal Chem 781:251–256
Steel AB, Herne TM, Tarlov MJ (1998) Electrochemical quantitation of DNA immobilized on gold. Anal Chem 70:4670–4677
Vincent M, Xu Y, Kong H (2004) Helicase-dependent isothermal DNA amplification. EMBO Rep 5:795–800
Wang W, Liu S, Ma C et al (2008) Determination of physiological thiols by electrochemical detection with piazselenole and its application in rat breast cancer cells 4T-1. J Am Chem Soc 130:10846–10847
Wang Q, Zheng H, Gao X et al (2013) A label-free ultrasensitive electrochemical aptameric recognition system for protein assay based on hyperbranched rolling circle amplification. Chem Commun 49:11418–11420
White RJ, Phares N, Lubin AA et al (2008) Optimization of electrochemical aptamer-based sensors via optimization of probe packing density and surface chemistry. Langmuir 24:10513–10518
Wilhelm J, Pingoud A (2003) Real-time polymerase chain reaction. ChemBioChem 4:1120–1128
Willner I, Zayats M (2007) Electronic aptamer-based sensors. Angew Chem Int Ed 46:6408–6418
Won BY, Shin S, Baek S et al (2011) Investigation of the signaling mechanism and verification of the performance of an electrochemical real-time PCR system based on the interaction of methylene blue with DNA. Analyst 136:1573–1579
Xuan F, Hsing IM (2014) Triggering hairpin-free chain-branching growth of fluorescent DNA dendrimers for nonlinear hybridization chain reaction. J Am Chem Soc 136:9810–9813
Xuan F, Fan TW, Hsing IM (2015) Electrochemical interrogation of kinetically-controlled dendritic DNA/PNA assembly for immobilization-free and enzyme-free nucleic acids sensing. ACS Nano 9:5027–5033
Yeung SS, Lee TM, Hsing IM (2006) Electrochemical real-time polymerase chain reaction. J Am Chem Soc 128:13374–13375
Yeung SS, Lee TM, Hsing IM (2008) Electrochemistry-based real-time PCR on a microchip. Anal Chem 80:363–368
Yu N, Wang Z, Wang C et al (2017) Combining padlock exponential rolling circle amplification with $CoFe_2O_4$ magnetic nanoparticles for microRNA detection by nanoelectrocatalysis without a substrate. Anal Chim Acta 962:24–31

Yurke B, Turberfield AJ, Mills Jr AP et al (2000) A DNA-fuelled molecular machine made of DNA. Nature 406:605–608

Zhang DY, Seelig G (2011) Dynamic DNA nanotechnology using strand-displacement reactions. Nat Chem 3:103–113

Zhang S, Tan Q, Li F et al (2007) Hybridization biosensor using diaquabis[N-(2-pyridinylmethyl)benzamide-κ2N, O]-cadmium(II) dinitrate as a new electroactive indicator for detection of human hepatitis B virus DNA. Sensors Actuat B-Chem 124:290–296

Zhang S, Xia J, Li X (2008) Electrochemical biosensor for detection of adenosine based on structure-switching aptamer and amplification with reporter probe DNA modified Au nanoparticles. Anal Chem 80:8382–8388

Zhang X, Qi B, Li Y et al (2009a) Amplified electrochemical aptasensor for thrombin based on bio-barcode method. Biosens Bioelectron 25:259–262

Zhang X, Su H, Bi S et al (2009b) DNA-based amplified electrical bio-barcode assay for one-pot detection of two target DNAs. Biosens Bioelectron 24:2730–2734

Zhang H, Fang C, Zhang S (2011) Ultrasensitive electrochemical analysis of two analytes by using an autonomous DNA machine that works in a two-cycle mode. Chem Eur J 17:7531–7537

Zhong H, Lei X, Hun X et al (2009) Design of one-to-one recognition triple Au nanoparticles DNA probe and its application in the electrochemical DNA biosensor. Chem Commun 6958–6960

Zhou LY, Zhang XY, Wang GL et al (2012) A simple and label-free electrochemical biosensor for DNA detection based on the super-sandwich assay. Analyst 137:5071–5075

Chapter 8
The Application of DNA Amplification Strategies in the Field of Photoelectrochemical Biosensor

Xiaoru Zhang

Abstract In this section, the strategy for isothermal amplification of nucleic acids has been applied in photoelectrochemistry. Based on the signal format, the main established strategies for PEC sensor can be classified as steric hindrance, biocatalytic precipitation, in situ generation of electron donor/acceptor, quenching effect, DNA conformational change, introduction of photoelectric active materials, and so on. Herein, we provide a comprehensive overview of the application of DNA amplification in different photoelectrochemical modes. Using illustrative examples, this brief review highlights the current advances in this topic.

8.1 Introduction

The photoelectrochemical (PEC) process refers to photovoltaic conversion resulting from electron excitation and subsequent charge transfer of a photoelectrochemically active material produced by an applied light (Zhao et al. 2015a; Hagfeldt et al. 2010; Qu and Duan 2013). The principle of photoelectrochemistry has been applied to solar cells for decades (Arias et al. 2010; Youngblood et al. 2009). The PEC biosensor is a recently emerged yet vibrantly developing analytical method for biological assays (Yu et al. 2015; Li et al. 2018a; Zhang et al. 2011). Benefiting from its separate source for photoirradiation and electrochemical detection, PEC assay has received substantial attention owing to its low background signal and high sensitivity. On the other hand, compared with the optical assay such as fluorescence, chemiluminescence (CL), and electrochemiluminescence (ECL), which use complex and expensive optical imaging instruments, the use of electronic detection makes the photoelectrochemical device simple and low cost (Zhang et al. 2013a, 2017; Bettazzi and Palchetti 2018). To date, many different kinds of target analytes such as proteins, metal ions, cells, microRNA, and DNA have been detected suc-

X. Zhang (✉)
Shandong Key Laboratory of Biochemical Analysis, College of Chemistry and Molecular Engineering, Qingdao University of Science and Technology, Qingdao 266042, Shandong, People's Republic of China
e-mail: zhangxr7407@126.com

S. Zhang et al. (eds.), *Nucleic Acid Amplification Strategies for Biosensing, Bioimaging and Biomedicine*, https://doi.org/10.1007/978-981-13-7044-1_8

cessfully by PEC biosensor (Haddour et al. 2006; Willner et al. 2001; Hojeij et al. 2008).

As we all know, photoactive material plays an important role in the performance of the PEC sensors. According to the types of charge carrier, inorganic semiconductor material involved in PEC detection could be divided into two groups: n-type and p-type (Hisatomi et al. 2014). Previous works mainly relied on the photoanodes of n-type semiconductors such as CdSe, CdS, ZnO, and TiO_2 (Yan et al. 2014; Zhao et al. 2013). The ejection of the electrons from conduction band to the electrode, with the concomitant transfer of electrons from electron donor in the solution (for example, H_2O_2, dopamine, ascorbic acid, thiol compounds, and nicotinamide adenine dinucleotide), yields an anodic photocurrent. In contrast, p-type semiconductor-based photocathode sensor needs electron acceptor rather than electron donor to produce cathodic photocurrent. The most commonly used electron acceptor is oxygen (Zhao et al. 2012a, b; Cheng et al. 2012).

With the in-depth study on the isothermal amplification of nucleic acids, it has been referred as an efficient amplification tool by means of several distinct strategies including strand-displacement amplification (SDA), hybridization chain reaction (HCR) (Zhao et al. 2015b), rolling circle amplification (RCA), and loop-mediated isothermal amplification (LAMP). Recently, these nucleic acid amplification strategies have also been utilized in PEC assay to increase the detection sensitivity. Here, we provide a comprehensive review from the viewpoint of different action modes of the amplification process in PEC biosensor.

8.2 Amplify Electron Donor and Electron Acceptor

Generally, the PEC sensing system is composed of an appropriate PEC transducer referring to photoexcited materials and electron donor or electron acceptors. As a result, when electron donor or electron acceptor is generated during the target recognition process, obvious photocurrent change can be found due to the charge separation. Based on this idea, some works were focused on producing more electron donor or electron acceptor using DNA amplification strategies.

Ye et al. (2016) showed a new PEC platform with an electron donor as a flexible trigger, which promoted the effective consumption of the electron donor, resulting in an enhanced signal. Hairpins (H1 and H2) modified dibenzocyclooctyne (DBCO) can ligate azide (N_3) functioned dopamine (DA) via click reaction to efficiently introduce DA. The enzyme-free HCR ensures lots of DA attached to the substrate. As a result, Bi_2S_3@MoS_2 nanoflowers decorated on the electrode yield high photoactivity under visible-light illumination with effective consumption of DA electron donor. This method was successfully employed to detect miRNA-141 with highly specific response (Fig. 8.1).

Qiu et al. (2018) devised a near-infrared light-to-UV light-mediated PEC sensor for the detection of carcinoembryonic antigen (CEA) using core-shell $NaYF_4$:Yb, Tm@TiO_2 upconversion microrods. As shown in Fig. 8.2, the guanine (G)-rich prod-

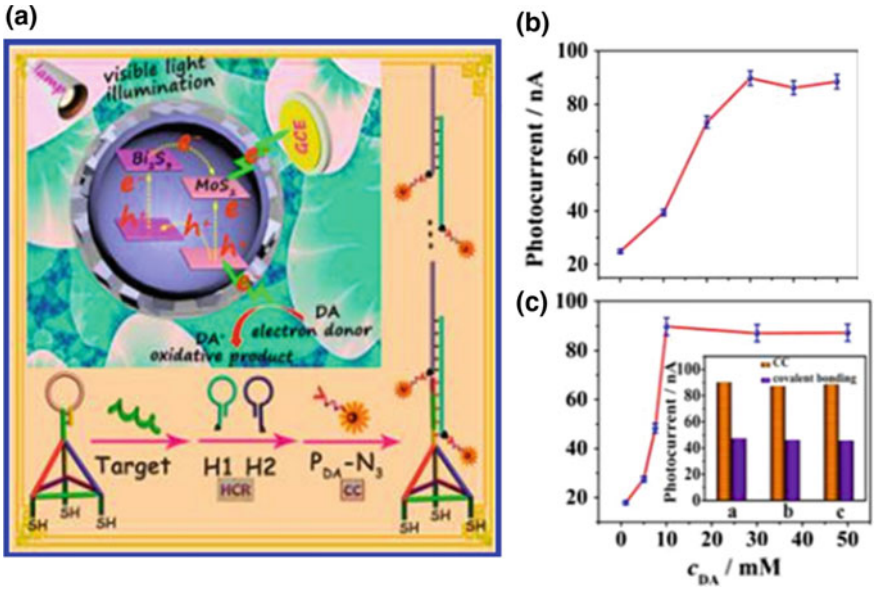

Fig. 8.1 **a** Schematic illustration of the amplification of electron donor dopamine using HCR method for ultrasensitively miRNA assay; **b** HCR hybridization time; and **c** DA concentration. Reprinted with the permission from Ye et al. (2016). Copyright 2016 American Chemical Society

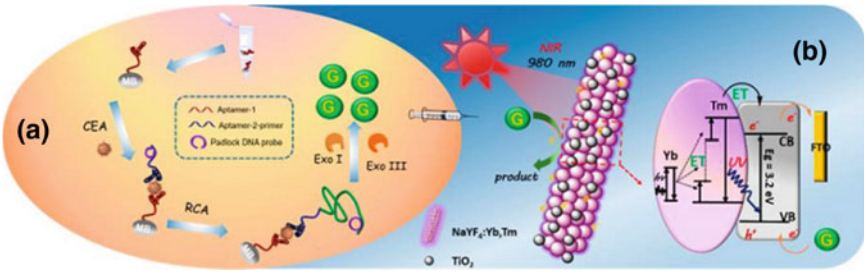

Fig. 8.2 **a** Schematic illustration the assembly of sandwich-type assay format and the released process of guanine (G) bases followed by the RCA reaction; **b** diagram of energy transfer (ET) among lanthanide ion and TiO_2 under near-IR irradiation. Reprinted with the permission from Qiu et al. (2018). Copyright 2018 American Chemical Society

uct generated by RCA reaction was cleaved by exonuclease I and exonuclease III (Exos I/III), thereby resulting in the formation of numerous individual guanine bases to enhance the photocurrent of upconversion microrods under 980 nm near-IR illumination.

Very recently, Zhang et al. developed another electron acceptor: hemin/G-quadruplex (Zhang et al. 2018). In this assay, prostate-specific antigen (PSA) was detected using p-type Cu-doped $Zn_{0.3}Cd_{0.7}S$ as the photosensitive semiconductor

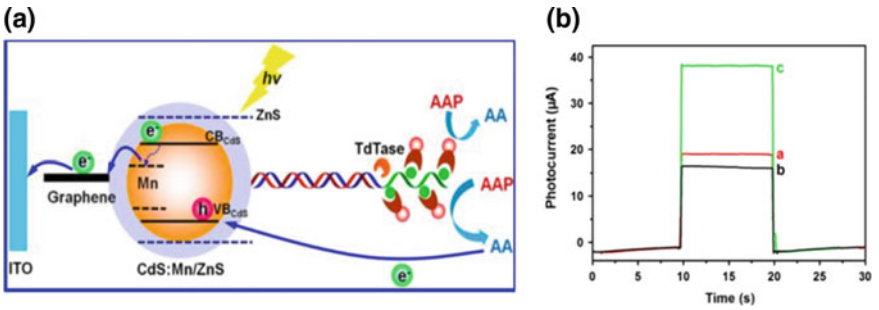

Fig. 8.3 **a** Mechanism of photocurrent generation of the HTLV-II DNA PEC biosensor; **b** photocurrent response of the different modified ITO electrodes containing 10 mM AAP: (a) GRCdS:Mn/ZnS; (b) GR-CdS:Mn/ZnS/pDNA/tDNA (1 nM)/dUTP-TdT; (c) GR-CdS:Mn/ZnS/pDNA/tDNA (1 nM)/dUTP-TdT/AvALP. Reprinted with the permission from Shen et al. (2015). Copyright 2011 American Chemical Society

material and target-triggered rolling circle amplification (RCA) for signal amplification. In this work, long single-stranded DNA generated by the RCA reaction ensures the introduction of G-rich DNA and the formation of long single-stranded DNA/G-quadruplex/hemin. After digested by Exo III, hemin/G-quadruplex is released into the solution. The free hemin/G-quadruplex can act as efficient electron acceptor which can receive electrons from the CB of Cu-doped $Zn_{0.3}Cd_{0.7}S$, resulting in the enhancement of the cathode photocurrent.

In addition to increasing the electron donor or electron acceptor directly, some work aimed at utilizing DNA amplification strategy to introduce more enzyme, which could catalyze substrates to generate more electron donors or electron acceptors. Shen et al. (2015) reported a dual signal amplification PEC assay combined terminal deoxynucleotidyl transferase (TdT)-mediated extension with enzymatic amplification. As shown in Fig. 8.3a, due to the amplification effect of TdT enzymes, multiplex dUTP biotin was incorporated into 3′-OH terminal of tDNA and thereby more avidin–alkaline phosphatase was assembled. The immobilized alkaline phosphatase could catalyze the hydrolysis of 2-phospho-L-ascorbic acid trisodium salt (AAP) and generate more electron donor–ascorbic acid (AA). The photocurrent response of the different modified ITO electrodes is shown in Fig. 8.3b. In addition to TdT-mediated extension strategy, HCR was also used for similar cascade signal amplification (Shi et al. 2018; Xiong et al. 2018).

8.3 Steric Hindrance

8.3.1 Under Catalysis of the Enzyme

Recently, enzymatic biocatalytic precipitation (BCP), involving the formation of insoluble products on electronic transducers, has been utilized as an important route for sensing and biorecognition events (Zhang et al. 2015; Zhao et al. 2012b; Gong et al. 2016). However, the use of natural enzymes often suffers from high cost and instability. To overcome these defects, numerous studies have resorted to the use of various nonenzymatic enzyme mimicking. Among them, the HRP-mimicking enzymes can be easily enriched through DNA amplification method. In Ref. (Huang et al. 2018a), photoactive material 3,4,9,10-perylene tetracarboxylic acid (PTCA) was decorated on the electrode after conjugated with PEI and nano-Au. Target thrombin was recognized via binding with two aptamers. Three-dimensional DNA networks with abundant manganese porphyrin (MnPP) were immobilized on electrode via complementary base pairing. MnPP was used simultaneously as quencher and HRP-mimicking enzyme to accelerate the generation of precipitation benzo-4-chlorohexadienone (4-CD) for further reducing the photocurrent of PTCA. Thus, a signal-off PEC aptasensor with high sensitivity was obtained.

In addition to the above metal–organic framework, other nonenzymatic enzyme mimickings were also used in PEC sensor such as silver halides (Gong et al. 2016) and hemin/G-quadruplex composition (Zhuang et al. 2015). Zhuang et al. reported a novel PEC sensing platform for monitoring the activity of T4 polynucleotide kinase (PNK) based on gold nanoparticle-decorated g-C_3N_4 nanosheets. As shown in Fig. 8.4, double-hairpin-based isothermal amplification strategy and DNAzyme-assisted biocatalytic precipitation were applied, which could induce to generate a lot of hemin/G-quadruplex based. Subsequently, this DNAzyme could catalyze the oxidation of 4-chloro-1-naphthol (4-CN) giving an insoluble precipitation on the Au NP/g-C_3N_4 surface, thus the photocurrent is gradually inhibited with the increasing activity of PNK.

8.3.2 Without Catalysis of the Enzyme

Introducing SiO_2 NPs is a more direct approach for the increase of steric hindrance. Zheng et al. (2016) reported a self-enhanced PEC platform based on a functionalized nanocapsule packaged with both donor-acceptor-type photoactive material and its sensitizer, which was applied for both ultrasensitive estimation of microRNA in different cancer cells and pharmacodynamics evaluation on cancer cells. As shown in Fig. 8.5, by combination of RCA reaction with the duplex-specific nuclease (DSN) and Exo III enzyme-assisted target quadratic recycling strategy, the hairpin DNA on

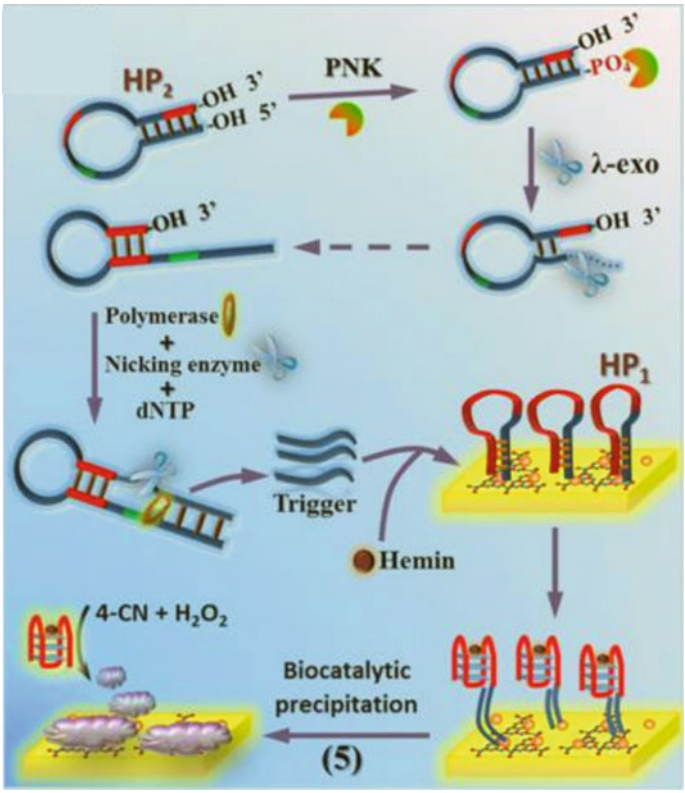

Fig. 8.4 Schematic Illustration of PEC detection platform toward monitoring the PNK activity. Reprinted with the permission from Zhuang et al. (2015). Copyright 2015 American Chemical Society

the SiO_2 nanoparticles (NPs) could be cleaved by target quadratic recycling strategy. After hybridized with the capture DNA on the modified electrode surface, the initial photocurrent signal could be efficiently decreased by the SiO_2 NPs via increasing the steric hindrance of the electrode and depressing the transference of electrons.

Later, the same group reported an ultrasensitive PEC biosensor for p53 gene detection using $[Ru(dcbpy)_2dppz]^{2+}$/Rose Bengal dyes co-sensitized C_{60} NPs structure as a photoactive indicator and SiO_2 NPs-labeled DNA sequences as an efficient quenching element (Wang et al. 2018). Nt.BstNB I enzyme-assisted target recycling amplification was employed to convert a limited quantity of target to numerous SiO_2 NPs-labeled DNA sequences, resulting in a sharp decrement of photocurrent since a dramatic increment of steric hindrance on the modified electrode surface.

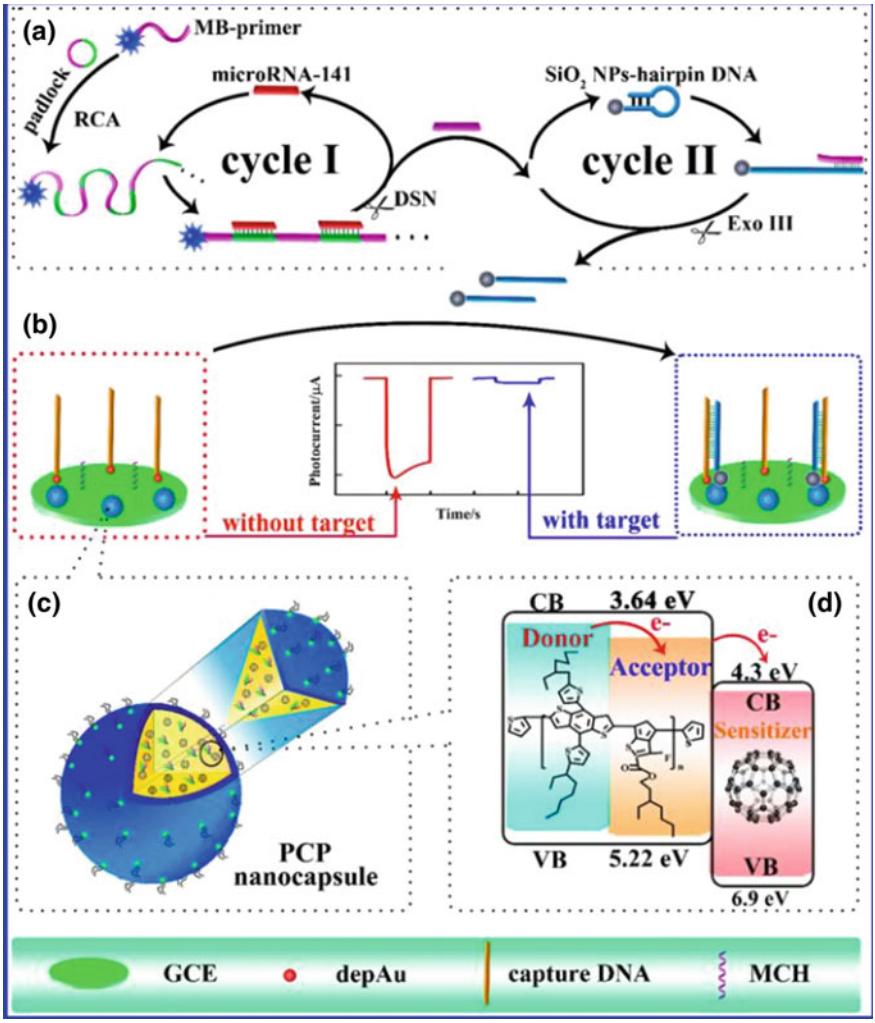

Fig. 8.5 Schematic diagram of **a** quadratic enzyme-assisted target recycling amplification strategy for the biosensor; **b** fabrication of the biosensor; **c** enlarged view of one nanocapsule; and **d** the electron-transfer route in one nanocapsule. Reprinted with the permission from Zheng et al. (2016). Copyright 2016 American Chemical Society

8.4 Producing Quenching Effect After DNA Amplification Process

Some signal-off PEC sensors are designed not from steric hindrance rout but from quenching effect. For example, manganese porphyrin (MnPP) can cause signal quenching of nano-C_{60}/CdTe QDs. HCR was applied to increase the immobilizing amount of MnPP owing to the super stability of MnPP in the HCR-based DNA duplex, which could reduce the background signal and improve the detection sensitivity. In

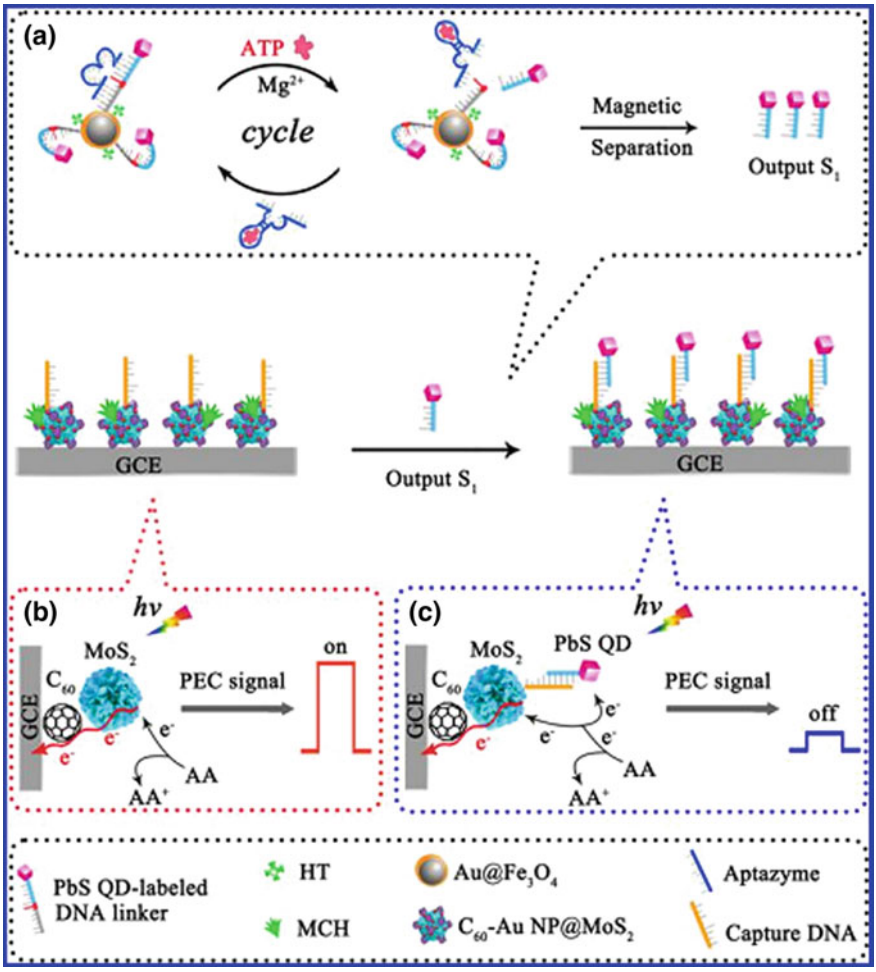

Fig. 8.6 ATP-mediated aptazyme cycling amplification procedure (**a**); schematic illustrations of the photocurrent-generating mechanisms (**b**); and photocurrent quenching mechanisms (**c**). Reprinted with the permission from Li et al. (2017a). Copyright 2011 American Chemical Society

the presence of thrombin, the formation of an aptamer–thrombin complex lead to the releasement of quencher MnPP from the sensing interface, and the PEC signal was recovered accordingly (Li et al. 2016).

Li et al. reported a novel signal-off PEC biosensor for ultrasensitive ATP detection. In this work, n-type C_{60}-Au NP@MoS_2 composite material was used as a signal indicator, and a p-type PbS QD was used as an efficient signal quencher (Li et al. 2017a). In this sensing system, the p-type PbS QDs could compete with C_{60}-Au NP@MoS_2 to absorb light energy and capture electron donor, which led to the retardation of the electron transfer. With the aid of target-mediated aptazyme cycling amplification strategy, a small amount of ATP was converted into plenty of output S1. Subsequently, PbS QD-labeled output S1 was used to amplify the quenching effect furthermore (see Fig. 8.6).

In the above work, MnPP and PbS QD can cause efficient signal quenching effect of photoactive material directly. In Zhao's work (Zhao et al. 2018), photoactive material CdTe QDs was used to react with dissolved Ag^+ through ion-exchange reaction, which led to the formation of inactive of AgTe QD and the decrease of photocurrent intensity. To further increase the detection sensitivity, target-triggering cascade multiple-cycle amplification was applied. In this work, nicking endonuclease-assisted target DNA recycling produced abundant DNA with cytosine (C)-rich loops, which were employed to synthesize silver nanoclusters (AgNCs). After treated with HNO_3, numerous Ag^+ were generated to trigger the ion-exchange reaction, which resulted in significantly amplified decrease of photocurrent and the improved detection sensitivity.

8.5 Producing Enhance Effect After DNA Amplification Process

In many research works, DNA amplification process can lead to the introduction of plenty of DNA probe on the electrode, which may favor the photocurrent enhancement. This always gives signal on photoelectrochemical biosensor.

λ-Exonuclease (λ-Exo) can selectively use double-strand DNA with one 5′-phosphorylated end as a substrate and catalyzes stepwise hydrolysis of the 5-phosphorylated strand in the direction of 5′ to 3′. Shi et al. developed an enhanced PEC DNA biosensor through coupling inorganic–organic nanocomposites with λ-Exo-assisted target recycling. As shown in Fig. 8.7, when tDNA and λ-Exo were added to the hDNA-modified electrode, hDNA could hybridize with tDNA. Then, λ-Exo-assisted tDNA recycling was initiated and plenty of short DNA (sDNA) fragments were produced. These sDNA fragments immobilized on the electrode could hybridize with CdTe/TCPP-labeled pDNA. As a result, the photocurrent signal increased dramatically by the sensitization of CdTe/TCPP inorganic–organic nanocomposites (Shi et al. 2016).

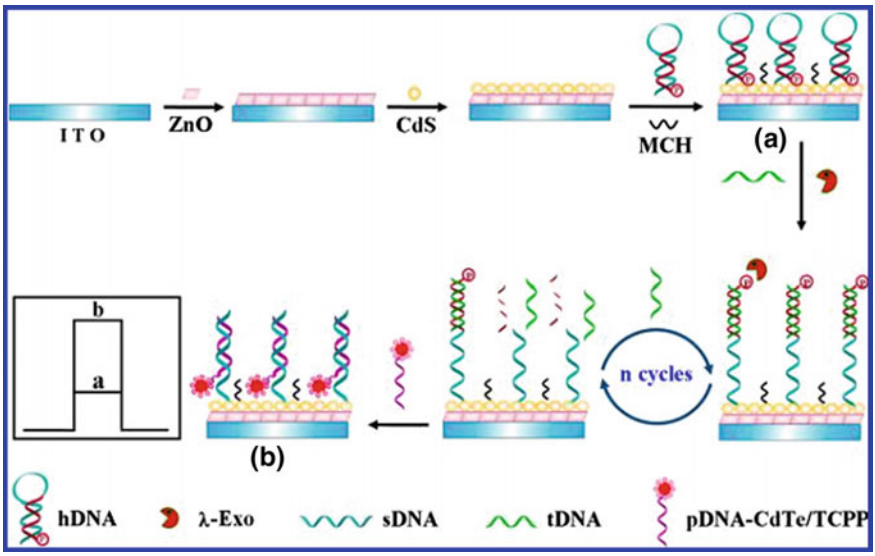

Fig. 8.7 Build produce of the designed PEC DNA biosensor. Reprinted with the permission from Shi et al. (2016). Copyright 2016 American Chemical Society

DNA walkers move autonomously along a prescribed track initiated by a series of reactions, including enzymatic cleavage, hybridization, and strand displacement (Cha et al. 2015). Recently, DNA walkers were also applied in the PEC assay. Lv et al. designed Z-scheme double photosystems for sensitive detection of PSA using a three-dimensional (3D) DNA walker (Fig. 8.8) (Lv et al. 2018). DNA walker strand was immobilized on magnetic bead by partial hybridization with PSA aptamer. In the presence of target PSA, DNA walker strand was released, which opened hairpin DNA1 immobilized on the Au NPs@$BiVO_4$ nanohybrids. Then strand-displacement reaction of the hairpin DNA2 led to the releasement of DNA walker to trigger the next-step reaction. In this way, numerous CdS QDs-H2 conjugates were assembled onto the surface of Au NPs@$BiVO_4$ nanohybrids, and the photocurrent was enhanced through the formation of 'Z-scheme' system on the Au NPs@$BiVO_4$ with the introduction of CdS QDs.

Ye et al. developed a label-free PEC sensor using G^- wire-enhanced method for highly sensitive detection of MicroRNA in cancer cells (Ye et al. 2017). As depicted in Fig. 8.9, ultrathin copper phosphate nanosheets (CuPi NSs) combined with Au nanoparticles (Au-CuPi NSs) were utilized as the photocathode material. Meanwhile, both the DNA duplex structure and DNA 4J architectures could be nicked by Nb.BbvCI and released c-myc regions, which form highly ordered G-wire superstructures via a π–π stacking interaction in the presence of Mg^{2+}. Finally, TSPP was coupled on the substrate via the unique G-wire superstructure to enhance the PEC response, thus realizing the highly efficient and sensitive miRNA assay.

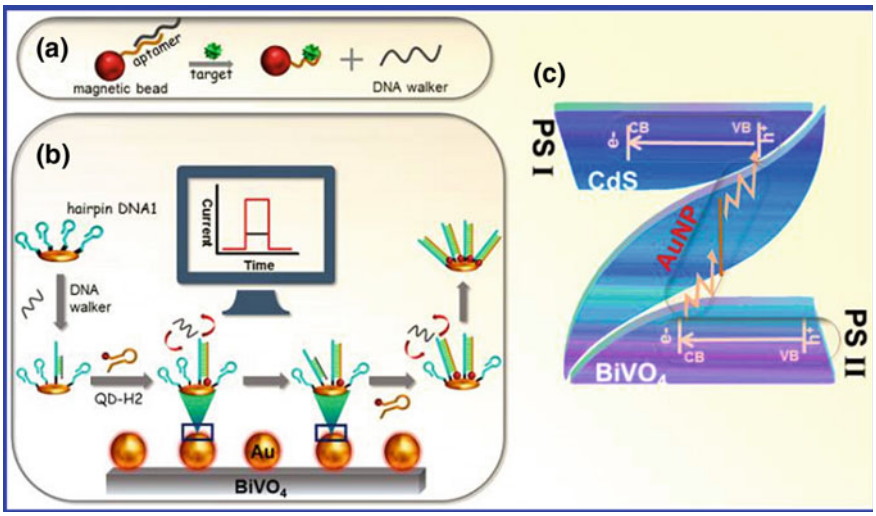

Fig. 8.8 Schematic illustration of double photosystem-based 'Z-scheme' PEC sensing mode. **a** target PSA-induced release of DNA walker strand; **b** DNA walker process; and **c** 'Z-scheme' double photosystems. Reprinted with the permission from Lv et al. (2018). Copyright 2018 American Chemical Society

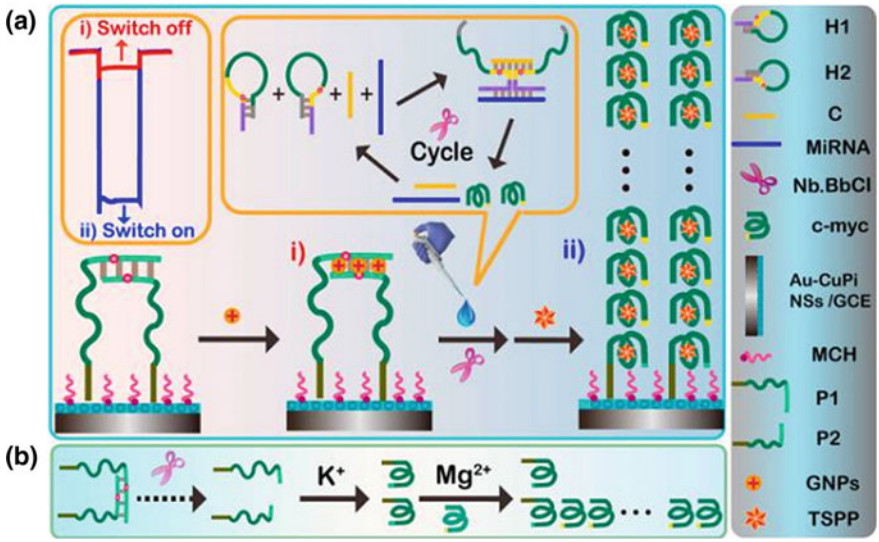

Fig. 8.9 Schematic diagrams of **a** the label-free "off–on" PEC platform fabrication for miRNA assay and **b** the G-wire formation. Reprinted with the permission from Ye et al. (2017). Copyright 2017 American Chemical Society

DNA nanotechnology provides new opportunities for the design of biosensor. Taking advantage of the programmable self-assembly ability, DNA is considered as a powerful building material for the creation of nanostructures with specific shape and function (Shen et al. 2018). Thereby, it is possible to develop PEC DNA sensing platforms by assembly of the DNA layer on an electrode to form 3D DNA networks (Huang et al. 2018a, b; Da et al. 2018). Da et al. developed a 'signal-off' PEC aptasensor based on assembly and disassembly of an aptamer-bridged 3D DNA network structure for the sensitive detection of vascular endothelial growth factor (VEGF165). By repeated assembling DNA D1 and D2 on the g-C3N4 modified electrode, the VEGF165 aptamer-bridged DNA networks could be obtained. This DNA network provided an excellent platform for the immobilization of methylene blue (MB), which could facilitate the electron transport through the DNA helix structure and suppress the recombination of electron–hole pairs generated by g-C_3N_4. In the presence of the target VEGF165, the DNA network could be destroyed through the formation of aptamer–VEGF165 complex, leading to a remarkable decrease of photocurrent.

8.6 DNA Conformational Change

Inspired by the work of electrochemical DNA (E-DNA), our group developed a method for the transduction of DNA conformational change into a readily detectable PEC signal (Zhang et al. 2013b). Photosensitizer $Ru(bpy)_2(dcbpy)$-tagged DNA stem–loop structures were self-assembled onto a nanogold-modified ITO electrode. To improve the sensitivity of the developed PEC biosensor, isothermal circular strand-displacement reaction was applied. Under the action of polymerase Klenow fragment and dNTP, polymerization reaction was initiated and the target was displaced. Thus, even minute amounts of targets could cause obvious photocurrent decrease. Therefore, by monitoring the decrease of photocurrent intensities, target DNA could be detected easily and sensitively.

Zheng et al. developed a ratiometric PEC assay for the determination of microRNA in cells based on target DNA recycling amplification and electron-transfer tunneling distance change (Zheng et al. 2017). As shown in Fig. 8.10, in absence of the target, an initial photocurrent signal at a wavelength of 460 nm was produced by CdS QDs-labeled hairpin DNA (signal probe 1) in close proximity to the electrode. In the presence of target, a DSN enzyme-assisted target recycling was introduced to release abundant product DNA from hairpin DNA. Subsequently, the binding-induced four-way junction DNA nanomachine could be formed by opening the signal probe 1 with the help of SiO_2@MB-labeled DNA (signal probe 2), assistant DNA and product

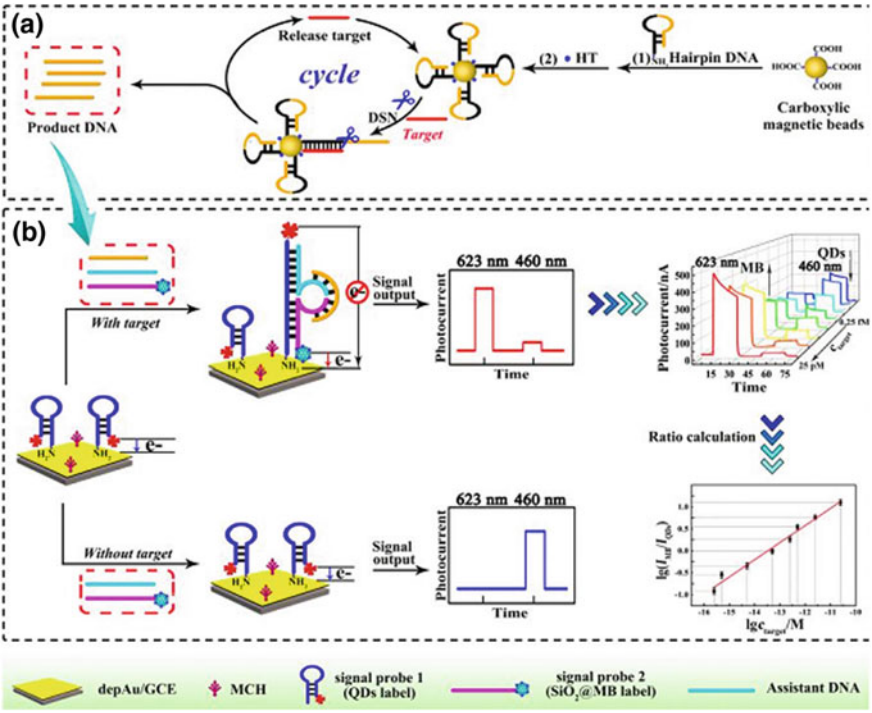

Fig. 8.10 Schematic diagram of **a** signal transduction amplification strategy and **b** fabrication procedure for the ratiometric PEC Assay. Reprinted with the permission from Zheng et al. (2017). Copyright 2017 American Chemical Society

DNA. As a result, photocurrent signal at 460-nm wavelength was reduced due to the increased distance of CdS QDs to the electrode, and photocurrent signal at 623-nm wavelength was enhanced due to the close proximity of SiO_2@MB to the electrode.

8.7 DNA Based Nanocarrier

DNA based nanocarrier was used to enhance the loaded capacity of photoactive or photopassive material and as a result amplified the enhancement or inhibition effect. Our group had taken advantage of the dual-quenched effect of PEC nanoparticles (Zhang et al. 2012), which relied on the electron transfer of bipyridinium relay and energy transfer of Au NPs. The nanoparticles could carry numerous bipyridinium. Carboxyl-functionalized graphene and CdSe nanoparticles were assembled as photoactive film. The hybridization between capture DNA and aptamer attached on the nanoparticle led to the dramatic decrease of PEC intensity, while the recognition

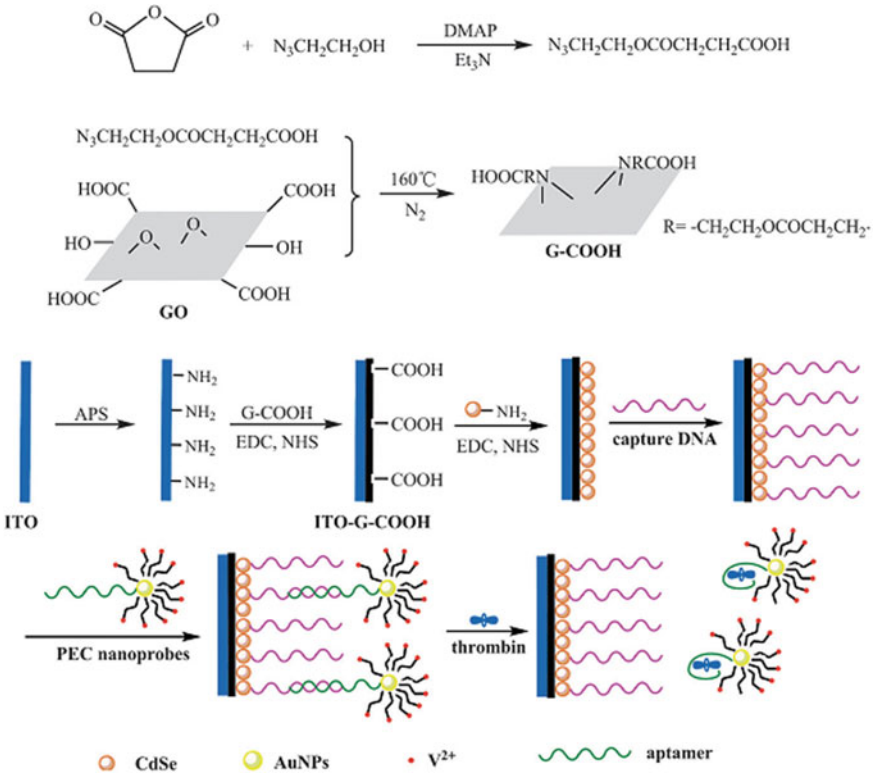

Fig. 8.11 Schematic diagram for preparation of carboxyl-functionalized graphene and the fabrication of amplified signal-on thrombin biosensor. Reproduced from Zhang et al. (2012) by permission of John Wiley & Sons Ltd.

of an aptamer with target thrombin led to the removement of nanoparticle and the restoration of the PEC signal (Fig. 8.11).

Li et al. developed visible-light induced PEC platform based on cyclometalated iridium(III) complex (Li et al. 2017a, b). $[(C6)_2Ir(dcbpy)]^+PF_6^-$ (C6 = coumarin 6, dcbpy = 2,2′-bipyridine-4,4-dicarboxylic acid) and P-DNA were assembled on the Au NPs to give nanoparticle probe, which contained a lot of PEC active species. Exo III cleavage led to target recycling and release of numerous secondary target fragment (T-DNA), which successively hybridized with the hairpin probe (HP3) on the electrode. Accordingly, signal nanoprobe was captured through hybridization of the released DNA fragment caged in HP3 with P-DNA attached to the Au NPs of nanoprobe, leading to a remarkable photocurrent response (see Fig. 8.12).

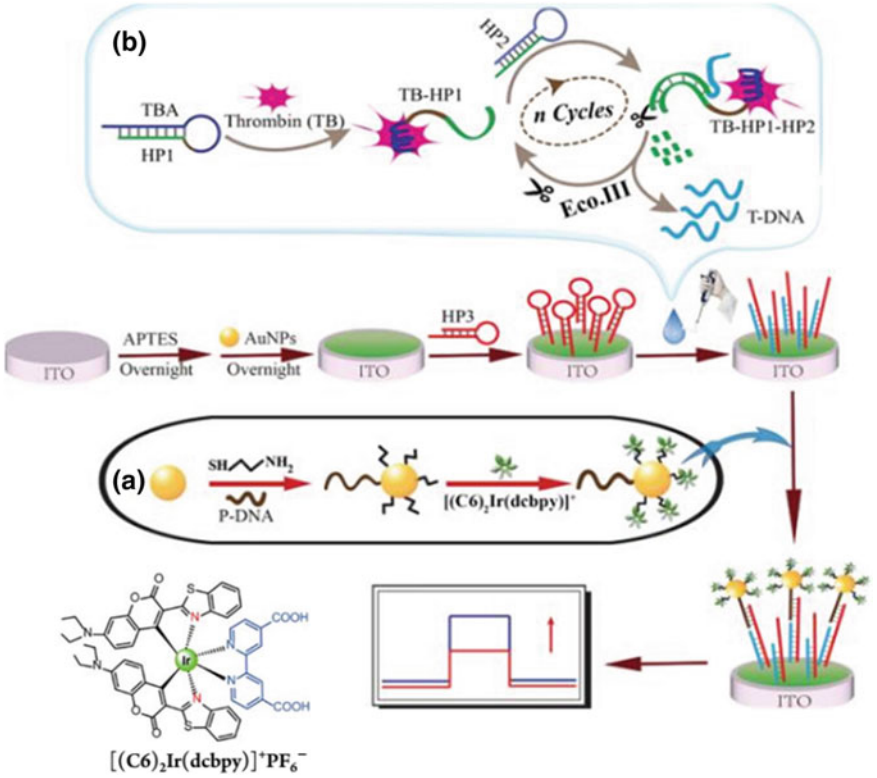

Fig. 8.12 Illustration of exonuclease III-assisted recycling amplification strategy for PEC detection of thrombin: **a** schematic preparation process of Au NPs nanoprobes and **b** schematic process of thrombin recognition and exonuclease III-assisted recycling amplification. Reprinted with the permission from Li et al. (2017a, b). Copyright 2011 American Chemical Society

DNA tetrahedron (TET) as an important kind of DNA nanostructures holds potential applications due to its easy preparation, structural stability, mechanical rigidity, and high loading capacity (Meng et al. 2016; Li et al. 2018b). Recently, Li's group (Li et al. 2018c) employed DNA TET as the nanocarrier to immobilize the photoactive material CdTe QDs and its signal enhancer methylene blue (MB) for forming the TET-QDs-MB complex as signal probe. Using this method, the loading capacity for CdTe QDs and MB was enhanced. At the same time, it could avoid direct modification of photoactive materials on sensing interface and produce a near-zero background noise to improve the sensitivity of this PEC biosensor (see Fig. 8.13).

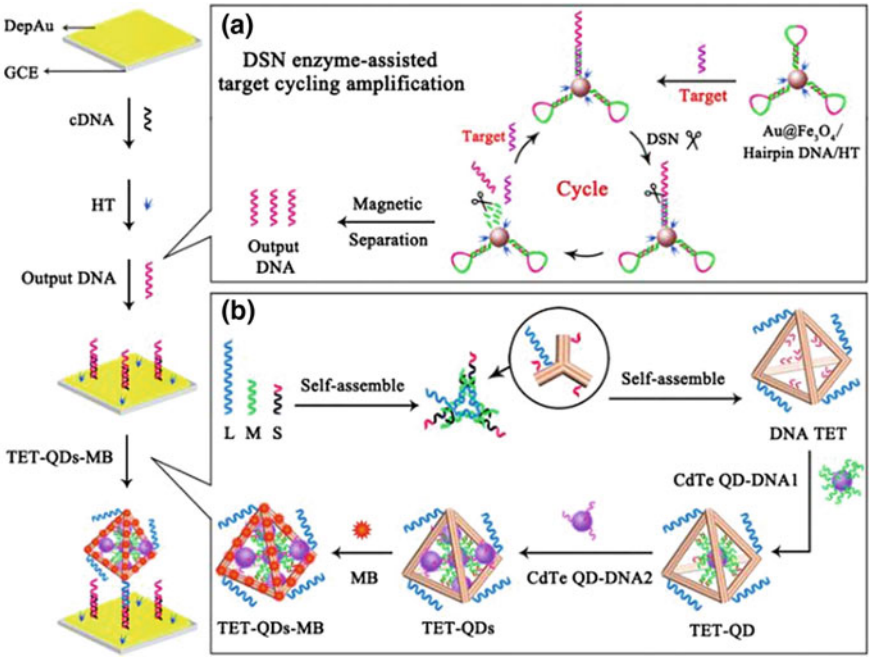

Fig. 8.13 Schematic diagrams of this proposed PEC biosensor for miRNA-141 determination. **a** DSN enzyme-assisted target cycling amplification strategy; **b** preparation of the DNA TET-CdTe QDs-MB complex. Reprinted with the permission from Li et al. (2018c). Copyright 2011 American Chemical Society

References

Arias AC, Mackenzie JD, Mcculloch I et al (2010) Materials and applications for large area electronics: solution-based approaches. Chem Rev 110:3–24

Bettazzi F, Palchetti I (2018) Photoelectrochemical genosensors for the determination of nucleic acid cancer biomarkers. Curr Opin Electrochem 12:51–59

Cha TG, Pan J, Chen HR et al (2015) Design principles of DNA enzyme-based walkers: translocation kinetics and photoregulation. J Am Chem Soc 137:9429–9437

Cheng LY, Zhou J, Zou Q et al (2012) A nanohybrid of graphene oxide–fluorescein derived silyl ether for photocurrent generation triggered by F^- ions. Rsc Adv 2:4623–4626

Da HM, Liu HY, Zheng YN et al (2018) A highly sensitive VEGF165 photoelectrochemical biosensor fabricated by assembly of aptamer bridged DNA networks. Biosens Bioelectron 101:213–218

Gong LS, Dai H, Zhang SP et al (2016) Silver iodide-chitosan nanotag induced biocatalytic precipitation for self-enhanced ultrasensitive photocathodic immunosensor. Anal Chem 88:5775–5782

Haddour N, Chauvin J, Gondran C et al (2006) Photoelectrochemical immunosensor for label-free detection and quantification of anti-cholera toxin antibody. J Am Chem Soc 128:9693–9698

Hagfeldt A, Boschloo G, Sun LC et al (2010) Dye-sensitized solar cells. Chem Rev 110:6595–6663

Hisatomi T, Kubota J, Domen K (2014) Recent advances in semiconductors for photocatalytic and photoelectrochemical water splitting. Chem Soc Rev 43:7520–7535

Hojeij M, Su B, Tan S et al (2008) Nanoporous photocathode and photoanode made by multilayer assembly of quantum dots. ACS Nano 2:984–992

Huang LJ, Zhang L, Yang L et al (2018a) Manganese porphyrin decorated on DNA networks as quencher and mimicking enzyme for construction of ultrasensitive photoelectrochemistry aptasensor. Biosens Bioelectron 104:21–26

Huang LG, Yang L, Zhu CC et al (2018b) Methylene blue sensitized photoelectrochemical biosensor with 3,4,9,10-perylene tetracarboxylic acidfilm as photoelectric material for highly sensitive Pb^{2+} detection. Sens Actuators B 274:458–463

Li MJ, Zheng YN, Liang WB et al (2016) An ultrasensitive "on-off-on" photoelectrochemical aptasensor based on signal amplification of a fullerene/CdTe quantum dots sensitized structure and efficient quenching by manganese porphyrin. Chem Commun 52:8138–8141

Li MJ, Zheng YN, Liang WB et al (2017a) Using p-type PbS quantum dots to quench photocurrent of fullerene-AuNP@MoS_2 composite structure for ultrasensitive photoelectrochemical detection of ATP. ACS Appl Mater Interfaces 9:42111–4212

Li CX, Lu WS, Zhu M et al (2017b) Development of visible-light induced photoelectrochemical platform based on cyclometalated iridium (III) complex for bioanalysis. Anal Chem 89:11098–11106

Li Y, Chen FT, Luan ZZ et al (2018a) A versatile cathodic "signal-on" photoelectrochemical platform based on a dual-signal amplification strategy. Biosens Bioelectron 119:63–69

Li C, Hu XL, Lu JY et al (2018b) Design of DNA nanostructure-based interfacial probes for the electrochemical detection of nucleic acids directly in whole blood. Chem Sci 9:979–984

Li MJ, Xiong C, Zheng YN et al (2018c) Ultrasensitive photoelectrochemical biosensor based on DNA tetrahedron as nanocarrier for efficient immobilization of CdTe QDs-methylene blue as signal probe with near-zero background noise. Anal Chem 90:8211–8216

Lv SZ, Zhang KY, Zeng YY et al (2018) Double photosystems-based 'Z-scheme' photoelectrochemical sensing mode for ultrasensitive detection of disease biomarker accompanying three-dimensional DNA walker. Anal Chem 90:7086–7093

Meng HM, Liu H, Kuai HL et al (2016) Aptamer-integrated DNA nanostructures for biosensing, bioimaging and cancer therapy. Chem Soc Rev 45:2583–2602

Qiu Z, Shu J, Tang D (2018) Near-infrared-to-ultraviolet light-mediated photoelectrochemical aptasensing platform for cancer biomarker based on core-shell NaYF4:Yb, Tm@TiO_2 upconversion microrods. Anal Chem 90:1021–1028

Qu YQ, Duan XF (2013) Progress, challenge and perspective of heterogeneous photocatalysts. Chem Soc Rev 42:2568–2580

Shen QM, Han L, Fan GH et al (2015) "Signal-on" photoelectrochemical biosensor for sensitive detection of human T-Cell lymphotropic virus type II DNA: dual signal amplification strategy integrating enzymatic amplification with terminal deoxynucleotidyl transferase-mediated extension. Anal Chem 87:4949–4956

Shen HJ, Wang YQ, Wang J et al (2018) Emerging biomimetic applications of DNA nanotechnology. ACS Appl Mater Interface. https://doi.org/10.1021/acsami.8b06175

Shi XM, Fan GC, Shen QM et al (2016) Photoelectrochemical DNA biosensor based on dual-signal amplification strategy integrating inorganic-organic nanocomposites sensitization with λ-exonuclease-assisted target recycling. ACS Appl Mater Interfaces 8:35091–35098

Shi XM, Fan GC, Tang X et al (2018) Ultrasensitive photoelectrochemical biosensor for the detection of HTLV-I DNA: a cascade signal amplification strategy integrating λ-exonuclease aided target recycling with hybridization chain reaction and enzyme catalysis. Biosens Bioelectron 109:190–196

Wang HH, Li MJ, Zheng YN et al (2018) An ultrasensitive photoelectrochemical biosensor based on [Ru(dcbpy)2dppz]2+/Rose Bengal dyes co-sensitized fullerene for DNA detection. Biosens Bioelectron 120:71–76

Willner I, Patolsky F, Wasserman J et al (2001) Photoelectrochemistry with controlled DNA-cross-linked CdS nanoparticle Arrays. Angew Chem Int Ed 40:1913–1916

Xiong EH, Yan XX, Zhang XH et al (2018) A new photoelectrochemical biosensor for ultrasensitive determination of nucleic acids based on a three-stage cascade signal amplification strategy. Analyst 143:2799–2806

Yan K, Wang R, Zhang JD et al (2014) A photoelectrochemical biosensor for o-aminophenol based on assembling of CdSe and DNA on TiO_2 film electrode. Biosens Bioelectron 53:301–304

Ye C, Wang MQ, Gao ZF et al (2016) Ligating dopamine as signal trigger onto the substrate via metal-catalyst-free click chemistry for "signal-on" photoelectrochemical sensing of ultralow MicroRNA levels. Anal Chem 88:11444–11449

Ye C, Wang MQ, Luo HQ et al (2017) Label-free photoelectrochemical "Off-On" platform coupled with G-wire-enhanced strategy for highly sensitive microRNA sensing in cancer cells. Anal Chem 89:11697–11702

Youngblood WJ, Lee SHA, Kobayashi Y et al (2009) Photoassisted overall water splitting in a visible light-absorbing dye-sensitized photoelectrochemical cell. J Am Chem Soc 131:926–927

Yu X, Wang Y, Chen X et al (2015) White-light-exciting, layer-by-layer-assembled ZnCdHgSe quantum dots/polymerized ionic liquid hybrid film for highly sensitive photoelectrochemical immunosensing of neuron specific enolase. Anal Chem 87:4237–4244

Zhang XR, Li SG, Jin X et al (2011) A new photoelectrochemical aptasensor for the detection of thrombin based on functionalized graphene and CdSe nanoparticles multilayers. Chem Commun 47(17):4929–4931

Zhang XR, Xu YP, Yang YQ et al (2012) A new signal-on photoelectrochemical biosensor based on a graphene/quantum-dot nanocomposite amplified by the dual-quenched effect of bipyridinium relay and AuNPs. Chem Eur J 18:16411–16418

Zhang XR, Guo YS, Liu MS et al (2013a) Photoelectrochemically active species and photoelectrochemical biosensors. Rsc Adv 3:2846–2857

Zhang XR, Xu YP, Zhao YQ et al (2013b) A new photoelectrochemical biosensors based on DNA conformational changes and isothermal circular strand-displacement polymerization reaction. Biosens Bioelectron 39:338–341

Zhang XR, Chen J, Liu HX et al (2015) Quartz crystal microbalance detection of protein amplified by nicked circling, rolling circle amplification and biocatalytic precipitation. Biosens Bioelectron 65:341–345

Zhang N, Zhang L, Ruan YF et al (2017) Quantum-dots-based photoelectrochemical bioanalysis highlighted with recent examples. Biosens Bioelectron 94:207–218

Zhang K, Lv S, Lu M et al (2018) Photoelectrochemical biosensing of disease marker on p-type Cu-doped Zn0.3Cd0.7S based on RCA and exonuclease III amplification. Biosens Bioelectron 117:590–596

Zhao WW, Dong XY, Wang J et al (2012a) Immunogold labeling-induced synergy effect for amplified photoelectrochemical immunoassay of prostate-specific antigen. Chem Commun 48:5253–5255

Zhao WW, Ma ZY, Yu PP et al (2012b) Highly sensitive photoelectrochemical immunoassay with enhanced amplification using horseradish peroxidase induced biocatalytic precipitation on a CdS quantum dots multilayer electrode. Anal Chem 84:917–923

Zhao WW, Shan S, Ma ZY et al (2013) Acetylcholine esterase antibodies on BiOI nanoflakes/TiO_2 nanoparticles electrode: a case of application for general photoelectrochemical enzymatic analysis. Anal Chem 85:11686–11690

Zhao WW, Xu JJ, Chen HY (2015a) Photoelectrochemical bioanalysis: the state of the art. Chem Soc Rev 46:729–741

Zhao YY, Chen F, Li Q et al (2015b) Isothermal amplification of nucleic acids. Chem Rev 115:12491–12545

Zhao Y, Tan L, Gao XS et al (2018) Silver nanoclusters-assisted ion-exchange reaction with CdTe quantum dots for photoelectrochemical detection of adenosine by target-triggering multiple-cycle amplification strategy. Biosens Bioelectron 110:239–245

Zheng YN, Liang WB, Xiong CY et al (2016) Self-enhanced ultrasensitive photoelectrochemical biosensor based on nanocapsule packaging both donor-acceptor-type photoactive material and its sensitizer. Anal Chem 88:8698–8705

Zheng YN, Liang WB, Xiong CY et al (2017) Universal ratiometric photoelectrochemical bioassay with target nucleotide transduction amplification and electron-transfer tunneling distance regulation strategies for ultrasensitive determination of microRNA in cells. Anal Chem 89:9445–9451

Zhuang JY, Lai WQ, Xu MD et al (2015) Plasmonic AuNP/gC_3N_4 nanohybrid-based photoelectrochemical sensing platform for ultrasensitive monitoring of polynucleotide kinase activity accompanying DNAzyme-catalyzed precipitation amplification. ACS Appl Mater Interfaces 7:8330–8338

Chapter 9
Nucleic Acid Amplification Strategy-Based Nanopore Sensors

Dongmei Xi and Min Liu

Abstract Nanopore sensing has developed into a powerful tool for single-molecule analysis in a rapid, low-cost, and label-free way. Generally, nanopores include biological nanopores, solid-state nanopores, and hybrid nanopores. Over the past two decades, nanopores have been used for a wide range of applications including gene sequencing and detection of various analytes. To improve the sensitivity of the nanopore sensors, signal amplification technologies, including isothermal amplification and thermocycling amplification, have been introduced into the nanopore system, although the reports are still rare. This chapter focuses on the combination of the signal amplification strategies and nanopore technique in the detection of various analytes.

9.1 Introduction

Biological cells utilize ion channels to gate the flow of ions across the cell membrane, maintain cell osmotic balance, and stabilize cell volume (Eisenberg 1998; Perozo et al. 2002). Inspired by this natural phenomenon, different biomimetic nanopores with different characteristics have emerged as an attractive, powerful, and sensitive single-molecule platform that has been used for a wide range of applications (Bayley and Cremer 2001; Pennisi 2014; Wanunu et al. 2009; Cao and Long 2018; Liu and Wu 2016; Long et al. 2018; Shang et al. 2018). Reported applications of these nanopores include rapid gene sequencing (Deamer et al. 2016; Branton et al. 2008; Cherf et al. 2012; Manrao et al. 2012) and the detection of various analytes such as metal ions (Braha et al. 2000; Wen et al. 2011), small molecules (Cao et al. 2014; Movileanu et al. 2003), DNA and microRNA (Xi et al. 2016; Liu et al. 2013a, b, c; Wanunu

D. Xi (✉) · M. Liu (✉)
Shandong Provincial Key Laboratory of Detection Technology for Tumour Markers, College of Chemistry and Chemical Engineering, Linyi University, Linyi 276005, Shandong, People's Republic of China
e-mail: dongmxi@126.com

M. Liu
e-mail: minliu548646@163.com

S. Zhang et al. (eds.), *Nucleic Acid Amplification Strategies for Biosensing, Bioimaging and Biomedicine*, https://doi.org/10.1007/978-981-13-7044-1_9

et al. 2010), peptides (Stefureac et al. 2012; Wang et al. 2013), and proteins (Bell and Keyser 2015; Kong et al. 2016; Zhou et al. 2016). As the key components of nanopore-based applications, nanopores can be broadly sorted into two categories, biological and solid state (Deng et al. 2015; Stoloff and Wanunu 2013; Zhang et al. 2016; Lindsay 2016; Haque et al. 2013; Shi et al. 2017). In general, the biological nanopores are nanoscale holes embedded in electrically insulating membranes (Cao and Long 2018; Schmidt et al. 2016; Göpfrich et al. 2016; Li et al. 2015), while the solid-state ones are tiny openings fabricated in thin inorganic or polymeric membranes (Wang et al. 2017; Buchsbaum et al. 2014; Zhang et al. 2017a, b; Liu et al. 2013a, b, c; Long et al. 2018). Both of these two types of nanopores have the ability to confine the target of interest in a nanoscale cavity. To combine merits from both the biological and solid-state nanopores, hybrid nanopore platforms have also been developed recently (Hall et al. 2010).

9.1.1 Biological Nanopores

By mimicking the functions of natural ion channels, α-hemolysin (α-HL) nanopore embedded in a lipid membrane was firstly fabricated that could monitor the transport of ions and small molecules through membranes (Kasianowicz et al. 1996). This protein pore has a cap domain with a large vestibule (with 2.6 nm opening and a wider 4.6 nm interior diameter) and a transmembrane β-barrel (with 5 nm length) (Song et al. 1996). Since the landmark demonstration of nucleotide detection with α-HL (Kasianowicz et al. 1996), nanopore sensors have been developed mainly for DNA sequencing (Laszlo et al. 2014; An et al. 2012; Deamer et al. 2016; Astier et al. 2016) and detection of a wide range of analytes (Xi et al. 2018; Shang et al. 2018; Bayley and Cremer 2001; Howorka and Siwy 2009; Cao and Long 2018; Ying et al. 2013). The principle of nanopore sensing relies on monitoring the ionic current fluctuation through nanopores (Liu and Wu 2016, Fig. 9.1). When an analyte binds within the nanopore, the ionic current will be modulated and current fluctuation events can be recorded. The current amplitude change and the dwell time of the events reveal the identity of the analyte, and the frequency of the events reveals its concentration.

To date, a variety of biological nanopores with various characteristics have been developed besides the widely used α-HL, including Mycobacterium smegmatis porin A (MspA) (Butler et al. 2008), aerolysin (Parker et al. 1994; Cao et al. 2016), Cytolysin A (ClyA) (Soskine et al. 2013), FhuA (Mohammad et al. 2012), bacteriophage phi29 motor protein (Wendell et al. 2009), and outer membrane protein G (OmpG) (Chen et al. 2008). Each protein pore has corresponding characteristics in terms of size, surface properties, and gating behaviors that can be separately exploited for different applications. Take the pore size (here, the pore size was defined as the narrowest constriction of the protein pores in their native forms) as an example, α-HL (~1.4 nm) (Song et al. 1996), MspA (~1.2 nm) (Faller 2004), OmpG (~1.3 nm) (Subbarao and Berg 2006), and aerolysin (~1.0 nm) (Parker et al. 1994; Degiacomi

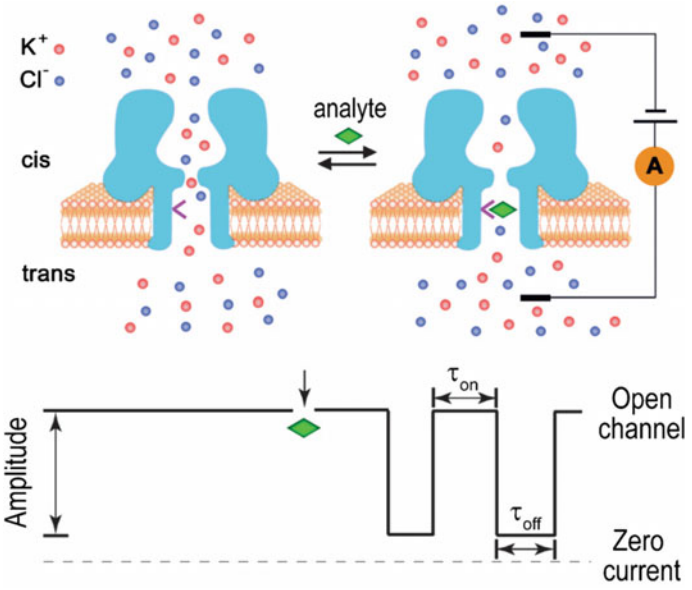

Fig. 9.1 Principle of nanopore sensing, top: reversible binding of the analyte (green rhomb) to a binding site (pink) inside the protein pore. Bottom: stochastic current trace showing blockade amplitude and duration, which allow identification of the analyte. Reproduced from Liu and Wu (2016) by permission of John Wiley & Sons Ltd.

et al. 2013) are more suitable for ssDNA translocation studies in their native, folded confirmations. ClyA (~3.3 nm) (Mueller et al. 2009) and phi29 motor (~3.6 nm) (Guasch et al. 2002), on the other hand, are large enough to allow the passage of dsDNA molecules.

To tune the functionality of the biological nanopores for specific applications, two common strategies have been employed in the nanopore sensing. The first one is to create sensing elements inside nanopores by site-directed mutagenesis and chemical modifications (Cheley et al. 2002; Wu and Bayley 2008). By introducing hydrophobic, aromatic, charged functional groups inside the nanopore, molecular recognition between nanopore and analytes could be adjusted. The second one is the utilization of molecular adapters, such as cyclic peptides (Sanchez-Quesada et al. 2000), cyclodextrins (Gu et al. 1999), and cucurbiturils (Braha et al. 2010), which could greatly enhance the identification of various analytes. For example, Bayley group has recently developed a truncated-barrel mutant (TBM) α-HL and incorporated CD adaptor molecule within the truncated pore for identification of four mononucleotides (Ayub et al. 2015). More precise mutations or modifications are expected to be employed in various biological nanopores in the coming research.

9.1.2 Solid Nanopores

Fabrication of solid-state nanopores with subnanometer control is another breakthrough in nanopore sensing. Those pores have the distinct feature of a wide range of possible diameters (1–100 nm). Generally, the principle of solid nanopore-based analysis can be described as follows: Analytes access or attach on the inner surface of a nanopore, change the effective diameter, or affect the charge transfer of the inner surface, leading to ionic current changes that can be detected (Liu et al. 2016a, b; Chen et al. 2013; Arjmandi-Tash et al. 2016).

To date, a variety of solid-state nanopore materials along with various fabrication approaches have been exploited. With synthetic membranes such as silicon nitride (SiNx) and silica (SiO_2), nanopores with diameters comparable to biological nanopores have been successfully fabricated via ion beam sculpting (Li et al. 2001) or electron beam lithography (Storm et al. 2003). Soon afterward, solid-state nanopores in porous polymer membranes fabricated via the track-etch technique (Li et al. 2004), alumina produced by the anodic oxidation method (Yuan et al. 2004), and block copolymer obtained by self-assembly of two or more chemically distinct polymer blocks (Noshay and McGrath 2013) have also been reported. Another attractive alternative is the direct fabrication of ultrathin pores within atomically thin membranes made from two-dimensional (2D) materials, including graphene (Garaj et al. 2010; Merchant et al. 2010; Fischbein and Drndic 2008), boron nitride (BN) (Liu et al. 2013a, b, c), molybdenum disulfide (MoS_2) (Liu et al. 2014), and hafnium oxide (HfO_2) (Larkin et al. 2013). Monolayers of 2D materials represent the thinnest materials with thickness comparable to the spacing between DNA bases, thus holding promise of superb spatial resolution. In recent years, glass nanopores fabricated by laser-assisted pulling have emerged as a cost-effective and versatile source of nanopores for single-molecule detection (Steinbock et al. 2010; Sze et al. 2017). They have a wide range of diameters, and a fast, cheap, and user-friendly fabrication process, drawing more and more researchers' attention. Long group has done a series of pioneering work with glass nanopore recently (Gao et al. 2018; Ying et al. 2018a, b). They have firstly used a two-step 3D fabrication process to develop a modified asymmetric glass nanopore electrode with a diameter down to 90 nm, which allowed for the detection of redox metabolism in living cells (Ying et al. 2018a, b).

Compared with the biological nanopore, the solid-state type possesses several unique advantages, including easy control over nanopore geometry and surface properties, superior thermal and chemical stability over a wide range of conditions (i.e., pH, temperature, concentration), as well as good compatibilities with existing semiconductor and microfluidics fabrication techniques (Siwy and Howorka 2010; Venkatesan 2011; Drndic 2014; Long et al. 2018). Up to now, solid nanopores have evolved into powerful tools with wide applications ranging from gene sequencing (Heerema and Dekker 2016; Feng et al. 2015) to stochastic sensing studies, such as detection of nucleic acids (Plesa et al. 2016; Zahid et al. 2016), proteins (Li et al. 2013; Wang et al. 2015), small molecules (Guo et al. 2015), and protein–DNA interactions (Marshall et al. 2015; Japrung et al. 2014). During the past several years,

intense efforts have been undertaken to improve the sensing performance of the solid nanopores. New pores are expected to be employed for nanopore sensing in the coming decades.

9.1.3 Hybrid Nanopores

To combine merits from both biological and solid-state nanopores and further expand the applications of nanopore sensing, increasing efforts have been put into the development of hybrid nanopore platforms. The first hybrid nanopore was created by Dekker, Bayley, and co-workers by inserting a single, preassembled α-HL protein pore into a SiNx pore (Hall et al. 2010). To guide entry of the α-HL pore into the SiNx pore in a specific orientation, a long dsDNA was tethered to the β-barrel of the α-HL to pull the protein pore into proper alignment as the DNA translocates the solid pore. Insertion of the dsDNA-conjugated α-HL pore was achieved through application of a potential across the SiNx membrane. In a novel design by Noy and co-workers, short carbon nanotubes (CNTs) can spontaneously insert into lipid bilayers and live cell membranes to form channels that exhibit a unitary conductance of 70–100 picosiemens under physiological conditions (Geng et al. 2014). Translocation of ssDNA through a CNT porin in the lipid bilayer has also been studied. Hybrid nanopore platforms possess the advantages of atomic-precision structural reproducibility and surface-modification adaptability of protein pores while also bypassing the instability of the lipid bilayer, and are expected to play increasing roles in nanopore sensing.

9.1.4 The Significance of the Combination of the Nanopore and Nucleic Acid Amplification Techniques

Ultrasensitive bioassays are fundamental to laboratory research, pharmacogenomics, and diagnosis of genetic or infectious disease. Up to now, a variety of nucleic acid amplification technologies have been developed for the fabrication of biosensors to improve the sensitivity. These amplification strategies can be grouped into two major categories, including isothermal amplification and thermocycling amplification. Many isothermal amplification strategies have been proposed utilizing rolling-circle amplification (RCA), enzyme-assisted cycling, strand-displacement amplification (SDA), helicase-dependent amplification (HDA), hybridization chain reaction (HCR), and loop-mediated isothermal amplification (LAMP), etc. Thermocycling amplification techniques include polymerase chain reaction (PCR) and ligase chain reaction (LCR). To improve the sensitivity of the nanopore sensors, some signal amplification technologies have been introduced into the nanopore system, although

the reports are still rare. This chapter focuses on the combination of the signal amplification strategies and nanopore technique in the detection of various analytes.

9.2 The Combination of Enzymatic Isothermal Amplification Reaction and Nanopore Sensors

9.2.1 Detection of Cancer Cells

Accurate diagnosis of cancer at its earliest stage is of importance to improve the cure rate. It has been demonstrated that cancer originating from genetic abnormalities can usually cause the affected cells to behave abnormally at molecular level. Different from normal cells, cancer cells have specific extracellular or intracellular biomarkers, and important cancer biomarkers would facilitate the monitoring of the biological processes associated with cancers. Therefore, the development of methods for selective and sensitive detection of cancer cells would greatly improve early diagnosis and prognosis of cancer.

Recently, our group present an ultrasensitive nanopore-based strategy for detection of Ramos cells (human Burkitt's lymphoma cells), by combining the enzymatic signal amplification with an aerolysin nanopore sensor (Xi et al. 2018). Aerolysin is a heptameric pore-forming toxin from *Aeromonas hydrophila*. It allows spontaneous insertion into the lipid bilayer leading to a nanoscale pore with diameter in a range from 1.0 to 1.7 nm (Tsitrin et al. 2002; Parker et al. 1994). Since its emergence as a nanopore to analyze the translocation of α-helix peptides through single pore (Radu et al. 2006), aerolysin has been applied to study the dynamics of proteins (Pastoriza-Gallego et al. 2011; Payet et al. 2012), oligosaccharides (Fennouri et al. 2012), and kinetics of enzymatic degradation (Fennouri et al. 2013). Recently, aerolysin was first utilized by Long group to discriminate oligonucleotides of different lengths, exhibiting impressive advantage in sensing nucleic acids (Cao et al. 2016). Despite its good performance, aerolysin has been utilized rarely in quantitative determination of the analytes. In our report, as shown in Fig. 9.2, a biotinylated aptamer of Ramos cells was first hybridized with a cDNA portion, and the obtained dsDNA was immobilized on a magnetic bead. Since the microbead–aptamer–cDNA complex was too large to enter the aerolysin, no transport events could be observed when the complex is subjected to a nanopore test. However, the addition of Ramos cells would result in the unfolding of the aptamer-cDNA duplex and cause the release of the cDNA, which subsequently triggers the enzymatic cycling amplification. This process ultimately produced a large number of outputs DNA, which could quantitatively produce characteristic current events when translocated through aerolysin. By introducing the signal amplification strategy into the nanopore sensor, the method exhibits excellent sensitivity, and Ramos cells with a number as low as five cells could be determined (Fig. 9.3). With good selectivity, the approach can further allow for the determination of cancer cells in human serum.

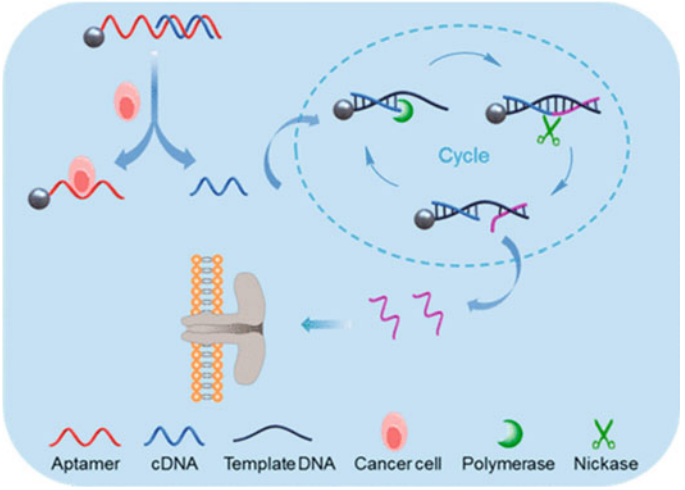

Fig. 9.2 Schematic representation of the cancer cell detection based on aptamer recognition and enzymatic cycling amplification with an aerolysin nanopore. Reprinted with the permission from Xi et al. (2018). Copyright 2018 American Chemical Society

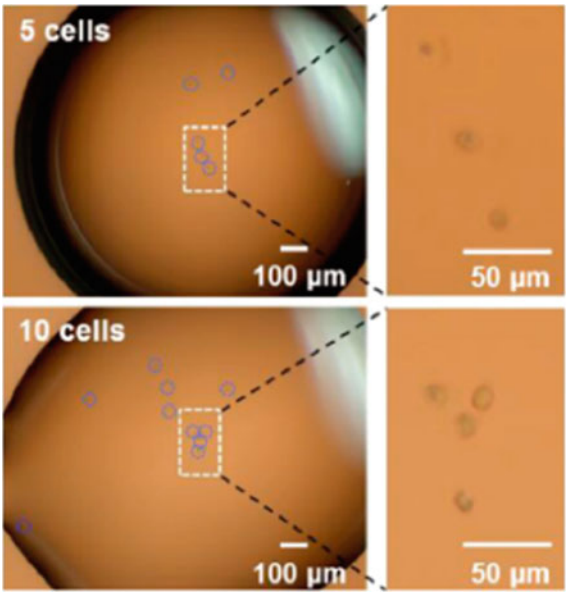

Fig. 9.3 Images of the five and ten cells obtained with the inverted fluorescence microscope. Reprinted with the permission from Xi et al. (2018). Copyright 2018 American Chemical Society

Compared with the conventional methods, this simple, label-free nanopore-based strategy opens a new horizon for the ultrasensitive detection of cancer cells, holding great promise for potential applications in early diagnosis of cancers. Meanwhile, this assay would open up a wide application of aerolysin to the quantitative determination of a variety of analytes.

9.2.2 Detection of MicroRNAs

MicroRNA (miRNA) is a group of short non-coding RNA molecules that can complement to a part of one or more messenger RNAs (mRNAs), thereby resulting in translational inhibition or degradation of mRNA, which eventually regulates gene expression. Aberrant expression of miRNAs has been found in various types of tumors, and different types of cancers have distinct miRNA profiles. Therefore, miRNAs can be used as a diagnostic biomarker to screen, monitor, or early diagnose cancer. However, because of their small size, highly homologous sequences, and low-level expression, accurate measurement of miRNAs remains a highly challenging task.

Recently, Kawano group reported a method for the detection of ultralow concentration miRNA by combining isothermal amplification and nanopore technology (Zhang et al. 2017a, b). Using miR-20a as the input and poly-thymines as the output molecules, the amplification system was constructed based on isothermal amplification (Hiratani et al. 2017; Zhang et al. 2014). Under asymmetric conditions, the amplified DNA at the concentration of 1 fM could be determined by α-HL nanopore (Fig. 9.4).

In addition, asymmetric nanopore detection for the polyT(20) generated by isothermal enzyme reaction in the presence of miR-20a was also realized. As shown in Fig. 9.5, DNA polyT(20) was transcribed and amplified at the concentrations of miR-20a ranging from 1 fM to 10 pM. The output polyT(20) could be measured and quantified by nanopore using the asymmetric solution method. So far, 1 fM of miRNA is the lowest concentration that can be detectable with nanopore. Based

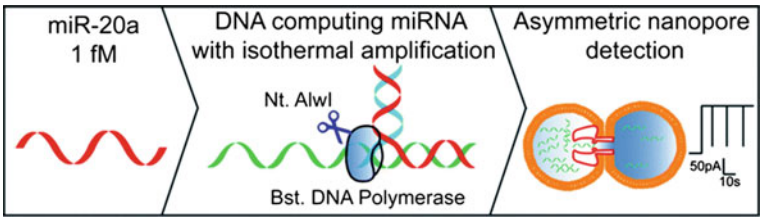

Fig. 9.4 Schematic diagram of miR-20a detection by isothermal amplification and asymmetric nanopore measurement. Reproduced from Zhang et al. (2017a, b) by permission of The Royal Society of Chemistry

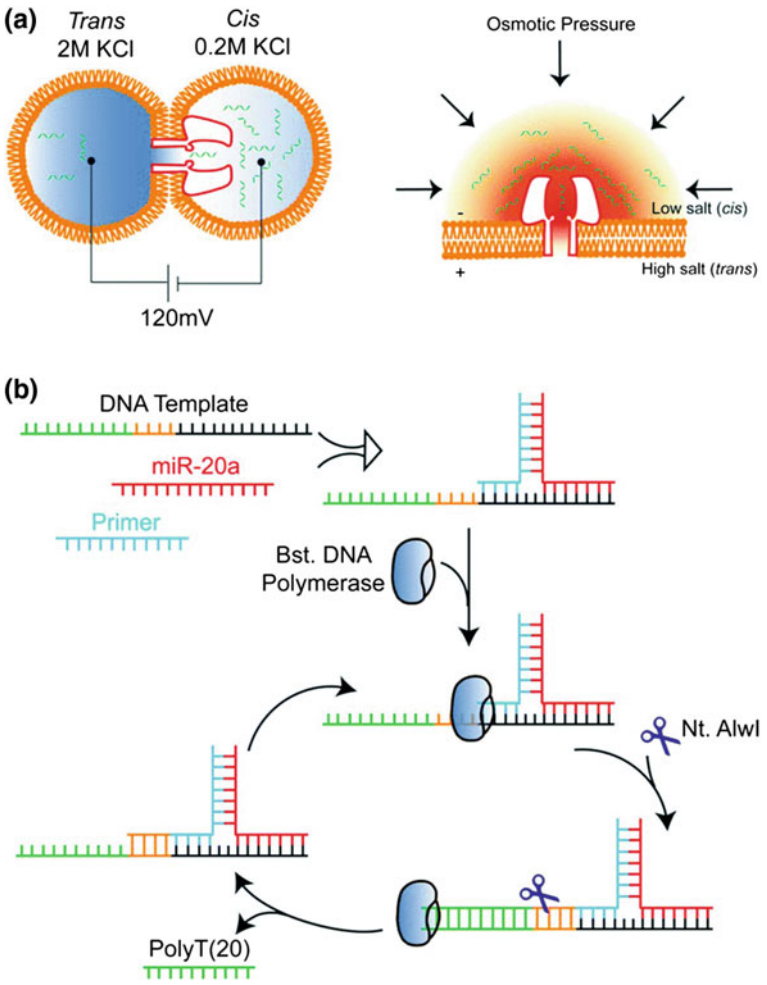

Fig. 9.5 **a** Schematic illustration of asymmetric nanopore detection for the generated PolyT(20). **b** Schematic illustration of PolyT(20) Generation by isothermal enzyme reaction in the presence of miR-20a. Reproduced from Zhang et al. (2017a, b) by permission of The Royal Society of Chemistry

on that, different miRNAs can be specifically amplified by simply changing the nucleotide sequence of the DNA template and the primer according to the target DNA. This is a promising method for the detection of ultralow concentrations of miRNAs with nanopore and can be used for the diagnosis of related diseases in which miRNA markers has been established.

Another report in Kawano's group presented an isothermal reaction amplification system that automatically produces large amounts of antisense DNA drugs after detecting miRNA in small-cell lung cancer (Hiratani et al. 2017). They also success-

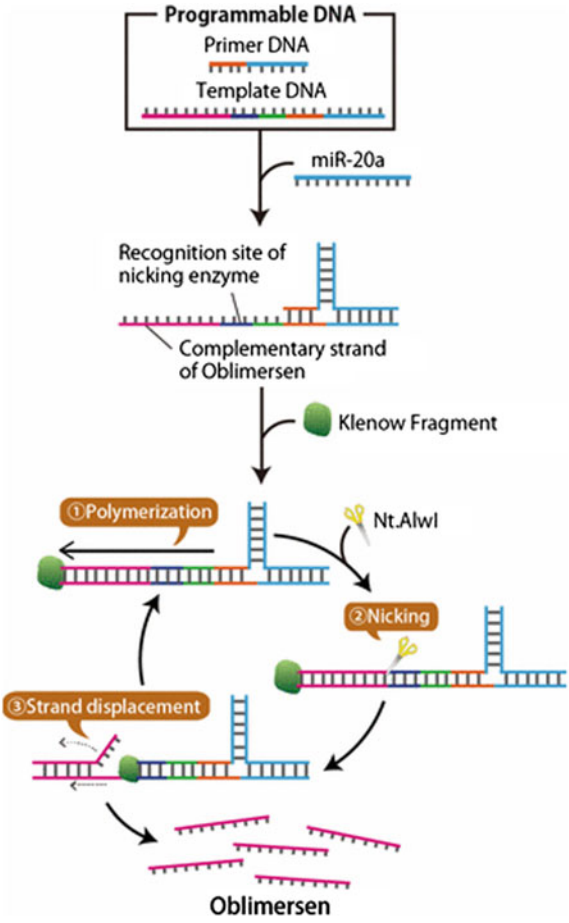

Fig. 9.6 Schematic illustration of miRNA detection and oblimersen generation. Reprinted with the permission from Hiratani et al. (2017). Copyright 2017 American Chemical Society

fully quantified the amount of the generated drug molecule by nanopore measurement with high accuracy. In detail, a DNA-strand polymerization reaction using a nicking endonuclease and DNA polymerase was selected (Komiya and Yamamura 2015). In order to achieve the autonomous amplification of oblimersen after discriminating miR-20a, an isothermal DNA reaction was carried out with enzymes and three-way junction (3WJ) structure (Fig. 9.6, Zhang et al. 2017a, b). Based on the amplification reaction, a theranostic system for small-cell lung cancer (SCLC) was constructed. The theranostic system and the model of oblimersen translocation through the α-HL nanopore are shown in Fig. 9.7. After isothermal amplification of miR-20a using a 3WJ structure, the antisense drug oblimersen could be amplified and the output molecule oblimersen was quantified with nanopore. Results indicated that more than 20-fold oblimersen was amplified from miR-20a, which meets the dosage requirement for SCLC therapy. This autonomous amplification strategy is an effective candidate for a wide range of theranostic with antisense oligonucleotides.

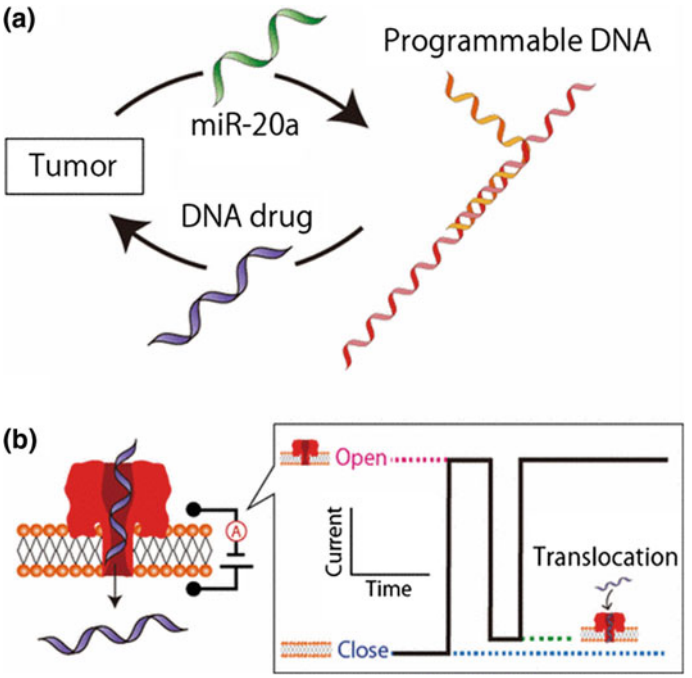

Fig. 9.7 **a** Schematic illustration of the theranostic system for small-cell lung cancer. **b** Schematic diagram of oblimersen translocation through the α-HL nanopore. Reprinted with the permission from Hiratani et al. (2017). Copyright 2017 American Chemical Society

9.3 The Combination of Hybridization Chain Reaction Amplification and Nanopore Sensors

A variety of solid-state nanopores have been exploited and utilized for detecting various targets. Among them, the porous anodized aluminum oxide (AAO) film possesses the advantages of uniform pore diameter, adjustability, high pore density, and close pore spacing (Lee and Park 2014), and has been used in nanopore sensing. In addition, the AAO nanopore membrane has a symmetrical cylindrical pore, so the ion current can be reduced by adjusting the pore size to study the development of biosensors. Recently, Zhao et al. designed target-triggered hybridization chain reaction amplification (HCR) on the surfaces of a highly efficient nanostructure assembly of AAO nanopore membrane, providing a simple, label-free, and sensitive nanopore biosensor for DNA detection (Zhao et al. 2017). In this work, HCR can efficiently assemble long dsDNA complexes on the surface of nanopore membranes, effectively reducing pore size and ionic current. Survivin mRNA was selected as a model target for its high expression in a variety of cancer cells. The analytical principle of the unlabeled nanopore biosensor was illustrated in Fig. 9.8. Compared with the traditional non-amplified nanopore biosensor, the detection sensitivity was signifi-

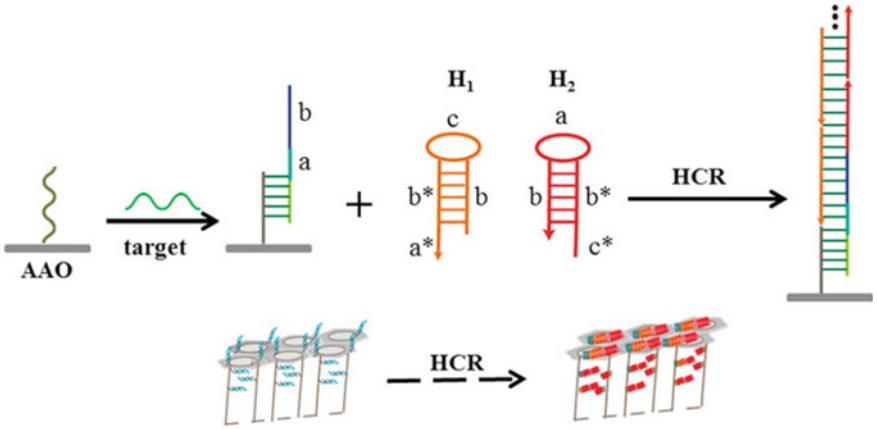

Fig. 9.8 Illustration of the HCR assembly on the surface of AAO nanopore membrane. Reprinted from Zhao et al. (2017). Copyright 2017, with permission from Elsevier

cantly improved by using large-size HCR products to enhance current blockage. This method exhibits desirable selectively and applicability in the detection of biological samples with surviving mRNA as a model target, and provides a new paradigm for unlabeled nucleic acid amplification strategies of ultrasensitive nanopore biosensors.

9.4 The Combination of Loop-Mediated Isothermal Amplification and Nanopore Sensors

Malaria is a mosquito infection caused by five protozoan parasites and is a serious public health problem in tropical and subtropical regions of the world. These parasites are dependent on the species of plasmodium and select appropriate antimalarial drugs based on accurate identification of pathogens. It is important to identify pathogens correctly before standard experience chemotherapy begins and after the initial diagnosis. Therefore, there is an urgent need for a simple molecular diagnostic method corresponding to the latest classification of Plasmodium to distinguish plasmodium.

The MinION™ nanopore sequencer is a pocket-sized and USB-connected portable real-time sequencer. It possesses the advantages of the portability, small platform, long reads, and real-time sequencing. In particular, sequence data can be made available in real time as they are generated, and MinION™ can be used in various clinical situations (Kugelman et al. 2015; Quick et al. 2016). In addition, loop-mediated isothermal amplification (LAMP) methods have already been used for the diagnoses of several infectious diseases in clinical, including malaria, and even in resource-limited areas, also are promising molecular technologies with high validity (Adams et al. 2014; Patel et al. 2013).

In the combination of LAMP and MinION™ nanopore sequencer, Imai et al. constructed a fast and easy diagnostic procedure for human malaria, and six species of Plasmodium were identified using this diagnostic procedure, including two P. ovale subspecies (Imai et al. 2017). Specifically, the LAMP method uses a set of four primers specially designed to recode six distinct sequences on the target DNA and relies on an automatic cycling process under isothermal conditions. In addition, the method enabled rapid library preparation (within 30 min), and the real-time sequencing data can be sequenced and analyzed by multiple sequencing and flow cytometry through the rapid barcode sequencing kit. Therefore, the MinION™ sequencer combined with the LAMP help to provide accurate diagnoses and appropriate treatments for malaria patients, and it also would be convenient used in a variety clinical setting.

9.5 The Combination of Rolling-Circle Amplification and Nanopore Sensors

Resistive pulse sensing (RPS) is a promising label-free alternative. The sensing principle is similar to the Coulter counter, and the sensor depends on the object passing through the nanopore from one compartment to another. A voltage applied between two electrolytic-filled compartments causes an ionic current between the compartments, which are temporarily blocked by particles passing through the pores. The amplitude of the current pulse event is proportional to the volume of the particle, while the width corresponds to the duration of the particle, which provides information about the charge, shape, or modification of the particle (Ito et al. 2003; Kececi et al. 2008; Roberts et al. 2010; Vogel et al. 2012). RPS nanoparticles can be used to distinguish DNA functionalized particles from unmodified particles (Roberts et al. 2010; Steinbock et al. 2009).

Recently, Kühnemund et al. proposed the concept of unlabeled digital quantification of rolling-circle amplification (RCA) products (RCPs) using RPS nanopore (Kühnemund and Nilsson 2014). In this design, DNA was captured on magnetic particles, targeted by a locked probe and amplified by RCA (Fig. 9.9a). Then the particles were measured one by one with RPS (Fig. 9.9b), and the particles with single attached RCPs were identified by their unique characteristics. To be more precise, the blockade magnitude, baseline duration, and full-width half-maximum were analyzed, and the particles with attached RCPs were allowed to be identified from the blank particles (Fig. 9.9c). The results showed the size distribution of RCA products, which was obtained for the first time by the method of true label-free size representation. This strategy can be used in the digitized quantization of DNA molecules with excellent sensitivity and can also be well applied to the portable, simple and inexpensive DNA sensing technology.

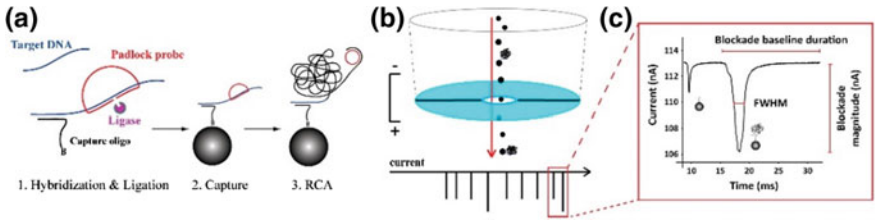

Fig. 9.9 Assay concept of the digital DNA quantification method using RCA on magnetic beads with RPS nanopore read out. Reprinted from Kühnemund and Nilsson (2014). Copyright 2014, with permission from Elsevier

9.6 The Combination of Polymerase Chain Reaction and Nanopore Sensors

DNA undergoes damage caused by oxidation, deamination, or alkylation, leading to the formation of various base lesions (Lonkar and Dedon 2011; Gates 2009; Cadet et al. 2014). The location of the modification occurring in the genome is critical because it enables understanding the origin of genetic mutations resulting from these lesions. Identification of the chemical identity and location of lesions is crucial for determining the molecular etiology of diseases. However, DNA lesions exist in low levels in the genome and cannot be amplified by standard PCR because they display both altered base pairing and are frequently pause or stop sites for polymerases.

Here, Riedl et al. presented a method for PCR amplification of lesion-containing DNA in which the site and identity could be marked, copied, and sequenced (Fig. 9.10, Riedl et al. 2015). In this report, the base excision repair (BER) pathway was used to yield gaps in DNA, and the nucleotides were inserted by passing the 'A rule'; these markers were exponential PCR amplification; the identity of the lesion was determined by the BER enzymes, avoiding lengthy synthesis of lesion-specific markers.

The key to this approach is the use of a marker nucleotide with a selective, complementary partner that allows for high-fidelity PCR amplification of the marked DNA. Herein, the dNaM or $dMMO_2$ nucleotides bases were selected to pair with d5SICS to form a set of unnatural base pairs (Fig. 9.11) (Malyshev et al. 2009; Seo et al. 2009). Sanger sequencing confirms the potential for this approach to locate lesions by marking, amplifying, and sequencing a lesion in the KRAS gene. Detection with the α-HL nanopore is realized to analyze the marker nucleotides in individual DNA strands with the potential to identify multiple lesions per strand. This newly developed nanopore sequencing method has great potential for detecting and sequencing non-native nucleotide that is currently only achievable by single-molecule real-time sequencing (SMRT).

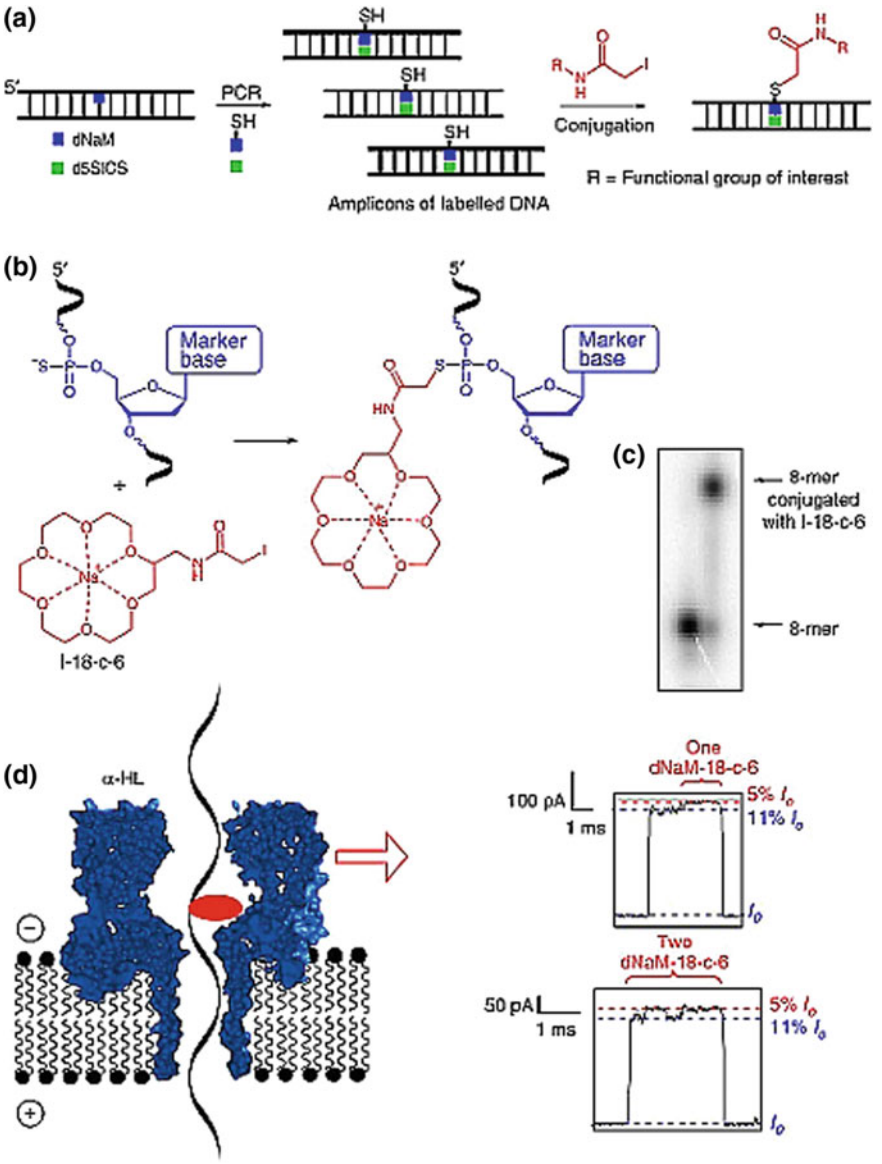

Fig. 9.10 New method for detection of marker nucleotides with the α-HL nanopore. **a** PCR amplification with $dNaM^{\alpha S}TP$ and labeling of DNA containing phosphorothioate by an iodoacetamide. **b** Reaction for phosphorothioate-containing DNA labeling by I-18-c-6. **c** Gel-shift analysis of labeled 8-mer by I-18-c-6 to confirm the reaction yield. **d** Translocation of DNA labeled by I-18-c-6 through the α-HL nanopore providing a modulation in the deep-blockage current level observed as the 11% Io signal decreasing to 5% Io that signals the presence of the crown ether and the marker nucleotide (i.e., Lesion). Reprinted by permission from Macmillan Publishers Ltd.: Riedl et al. (2015), copyright 2015

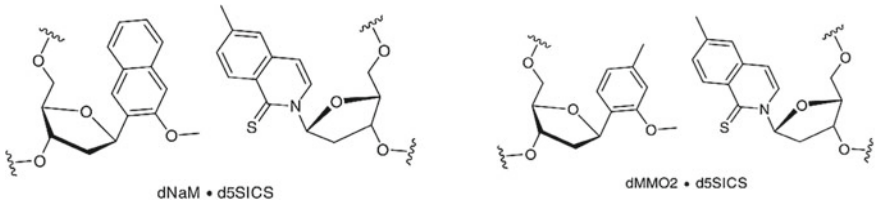

Fig. 9.11 Unnatural base pairs used for labeling of DNA lesions. The dNaM·d5SICS and $dMMO_2$·d5SICS unnatural base pairs utilized for labeling DNA lesions with a third, amplifiable marker base pair. Reprinted by permission from Macmillan Publishers Ltd.: Riedl et al. (2015), copyright 2015

9.7 Others

Besides the nucleic acid amplification strategies mentioned above, there are many other methods that have been used in nanopore sensing. Among which, the supersandwich structure is also a widely used signal amplification method. In particular, a highly efficient nanofluidic gating system was reported by Xia, Guo, and coworkers through inserting supersandwich structures into alumina nanopores (Jiang et al. 2012). It was found that the DNA supersandwich structures could reduce the effective diameter of the nanochannels through self-assembling into the alumina nanochannels, leading to the transformation of the open-to-close state of the nanopores. Through DNA-ATP-binding interactions, the close-to-open process of the nanopores would lead to the disassembly of the supersandwich structures (Fig. 9.12). This device could fulfill the logic operations, in which multiple signal probes assembled via multiple target DNAs, and then acted as a whole. The nanofluidic device enables built-in signal amplification for future nanofluidic biosensing and modular DNA computing on solid-state substrates.

In another report by Xia, Guo, and co-workers, a more complex DNA nanostructure was grafted onto the inner surface of the polyethylene terephthalate (PET) nanopores, with multiple target-binding sites on each of its long concatamers. However, the supersandwich structure in the PET nanopores contained only one target DNA, achieving a built-in signal amplification, which greatly lowers the detection limit (Fig. 9.13) (Liu et al. 2013a, b, c). In detail, this sensor was based on the self-assembly and disassembly of supramolecular DNA nanostructures in nanopores (two-way sensing), which turns off or on an intelligent nanofluidic switch, thus affecting the effective diameter of the nanopores. By coordinating the improved structure into the nanopores, a device for detecting subnanomolar DNA was designed. The nanofluidic sensing system possessed a high specificity for DNA analysis and high sensitivity with the detection limit of 10 fM. In addition, ATP aptamer sequence was introduced into the capture and signal probes, and enabled a sensitive measurement of ATP with the detection limit down to 1 nM. In the future, this sensing strategy may be developed into real-time detection approach for disease-related molecular

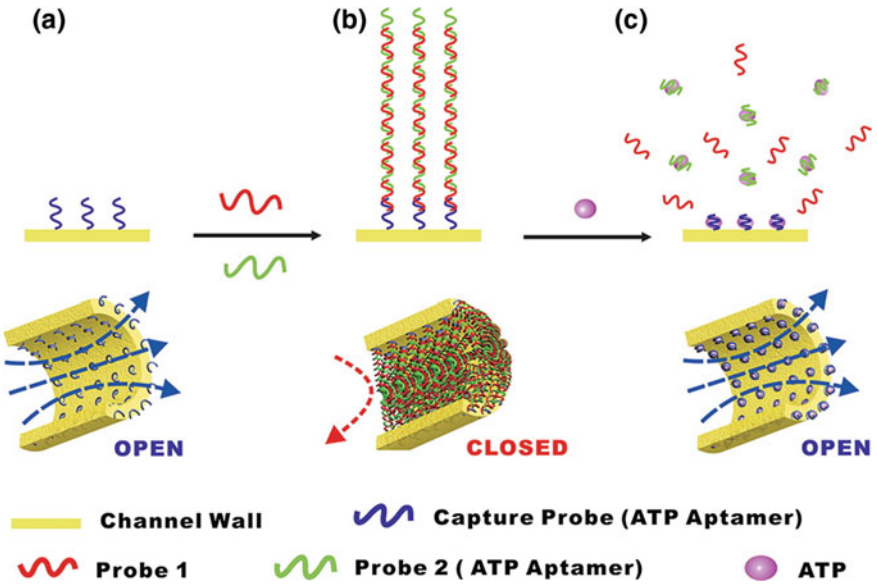

Fig. 9.12 Gating of alumina nanochannels by DNA supersandwich assemblies and ATP. The nanochannels are first modified with the capture DNA probes (**a**). The DNA supersandwich structures initiate from the immobilized capture probes and compose repeated units of partially hybridized DNA probes 1 and 2 (**b**). The formed long DNA concatamers efficiently block the pathway for ion transport across the nanochannels, yielding an extremely low conducting state. Since the capture probe and probe 2 contain an ATP-binding sequence (CCTGGGGGATATTGCGGAGGAAGG), the supersandwich structures are disassembled by ATP that reopens the conducting pathway (**c**). Reprinted with the permission from Jiang et al. (2012). Copyright 2012 American Chemical Society

targets, holding great potential for practical applications in biotechnology and life science.

Liu et al. also designed a nanopore platform for Zn^{2+} detection based on both DNA supersandwich and Zn^{2+}-requiring DNAzymes (Liu et al. 2016a, b). Due to the multiple amplification of nucleic acids, DNA supersandwich structures were formed and seriously blocked the nanopore. At the same time, DNA supersandwich structure was bound to the sessile probe (SP) of the substrate in the nanopore and was partially hybridized with DNAzymes. In the presence of Zn^{2+}, the Zn^{2+}-requiring DNAzyme dissected the SP into two fragments, while the DNA supersandwich structures were stripped and the ionic pathway was not obstructed. When the DNA supersandwich structure was decorated and stripped, a sharp drop appears in the I-V diagram and a continuous complete recovery of the current occurs (Fig. 9.14). In this system, the reliable detection limit of Zn^{2+} is as low as 1 nM. Discrimination between different types of ions (Cu^{2+}, Hg^{2+}, Pb^{2+}) was achieved.

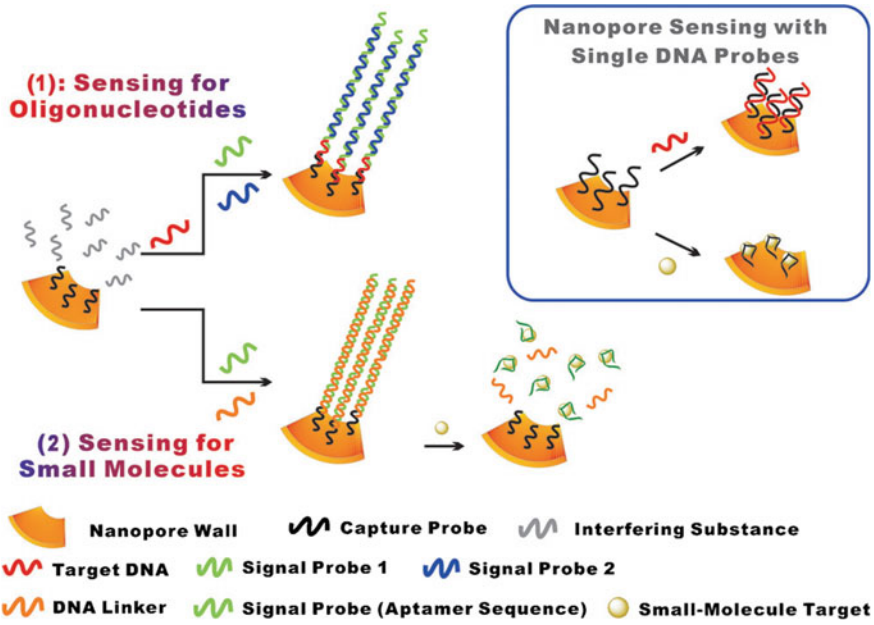

Fig. 9.13 In conventional DNA-based nanopore sensors, a single capture DNA hybridizes to a single target strand or binds to a single molecular target (inset). Here we improved this sensing strategy by integrating a more complex DNA nanostructure within the nanopores. To detect oligonucleotides (1), a capture probe (CP) is grafted onto the nanopores. When the target DNA is present, it is first captured by the CP. To amplify this hybridization event, repeated units of signal probes hybridize to each other from the free end of the target DNA, creating long concatamers (supersandwich). To detect small molecules (2), such as ATP, predesigned signal probes containing an aptamer sequence for ATP are used. The disassembly of the DNA nanostructures can therefore be used for sensing. Reproduced from Liu et al. (2013a, b, c) by permission of John Wiley & Sons Ltd.

9.8 Conclusion and Perspectives

In this chapter, we have summarized remarkable advances in the development of novel ultrasensitive nanopore sensors based on nucleic acid amplification strategies. Further construction of nucleic acid amplification reactions on smartly designed nanopore sensors will be widely applied in this rapidly evolving field. To date, however, the nanopore technology is still mainly used for in vitro detection, and the study on intracellular analysis is just the beginning. With the rapid development of pore materials and the continuous improvement of related instruments, combination of the nanopore technology and nucleic acid amplification strategies will play an important role in the field of cell analysis and even in vivo assay. This will not only promote the development of basic research, but is also expected to be applied in areas such as diagnosis of major diseases and personalized medicine.

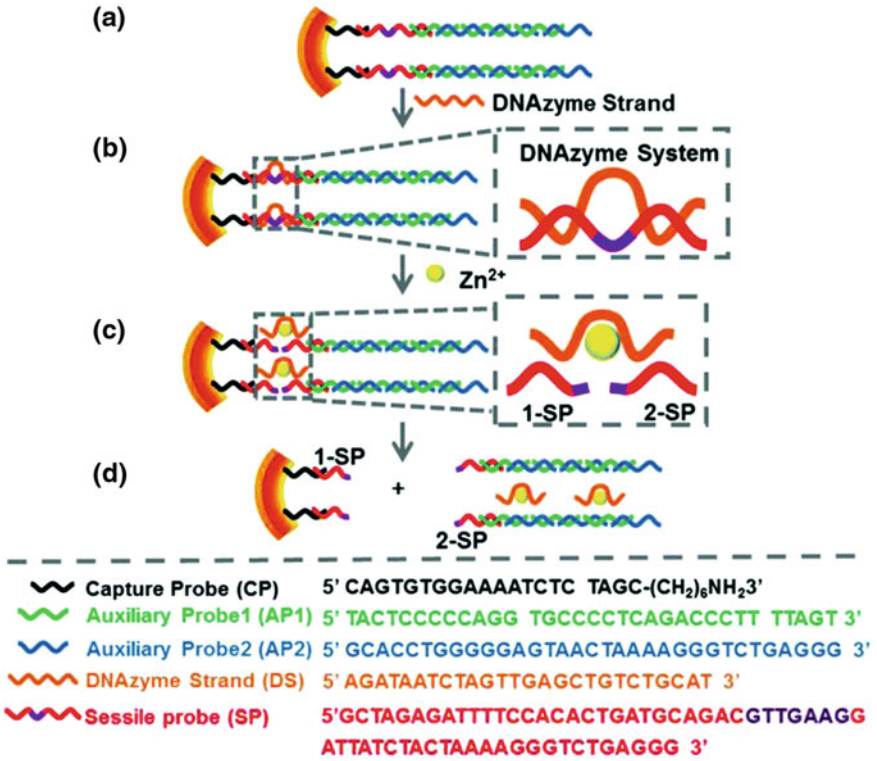

Fig. 9.14 Working mechanism of the Zn^{2+} detection in the nanopores based on DNA supersandwich structures and Zn^{2+}-requiring DNAzyme. **a** Formation of DNA supersandwich structures on the internal surface of nanopore by bridging of CPs and SPs of the substrate; **b** formation of DNAzyme system through partially hybridization between Zn^{2+}-requiring DNAzyme and SPs; **c** fragmentation of SPs into two parts in the presence of Zn^{2+}; **d** the peeling of DNA supersandwich structures from the internal surface of nanopores. All DNA sequences are listed. Reproduced from Liu et al. (2016a, b) by permission of The Royal Society of Chemistry

References

Adams ER, Gomez MA, Scheske L et al (2014) Sensitive diagnosis of cutaneous leishmaniasis by lesion swab sampling coupled to qPCR. Parasitology 141:1891–1897

An N, Fleming AM, White HS et al (2012) Crown ether-electrolyte interactions permit nanopore detection of individual DNA abasic sites in single molecules. Proc Natl Acad Sci USA 109(29):11504–11509

Arjmandi-Tash H, Belyaeva LA, Schneider GF (2016) Single molecule detection with graphene and other two-dimensional materials: nanopores and beyond. Chem Soc Rev 45:476–493

Astier Y, Braha O, Bayley H (2016) Toward single molecule DNA sequencing: direct identification of ribonucleoside and deoxyribonucleoside 5'-monophosphates by using an engineered protein nanopore equipped with a molecular adapter. J Am Chem Soc 128(5):1705–1710

Ayub M, Stoddart D, Bayley H (2015) Nucleobase recognition by truncated α-hemolysin pores. ACS Nano 9(8):7895–7903

Bayley H, Cremer PD (2001) Stochastic sensors inspired by biology. Nature 413(6852):226–230
Bell NA, Keyser UF (2015) Specific protein detection using designed DNA carriers and nanopores. J Am Chem Soc 137(5):2035–2041
Braha O, Gu LQ, Zhou L et al (2000) Simultaneous stochastic sensing of divalent metal ions. Nat Biotechnol 18(9):1005–1007
Braha O, Webb J, Gu LQ et al (2010) Carriers versus adapters in stochastic sensing. Chemphys Chem 6(5):889–892
Branton D, Deamer DW, Marziali A et al (2008) The potential and challenges of nanopore sequencing. Nat Biotechnol 26(10):1146–1153
Buchsbaum SF, Nguyen G, Howorka S et al (2014) DNA-modified polymer pores allow pH- and voltage-gated control of channel flux. J Am Chem Soc 136(28):9902–9905
Butler TZ, Pavlenok M, Derrington IM et al (2008) Single-molecule DNA detection with an engineered MspA protein nanopore. Proc Natl Acad Sci USA 105(52):20647–20652
Cadet J, Wagner JR, Shafirovich V et al (2014) One-electron oxidation reactions of purine and pyrimidine bases in cellular DNA. Int J Radiat Biol 90:423–432
Cao C, Long YT (2018) Biological Nanopores: Confined spaces for electrochemical single-molecule analysis. Acc Chem Res 51(2):331–341
Cao C, Ying YL, Gu Z et al (2014) Enhanced resolution of low molecular weight poly(ethylene glycol) in nanopore analysis. Anal Chem 86(24):11946–11950
Cao C, Ying YL, Hu ZL et al (2016) Discrimination of oligonucleotides of different lengths with a wild-type aerolysin nanopore. Nat Nanotechnol 11:713–718
Cheley S, Gu LQ, Bayley H (2002) Stochastic sensing of nanomolar inositol 1,4,5-trisphosphate with an engineered pore. Chem Biol 9(7):829–838
Chen M, Khalid S, Sansom MS et al (2008) Outer membrane protein G: engineering a quiet pore for biosensing. Proc Natl Acad Sci USA 105(17):6272–6277
Chen L, Si W, Zhang L et al (2013) Chiral selective transmembrane transport of amino acid through artificial channels. J Am Chem Soc 135(6):2152–2155
Cherf GM, Lieberman KR, Rashid H et al (2012) Automated forward and reverse ratcheting of DNA in a nanopore at 5-Å precision. Nat Biotechnol 30(4):344–348
Deamer D, Akeson M, Branton D (2016) Three decades of nanopore sequencing. Nat Biotechnol 34(5):518–524
Degiacomi MT, Iacovache I, Pernot L et al (2013) Molecular assembly of the aerolysin pore reveals a swirling membrane-insertion mechanism. Nat Chem Biol 9(10):623–629
Deng T, Li M, Wang Y et al (2015) Development of solid-state nanopore fabrication technologies. Sci Bull 60(3):304–319
Drndic M (2014) Sequencing with graphene pores. Nat Nanotechnol 9(10):743
Eisenberg B (1998) Ionic channels in biological membranes: natural nanotubes. Acc Chem Res 31(3):117–123
Faller M (2004) The structure of a mycobacterial outer-membrane channel. Science 303(5661):1189–1192
Feng J, Liu K, Bulushev RD et al (2015) Identification of single nucleotides in MoS_2 nanopores. Nat Nanotechnol 10(12):1070–1076
Fennouri A, Przybylski C, Pastoriza-Gallego M et al (2012) Single molecule detection of glycosaminoglycan hyaluronic acid oligosaccharides and depolymerization enzyme activity using a protein nanopore. ACS Nano 6(11):9672–9678
Fennouri A, Daniel R, Pastoriza-Gallego M et al (2013) Kinetics of enzymatic degradation of high molecular weight polysaccharides through a nanopore: experiments and data-modeling. Anal Chem 85(18):8488–8492
Fischbein MD, Drndic M (2008) Electron beam nanosculpting of suspended graphene sheets. Appl Phys Lett 93(11):113107
Gao R, Ying YL, Li YJ et al (2018) A 30 nm nanopore electrode: facile fabrication and direct insights into the intrinsic feature of single nanoparticle collisions. Angew Chem Int Ed 57(4):1011–1015

Garaj S, Hubbard W, Reina A et al (2010) Graphene as a subnanometre trans-electrode membrane. Nature 467(7312):190–193
Gates K (2009) An overview of chemical processes that damage cellular DNA: spontaneous hydrolysis, alkylation, and reactions with radicals. Chem Res Toxicol 22:1747–1760
Geng J, Kim K, Zhang J et al (2014) Stochastic transport through carbon nanotubes in lipid bilayers and live cell membranes. Nature 514(7524):612–615
Göpfrich K, Li CY, Mames I et al (2016) Ion channels made from a single membrane-spanning DNA duplex. Nano Lett 16(7):4665–4669
Gu LQ, Braha O, Conlan S et al (1999) Stochastic sensing of organic analytes by a pore-forming protein containing a molecular adapter. Nature 398(6729):686–690
Guasch A, Pous J, Ibarra B et al (2002) Detailed architecture of a DNA translocating machine: the high-resolution structure of the bacteriophage φ29 connector particle. J Mol Biol 315(4):670–676
Guo W, Hong F, Liu N et al (2015) Target-specific 3D DNA gatekeepers for biomimetic nanopores. Adv Mater 27(12):2090–2095
Hall AR, Scott A, Rotem D et al (2010) Hybrid pore formation by directed insertion of alpha hemolysin into solid-state nanopores. Nat Nanotechnol 5(12):874–877
Haque F, Li J, Wu HC et al (2013) Solid-state and biological nanopore for real-time sensing of single chemical and sequencing of DNA. Nano Today 8(1):56–74
Heerema SJ, Dekker C (2016) Graphene nanodevices for DNA sequencing. Nat Nanotechnol 11(2):127–136
Hiratani M, Ohara M, Kawano R (2017) Amplification and quantification of an antisense oligonucleotide from target microRNA using programmable DNA and a biological nanopore. Anal Chem 89(4):2312–2317
Howorka S, Siwy Z (2009) Nanopore analytics: sensing of single molecules. Chem Soc Rev 38:2360–2384
Imai K, Tarumoto N, Misawa K et al (2017) A novel diagnostic method for malaria using loop-mediated isothermal amplification (LAMP) and MinION™ nanopore sequencer. BMC Infect Dis 17(1):621
Ito T, Sun L, Crooks RM (2003) Simultaneous determination of the size and surface charge of individual nanoparticles using a carbon nanotube-based coulter counter. Ana Chem 75(10):2399–2406
Japrung D, Bahrami A, Nadzeyka A et al (2014) SSB Binding to single-stranded DNA probed using solid-state nanopore sensors. J Phys Chem B 118(40):11605–11612
Jiang Y, Liu N, Wei G et al (2012) Highly-efficient gating of solid-state nanochannels by DNA supersandwich structure containing ATP aptamers: a nanofluidic implication logic device. J Am Chem Soc 134(37):15395–15401
Kasianowicz JJ, Brandin E, Branton D et al (1996) Characterization of individual polynucleotide molecules using a membrane channel. Proc Natl Acad Sci USA 93(24):13770–13773
Kececi K, Sexton LT, Buyukserin F et al (2008) Resistive-pulse detection of short dsDNAs using a chemically functionalized conical nanopore sensor. Nanomedicine 3(6):787–796
Komiya K, Yamamura M (2015) Cascading DNA generation reaction for controlling DNA nanomachines at a physiological temperature. New Generat Comput 33(3):213–229
Kong J, Bell NA, Keyser UF (2016) Quantifying nanomolar protein concentrations using designed DNA carriers and solid-state nanopores. Nano Lett 16(6):3557–3562
Kugelman JR, Wiley MR, Mate S et al (2015) Monitoring of ebola virus makona evolution through establishment of advanced genomic capability in liberia. Emerg Infect Dis 21:1135–1143
Kühnemund M, Nilsson M (2014) Digital quantification of rolling circle amplified single DNA molecules in a resistive pulse sensing nanopore. Biosens Bioelectron 67:11–17
Larkin J, Henley R, Bell DC et al (2013) Slow DNA transport through nanopores in hafnium oxide membranes. ACS Nano 7(11):10121–10128
Laszlo AH, Derrington IM, Ross BC et al (2014) Decoding long nanopore sequencing reads of natural DNA. Nat Biotechnol 32(8):829–833

Lee W, Park SJ (2014) Porous anodic aluminum oxide: anodization and templated synthesis of functional nanostructures. Chem Rev 114(15):7487–7556
Li J, Stein D, McMullan C et al (2001) Ion-beam sculpting at nanometre length scales. Nature 412(6843):166–169
Li N, Yu S, Harrell CC et al (2004) Conical nanopore membranes. Preparation and transport properties. Anal Chem 76(7):2025–2030
Li W, Bell NAW, Hernández-Ainsa S et al (2013) Single protein molecule detection by glass nanopores. ACS Nano 7(5):4129–4134
Li T, Liu L, Li Y et al (2015) A universal strategy for aptamer-based nanopore sensing through host-guest interactions inside α-hemolysin. Angew Chem Int Ed 54(26):7568–7571
Lindsay S (2016) The promises and challenges of solid-state sequencing. Nat Nanotechnol 11(2):109–111
Liu L, Wu HC (2016) DNA-based nanopore sensing. Angew Chem Int Edit 55(49):15216–15222
Liu N, Jiang Y, Zhou Y et al (2013a) Two-way nanopore sensing of sequence-specific oligonucleotides and small-molecule targets in complex matrices using integrated DNA supersandwich structures. Angew Chem Int Edit 125(7):2061–2065
Liu L, Yang C, Zhao K et al (2013b) Ultrashort single-walled carbon nanotubes in a lipid bilayer as a new nanopore sensor. Nat Commun 4(1):2989–2997
Liu N, Jiang Y, Zhou Y et al (2013c) Two-way nanopore sensing of sequence-specific oligonucleotides and small-molecule targets in complex matrices using integrated DNA supersandwich structures. Angew Chem Int Edit 52(7):2007–2011
Liu K, Feng J, Kis A et al (2014) Atomically thin molybdenum disulfide nanopores with high sensitivity for DNA translocation. ACS Nano 8(3):2504–2511
Liu N, Yang Z, Ou X et al (2016a) Nanopore-based analysis of biochemical species. Microchim Acta 183(3):955–963
Liu N, Hou R, Gao P et al (2016b) Sensitive Zn^{2+} sensor based on biofunctionalized nanopores via combination of DNAzyme and DNA supersandwich structures. Analyst 141(12):3626–3629
Long Z, Zhan S, Gao P et al (2018) Recent advances in solid nanopore/channel analysis. Anal Chem 90(1):577–588
Lonkar P, Dedon PC (2011) Reactive species and DNA damage in chronic inflammation: reconciling chemical mechanisms and biological fates. Int J Cancer 128:1999–2009
Malyshev DA, Seo YJ, Ordoukhanian P et al (2009) PCR with an expanded genetic alphabet. J Am Chem Soc 131:14620–14621
Manrao EA, Derrington IM, Laszlo AH et al (2012) Reading DNA at single-nucleotide resolution with a mutant MspA nanopore and phi29 DNA polymerase. Nat Biotechnol 30(4):349–353
Marshall MM, Ruzicka J, Zahid OK et al (2015) Nanopore analysis of single-stranded binding protein interactions with DNA. Langmuir 31(15):4582–4588
Merchant CA, Healy K, Wanunu M et al (2010) DNA translocation through grapheme nanopores. Nano Lett 10:2915–2921
Mohammad MM, Iyer R, Howard KR et al (2012) Engineering a rigid protein tunnel for biomolecular detection. J Am Chem Soc 134(22):9521–9531
Movileanu L, Cheley S, Bayley H (2003) Partitioning of individual flexible polymers into a nanoscopic protein pore. Biophys J 85(2):897–910
Mueller M, Grauschopf U, Maier T et al (2009) The structure of a cytolytic [agr]-helical toxin pore reveals its assembly mechanism. Nature 459(7247):726–730
Noshay A, McGrath JE (2013) Block copolymers: overview and critical survey. Elsevier, New York
Parker MW, Buckley JT, Postma JP et al (1994) Structure of the aeromonas toxin proaerolysin in its water-soluble and membrane-channel states. Nature 367(6460):292–295
Pastoriza-Gallego M, Rabah L, Gibrat G et al (2011) Dynamics of unfolded protein transport through an aerolysin pore. J Am Chem Soc 133(9):2923–2931
Patel JC, Oberstaller J, Xayavong M et al (2013) Real-time loop-mediated isothermal amplification (RealAmp) for the species-specific identification of Plasmodium vivax. PLoS ONE 8:e54986

Payet L, Martinho M, Pastoriza-Gallego M et al (2012) Thermal unfolding of proteins probed at the single molecule level using nanopores. Anal Chem 84(9):4071–4076
Pennisi E (2014) DNA sequencers still waiting for the nanopore revolution. Science 343(6173):829–830
Perozo E, Cortes DM, Sompornpisut P et al (2002) Open channel structure of MscL and the gating mechanism of mechanosensitive channels. Nature 418(6901):942–948
Plesa C, Verschueren D, Pud S et al (2016) Direct observation of DNA knots using a solid-state nanopore. Nat Nanotechnol 153
Quick J, Loman NJ, Duraffour S et al (2016) Real-time, portable genome sequencing for Ebola surveillance. Nature 530:228–232
Radu S, Yi-Tao L, Heinz-Bernhard K et al (2006) Transport of alpha-helical peptides through alpha-hemolysin and aerolysin pores. Biochemistry 45(30):9172–9179
Riedl J, Yun D, Fleming AM et al (2015) Identification of DNA lesions using a third base pair for amplification and nanopore sequencing. Nat Commun 6:8807
Roberts GS, Kozak D, Anderson W et al (2010) Tunable nano/micropores for particle detection and discrimination: scanning ion occlusion spectroscopy. Small 6(23):2653–2658
Sanchez-Quesada J, Ghadiri MR, Bayley H et al (2000) Cyclic peptides as molecular adapters for a pore-forming protein. J Am Chem Soc 122(48):11757–11766
Schmidt J et al (2016) Membrane platforms for biological nanopore sensing and sequencing. Curr Opin Biotechnol 39(1):17–27
Seo YJ, Hwang GT, Ordoukhanian P et al (2009) Optimization of an unnatural base pair toward natural-like replication. J Am Chem Soc 131:3246–3252
Shang J, Li Z, Liu L et al (2018) Label-free sensing of human 8-oxoguanine DNA glycosylase activity with a nanopore. ACS Sensors 3(2):512–518
Shi W, Friedman AK, Baker LA (2017) Nanopore sensing. Anal Chem 89(1):157–188
Siwy ZS, Howorka S (2010) Engineered voltage-responsive nanopores. Chem Soc Rev 39(3):1115–1132
Song L, Hobaugh MR, Shustak C et al (1996) Structure of staphylococcal α-hemolysin, a heptameric transmembrane pore. Science 274(5294):1859–1866
Soskine M, Biesemans A, De Maeyer M et al (2013) Tuning the size and properties of ClyA nanopores assisted by directed evolution. J Am Chem Soc 135(36):13456–13463
Stefureac IR, Kachayev A, Lee SJ et al (2012) Modulation of the translocation of peptides through nanopores by the application of an AC electric field. Chem Commun 48(13):1928–1930
Steinbock LJ, Stober G, Keyser UF (2009) Sensing DNA-coatings of microparticles using micropipettes. Biosens Bioelectron 24(8):2423–2427
Steinbock LJ, Otto O, Chimerel C et al (2010) Detecting DNA folding with nanocapillaries. Nano Lett 10(7):2493–2497
Stoloff DH, Wanunu M (2013) Recent trends in nanopores for biotechnology. Curr Opin Biotechnol 24(4):699–704
Storm A, Chen J, Ling X et al (2003) Fabrication of solid-state nanopores with single-nanometre precision. Nat Mater 2(8):537–540
Subbarao GV, Berg BVD (2006) Crystal structure of the monomeric porin OmpG. J Mol Biol 360(4):750–759
Sze J, Ivanov AP, Cass A et al (2017) Single molecule multiplexed nanopore protein screening in human serum using aptamer modified DNA carriers. Nat Commun 8(1):1552
Tsitrin Y, Morton CJ, Elbez C et al (2002) Conversion of a transmembrane to a water-soluble protein complex by a single point mutation. Nat Struct Biol 9(10):729–733
Venkatesan BMK (2011) Solid-state nanopore sensors for nucleic acid analysis. Nat Nanotechnol 6(10):615–624
Vogel R, Anderson W, Eldridge J et al (2012) A variable pressure method for characterizing nanoparticle surface charge using pore sensors. Anal Chem 84(7):3125–3131
Wang HY, Gu Z, Cao C et al (2013) Analysis of a single α-synuclein fibrillation by the interaction with a protein nanopore. Anal Chem 85(17):8254–8261

Wang C, Fu Q, Wang X et al (2015) Atomic layer deposition modified track-etched conical nanochannels for protein sensing. Anal Chem 87(16):8227–8233
Wang R, Sun Y, Zhang F (2017) Temperature-sensitive artificial channels through pillar[5]arene-based host-guest interactions. Angew Chem Int Ed 56(19):5294–5298
Wanunu M, Sutin J, Meller A (2009) DNA profiling using solid-state nanopores: detection of DNA-binding molecules. Nano Lett 9(10):3498–3502
Wanunu M, Dadosh T, Ray V et al (2010) Rapid electronic detection of probe-specific microRNAs using thin nanopore sensors. Nat Nanotechnol 5(11):807–814
Wen S, Zeng T, Liu L et al (2011) Highly sensitive and selective DNA-based detection of mercury (II) with α-hemolysin nanopore. J Am Chem Soc 133(45):18312–18317
Wendell D, Jing P, Geng J et al (2009) Translocation of double stranded DNA through membrane adapted phi29 motor protein nanopore. Nat Biotechnol 4(11):765–772
Wu HC, Bayley H (2008) Single-molecule detection of nitrogen mustards by covalent reaction within a protein nanopore. J Am Chem Soc 130(21):6813–6819
Xi D, Shang J, Fan E et al (2016) Nanopore-based selective discrimination of microRNAs with single-nucleotide difference using locked nucleic acid-modified probes. Anal Chem 88(21):10540–10546
Xi D, Li Z, Liu L et al (2018) Ultrasensitive detection of cancer cells combining enzymatic signal amplification with an aerolysin nanopore. Anal Chem 90:1029–1034
Ying YL, Zhang J, Gao R et al (2013) Nanopore-based sequencing and detection of nucleic acids. Angew Chem Int Ed 52(50):13154–13161
Ying YL, Li YJ, Mei J et al (2018a) Manipulating and visualizing the dynamic aggregation-induced emission within a confined quartz nanopore. Nat Commun 9(1):3657
Ying YL, Hu YX, Gao R et al (2018b) Asymmetric nanopore electrode-based amplification for electron transfer imaging in live cells. J Am Chem Soc 140(16):5385–5392
Yuan J, He F, Sun D et al (2004) A simple method for preparation of through-hole porous anodic alumina membrane. Chem Mater 6(10):1841–1844
Zahid OK, Wang F, Ruzicka JA et al (2016) Sequence-specific recognition of microRNAs and other short nucleic acids with solid-state nanopores. Nano Lett 16:2033–2039
Zhang Q, Chen F, Xu F et al (2014) Target-triggered three-way junction structure and polymerase/nicking enzyme synergetic isothermal quadratic DNA machine for highly specific, one-step, and rapid microRNA detection at attomolar level. Anal Chem 86(16):8098–8105
Zhang H, Tian Y, Jiang L (2016) Fundamental studies and practical applications of bio-inspired smart solid-state nanopores and nanochannels. Nano Today 11(1):61–81
Zhang H, Hiratani M, Nagaoka K et al (2017a) MicroRNA detection at femtomolar concentrations with isothermal amplification and a biological nanopore. Nanoscale 9(42):16124–16128
Zhang Z, Sui X, Li P et al (2017b) Ultrathin and ion-selective janus membranes for high-performance osmotic energy conversion. J Am Chem Soc 139(26):8905–8914
Zhao T, Zhang HS, Tang H et al (2017) Nanopore biosensor for sensitive and label-free nucleic acid detection based on hybridization chain reaction amplification. Talanta 175:121–126
Zhou S, Wang L, Chen X et al (2016) Label-free nanopore single-molecule measurement of trypsin activity. ACS Sens 1(5):607–613

Chapter 10
Nucleic Acid Amplification Strategies Based on QCM

Lishang Liu

Abstract As a sensitive mass sensor, quartz crystal microbalance (QCM) has been applied in measurement of various phenomena such as deposition kinetics, cell growth, molecular recognition, chirality discrimination, environmental pollutant detection, cancer biomarker detection, conformational arrangement, and so on. Using a direct, no amplification QCM assay, nanomolar sensitivity of DNA is reported for analyte monitoring, whereas attomolar sensitivity has been reported for amplified detection. To analyze trace levels of small molecules of nucleic acid, several classical signal amplification strategies such as polymerase chain reaction (PCR) or hybridization chain reaction (HCR) via elongate DNA for improving the detection limit of QCM. Besides, particle conjugation, biocatalyzed precipitation, and surface crystallization have been employed for enhancing the sensitivity via mass amplification.

10.1 Introduction of QCM

Piezoelectric materials such as quartz can be used to detect mass change due to their piezoelectric properties. Quartz crystal microbalance (QCM) is an acoustic sensor composed of a piece of quartz crystal with gold electrodes on both of two sides. The quartz crystal can be properly cut and upon stimulation of alternative potential; the quartz vibrates at a resonant frequency infinitely. This frequency is very sensitive to the mass of the crystal and can be determined with very high precision. With materials deposited on the QCM gold surface, the resonant frequency varies according to the attachment's mass and physical property. The mass sensing ability of QCM is extremely sensitive, and the adsorbed mass at the QCM-surface can be detected down to a few ng/cm^2 by measuring the change of a quartz crystal resonator. With the capability of discriminating dissipation factor (D), a special QCM is called QCM-D. Information about the structure variation of the attached layer can be known

L. Liu (✉)
Shandong Provincial Key Laboratory of Detection Technology for Tumour Markers, College of Chemistry and Chemical Engineering, Linyi University, Linyi 276005, People's Republic of China
e-mail: liulishanghao@126.com

S. Zhang et al. (eds.), *Nucleic Acid Amplification Strategies for Biosensing, Bioimaging and Biomedicine*, https://doi.org/10.1007/978-981-13-7044-1_10

through dissipation factor. Attributed to its compatibility with essentially any type of substrate material QCM has become a versatile analyzing tool.

Without any disturbance, the quartz vibrates infinitely at a basic frequency. However, when the oscillation is disturbed by an adsorbed material, the oscillation wave propagation from the QCM surface varies with the properties of the adsorbed material. The frequency of the shear wave of the oscillating quartz crystal, called the resonant frequency, is linearly correlated with the rigid mass loading on the quartz surface, as described by Sauerbrey's equation for the idealized mode (Sauerbrey 1959):

$$\Delta f = -\frac{2f_0^2}{A\sqrt{\mu_q \rho_q}}\Delta m$$

where Δf_m is the resonant frequency shift due to the loaded mass on the sensor Δm, f_0 is the fundamental frequency of the resonator (9 MHz), A is the active area of the quartz crystal, called the electrode surface (0.2 cm^2), ρ_q is the density of the quartz crystal (2.648 g/cm^2), and μ_q is its shear modulus (2.947×10^{11} dyn/cm^2).

According to the above equation, the correlation between the frequency shift and the mass change of the QCM sensor is linear. Initially working as an ultrasensitive gravimetric balance, further, QCM technique draws substantial attention and has become one of the most important tools in fundamental surface science (Becker and Cooper 2011; Liu et al. 2017, 2019; Speight and Cooper 2012). Fluid-based QCM detection spans the nanomolar range: Nanomolar sensitivity of DNA is reported for continuous analyte monitoring using a direct, no amplification assay, whereas attomolar sensitivity has been reported for amplified detection. To analyze trace levels of small molecules, several classical signal amplification strategies have been employed for enhancing the sensitivity via mass amplification.

10.2 Nucleic Acid Amplification Based on QCM: RCA/HCR Strategy

Mass increment of DNA strand can be realized by rolling circle amplification (RCA), hybridized chain reaction (HCR), and bio-bar-code probe assemble and so on. This mass increment caused by target recognition can be used for signal amplification of QCM detection.

The QCM and surface plasmon resonance (SPR) sensing platforms are applied in a detection of human a-thrombin, a biomarker of blood block formation in tumor transfer (Falanga et al. 2015; Hao et al. 2017). Signal amplification was realized by combination of aptamer-based RCA and bio-bar-coded AuNP. The capture probe modified on gold ship surface contains aptamer part and primer part. Aptamer with a loop structure can recognize target specifically. The primer part can initiate the RCA process after its reconstruction followed target reorganization with aptamer.

The long sequences generated by RCA increase the mass sensed by QCM chip and realized signal amplification of thrombin recognition. For secondary signal amplification, AuNP labeled bio-bar-coded probes were introduced. A large amount of AuNP labeled bio-bar-coded probes were assembled on the RCA products and caused obvious mass increase; thus, the QCM detection signal of thrombin recognition was further enhanced (He et al. 2014).

A QCM measurement combined with surface plasmon resonance (SPR) is designed to detect DNA and lysozyme. RCA and template-enhanced hybridization processes (TEHP) amplified the signal of QCM measurement. After triggered by aptamer recognition of target molecule, the released complementary strand was used as the catalyst of template-enhanced hybridization processes (TEHP). The RCA reaction occurred with the assistance of DNAzyme. Biocatalytic precipitation (BCP) was stimulated by the horseradish peroxidase captured on electrode surface insoluble products on the electrode surface amplified the sensor response greatly. The detection scheme of lysozyme is presented in Fig. 10.3 (Sun et al. 2017).

A duplex formed after the aptamer S1 immobilized on magnetic beads hybridized with strand S2. With lysozyme binding with S1, DNA S2 (i.e., the target DNA) released spontaneously and triggered the TEHP. After TEHP, the RCA reaction was initiated and a long strand of DNA containing many repeat sequences was obtained. The biotinylated probe hybridized to repeat units and bind with the streptavidin-HRP In the presence of H_2O_2, the horseradish peroxidase-catalyzed oxidation of 4-chloro-1-naphthol occurred. Therefore, a large amount of precipitate deposited on the surface of QCM sensor and amplified the frequency shift obviously.

In HCR, with the presence of special sequence, two stable nucleotide with stem-loop structures hybridize with each other and further assemble to a nucleotide nanowire (Ge et al. 2014). Without the necessity of enzyme, the HCR has been applied in various amplification strategies (Fig. 10.1).

A QCM-D biosensing platform combining the amplification capability of self-assembled DNA nanostructures via HCR has been developed for nucleic acids detection (Tang et al. 2012). A most common genetic alteration in human cancers, p53 gene fragment was analyzed. The rationale of the DNA nanostructure amplified QCM-D biosensor for target p53 is shown in Fig. 10.4. The sequence of the capture probe immobilized on gold ship surface was designed precisely so that the initiator domain was protected by hairpin initially. The hybridization of target p53 with CP unfolded the closed CP hairpin to free the initiator domain. Due to the low mass of target p53, a very small signal of QCM was observed. As amplification strategy, two additional hairpins were added to facilitate cross-hybridization on the initiator domain and finally formed a one-dimensional helix nanosturcture. The frequency shift of QCM was significantly enlarged accompanied with a remarkable dissipation signal increase. The one-dimensional helix nanosturcture around 4 μm was observed clearly by AFM. The detection of p53 with a direct detection limit of 20 nM was successfully amplified by HCR with a detection limit of 0.1 nM.

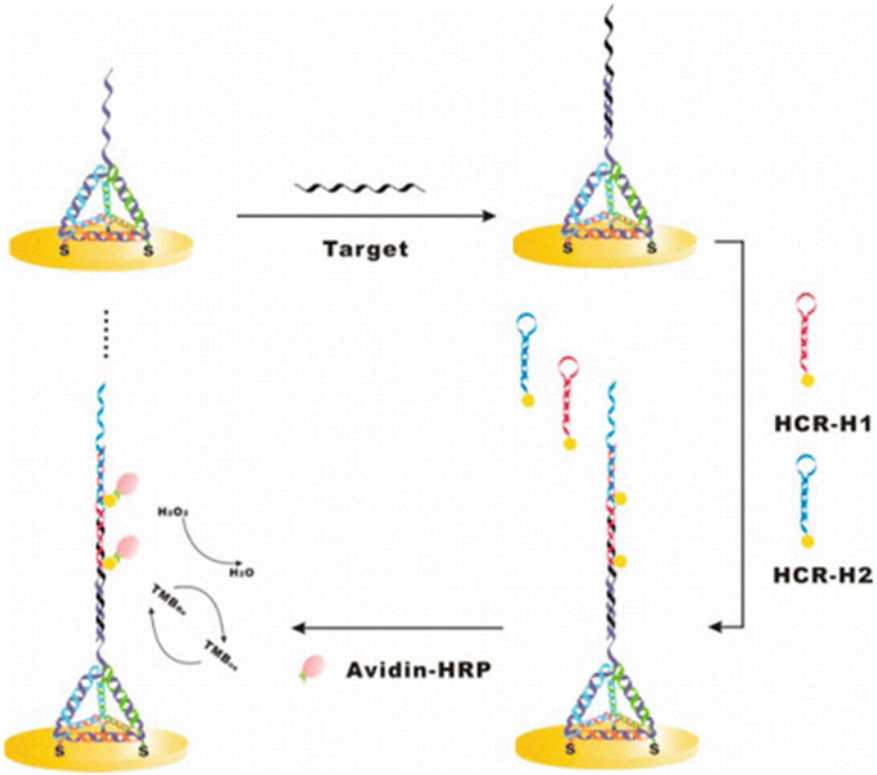

Fig. 10.1 Schematic illustration of DNA detection. Probes are immobilized on a 3D tetrahedral scaffold, and signal is amplified by hybridization chain reaction (HCR). Reprinted with the permission from Ge et al. (2014). Copyright 2014 American Chemical Society

10.3 Nucleic Acid Amplification Based on QCM: Biomolecule Conjugation Strategy

Liu et al. developed a target-triggered in situ layer-by-layer assembled DNA-streptavidin (SA) dendrimer nanostructure on the chip surface as an efficient mass amplifier (Zhao et al. 2015). They designed the two building blocks (DNA1-SA and DNA2-SA) for assembling the DNA-SA dendrimer nanostructure, which based on the fact that one SA molecule has four binding sites for coupling with the biotinylated single-strand DNA. They prepared the building block DNA1-SA by incubating a 30-nt linker DNA sequence and SA successively. The building block DNA2-SA was also prepared similarly. The model nucleic acid target, the 32-nt p53 gene fragment related to human cancers (abbreviated as target p53), was injected to hybridize with the hairpin capture probe on god chip. The closed hairpin was opened through a strand displacement process. The newly exposed sticky end of CP further binds with DNA1-SA. Sequentially, by alternately injecting DNA2-SA and DNA1-SA,

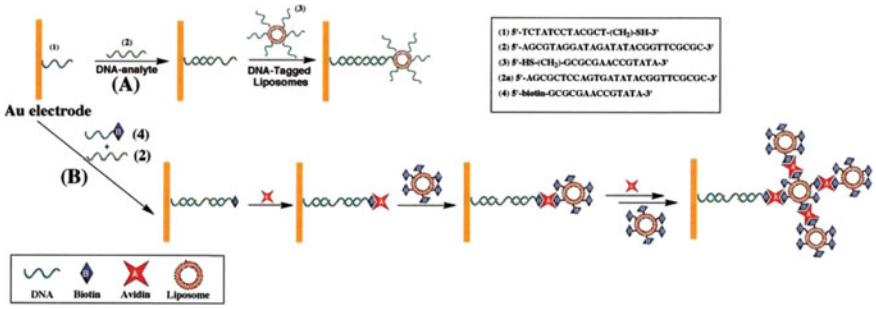

Fig. 10.2 Microgravimetric amplified assay of a target DNA by an oligonucleotide-functionalized liposome (**a**) and by an avidin/biotin-functionalized liposome (**b**). Reprinted with the permission from Patolsky et al. (2000). Copyright 2000 American Chemical Society

the layer-by-layer assembled DNA-SA dendrimer nanostructure is constructed on the chip surface in a simple and enzyme-free manner. The amplified frequency shift of the crystal chip as the output signal confirmed that the DNA-SA dendrimer nanostructure is an efficient mass amplifier. This novel sensing strategy integrates two advantages: (1) the target-triggered in situ layer-by-layer assembly of the DNA-SA dendrimer nanostructure is very simple and specific, which dramatically enhances sensitivity of the sensing platform, and (2) the QCM technique enables a label-free detection in real time. It is notable that both the assembly of DNA-SA dendrimer nanostructure and the sensing procedures here can be conducted facilely, with no need for complex separation processes or enzymatic reactions.

Taking the sequence of TS 4I-N gene in which mutations lead to Tay-Sachs genetic disorder as target, amplification of the oligonucleotide-DNA sensing processes by antibodies by QCM assay was reported by Bardea et al. (1998). Frequency shift of 2 Hz is observed for 0.6 μg/mL target DNA, achieving its detection limit. The association of anti-dsDNA antibody resulted in a frequency change of 14 Hz, and the further association of anti-mouse Fc-antibody (secondary antibody) resulted in a further decrease of 8 Hz.

The amplified oligonucleotide-DNA recognition of QCM using functionalized liposomes was realized by Patolsky et al. (2000). The oligonucleotide-tagged liposomes and biotin-tagged liposomes worked as amplifying probes with an impressive improved sensitivity (Fig. 10.2). The lower sensitivity limit for the detection of target DNA by amplification of oligonucleotide-tagged liposomes was estimated to be 5×10^{-12} M (Fig. 10.2b). A two-step amplification route was realized by applying biotinylated oligonucleotide, avidin, and biotin-tagged liposome (Fig. 10.2b). Using the two-step amplification route, the lower sensitivity limit for sensing of analyte DNA is 1×10^{-13} M.

10.4 Nucleic Acid Amplification Based on QCM: Nanoparticle Conjugation Strategy

Due to the unique chemical, optical, electrical, and biological properties, nanomaterials such as gold nanoparticles, magnetic beads, and quantum dots have been applied in many fields (Nam et al. 2003; Liu et al. 2009, 2010). Metal nanoparticles with big molecule weight can also be designed as mass amplifier for QCM sensing (Mo et al. 2005; Nie et al. 2007; Pang et al. 2007; Chen et al. 2010; Hao et al. 2011; Uludag and Tothill 2012).

A QCM sensor was developed by layer-by-layer assembly of mercaptopropionic acid, gold nanoparticle functionalized with polyethylene glycol (AuNPPEG), capture DNA, target BRCA1 DNA and DNA labeled with gold nanoparticle reporter on gold electrode (Rasheed and Sandhyarani 2015). Mercaptopropionic acid and functionalized gold nanoparticles ($AuNP_{PEG}$) were immobilized on the gold electrode surface (Au electrode) before the immobilization of DNA-c. The sensor relies on the hybridization of the probes with their complementary target immobilized on the electrode. The DNA probes are hybridized by "sandwich" hybridization scheme, which involves capture probe DNA on the $AuNP_{PEG}$ hybridize to one half of the target DNA and reporter probe DNA labeled with gold nanoparticles hybridize to the other half of target DNA. The highest sensitivity obtained for the sensor is greatly due to the presence of two gold nanoparticles in the sensor design.

Dengue virus is nowadays a most important arthropod-spread virus affecting human being. Dengue virus causes infections which resulted in clinical symptoms such as dengue fever dengue hemorrhagic fever and dengue shock syndrome and so on. Chen et al. developed a circulating-flow QCM detecting platform for dengue virus measurement (Chen et al. 2009). Two kinds of specific AuNP probes were designed and linked onto the QCM sensor surface to amplify the signal of target DNA. The AuNP probes used work as verifiers to specifically recognize target sequences and as amplifiers simultaneously.

Abdul et al. achieved a detection limit of 100 aM for the target BRCA1 gene using gold nanoparticle conjugated DNA-r in the traditional sandwich assay (Rasheed and Sandhyarani Abdul-Rasheed and Sandhyarani 2016). The gold nanoparticle clusters conjugated with DNA-r are used for the hybridization with target DNA. The hybridization of reporter probe DNA conjugated with AuNPC (DNA-AuNPC) with the target DNA (DNA-t) produces a large increase of mass on the surface even at ultralow concentration of DNA-t. A detection of 10 aM target DNA was achieved by the method.

10.5 Nucleic Acid Amplification Based on QCM: Metal Reduction Strategy

Because of its high electrical conductivity and excellent stability of AgNCs, DNA-templated deposition of AgNCs has large potential for biology, electricity, and other areas. The DNA-templated deposition of AgNCs is based on selective localization of silver ions along the DNA through Ag^+/Na^+ ion-exchange. Ag^+ ions are reduced by reducing agents to generate AgNCs. This method can be applied for signal amplification in QCM analysis. Zhou et al. reported a DNA QCM biosensor based on DNA templated in situ formation of AgNCs for signal amplification (Zhou et al. 2016).

AgNCs as the mass contribution amplifiers can be employed for enhancing detective sensitivity in the QCM biosensor (Fig. 10.3). A signal amplification strategy based on deposited-AgNCs along DNA combined with QCM biosensor was designed to highly sensitive detect nucleic acid. The target DNA was captured by the probe DNA-modified gold chip of QCM sensor, then silver cluster deposited along DNA to amplify the detecting signal of QCM. DNA-templated AgNCs based on selective localization of silver ions along the DNA through Ag^+/Na^+ ion exchange and AgNCs were then formed on the DNA skeleton by in situ chemical reduction of electrostatically absorbed Ag(I). They were characterized with TEM and AFM. The signal amplification protocol can be applied in straightforward and cost-effective detection of small molecule by QCM biosensor.

10.6 Nucleic Aid Amplification Based on QCM: Enzymatic Catalyzed Insoluble Deposition Strategy

It is reported that biocatalyzed precipitation on electronic transducers provides a means to amplify biochemical detection events as shown in Fig. 10.4 (Patolsky et al. 1999). Enzymes or oligonucleotides attached to electrodes or quartz crystals were found to act as sensitive sensing interfaces for the respective substrates or complementary DNA. Mass changes occurring on the crystal as a result of the biocatalyzed precipitation of an insoluble product are reflected by changes in the resonance frequency (Fig. 10.4). The biocatalytic precipitation of an insoluble product on the transducer provides an amplification route for the formation of the complex between the sensing interface and the mutant DNA.

The specific detection of DNA with single-base mismatch detection ability is a major challenge in DNA bioelectronics. Willner et al. reported on the amplified detection of a single-base mismatch in DNA by the polymerase-induced incorporation of a biotin-labeled base, complementary to the base mismatch. Coupling of an enzyme-avidin conjugate to the biotin label enabled the amplified detection of the mutant by the biocatalyzed precipitation of an insoluble product on the transducer. The method enabled the analysis of polymorphic blood samples with the ability to differentiate the homozygotic or heterozygotic genes from the normal gene. In another work, they

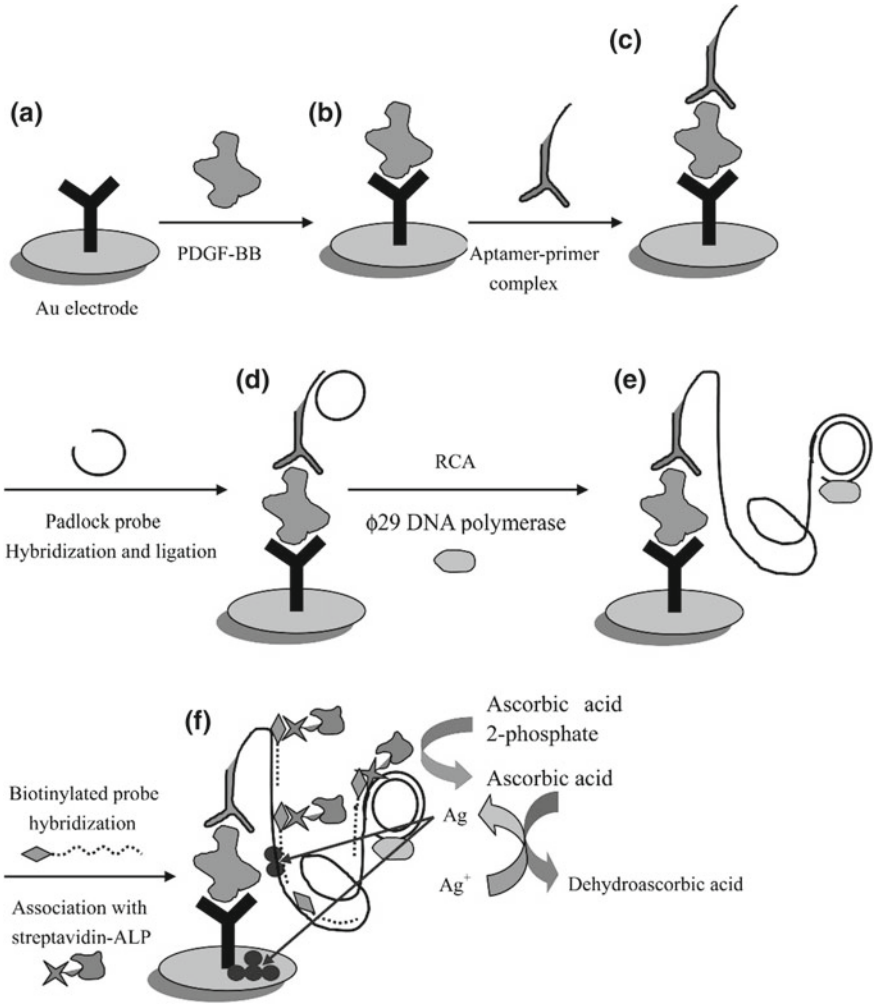

Fig. 10.3 Schematic outline of the aptamer-RCA immunosensor based on enzymatic silver deposition. Reprinted with the permission from Zhou et al. (2007). Copyright 2007 American Chemical Society

described three different methods to detect and amplify a single-base mismatch in a target DNA. They employed liposomes, Au-nanoparticles, or catalytic/biocatalytic components that chemically amplify the base mismatch recognition event.

The study has compared three different methods to detect and amplify a single-base mismatch in DNA (Willner et al. 2002). All methods are based on the polymerase I-induced coupling of a biotinylated base complementary to the mutation site and the subsequent detection of the biotin label in the hybrid assembly. Three methods are described to amplify the existence of the biotin label in the double-stranded assembly:

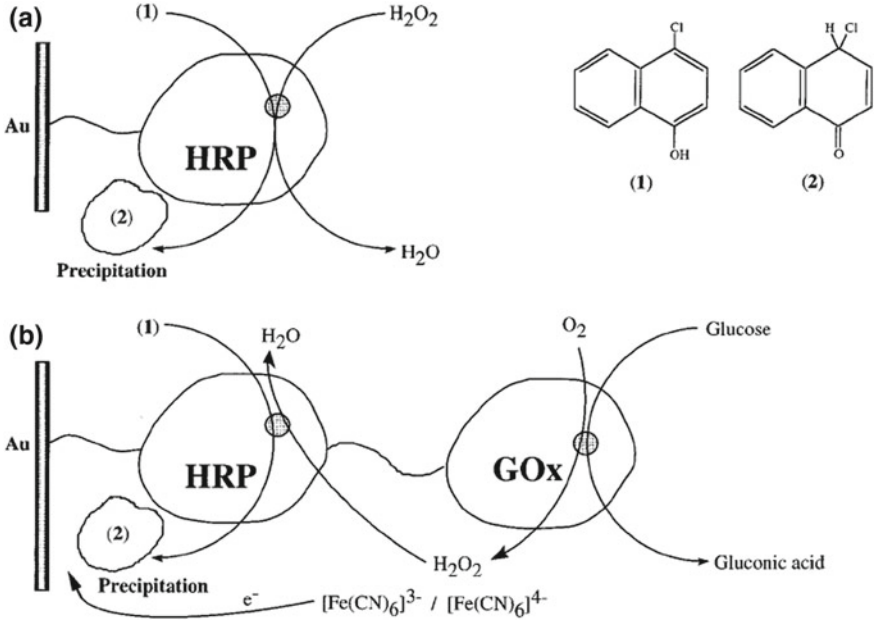

Fig. 10.4 Precipitation of the insoluble insulating material on QCM sensor surface. Reprinted with the permission from Patolsky et al. (1999). Copyright 1999 American Chemical Society

(i) the use of avidin- and biotin-labeled liposomes as a particulate amplifying unit; (ii) the use of avidin–alkaline phosphatase as a biocatalytic agent that generates an insoluble product on the piezoelectric crystal; and (iii) the use of an avidin-Au-nanoparticle conjugate that stimulates the catalyzed electroless deposition of gold. All the three methods lead to ultrasensitive tools for the detection of the mutant. Methods (i) and (ii) lead to a sensitivity limit in the range of 10^{-12}–10^{-13} M, whereas method (iii) leads to a record sensitivity of 3×10^{-16} M. The sensitivity reached by methods (i) and (ii) is clearly not optimized.

10.7 Amplification Based on QCM: In Situ Crystallization Strategy

The crystallization process has been reported to generate obvious frequency shift of QCM (Liu et al. 2013, 2015, 2016). Surface selective crystallization on gold surface can be realized by controlled self-assembled monolayers (SAMs) of ω-terminated alkanethiols ($HS(CH_2)nX$). Aizenberg et al. demonstrated that functional groups like –COOH and –OH can obviously enhance the $CaCO_3$ crystal growth, conversely, groups like $–CH_3$ and $–N(CH_3)_3$ can significantly inhibit crystal growth (Aizenberg

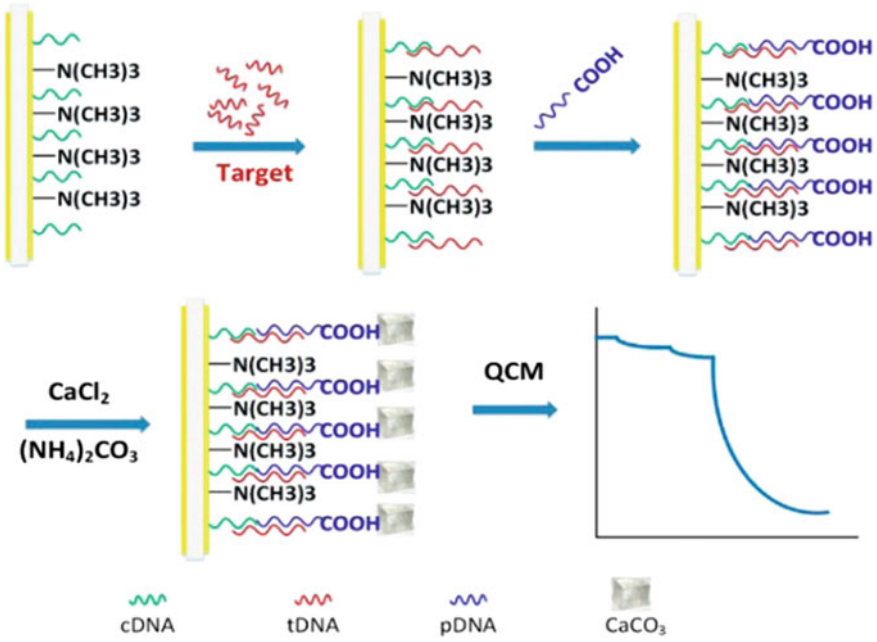

Fig. 10.5 DNA detection by in situ selective crystallization amplified QCM. Reprinted with the permission from Liu et al. (2017). Copyright 2017 American Chemical Society

et al. 1999a, b; Han and Aizenberg 2003; Kim et al. 2013). Combing the advantage of surface selective crystallization and the mass effect of $CaCO_3$, in situ selective nucleation could work as an effective signal amplification strategy for QCM to improve the detection sensitivity.

Liu et al. reported a novel method using in situ selective crystallization of $CaCO_3$ to improve the QCM sensitivity as a DNA sensor as shown in Fig. 10.5 (Liu et al. 2017). After the immobilization of DNAs (cDNA) on gold surface, a thiolate $–N(CH_3)_3$ was utilized instead of MCH and functioned as blocker of $CaCO_3$ nucleation. With the introduction of target DNA (tDNA), probe DNA (pDNA) labeled with –COOH hybridized on gold surface providing nucleation cites for $CaCO_3$. The –COOH group on gold surface captured Ca^{2+} and react with CO_2, realizing surface selective nucleation of $CaCO_3$ on sensor surface.

Significant frequency shift was observed when $CaCO_3$ nucleation took place. Frequency decreased more than 10,000 Hz after the crystallization amplification, which is thousands folds of the direct detection. With DNA of higher concentration, the crystals amount found on QCM sensor surface were also increase. A detection limit of 2 aM and a wide linear range from 10 aM to 1 nM are achieved for DNA.

Applying a DNA aptamer, cancer cells were also detected using the in situ crystallization amplification strategy as shown in Fig. 10.6. A limitation of 5 Ramos

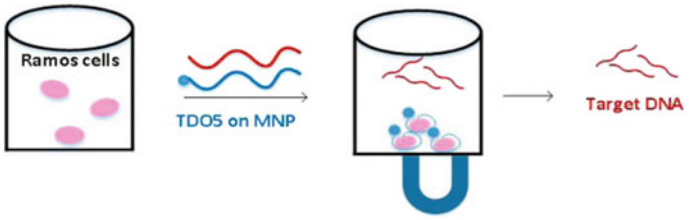

Fig. 10.6 Ramos cell detection by in situ selective crystallization amplified QCM. Reprinted with the permission from Liu et al. (2017). Copyright 2017 American Chemical Society

cells was achieved. The amplification strategy of in situ $CaCO_3$ crystallization is enzyme-free, straightforward, ultrasensitive, and selective.

10.8 Conclusion

Direct detection by QCM is limited by the sensitivity of QCM instrument. This chapter introduced several QCM signal enhance strategy based on mass amplification. The utilization of mass amplification strategy enhanced the detection sensitivity, lowered the detection limit, and expanded the scope of QCM application. The signal amplification strategy of QCM is mainly based on mass amplification include biomolecule conjugation, DNA polymerization hybridization, nanoparticle conjugation, enzymatic catalyzed insoluble deposition, metal reduction, and in situ crystallization and so on. The QCM-based detection strategies have the advantages of easy operation, high sensitivity, real-time detection, and so on. Along with the signal amplification strategy, the further cooperation of QCM with multiple platforms such as electrical station and SEM could provide multichannel information. Beside the broad application in quantitative assay, the QCM also has shown potential in detection of molecular interaction, structure transformation, visco-elasticity assay, and so on.

References

Abdul-Rasheed P, Sandhyarani N (2015) Attomolar detection of BRCA1 gene based on gold nanoparticle assisted signal amplification. Biosens Bioelectron 65:333–340

Abdul-Rasheed P, Sandhyarani N (2016) Quartz crystal microbalance genosensor for sequence specific detection of attomolar DNA targets. Anal Chim Acta 905:134–139

Aizenberg J, Black AJ, Whitesides GM (1999a) Control of crystal nucleation by patterned self-assembled monolayers. Nature 398(6727):495–498

Aizenberg J, Black AJ, Whitesides GM (1999b) Oriented growth of calcite controlled by self-assembled monolayers of functionalized alkanethiols supported on gold and silver. J Am Chem Soc 121(18):4500–4509

Bardea A, Dagan A, Ben-Dov I et al (1998) Amplified microgravimetric quartz-crystal-microbalance analyses of oligonucleotide complexes: a route to a Tay-Sachs biosensor device. Chem Commun 7:839–840

Becker B, Cooper MA (2011) A survey of the 2006–2009 quartz crystal microbalance biosensor literature. J Mol Recognit 24(5):754–787

Chen SH, Chuang YC, Lu YC et al (2009) A method of layer-by-layer gold nanoparticle hybridization in a quartz crystal microbalance DNA sensing system used to detect dengue virus. Nanotechnology 20(21):215501

Chen Q, Tang W, Wang D et al (2010) Amplified QCM-D biosensor for protein based on aptamer-functionalized gold nanoparticles. Biosens Bioelectron 26(2):575–579

Falanga A, Marchetti M, Verzeroli C et al (2015) Measurement of thrombin generation is a positive predictive biomarker of venous thromboembolism in metastatic cancer patients enrolled in the hypercan study. Blood 126(23):654

Ge Z, Lin M, Wang P et al (2014) Hybridization chain reaction amplification of MicroRNA detection with a tetrahedral DNA nanostructure-based electrochemical biosensor. Anal Chem 86(4):2124–2130

Han YJ, Aizenberg J (2003) Face-selective nucleation of calcite on self-assembled monolayers of alkanethiols: effect of the parity of the alkyl chain. Angew Chem Int Ed 42(31):3668–3670

Hao RZ, Song HB, Zuo GM et al (2011) DNA probe functionalized QCM biosensor based on gold nanoparticle amplification for Bacillus anthracis detection. Biosens Bioelectron 26(8):3398–3404

Hao T, Wu X, Xu L et al (2017) Ultrasensitive Detection of prostate-specific antigen and thrombin based on gold-upconversion nanoparticle assembled pyramids. Small 13(19):1603944

He P, Liu L, Qiao W et al (2014) Ultrasensitive detection of thrombin using surface plasmon resonance and quartz crystal microbalance sensors by aptamer-based rolling circle amplification and nanoparticle signal enhancement. Chem Commun 50(12):1481–1484

Kim P, Kreder MJ, Alvarenga J et al (2013) Hierarchical or not? effect of the length scale and hierarchy of the surface roughness on omniphobicity of lubricant-infused substrates. Nano Lett 13(4):1793–1799

Liu GD, Mao X, Phillips JA et al (2009) Aptamer-nanoparticle strip biosensor for sensitive detection of cancer cells. Anal Chem 81(24):10013–10018

Liu LS, Liu HN, Li S et al (2010) Fabrication and characterization of streptavidin gamma-Fe_2O_3@Au nanocomposites for biological application. Acta Chim Sin 68(20):2041–2046

Liu LS, Kim J, Chang SM et al (2013) Quartz crystal microbalance technique for analysis of cooling crystallization. Anal Chem 85(9):4790–4796

Liu LS, Kim JM, Kim WS (2015) Simple and reliable quartz crystal microbalance technique for determination of solubility by cooling and heating solution. Anal Chem 87(6):3329–3335

Liu LS, Kim JM, Kim WS (2016) Quartz crystal microbalance technique for in situ analysis of supersaturation in cooling crystallization. Anal Chem 88(11):5718–5724

Liu LS, Wu C, Zhang S (2017) Ultrasensitive detection of DNA and ramos cell using in situ selective crystallization based quartz crystal microbalance. Anal Chem 89(7):4309–4313

Liu LS, Jiang Y, Li XM et al (2019) The application of signal amplification strategies based on QCM in the detection of tumor marker. Sci Sin Chim 2:276–284

Mo Z, Wang H, Liang Y et al (2005) Highly reproducible hybridization assay of zeptomole DNA based on adsorption of nanoparticle-bioconjugate. Analyst 130(12):1589–1594

Nam JM, Thaxton CS, Mirkin CA (2003) Nanoparticle-based bio-bar codes for the ultrasensitive detection of proteins. Science 301(5641):1884–1886

Nie LB, Yang Y, Li S et al (2007) Enhanced DNA detection based on the amplification of gold nanoparticles using quartz crystal microbalance. Nanotechnology 18(30):305501

Pang LL, Li JS, Jiang JH et al (2007) A novel detection method for DNA point mutation using QCM based on Fe3O4/Au core/shell nanoparticle and DNA ligase reaction. Sens Actuators B-Chem 127(2):311–316

Patolsky F, Zayats M, Katz E et al (1999) Precipitation of an insoluble product on enzyme monolayer electrodes for biosensor applications: characterization by faradaic impedance spectroscopy,

cyclic voltammetry, and microgravimetric quartz crystal microbalance analyses. Anal Chem 71(15):3171–3180

Patolsky F, Lichtenstein A, Willner I (2000) Amplified microgravimetric quartz-crystal-microbalance assay of DNA using oligonucleotide-functionalized liposomes or biotinylated liposomes. J Am Chem Soc 122(2):418–419

Sauerbrey GZ (1959) The use of quartz oscillators for weighing thin films and for microweighing. Z Phys 155:206–222

Speight RE, Cooper MA (2012) A survey of the 2010 quartz crystal microbalance literature. J Mol Recognit 25(9):451–473

Sun W, Song W, Guo X et al (2017) Ultrasensitive detection of nucleic acids and proteins using quartz crystal microbalance and surface plasmon resonance sensors based on target-triggering multiple signal amplification strategy. Anal Chim Acta 978:42–47

Tang W, Wang D, Xu Y et al (2012) A self-assembled DNA nanostructure-amplified quartz crystal microbalance with dissipation biosensing platform for nucleic acids. Chem Commun 48(53):6678–6680

Uludag Y, Tothill IE (2012) Cancer biomarker detection in serum samples using surface plasmon resonance and quartz crystal microbalance sensors with nanoparticle signal amplification. Anal Chem 84(14):5898–5904

Willner I, Patolsky F, Weizmann Y et al (2002) Amplified detection of single-base mismatches in DNA using microgravimetric quartz-crystal-microbalance transduction. Talanta 56(5):847–856

Zhao Y, Wang H, Tang W et al (2015) An in situ assembly of a DNA-streptavidin dendrimer nanostructure: a new amplified quartz crystal microbalance platform for nucleic acid sensing. Chem Commun 51(53):10660–10663

Zhou L, Ou LJ, Chu X et al (2007) Aptamer-based rolling circle amplification: a platform for electrochemical detection of protein. Anal Chem 79(19):7492–7500

Zhou L, Lu P, Zhu M et al (2016) Silver nanocluster based sensitivity amplification of a quartz crystal microbalance gene sensor. Microchim Acta 183(2):881–887

Part III
Nucleic Acid Amplification Strategies for Bioimaging

Chapter 11
Nucleic Acid Amplification Strategy-Based Fluorescence Imaging

Qiong Li

Abstract Nucleic acid amplification techniques can be grouped into two major categories, including isothermal amplification and thermocycling amplification. Isothermal amplification techniques include rolling-circle amplification (RCA), strand-displacement amplification (SDA), helicase-dependent amplification (HDA), and hybridization chain reaction (HCR). And polymerase chain reaction (PCR) and ligase chain reaction (LCR) have been known as thermocycling amplification techniques. Now nucleic acid amplification techniques were widely applied in cellular imaging based on fluorescent techniques. In this section, we attempt to summarize recent development of nucleic acid amplification techniques for bio-analysis, including the detection of miRNA, mRNA, ATP, telomerase, pH, and metal ions in cells and biomolecules in cell surface. We also consider the current challenges and our perspectives of nucleic acid amplification techniques for bio-imaging.

11.1 Introduction

Many components in cells, such as microRNA (miRNA), message RNA (mRNA), ATP, and telomerase, play significant roles to maintain normal functions in diverse range of cellular processes. For instance, miRNAs are significant to cell differentiation, proliferation, apoptosis, gene expression, and many other biological processes because of the regulation of gene expression through the promotion of the degradation or the inhibition of the translation of the target mRNAs. mRNA conveys genetic information from DNA to the ribosome and specify the amino acid sequence of the protein products of gene expression. Metal ions are essential in biological systems on account of metal homeostasis. Much clinical evidence suggests that abnormal biomolecule expression is closely related to serious diseases such as cancers. So they are usually regarded as biomarkers for various diseases. However, these molecules

Q. Li (✉)
Shandong Provincial Key Laboratory of Detection Technology for Tumour Markers, College of Chemistry and Chemical Engineering, Linyi University, Linyi 276005, Shandong, People's Republic of China
e-mail: qiongli7@163.com

S. Zhang et al. (eds.), *Nucleic Acid Amplification Strategies for Biosensing, Bioimaging and Biomedicine*, https://doi.org/10.1007/978-981-13-7044-1_11

in cell have a low-level abundance even the abundance will down-regulate when associated with serious diseases. So it is easy to detect these biomolecules with low abundance in cells on basis of nucleic acid amplification techniques.

In recent years, many kinds of nanomaterials have been widely developed, such as noble metal nanoparticles, inorganic semiconductor quantum dots, silica nanoparticles, graphene, and novel two-dimensional (2D) layered nanomaterials analogous to graphene. These nanomaterials attract considerable attention due to their outstanding characteristics such as large surface areas, high loading capacity, high stability, and excellent biocompatible feature and have been widely applied in biological field as micro-interfaces. On this basis, the micro-interfaces acted as a good cellular transporter combined with nucleic acid amplification techniques and have established their enormous potential in biosensing analysis of targets inside cells.

11.2 Nucleic Acid Amplification Techniques for Cellular Imaging

Nucleic acids could carry genetic information and regulate intracellular molecules so they play fundamental roles in many critical biological systems. Reagents developed from nucleic acids represent an essential tool in detection and regulation of gene expression and protein activity in biomedical field. There are still a number of challenges for nucleic acid reagents in cell biology and theranostics, for example, the efficiency of their delivery into different cells and the sensitivity for target detection and regulation. DNA/RNA nanostructures represent an attractive option for intracellular delivery of nucleic acids. Spherical nucleic acids and self-assembled nucleic acid nanostructures are typical examples of nucleic reagents. These nucleic acid nanostructures have displayed their capacity to enter diverse cells with no aid of cationic carriers and provided a powerful platform for developing diagnostic assays, therapeutic drugs, and gene regulation agents in applications of cellular and in vivo analysis. Nevertheless, for intracellular detection and regulation, a detection limit of current nucleic acid nanostructures was typically at the nanomolar level, which was largely resulted from no signal amplification mechanisms in these methods, so challenges, signal amplification strategies achieved through a nanomachine constructed with specific nucleic acids in living cells, remain to be resolved. Nucleic acid amplification techniques can be grouped into two major categories, including isothermal amplification and thermocycling amplification. Isothermal amplification techniques include HCR, CHA, RCA, SDA, and HAD. And thermocycling amplification techniques include PCR and LCR. Now nucleic acid amplification techniques are widely applied in cellular imaging based on fluorescent techniques. Many nucleic acid amplification techniques have been developed for bio-analysis, including the detection of miRNA, mRNA, ATP, telomerase, pH, and metal ions in cells and some proteins in cell surface.

11.2.1 HCR for Biomolecule Imaging in Cells

11.2.1.1 HCR for miRNA Imaging in Cells

Various strategies have been designed to challenge effective signal amplification of miRNAs in living cells. Figure 11.1 illuminates the concept for amplification and two-color imaging of miRNA in living cells based on HCR and GO (Li et al. 2016a, b). Here to simultaneously detect two kinds of miRNAs miR-21 and let-7a within the same living cell, workers designed two pairs of hairpin probes labeled with FAM and ROX, respectively. The hairpin probes H1 and H2 with fluorophore FAM at the sticky end were specifically designed to detect miR-21. The hairpin probes H3 and H4 attached with fluorophore ROX were specifically designed to detect let-7a. Hairpin DNA probes and the GO self-assembly formed a probe/GO complex due to noncovalent p-p stacking interactions between the hexagonal cells of graphene and the ring of nucleobases. GO efficiently quenched the fluorescence of the dye labeled on the probes. The hairpin probes were carried into cells by GO via non-destructive clathrin-mediated endocytosis. The hairpin probe/GO complex provided a fluorescence-sensing platform for imaging of intracellular miRNAs. In the presence of miR-21 in cells, an HCR between H1 and H2 was triggered by each miR-21 to yield long dsDNA with collected fluorophores. Remarkable fluorescence enhancement was obtained because of weak interaction between the dsDNA and GO. One miR-21 molecule could be effectively amplified by several FAM fluorophores, and green fluorescence was imaged in the cells. Similar to miR-21, let-7a could specifically trigger an HCR between H3 and H4, so that cellular let-7a miRNAs were amplified and imaged by the red ROX fluorescence. Compared with let-7a, let-7b, let-7c, and anti-miR-21, the H1 and H hairpin probes exhibited excellent specificity for miR-21. This amplification strategy simultaneously succeeded imaging the two miRNAs at different expression levels in the same living cells with a detection limit of 0.18 pM for miR-21.

For miRNA imaging in living cells, a protein scaffolded DNA tetrad, shown in Fig. 11.2, was developed (Huang et al. 2018a, b). As the proof-of-principle, intracellular miR-21 imaging was demonstrated using cHCR. Workers designed two biotinylated hairpin probes H1 and H2, one attaching Cy3 fluorescence dye as a donor and the other choosing Cy5 as fluorescence acceptor. Here DNA tetrads were synthesized by separately displaying H1 and H2 probes on SA. miRNA would open the hairpin probe H1, then, a cascade of alternating hybridization initialized HCR between H1 and H2 and induced crosslinking of the tetrads to form 3D crosslinked hydrogel networks. In this design, donors Cy3 and acceptors Cy5 are brought into close proximity leading to the Föster resonant energy transfer (FRET) in the presence of miRNA. The cHCR between H1 and H2 probes and FRET from Cy3 to Cy5 do not occur without miRNA. Therefore, the cHCR products indicate the expression of target miRNA. In comparison with other nucleic acid probes, this probe can quickly enter live cells without the aid of transfection carriers and efficiently escape from lysosome. And this probe affords high sensitivity and spatial resolution for imaging because of 3D

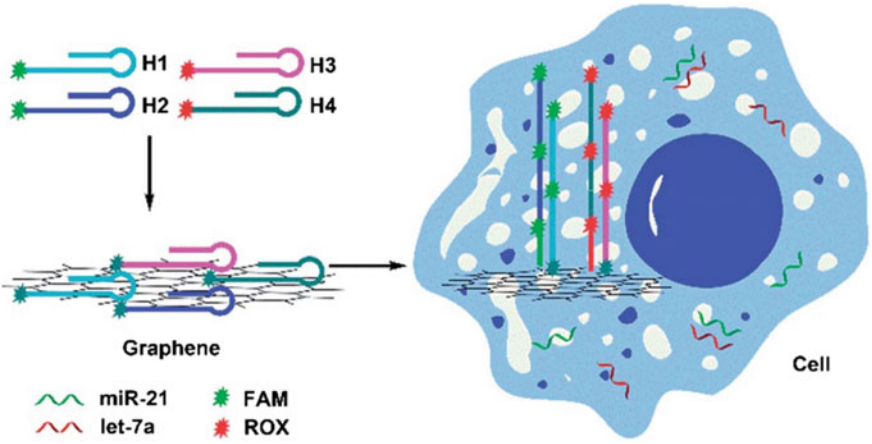

Fig. 11.1 Scheme for amplification and two-color imaging of miRNA in living cells based on HCR and GO. Reproduced from Li et al. (2016a, b) by permission of The Royal Society of Chemistry

crosslinked hydrogel networks induced by HCR. Finally, the result, dual-emission ratiometric imaging obtained by FRET in this design, confers improved precision and avoids the false signal in complex biological environment.

Using a ratiometric method to detect intracellular miRNAs, especially for the down-regulated ones, recently Li and co-workers developed a biodegradable MnO_2 nanosheet-mediated HCR strategy (Li et al. 2017a, b). Similar to graphene nanomaterial, MnO_2 nanosheets exhibit efficient fluorescent quenching ability to organic dye attached to ssDNAs (Fan et al. 2015). In addition, glutathione (GSH) in cells can degrade MnO_2 nanosheets to significantly decrease the cytotoxicity. Therefore, MnO_2 nanosheets are employed as promising delivery and sensing intermediates for living cells. In this design, the FRET donor and acceptor organic dyes were separately labeled to two hairpin DNAs. Then they were delivered into living cells by MnO_2 nanosheets, and upon entering cells, the hairpin DNAs can be released due to the displacement reactions by other proteins or nucleic acids (Xuan et al. 2015) and the MnO_2 nanosheets would be degraded by cellular GSH. With the presence of down-regulated miRNAs in cells, the hairpins can be triggered to assemble into dsDNA polymers and the FRET pairs were drawn into close proximity, which activated significantly amplified FRET signals as indicators for detecting the trace miRNAs in living cells. Compared to other reported intracellular sensing methods, this design described herein thus is obviously advantageous with low cytotoxicity because of employing biodegradable MnO_2 nanosheets, and high accurateness resulted from the FRET-based approach, which can minimize false-positive signals. Given the virtue of MnO_2 nanosheets, Wang's group also constructed a live cell miRNA imaging method utilizing MnO_2 nanosheet-mediated DD-A HCR (Ou et al. 2017). They chose MnO_2 nanosheets to deliver DNA hair probes into live cells and upon the degradation of

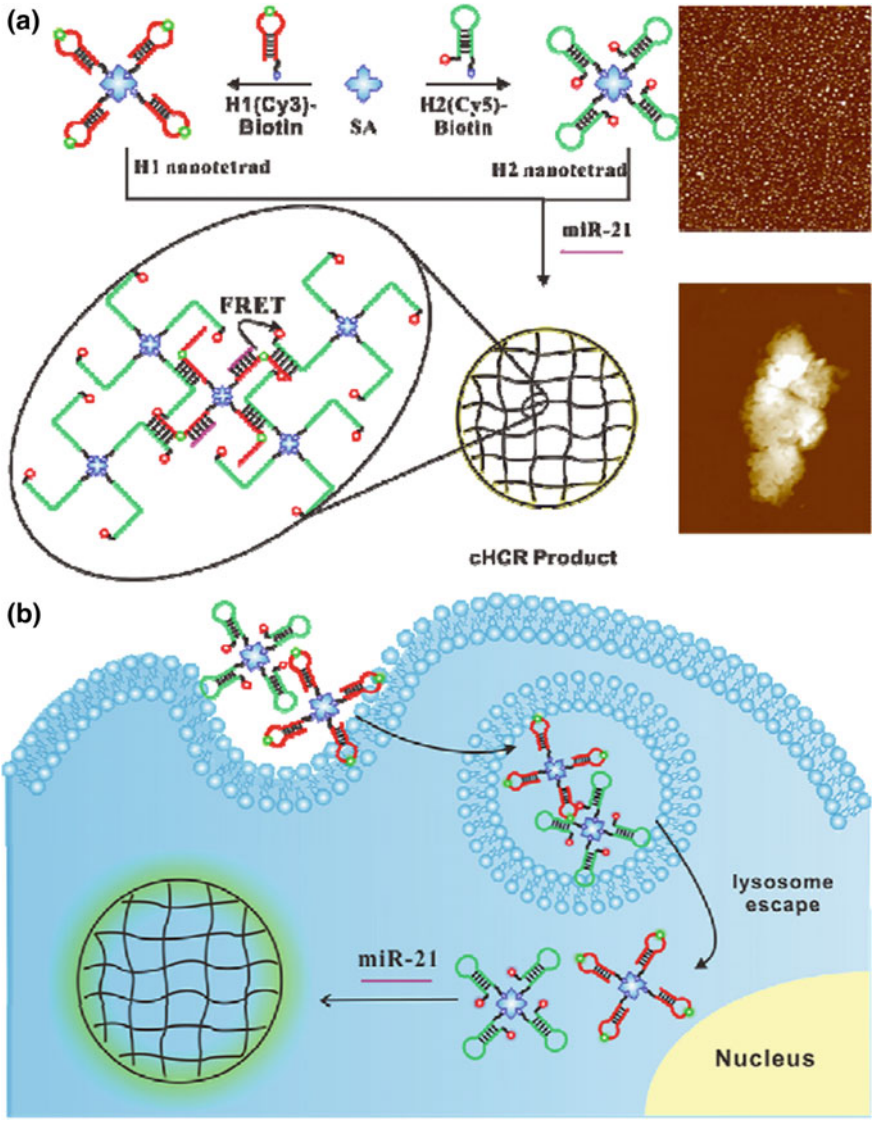

Fig. 11.2 Illustration of **a** DNA tetrad-enabled cHCR and **b** ultrasensitive intracellular miRNA imaging strategy. Reproduced from Huang et al. (2018a, b) by permission of The Royal Society of Chemistry

MnO_2 nanosheets by cellular GSH the miRNA would be detected and imaged by significantly enhanced DD-A FRET signals.

There are also many approaches developed for amplifying the signal of miRNAs with low abundance and imaging in living cells. For example, based on isothermal enzyme-free HCR, Wei and co-workers constructed a signal amplification platform using two-layered concatenated HCR-1/HCR-2 circuit (cHCR) with synergistic amplification performance (Wei et al. 2018). The downstream HCR (HCR-2) transduction amplifier was triggered by the amplicon product of the upstream HCR (HCR-1) layer. The cHCR imaging system exhibits concomitant improvements in the convenience and programmability for intracellular biomarkers, leading to an accurate in situ diagnoses and effective treatment of key diseases. In the past work, we established a miRNA imaging method in single cells by orderly aggregating nucleic acid on mesoporous silica nanoparticles (MSNs) using electrostatic self-assembly (Wang et al. 2016). Song described an intracellular DNA and miRNA sensing approach using HCR based on metal-organic framework (MOF) nanosheets (MnDMS) (Song 2017). The miRNA probes were assembled on MnDMS nanosheets, leading to efficient fluorescence quenching of the fluorophore linked to ssDNA and miRNA. In presence of the target, MnDMS nanosheets would release probes labeled with fluorophores and the obvious fluorescence would be observed.

11.2.1.2 HCR for mRNA Imaging in Cells

mRNAs play a fundamental role in conveying the genetic blueprint encoded by DNA to proteins. Abnormal expression of mRNA has been widely used as biomarkers for the diagnosis of various diseases such as cancer (Santangelo et al. 2004, 2007; Li et al. 2012; Pan et al. 2013). Probes based on HCR could be used for directly detecting and imaging of endogenous mRNA in living cells. So for the diagnosis of diseases by detecting mRNAs, HCR affords valuable approaches (Xia et al. 2017). Jiang's group utilized gold nanoparticles (AuNP) to develop an electrostatic DNA nanoassembly based on HCR for imaging mRNA in living cells (Wu et al. 2015a, b). In this design, AuNP chosen as a core acts as a well-defined template, then cysteine-terminated cationic peptides and fluorophore-labeled nucleic acid probes self-assembled as an interlayer and outer layer on the core surface for signal amplification. In the self-assembly nanostructure, fluorophores labeled at the nucleic acid probes could be efficiently quenched due to surface energy transfer (SET). The survivin mRNA, overexpressed in many cancers, was chosen as the model target. They designed two hairpin-structured DNA probes H1 and H2, which was labeled with a FRET pair, carboxyfluorescein (FAM) as the donor and tetramethylrhodamine (TMR) as the acceptor, respectively. Because of efficient quenching by the gold core, H1 and H2 probes assembled on the peptide-coated particles exhibited very weak fluorescence signals for both fluorophores (Wu et al. 2013; Paliwoda et al. 2014). As shown in Fig. 11.3, the hybridization between mRNA target and H1 was triggered and produced a single-stranded tail in H1, which might dissociate or increase the mobility of H1 on the particles, facilitating its hybridization with H2 and restoring a single-strand tail

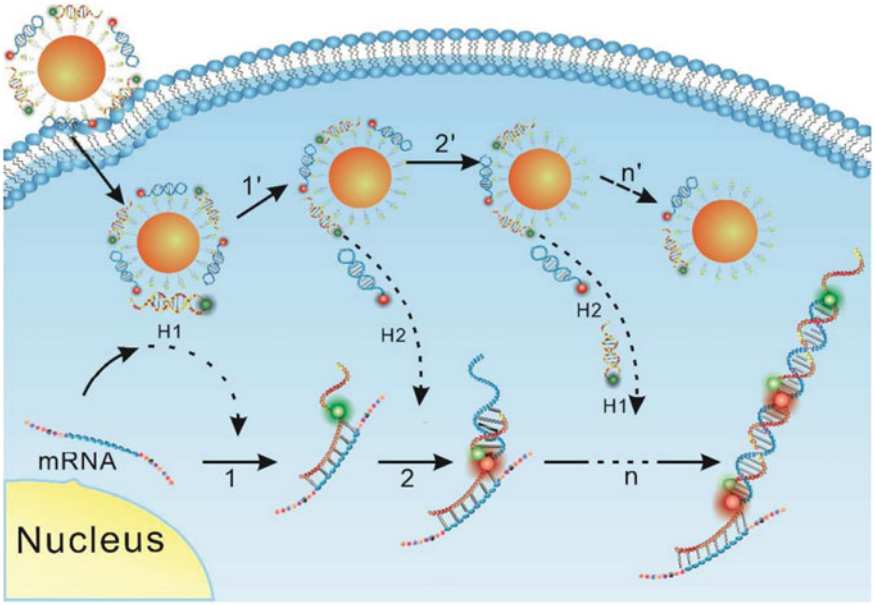

Fig. 11.3 Illustration of intracellular HCR for mRNA detection. Reprinted with the permission from Wu et al. (2015a, b). Copyright 2015 American Chemical Society

in H2 with the same sequence of target. In this way, a chain reaction is triggered for alternating hybridization between H1 and H2, producing a chain-like assembly of H1 and H2 (Li et al. 2013). The HCR product had a rigid duplex conformation, which had decreased affinity to the nanoassembly and thus dissociated from the surface. The dissociated product also draws the FRET pair into close proximity leading a FRET signal as an indicator for target mRNA expression. This HCR amplification based on electrostatic nucleic acid assembly is an invaluable approach for detecting mRNAs with low abundance and diagnosing related diseases.

Compared to standard HCR, branched HCR (bHCR) exhibits enhanced sensitivity under stringent hybridization conditions. Jiang's group exploited a fluorescence in situ hybridization (FISH) strategy based on a bHCR for intracellular mRNA imaging to specifically resolve single-nucleotide variation (Tang et al. 2017). In the FISH experiment, two new designs, ligase-mediated mutation discrimination of target mRNA and bHCR-based signal-amplified detection of individual ligated products, played crucial roles on this strategy. They utilized ligase-mediated mutation discrimination to convert individual mRNA into a ligated DNA molecule-tagged bHCR initiator with high specificity and efficiency. In order to realize sensitive and specific detection of individual mRNA, target mRNA was reversely transcribed into localized cDNA using a locked nucleic acid (LNA) primer, which could protect the complementary RNA from degradation during RNase H treatment, allowing the LNA primed cDNA to anchor on target mRNA in situ. In their study, to avoid topological

constraints in circular probes and achieve efficient ligation, they chose linear DNA probes, constructed with one anchor probe and two allelic probes, which flank the polymorphic site. Catalyzed by DNA ligase, the pair of DNA probes perfectly matching cDNA is specifically ligated, while mismatched DNA probes remain unligated. With unligated probes readily removed at a controlled temperature, the ligation product is stably immobilized on cDNA due to its much higher melting temperature. A single-stranded tail with the sequence encoded for a polymorphic site in each allelic probe was incorporated to initiate bHCR from anchored ligation product. Accordingly, a target mRNA with its single-nucleotide variation is converted into a ligated DNA with an encoded single-stranded tail, which is anchored on target mRNA acting as the initiator for subsequent bHCR detection.

In Jiang's another research, they further reported a novel bHCR circuit for efficient signal-amplified imaging of mRNA in living cells (Liu et al. 2018a, b). The hierarchical coupling of two HCR circuits in a single reaction was the crucial design in this bHCR strategy. Two hairpin probes H1 and H2 were used for designing the primary linear HCR circuit. The presence of target mRNA triggered two hairpin probes to form the backbone chain of the hyperbranched assembly. They distinctly designed the loop region of H1 and the toehold region of H2, in which two split initiator fragments of the secondary HCR are incorporated, respectively. The backbone assembled in presence of target mRNA, and these split initiator fragments are bright into close proximity, activating the secondary HCR circuit and enabling branched growth of chain-like assembly between hairpin probes H3 and H4. The hierarchical coupling of the primary and the secondary HCR circuits was able to generate a hyperbranched, brush-like assembly with a single mRNA target as the initiator. A fluorophore FAM and a quencher BHQ1 were labeled in the stem region of H3 forming F-H3 to light up the mRNA target. The F-H3 probe exhibited a low fluorescence background in its folded, hairpin state while showed enhanced fluorescence in the hyperbranched assembly in which H3 is extended by hybridization with H4. Upon entering into cells, the probes H1, H2, H3, and H4 formed a hyperbranched, highly fluorescent assembly triggered by each single mRNA target, realizing mRNA imaging in situ with high-contrast and spatial resolution. Hence, this approach offered a useful platform for intracellular mRNA imaging in situ with high sensitivity.

To analyze the expression of tumor-related mRNA, Wang's group developed a FRET-based HCR, which was initiated by the target mRNA (Huang et al. 2016). Then, HCR produced multiple DNA repeating units generating a FRET signal for each one. As illustrated in Fig. 11.4, three programmable DNA hairpins (H1, H2, and H3) were used in this design. H1 was designed to hybridize the target TK1 mRNA with a complementary sequence. A FRET pair TAMRA as an acceptor and FAM as a donor was separately labeled on H2 and H3 at the appropriate positions. The presence of target opened H1 (step 1), producing H1 pairs with the sticky end of H2, which would open the hairpin by an unbiased strand-displacement interaction (step 2). The resulting H2 exposed at the sticky end of H3 and opened the hairpin to attach on the sticky end of H3, which can open H2 again (step 3). In presence of target, chain reaction of hybridization events between alternating H2 and H3 hairpins, which generated and amplified the FRET signal, could be cycled to form a nicked

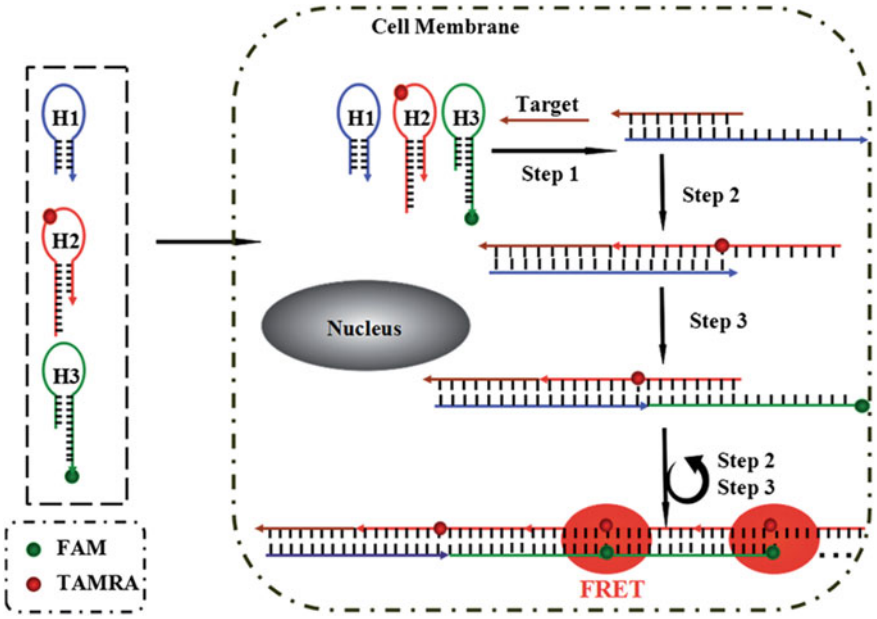

Fig. 11.4 Working principle for in situ detection of TK1 mRNA using the FRET-based HCR method. Reproduced from Wu et al. (2015a, b) by permission of The Royal Society of Chemistry

duplex (repeat steps 2 and 3). However, with no target the hairpins stay metastable because of the closed formation of the hairpin stems. A FRET-based approach for the analysis of target expression used in this system could avoid multiple washing steps and prevent false-positive signals resulted from probe accumulation or degradation in quencher/dye systems.

A study on detecting mRNA transcript abundance and localization in single cells with single-molecule fluorescence in situ hybridization (smFISH) was reported (Burke et al. 2017). In this system, RNA in situ hybridization and HCR was used to measure translation of unmodified endogenous mRNA transcripts in single fixed cells. This method was described as a fluorescence assay to detect ribosome interactions with mRNA (FLARIM), which revealed interactions between individual mRNAs and ribosomes to provide a measure of the extent of active translation of the target mRNA species. No genetic manipulation of cells was required in this method, which was almost suitable for any mRNA of interest. As ribosome profiling extends RNA-seq to quantify mRNAs bound by ribosomes, FLARIM extends smFISH to identify ribosome-bound mRNAs and to monitor the changes in ribosome–mRNA interaction that accompany cellular perturbations. The subcellular locations where mRNAs interacted with ribosomes could be determined utilizing fixed cell images resulting from FLARIM.

11.2.1.3 HCR for Detection of Circulating Tumor Cells

The detection and analysis of circulating tumor cells (CTCs) have been considered as an important platform for predictive cancer diagnosis. DNA-templated magnetic nanoparticle (MNP)-quantum dot (QD)-aptamer copolymers (MQAPs) was designed for magnetic isolation and detection of CTCs with both high capture efficiency (CE) and capture purity, shown in Fig. 11.5 (Li et al. 2018a, b). They chose DNA molecules as templates to design a nanostructure with several functionalities such as magnetic, fluorescent, and biorecognition functionalities. In this way, each functionality of the assembly could be rationally programmed and amplified. Compared to MNPQD-aptamer monomers (MQAMs), MQAPs designed in this method enhanced magnetic response at single cell level to efficiently isolate CTCs. This approach offered a practical platform for biomedical applications with bio-inspired construction of inorganic magneto-fluorescent materials with programmable properties.

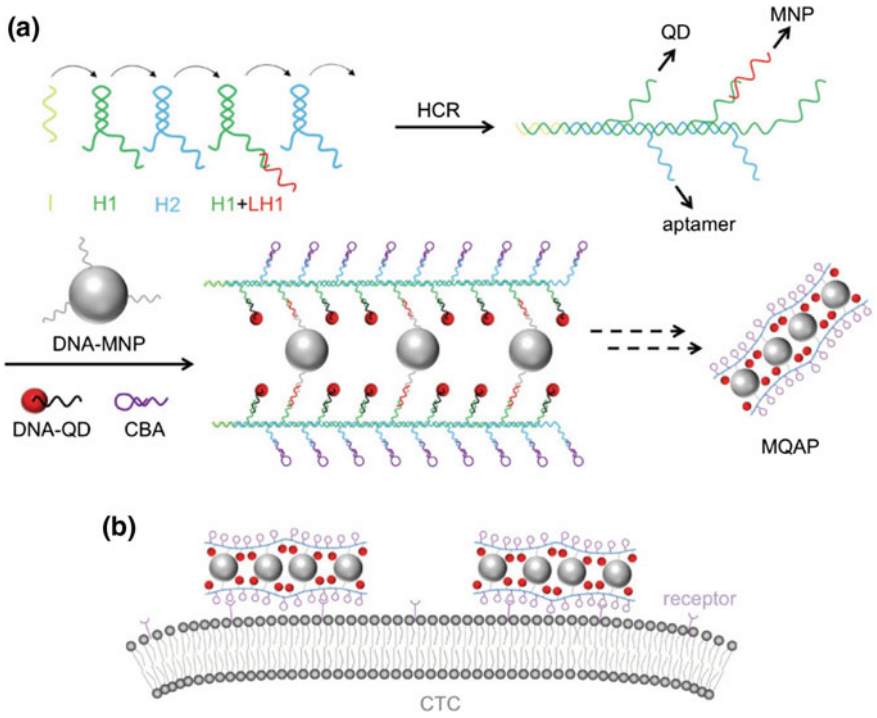

Fig. 11.5 Schematic illustration of MQAPs for magnetic isolation of CTCs. **a** Construction of MQAPs in two steps: (i) hybridization chain reaction mediated formation of the polymeric DNA template and (ii) co-assembly of DNA-QDs, DNA-MNPs, and DNA aptamers with the DNA template. **b** Multivalent binding between MQAPs and cell surface receptors for CTC isolation and detection. Reproduced from Li et al. (2018a, b) by permission of John Wiley & Sons Ltd.

Using porous DNA hydrogels, as shown in Fig. 11.6, based on aptamer-trigger clamped hybridization chain reaction (atcHCR) an approach was illustrated to in situ identify and subsequent cloak/decloak CTCs, which were then used for live cell analysis (Song et al. 2017). In this method, authors employed a DNA staple strand with aptamer-toehold biblocks, which specifically recognized epithelial cell adhesion molecule (EpCAM) on the CTC surface, to trigger subsequent atcHCR via toehold-initiated branch migration. Living CTCs could be directly captured by porous DNA hydrogel by cloaking of single/cluster of CTCs. Upon controlled and defined chemical stimuli, living CTCs cloaked in the DNA hydrogel could be released without damages for subsequent culture and live cell analysis.

For the efficient isolation and detection of CTCs in whole blood, Ding and co-workers designed and prepared a new NIR Ag_2S nanoprobe combined with immune-magnetic spheres based on HCR signal amplification (Ding et al. 2018). In this design, workers constructed Ag_2S nanoprobe with DNA1-labeled Ag_2S nanodots (DNA1-Ag_2S) through HCR. DNA1-Ag_2S and aptamer, which could specially bind with MUC1 overexpressed in MCF-7 cells, were firstly assembled with the hairpin DNA sequence H1 and H2, respectively. Upon hybridizing, the presence of initiator-triggered assembling to form multiple Ag_2S nanodot–aptamer nanoassembly, named as Ag_2S nanoassembly. The NIR fluorescence signal intensities of nanoprobe were greatly enhanced due to multiple Ag_2S nanodots assembled in each Ag_2S assembly with multibranched structures, which produced the high sensitivity for cell imaging. Compared to the probe with one aptamer per fluorescence nanoparticle, the multi-aptamer structures on assembly largely enhanced the binding ability with tumor cells. Furthermore, magnetic nanospheres (MNs) modified with anti-EpCAM antibody (anti-EpCAM-MNs) were used to isolate the target cells due to the specific binding with EpCAM on the surfaces of MCF-7 cells. The combination of the Ag_2S nanoassembly with anti-EpCAM-MNs showed highly efficient separation and analysis of CTCs with the feature of capturing and detecting as low as six cancer cells in artificial clinical samples.

11.2.1.4 HCR for Detection of Other Biotic Environment

Similar to the above-mentioned report, Li and co-workers also reported quantum dots and DNA assembly with multibranched structures for molecular imaging on surface of cancer cells in the previous study (Li et al. 2016a, b). They synthesized polymers with QD monomer (M1) and aptamer monomer (M2) through HCR. The overhangs of the reactive hairpin unit (H1 or H2) were used for separate conjugation with the functional unit (QDs or aptamer). In this design, the imaging sensitivity of QAPs was significantly improved over QAMs, and biomolecule PTK7 imaging on surface of cancer cells was realized at very low QD concentration of 5 nM. As illustrated in Fig. 11.7, another study on PTK7 imaging on cell surface was reported for activatable theranostics based on structure-switching aptamer-triggered hybridization chain reaction (SATHCR) (Wang et al. 2015). To prove the concept, the aptamer probe was designed using sgc8c as the model system with a molecular

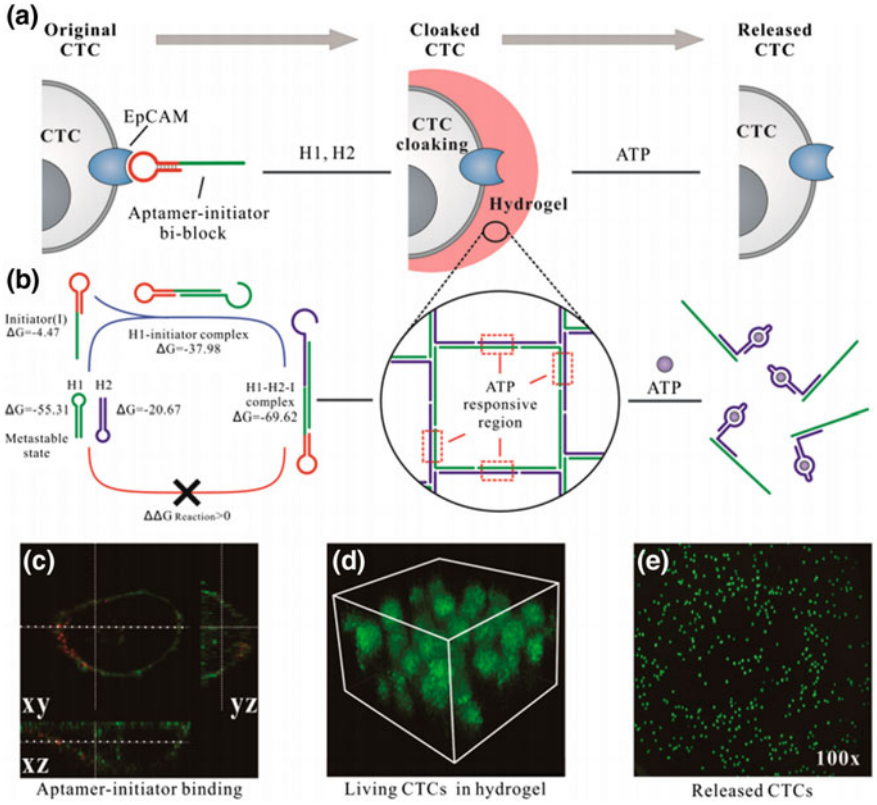

Fig. 11.6 DNA gelation-based cloaking and decloaking of CTCs. **a** At the initial solution phase, the MCF-7 cells were dispersed in solution. The aptamer-initiator biblocks were able to specifically bind to the EpCAM on cell surface that could then trigger the atcHCR reaction to assemble DNA hydrogel. The ATP was used to destroy the DNA hydrogel with designed ATP-responsive region in DNA hydrogel that cloaked on cell surface. **b** DNA hairpins H1 and H2 were trapped in metastable state. Without DNA initiator, H1 and H2 could not hybridize. With DNA initiator, the H1 was opened and triggered the subsequent hybridization chain reaction. **c** Confocal images of aptamer-initiator biblocks (red) colocalized with DiO-stained lipid on cell membrane (green). **d** The 3D stack of MCF-7 cells cloaked in DNA hydrogel with FDA staining in green which show multilayered cells in hydrogel. Stack height: 40 μm. **e** By adding the ATP, the MCF-7 cells were released and dispersed in solution. Reprinted with the permission from Song et al. (2017). Copyright 2017 American Chemical Society

recognition functionality and activatable ability to initiating HCR via two hairpin probes, signal probe H1 and drug probe H2 tagged with Cy5 as a donor and BHQ3 as an acceptor, respectively. The drug probe H2 was linked with a synthesized pro-drug c,c,t-[$Pt(NH_3)_2Cl_2(OH)(O_2CCH_2CH_2COOH)$]. The AP would not trigger HCR without target protein leading to no fluorescence signal for diagnostic imaging and internalized drug probes for tumor therapy. Upon binding to PTK7, the AP underwent structure switching and activated a single-stranded initiator sequence triggering

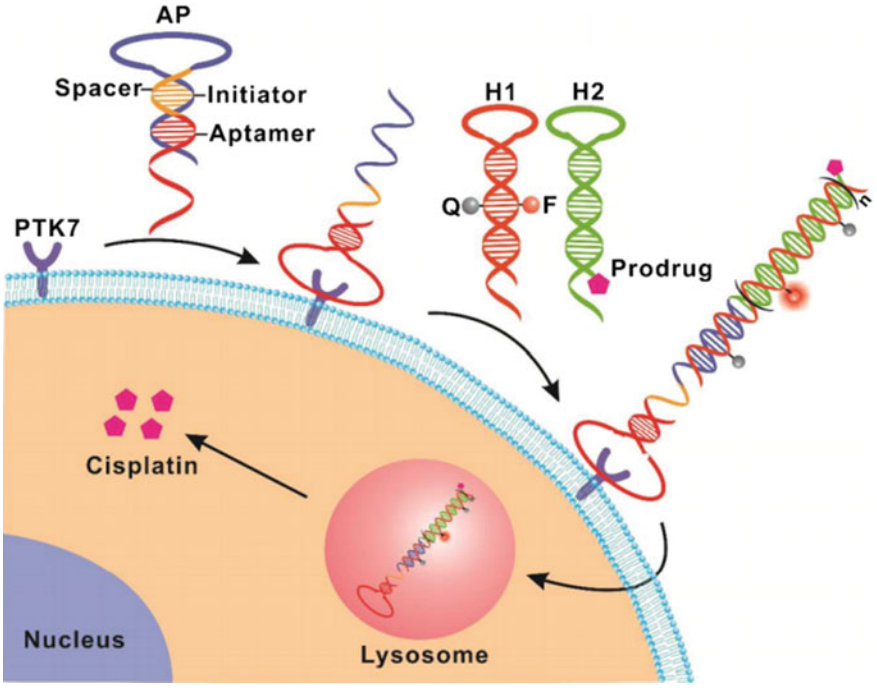

Fig. 11.7 Illustration of SATHCR for activatable theranostics. Reprinted with the permission from Wang et al. (2015). Copyright 2015 American Chemical Society

a real-time HCR with probes H1 and H2. An amplified fluorescence signal is activated in the chain-like HCR product due to the separation of fluorophores from quenchers producing real-time fluorescence signal of tumor cells. The HCR product also accumulated a high load of prodrug, which was taken in cells and led selective cytotoxicity to tumor cells via reduction of the conjugated prodrug into cisplatin by cytosolic thiols.

Recently, Zhang et al. developed a biosensing method based on HCR for the detection of intracellular telomerase activity (Zhang et al. 2018). pH modulates diverse cellular events and plays an important role in many biological processes. Jiang's group illustrated a sensitive sensing and imaging of intracellular pH method based on a pH-responsive, fully reversible hybridization chain assembly (Liu et al. 2017). The triplex-forming sequence (TFS) would induce a cascade of strand displacement and DNA assembly after forming DNA triplex by using the Hoogsteen base pairs at acidic pH. The results showed that the HCR signal was responsible in physiological pH ranges with reversibility.

11.2.2 CHA for Biomolecule Imaging in Cells

11.2.2.1 CHA for miRNA Imaging in Cells

In recent years, a lot of work about detection and imaging of miRNA in cells, especially cancer cells, based on CHA have been reported. For example, Wang's group recently designed gold nanoparticles based hairpin-locked-DNAzyme for amplified miRNA imaging in living cells (Yang et al. 2017). As shown in Fig. 11.8, the probe was constructed with an AuNP and hairpin-locked-DNAzyme strands. The AuNP core was employed as a cellular transporter and fluorescence quencher. The fluorophore of FAM and thiol were labeled at the 5′ end and the 3′ end of hairpin-locked-DNAzyme strands, respectively, which consisted four essential structural sections, including a target-binding sequence, a DNAzyme sequence which is a Mg^{2+}-dependent 10-23 DNAzyme (Mei et al. 2003), substrate sequence with a cleavage site and a linker. The linker, which was composed of poly T and used to attach with the 10-23 DNAzyme and its substrate, was hybridized to poly A to form the hairpin structure. With no target miRNA, the hairpin-locked-DNAzyme strand could form hairpin structure via intramolecular hybridization, which could inhibit the catalytic activity of DNAzyme strand leading fluorescence quenching due to drawing fluorophores onto the AuNP surface. The presence of target miRNA-triggered target–probe hybridization to open the hairpin and form the active secondary structure in the catalytic cores and then yielded an 'active' DNAzyme. With the aid of Mg^{2+}, DNAzyme cleaved the self-strand at the facing ribonucleotide moiety into two shorter fragments separated with the target because of the lower affinity leading to fluorescence recovery. Meanwhile, the intact miRNA strand (target) was released and bound to adjacent hairpin-locked-DNAzyme strand to activate another cycle for significant signal enhancement with high detection sensitivity.

Recently, Liu and co-workers established a miRNA imaging platform based on CHA using gold nanoflower (AuNF) modified with polydopamine (Liu et al. 2018a, b). As described in their paper, folic acid and dye-labeled hairpin DNA 1 (H1) and hairpin DNA 2 (H2) were separately employed as the targeted moiety, the recognition and amplification elements to modify DA-AuNF by noncovalent interactions for yielding hairpin DNA functionalized DA-AuNF (HDA-AuNF) which was in "off" state due to the FRET between the dye and DA-AuNF. Upon the nanovector delivered into cells mediated by folate receptor, the target miRNA-21 specifically recognized and opened H1 on the HDA-AuNF. The H1-target conjugate with exposing sticky end could be dissociated by H2 via strand displacement to release the target for the next cycle, leading to multiple signal outputs for imaging and sensitive detection of intracellular miRNA. Other nanovectors, such as carbon nitride nanosheets and graphene oxide (GO), were chosen as cellular carriers to amplify detection signal for miRNA in living cells based on CHA (Liao et al. 2018; Liu et al. 2016).

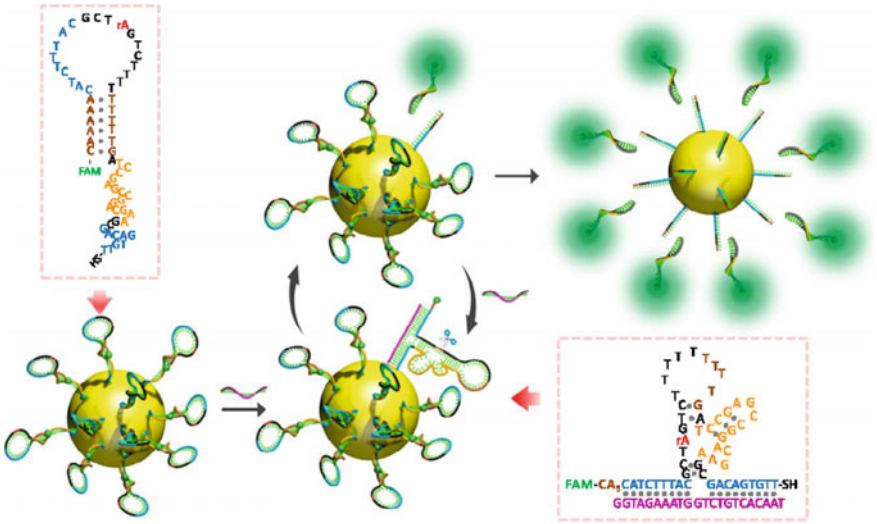

Fig. 11.8 Working mechanism of the AuNP-based hairpin-locked-DNAzyme probe for miRNA detection. Reprinted with the permission from Yang et al. (2017). Copyright 2017 American Chemical Society

11.2.2.2 CHA for mRNA Imaging in Cells

CHA offers a useful platform for development of DNA nanomachines, constructed with multiple DNA sequences in response to a single trigger, which could be used for biosensing and imaging of low-abundance biomolecules. For example, Jiang's group reported an approach to reconstruct DNAzymatic amplifier nanomachine induced by mRNA target via CHA, and the nanomachine then was used to elicit concurrent mRNA imaging and gene silencing in living cells (Li et al. 2018a, b). To verify the concept, they chose a tumor-related biomarker GalNAc-T mRNA as the model target to demonstrate the design (Li et al. 2012). Two hairpin probes H1 and H2 were separately designed as the signal unit and the therapy unit in the nanodevice. A fluorophore Cy5 and a quencher BHQ2 were attached onto the signal unit H1 and its complementary base, respectively, to light up the target mRNA. Therapy unit H2 is designed to block a part of the enzyme strand of DNAzyme in the stem region to activate gene therapy. 10-23 DNAzyme was chosen to cleave the target gene human early growth response-1 (EGR-1). The presence of target GalNAc-T mRNA initiated the CHA to form multiple H1-H2 duplex products, activating an amplified fluorescence signal due to the dissociation of fluorophores from quenchers. Meanwhile, the conformational changes of hairpin probes completely restore the enzyme strand from H2, allowing reconstruction of DNAzyme for activatable gene silencing. Intracellular mRNA target would trigger the generation of multiple H1-H2 duplex products for concurrent sensitive mRNA imaging with a low limit of detection estimated to be 9 pM. Because the activity of DNAzyme is inhibited and is selectively

activated by the target mRNA, this approach could improve the selectivity of therapy with low side effect.

For monitoring targets of interest, especially for analytes with low abundance in live cells, enzyme-free amplification techniques still remain a challenge. To meet this challenge, Su et al. demonstrated the design and fabrication of a CHA-based theranostic nanoplatform for sensitive and specific intracellular mRNA-triggered fluorescence-guided therapy (Su et al. 2017). In this design, Cy5 attached on duplex DNA was chosen as the near-infrared (NIR) fluorescence reporter of CHA, and AuNRs were chosen as the fluorescence quencher and PTT agent due to the strong surface plasmon absorption at NIR region and high photothermal conversion efficiency. This nanoplatform relied on two intracellular mRNA triggerable hairpin DNAs which were assembled to the Cy5 linking duplex DNA on the surface of AuNRs for enabling fluorescence amplification. The fluorescence of Cy5 was quenched by AuNRs without target mRNA, and the presence of target mRNA would light up the fluorescence of Cy5. Compared to the always-on systems, the "off" to "on" process effectively avoided the "false-positive" signal. Thus, the "off" to "on" theranostic nanoplatform offered synergistic advantages of enzyme-free signal amplification from CHA and the high photothermal effect from AuNRs for mRNA-triggered fluorescence imaging-guided PTT.

For another enzyme-free amplification technique, hairpin DNA cascade amplifier (HDCA) was developed to visualize low-expression mRNA with high signal gain in live cells. This HDCA was constructed with two major components: a catalytic element consisting of two hairpin-shaped metastable DNA substrates, whose conformational transformations can be catalytically triggered upon target mRNA binding, and the reporting moiety containing a hybridized DNA duplex with a fluorophore (Rep-F) and quencher (Rep-Q) (Wu et al. 2015a, b). As shown in Fig. 11.9, a pair of metastable hairpin DNA substrates, H1 and H2, remained intact with no target mRNA, since their cross-reactivity was effectively blocked by intramolecular hybridization. However, H1 and H2 will form a stable hybridized duplex triggered by target mRNA, which was released, instead of being consumed, to catalyze the next catalytic round. The H1-H2 duplex dehybridized the reporting moiety, resulting in a restoration of the initially quenched fluorescent signal which lighted up cells. In this HDCA, the target mRNA acted as catalyst and circularly generated signal outputs to achieve signal amplification.

11.2.2.3 CHA for Other Biomolecule Imaging in Cells

There are also many approaches developed for amplifying the signal of biomolecules with low abundance and imaging in living cells. For example, a catalytic hairpin assembly RNA circuit that was genetically encoded, termed CHARGE, was developed by Karunanayake Mudiyanselage et al. (2018) In the design, Broccoli was separated into Broc and Coli with no fluorescence, and two CHA hairpins, H1 and H2, were separately linked to Broc and Coli (Alam et al. 2017). In presence of target, hybridization between H1 and H2 was triggered to form Broccoli, leading to fluores-

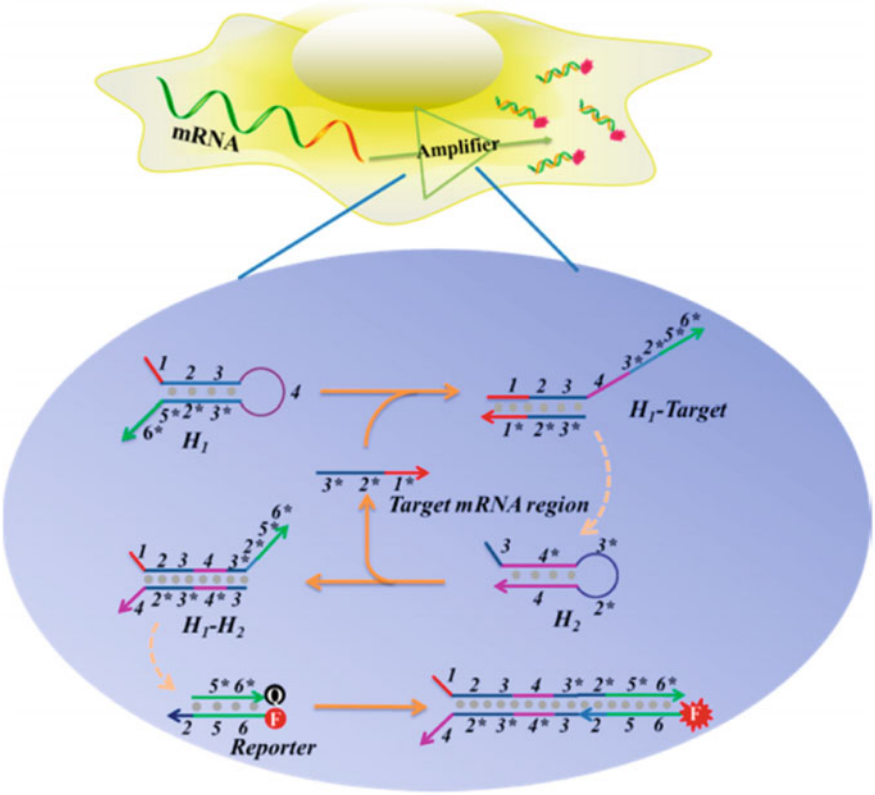

Fig. 11.9 Illustration of hairpin DNA cascade amplifier (HDCA) for catalytic signal enhancement of specific mRNA expression in living cells. After transfection into live cells, the catalytic HDCAs are initiated by specific target mRNA to repeatedly yield many H1–H2 duplexes, which further destabilize the reporter moiety and fluoresce inside the cells. Reprinted with the permission from Wu et al. (2015a, b). Copyright 2014 American Chemical Society

cent restoration of DFHBI-1T as an indicator for target. As described in the report, one target RNA can catalytically activate tens-to-hundreds of Broccoli fluorescence. So this approach they constructed provides a robust fluorescence signal and can be used for RNA imaging in live cells with high sensitivity.

Metal ions play critical roles in numerous biological processes. It is important to detect and monitor intracellular concentrations of metal ions because their concentration may affect normal functions. Toward this goal, Jiang's group designed the DzCHA probe that consisted of two parts: a Na^+-specific NaA43 DNAzyme and CHA amplification triggered by the cleaved product of the DNAzyme (Wu et al. 2017). The substrate strand at the rA position would be cleaved by the DNAzyme in the presence of Na^+. Upon being released from the substrate strand, the cleaved fragment became the initiator DNA (I) for the CHA amplification using two hairpin DNA

molecules (H1 and H2). The H1 and H2 remain intact because the cross-reactivity is blocked by their intramolecular hybridization to form loops without free initiator DNA. Once the initiator DNA (I) is released, it will bind to H1 through toehold-assisted hybridization to open H1. Upon generating single-stranded portion on H1, H2 was opened through strand-displacement reaction, leading the fluorescence signal turn-on. As a result of forming a stronger duplex between H1 and H2, I fragment was released, instead of being consumed, to catalyze the next circuit, generating multiple signal outputs to achieve signal amplification for endogenous Na^+ detection.

For ATP detection and imaging in living cells, the approach based on aptazyme technology was established (Yang et al. 2016). In this design, ATP aptamer and AuNPs were employed to construct the probe to elucidate the principle of this method. This method provides a new platform to intracellular ATP imaging with high selectivity and low detection limit of 100 nM.

11.2.3 SDA for Biomolecule Imaging in Cells

11.2.3.1 SDA for miRNA Imaging in Cells

In recent years, many strategies based on SDA, which is used to achieve target induction and signal amplification, have been reported. For example, Bai and co-workers employed gold nanoparticles (AuNP) as a scaffold to hold DNA to form a tetrahedral DNA nanostructure (TDN) (Bai et al. 2018). AuNPs exhibited fluorescence quenching effects and a large surface area to fabricate a fluorescence resonance energy transfer-based nanosensor (Au-TDNN). In the presence of miR-21 (target), the fluorescent dye-labeled detection probe on Au-TDNNs would be separated from AuNPs, which blocked the fluorescent quenching, producing an intensive fluorescence signal as an indicator for miRNA detection. Dai and co-workers also design a probe for miRNA quantitative detection utilizing SDA techniques (Dai et al. 2018). As shown in Fig. 11.10, they developed an intracellular miRNAs detection method based on a near-infrared (NIR) laser-induced target SDA mechanism. In this work, two types of hairpin probes, one was programmable oligonucleotide hairpin probes of hairpin assistant probe and the other was dye-labeled hairpin detection probe (HDP), were separately designed on the terminal and side surfaces of AuNRs (THP-AuNRs). In the THP-AuNRs, fluorescence of HDP was quenched by the AuNRs. The presence of target miRNAs separated the fluorescent dye from the surface of the AuNRs, leading to recovery of fluorescence. In the THP-AuNRs, a DNA linker connected the HAP to the terminal surface. The HAP was thermodynamically released from the terminal surface of AuNRs due to the photothermal effect of AuNRs with the 808 nm NIR laser irradiating. The released HAP displaced the hybridized target miRNAs on the THP-AuNPs, triggering a target SDA for sensitive miRNAs detection. The designed strategy provided excellent analytical performance in miRNAs analysis in living cells and multicellular tumor spheroids (MCTS). Notably, a quantitative method in single living cells was realized using a linear regression equation derived from miRNA

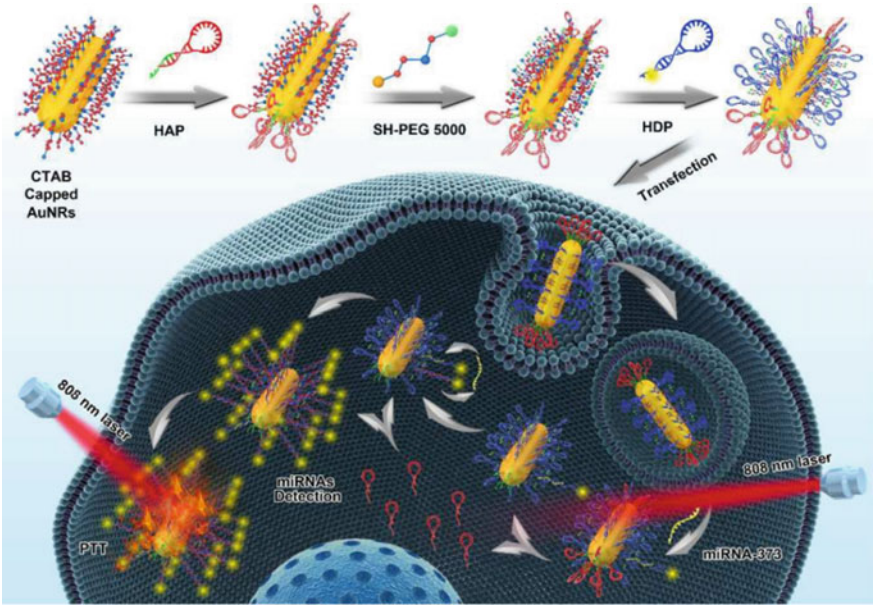

Fig. 11.10 Schematic illustration of THP-AuNRs nanopore and intracellular miRNA-amplified analysis in single living cells. The top row shows the principle of HAP and HDP modified to AuNRs. The bottom row shows the principle of detection based on THP-AuNRs nanoprobe through NIR irradiation-triggered SDA. Reproduced from Dai et al. (2018) by permission of The Royal Society of Chemistry

mimics based on the NIR-triggered SDA strategy because of its high sensitivity. For highly sensitive multiple intracellular miRNA detection, this group also developed an ATP self-powered SDCA system based on mesoporous silica-coated copper sulfide nanoparticles (CuS@mSiO_2) (Meng et al. 2018). CuS@mSiO_2 loaded with numerous ATPs was modified with the Y-motif DNA structure (CuS@mSiO_2/Y-ATP) through a disulfide bond (–S–S–) with one terminal containing a folded DNA strand (rich in cytosine and guanine) to improve the encapsulation efficiency and reduce the cargo leakage. After cellular uptake, the folded DNA strands were unlocked by forming a C-G·C^+ triplex DNA structure and accelerated the rupture of the disulfide bond (–S–S–) to release numerous ATPs in an acidic microenvironment. ATP was enhanced released from the nanoprobe due to the photothermal effect of the CuS core with the near-infrared (NIR) laser irradiation. The presence of target miRNAs in living cells triggered the corresponding strand displacement, and the endogenous and released ATP acted as fuel for SDCA, producing fluorescent signal as an indicator for miRNA target detection. In this report, the endogenous and released ATP powered the SDCA strategy instead of additional external catalytic fuel for intracellular miRNA analysis, enabling facile and accurate differentiation between normal cells and different types of cancer cell using intracellular miRNA imaging.

A DNA-fueled molecular machinery approach for sensitive detection of let-7a miRNAs in living cells with target-triggered recycling amplifications was reported (Li et al. 2017a, b). The nanoprobe was constructed with gold nanoparticles modifies with dsDNA, which were doubly labeled with FAM and TAMRA, and unfolded hairpin sequences together with the DNA fuels. Once the molecular machine was uptaken by cells, the function would be triggered by the target let-7a miRNA sequences and led to recycle the let-7a sequences through two cascaded TSDRs with the aid of the DNA fuel strands, leading to the release of many hairpin sequences from the dsDNA-AuNPs. The FAM and TAMRA were brought into close proximity, because of the restoration of the hairpin structures, to generate amplified FRET signals as an indicator for let-7a detection in living cells. As shown in Fig. 11.11, a nanomachine containing a DNA coated AuNP assembly (DNA-AuNP), a walking leg (W), and a fuel (F) was designed (Liang et al. 2017). In this design, a three-stranded substrate complex (A/B/C) and affinity ligand (L) were conjugated on a single AuNP. Substrate A tethered to the AuNP through a thiol at 5′ end along with B co-hybridizes to C labeled at 3′ end with FAM, forming a sandwich structure with a toehold at the 5′ end (toehold 1) and a B-sequestered toehold in the middle (toehold 2). In this nanomachine, the FAM fluorescence emission was almost quenched by AuNP. The W was drawn into a close proximity to the AuNP surface by binding L and W to T, which was designed to separately embed in L and W as the recognition sequences for target. The close proximity made W tethered to the AuNP to form a walkable leg with capability to perform highly effective intramolecular hybridization. And entropy-driven catalytic reaction was triggered as follows: W interacted with C via toehold 1 and displaced B from C via toehold-mediated strand displacement to expose toehold 2 on C. F hybridized to toehold 2 and triggered branch migration to form duplex C/F, resulting in the complete disassembly of the A/B/C complex and concurrent restoration of initially quenched FAM emission of C. The interaction of C with F liberated W to move along the DNA-AuNP track to react with a new toehold 1, triggering autonomous surface-bound A/B/C disassembly and continuous production of the fluorescence signal from the formation of duplex C/F.

Recently, Wu's group designed a ^{3HP}SDA nanomachine for target miRNA-triggered catalytic assembly to amplify fluorescence signal as an indicator for miRNA detection (Xue et al. 2018). Shen and co-workers utilized AuNPs to design photocaged DNA sensors based on SDA for miRNA detection (Shen et al. 2018).

11.2.3.2 SDA for Other Biomolecule Imaging in Cells

SDA strategies designed for cellular imaging have been widely reported including ATP detection and mRNA detection in living cells (Gao et al. 2018; He et al. 2018). Tan's group developed an entropy-driven 3D DNA amplifier (EDTD) able to operate within living cells to detect a specific intracellular mRNA target, shown in Fig. 11.12 (He et al. 2018). The EDTD probe was constructed with the entropy beacon tetrahedron (ET) module and the fuel tetrahedron (FT) module. In their design, an autonomous DNA circuit inside living cells could be specifically initiated by mRNA

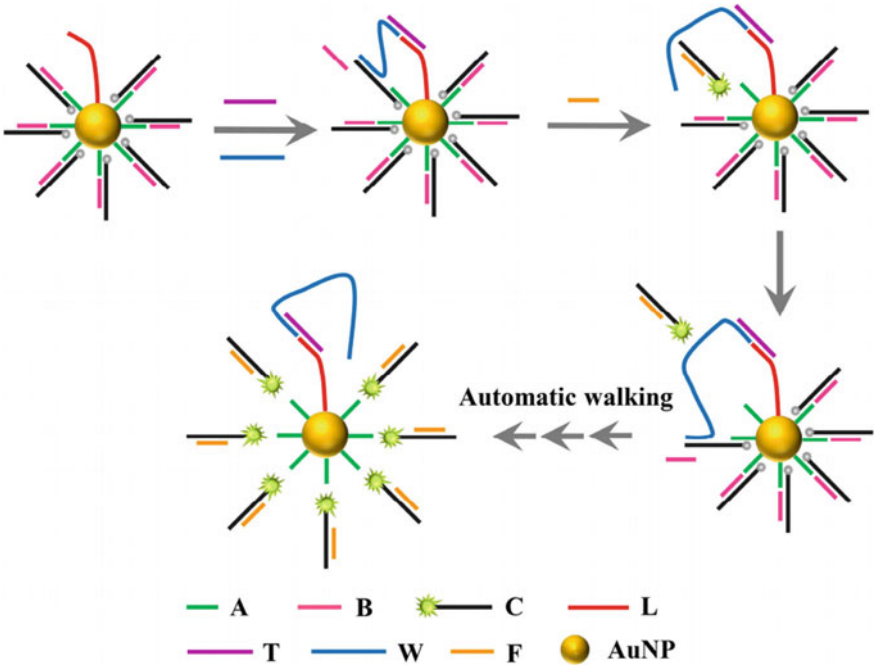

Fig. 11.11 Schematic illustration of the operation of entropy-driven DNA nanomachine for miRNAs analysis. Reproduced from Liang et al. (2017) by permission of John Wiley & Sons Ltd.

target/EDTD interaction owing to the exclusive entropy-driven force, leading obvious signal amplification for ultrasensitive detection of the target mRNA. Biostability and cellular uptake efficiency of DNA machines, which were usually recognized as prerequisites for in vivo applications, were significantly enhanced due to molecular engineering of a unique DNA tetrahedral framework into the DNA amplifier. This programmable DNA machine presented a simple and modular amplification mechanism for the detection of intracellular biomarkers. Moreover, this study provides a potentially valuable molecular tool for understanding the chemistry of cellular systems and offers a design blueprint for further expansion of DNA nanotechnology in living systems.

11.2.4 RCA for Biomolecule Imaging in Cells

In recent years, many nanoprobes based on RCA strategies have been widely designed and applied in cellular imaging including ATP, miRNA, and mRNA detection in living cells, and detection of cancer cells, and delivery of siRNA into cancer cells. For example, Larsson and co-workers presented a method for in situ detection and geno-

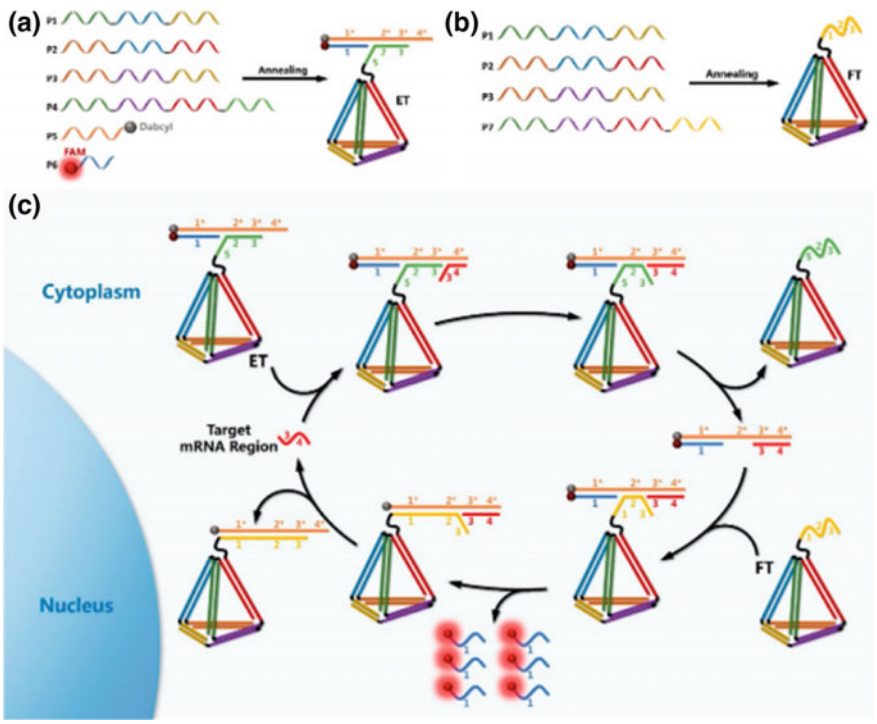

Fig. 11.12 Assembly of the ET module (**a**) and the FT module (**b**); **c** mechanism of EDTD for catalytic signal enhancement of specific mRNA expression in living cells. Reprinted with the permission from He et al. (2018). Copyright 2018 American Chemical Society

typing of individual mRNA molecules with padlock probes utilizing target-primed RCA (Larsson et al. 2010). In this report, they accomplished transcript detection in situ by first converting the mRNA into localized cDNA molecules, which could be detected with padlock probes and target-primed RCA. Genotyping of individual transcript molecules was highly specific with cDNA due to the specificity of the padlock probe ligation. For in situ mRNA detection in single cells, Li's group developed a robust method to directly detect mRNA. They employed Splint R, a recently discovered ligase, to efficiently catalyze ligation of the padlock probe by a RNA template for mRNA detection without reverse transcription (Deng et al. 2017). In their work, they introduced an extra short DNA sequence acting as the primer to perform in situ RCA instead of using mRNA as primer. In our group, we also designed probes for biomolecules detection using RCA techniques. For example, as shown in Fig. 11.13, DNA RCA based on click chemistry reaction was designed for imaging cell surface glycosylation with improved detection sensitivity. The click chemistry between the azide group of azido-sugars, which were integrated into glycans, and alkyne-functionalized DNA enhanced the labeling efficiency of DNA on the cell surface. An in situ RCA reaction would be initiated by the assembled DNA with the presence

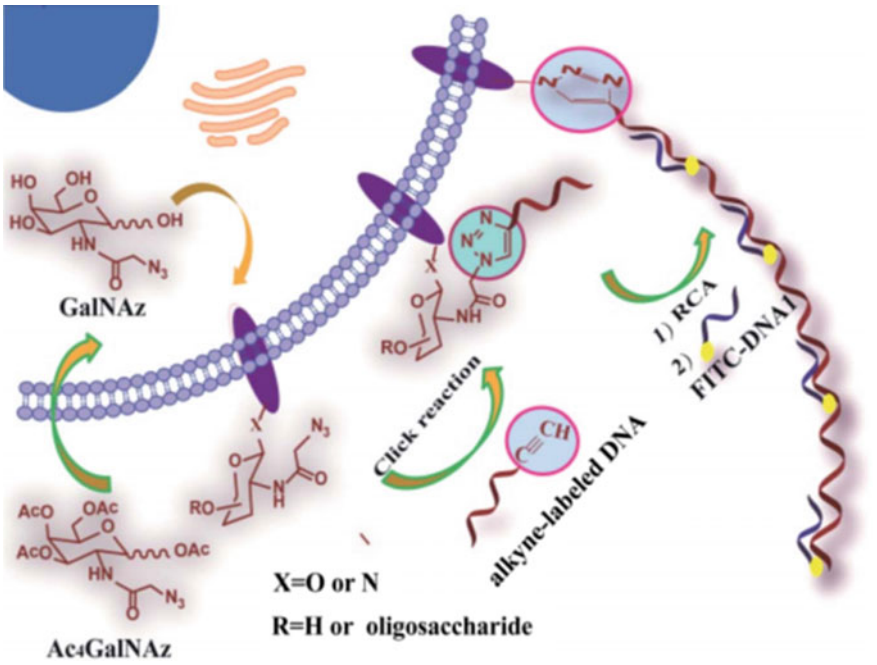

Fig. 11.13 General strategy for DNA RCA-assisted metabolic labeling of cell surface glycans. Reproduced from Zhang et al. (2016a, b) by permission of The Royal Society of Chemistry

of phi29 DNA polymerase and dNTPs, producing a long tandem repeated sequence. The RCA product would hybridized with large amount of FITC-labeled DNA generating an enhanced fluorescence as a detectable signal. This method can provide information about the localization and distributions of carbohydrates on the cell surface by using relatively low concentration of azido-sugar (Zhang et al. 2016a, b).

Recently in our group, a study on telomere detection and drug delivery based on RCA was reported (Zhang et al. 2017). In this design, new nuclear-shell biopolymers were formed on silica nanoflowers by telomere elongation. Telomerase could elongate the telomere primers, resulting in inner chain substitution followed by the release of RCA-primers and the trapped drug, which triggered the RCA of signal molecules, attached with fluorescence labels and self-assembled into the nuclear-shell offering significantly amplified signal. DOX could be released in response to telomerase activity for specific cancer treatments. This method could be used for human telomerase activity monitoring with high sensitivity. The discrepancy of telomerase activity between normal and tumor cells could be utilized to target drug release and improve diagnosis–treatment processes. For another work, based on RCA we constructed the novel nucleic acid–graphene oxide self-assembly, nucleic acid molecular aggregate self-assembled on graphene oxide nanoplates, and a functionalized triple-helix probe (THP) (Zhang et al. 2016a, b). The functionalized THP, which consisted with the

aptamer region for target recognition and the trigger DNA region for RCA, was firstly used for miRNA imaging in single cells. In this design, nucleic acid molecular aggregates, which were composed with the RCA products and fluorescence molecule-labeled DNA by hybridization, could partly self-assemble on graphene oxide nanoplates, and the other part were free, which led to the quenched fluorescence recovery. This method could be applied in low-abundance miRNA detection and imaging in single cells.

The use of self-propelled nanowires (AuNWs) for selective and rapid intracellular siRNA delivery utilizing a hybrid siRNA-DNA nanotechnology platform was described in this work (Esteban-Fernandez de Avila et al. 2016). In this approach, gene silencing relied on the accelerated intracellular delivery of green fluorescence protein targeted siRNA (siGFP), hybridized to RCA DNA structures carried by the US-propelled AuNWs. Once inside the cell, the siGFP was responsible for silencing the formation of new fluorescent proteins, as indicated by the rapid loss of the green fluorescence, which reflected an effective intracellular siRNA delivery. Different from other approaches using either membrane fusion or receptor-related endocytosis to enter the cell, these ultrasound-powered nanomotors pierced and traveled inside the cell. The nanomotor-based gene silencing method would be widely used for many cell lines.

11.2.5 PCR for Biomolecule Imaging in Cells

Based on programmable signal sequence, Jiang's group developed a novel strategy, using small molecule linked with DNA, to realize protein biomarker, on living cell surface, detection and imaging in situ and washing-free, developed (Huang et al. 2018a, b). Compared to the former study, in this method they deactivated the non-bound probes to achieve wash-free detection of proteins on cell surface. Hence, in this strategy the signal-to-background ratio was enhanced and this method provided a platform for signal reporting and amplification of various functional nucleic acids. Additionally, this strategy provided a label-free method for membrane protein detection because of no fluorescence or radiolabeling labeling.

Given the disruptiveness and restrictive, such as only provided snapshots of phenotypic traits, of molecular evaluation of reprogramming, gene reporter might risk insertional mutagenesis during viral transfection. So, Wiraja et al. demonstrated the utilization of a non-integrative nanosensor to visualize key reprogramming events in situ within live cells (Wiraja et al. 2018). Principally based on sustained intracellular release of encapsulated molecular probes, nanosensors successfully monitored mesenchymal-epithelial transition, pluripotency acquisition, and transdifferentiation events. Tracking the dynamic expression of four pivotal biomarkers (i.e., THY1, E-CADHERIN, OCT4, and GATA4 mRNA), nanosensor signal showed great agreement with PCR and gene reporter imaging ($R^2 > 0.9$). Such facile, versatile nanosensor-enabled real-time monitoring of low-frequency reprogramming events is

thereby useful for high-throughput assessment, optimization, and biomarker-specific cell enrichment.

11.3 Conclusion and Perspectives

These nucleic acid amplification strategies were widely developed and used for many biomarker detection and imaging in living cells or on cell surface. These strategies were designed to be facile and versatile, and the methods could be sensitively and specially used to detect biomolecules with low abundance or down-regulated properties in tumor cells. However, the nucleic acid amplification strategy used for in vivo imaging is rarely reported now. The current and oncoming challenges provide new opportunities for further research and development of improved analytical methods for all aspects of detection abilities, including accuracy, selectivity, efficiency, sensitivity, and application rang such as efficient multimode clinical detection, small animal in vivo imaging and the study of integrated diagnosis and treatment. If we can overcome the stability problem of probes in enzyme resistance inside cells, an isothermal amplification strategy-assisted modern optical method could be a strong tool in understanding life processes, and then help us to diagnose and treat cancers at a higher level. With the rapid development of nanomaterials and analytical methodology, it is expected that more excellent and simple-to-handle gentle amplification strategies could emerge brilliantly to build smart optical biosensing platforms for the sensitive assay of many malignant diseases with low cost, less time, ease of operation, and high sensitivity. Therefore, real clinical applications for accurate and minimally invasive diagnosis even with portable POC devices, precise and efficient drug delivery, and disease therapeutics could be realized.

References

Alam KK, Tawiah KD, Lichte MF et al (2017) A fluorescent split aptamer for visualizing RNA-RNA assembly in vivo. ACS Synth Biol 6:1710–1721

Bai S, Xu B, Guo Y et al (2018) High-discrimination factor nanosensor based on tetrahedral DNA nanostructures and gold nanoparticles for detection of miRNA-21 in live cells. Theranostics 8:2424–2434

Burke KS, Antilla KA, Tirrell DA (2017) A fluorescence in situ hybridization method to quantify mRNA translation by visualizing ribosome-mRNA interactions in single cells. ACS Cent Sci 3:425–433

Dai W, Dong H, Guo K et al (2018) Near-infrared triggered strand displacement amplification for microRNA quantitative detection in single living cells. Chem Sci 9:1753–1759

Deng R, Zhang K, Sun Y et al (2017) Highly specific imaging of mRNA in single cells by target RNA-initiated rolling circle amplification. Chem Sci 8:3668–3675

Ding C, Zhang C, Yin X et al (2018) Near-infrared fluorescent Ag_2S nanodot-based signal amplification for efficient detection of circulating tumor cells. Anal Chem 90:6702–6709

Esteban-Fernandez de Avila B, Angell C, Soto F et al (2016) Acoustically propelled nanomotors for intracellular siRNA delivery. ACS Nano 10:4997–5005
Fan HH, Zhao ZL, Yan GB et al (2015) A smart dnazyme–MnO_2 nanosystem for efficient gene silencing. Angew Chem Int Ed 127:4883–4887
Gao F, Wu J, Yao Y et al (2018) Proximity hybridization triggered strand displacement and DNAzyme assisted strand recycling for ATP fluorescence detection in vitro and imaging in living cells. RSC Adv 8:28161–28171
He L, Lu D, Liang H et al (2018) mRNA-initiated, three-dimensional DNA amplifier able to function inside living cells. J Am Chem Soc 140:258–263
Huang J, Wang H, Yang X et al (2016) Fluorescence resonance energy transfer-based hybridization chain reaction for in situ visualization of tumor-related mRNA. Chem Sci 7:3829–3835
Huang DJ, Huang ZM, Xiao HY et al (2018a) Protein scaffolded DNA tetrads enable efficient delivery and ultrasensitive imaging of miRNA through crosslinking hybridization chain reaction. Chem Sci 9:4892–4897
Huang DJ, Wu Z, Yu RQ et al (2018b) Small molecule-linked programmable DNA for washing-free imaging of cell surface biomarkers. Talanta 190:429–435
Karunanayake Mudiyanselage A, Yu Q, Leon-Duque MA et al (2018) Genetically encoded catalytic hairpin assembly for sensitive RNA imaging in live cells. J Am Chem Soc 140:8739–8745
Larsson C, Grundberg I, Soderberg O et al (2010) In situ detection and genotyping of individual mRNA molecules. Nat Methods 7:395–397
Li N, Chang C, Pan W et al (2012) A multicolor nanoprobe for detection and imaging of tumor-related mRNAs in living cells. Angew Chem Int Ed 51:7426–7430
Li F, Zhang H, Wang Z et al (2013) Dynamic DNA assemblies mediated by binding-induced DNA strand displacement. J Am Chem Soc 135:2443–2446
Li L, Feng J, Liu H et al (2016a) Two-color imaging of microRNA with enzyme-free signal amplification via hybridization chain reactions in living cells. Chem Sci 7:1940–1945
Li Z, He X, Luo X et al (2016b) DNA-programmed quantum dot polymerization for ultrasensitive molecular imaging of cancer cells. Anal Chem 88:9355–9358
Li D, Zhou W, Yuan R et al (2017a) A DNA-fueled and catalytic molecule machine lights up trace under-expressed microRNAs in living cells. Anal Chem 89:9934–9940
Li J, Li D, Yuan R et al (2017b) Biodegradable MnO_2 nanosheet-mediated signal amplification in living cells enables sensitive detection of down-regulated intracellular microRNA. ACS Appl Mater Interfaces 9:5717–5724
Li JJ, Li WN, Du WF et al (2018a) Target induced reconstruction of DNAzymatic amplifier nanomachines in living cells for concurrent imaging and gene silencing. Chem Commun 54:10626–10629
Li Z, Wang G, Shen Y et al (2018b) DNA-templated magnetic nanoparticle-quantum dot polymers for ultrasensitive capture and detection of circulating tumor cells. Adv Funct Mater 28:1707152
Liang CP, Ma PQ, Liu H et al (2017) Rational engineering of a dynamic, entropy-driven DNA nanomachine for intracellular microRNA imaging. Angew Chem Int Ed Engl 56:9077–9081
Liao X, Li L, Pan J et al (2018) In situ biosensor for detection miRNA in living cells based on carbon nitride nanosheets with catalytic hairpin assembly amplification. Luminescence 33:190–195
Liu HY, Tian T, Ji DD et al (2016) A Graphene-enhanced imaging of microRNA with enzyme-free signal amplification of catalyzed hairpin assembly in living cells. Biosens Bioelectron 85:909–914
Liu L, Liu JW, Huang ZM et al (2017) Proton-fueled, reversible DNA hybridization chain assembly for pH sensing and imaging. Anal Chem 89:6944–6947
Liu J, Du P, Zhang J et al (2018a) Sensitive detection of intracellular microRNA based on a flowerlike vector with catalytic hairpin assembly. Chem Commun 54:2550–2553
Liu L, Liu JW, Wu H et al (2018b) Branched hybridization chain reaction circuit for ultrasensitive localizable imaging of mRNA in living cells. Anal Chem 90:1502–1505
Mei SH, Liu ZJ, Brennan JD et al (2003) An efficient RNA-cleaving DNA enzyme that synchronizes catalysis with fluorescence signaling. J Am Chem Soc 125:412–420
Meng X, Dai W, Zhang K et al (2018) Imaging multiple microRNAs in living cells using ATP self-powered strand-displacement cascade amplification. Chem Sci 9:1184–1190

Ou M, Huang J, Yang XH et al (2017) Live-cell microRNA imaging through MnO_2 nanosheet mediated DD-A hybridization chain reaction. Chem Biochem Commun 19:147–152
Paliwoda RE, Li F, Reid S et al (2014) Sequential strand displacement beacon for detection of DNA coverage on functionalized gold nanoparticles. Anal Chem 86:6138–6143
Pan W, Zhang T, Yang H et al (2013) Multiplexed detection and imaging of intracellular mRNAs using a four-color nanoprobe. Anal Chem 85:10581–10588
Santangelo PJ, Nix B, Tsourkas A et al (2004) Dual FRET molecular beacons for mRNA detection in living cells. Nucleic Acids Res 32:e57
Santangelo DS, Giljohann DA, Hill HD et al (2007) Nano-flares: probes for transfection and mRNA detection in living cells. J Am Chem Soc 129:15477–15479
Shen Y, Li Z, Wang G et al (2018) Photocaged nanoparticle sensor for sensitive microRNA imaging in living cancer cells with temporal control. ACS Sens 3:494–503
Song WJ (2017) Intracellular DNA and microRNA sensing based on metal-organic framework nanosheets with enzyme-free signal amplification. Talanta 170:74–80
Song P, Ye D, Zuo X et al (2017) DNA hydrogel with aptamer-toehold-based recognition, cloaking, and decloaking of circulating tumor cells for live cell analysis. Nano Lett 17:5193–5198
Su FX, Yang CX, Yan XP (2017) Intracellular messenger RNA triggered catalytic hairpin assembly for fluorescence imaging guided photothermal therapy. Anal Chem 89:7277–7281
Tang Y, Zhang XL, Tang LJ et al (2017) In situ imaging of individual mRNA mutation in single cells using ligation-mediated branched hybridization chain reaction (ligation-bHCR). Anal Chem 89:3445–3451
Wang YM, Wu Z, Liu SJ et al (2015) Structure-switching aptamer triggering hybridization chain reaction on the cell surface for activatable theranostics. Anal Chem 87:6470–6474
Wang Y, Yu Z, Zhang Z et al (2016) Orderly nucleic acid aggregates by electrostatic self-assembly in single cells for miRNA detection and visualizing. Analyst 141:2861–2864
Wei J, Gong X, Wang Q et al (2018) Construction of an autonomously concatenated hybridization chain reaction for signal amplification and intracellular imaging. Chem Sci 9:52–61
Wiraja C, Yeo DC, Tham KC et al (2018) Real-time imaging of dynamic cell reprogramming with nanosensors. Small 14:e1703440
Wu P, Hwang K, Lan T et al (2013) A DNAzyme-gold nanoparticle probe for uranyl ion in living cells. J Am Chem Soc 135:5254–5257
Wu C, Cansiz S, Zhang L et al (2015a) A nonenzymatic hairpin DNA cascade reaction provides high signal gain of mRNA imaging inside live cells. J Am Chem Soc 137:4900–4903
Wu Z, Liu GQ, Yang XL et al (2015b) Electrostatic nucleic acid nanoassembly enables hybridization chain reaction in living cells for ultrasensitive mRNA imaging. J Am Chem Soc 137:6829–6836
Wu Z, Fan H, Satyavolu NSR et al (2017) Imaging endogenous metal ions in living cells using a DNAzyme-catalytic hairpin assembly probe. Angew Chem Int Ed 56:8721–8725
Xia Y, Zhang R, Wang Z et al (2017) Recent advances in high-performance fluorescent and bioluminescent RNA imaging probes. Chem Soc Rev 46:2824–2843
Xuan F, Fan TW, Hsing I-M (2015) Electrochemical interrogation of kinetically-controlled dendritic DNA/PNA assembly for immobilization-free and enzyme-free nucleic acids sensing. ACS Nano 9:5027–5033
Xue C, Zhang SX, Ouyang CH et al (2018) Target-induced catalytic assembly of y-shaped DNA and its application for in situ imaging of microRNAs. Angew Chem Int Ed 57:9739–9743
Yang Y, Huang J, Yang X et al (2016) Aptazyme-gold nanoparticle sensor for amplified molecular probing in living cells. Anal Chem 88:5981–5987
Yang J, Huang J, Yang XH et al (2017) Gold nanoparticle based hairpin-locked-DNAzyme probe for amplified miRNA imaging in living cells. Anal Chem 89:5850–5856
Zhang X, Li R, Chen Y et al (2016a) Applying DNA rolling circle amplification in fluorescence imaging of cell surface glycans labeled by a metabolic method. Chem Sci 7:6182–6189
Zhang Z, Wang Y, Zhang N et al (2016b) Self-assembly of nucleic acid molecular aggregates catalyzed by a triple-helix probe for miRNA detection and single cell imaging. Chem Sci 7:4184–4189

Zhang Z, Jiao Y, Zhu M et al (2017) Nuclear-shell biopolymers initiated by telomere elongation for individual cancer cell imaging and drug delivery. Anal Chem 89:4320–4327
Zhang Z, Zhong C, Yuan T et al (2018) A hybridization chain reaction amplification strategy for fluorescence imaging of human telomerase activity in living cells. Methods Appl Fluoresc 6:045003

Chapter 12
Surface-Enhanced Raman Spectroscopy for Bioimaging Based on Nucleic Acid Amplification Strategies

Shanwen Hu

Abstract Surface-enhanced Raman scattering (SERS) has been widely used on biosensing and bioimaging, especially for nucleic acid analysis. However, some problems such as target identification and signal uniformity limit its development. When introducing nucleic acid amplification strategies into SERS detections, some inspiring works have been reported. Herein, we first made a brief tutorial on SERS technique, then we reviewed recent works on SERS bioimaging based on nucleic acid amplification strategies, and at last, we made an outlook on the development of this topic.

12.1 A Brief Tutorial on SERS

Surface-enhanced Raman scattering (SERS) is firstly observed in 1973 on a roughened silver electrode to detect adsorbed pyridine and then correctly interpreted in 1977 (Campion and Kambhampati 1998). In 1997, scientists were inspired by the fact that the signal strength of Raman scattering can be evenly matched with that of fluorescence (Fig. 12.1) (Kneipp et al. 1999). During the last two decades, SERS technique undergoes a blooming age, in view of development in nanomaterials and Raman instrument. Nowadays, scientists majored in many fields, including chemistry, physics, material, and life sciences, are expanding our knowledge on SERS and exploiting its huge potential in numerous approaches (Bantz et al. 2011).

The mechanisms of SERS phenomenon can be classified into two types: electromagnetic enhancement and chemical enhancement. Electromagnetic enhancement relies heavily on noble metal nanoparticles. A molecule with Raman scattering effect is subjected to electromagnetic fields (EF) generated on the metal surfaces, results in stronger polarization of the molecule, leading to high SERS signals. Electromagnetic enhancement is counting for the major component of the enhancement mechanism, reported enhancement contribution of 10^4–10^7. Chemical enhancement results from

S. Hu (✉)
Shandong Provincial Key Laboratory of Detection Technology for Tumour Markers, College of Chemistry and Chemical Engineering, Linyi University, Linyi 276005, People's Republic of China
e-mail: shanwenhu@126.com

S. Zhang et al. (eds.), *Nucleic Acid Amplification Strategies for Biosensing, Bioimaging and Biomedicine*, https://doi.org/10.1007/978-981-13-7044-1_12

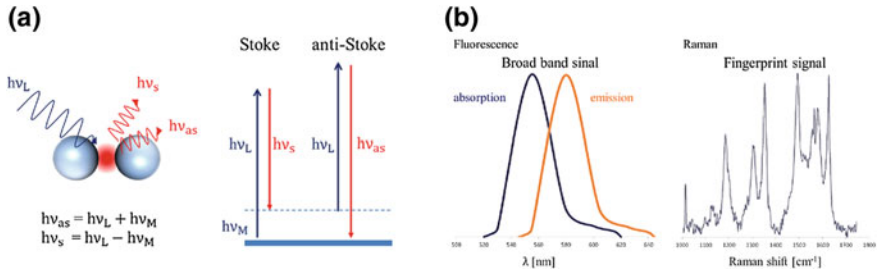

Fig. 12.1 Principle of Raman scattering, **a** stoke and anti-stoke modes, and **b** the comparison between fluorescence and Raman scattering spectra. Reprinted with permission from Lee and Tseng (2018). Copyright 2018 AIP publishing

charge transfer between metal and molecules adsorbed on plasmonic nanoparticles surfaces. Compared with electromagnetic enhancements, chemical enhancements are usually smaller, at range of $10–10^2$, depending on the chemical structure of molecules (Laing et al. 2017; Kahraman et al. 2017).

Since electromagnetic enhancement counts for most of SERS phenomenon, research mainly focuses on fabricating novel plasmonic substrates to obtain higher enhancement factors, via modulating physical properties such as particle size, shape, or composition of plasmonic particles (Fig. 12.2) (Du et al. 2018). The resonance frequency changed with the physical characteristics of nanoparticles. Higher SERS EFs can be achieved when the wavelength of the SPs (defined as λ_{SP}) is between the excitation wavelength (defined as λ_{exc}) and the wavelength of Raman signal (defined as λ_{RS}). Theoretical and experimental results indicate that EF reaches a maximum when $\lambda_{SP} = 1/2(\lambda_{exc} + \lambda_{RS})$. The EF on surface of nanoparticles also changes with physical properties. Thus, it is of essential meanings to generate intense electric fields on SERS substrate (Kneipp et al. 1999).

Besides physical properties of metallic nanoparticles mentioned above, there are other factors could effect plasmonic properties and which in turn contribute to SERS signals, such as molecule–substrate distance, type of structures (colloids and solid substrates), and aggregation status.

12.2 Fundamental Aspects of SERS Bioimaging

Identification of target molecules is always a key issue for applications ranging from health care to homeland security. SERS is especially helpful since it is capable of obtaining "fingerprinting" spectra from molecules similar in structure with high sensitivity. Furthermore, water has minimal background signal in SERS detection, which is beneficial for analysis of aqueous samples (Li et al. 2014; Cialla-May et al. 2017).

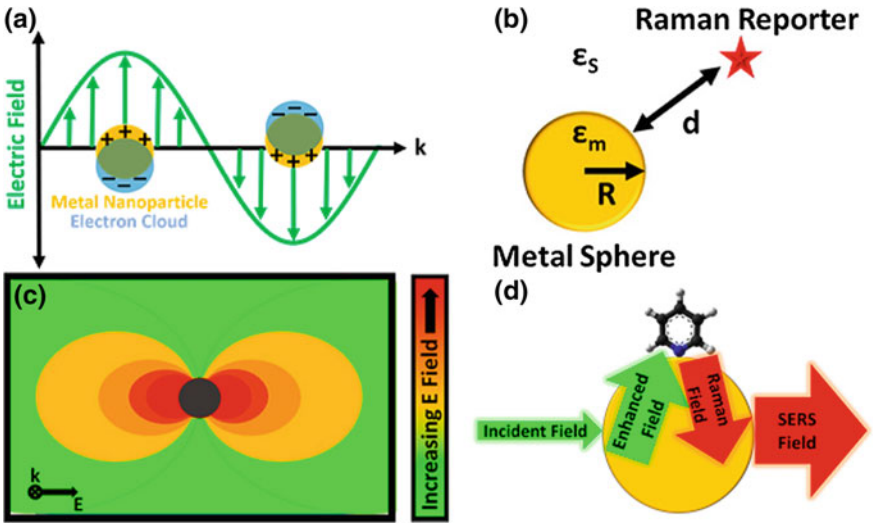

Fig. 12.2 **a** Illustration of the oscillating electron cloud, which moves in opposite direction of the electric field vector, for a nanoparticle smaller than the wavelength of light. **b** Depiction of the parameters. **c** Emitted dipole field of a metallic nanoparticle under light excitation. **d** EM enhancement of both the incident field and the scattered field. Reprinted with the permission from Lane et al. (2015). Copyright 2015 American Chemical Society

SERS bioimaging shows further advantages over other typical analysis techniques for the following aspects: (1) Widths of Raman peaks are normally 10–100 times narrower than fluorescence peaks, minimizing the overlap between different peaks; (2) SERS signal can be generated from SERS-active molecule within the zone of electromagnetic enhancement as long as the laser excitation wavelength is matched with the substrate LSPR wavelength, thus a single excitation source can be used for multiple labels; and (3) SERS labels are not susceptible to photobleaching (Ding et al. 2017).

Considering all these advantages, SERS detection is playing more and more important roles in biosensing applications. Herein in order to gain a better understanding of nucleic acid-based SERS detection, we first introduce some fundamental aspects of SERS biosensing in this section.

There are two types of SERS probes namely colloidal suspensions and solid substrates. As mentioned above, molecules must be bound to noble metal nanostructures in the range of 1–4 nm. Since this distance is determined by interactions between molecules and nanosurfaces, the SERS activity is stronger when the target molecules possess the opposite charge with the nanosurfaces. The reduced zeta potential of nanoparticles often caused aggregation, leading to increased SERS signals. However, large aggregates limit the generation of hot spots, and small-sized aggregates seem to be optimum for largest EFs (Cardinal et al. 2017).

12.2.1 SERS Substrate

As mentioned before, there are two mechanisms attributed to SERS effect, namely chemical enhancement, which is based on the charge transfer between substrate and analytes, and electromagnetic field (EF) enhancement, which relies on the metallic nanoparticles. Hence, most efforts to develop EF-based SERS sensors are focused on various SERS-active substrates based on new metal nanomaterials (Betz et al. 2014; Wang et al. 2017a).

The mechanism of SERS phenomenon is thought to be the laser excites localized surface plasmons on the metal, when properly regulated to match the geometry and material on SERS substrate, resulting in a strong, localized electromagnetic field, which greatly enhances Raman scattering of molecules within a few nm of the substrate surface. There are additional reports of a chemical charge transfer mechanism, which contribute to the overall SERS effect. Since the SERS substrate material plays a key role in the surface enhancement phenomenon, efforts have been devoted to fabricating novel and efficient SERS substrates. A brief review about the major categories of SERS substrates is introduced in this section, not intending to be a completed list, but instead a brief outline for better understanding of SERS bioimaging.

Roughened electrode

An electrode possess nanoscale roughness can be used as a signal generator for both electrochemical and SERS detection. Ikeda, K presented an Pt monolayer electroded, shown in Fig. 12.3, helped to gain better understanding in electrochemical SERS study. SERS observations were conducted on atomically defined Pt surface, while the electronic effects induced by crystal orientation, surface metal layer formation, and electrochemical potential tuning were also investigated successfully (Hu et al. 2014). Brolo, AG developed a roughened silver electrode immersed in diluted solutions of Brilliant Green, to show Stokes and anti-Stokes SERRS intensity fluctuations (dos Santos et al. 2011). Advantages of such electrode lie in the convenience of fabrication, the controllable surface situation, and double signal obtainment.

Colloidal nanoparticles

Colloidal nanoparticles have been widely used as SERS substrates for decades. Nanoparticles such as Au or Ag can be synthetized conveniently in the laboratory, with tunable physical and chemical prospects. For example, Xiong, J reported 3D sword-shaped Cu crystals via a universal colloidal method on Al substrates (Zhao et al. 2018). Morphology control during synthesis is key factors to fabricate colloidal nanoparticles as highly efficient SERS platforms.

Thanks to the development of nanotechnology, both nanoparticle size and geometry can be easily tuned or controlled by modulating experimental conditions. Some inspiring works have demonstrated controlled nanoparticle geometry for SERS detection such as nanocubes (Park et al. 2018), octahedral (Yoon et al. 2017), cuboctahedra (Zhang et al. 2016), as well as core-shell (Jung et al. 2018) or alloyed particles

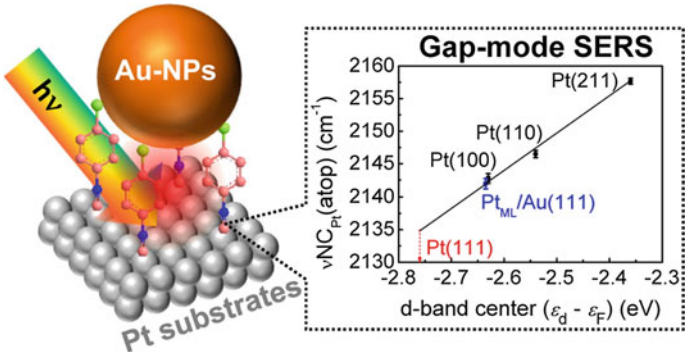

Fig. 12.3 **a** Schematic illustration of conventional SERS system on rough poly Pt. The Pt surface was covered with CPI. **b** Peak position as a function of the d-band center for various single crystalline Pt substrates. The linear fitting was conducted among Pt(100), Pt(110), and Pt(211). Reprinted with permission from Hu et al. (2014). Copyright 2014 American Chemical Society

(Schlucker 2014). Since the size, shape, and material of the particles all contributes to the resulting plasmonic resonance characteristics, research on SERS-based bioanalysis is closely related to nanotechnology.

Silicon

Silicon substrates are utilized as SERS substrate for their relatively low background within the Raman fingerprint region, aside from the characteristic peaks associated with the silicon crystal vibrations (Wang et al. 2015). The inkjet printer is used to fabricate the substrate for patterning designs. The brittleness of silicon wafers precludes them from being easily transported to the point of use, unless the wafers are immobilized on another support, for example, a glass slide. On-site SERS biosensing based on silicon substrate is bearing a blooming development (Shi et al. 2018; Meng et al. 2018).

Paper

Paper is drawing increasing attention as a substrate material for the features of lightweight, flexible, economical and portable, as well as power-free fluid transport via capillary action and the ability to store reagents within the fiber network. All of these features indicate that paper is very suitable for SERS sensor as supporting substrate (Hu et al. 2017). Recently, many works have reported that paper can be integrated with nanoparticles via different strategies, such as seeded growth, self-assembly, adsorption, brushing, inkjet printing, or in situ synthesis (Hu et al. 2018). So paper coupled with nanoparticles has great potential to be developed as SERS-active biosensors.

12.2.2 Labeled and Label-Free SERS Sensing

Raman reporter

Raman reporters are usually referred to molecules with large Raman cross sections, for example, chromophores such as malachite green, cyanine dyes, R6G, crystal violet, and Nile blue. The concentrations of targets molecules are related with amount of Raman reporters, so as to change the signal of targets to signal from the reporter, which is stronger enough to be distinguished from potential contaminants adsorbed on surface. Fluorescence signal is a common interference for SERS detection. So it is essential for the reporters to be firmly anchored to the surface so as to quench background emission (Wang et al. 2013b; Lane et al. 2015).

In recent years, the rational design of SERS reporters has been reported for improved stability and signal intensity (Banholzer et al. 2008). For example, Olivo and colleagues developed reporters based on triphenylmethine parent structures with a lipoic acid anchor group, which is more stable than single sulfur bond (Maiti et al. 2011). The Olivo group also fabricated a NIR resonant dye possessed 12-fold greater sensitivity than normal DTTC dyes, due to the extra stability introduced by a dithiol anchoring group (Maiti et al. 2012). Recently, chalcogenopyrylium dyes have been found to exhibit strong SERS signals in the NIR spectrum while having high affinity to substrate surfaces (Harmsen et al. 2015). Further explorations of Raman reporters would be beneficial to multiplexed tagging SERS applications (Kneipp et al. 2008; Wang et al. 2017a).

Label-free detection

Label-free methods have been used to directly identify biomolecules and obtain spectrum of molecules. By label-free determination of analytes, the spectral signatures of a single molecule down to fingerprint can be captured. For a long time, the signal of label-free is not strong enough to be distinguished from background. Nowadays, due to the improvement of Raman instrument and detection strategies, label-free signal can be read out and the signal intensity can also be related with target concentrations (Krafft et al. 2017; Wang et al. 2017b; Dasary et al. 2009).

12.2.3 Limitation of SERS Bioanalysis

Though numerous works have highlighted their SERS bioanalysis strategies, there are still some major limitations. First, the linkage between pre-embedded nanomaterials and substrates is usually not strong enough to bear the reagents during sample loading, which may lead to aggregation or detachment, resulting in uniformity. Second, nanoparticles are usually deposited on substrate in a random way, and it may restrict the generation of hot spot and reduce the uniformity. Third, fluorescence signal has the potential to mask SERS signals, even small amount of background fluorescence signal will lead to large disturbance. Finally, the practical issue of instrumentation

cost limits application of SERS out of biological laboratory; even though miniscale Raman spectrometers have been reported, for the most part, the cost of a laser, optics, spectrograph, and detector is high (Cardinal et al. 2017; Barhoumi et al. 2008; Laing et al. 2016).

12.3 SERS Bioanalysis Based on Nucleic Acid Amplification Strategies

12.3.1 Nucleic Acid in SERS Bioimaging

Aptamers for recognition

Aptamers are short single-strand DNAs or RNAs capable of recognizing targets with high affinity and specificity. A large number of aptamers have been screened via a combinatorial technique called systematic evolution of ligands by exponential enrichment (SELEX). Typically, more than 1010 random sequences are sent for target binding, and the ssDNAs/RNAs binding well to the target are then picked out. After PCR process, the products are subjected to the next round until the final sequences are identified as aptamers.

Aptamers play a vital role for biotarget recognition including metal ions, organic molecules, biomolecules, and even microorganisms/cells. In comparison with other target recognition molecules such as antibodies, aptamers show their advantages such as cost-effective synthesis, high binding affinities, and flexibility for signal transduction. Besides, it is easy to design probes in combination with following nucleic acid amplification process (Lee and Tseng 2018; Wang et al. 2010) (Fig. 12.4).

DNA detection in SERS

SERS has been widely used in DNA detection since its high sensitivity for readout (Ngo et al. 2016). Indirect sensing approaches are more popular, where a SERS reporter and ssDNA are immobilized onto nanoparticles and conformation will change after target recognition. Direct sensing methods have long been suffered from limitations such as weak signals and large background. However, in recent years large efforts have been devoted to these issues (Garcia-Rico et al. 2018). Target DNAs are determined after hybridization with probe on SERS-active substrate (Wang et al. 2013a). Due to the "hot spots" scattering on these SERS-active substrates, DNA targets detection with a limit low to 15–20 attomoles have been reported (Li et al. 2013) (Fig. 12.5).

RNA detection in SERS

When it comes to RNA detection on SERS substrate, most of the detection methods based on the Raman-labeled nanoparticle probes or least squares analysis failed to meet the requirement. The sensitivity is not sufficient to detect RNAs in clinically

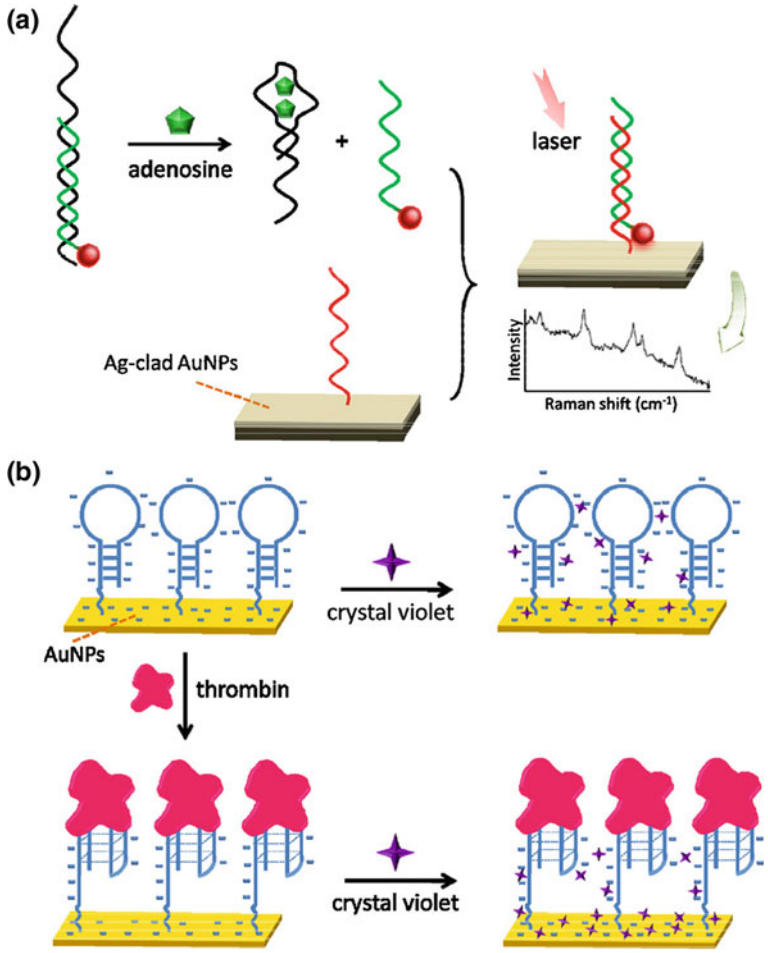

Fig. 12.4 SERS-based adenosine detection using structure-switching aptamer. **a** Short DNA strand released by target addition hybridizes with its probe DNA on SERS substrate and generates SERS signal (Chen et al. 2008). **b** Thrombin detection according to the different amount of CV molecules absorbed on SERS substrate due to target-induced different electrostatic effect of the anchored aptamer (Hu et al. 2009). Reprinted from Wang et al. (2010). Copyright 2010, with permission from Elsevier

relevant samples without an RNA enrichment treatment. For example, to detect circulating miRNAs in blood without PCR enrichment treatment, at least femtomolar sensitivity was needed (Pang et al. 2014).

Efforts have been devoted to detect RNA via SERS for clinical use, such as diagnosis of H5N1 (Wang et al. 2018b), cancer cells, and virus (Zou et al. 2018; Lee et al. 2017; Ali et al. 2014). Xu et al. described in vivo image of miRNA by SERS. They introduced side-by-side self-assembled plasmonic nanorod dimers into

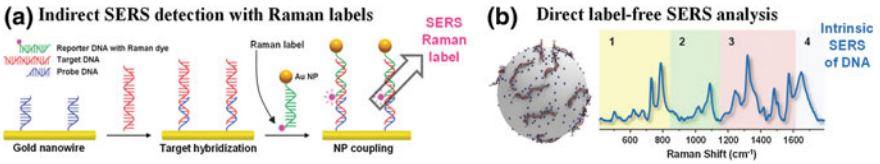

Fig. 12.5 **a** Schematic illustration of an indirect SERS approach for the detection of target single-stranded strands (ssDNAs) (Kang et al. 2010). **b** Schematic illustration of the acquisition of the intrinsic SERS spectrum of ssDNA strands directly adsorbed onto silver nanoparticles. Four major spectral regions of interest in representative SERS spectra of DNA. Reprinted from Garcia-Rico et al. (2018), by permission of The Royal Society of Chemistry

living cells, which give rise to a distinct intense plasmonic response. This work demonstrated potential for the real-time SERS bioimaging of biomarkers in living cells (Xu et al. 2018). Haldavnekar designed a label-free 3D semiconductor quantum probe for in vitro diagnosis of cancer. They observed an exponential increase in the SERS enhancement up to 10^6 at nanomolar concentration for potential bioimaging of DNA, RNA, or proteins up to single-cell level (Haldavnekar et al. 2018).

12.3.2 Distance Change Based on Nucleic Acid

The distance between Raman reporter and substrate is closely related with SERS signal intensity. A simple model for the distance dependence of the enhancement treats it as a near-field interaction of an oscillating dipole in the center of a sphere with a molecule at distance R from the center of the sphere, yielding a R^{-12} distance dependence. Hence, approaches have been promoted to build establish relevance between target molecules and the distance. The structure of aptamer or signal strand DNA will change after bonding with target molecules, leading to the approach or apart of labeled Raman reporter (Zhou et al. 2018; Lim et al. 2011).

The largest obstacle in utilizing operando SERS is the requirement that the reaction takes place within a few nanometers from the plasmonic surface (Zeng et al. 2016). If the catalytic reaction does not involve the plasmonic surface as the catalyst, then the whole catalytic system (i.e., the catalyst, reagents, and inert separation layer between the catalyst and plasmonic surface) must be incorporated near the surface in a way that optimizes the Raman signal during the experiment. Because a multitude of factors inherent to the catalytic reaction (not limited to the coverage, lifetime, and Raman scattering cross section of analyte species) will limit the SERS signal, the total distance between the analyte and plasmonic surface must be minimized to obtain appreciable signal (Qian and Nie 2008) (Fig. 12.6).

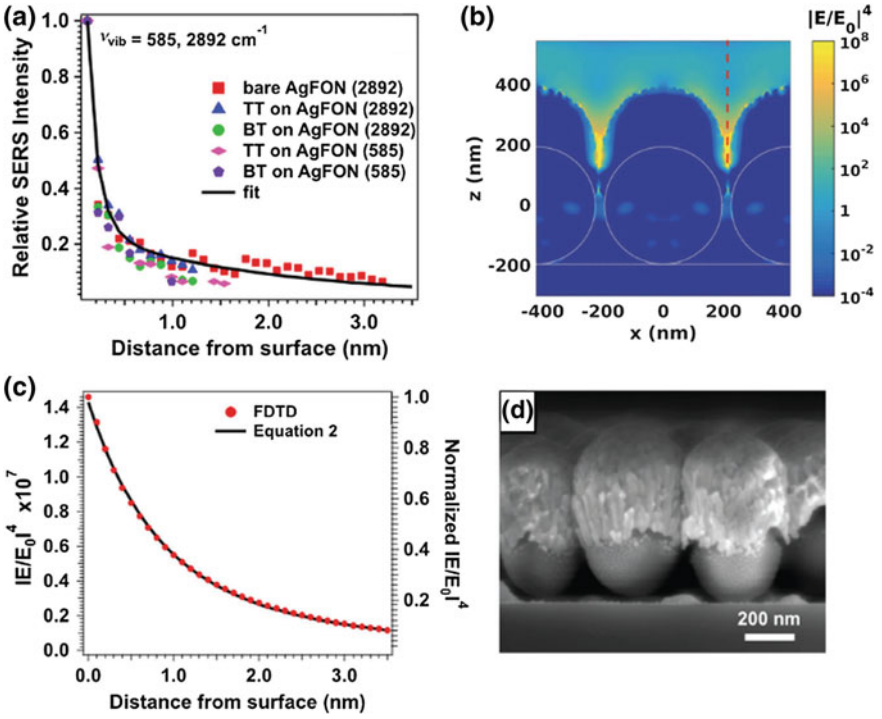

Fig. 12.6 Distance dependence of SERS. **a** SERS intensity decay of sym. C–H and sym. Al-CH_3. **b** Spatial distribution of local electric field enhancement from FDTD calculations of simulated Ag FON surface. **c** Near-field distance dependence profile at gap of simulated AgFON surface observed at the dashed red line in (B). **d** Side-view SEM micrograph of AgFON substrate used. Reprinted from Cardinal et al. (2017) by permission of The Royal Society of Chemistry

12.3.3 Aggregation Assisted by Nucleic Reactions

It is widely accepted that aggregation of nanoparticles can provide much higher SERS effect than single one. Thereby, target-induced aggregation of nanoparticles can be designed for novel "signal-on" SERS detection, which has a tremendous capacity for multiplex assays. However, since the uniformity of SERS signal during aggregation is especially out of control, substrates for homogenous and reproducible SERS analysis are still in demand (Guerrini and Graham 2012).

Chen, LX fabricated a silver nanoplatform for Hg^{2+} SERS detection. Spermine could bind AgNPs through Ag–N bonds and induce remarkable aggregation of labeled AgNPs, leading to strong SERS signal. At present of Hg^{2+}, the formation of the Hg–Ag alloy blocked the adsorption of spermine, resulting in the decrement of SERS signal (Chen et al. 2014). Some typical work based on target-induced aggregation of nanoparticles is shown in Fig. 12.7.

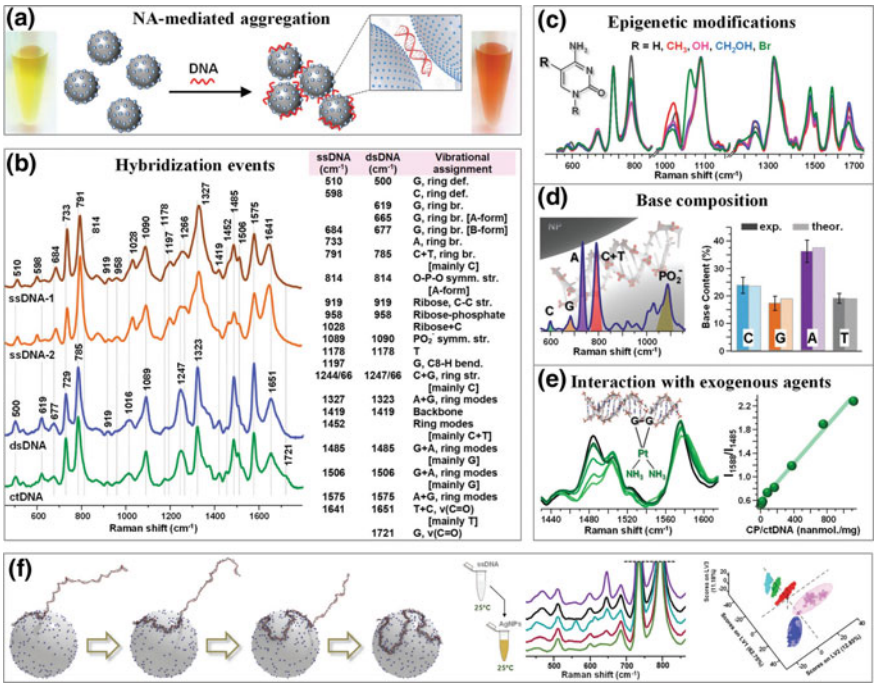

Fig. 12.7 **a** Schematic of DNA-mediated aggregation of positively charged Spermine-coated silver colloids (AgSp) into stable clusters in suspension (Morla-Folch et al. 2015). **b** Spectral differentiation of hybridization events. SERS spectra of two complementary 21-nt single strands and their corresponding duplex dsDNA. SERS spectra of double-stranded DNA isolated from the thymus of calves (ctDNA). (Panikkanvalappil et al. 2013) **c** Identification of chemically-modified cytosine variants in DNA. **d** Direct quantification of relative base composition in DNAs (Prado et al. 2014). **e** SERS monitoring of duplex DNA interactions with the chemotherapeutic drug cisplatin (CP) (Masetti et al. 2015). **f** Molecular dynamics simulation of the adsorption and wrapping process of a 141-nt ssDNA at low salt concentration (Morla-Folch et al. 2017). Reprinted from Garcia-Rico et al. (2018) by permission of The Royal Society of Chemistry

12.3.4 Cyclic Amplification Assisted Analysis

Rolling circle amplification (RCA)-assisted SERS

RCA is a simple and efficient in vitro DNA amplification technology, imitating internal rolling circle replication and generating a large number of repetitive sequences of target sequences. In the presence of DNA polymerase, the primer would extend and generate a long ssDNA product with thousands of repeated complementary sequences on the circular template. Linear RCA could generally achieve approximately 103-fold amplification in a short period, and the number could be further increased with the addition of a co-reagent DNA or protein. Therefore, it has been widely utilized

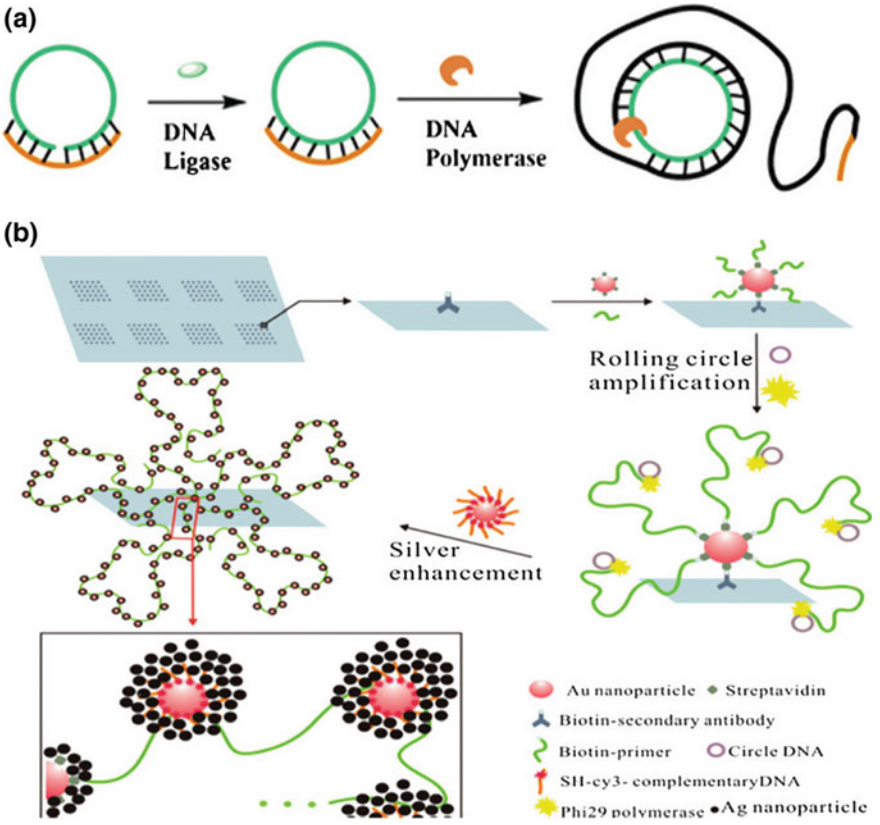

Fig. 12.8 Schematic illustration of RCA strategy and RCA-based sensitive SERS assays. **a** Schematic illustration of RCA strategy. **b** SERS assays based on nano rolling circle amplification (left) and nanohyperbranched rolling circle amplification (right) for protein microarrays. Reprinted with permission from Yan et al. (2012). Copyright (2012) American Chemical Society

in the diagnostic field for the detection of various DNA, RNA, or proteins combined with electrochemical or optical testing techniques (Ali et al. 2014).

RCA-assisted SERS detection interface was constructed according to the detection requirement. Hu and co-workers first combined the RCA reaction with SERS for the sensitive detection of nucleic acids on a gold electrode (Hu and Zhang 2010). In that work, target DNAs are sandwich-hybridized with the thiol-labeled capture probes and primer–probe. Then, the RCA reaction catalyzed with T4L DNA ligase induced an increasing amount of probe-modified gold nanoparticles hybridized with the long DNA strand, which significantly amplified the SERS signal and the detection sensitivity. Besides gold nanoparticles and gold nanorods were also combined with the long RCA product and showed more sensitive 35S promoter gene detection compared with a traditional assay without RCA (Guven et al. 2015) (Fig. 12.8).

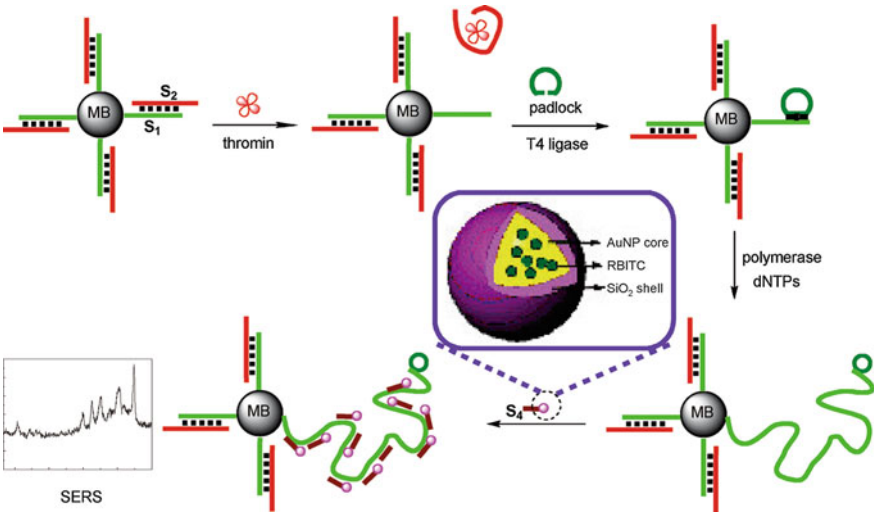

Fig. 12.9 Schematic illustration of the detection of thrombin by RCA–SERS strategy with core-shell tags. Reproduced from Li et al. (2015a) by permission of John Wiley & Sons Ltd.

In SERS assays, gold–silver staining methods were usually used for Raman scattering enhancement, attributed to the hot spots arising from the Ag nanoparticles grown around the fluorophore-labeled AuNPs (Cao et al. 2002). In order to increase these "hot spot" groups, Yan and co-workers reported a SERS sensing method employing an aldehyde-activated chip for protein micro-arrays with the help of nanoRCA and nanohyperbranched rolling circle amplification (HRCA) (Yan et al. 2012). Streptavidin-combined AuNPs (SA–AuNPs) were previously bound to the protein, and then, biotin-modified primers bonded to SA–AuNPs and simultaneously initiated the RCA reaction. Thus, the intensity of the Raman signal was detected for target protein analysis, with a detection limit lower than 10 zeptomolar. Considering that HRCA could create longer ssDNA and thus before efficient than RCA, they further designed a nanoHRCA strategy to achieve a much stronger SERS signal for protein micro-arrays than nanoRCA. Besides nucleic acids and proteins, some pathogenic microorganisms could also be sensitively detected using this RCA-assisted SERS assay method (Yao et al. 2017).

Li et al. reported an ultrasensitive SERS sensor based on RCA-increased "hot spot" for the detection of thrombin. The SERS probe is a sandwiched nanoplatform containing gold nanoparticle core, Raman label, and SiO_2 shell. At the surface of magnetic beads, they immobilized thrombin aptamers. When thrombin exists, the aptamer sequence was released, leaving the complementary ssDNA as primer for RCA reaction, resulting in long ssDNAs, which can bind with a large number of SERS probes. This method achieved a detection limit of 4.2×10^{-13} M, with good performance in real serum samples (Li et al. 2015b) (Fig. 12.9).

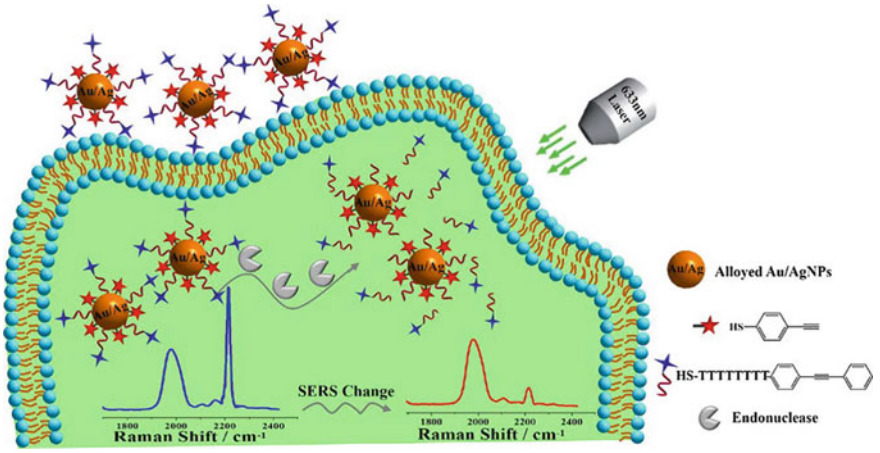

Fig. 12.10 Schematic illustration of the DNA–alkynes functionalized alloyed Au/AgNPs-based SERS nanosensor for ratio-metric detection of endonuclease. Reprinted with permission from Si et al. (2018). Copyright 2018 American Chemical Society

Endonuclease-assisted SERS

Endonuclease includes restriction endonucleases and nicking endonucleases (NEase). Restriction endonucleases are enzymes that catalyze the cleavage of specific double-stranded nucleotide sequences known as restriction sites. Benefiting from the unique character of NEase, which only catalyzes the hydrolysis of one strand of a duplex at specific recognition sites, many works further integrated it with strand displacement amplification (SDA) to further amplify the detection signals. Li et al. fabricated Au/Ag nanoparticles (NPs) as SERS substrate to determine the activity of endonuclease under in vitro and in living cells conditions, ssDNA carrying PEB acts as endonuclease responsive SERS signaling molecule and 4-thiophenylacetylene (TPA) acts as the internal standard molecule (Si et al. 2018; Ye et al. 2014b). Li et al. combined two-stage isothermal nucleic acid amplification with SERS readout to develop a signal-on detection platform. With help of exonuclease III, trigger DNA is generated to initiate HCR circles. The product structure tagged with SERS label is then anchored onto substrate for readout (Li et al. 2016) (Fig. 12.10).

In addition to the above-mentioned enzyme-assisted amplification strategies, enzyme-free nucleic acid isothermal amplification methods were also constructed on AuNP-based micro-reaction interfaces to obtain amplified SERS signal. For example, Ding et al. developed a HCR-assisted SERS biosensor for determination of mercuric ion Hg(II). The trigger DNA is identified by two hairpin probes for HCR to form a stable nicked dsDNA structure on magnetic beads, so as to generate a large number of binding sites for connection of AuNPs (with Raman-labeled DNA and streptavidin). The stable sandwich structure can be isolated by magnetic field and used in the following amplification step. By this means, Hg(II) can be determined with high sensitivity (Zhang et al. 2018; He et al. 2013).

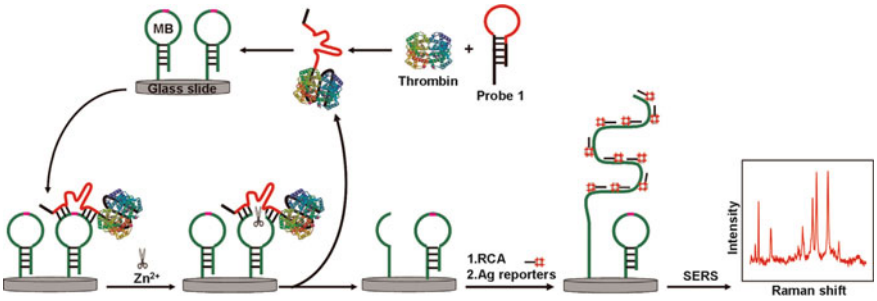

Fig. 12.11 Schematic illustration of SERS assay for thrombin detection based on DNAzyme assistant DNA recycling and rolling circle amplification. Reprinted from Gao et al. (2015). Copyright 2015, with permission from Elsevier

DNAzyme-assisted SERS

DNAzymes have shown its potential as molecular tools in biosensing and bioimaging. The catalytic activities of DNAzymes can be specifically triggered by cofactors and showed multiple enzymatic properties, which make DNAzymes capable of both molecule recognition and signal amplifiers. Combining with nanostructures, DNAzymes may be applied to novel fluorescent, colorimetric, SERS, electrochemical, and chemiluminescent analysis (Gong et al. 2015; Tian et al. 2017).

Gao and co-workers combined DNAzyme-assisted DNA recycling into SERS cycling for detection of thrombin. After thrombin binding with hairpins, the resulting DNAzyme can hybridize with the MB and activate by cofactor Zn^{2+}, while the remaining DNA can trigger RCA reaction. The long amplified RCA product can bind with Raman reporter-labeled AgNPs for SERS readout (Gao et al. 2015). Shi fabricated a SERS silicon chip for Pb^{2+} detection. The chip composed of core (Ag)-satellite (Au) nanoparticles on silicon surface. When DNAzyme is specifically activated by Pb^{2+} and cleaved the substrate strand into two free DNA strands, strong SERS signals could be generated (Shi et al. 2016) (Fig. 12.11).

In order to prepare gold nanorods (AuNRs) with high purity and density on graphene oxide (GO) , both two-step strategy of pre-sythesis–post assembly and one-step strategy of in situ growth have been explored, respectively. Observations of morphology and plasmonic bands reveal that both of the two approaches can yield AuNRs with high purity on GO; however, the former can generate more uniform-sized AuNRs on GO in contrast with the latter. Moreover, the AuNRs/GO and gold nanoparticle seed–SERS nanotags can be assembled to fabricate large-scaled superstructured plasmonic nanocomposities through DNAzyme–DNA substrate prehybridization and in situ hybridization, respectively, and disassembled via copper ions aided-DNAzyme–DNA substrate cleavage. As a result, an "on–off" aptasensor can be utilized as an ultrasensitive SERS substrate for detection of copper ions (Wang et al. 2018a; Tao and Wang 2018).

Fu et al. proposed a DNAzyme-linked plasmonic nanomachine for detection of lead ions. This DNAzyme could be activated by lead ions and catalyze a fracture

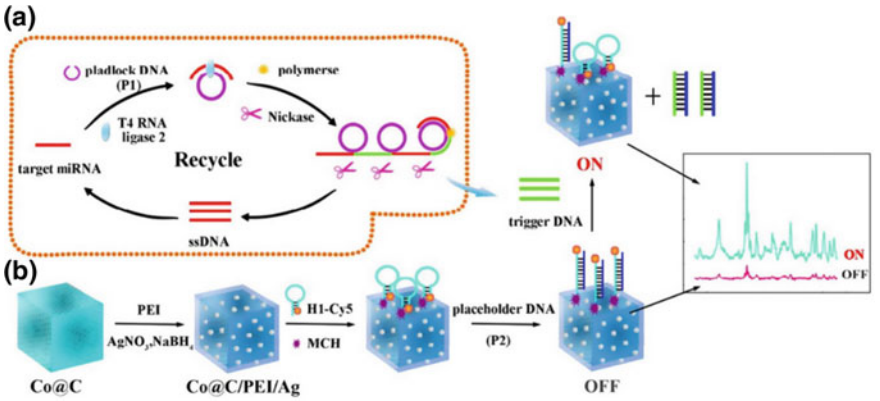

Fig. 12.12 Schematic Illustration of **a** RCA process; **b** SERS platform. Reprinted with permission from He et al. (2017). Copyright 2017 American Chemical Society

action of the substrate, changing the double chain structure into a flexible single strand, making the labeled nanoparticles fall to the metal film, which will exhibit a similar effect of a "hot spot" and remarkably enhance the SERS signal (Fu et al. 2014).

Rolling circle reaction-assisted SERS

Yuan et al. fabricated a rolling circle reaction-assisted SERS strategy named padlock probe-based exponential RCA (P-ERCA) for ultrasensitive detection of miRNA. On surface of a magnetic SERS substrate (Co@C/PEI/Ag), mi-155 triggered a RCA process for a long repeat sequence, which could be cleaved into two ssDNAs with help of nickase. One of the DNAs can initiate new cycle reactions to amplify trigger DNA, which would be hybridized with a Raman-labeled hairpin DNA for readout (He et al. 2017) (Fig. 12.12).

Li and co-workers have built a SERS protocol for the selective and sensitive assay of miRNA with the help of target-triggered rolling circle polymerization (RCP) and rolling circle transcription (RCT) (Li et al. 2015a). Ye designed a circular exponential amplification reaction to develop a direct sensing system for detection of multiple miRNAs in lung cancer cells with a limit of 0.5 fM, showing great potential for further clinical application in early diagnosis (Ye et al. 2014a).

12.4 Conclusions and Outlook

Numerous works have been proposed in developing SERS strategies for nucleic acid analysis both in vitro and in vivo. Well-designed SERS analysis allows high signal enhancements without giving rise to interference human body. The biocompatibility of nanoparticles has also been improved by careful selection of the substrate and

application of protective coatings. However, cytotoxicity still remains a concern preventing clinical application of SERS, and more and more research is necessary to explore the most safe and stable nanoprobes for clinical use. We predict the use of SERS bioimaging in a clinical environment that will eventually come true in next decades.

References

Ali MM, Li F, Zhang ZQ et al (2014) Rolling circle amplification: a versatile tool for chemical biology, materials science and medicine. Chem Soc Rev 43(10):3324–3341

An Q, Zhang P, Li JM et al (2012) Silver-coated magnetite-carbon core-shell microspheres as substrate-enhanced SERS probes for detection of trace persistent organic pollutants. Nanoscale 4(16):5210–5216

Banholzer MJ, Millstone JE, Lidong Q et al (2008) Rationally designed nanostructures for surface-enhanced Raman spectroscopy. Chem Soc Rev 37(5):885–897

Bantz KC, Meyer AF, Wittenberg NJ et al (2011) Recent progress in SERS biosensing. Phys Chem Chem Phys 13(24):11551–11567

Barhoumi A, Zhang D, Tam F et al (2008) Surface-enhanced Raman spectroscopy of DNA. J Am Chem Soc 130(16):5523–5529

Betz JF, Yu WW, Cheng Y et al (2014) Simple SERS substrates: powerful, portable, and full of potential. Phys Chem Chem Phys 16(6):2224–2239

Campion A, Kambhampati P (1998) Surface-enhanced Raman scattering. Chem Soc Rev 27(4):241–250

Cao YWC, Jin RC, Mirkin CA (2002) Nanoparticles with Raman spectroscopic fingerprints for DNA and RNA detection. Science 297(5586):1536–1540

Cardinal MF, Ende EV, Hackler RA et al (2017) Expanding applications of SERS through versatile nanomaterials engineering. Chem Soc Rev 46(13):3886–3903

Chen JW, Liu XP, Feng KJ, Liang Y, Jiang JH, Shen GL, Yu RQ (2008) Detection of adenosine using surface-enhanced Raman scattering based on structure-switching signaling aptamer. Biosens Bioelectron 24(1):66–71

Chen LX, Qi N, Wang XK et al (2014) Ultrasensitive surface-enhanced Raman scattering nanosensor for mercury ion detection based on functionalized silver nanoparticles. RSC Adv 4(29):15055–15060

Cialla-May D, Zheng XS, Weber K et al (2017) Recent progress in surface-enhanced Raman spectroscopy for biological and biomedical applications: from cells to clinics. Chem Soc Rev 46(13):3945–3961

Dasary SSR, Singh AK, Senapati D et al (2009) Gold nanoparticle based label-free SERS probe for ultrasensitive and selective detection of trinitrotoluene. J Am Chem Soc 131(38):13806–13812

Ding SY, You EM, Tian ZQ et al (2017) Electromagnetic theories of surface-enhanced Raman spectroscopy. Chem Soc Rev 46(13):4042–4076

dos Santos DP, Andrade GFS, Brolo AG et al (2011) Fluctuations of the Stokes and anti-Stokes surface-enhanced resonance Raman scattering intensities in an electrochemical environment. Chem Commun 47(25):7158–7160

Du S, Yu C, Tang L et al (2018) Applications of SERS in the detection of stress-related substances. Nanomaterials 8(10):757

Fu CC, Xu WQ, Wang HL et al (2014) DNAzyme-based plasmonic nanomachine for ultrasensitive selective surface-enhanced raman scattering detection of Lead ions via a particle-on-a-film hot spot construction. Anal Chem 86(23):11494–11497

Gao FL, Du LL, Tang DQ et al (2015) A cascade signal amplification strategy for surface enhanced Raman spectroscopy detection of thrombin based on DNAzyme assistant DNA recycling and rolling circle amplification. Biosens Bioelectron 66:423–430

Garcia-Rico E, Alvarez-Puebla RA, Guerrini L (2018) Direct surface-enhanced Raman scattering (SERS) spectroscopy of nucleic acids: from fundamental studies to real-life applications. Chem Soc Rev 47(13):4909–4923

Gong L, Zhao ZL, Lv YF et al (2015) DNAzyme-based biosensors and nanodevices. Chem Commun 51(6):979–995

Guerrini L, Graham D (2012) Molecularly-mediated assemblies of plasmonic nanoparticles for surface-enhanced Raman spectroscopy applications. Chem Soc Rev 41(21):7085–7107

Guven B, Boyaci IH, Tamer U et al (2015) Development of rolling circle amplification based surface-enhanced Raman spectroscopy method for 35S promoter gene detection. Talanta 136:68–74

Haldavnekar R, Venkatakrishnan K, Tan B (2018) Non plasmonic semiconductor quantum SERS probe as a pathway for in vitro cancer detection. Nat Commun 9:18

Harmsen S, Bedics MA, Wall MA et al (2015) Rational design of a chalcogenopyrylium-based surface-enhanced resonance Raman scattering nanoprobe with attomolar sensitivity. Nat Commun 6:9

He P, Zhang Y, Liu LJ et al (2013) Ultrasensitive SERS detection of lysozyme by a target-triggering multiple cycle amplification strategy based on a gold substrate. Chem-Eur J 19(23):7452–7460

He Y, Yang X, Yuan R et al (2017) "Off" to "On" Surface-enhanced Raman spectroscopy platform with padlock probe-based exponential rolling circle amplification for ultrasensitive detection of microRNA 155. Anal Chem 89(5):2866–2872

Hu J, Zheng PC, Jiang JH, Shen GL, Yu RQ, Liu GK (2009) Electrostatic interaction based approach to thrombin detection by surface-enhanced Raman spectroscopy. Anal Chem 81(1):87–93

Hu J, Tanabe M, Sato J et al (2014) Effects of atomic geometry and electronic structure of platinum surfaces on molecular adsorbates studied by gap-mode SERS. J Am Chem Soc 136(29):10299–10307

Hu JA, Zhang CY (2010) Sensitive detection of nucleic acids with rolling circle amplification and surface-enhanced raman scattering spectroscopy. Anal Chem 82(21):8991–8997

Hu SW, Qiao S, Pan JB et al (2018) A paper-based SERS test strip for quantitative detection of Mucin-1 in whole blood. Talanta 179:9–14

Hu SW, Qiao S, Xu BY et al (2017) Dual-functional carbon dots pattern on paper chips for Fe^{3+} and Ferritin analysis in whole blood. Anal Chem 89(3):2131–2137

Jung JH, Lee SY, Seo TS (2018) In vivo synthesis of nanocomposites using the recombinant escherichia coli. Small 14(42):7

Kahraman M, Mullen ER, Korkmaz A et al (2017) Fundamentals and applications of SERS-based bioanalytical sensing. Nanophotonics 6(5):831–852

Kang T, Yoo SM, Yoon I et al (2010) Patterned multiplex pathogen DNA detection by Au particle-on-wire SERS sensor. Nano Lett 10(4):1189–1193

Kneipp J, Kneipp H, Kneipp K (2008) SERS-a single-molecule and nanoscale tool for bioanalytics. Chem Soc Rev 37(5):1052–1060

Kneipp K, Kneipp H, Itzkan I et al (1999) Ultrasensitive chemical analysis by Raman spectroscopy. Chem Rev 99(10):2957

Krafft C, Schmitt M, Schie IW et al (2017) Label-free molecular imaging of biological cells and tissues by linear and nonlinear Raman spectroscopic approaches. Angew Chem Int Ed 56(16):4392–4430

Laing S, Gracie K, Faulds K (2016) Multiplex in vitro detection using SERS. Chem Soc Rev 45(7):1901–1918

Laing S, Jamieson LE, Faulds K et al (2017) Surface-enhanced Raman spectroscopy for in vivo biosensing. Nat Rev Chem 1(8):19

Lane LA, Qian XM, Nie SM (2015) SERS nanoparticles in medicine: from label-free detection to spectroscopic tagging. Chem Rev 115(19):10489–10529

Lee CW, Tseng FG (2018) Surface enhanced Raman scattering (SERS) based biomicrofluidics systems for trace protein analysis. Biomicrofluidics 12(1):19

Lee JM, Hwang A, Choi H et al (2017) A multivalent structure-specific RNA binder with extremely stable target binding but reduced interaction with nonspecific RNAs. Angew Chem Int Ed 56(50):15998–16002

Li M, Cushing SK, Liang HY et al (2013) Plasmonic nanorice antenna on triangle nanoarray for surface-enhanced Raman scattering detection of Hepatitis B Virus DNA. Anal Chem 85(4):2072–2078

Li XM, Wang LL, Li CX (2015a) Rolling-circle amplification detection of thrombin using surface-enhanced Raman spectroscopy with core-shell nanoparticle probe. Chem Eur J 21(18):6817–6822

Li XM, Zheng FW, Ren R (2015b) Detecting miRNA by producing RNA: a sensitive assay that combines rolling-circle DNA polymerization and rolling circle transcription. Chem Commun 51(60):11976–11979

Li Y, Qi XD, Lei CC et al (2014) Simultaneous SERS detection and imaging of two biomarkers on the cancer cell surface by self-assembly of branched DNA-gold nanoaggregates. Chem Commun 50(69):9907–9909

Li Y, Yu CF, Han HX et al (2016) Sensitive SERS detection of DNA methyltransferase by target triggering primer generation-based multiple signal amplification strategy. Biosens Bioelectron 81:111–116

Lim DK, Jeon KS, Hwang JH et al (2011) Highly uniform and reproducible surface-enhanced Raman scattering from DNA-tailorable nanoparticles with 1-nm interior gap. Nat Nanotechnol 6(7):452–460

Maiti KK, Dinish US, Samanta A et al (2012) Multiplex targeted in vivo cancer detection using sensitive near-infrared SERS nanotags. Nano Today 7(2):85–93

Maiti KK, Samanta A, Vendrell M et al (2011) Multiplex cancer cell detection by SERS nanotags with cyanine and triphenylmethine Raman reporters. Chem Commun 47(12):3514–3516

Masetti M, Xie HN, Krpetic Z et al (2015) Revealing DNA Interactions with Exogenous Agents by Surface-Enhanced Raman Scattering. J Am Chem Soc 137(1):469–476

Meng XY, Wang HY, Chen N et al (2018) A Graphene-silver nanoparticle-silicon sandwich SERS chip for quantitative detection of molecules and capture, discrimination, and inactivation of Bacteria. Anal Chem 90(9):5646–5653

Morla-Folch J, Gisbert-Quilis P, Masetti M, Garcia-Rico E, Alvarez-Puebla RA, Guerrini L (2017) Conformational SERS classification of K-Ras point mutations for cancer diagnostics. Angew Chem-Int Edit 56(9):2381–2385

Morla-Folch J, Xie HN, Gisbert-Quilis P et al (2015) Ultrasensitive direct quantification of nucleobase modifications in DNA by surface-enhanced raman scattering: The Case of Cytosine. Angew Chem Int Ed 54(46):13650–13654

Ngo HT, Wang HN, Fales AM et al (2016) Plasmonic SERS biosensing nanochips for DNA detection. Anal Bioanal Chem 408(7):1773–1781

Pang YF, Wang JF, Xiao R et al (2014) SERS molecular sentinel for the RNA genetic marker of PB1-F2 protein in highly pathogenic avian influenza (HPAI) virus. Biosens Bioelectron 61:460–465

Panikkanvalappil SR, Mahmoud MA, Mackey MA et al (2013) Surface-enhanced Raman spectroscopy for real-time monitoring of reactive oxygen species-induced DNA damage and its prevention by platinum nanoparticles. ACS Nano 7(9):7524–7533

Park JE, Lee Y, Nam JM (2018) Precisely shaped, uniformly formed gold nanocubes with ultrahigh reproducibility in single-particle scattering and surface enhanced Raman scattering. Nano Lett 18(10):6475–6482

Prado E, Colin A, Servant L et al (2014) SERS spectra of oligonucleotides as fingerprints to detect label-free RNA in microfluidic devices. J Phys Chem C 118(25):13965–13971

Qian XM, Nie SM (2008) Single-molecule and single-nanoparticle SERS: from fundamental mechanisms to biomedical applications. Chem Soc Rev 37(5):912–920

Schlucker S (2014) Surface-enhanced raman spectroscopy: concepts and chemical applications. Angew Chem Int Ed 53(19):4756–4795

Shi Y, Chen N, Su YY et al (2018) Silicon nanohybrid-based SERS chips armed with an internal standard for broad-range, sensitive and reproducible simultaneous quantification of lead(II) and mercury(II) in real systems. Nanoscale 10(8):4010–4018

Shi Y, Wang HY, Jiang XX et al (2016) Ultrasensitive, specific, recyclable, and reproducible detection of Lead ions in real systems through a polyadenine-assisted, surface enhanced raman scattering silicon chip. Anal Chem 88(7):3723–3729

Si YM, Bai YC, Qin XJ et al (2018) Alkyne-DNA-functionalized alloyed Au/Ag nanospheres for ratiometric surface-enhanced raman scattering imaging assay of endonuclease activity in live cells. Anal Chem 90(6):3898–3905

Tao GQ, Wang J (2018) Gold nanorod@nanoparticle seed-SERS nanotags/graphene oxide plasmonic superstructured nanocomposities as an "on-off" SERS aptasensor. Carbon 133:209–217

Tian AH, Liu Y, Gao JA (2017) Sensitive SERS detection of lead ions via DNAzyme based quadratic signal amplification. Talanta 171:185–189

Wang GQ, Wang YQ, Chen LX et al (2010) Nanomaterial-assisted aptamers for optical sensing. Biosens Bioelectron 25(8):1859–1868

Wang HN, Dhawan A, Du Y et al (2013a) Molecular sentinel-on-chip for SERS-based biosensing. Phys Chem Chem Phys 15(16):6008–6015

Wang YQ, Yan B, Chen LX (2013b) SERS tags: novel optical nanoprobes for bioanalysis. Chem Rev 113(3):1391–1428

Wang HY, Zhou YF, Jiang XX et al (2015) Simultaneous capture, detection, and inactivation of bacteria as enabled by a surface-enhanced raman scattering multifunctional chip. Angew Chem Int Ed 54(17):5132–5136

Wang XM, Zhang Z, Liu J et al (2017a) Stable Cu_2O@Au for accurate and rapid surface enhancement Raman scattering analysis of rhodamine B. Chin J Anal Chem 45(12):2026–2031

Wang ZY, Zong SF, Wu L et al (2017b) SERS-activated platforms for immunoassay: probes, encoding methods, and applications. Chem Rev 117(12):7910–7963

Wang LL, Wen YL, Li LY et al (2018a) Sensitive and label-free electrochemical lead ion biosensor based on a DNAzyme triggered G-quadruplex/hemin conformation. Biosens Bioelectron 115:91–96

Wang Y, Ruan QY, Lei ZC et al (2018b) Highly sensitive and automated surface enhanced raman scattering-based immunoassay for H5N1 detection with digital microfluidics. Anal Chem 90(8):5224–5231

Xu LG, Gao YF, Kuang H et al (2018) MicroRNA-directed intracellular self-assembly of chiral nanorod dimers. Angew Chem Int Ed 57(33):10544–10548

Yao L, Ye YW, Teng J et al (2017) In vitro isothermal nucleic acid amplification assisted surface-enhanced Raman spectroscopic for ultrasensitive detection of vibrio parahaemolyticus. Anal Chem 89(18):9775–9780

Ye LP, Hu J, Liang L et al (2014a) Surface-enhanced Raman spectroscopy for simultaneous sensitive detection of multiple microRNAs in lung cancer cells. Chem Commun 50(80):11883–11886

Ye SJ, Mao YN, Guo YY et al (2014b) Enzyme-based signal amplification of surface-enhanced Raman scattering in cancer-biomarker detection. Trac-Trends Anal Chem 55:43–54

Yoon J, Jang HJ, Jung I et al (2017) A close-packed 3D plasmonic superlattice of truncated octahedral gold nanoframes. Nanoscale 9(23):7708–7713

Zeng Z, Liu YY, Wei JJ (2016) Recent advances in surface-enhanced raman spectroscopy (SERS): finite-difference time-domain (FDTD) method for SERS and sensing applications. Trac-Trends Anal Chem 75:162–173

Zhang JW, Winget SA, Wu YR et al (2016) Ag@Au concave cuboctahedra: a unique probe for monitoring Au-catalyzed reduction and oxidation reactions by surface-enhanced Raman spectroscopy. ACS Nano 10(2):2607–2616

Zhang RY, Lv SP, Gong Y et al (2018) Sensitive determination of Hg(II) based on a hybridization chain recycling amplification reaction and surface-enhanced Raman scattering on gold nanoparticles. Microchim Acta 185(8):8

Zhao XH, Deng M, Rao GF et al (2018) High-performance SERS substrate based on hierarchical 3D Cu nanocrystals with efficient morphology control. Small 14(38):8
Zhou H, Liu J, Xu JJ et al (2018) Optical nano-biosensing interface via nucleic acid amplification strategy: construction and application. Chem Soc Rev 47(6):1996–2019
Zou YX, Huang SQ, Liao YX et al (2018) Isotopic graphene-isolated-Au-nanocrystals with cellular Raman-silent signals for cancer cell pattern recognition. Chem Sci 9(10):2842–2849

Part IV
Nucleic Acid Amplification Strategies for Biomedicine

Chapter 13
Nucleic Acid Amplification Strategies for In Vitro and In Vivo Metal Ion Detection

Beibei Xie and Zhongfeng Gao

Abstract Metal ions are critical to many biological, chemical, and environmental processes. In recent years, many nucleic acid-based biosensors have emerged for in vitro and in vivo metal ion detection. The structure of DNA is ideal for metal ion binding by both the nucleobases and phosphate backbone, although the essential biological role of DNA is to store genetic information. Three main groups of functional DNA were demonstrated for metal ion sensing: DNAzymes, G-quadruplex (also known as G4 structure), and mismatched DNA base pair. Combining with nucleic acid amplification strategies, many important metal ions can be sensitive determined down to the low parts-per-billion level. Here, we detailed the interaction between nucleic acid amplifications and metal ions, mainly including exonuclease-assisted circling, hybridization chain reaction, and rolling circle amplification. We also offer classic examples from the literature to reveal their impact in practical applications. Finally, we highlight the essential limitations that need to be addressed, and future research opportunities are discussed.

13.1 Introduction

Metal ions play critical roles in chemical environmental and biological systems (Zhou et al. 2017b). As most metal ions cannot be biodegraded and cause persistent pollution, they are easy to be ingested by the human body and cause serious harm to the human body (Jarup 2003; Saidur et al. 2017). Therefore, the in vitro and in vivo detection of metal ions is of great significance in the research fields of biomedicine, environment, and industry.

Traditional methods for the detection of metal ion, such as inductively coupled plasma mass spectrometry (Ashoka et al. 2009) and atomic absorption spectroscopy

B. Xie · Z. Gao (✉)
Shandong Provincial Key Laboratory of Detection Technology for Tumour Markers, College of Chemistry and Chemical Engineering, Linyi University, Linyi 276005, People's Republic of China
e-mail: gaozhongfeng@lyu.edu.cn

B. Xie
e-mail: xiaobei6907@163.com

S. Zhang et al. (eds.), *Nucleic Acid Amplification Strategies for Biosensing, Bioimaging and Biomedicine*, https://doi.org/10.1007/978-981-13-7044-1_13

(Giokas et al. 2004), need costly and bulky instrumentation and significant training to use properly, making it very difficult for in vitro and in vivo biosensing. Significant progress, to overcome these limitations, based on functional nucleic acid isothermal amplification techniques has been made in developing sensors and imaging agents for the detection of metal ions.

13.2 Functional Nucleic Acids for Metal Ion Detection

To detect metal ions, functional nucleic acids are mainly categorized into three groups: DNAzymes, mismatched DNA base pairs, and G-quadruplexes related to guanine (G)-rich DNA probes. To achieve sensitive detection, signal amplification strategies such as peroxidase-mimicking DNAzymes, cascade DNAzyme, protein-based enzymes (e.g., rolling circle amplification (RCA), nicking enzymes, exonuclease III, polymerase/DNase I, and so on), enzyme-free amplification (e.g., hybridization chain reaction (HCR)) are particularly used.

13.2.1 DNAzyme-Based Sensing Strategies

DNAzymes, screened via in vitro selections, have been commonly employed as highly selective recognition elements for a broad range of cofactors, such as Cu^{2+}, Pb^{2+}, Zn^{2+}, Ca^{2+}, Mg^{2+}, $UO_2{}^{2+}$, and Hg^{2+} (Liu et al. 2009; Peng et al. 2018). DNAzymes can bind with substrates associated with target ions. For example, Fig. 13.1a, b exhibits the main structure of DNAzymes that are highly selective to Pb^{2+} and Cu^{2+}, respectively. With the addition of certain ions, the activities of DNAzymes can be activated and cut into two components from the specific positions marked by the triangles. Then, the dsDNA dissociates from each other and produces several short ssDNA fragments. DNAzymes have significant efficient catalytic activities and recognition abilities, which are especially dependent on the target ions being detected. DNAzymes have been extensively used in electrochemical and optical sensors for the detection of metal ions in a simple, rapid, and stable manner (Huang et al. 2017; Zhou et al. 2017b).

13.2.2 G-quadruplex-Enabled Detection Platforms

G-quadruplexes, also known as G4 structure, in which four guanines form a square planar tetrad, have attracted extensive interest in recent years (Mohanty et al. 2013; Vummidi et al. 2013; Yang et al. 2009). Since metal ions play a key role in the preparation of G4 structure (Fig. 13.1c), G4 structures have been widely employed for the sensitive determination of various metal ions, including Na^+ and K^+. An

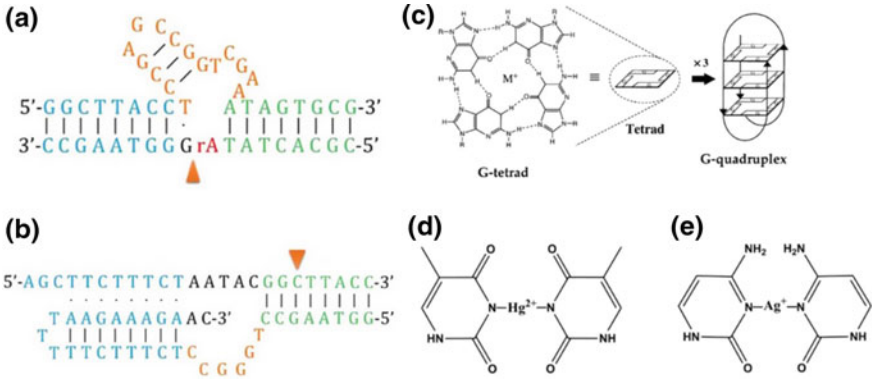

Fig. 13.1 Common functional nucleic acids used for metal ion detection: DNAzyme-specific complexes that are sensitive to **a** Pb^{2+} and **b** Cu^{2+}. **c** Illustration of the metal ion-mediated G-quadruplex structure. **d** T–Hg^{2+}–T and **e** C–Ag^{+}–C. Reprinted from Huang et al. (2017), Copyright 2017, with permission from Elsevier

interesting property of G4 structures is that its conformation can transform from single-strand structures to quadruplex states, which enables G4 structures compatible with diverse signaling mechanisms.

Traditionally, a ssDNA probe is designed with the two terminals that linked with a quencher and a fluorophore. It adopts a random coil structure and retains strong fluorescence intensity (Ueyama et al. 2002). However, it rearranges its configuration and forms a G-quadruplex structure upon the addition of K^{+}, which brings the quencher and fluorophore close to each other, thus allowing FRET process. The decrease of fluorescence reveals the presence of K^{+} selectively and accurately. Unlike the dual-labeled ssDNA probe, label-free ssDNA probe is also used, which provides the straightforward and cost-effective detection of K^{+}. The ssDNA probe is enabled to switch its random coil structure to a G-quadruplex structure in the presence of K^{+}. Riboflavin, a special ligand that has strong fluorescent signal by binding with G-quadruplexes, could be accommodated with G-quadruplex, producing a significant fluorescent signal.

13.2.3 Mismatched DNA Base Pair-Mediated Assays

Hybridization events between thymine (T) bases can be effectively induced to generate T–Hg^{2+}–T complexes in the presence of Hg^{2+} (Chiang et al. 2008; Li et al. 2009; Xue et al. 2008). The imino proton of T residues, as shown in Fig. 13.1d, can be replaced by Hg^{2+} to form T–Hg^{2+}–T complexes, which is much stable than the natural T-A base pair. Thus, T–Hg^{2+}–T coordination is a powerful protocol for Hg^{2+} detections. Similarly, Ag^{+} can link with cytosine (C) bases to induce the formation of C–Ag^{+}–C base pairs (Fig. 13.1e) (Hao et al. 2012; Yan et al. 2012; Zhao et al.

2010). Many efforts have already been initiated to establishing methods for effective and reliable detection of mercury and silver ions, which enable good use of metal ion-aided coordination chemistry: T–Hg^{2+}–T and C–Ag^{+}–C.

13.2.4 Nanomaterials for Signal Transduction and Amplification

With the development of nanomaterial and technology, functional nanomaterials have attracted extensive attention in nucleic acid amplification for in vitro and in vivo metal ion detection. Nanomaterials have significant electrical, optical, thermal, mechanical, and chemical properties, which can greatly improve the performance of biosensors. Notably, nanomaterials can serve as remarkable colorimetric indicators or fluorescence quenchers. Also, they can be used as efficient nanocarriers for superb signal enhancers or signaling probes to effectively amplify the readout signals, such as SERS and fluorescence polarization. The combination of nanomaterials with functional nucleic acid indicates high recognition affinity toward metal ions, enabling innovative biosensing nanoplatforms with advanced selectivity and sensitivity. In this chapter, the examples of metal ion biosensors on the basis of both nucleic acid amplification and advanced nanomaterials, such as carbon nanotubes (CNTs), quantum dots (QDs), gold nanoparticles (AuNPs), magnetic nanoparticles (MNPs), graphene oxide (GO), and so on, are illustrated.

13.3 Detection of Alkali Metal Ions

Alkali metal ions contain lithium ion (Li^{+}), sodium ion (Na^{+}), potassium ion (K^{+}), rubidium ion (Rb^{+}), and cesium ion (Cs^{+}). As general buffer salts, these metals have long been employed to screen charge repulsion in nucleic acid. Notably, Li^{+}, Na^{+}, and K^{+} play a critical role in biology process. Rb^{+} has not been demonstrated on biological functions yet. Cs^{+} is toxic to some degree. Until now, DNA-based biosensors were mainly established for Na^{+} and K^{+}.

Na^{+} is very important in organism. The increased concentration of Na^{+} might result in high blood pressure, water retention, and other physiological disorders (Grant et al. 2002; Jaitovich and Bertorello 2010). Twenty years ago, Geyer and Sen have in vitro selected DNAzyme using Na^{+} alone, as shown in Fig. 13.2a, when they tried to examine whether DNAzymes could be active without addition of divalent metals (Geyer and Sen 1997). In the presence of Na^{+}, the isolated DNAzyme was active; however, the secondary structure is not satisfied and the selectivity for other metals was not revealed, which might explain its lack of biosensing performances. In recent years, a few Na^{+}-specific DNAzymes have been demonstrated, and Lu et al., for example, selected a DNAzyme called NaA43 with a rate of 0.1 min^{-1} in 400 mM

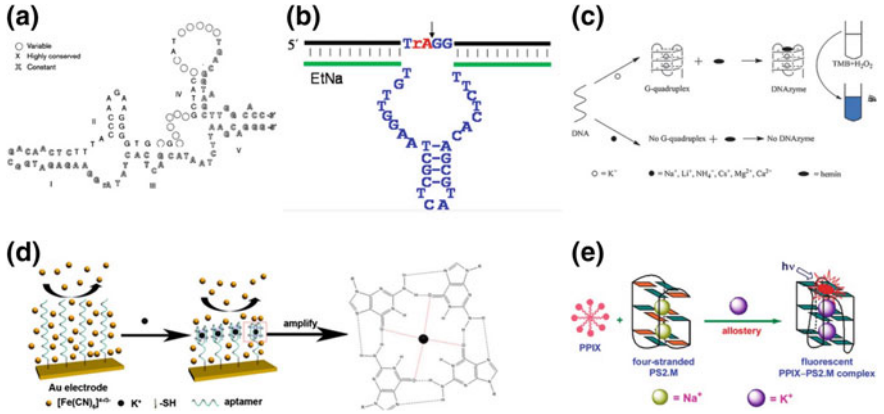

Fig. 13.2 **a** Proposed secondary structure of the Na^+ family DNAzymes. Reprinted from Geyer and Sen (1997), Copyright 1997, with permission from Elsevier and **b** secondary structures of the EtNa DNAzymes for Na^+ detection. Reproduced from Zhou et al. (2016) by permission of John Wiley & Sons Ltd. **c** The colorimetric detection of K^+. Reproduced from Yang et al. (2010) by permission of The Royal Society of Chemistry. **d** Illustration of the label-free electrochemical detection of K^+. Reprinted from Chen et al. (2013), Copyright 2013, with permission from Elsevier. **e** Turn-On fluorescent sensor for K^+ detection with G4 structure as the sensing element. Reprinted with the permission from Li et al. (2010). Copyright 2010 American Chemical Society

Na^+ specifically, while other mono-, di-, and trivalent metals are inactive (Torabi et al. 2015). Liu and coworkers isolated another DNAzyme called EtNa (Fig. 13.2b). Although the rate was slightly slower, about 0.06 min^{-1}, with much weaker Na^+ binding affinity in water, it showed excellent selectivity for Na^+ (Zhou et al. 2016).

Na^+ is able to promote the formation of G-quadruplex; however, it is generally less efficient than K^+. However, G-quadruplex with Na^+ specificity was developed by Tang et al. and it could be used for the detection of Na^+ (Sun et al. 2016). The authors chose a DNA sequence named p25, producing an antiparallel conformation with Na^+ but a hybrid-type conformation with K^+. Toward hemin, the binding affinities using these two conformations are different, and thus, the resulting hemin-p25 DNAzymes with peroxidase-like activity were employed for the detection of Na^+. However, to detect Na^+ using such method in complex biological samples has yet to be reported because of the high background ionic strength generating a high intracellular K^+ concentration for competition and nonspecific DNA condensation.

Using DNA for the detection of K^+ mainly relies on G4 structures. K^+ is coordinated by O6 groups of guanines from two consecutive stacked G-tetrads (Bhattacharyya et al. 2016; Mekmaysy et al. 2008). Many efforts have been conducted to improve selectivity to achieve its biological applications. It has been shown that K^+ sensitivity at nanomolar level with about 10^4-fold selectivity over Na^+ (Huang and Chang 2008; Qin et al. 2010). As shown in Fig. 13.2c–e, utilizing the K^+-sensitive G4 structures, researchers have achieved selective and sensitive determination of K^+ by colorimetric (Yang et al. 2010), electrochemical (Chen et al. 2013; Jarczewska et al.

2016), and fluorescent strategies (Lee et al. 2014; Li et al. 2010). Given these research progresses, using G4 structures for K^+ detection in biological samples, such as human serum and urine, has been achieved (Huang and Chang 2008; Yang et al. 2016). However, since many other metals could bind with G4 structures, new DNA sequences that can better selectively detect K^+ from Na^+ and other metal ions are still to be developed.

13.4 Detection of Alkaline Earth Metal Ions

Alkaline earth metals refer to beryllium ion (Be^{2+}), magnesium ion (Mg^{2+}), calcium ion (Ca^{2+}), strontium ion (Sr^{2+}), barium ion (Ba^{2+}), and radium (Ra^{2+}). Here, Be^{2+} is slightly toxic, Sr^{2+} usually acts as beta-ray source, Ba^{2+} is employed to help X-ray imaging, and Ra^{2+} shows radioactive property. Only Mg^{2+} and Ca^{2+} are the most important in biology.

13.4.1 Magnesium Ion Sensors

Magnesium ion, one of the most important, major intracellular divalent cation, is related to all nucleic acid in biological processes (Pechlaner and Sigel 2012; Anastassopoulou and Theophanides 2002; Auffinger et al. 2011). Mg^{2+} is demonstrated to be a critical cofactor for most ribozymes (Bowman et al. 2012). A recent molecular dynamics simulation reported by Li et al. indicates that Mg^{2+} specifically attaches to the negatively charged phosphate backbone and the major groove of G/C bases (Li et al. 2011).

Ju and coworkers reported a dual-potential ratiometric electrochemiluminescence (ECL) biosensing strategy on the basis of Mg^{2+}-specific DNAzyme-controlled ECL signals of CdS QDs and luminol (Cheng et al. 2014). Without addition of Mg^{2+}, the cathode ECL of the QDs is significantly quenched by electrochemiluminescence resonance energy transfer between Cy5 molecule and CdS QDs, while the anode ECL from Au@luminol is presented into the system (Fig. 13.3a). Conversely, in the presence of Mg^{2+}, the DNAzyme cleaves the substrate, releasing the Au@luminol and Cy5, which leads to the decrease of the anode ECL. Based on the ECL intensities, this method yields a detection limit as low as 2.8 μM of Mg^{2+} and achieves sensitive detection of Mg^{2+} in Hela cell extract.

Generally, Mg^{2+}-dependent DNAzyme is more commonly used as a universal tool for target detections, such as nucleic acid, protein, enzymatic activity, and other metal ions. For example, a new type of intracellular nanoprobe, named AuNP-based hairpin-locked-DNAzyme, was established to detect miRNA in living cells (Yang et al. 2017). Briefly, it contains hairpin-locked-DNAzyme strands and an AuNP (Fig. 13.3b). The hairpin-locked DNAzyme strand induces a hairpin structure via intramolecular hybridization in the absence of target, which could suppress the catalytic activity of DNAzyme and the fluorescence is quenched using the AuNP.

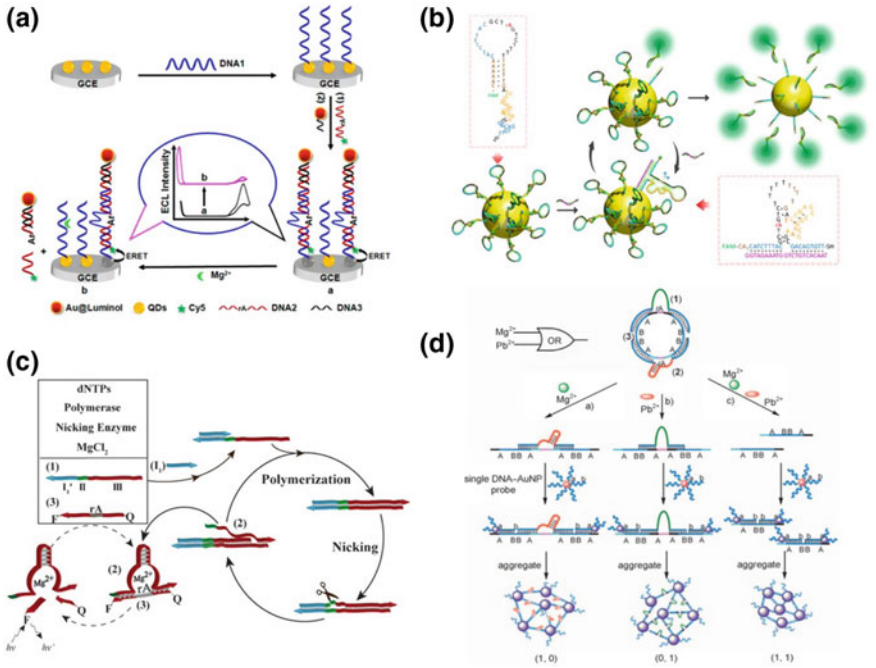

Fig. 13.3 **a** Illustration of ratiometric ECL approach initiated by Mg^{2+}-dependent DNAzyme for biosensing. Reprinted with the permission from Cheng et al. (2014). Copyright 2014 American Chemical Society. **b** Working mechanism of the AuNP-based hairpin-locked DNAzyme probe for miRNA detection. Reprinted with the permission from Yang et al. (2017). Copyright 2017 American Chemical Society. **c** Nucleic acid-controlled DNA machineries synthesizing Mg^{2+}-dependent DNAzymes for the logic-gate operations. Reproduced from Orbach et al. (2012) by permission of John Wiley & Sons Ltd. **d** Colorimetric logic gates based on DNA machineries structures and AuNPs. Reproduced from Bi et al. (2010) by permission of John Wiley & Sons Ltd.

However, the target–probe hybridization, in the presence of target, can open the hairpin and form the active secondary structure to yield an active DNAzyme, which then cleaves the self-strand with the aid of Mg^{2+}. The cleaved two shorter DNA fragments can be separated with the miRNA. In this case, the fluorophores are released from the AuNP and the fluorescence is increased. At the same time, the target is also released and attaches to another hairpin-locked DNAzyme strand to trigger another cycle of activation.

Due to its unique advantages, including site-specific, programmable, and reliable properties, it has been recently used to construct DNA machineries and logic gates. Willner's group used polymerase, nicking enzymes, and Mg^{2+}-dependent DNAzyme subunits to prepare DNA machines for the design of logic gates and for the development of amplified DNA detection schemes (Fig. 13.3c). They revealed the assembly of the OR, AND, and AND gates and discussed the interplay of the systems between biosensing and logic-gate functionalities (Orbach et al. 2012). We previ-

ously developed a complete set of two-input logic gates, including AND, OR, XOR, NOR, INHIBIT, XNOR, and NAND, based on the employment of ion-dependent DNAzymes as functional elements and the cofactor ions as inputs (Fig. 13.3d). The outputs of the gates perform the gate functions through AuNP-based colorimetric detection (Bi et al. 2010).

13.4.2 Calcium Ion Sensors

Ca^{2+} is an essential metal ion in biology process and in the environment, resulting in extensive research in developing biosensors for the detection of Ca^{2+}. While many proteins that are specific to Ca^{2+} are demonstrated, very few DNA or RNA can specifically bind to Ca^{2+}. Biosensors based on nucleic acid are interesting and attractive for its excellent programmability and high stability. Liu et al. reported an RNA-cleaving DNAzyme, termed EtNa, cooperatively binding with two Ca^{2+} but only one Mg^{2+} (Zhou et al. 2017a). Compared with four DNAzymes with known Ca^{2+}-dependent activity, the selectivity of EtNa for Ca^{2+} was the best. The EtNa was used for Ca^{2+} detection with excellent selectivity and a detection limit of 17 μM Ca^{2+}. The Ca^{2+} sensing in tap water was conducted, and the obtained result was comparable with that from standard ICP-MS method.

13.5 Detection of Lanthanide and Actinide Ions

Lanthanides represent an especially challenging classification of analytes, as these ions are very similar to each other. Lanthanides are belonging to hard Lewis acids with a high density of charge. These ions have strong affinity to the phosphate backbone of DNA and thus tend to coordinate with DNA molecules. For example, Ln^{3+} only binds to the negatively charged phosphate backbone of dsDNA by the loss of at least one hydration water (Gross and Simpkins 1981). Tb^{3+} binds with the phosphate backbone of the nucleotide monophosphates (Barry et al. 1971; Raj and Rao 1969). The resonance energy levels of Eu^{3+}, Ce^{3+}, and Tb^{3+} overlap with the triplet energy states of the nucleotide, leading to higher lanthanide luminescence by energy transfer (Yonuschot and Mushrush 1975). Thus, Tb^{3+} has been widely employed as an enhanced luminescent probe for nucleic acids (Chatterji 1988; Gross and Simpkins 1981). Ye et al. reported that GT-rich DNA sequence is highly effective in improving sensitized Tb^{3+} luminescence (Lin et al. 2014; Zhang et al. 2013).

In the early 1990s, Ln^{3+} has been reported for cleaving nucleic acids. Free Ln^{3+} ions at millimolar level cleave RNA nonspecifically through binding to the phosphate backbone and producing multinuclear complexes under alkaline conditions (Komiyama and Shigekawa 1999). In addition, Ce^{4+} and its complexes have been demonstrated to have more efficient in hydrolyzing DNA (Aiba et al. 2011). With a ribozyme or DNAzyme, site-specific cleavage was realized. For instance, in the

presence of Eu^{3+}, Yb^{3+}, or Ce^{3+} together with Zn^{2+}, DNAzymes for DNA cleavage were isolated (Dokukin and Silverman 2012). Introducing the lanthanide ions to the DNAzyme chemistry has generated several new signal amplifications for its detection.

Previous literature selected a Gd^{3+} aptamer (Edogun et al. 2016). By constructing a fluorescent strategy, the optimized conformation was characterized with a K_d of 330 nM Gd^{3+}, which could be transformed into a fluorescent biosensor with a detection limit of 80 nM. The biosensor was found to have excellent selectivity against several other ions, including divalent and trivalent metals.

Yttrium (Y^{3+}), a trivalent rare earth metal, has a similar size with holmium (Ho^{3+}), and its catalytic activity with the above-mentioned lanthanide-specific DNAzymes is also similar to that of Ho^{3+} (Huang et al. 2014, 2015, 2016). However, in vitro selection with Y^{3+} has not been reported yet. Adsorption of DNA by Y_2O_3 was investigated, indicating DNA phosphate backbone has essential for this adsorption reaction (Liu and Liu 2015). Also, Sc^{3+} is a trivalent rare earth metal; however, it is inactive with all known Ln^{3+}-dependent DNAzymes because it is much smaller than Y^{3+}.

Uranium is often employed for preparing power generation and nuclear weapons. Sensitive determination of uranium is a practical analytical need as a nuclear waste. In water, the most stable form of uranium is UO_2^{2+}. The Lu's group isolated a DNAzyme for UO_2^{2+} called 39E showing million-fold selectivity against other examined metals (Xiao et al. 2007). The 39E for the detection of UO_2^{2+} is down to 45 pM.

13.6 Detection of Post-transition Metal Ions

Post-transition metals are a set of metallic elements located after the transition metals in the periodic table, such as lead, bismuth, gallium, indium, thallium, and tin. Most of them are toxic, and their interactions with nucleic acid are barely reported except for lead. Here, we mainly review the nucleic acid amplification methods for lead ion detection.

Lead, one of the most toxic heavy metals, can pass through skin, respiratory organs, and digestive system into the blood. Lead is always accumulated in vital tissues and organs of the human body and causes reproductive, cardiovascular, neurological, and developmental disorders, especially in children (Wang et al. 2013). On the basis of Environmental Protection Agency (EPA), the safety limit is 15 ppb (0.07 μM) in drinking water, while the International Agency for Research on Cancer (IARC) defines a lower threshold of 10 ppb (48.26 nM) in water and food (Lu et al. 2015). Thus, it is very essential to develop the biosensing strategies for effective and routine monitoring of Pb^{2+}.

Plaxco et al. used the Pb^{2+}-dependent DNAzyme for electrochemical Pb^{2+} detection (Xiao et al. 2007) (Fig. 13.4a). The sensor contains a methylene-blue (MB)-modified catalytic DNA strand (1), which is used to hybridize with its complementary sequence (2). This complex is relatively rigid, preventing the MB from approaching the gold electrode to transfer electrons. With the addition of target Pb^{2+}, the catalytic

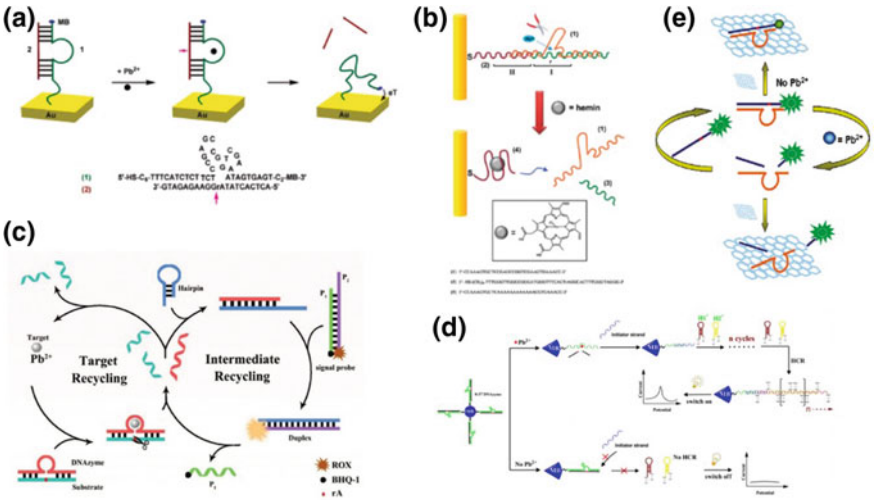

Fig. 13.4 **a** Schematic of electrochemical Pb^{2+} sensor based on the DNAzyme. Reprinted with the permission from Xiao et al. (2007). Copyright 2007 American Chemical Society. **b** Pb^{2+}-dependent DNAzyme-catalyzed reaction for Pb^{2+} detection based on a hemin/G-quadruplex structure. Reprinted with the permission from Pelossof et al. (2012). Copyright 2012 American Chemical Society. **c** Illustration of target–intermediate recycling amplification. Reproduced from Wen et al. (2017) by permission of The Royal Society of Chemistry. **d** Working mechanism of the DNAzyme-based electronic switch for Pb^{2+} detection based on HCR reaction. Reprinted from Zhuang et al. (2013), Copyright 2013, with permission from Elsevier. **e** Schematic of the DNAzyme-GO based fluorescence method for the detection of Pb^{2+}. Reprinted with the permission from Zhao et al. (2011). Copyright 2011 American Chemical Society

strand cleaves the substrate into two fragments, which dissociate from the complex, allowing the MB molecule to transfer electrons to the gold electrode. The directly measured detection limit of the proposed biosensor is 0.3 μM.

Similarly, Willner et al. used Pb^{2+}-dependent DNAzyme for electrochemical detection (Fig. 13.4b). With the addition of target Pb^{2+}, cleavage of the DNAzyme substrate proceeds, leading to the self-assembly of the hemin/G-quadruplex nanostructure label (Pelossof et al. 2012). The proposed sensing platform realizes sensitive detection of Pb^{2+} with a low detection limit of 5 fM.

Cai et al. proposed an ultrasensitive fluorescence method for intracellular determination of Pb^{2+} with a detection limit down to 0.3 nM by target–intermediate recycling amplification based on a strand displacement reaction and metal-aided DNAzyme catalysis (Fig. 13.4c). With the addition of Pb^{2+}, the DNAzyme cleaves the ribonucleotide in the substrate with excellent specificity, releasing the Pb^{2+} and DNAzyme. The released Pb^{2+} circularly activates another DNAzyme to realize the signal amplification. At the same time, the released DNAzyme could open the hairpin probe and trigger the intermediate recycling with the signal probe. In the intermediate recycling, the opened hairpin probe hybridizes with the P2 strand to form a completely

complementary DNA duplex, recovering the fluorescent signal. Thus, the DNAzyme was released and generated another intermediate recycling (Wen et al. 2017).

An enzyme-free strategy that couples a Pb^{2+}-specific DNAzyme with HCR was developed by Tang's group (Fig. 13.4d). Upon addition of Pb^{2+}, catalytic cleavage of substrate in the DNAzymes leads to the capture of the initiator strands by the conjugated catalytic strands that modified on MNPs. The captured DNA initiator strands induced the HCR process between two alternating hairpin probes modified with Fc to produce a nicked dsDNA on the MNPs. Massive Fc molecules were formed on the neighboring probes and thus amplified the electrochemical signal within the applied potential. This sensor displayed a detection limit of 37 pM and robust applications in groundwater or drinking water (Zhuang et al. 2013).

Yu et al. developed a GO-DNAzyme-based strategy for amplified turn-on fluorescent detection of Pb^{2+} (Fig. 13.4e). The DNAzyme strand is hybridized with the substrate strand by only five base pairs, allowing fluorophore attached to the GO surface to afford a high quenching efficiency and a low background signal. The FAM-labeled hybrid acts as both signal reporter and a molecular recognition module and GO as a quencher. Upon addition of Pb^{2+}, the substrate strand can be digested into two short segments, releasing the FAM-labeled portion and recovering the fluorescence. The biosensor shows a high sensitivity toward the Pb^{2+} with a low detection limit of 300 pM (Zhao et al. 2011).

Fan and coworkers proposed a novel detection platform using enzyme synergetic isothermal quadratic DNA machine (Xu et al. 2013). This platform integrates an NEase-aided signal amplification module and strand displacement amplification (SDA) module into a one-step system to realize ultrasensitive analysis of Pb^{2+} (detection limit down to 30 fM) within a short sensing time (40 min). The obtained results for the detection of Pb^{2+} in complex environmental water samples using the proposed sensing system are consistent with those obtained by ICP-MS (Zhang et al. 2014).

With the help of RCA and DNAzyme, Zhang et al. developed highly selective and sensitive electrochemical sensing system for the detection of Pb^{2+} (Tang et al. 2013). The DNAzyme could be activated in the presence of Pb^{2+} to digest the DNAzyme into two short DNA fragments. A long ssDNA probe with repeating sequence was generated after RCA reaction. Subsequently, CdS QD-labeled ssDNA were employed as signaling probes to hybridize with the long ssDNA product. Owing to the significant signal amplification by the massive QDs and the low background signal by magnetic separation, a low concentration of 7.8 pM Pb^{2+} could be detected.

Exonuclease-aided DNA recycling is a powerful strategy for signal-amplified detection of Pb^{2+}. Zuo et al. proposed a Pb^{2+} induced exonuclease III-assisted DNA recycling system to enhance the sensitivity of detection (Xu et al. 2013). With the addition of Pb^{2+}, the substrate DNA segments were digested and released from the dsDNA. The disassociated DNAzyme was employed as a primer of the exonuclease-assisted recycling system which can significantly amplify the fluorescent intensity by continuously recycling the DNAzyme. The detection limit of Pb^{2+} was down to 5 pM with excellent selectivity.

Similarly, Yu et al. proposed an isothermal signal-amplified DNAzyme method for the specific and sensitive quantification of Pb^{2+} (Li et al. 2014). In the presence

of Pb^{2+}, an RNA probe containing DNA substrate was digested by the DNAzyme, efficiently removing the 2′,3′-cyclic phosphate of the digested substrate by exonuclease III. The remaining portion of the ssDNA was subsequently employed as the primer for SDA reaction. The proposed assay could sensitively detect 200 pM Pb^{2+}.

13.7 Detection of Transition Metals

In recent years, nonspecific interactions between transition metal ions and DNA have been investigated by diverse methods, which collectively imply transition metals prefer nucleic acid bases to the phosphate with the following binding affinity: $Hg^{2+} > Cu^{2+} > Cd^{2+} > Zn^{2+} > Mn^{2+} > Ni^{2+}$, $Co^{2+} > Fe^{2+}$ (Duguid et al. 1993). Many reports have been shown to select their DNAzymes and aptamers. Although DNAzymes have been developed for Cd^{2+} detection, none of the DNAzymes were highly selective for Cd^{2+}. Furthermore, no nucleic acid-based high-performance sensors for manganese, cobalt, iron, molybdenum, nickel, and tungsten are reported yet. Noble metals, including gold, silver, platinum, and palladium, are transition metals as well. These metals are not endogenous ions in living organisms and barely participate in native biological processes. Silver and platinum are often used to form stable metal nanoparticles for DNA adsorption. Palladium usually coexists with platinum, and no DNA-based biosensors have been reported for palladium detection yet. Thus, the sensitive detection of Cu^{2+}, Hg^{2+}, Zn^{2+}, and Ag^{+} is mainly discussed.

13.7.1 Copper Ion Sensors

Copper, a broadly used metal worldwide, can leak into the environment by numerous ways. Copper with low concentration is a critical nutrient for human body. But gastrointestinal disturbance might occur when exposed to high level of copper even for a short period of time, while long-term exposure causes the damage of kidney or liver (Georgopoulos et al. 2001). The US EPA has set the limit of copper to be 1.3 ppm (~20 μM) in drinking water (Georgopoulos et al. 2001). Hence, it is very important to detect the concentration of Cu^{2+} in the environment.

Breaker et al. isolated DNA-cleaving DNAzymes by using Cu^{2+} as a metal cofactor (Carmi et al. 1996, 1998). Based on the discovery, Lu et al. developed a Cu^{2+}-dependent DNA-cleaving DNAzyme sequences for a Cu^{2+} detection (Liu and Lu 2007a) (Fig. 13.5a). The DNAzyme contained two DNA strands that formed a complex. A FAM fluorophore at the 3′-end and a quencher at the 5′-end are labeled on the substrate, while the enzyme modified a 5′-quencher. In the presence of Cu^{2+}, the substrate could be cleaved irreversibly at the cleavage site (the guanine in red). After that, the digested segments were released because of the low affinities to the enzyme, resulting in increased fluorescence. They obtained a low detection limit of 35 nM with excellent practicability for detecting Cu^{2+} in drinking water.

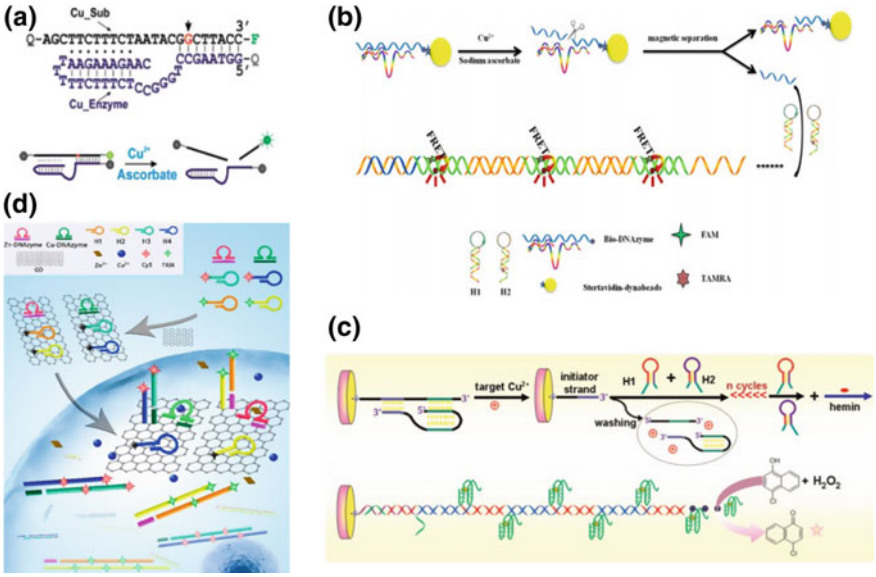

Fig. 13.5 **a** Illustration of the Cu^{2+}-specific DNAzyme for fluorescence detection. Reprinted with the permission from Liu and Lu (2007a). Copyright 2007 American Chemical Society. **b** Schematic illustration of DNAzyme-based fluorescent assay using HCR with FRET technique. Reprinted from Chen et al. (2016), Copyright 2016, with permission from Elsevier. **c** Schematic illustration of Cu^{2+}-specific DNAzyme-based electrochemical biosensor based on target-induced HCR for sensing of Cu^{2+}. Reprinted from Xu et al. (2015), Copyright 2015, with permission from Elsevier. **d** Signal amplification method for the sensitive fluorescence imaging of Cu^{2+} and Zn^{2+} in living cells. Reprinted with the permission from Si et al. (2018). Copyright 2018 American Chemical Society

Combining Cu^{2+}-dependent DNAzyme with HCR signal amplification, Guo and coworkers demonstrated the amplified detection of Cu^{2+} using fluorescence resonance energy transfer (FRET) method (Chen et al. 2016) (Fig. 13.5b). With the addition of Cu^{2+} ion, the DNAzyme attached on MNPs was selectively digested and released, initiating the HCR process of hairpin H1 and H2 modified with TAMRA as the acceptor and FAM as the donor, respectively. Long nicked duplexes were self-assembled to provide the acceptor and the donor in close proximity, leading to a FRET process. They achieved a limit of detection of 0.5 nM Cu^{2+} and successfully applied for detection in tap water with satisfactory results. Similarly, Tang et al. designed an impedimetric biosensor by coupling Cu^{2+}-induced hemin/G-quadruplex-based DNAzyme with enzymatic catalytic precipitation technique (Fig. 13.5c). Under the optimal conditions, the electrochemical resistance increased with raising Cu^{2+} concentration and exhibited a detection limit down to 60 fM (Xu et al. 2015).

Using polymerase/endonuclease reaction, He et al. realized amplified fluorescent detection of Cu^{2+} (He et al. 2014). With the addition of Cu^{2+}, the enzyme strand induces catalytic processes to cleave substrate strand, releasing DNAzyme substrates acting as primers to initiate the Klenow fragment polymerization. The

double-stranded niking site is cut by Nb.BbvCI endonuclease, opening a new site for a new replication. Thus, the complete dsDNA is regenerated to trigger another cycle of nicking, polymerization, and displacement. With the assistance of GO, Quan et al. designed a "turn-on" fluorescent biosensor for Cu^{2+} detection based on graphene–DNAzyme catalytic beacon (Liu et al. 2011). Owing to the excellent surface quenching property, GO acts as both "quencher" and "scaffold" of the Cu^{2+}-dependent DNAzyme, promoting the formation of self-assembled graphene-quenched DNAzyme complex. However, with the addition of Cu^{2+}, the graphene–DNAzyme conformation is disturbed, producing internal DNA cleavage-dependent effect. Thus, the quenched fluorescence in graphene–DNAzyme is rapidly recovered. Based on the change of fluorescence, they achieved a detection limit as low as 0.365 nM. Recently, Tang and coworkers used GO as intracellular transport carrier to load DNAzyme and hairpin probe into the cell (Fig. 13.5d). The sensor enabled the imaging of Cu^{2+} and Zn^{2+} by signal amplification based on DNA self-assembly under DNAzyme catalysis and reached low detection limits of 80 pM and 100 pM, respectively (Si et al. 2018).

13.7.2 Mercury Ion Sensors

As T-T mismatched base pairs revealed, Ono and coworkers first established a biosensor for the detection of Hg^{2+} in 2004 (Ono and Togashi 2004), as shown in Fig. 13.6a. They designed an ssDNA probe comprising T-rich bases with a quencher and a fluorophore labeled at the ends. Without addition of Hg^{2+}, the DNA probe tends to adopt a random coil conformation with the quencher and fluorophore being away from each other. In the presence of Hg^{2+}, the DNA probe formed a hairpin structure owing to the T–Hg^{2+}–T complexes at the ends, which bring the quencher and fluorophore into close proximity, resulting in significant fluorescence quenching. The decrease of fluorescence is greatly influenced by the concentration of Hg^{2+}. Although this turn-off strategy provides an unsatisfactory sensitivity (about 40 nM), it brings a new and potential method for Hg^{2+} detection by T–Hg^{2+}–T coordination as the basic recognition elements.

Hong et al. developed a signal-on electrochemical method for sensitive and selective detection of Hg^{2+} based on nicking endonuclease-assisted (NEase) target recycling and HCR amplification tactics (Fig. 13.6b). Upon addition of Hg^{2+}, PB probe hybridized with PA probe to form dsDNA by T–Hg^{2+}–T coordination, which automatically induced NEase to efficiently digest duplex region from the recognition sites, spontaneously releasing Hg^{2+} and PB and leaving the remnant initiators. The dissociated Hg^{2+} and PB could be reused to trigger the next cycle, and more initiators were produced. The HCR events occurred on the electrode surface triggered by the initiators, resulting in a significant signal increase. They obtained a linear range from 10 pM to 50 nM and a detection limit down to 1.6 pM (Hong et al. 2017).

Li's group developed a novel guanine nanowire (G-wire)-based approach for signal amplification (Gao et al. 2016). On the basis of Hg^{2+}-induced Exo III-aided

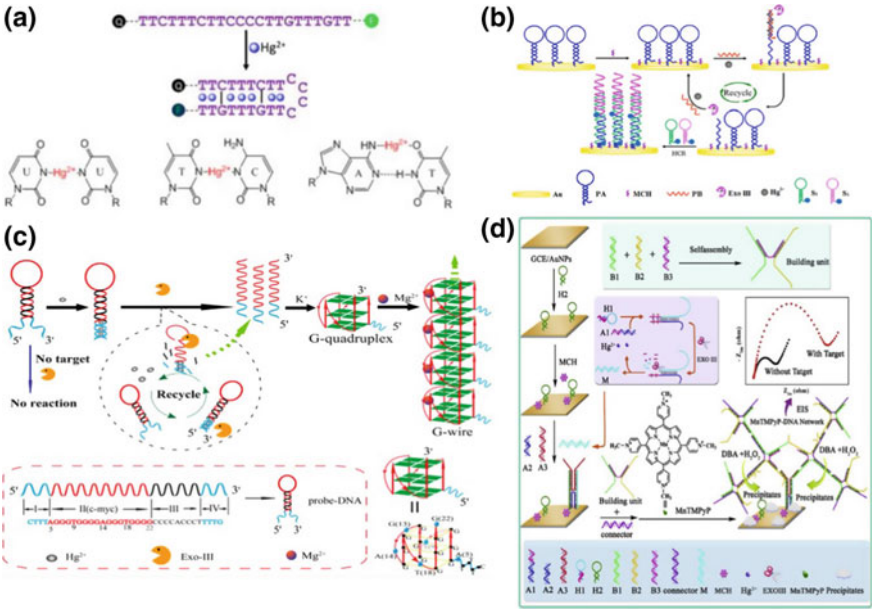

Fig. 13.6 **a** Schematic diagram of T–Hg^{2+}–T coordination. Reproduced from Ono and Togashi (2004) by permission of John Wiley & Sons Ltd. **b** Illustration of electrochemical sensor based on NEase assisted recycling and HCR strategy for the detection of Hg^{2+}. Reprinted from Hong et al. (2017), Copyright 2017, with permission from Elsevier. **c** Illustration of the label-free RRS aptasensor based on Exo III-assisted recycling and G-wire amplification for Hg^{2+} detection. Reprinted with the permission from Ren et al. (2016). Copyright 2016 American Chemical Society. **d** Schematic diagram of the impedimetric biosensor based on DNA network for Hg^{2+} detection. Reprinted from Xie et al. (2018), Copyright 2018, with permission from Elsevier

recycling and growth of G-wires for signal amplification, they designed a label-free and signal-on resonance Rayleigh scattering (RRS) aptasensor for detection of Hg^{2+} (Fig. 13.6c). The hairpin DNA probe was designed as a signal probe to recognize Hg^{2+} by T–Hg^{2+}–T structure, which automatically induced Exo III digestion to recycle the target and liberate the G-quadruplex sequence. The free G-quadruplex sequences can be self-assembled into G-wire superstructure with addition of Mg^{2+}, resulting in the dramatically amplification of RRS intensity. The limit of detection was down to 20.0 pM, and it successfully applied to test tap water and river water samples (Ren et al. 2016).

Xie et al. constructed a highly sensitive impedimetric biosensor to detect Hg^{2+} (Fig. 13.6d). With the addition of Hg^{2+}, T–Hg^{2+}–T structures initiated the Exo III-catalyzed target recycling and generated free ssDNA to promote the information of DNA networks on electrode surface, which could efficiently immobilize the porphyrin manganese (MnTmPyP). The formed MnTMPyP-dsDNA complex produced an insoluble precipitate on the electrode surface, significantly increasing the resis-

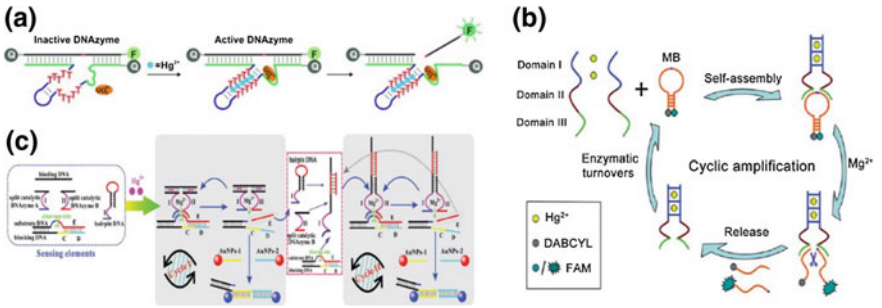

Fig. 13.7 **a** Schematic presentation of the DNAzyme sensor for the detection of Hg^{2+}. Reproduced from Liu and Lu (2007b) by permission of John Wiley & Sons Ltd. **b** Schematic of target-induced DNAzyme cascade for the amplified fluorescence detection of Hg^{2+}. Reproduced from Qi et al. (2012) by permission of The Royal Society of Chemistry. **c** Schematic presentation of the DNAzyme cascade for the amplified colorimetric detection of Hg^{2+}. Reproduced from Chen et al. (2017) by permission of The Royal Society of Chemistry

tance signal for the quantitative determination of Hg^{2+}. This platform obtained a detection limit of 1.47 pM (Xie et al. 2018).

DNAzyme is also a powerful tool to design sensitive strategies for Hg^{2+} detection. Liu and Lu first designed a turn-on allosteric DNAzyme catalytic beacons triggered by T–Hg^{2+}–T structure for ultrahigh sensitive and selective detection of aqueous mercury ions (Liu and Lu 2007b) (Fig. 13.7a). Zhao et al. reported that T–Hg^{2+}–T structure could activate Mg^{2+}-dependent DNAzyme in the presence of Hg^{2+} (Fig. 13.7b), leading to hybridize with a hairpin-structured substrate to release the fluorescent signal (Qi et al. 2012). Chen et al. designed a sensitive colorimetric method for visual detection of Hg^{2+} based on T–Hg^{2+}–T triggered DNAzyme cyclic amplification (Chen et al. 2017) (Fig. 13.7c).

13.7.3 Zinc Ion Sensors

Shen et al. reported a sensitive biosensor based on G-quadruplex for fluorescent determination of Zn^{2+} with a detection limit down to 0.91 μM. The thioflavin T was bound to the G-quadruplex in the absence of Zn^{2+}, leading to the significant enhancement of fluorescent signal, while with the addition of Zn^{2+}, thioflavin T was released by displacement of Zn^{2+}, resulting in a remarkable decrease of fluorescence (Guo et al. 2015).

Cellular fluorescent detection of Zn^{2+} has been reported. Fan and coworkers presented a dual-purpose fluorescent strategy to simultaneously monitor cellular $Cu^{2+}$and Zn^{2+} (Fig. 13.8a). As is shown, the probe comprised Cu^{2+}-specific DNAzymes, Zn^{2+}-specific DNAzymes, and AuNPs. To realize the synchronous imaging of cellular $Cu^{2+}$and Zn^{2+}, dual-purpose AuNPs were designed labeled

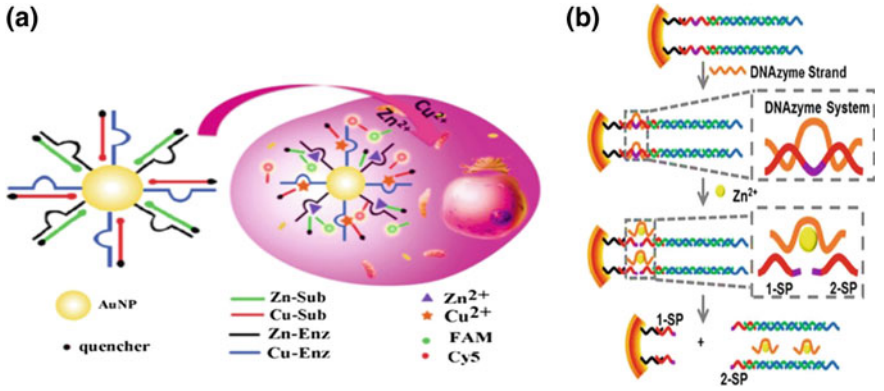

Fig. 13.8 **a** two DNAzyme-modified AuNPs were used to fabricate fluorescent biosensor for synchronous imaging of Zn^{2+} and Cu^{2+} in living cells. Reprinted with the permission from Li et al. (2015). Copyright 2015 American Chemical Society. **b** Electrochemical nanopore biosensor based on DNA supersandwich amplification for Zn^{2+} detection. Reproduced from Liu et al. (2016) by permission of The Royal Society of Chemistry

with two-color fluorophore-based DNAzyme probes. The fluorophores were greatly quenched by the AuNPs and quencher. In the presence of $Cu^{2+}$and Zn^{2+}, the substrate strands could be digested into two short fragments, when the nanoprobes were transported into the living cells, resulting in the separation of the fluorophore-modified DNA fragments, which generated significant fluorescent signals corresponding to the concentration and location of Cu^{2+} and Zn^{2+} (Li et al. 2015).

Traditional electrochemical biosensor contains immobilized nanomaterials and DNA probes on the surface. Nevertheless, Xia and colleagues developed an electrochemical nanopore biosensor for Zn^{2+} detection based on HCR amplification and Zn^{2+}-specific DNAzyme (Fig. 13.8b). As is shown, the HCR structures were formed by the multiple hybridization of DNA, leading to heavy blockage of nanopores and a significant current decrease in an I-V plot. The DNA supersandwich contains the SP probe, which could hybridize with the Zn^{2+}-specific DNAzyme. With the addition of Zn^{2+}, the SP was digested into two short segments, releasing the DNA supersandwich structures. In this case, the ionic pathway was smooth, leading to a rapid and complete rehabilitation of the current with a detection limit of 1 nM (Liu et al. 2016).

13.7.4 Silver Ion Sensors

For Ag^{+} detection, cytosine-rich DNA probes have been commonly employed. Similar to the specific interaction between thymine and Hg^{2+}, Ag^{+} was demonstrated to selectively stabilize cytosine–cytosine mismatches.

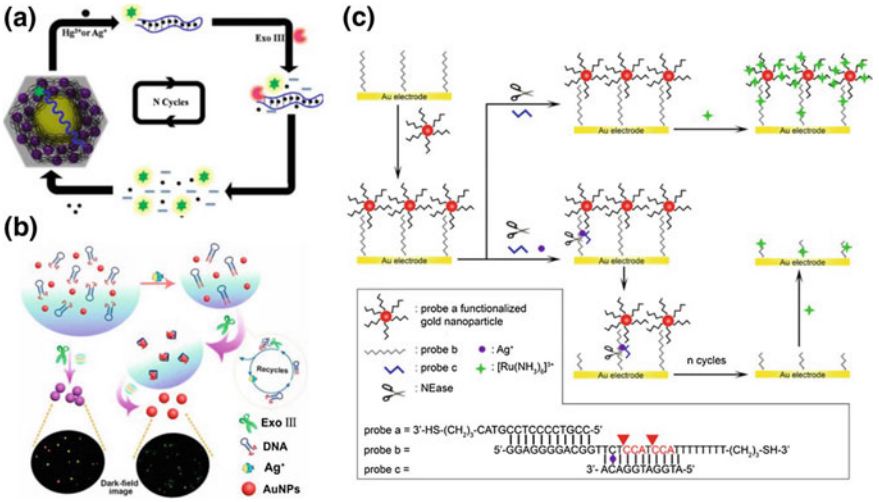

Fig. 13.9 Schematic illustration of **a** Exo III amplified fluorescent sensing system for the detection of Hg^{2+} and Ag^{+} based on metal-polydopamine framework. Reprinted with the permission from Ravikumar et al. (2018). Copyright 2018 American Chemical Society. **b** Detecting Ag^{+} based on C–Ag^{+}–C coordination chemistry by dark-field microscopy. Reprinted with the permission from Li et al. (2018). Copyright 2018 American Chemical Society. **c** Electrochemical strategy based on AuNPs and cleavage-mediated dual signal amplification for Ag^{+} detection. Reprinted with the permission from Miao et al. (2013). Copyright 2013 American Chemical Society

Exo III is frequently used to catalyze the stepwise removal of mononucleotides of dsDNA. The addition of Ag^{+} will trigger the formation of C–Ag^{+}–C hybrid, enabling Exo III to digest the generated hybrid duplex. Based on the principle, scientists have developed numerous strategies for colorimetric, electrochemical, fluorescent assays, and so on. Combining Exo III-aided strategy with nanomaterials, the sensing performance might be improved due to the unique superiority of nanomaterials. For example, Panneerselvam et al. proposed a metal–polydopamine framework with specific molecular probe as an effective fluorescent quencher (Fig. 13.9a) (Ravikumar et al. 2018). They achieved simultaneous detection of Hg^{2+} and Ag^{+} with the aid of Exo III. Integrating with AuNPs, colorimetric signal amplification strategy was developed for Ag^{+} detection at the femtomolar level using dark-field microscope (Fig. 13.9b) (Li et al. 2018).

Polymerization, DNAzyme, and nuclease-assisted amplification techniques have also been employed. Bi et al. studied Ag^{+}- and Hg^{2+}-triggered ligase activity and then established an RCA-based molecular logic gate to detect these two metal ions (Fig. 13.3d) (Bi et al. 2010). Miao et al. developed a gold nanoparticles and nicking endonuclease cleavage-based dual signal amplification method for the detection of Ag^{+} by electrochemical readout (Fig. 13.9c). They achieve a low detection limit of 470 fM with satisfactory selectivity and practicability in lake water and drinking water samples (Miao et al. 2013).

13.8 Conclusion

Heavy metal ions have a great influence on human health. How to detect the metal ions rapidly in vitro and in vivo with low cost and real time has become a challenge that needs to be addressed urgently. Nucleic acid amplifications have been extensively used in the development of biosensors to detect metal ions because they are highly sensitive, programmable, and stable. At present, the biosensors mainly include four detection strategies, DNAzyme, G4 structure, mismatched DNA base pair, and nanomaterial-based amplifications by fluorescent, colorimetric, and electrochemistry readout. Although nucleic acid biosensors demonstrate many merits, several limits are still existed. First, the reported biosensors are mainly focused on the detection of K^+, Mg^{2+}, Hg^{2+}, Pb^{2+}, Cu^{2+}, Zn^{2+}, and Ag^+, and other metal ions are less investigated. Second, the current studies mostly stay in the theoretical and laboratory level, and the relevant practical applications are few. Thus, nucleic acid amplifications urgently need to be improved in many areas, e.g., discover new signal amplification methods, promote binding nucleophilicity, enhance the sensitivity by combining nucleic acid amplifications with nanomaterials, such as carbon nanotubes, graphene oxide, gold nanoparticles, quantum dots, etc., extend the detection range of metal ions, improve detection approaches for metal ions detection in vivo, complete high-throughput assays, explore multiple metal ion detections, and develop easy to operate, simple, repeatable, real-time, and stable quantitative biosensors for in situ detection.

References

Aiba Y, Sumaoka J, Komiyama M (2011) Artificial DNA cutters for DNA manipulation and genome engineering. Chem Soc Rev 40:5657–5668

Anastassopoulou J, Theophanides T (2002) Magnesium-DNA interactions and the possible relation of magnesium to carcinogenesis. Irradiation and free radicals. Crit Rev Oncol Hematol 42:79–91

Ashoka S, Peake BM, Bremner G et al (2009) Comparison of digestion methods for ICP-MS determination of trace elements in fish tissues. Anal Chim Acta 653:191–199

Auffinger P, Grover N, Westhof E (2011) Metal ion binding to RNA. Met Ions Life Sci 9:1–35

Barry CD, North AC, Glasel JA et al (1971) Quantitative determination of mononucleotide conformations in solution using lanthanide ion shift and broadenine NMR probes. Nature 232:236–245

Bhattacharyya D, Mirihana AG, Basu S (2016) Metal cations in G-quadruplex folding and stability. Front Chem 4:38

Bi S, Yan Y, Hao S et al (2010) Colorimetric logic gates based on supramolecular DNAzyme structures. Angew Chem Int Ed 49:4438–4442

Bowman JC, Lenz TK, Hud NV et al (2012) Cations in charge: magnesium ions in RNA folding and catalysis. Curr Opin Struct Biol 22:262–272

Carmi N, Shultz LA, Breaker RR (1996) In vitro selection of self-cleaving DNAs. Chem Biol 3:1039–1046

Carmi N, Balkhi SR, Breaker RR (1998) Cleaving DNA with DNA. Proc Natl Acad Sci USA 95:2233–2237

Chatterji D (1988) Terbium(III) induced Z to A transition in poly(dG-m5dC). Biopolymers 27:1183–1186

Chen Z, Chen L, Ma H et al (2013) Aptamer biosensor for label-free impedance spectroscopy detection of potassium ion based on DNA G-quadruplex conformation. Biosens Bioelectron 48:108–112

Chen Y, Chen L, Ou Y et al (2016) DNAzyme-based biosensor for Cu^{2+} ion by combining hybridization chain reaction with fluorescence resonance energy transfer technique. Talanta 155:245–249

Chen J, Pan J, Chen S (2017) A naked-eye colorimetric sensor for Hg^{2+} monitoring with cascade signal amplification based on target-induced conjunction of split DNAzyme fragments. Chem Commun 53:10224–10227

Cheng Y, Huang Y, Lei J et al (2014) Design and biosensing of Mg^{2+}-dependent DNAzyme-triggered ratiometric electrochemiluminescence. Anal Chem 86:5158–5163

Chiang CK, Huang CC, Liu CW et al (2008) Oligonucleotide-based fluorescence probe for sensitive and selective detection of mercury(II) in aqueous solution. Anal Chem 80:3716–3721

Dokukin V, Silverman SK (2012) Lanthanide ions as required cofactors for DNA catalysts. Chem Sci 3:1707–1714

Duguid J, Bloomfield VA, Benevides J et al (1993) Raman spectroscopy of DNA-metal complexes. I. Interactions and conformational effects of the divalent cations: Mg, Ca, Sr, Ba, Mn Co, Ni, Cu, Pd, and Cd. Biophys J 65:1916–1928

Edogun O, Nguyen NH, Halim M (2016) Fluorescent single-stranded DNA-based assay for detecting unchelated Gadolinium(III) ions in aqueous solution. Anal Bioanal Chem 408:4121–4131

Gao ZF, Huang YL, Ren W et al (2016) Guanine nanowire based amplification strategy: enzyme-free biosensing of nucleic acids and proteins. Biosens Bioelectron 78:351–357

Georgopoulos PG, Roy A, Yonone-Lioy MJ et al (2001) Environmental copper: its dynamics and human exposure issues. J Toxicol Environ Health B Crit Rev 4:341–394

Geyer CR, Sen D (1997) Evidence for the metal-cofactor independence of an RNA phosphodiester-cleaving DNA enzyme. Chem Biol 4:579–593

Giokas DL, Tsogas GZ, Vlessidis AG et al (2004) Metal ion determination by flame atomic absorption spectrometry through reagentless coacervate phase separation-extraction into lamellar vesicles. Anal Chem 76:1302–1309

Grant FD, Romero JR, Jeunemaitre X et al (2002) Low-renin hypertension, altered sodium homeostasis, and an alpha-adducin polymorphism. Hypertension 39:191–196

Gross DS, Simpkins H (1981) Evidence for two-site binding in the terbium(iii)-nucleic acid interaction. J Biol Chem 256:9593–9598

Guo Y, Sun Y, Shen X et al (2015) Label-free detection of Zn(2 +) based on G-quadruplex. Anal Sci 31:1041–1045

Hao C, Xua L, Xing C et al (2012) Oligonucleotide-based fluorogenic sensor for simultaneous detection of heavy metal ions. Biosens Bioelectron 36:174–178

He JL, Zhu SL, Wu P et al (2014) Enzymatic cascade based fluorescent DNAzyme machines for the ultrasensitive detection of Cu(II) ions. Biosens Bioelectron 60:112–117

Hong M, Wang M, Wang J et al (2017) Ultrasensitive and selective electrochemical biosensor for detection of mercury (II) ions by nicking endonuclease-assisted target recycling and hybridization chain reaction signal amplification. Biosens Bioelectron 94:19–23

Huang CC, Chang HT (2008) Aptamer-based fluorescence sensor for rapid detection of potassium ions in urine. Chem Commun 1461–1463

Huang PJ, Vazin M, Liu J (2014) In vitro selection of a new lanthanide-dependent DNAzyme for ratiometric sensing lanthanides. Anal Chem 86:9993–9999

Huang PJ, Vazin M, Matuszek Z et al (2015) A new heavy lanthanide-dependent DNAzyme displaying strong metal cooperativity and unrescuable phosphorothioate effect. Nucleic Acids Res 43:461–469

Huang PJ, Vazin M, Liu J (2016) In Vitro selection of a DNAzyme cooperatively binding two lanthanide ions for RNA cleavage. Biochemistry 55:2518–2525

Huang J, Su X, Li Z (2017) Metal ion detection using functional nucleic acids and nanomaterials. Biosens Bioelectron 96:127–139

Jaitovich A, Bertorello AM (2010) Intracellular sodium sensing: SIK1 network, hormone action and high blood pressure. Biochim Biophys Acta 1802:1140–1149
Jarczewska M, Górski Ł, Malinowska E (2016) Application of DNA aptamers as sensing layers for electrochemical detection of potassium ions. Sensor Actuat B: Chem 226:37–43
Jarup L (2003) Hazards of heavy metal contamination. Br Med Bull 68:167–182
Komiyama MTN, Shigekawa H (1999) Hydrolysis of DNA and RNA by lanthanide ions: mechanistic studies leading to new applications. Chem Commun 1443–1451
Lee J, Park J, Lee HH et al (2014) DNA-templated silver nanoclusters as label-free, sensitive detection probes for potassium ions and nitric oxide. J Mater Chem B 2:2616–2621
Li T, Dong S, Wang E (2009) Label-free colorimetric detection of aqueous mercury ion Hg^{2+} using Hg^{2+}-modulated G-quadruplex-based DNAzymes. Anal Chem 81:2144–2149
Li T, Wang E, Dong S (2010) Parallel G-quadruplex-specific fluorescent probe for monitoring DNA structural changes and label-free detection of potassium ion. Anal Chem 82:7576–7580
Li W, Nordenskiold L, Mu Y (2011) Sequence-specific Mg^{2+}-DNA interactions: a molecular dynamics simulation study. J Phys Chem B 115:14713–14720
Li W, Yang Y, Chen J et al (2014) Detection of lead(II) ions with a DNAzyme and isothermal strand displacement signal amplification. Biosens Bioelectron 53:245–249
Li L, Feng J, Fan Y et al (2015) Simultaneous imaging of Zn^{2+} and Cu^{2+} in living cells based on DNAzyme modified gold nanoparticle. Anal Chem 87:4829–4835
Li J, Xi H, Kong C et al (2018) "Aggregation-to-deaggregation" colorimetric signal amplification strategy for Ag^{+} detection at the femtomolar level with dark-field microscope observation. Anal Chem 90:11723–11727
Lin WT, Huang PJ, Pautler R et al (2014) The group trend of lanthanides binding to DNA and DNAzymes with a complex but symmetric pattern. Chem Commun 50:11859–11862
Liu B, Liu J (2015) Comprehensive screen of metal oxide nanoparticles for dna adsorption, fluorescence quenching, and anion discrimination. ACS Appl Mater Interfaces 7:24833–24838
Liu J, Lu Y (2007a) A DNAzyme catalytic beacon sensor for paramagnetic Cu^{2+} ions in aqueous solution with high sensitivity and selectivity. J Am Chem Soc 129:9838–9839
Liu J, Lu, Y (2007b) Rational design of "turn-on" allosteric DNAzyme catalytic beacons for aqueous mercury ions with ultrahigh sensitivity and selectivity. Angew Chem Int Ed 46:7587–7590
Liu J, Cao Z, Lu Y (2009) Functional nucleic acid sensors. Chem Rev 109:1948–1998
Liu M, Zhao H, Chen S et al (2011) A "turn-on" fluorescent copper biosensor based on DNA cleavage-dependent graphene-quenched DNAzyme. Biosens Bioelectron 26:4111–4116
Liu N, Hou R, Gao P et al (2016) Sensitive Zn^{2+} sensor based on biofunctionalized nanopores via combination of DNAzyme and DNA supersandwich structures. Analyst 141:3626–3629
Lu L, Si JC, Gao ZF et al (2015) Highly selective and sensitive electrochemical biosensor for ATP based on the dual strategy integrating the cofactor-dependent enzymatic ligation reaction with self-cleaving DNAzyme-amplified electrochemical detection. Biosens Bioelectron 63:14–20
Mekmaysy CS, Petraccone L, Garbett NC et al (2008) Effect of O6-methylguanine on the stability of G-quadruplex DNA. J Am Chem Soc 130:6710–6711
Miao P, Ning L, Li X (2013) Gold nanoparticles and cleavage-based dual signal amplification for ultrasensitive detection of silver ions. Anal Chem 85:7966–7970
Mohanty J, Barooah N, Dhamodharan V et al (2013) Thioflavin T as an efficient inducer and selective fluorescent sensor for the human telomeric G-quadruplex DNA. J Am Chem Soc 135:367–376
Ono A, Togashi H (2004) Highly selective oligonucleotide-based sensor for mercury(II) in aqueous solutions. Angew Chem Int Ed 43:4300–4302
Orbach R, Mostinski L, Wang F et al (2012) Nucleic acid driven DNA machineries synthesizing Mg^{2+}-dependent DNAzymes: an interplay between DNA sensing and logic-gate operations. Chem Eur J 18:14689–14694
Pechlaner M, Sigel RK (2012) Characterization of metal ion-nucleic acid interactions in solution. Met Ions Life Sci 10:1–42

Pelossof G, Tel-Vered R, Willner I (2012) Amplified surface plasmon resonance and electrochemical detection of Pb^{2+} ions using the Pb^{2+}-dependent DNAzyme and hemin/G-quadruplex as a label. Anal Chem 84:3703–3709

Peng H, Newbigging AM, Wang Z et al (2018) DNAzyme-mediated assays for amplified detection of nucleic acids and proteins. Anal Chem 90:190–207

Qi L, Zhao Y, Yuan H et al (2012) Amplified fluorescence detection of mercury(II) ions Hg^{2+} using target-induced DNAzyme cascade with catalytic and molecular beacons. Analyst 137:2799–2805

Qin H, Ren J, Wang J et al (2010) G-quadruplex-modulated fluorescence detection of potassium in the presence of a 3500-fold excess of sodium ions. Anal Chem 82:8356–8360

Raj NB, Rao MS (1969) Metal ion-nucleic acid interactions. I. A method for the fractionation of rat liver ribonucleic acids into transfer ribonucleic acid and ribosomal ribonucleic acids using Zn-II as a precipitant. Biochemistry 8:1277–1284

Ravikumar A, Panneerselvam P, Morad N (2018) Metal-polydopamine framework as an effective fluorescent quencher for highly sensitive detection of Hg(II) and Ag(I) ions through exonuclease III activity. ACS Appl Mater Interfaces 10:20550–20558

Ren W, Zhang Y, Chen HG et al (2016) Ultrasensitive label-free resonance rayleigh scattering aptasensor for Hg^{2+} Using Hg^{2+}-triggered exonuclease III-assisted target recycling and growth of G-wires for signal amplification. Anal Chem 88:1385–1390

Saidur MR, Aziz AR, Basirun WJ (2017) Recent advances in DNA-based electrochemical biosensors for heavy metal ion detection: a review. Biosens Bioelectron 90:125–139

Si H, Sheng R, Li Q et al (2018) Highly sensitive fluorescence imaging of Zn^{2+} and Cu^{2+} in living cells with signal amplification based on functional DNA self-assembly. Anal Chem 90:8785–8792

Sun H, Chen H, Zhang X et al (2016) Colorimetric detection of sodium ion in serum based on the G-quadruplex conformation related DNAzyme activity. Anal Chim Acta 912:133–138

Tang S, Tong P, Li H et al (2013) Ultrasensitive electrochemical detection of Pb(2 +) based on rolling circle amplification and quantum dots tagging. Biosens Bioelectron 42:608–611

Torabi SF, Wu P, McGhee CE et al (2015) In vitro selection of a sodium-specific DNAzyme and its application in intracellular sensing. Proc Natl Acad Sci USA 112:5903–5908

Ueyama H, Takagi M, Takenaka S (2002) A novel potassium sensing in aqueous media with a synthetic oligonucleotide derivative. Fluorescence resonance energy transfer associated with Guanine quartet-potassium ion complex formation. J Am Chem Soc 124:14286–14287

Vummidi BR, Alzeer J, Luedtke NW (2013) Fluorescent probes for G-quadruplex structures. ChemBioChem 14:540–558

Wang Z, Wu L, Shen B et al (2013) Highly sensitive and selective cartap nanosensor based on luminescence resonance energy transfer between NaYF4:Yb, Ho nanocrystals and gold nanoparticles. Talanta 114:124–130

Wen ZB, Liang WB, Zhuo Y et al (2017) An efficient target-intermediate recycling amplification strategy for ultrasensitive fluorescence assay of intracellular lead ions. Chem Commun 53:7525–7528

Xiao Y, Rowe AA, Plaxco KW (2007) Electrochemical detection of parts-per-billion lead via an electrode-bound DNAzyme assembly. J Am Chem Soc 129:262–263

Xie S, Tang Y, Tang D et al (2018) Highly sensitive impedimetric biosensor for Hg^{2+} detection based on manganese porphyrin-decorated DNA network for precipitation polymerization. Anal Chim Acta 1023:22–28

Xu H, Xu P, Gao S et al (2013) Highly sensitive recognition of Pb^{2+} using Pb^{2+} triggered exonuclease aided DNA recycling. Biosens Bioelectron 47:520–523

Xu M, Gao Z, Wei Q et al (2015) Hemin/G-quadruplex-based DNAzyme concatamers for in situ amplified impedimetric sensing of copper(II) ion coupling with DNAzyme-catalyzed precipitation strategy. Biosens Bioelectron 74:1–7

Xue X, Wang F, Liu X (2008) One-step, room temperature, colorimetric detection of mercury Hg^{2+} using DNA/nanoparticle conjugates. J Am Chem Soc 130:3244–3245

Yan G, Wang Y, He X et al (2012) A highly sensitive electrochemical assay for silver ion detection based on un-labeled C-rich ssDNA probe and controlled assembly of MWCNTs. Talanta 94:178–183

Yang P, De Cian A, Teulade-Fichou MP et al (2009) Engineering bisquinolinium/thiazole orange conjugates for fluorescent sensing of G-quadruplex DNA. Angew Chem Int Ed 48:2188–2191

Yang X, Li T, Li B et al (2010) Potassium-sensitive G-quadruplex DNA for sensitive visible potassium detection. Analyst 135:71–75

Yang L, Qing Z, Liu C et al (2016) Direct fluorescent detection of blood potassium by ion-selective formation of intermolecular g-quadruplex and ligand binding. Anal Chem 88:9285–9292

Yang Y, Huang J, Yang X et al (2017) Gold nanoparticle based hairpin-locked-dnazyme probe for amplified mirna imaging in living cells. Anal Chem 89:5850–5856

Yonuschot G, Mushrush GW (1975) Terbium as a fluorescent probe for DNA and chromatin. Biochemistry 14:1677–1681

Zhang M, Le HN, Jiang XQ et al (2013) Time-resolved probes based on guanine/thymine-rich DNA-sensitized luminescence of terbium(III). Anal Chem 85:11665–11674

Zhang Q, Chen F, Xu F et al (2014) Target-triggered three-way junction structure and polymerase/nicking enzyme synergetic isothermal quadratic DNA machine for highly specific, one-step, and rapid microRNA detection at attomolar level. Anal Chem 86:8098–8105

Zhao C, Qu K, Song Y et al (2010) A reusable DNA single-walled carbon-nanotube-based fluorescent sensor for highly sensitive and selective detection of Ag + and cysteine in aqueous solutions. Chemistry 16:8147–8154

Zhao XH, Kong RM, Zhang XB et al (2011) Graphene-DNAzyme based biosensor for amplified fluorescence "turn-on" detection of Pb^{2+} with a high selectivity. Anal Chem 83:5062–5066

Zhou W, Saran R, Chen Q et al (2016) A New Na^{+}-dependent RNA-cleaving DNAzyme with over 1000-fold rate acceleration by ethanol. ChemBioChem 17:159–163

Zhou W, Saran R, Huang PJ et al (2017a) An exceptionally selective DNA cooperatively binding two Ca^{2+} ions. Chembiochem 18:518–522

Zhou W, Saran R, Liu J (2017b) Metal sensing by DNA. Chem Rev 117:8272–8325

Zhuang J, Fu L, Xu M et al (2013) DNAzyme-based magneto-controlled electronic switch for picomolar detection of lead (II) coupling with DNA-based hybridization chain reaction. Biosens Bioelectron 45:52–57

Chapter 14
The Application of Nucleic Acid Amplification Strategies in Theranostics

Yanxialei Jiang

Abstract Targeting nanoparticles equipped with diagnosis "tools" to malignant cells or tissues for optimal therapy is a popular concept of theranostics. As one of the most reliable and sensitive diagnosis "tools," nucleic acid detection is of growing practical interest with respect to molecular diagnostics of cancer and other genetic diseases. Particularly, PCR-based and other nucleic acid amplification strategies are most widely used in theranostics. This chapter aims at systematization and critical summarization of the applications of DNA- or RNA-targeted nucleic acid amplification strategies in theranostics.

14.1 Introduction

Cancer is the first leading cause of disease-associated death in China (Chen et al. 2016) and the second leading cause of death in the USA (Olaku, Taylor 2017) in decades. Current treatment modalities for tumors or cancers mainly focus on surgery, radiotherapy, chemotherapy, and immunotherapy, among which medicine treatment is still the most widely used therapeutic way for various types of tumors or cancers (Xiao et al. 2017). Nevertheless, typical anticancer therapies, such as radiotherapy and chemotherapy, cannot always work for the patients, even they helpful, they may not cure the patients completely (Weeks et al. 2012). Besides, radiotherapy and chemotherapy are also well known as their adverse side effects due to the treatment cannot distinguish the similarity between cancerous cells and healthy human cells (Emmenegger and Kerbel 2010; Karimi et al. 2016; Abou-Elkacem et al. 2016; Fan et al. 2016; Park et al. 2016). What's more, drug resistance, insufficient curative effect, and tumor relapse during therapeutic process are still the huge challenges when patients treated by conventional cytotoxic drugs or molecularly targeted therapeutics (Al-Lazikani et al. 2012; Yano et al. 2012), and the efficacy of typical anticancer therapies is usually limited in clinic.

Y. Jiang (✉)
Shandong Provincial Key Laboratory of Detection Technology for Tumour Markers, College of Chemistry and Chemical Engineering, Linyi University, 276005 Linyi, People's Republic of China
e-mail: jyxialei@126.com

S. Zhang et al. (eds.), *Nucleic Acid Amplification Strategies for Biosensing, Bioimaging and Biomedicine*, https://doi.org/10.1007/978-981-13-7044-1_14

The ability to kill diseased cancerous cells while causing less harm to the normal cells is of great significance to reduce adverse side effects during therapeutic process especially in radiotherapy and chemotherapy. How to distinguish healthy cells and cancerous cells, how to achieve tumor cells specific targeting, are the vital factors in a cancer cure process. Particularly, a typical adopted strategy is to design a cancerous cells target-specific drug delivery system (DDS) that can transport an effective dosage of anticancer drugs to targeted cells, cancerous tissues or diseased area of the body (Nicolas et al. 2013; Ge and Liu 2013; Chen et al. 2014; Frandsen and Ghandehari 2012), and sustained release drug over a period of time in a controlled manner to increase survival of drugs (Bertrand and Leroux 2012).

Generally speaking, theranostics is a process combined diagnosis and therapy, popularly in cancer. Cancerous cells target-specific DDS accelerates the advancement of therapy; at the same time, more effective and reliable early tumor detection and diagnosing methods have also been put forward result from the clinical needs, which are also significant for cancer therapy in theranostics. The technology of nucleic acid amplification strategy opens up avenues for meeting this clinical diagnosis requirement in theranostics. Hybridization chain reaction (HCR), rolling-circle amplification (RCA), the strand displacement reaction (SDR), loop-mediated amplification (LAMP), and target-recycling amplification with endonuclease, exonuclease, and polymerase, and these nucleic acid amplification strategies have already become powerful tools for early diagnosis of cancer, due to their high sensitivity, excellent stability, and subtly designability, which demonstrate good prospects to meet clinical requirements, and assist DDS employed in theranostics.

14.2 Theranostics

"Theranostics," generally, points out emphatically the inseparability of diagnosis and therapy, the pillars of medicine (Baum and Kulkarni 2012). It means that "we know which sites require treatment and confirm that those sites have been treated." The term "theranostics" was first used by John Funkhouser at the beginning of the 1990s, while the concept of personalized medicine appeared at the same time (Choudhury and Gupta 2018). Theranostics provides a clinical transition from conventional disease trial and wrong medicine treatment to much more personalized and precision medicine time. Theranostics should have the ability to cure patients with more accurate diagnosis and more specific therapy plan.

Diagnostic and therapeutic agents can be formulated as a single theranostic platform and then can be attached to a biological ligand for cancerous cells or area targeting (Muthu et al. 2014). The use of aptamers as targeting ligands which conjugated to DDS nanoparticles as nanotheranostic system has been substantially studied (Vandghanooni et al. 2018). For example, Mosafer et al. (2017) loaded SPIONs and doxorubicin simultaneously into poly (lactic-co-glycolic acid) (PLGA) nanoparticles and then modified PLGA nanoparticles with AS1411 aptamer for tumor cell-targeted theranostic purposes. It turned out that the AS1411 aptamer-conjugated

PLGA nanoparticles enhanced its cellular uptake and cytotoxicity effect of doxorubicin in murine C26 cells.

Nanotechnology has been proved to be a promising platform for theranostic in recent advances. Nanoparticle-based contrast drug agents in theranostic offer improved capabilities for specific cancer targeting, high-resolution imaging, and prolonged circulation times in comparison with the custom used methods (Hahn et al. 2011). Even though theranostic has drawn world widely particular interest in cancer therapy since it shows significantly more advantages compared to typical radiotherapy and chemotherapy, its application also raises critical questions simultaneously. For example, is the optimal nanoparticles used in DDS for patients' therapy also the optimal nanoparticles used for cancer diagnostics (Dreifuss et al. 2015)?

14.3 DDS Applied in Theranostics

Nanotechnology has already involved in all fields of biochemical and chemical science and technology,according to its high financial investment and rapid development (Heath 2015). Simultaneously, nanotechnology breaks a new ground for drug delivery, especially for tumor-targeted drug delivery system (DDS). In 2004, National Cancer Institute (NCI) launched the NCI Alliance for Nanotechnology in Cancer to exploit the nanotechnology to fight cancer (Hull et al. 2014; Farrell et al. 2010).

Targeted DDS, as its name means, is to deliver the loaded cargos or treatment drugs to the interested site while reducing or avoiding the cargos or treatment drugs distribution to normal tissue or cells (Bae and Park 2011). For decades, several series of nanocarriers applied in DDS have been used for anticancer drugs delivery, including liposomes (Felfoul et al. 2016; Sharma and Sharma 1997; Gregoriadis and Florence 1993; Drummond et al. 2000), organic nanoparticles (Horcajada et al. 2010a, b), inorganic nanoparticles (Rotello 2008; Liong et al. 2008; Vivero-Escoto et al. 2010; Zhi et al. 2006), hybrid nanoparticles (Hrkach et al. 2012), polymeric micelles (Matsumura and Kataoka 2009; Norased et al. 2006, Bae et al. 2003), polymer-drug conjugates (Zhu et al. 2013), nanogels (Du et al. 2010; Jung-Kwon et al. 2008), as shown in Fig. 14.1.

In addition to solubilizing poorly soluble drugs and protecting drugs from cellular degradation, the drug-loaded nanocarriers in DDS could prolong the circulation time of released drugs and selectively deliver them to the targeted tumor tissue, tumor cells, or subcellular organelle (Shi et al. 2017). Besides, the released drugs from the nanocarriers can be controlled in a spatiotemporal manner, sustained release drug over a period of time, achieving their pharmacological activities only at the targeted site (Dai et al. 2012). FDA has already approved several nanotechnology-based antitumor preparations for decades, such as Doxil® (PEGylated liposomal doxorubicin (DOX)) and Abraxane® (paclitaxel (PTX) loaded albumin nanoparticles) (Hare et al. 2017).

Even though targeting nanocarriers to malignant tissues, tumor cells, or subcellular organelle to improve diagnosis and therapy is a popular concept, the literature

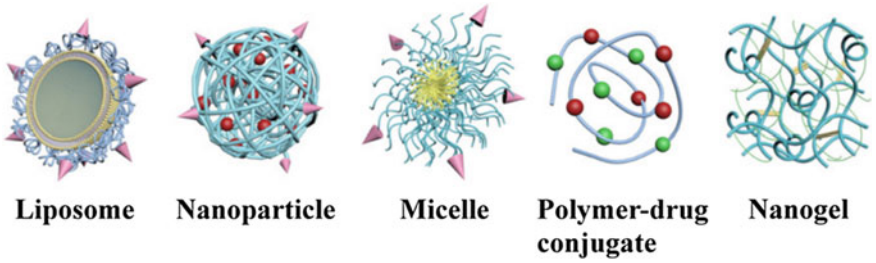

Fig. 14.1 Illustration of several representative nanomedicines for cancer therapy, including liposome, nanoparticle, polymer micelle, polymer–drug conjugate, and nanogel. Reprinted from Dai et al. (2017). Copyright 2017, with permission from Elsevier

survey during the past 10 years turned out that only 0.7% (median) of the administered nanocarriers is delivered to the targeted solid tumor. This has a negative effect on nanotechnology for human clinic use with respect to manufacturing, financial investment, toxicity, and imaging and therapeutic efficacy (Table 14.1) (Wilhelm et al. 2016).

14.4 Nucleic Acid Amplification Strategies Applied in Theranostics

For a particular disease, such as cancer, there is a growing significant interest in theranostic approaches that permit concurrent diagnosis and treatment with therapeutic development. With the increased insights into delivery kinetics and biological response, the theranostic may help open the field of medicine toward to an era of more effective and precise treatment (Peer et al. 2007; Conway et al. 2014). Unfortunately, probing and detection low-abundance cancer biomarker and transporting a high-load drug nanocarrier to specifically targeted tumor cells and, particularly, their combination still are a major challenge nowadays. Currently, theranostic approaches for probing and detection in cancer typically rely on targeting tumor-associated biomarkers with aptamer, antibodies or other ligands, which allows an accumulation of signal reporters or drug payloads in tumors and thus renders contrast imaging and selective treatment (Andersen et al. 2009). However, the lack of intelligent designs for probing and detection in diagnosis step in theranostic leads to limited imaging sensitivity and increased background interference (Bhuniya et al. 2014). The pursuit of activatable probe and detection designs represents a vital effort in cancer theranostics.

Table 14.1 Delivery efficiency and the number of data sets. Reprinted from Wilhelm et al. (2016), with kind permission from Springer Science + Business Media

Category	Delivery efficiency [%ID]*	Number of data sets
All data sets	0.7	232
Year		
2005	1.4	8
2006	0.7	8
2007	1.0	24
2008	0.3	8
2009	0.9	11
2010	0.8	14
2011	0.7	27
2012	0.7	14
2013	0.5	35
2014	0.8	38
2015	0.5	45
Mateiral		
Inorganic	0.8	86
Organic	0.6	137
Inorganic material		
Gold	1.0	45
Iron oxide	0.6	8
Silica	0.4	13
Quantum dots	0.9	5
Other	0.6	14
Organic material		
Dendrimers	1.4	7
Liposomes	0.5	27
Polymeric	0.6	62
Hydrogels	0.5	18
Other	0.9	23
Targeting strategy		
Passive	0.6	175
Active	0.9	57

14.4.1 Theranostics Based on DNA Rolling-Circle Amplification

Rolling-circle amplification (RCA) is an isothermal nucleic acid amplification technique, and a variety of biomarkers such as genes, microRNAs, proteins with ultra-low cellular abundance have been successfully detected using developed RCA-based probes. In recent decades, various approaches have been achieved to improve the RCA technique, and it has become an attractive detection tool for biomedical applications. In this section, I will summarize the RCA-DDS combined cancer clinical applications, making an outlook on the trends of the related research fields in the future (Wang et al. 2015a; Chen et al. 2015).

In most assays based on RCA, the quantification of the target is achieved through the RCA product quantification. The RCA products not only can turn into nanostructures by self-assembly, but also can form solubilized threads. Zhang's group synthesized MNP/DNA-SP as nanocarrier and doxorubicin embedded in MNP/DNA-SP as therapy drug to constructed a DDS (Guo et al. 2017b). By modification of different functional elements in the surface of MNP/DNA-SP, such as aptamers and disulfide linkages, the synthesized MNP/DNA-SP-DOX can be used for targeted GSH or CEM cells detection and doxorubicin delivery, resulting in the relief of cell apoptosis in target GSH or CEM cells, as shown in Fig. 14.2. For those that have not yet been screened by their aptamers specifically, functional element (e.g., FA) modified poly T tailed sequences were taken to MNP/DNA-SP by terminal transferase-mediated chain elongation. Different functional elements as ligands for different targets can be incorporated into MNP/DNA-SP, which can achieve versatile targeted and detection applications. The advantages of MNP/DNA-SP-DOX cargo displayed high selectivity, superior biocompatibility, and convenient drug delivery. The potent antitumor efficacy of DOX delivered by the biocompatible MNP/DNA-SP nanocarrier was also tested in a model of xenografted tumors of mice. Consequently, the result is a combination of traceable targeted detection and drug delivery that serves as a multifunctional MNP/DNA-SP, which will provide a novel theranostic platform for cancer targets detection and may also approve other clinical applications.

Considering the requirement for combination of cancer clinical diagnosis and therapy, Guo and her co-workers developed a magnetic nanoparticle (MNP)-based cellular DDS for DOX cellular load and release to kill cancerous cells (Guo et al. 2017a). As shown in Fig. 14.3, MNPs surface was modified with RNA nanoflowers (RNA NF) through biotin–avidin conjugation (MNP/RNA NF), and RNA NF was produced based on rolling-circle transcription (RCT). To realize the specific targeting cancerous cell delivery, they employed folic acid (FA) as active targeting ligands to functionalize MNP/RNA NF and constructed FA/MNP/RNA NF nanostructure. While for specific binding, folate receptors (FRs) is a wise choice for specific binding of FA, which is overexpressed on the cancer cell membrane, while low expressed in the normal cell. The anticancer drug DOX as well as the photosensitizer TMPyP4, which could generate reactive oxygen species (ROS) with 650 nm light, was both loaded into this FA/MNP/RNA NF nanocarrier. The result showed that

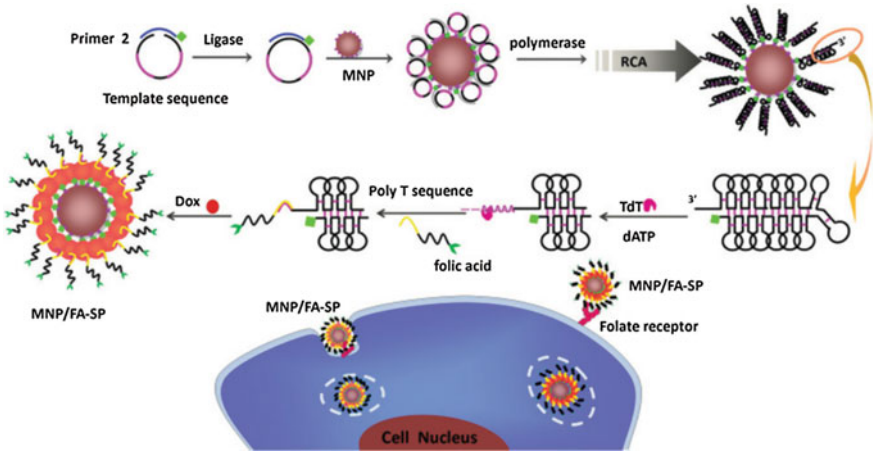

Fig. 14.2 Schematic diagram of folic acid decorated MNP/DNA-SP for cellular targeted drug delivery Reproduced from Guo et al. (2017a, b) by permission of the Royal Society of Chemistry

FA/MNP/RNA NF nanocarrier has better treatment efficacy than DOX traditional delivery way. Additionally, FA/MNP/RNA NF could also be used as a probe for HeLa cells' detection, and it can detect as low as 50 cells (Guo et al. 2017b). Thus, the nucleic acid amplification technique assisted by MNPs holds great promise for potential applications in cancer diagnostics and therapeutics.

14.4.2 Theranostics Based on Hybridization Chain Reaction

Hybridization chain reaction (HCR), in which stable DNA monomers assemble only upon exposure to a target DNA fragment (Dirks and Pierce 2004). Generally speaking, two stable DNA hairpins' species coexist in reaction solution and then introduce initiator strands to trigger a cascade of hybridization processes that yields nicked double helices analogous to alternating copolymers. By coupling HCR to aptamer triggers, amplification of more diverse recognition reactions can be achieved. In HCR, this functionality allows DNA to act as an amplifying transducer for biosensing applications.

Based on the feature and function of the telomerase primer and its extension products (Qian et al. 2013, 2014), Zhang and her co-workers proposed a new strategy for synthesis a novel nuclear-shell biopolymers initiated by telomere elongation and can be used for telomerase activity detection and drug delivery to cancer cells (Zhang et al. 2017). As shown in Fig. 14.4, telomerase can elongate the telomere primers, which resulting in inner chain substitution followed by the release of RCA primers and loaded drug. A core nanoball, an outer shell of RCA, biopolymers labeled with fluorescence probes constituted the nuclear-shell self-assembly body. After equipped

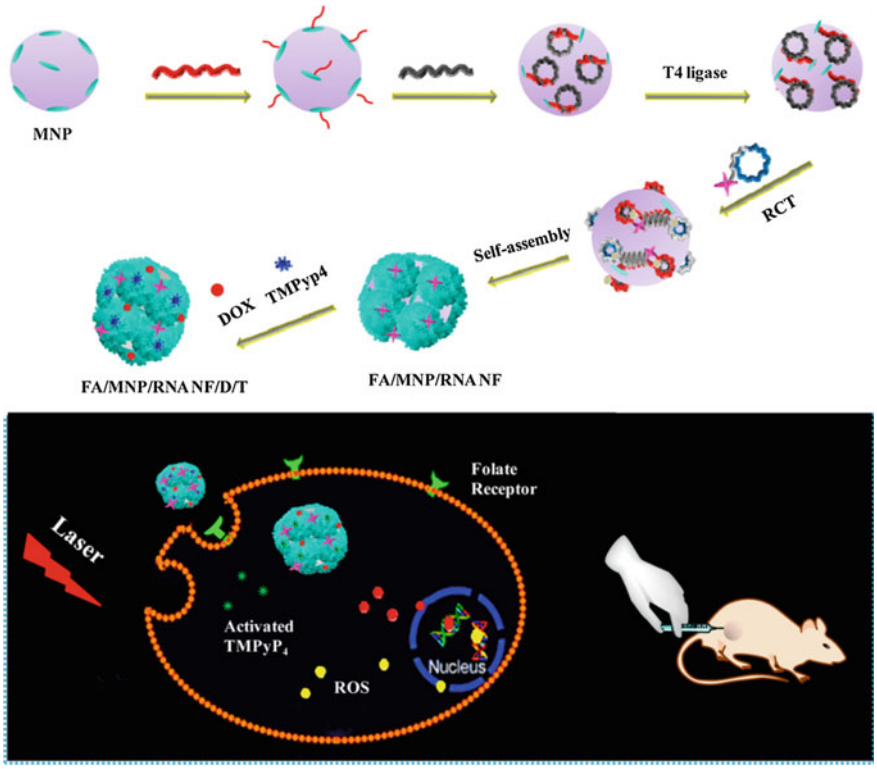

Fig. 14.3 Schematic diagram of magnetic nanoparticle-based co-delivery system Reprinted with the permission from Guo et al. (2017a, b). Copyright 2017 American Chemical Society

this platform with functionalized silica-nanoflowers (FSNFs), it was supported to detect and monitor telomerase activity and to achieve drug delivery to cancer cells. The results showed that the nuclear-shell self-assembly body, which was the product of RCA, displayed high sensitivity and activity for monitoring cellular telomerase, and efficient signal amplification effect. Consequently, as RCA product, the nuclear-shell biopolymer can efficiently deliver drugs to targeted cancer cells, which reduce the undesired death of healthy cells, might prove a new way for diagnosis–treatment processes in theranostics.

By applying a structure-switching aptamer-triggered HCR on cell surface, Chu's group developed a novel activatable theranostic approach. It is the first time that achieves real-time activation and amplification for fluorescence imaging and targeting therapy use an aptamer platform (Wang et al. 2015b). The aptamer probe (AP) used in this system is designed to trigger HCR on binding to the target cell via structure switching, instead of initiating HCR in its free state, skillfully. The HCR not only amplifies fluorescence signals from a fluorescence-quenched probe (H1) for activatable tumor imaging but also accumulates high-load prodrugs from a drug-labeled

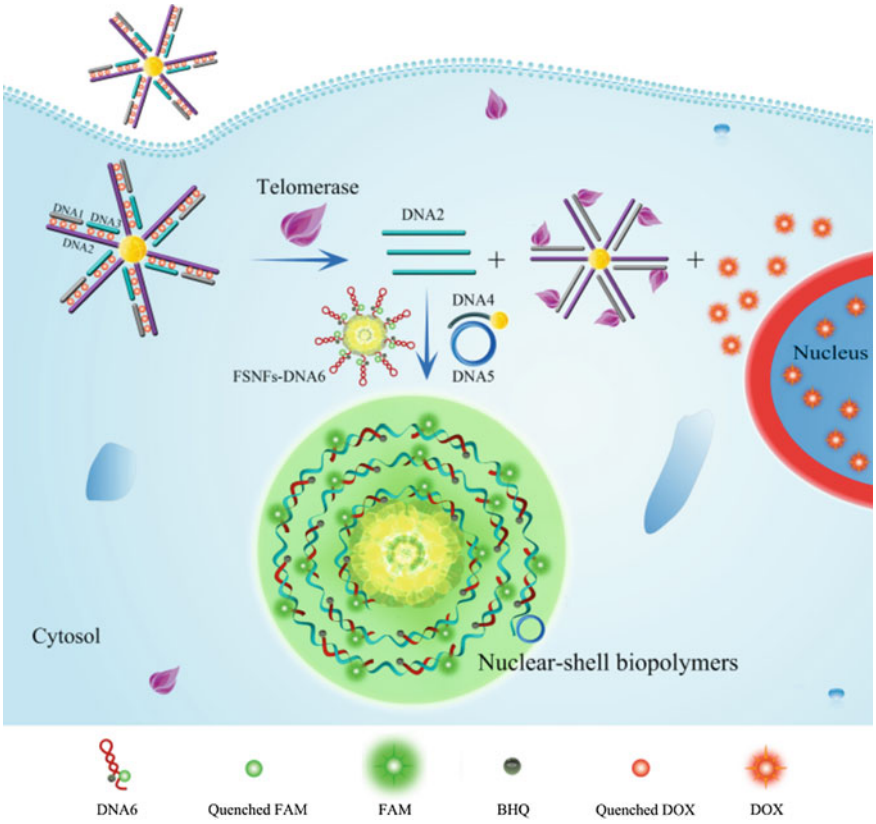

Fig. 14.4 Illustration of telomerase activity monitoring and drug delivery based on novel nuclear-shell biopolymers in individual cancer cells. Reprinted with the permission from Zhang et al. (2017). Copyright 2017 American Chemical Society

probe (H2) and induces its uptake and conversion into cisplatin in cells for selective tumor therapy. The in vitro result showed that this approach affords efficient signal amplification for fluorescence detection of target protein tyrosine kinase-7 (PTK7) with a detection limit of 1 pM. Live cell studies also reveal that this approach provides high-contrast fluorescence imaging and highly sensitive detection of tumor cells, while renders high-efficiency drug delivery into tumor cells via an endocytosis pathway. The results imply the potential of the HCR approach as a promising platform for early-stage disease diagnosis and precise cancer therapy (Fig. 14.5).

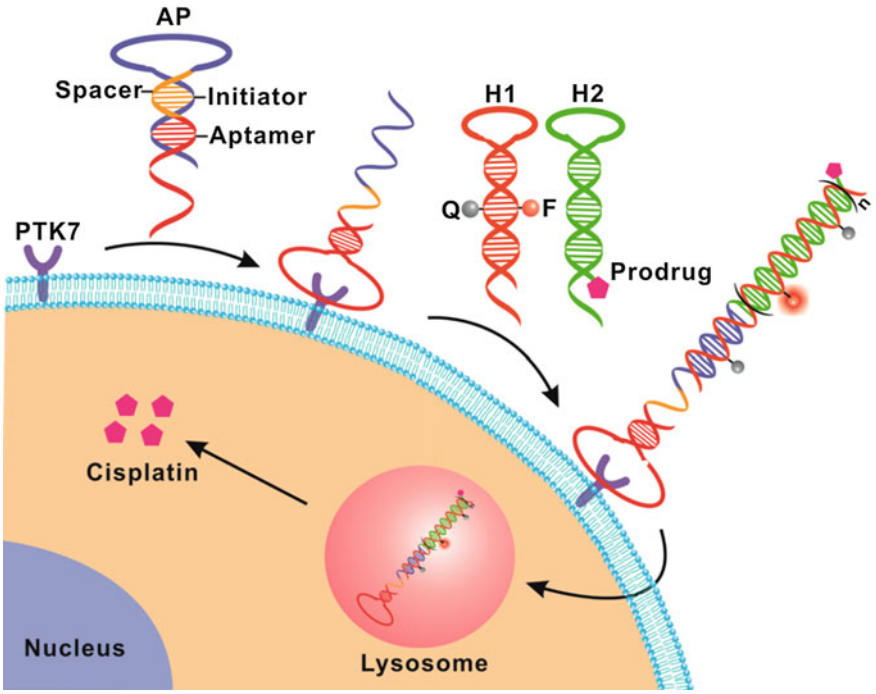

Fig. 14.5 Illustration of SATHCR for activatable theranostics. Reprinted with the permission from Wang et al. (2015a, b). Copyright 2015 American Chemical Society

14.4.3 Theranostics Based on Aptamer-Incorporated Nucleic Acid Amplification

Definitely, in theranostics, it is essential to monitor the expression of low-abundance biomarkers and transport a high-load drug to target cancer cells (Srinivasarao et al. 2015). Aptamers are single RNA or DNA strand with unique intramolecular conformations for selective binding to various targets. Aptamer-ligand recognition depends on the precise stacking of flat moieties, specific hydrogen bonding, and molecular shape complementarity (Bock et al. 1992; Jayasena 1999; Hermann and Patel 2000). Aptamer possesses dominant advantages over antibodies in terms of size, synthetic accessibility, and chemical modification. Therefore, aptamers are under worldwide development as a potential diagnostic or therapeutic tool in theranostics (Table 14.2) (Keefe et al. 2010).

In theranostics, the applied aptamers are functionalized with therapeutic agents or imaging probes (Wang et al. 2014; Kruspe and Hahn 2014). How to discriminate different types of cancer cells still remains challenging in the detection step due to the subtle differences in cancer cell expression of membrane receptors. Zhang's group developed a multicolor cell imaging method for distinguishing different types

Table 14.2 Aptamers to targets of therapeutic interest. Reprinted from Keefe et al. (2010), with kind permission from Springer Science + Business Media

Target (alternative name)	K_d (nM)	Therapeutic applications	Refs
α-thrombin	25	Prevent thrombosis	9
HIV-1 reverse transcriptase	1	Inhibit viral replication	134
HIV-1 Rev	<1	Inhibit viral replication	135
Fibroblast growth factor 2, basic	0.35	Prevent angiogenesis	136
Respiratory syncytial virus	40	Prevent infection	137
HIV-1 integrase	10	Inhibit viral replication	138
Vascular endothelial growth factor	0.1	Prevent neovascularization	139
Platelet-derived growth factor	0.1	Prevent tumor development	83
Immunoglobulin E	10	Prevent allergies	140
L-Selectin	3	Modulate inflammation	141
D.Adenosine	1100	Unknown	39
Acetylcholine-specific auto-antibodies	60	Treat myasthenia gravis	142
Interferon-γ	68	Modulate inflammation and immune response	143
Keratinocyte growth factor	0.0002	Treat epithelial hyperproliferative disease	144
Neutrophil elastase	n/o	Modulate inflammation	145
P-selectin	0.04	Inhibit viral adhesion	146
Acetycholine receptor	2	Control neurotransmission	147
Phospholipase A_2	118	Treat ARDS, septic shock	148
Protein tyrosine phosphatase	18	Inhibit oncogenesis, viral regulation	149
Activated protein C	110	Prevent thrombosis	150
CD4	0.5	Modulate immune response	151
Nuclear factor-κB	1	Treat chronic inflammtory disease	152
Lymphocyte function-associated antigen 1	500	Prevent tumor development, modulate inflammation	153
Cytohesin 1	5	Modulate cytoskeletal reorganization	154
α v β 3 integrin	2	Prevent tumor development	155, 156

of cancer cells with fluorophore-tagged aptamers (Fig. 14.6) (Wang et al. 2014). Aptamer sequence and aptamer-labeled dyes affect the recognition process between aptamers and cancer cells. For different cancer cell lines, even though they own the same biomarkers, when interact the fluorophore-tagged aptamers with different cancer cell lines in different degree, the result turned out that there is a distinct color to discriminate different types of cancer cells at single cell level. Based on cross-reactive ability of the fluorophore-tagged aptamers, distinguish the cancer cells from

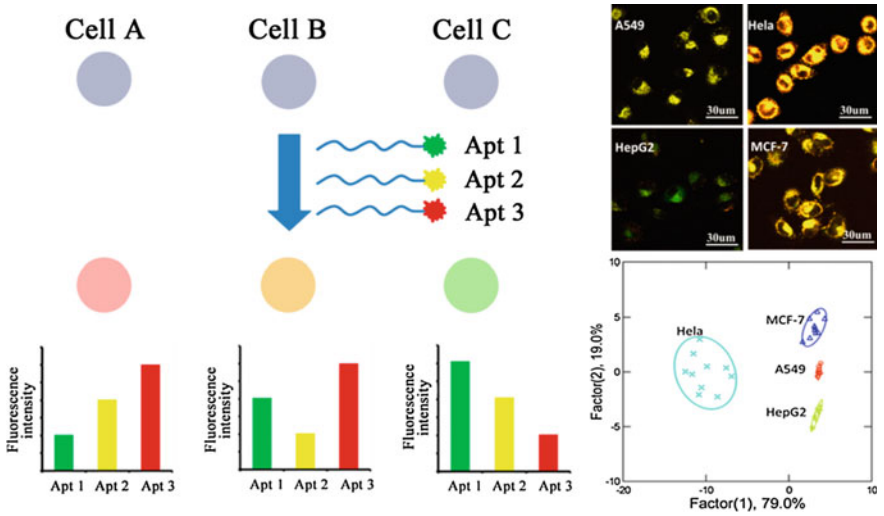

Fig. 14.6 Schematic presentation of the multicolor imaging for single cell typing with fluorophore-tagged aptamers. Reprinted with the permission from Wang et al. (2014). Copyright 2014 American Chemical Society

large quantities of normal cells quickly, and identify different types of the cancer cells are achieved, simultaneously. These fluorophore-tagged aptamers have a promising application for cancer diagnostic and therapy in the future.

As one of the class of therapeutic nucleoside and nucleobase analogues drugs, 5-fluorouracil (5-FU) has been used in cancer therapy and in the treatment of various diseases for decades (Longley et al. 2003). Therefore, in DDS, nanoparticles, nanogels, and nanopolymers are mainly focus on 5-FU cellular delivery for cancer therapy (Burke et al. 2014). By applying a cell-specific cytotoxic aptamer, Sven's group found that it can be prepared in a one-step enzymatic reaction by incorporating multiple units of a nucleoside analogue directly into an aptamer that targets a cytokine receptor. In targeted cancer cells, the controlled cellular release of 5-FU is initiated by intracellular nucleolytic hydrolysis of the cell-specific cytotoxic aptamer (Kruspe and Hahn 2014). Cytotoxic nucleoside and nucleobase analogues, such as 5-fluoro-2'-deoxyuridine (5-FUdR), are advantageous drugs for receptor-mediated active targeting as they benefit from this intracellular turnover. As showed in Fig. 14.7, 5-FUdR becomes part of the aptamer molecule itself, replacing all the uridines in the original aptamer. The controlled release of the drug inside the target cells is mediated through naturally occurred degradation by lysosomal nucleases. The hydrolysis of the aptamer would yield 5-FUdR, which could escape the lysosome by active nucleoside transporters, which normally serve as recycling gateways for lysosomal degraded nucleic acids (Fig. 14.7).

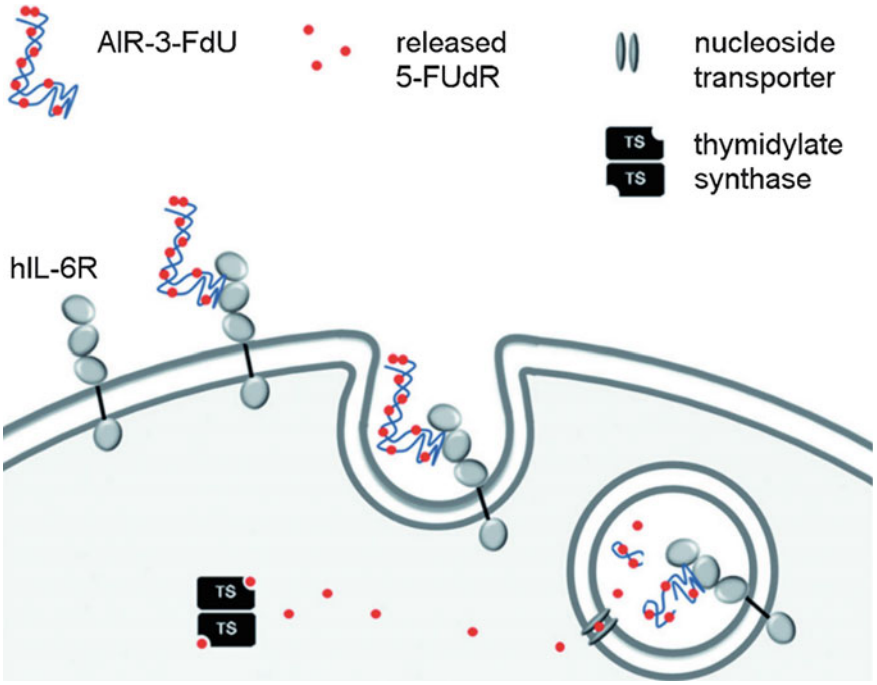

Fig. 14.7 Principle of drug delivery by AIR-3-FdU. The 5-FUdR-modified aptamer (AIR-3-FdU) binds to the human interleukin-6 receptor on the cell surface and is internalized. Reproduced from Kruspe and Hahn (2014) by permission of John Wiley& Sons Ltd.

14.5 Conclusion

Theranostics is a prosperous field of cancer which combines specific targeted cancer therapy with specific cancer biomarkers-targeted diagnosis. Theranostics uses specifically diagnostic ways in the human body, to acquire diagnostic images and also to deliver a therapeutic dose of medicine to the patient. It applies nanoscience to unite diagnostic and therapeutic applications to form a single agent, allowing for diagnosis, drug delivery, and treatment response monitoring. Besides, theranostics provides a transition from conventional medicine therapy to a contemporary personalized and precision medicine approach.

In theranostics, the nucleic acid amplification strategy-based diagnostic method recognize the particular biomarkers on a tumor, amplify the signal, and allow loaded therapy drug released to specifically targets on the tumor, rather than more broadly the disease and location it presents. This contemporary form of treatment moves away from the one-medicine-fits-all and trial-and-error medicine approach, to offering the right treatment, for the right patient, at the right time, with the right dose, providing a more targeted, accurate and efficient pharmacotherapy in the form of theranostics.

This chapter covers part of the reported applications, and many efforts have been made to develop diagnostic and theraputic assays using nucleic acid amplification combined DDS in theranostics. In the past decade, DNA- or RNA-targeted nucleic acid amplification has been well developed to help in the detection and quantification of cancer biomarkers and cells in patient-derived blood and tissue samples as well as the patient's body. While tumor is a heterogeneous tissue consisting of different types of cancer or cancer-associated cells, it may vary between different patients or even between different cancer stages in an individual patient. Therefore, currently, the discovery of new and effective diagnostic and prognostic DDS cargoes seems necessary in theranostics.

References

Abou-Elkacem L, Wilson KE, Johnson SM et al (2016) Ultrasound molecular imaging of the breast cancer neovasculature using engineered fibronectin scaffold ligands: a novel class of targeted contrast ultrasound agent. Theranostics 6:1740–1752

Al-Lazikani B, Banerji U, Workman P (2012) Combinatorial drug therapy for cancer in the post-genomic era. Nat Biotechnol 30:679–692

Andersen ES, Dong M, Nielsen MM et al (2009) Self-assembly of a nanoscale DNA box with a controllable lid. Nature 459:73–76

Bae Y, Fukushima S, Harada A et al (2003) Design of environment-sensitive supramolecular assemblies for intracellular drug delivery: polymeric micelles that are responsive to intracellular pH change. Angew Chem Int Ed 42:4640–4643

Bae YH, Park K (2011) Targeted drug delivery to tumors: myths, reality and possibility. J Control Release 153:198–205

Baum RP, Kulkarni HR (2012) Theranostics: from molecular imaging using Ga-68 labeled tracers and PET/CT to personalized radionuclide therapy—the bad berka experience. Theranostics 2:437–447

Bertrand N, Leroux JC (2012) The journey of a drug-carrier in the body: an anatomo-physiological perspective. J Control Release 161:152–163

Bhuniya S, Maiti S, Kim EJ et al (2014) An activatable theranostic for targeted cancer therapy and imaging. Angew Chem Int Ed 53:4469–4474

Bock LC, Griffin LC, Latham JA et al (1992) Selection of single-stranded DNA molecules that bind and inhibit human thrombin. Nature 355:564–566

Burke CW, Et Alexander, Timbie K et al (2014) Ultrasound-activated agents comprised of 5FU-bearing nanoparticles bonded to microbubbles inhibit solid tumor growth and improve survival. Mol Ther 22:321–328

Chen G, Liu D, He C et al (2015) Enzymatic synthesis of periodic DNA nanoribbons for intracellular pH sensing and gene silencing. J Am Chem Soc 137:3844–3851

Chen KJ, Chaung EY, Wey SP et al (2014) Hyperthermia-mediated local drug delivery by a bubble-generating liposomal system for tumor-specific chemotherapy. ACS Nano 8:5105–5115

Chen W, Zheng R, Baade PD et al (2016) Cancer statistics in China, 2015. CA Cancer J Clin 66:115–132

Choudhury P, Gupta M (2018) Differentiated thyroid cancer theranostics: radioiodine and beyond. Br J Radiol 91:20180136

Conway JR, Carragher NO, Timpson P (2014) Developments in preclinical cancer imaging: innovating the discovery of therapeutics. Nat Rev Cancer 14:314–328

Dai W, Jin W, Zhang J et al (2012) Spatiotemporally controlled co-delivery of anti-vasculature agent and cytotoxic drug by octreotide-modified stealth liposomes. Pharm Res 29:2902–2911

Dai W, Wang X, Song G et al (2017) Combination antitumor therapy with targeted dual nanomedicines. Adv Drug Deliv Rev 115:23–45
Dirks RM, Pierce NA (2004) Triggered amplification by hybridization chain reaction. Proc Natl Acad Sci U S A 101:15275–15278
Dreifuss T, Betzer O, Shilo M et al (2015) A challenge for theranostics: is the optimal particle for therapy also optimal for diagnostics? Nanoscale 7:15175–15184
Drummond DC, Zignani M, Leroux JC (2000) Current status of pH-sensitive liposomes in drug delivery. Prog Lipid Res 39:409–460
Du JZ, Sun TM, Song WJ et al (2010) A tumor-acidity-activated charge-conversional nanogel as an intelligent vehicle for promoted tumoral-cell uptake and drug delivery. Angew Chem Int Ed 49:3621–3626
Emmenegger U, Kerbel RS (2010) Cancer: chemotherapy counteracted. Nature 468:637–638
Fan CH, Cheng YH, Ting CY et al (2016) Ultrasound/magnetic targeting with SPIO-DOX-microbubble complex for image-guided drug delivery in brain tumors. Theranostics 6:1542–1556
Farrell D, Alper J, Ptak K et al (2010) Recent advances from the national cancer institute alliance for nanotechnology in cancer. ACS Nano 4:589–594
Felfoul O, Mohammadi M, Taherkhani S et al (2016) Magneto-aerotactic bacteria deliver drug-containing nanoliposomes to tumour hypoxic regions. Nat Nanotechnol 11:941–947
Frandsen JL, Ghandehari H (2012) Recombinant protein-based polymers for advanced drug delivery. Chem Soc Rev 41:2696–2706
Ge Z, Liu S (2013) Functional block copolymer assemblies responsive to tumor and intracellular microenvironments for site-specific drug delivery and enhanced imaging performance. Chem Soc Rev 42:7289–7325
Gregoriadis G, Florence AT (1993) Liposomes in drug delivery. Drugs 45:15–28
Guo Y, Li S, Wang Y et al (2017a) Diagnosis-therapy integrative systems based on magnetic RNA nanoflowers for co-drug delivery and targeted therapy. Anal Chem 89:2267–2274
Guo Y, Wang Y, Li S et al (2017b) DNA-spheres decorated with magnetic nanocomposites based on terminal transfer reactions for versatile target detection and cellular targeted drug delivery. Chem Commun 53:4826–4829
Hahn MA, Singh AK, Sharma P et al (2011) Nanoparticles as contrast agents for in-vivo bioimaging: current status and future perspectives. Anal Bioanal Chem 399:3–27
Hare JI, Lammers T, Ashford MB et al (2017) Challenges and strategies in anti-cancer nanomedicine development: an industry perspective. Adv Drug Deliv Rev 108:25–38
Heath JR (2015) Nanotechnologies for biomedical science and translational medicine. Proc Natl Acad Sci U S A 112:14436–14443
Hermann T, Patel DJ (2000) Adaptive recognition by nucleic acid aptamers. Science 287:820–825
Horcajada P, Chalati T, Serre C et al (2010a) Porous metal-organic-framework nanoscale carriers as a potential platform for drug delivery and imaging. Nat Mater 9:172–178
Horcajada P, Serre C, Valletregí M et al (2010b) Metal-organic frameworks as efficient materials for drug delivery. Angew Chem Int Ed 45:5974–5978
Hrkach J, Von Hoff D, Mukkaram Ali M et al (2012) Preclinical development and clinical translation of a PSMA-targeted docetaxel nanoparticle with a differentiated pharmacological profile. Sci Transl Med 4:128–139
Hull LC, Farrell D, Grodzinski P (2014) Highlights of recent developments and trends in cancer nanotechnology research–view from NCI Alliance for Nanotechnology in Cancer. Biotechnol Adv 32:666–678
Jayasena SD (1999) Aptamers: an emerging class of molecules that rival antibodies in diagnostics. Clin Chem 45:1628–1650
Jun Kwon OH, Ray D, Daniel J et al (2008) The development of microgels/nanogels for drug delivery applications. Prog Polym Sci 33:448–477
Karimi M, Ghasemi A, Sahandi Zangabad P et al (2016) Smart micro/nanoparticles in stimulus-responsive drug/gene delivery systems. Chem Soc Rev 45:1457–1501
Keefe AD, Pai S, Ellington A (2010) Aptamers as therapeutics. Nat Rev Drug Discov 9:537–550

Kruspe S, Hahn U (2014) An aptamer intrinsically comprising 5-fluoro-2′-deoxyuridine for targeted chemotherapy. Angew Chem Int Ed 53:10541–10544
Liong M, Lu J, Kovochich M et al (2008) Multifunctional inorganic nanoparticles for imaging, targeting, and drug delivery. ACS Nano 2:889–896
Longley DB, Harkin DP, Johnston PG (2003) 5-fluorouracil: mechanisms of action and clinical strategies. Nat Rev Cancer 3:330–338
Matsumura Y, Kataoka K (2009) Preclinical and clinical studies of anticancer agent-incorporating polymer micelles. Cancer Sci 100:572–579
Mosafer J, Abnous K, Tafaghodi M et al (2017) In vitro and in vivo evaluation of anti-nucleolin-targeted magnetic PLGA nanoparticles loaded with doxorubicin as a theranostic agent for enhanced targeted cancer imaging and therapy. Eur J Pharm Biopharm 113:60–74
Muthu MS, Leong DT, Mei L et al (2014) Nanotheranostics—application and further development of nanomedicine strategies for advanced theranostics. Theranostics 4:660–677
Nicolas J, Mura S, Brambilla D et al (2013) Design, functionalization strategies and biomedical applications of targeted biodegradable/biocompatible polymer-based nanocarriers for drug delivery. Chem Soc Rev 42:1147–1235
Norased N, Bey E, Ren J et al (2006) Multifunctional polymeric micelles as cancer-targeted, MRI-ultrasensitive drug delivery systems. Nano Lett 6:2427–2430
Olaku OO, Taylor EA (2017) Cancer in the medically underserved population. Prim Care 44:87–97
Park SH, Zheng JH, Nguyen VH et al (2016) RGD peptide cell-surface display enhances the targeting and therapeutic efficacy of attenuated salmonella-mediated cancer therapy. Theranostics 6:1672–1682
Peer D, Karp JM, Hong S et al (2007) Nanocarriers as an emerging platform for cancer therapy. Nat Nanotechnol 2:751–760
Qian R, Ding L, Ju H (2013) Switchable fluorescent imaging of intracellular telomerase activity using telomerase-responsive mesoporous silica nanoparticle. J Am Chem Soc 135:13282–13285
Qian R, Ding L, Yan L et al (2014) Smart vesicle kit for in situ monitoring of intracellular telomerase activity using a telomerase-responsive probe. Anal Chem 86:8642–8648
Rotello VM (2008) Advanced drug delivery reviews theme issue: “inorganic nanoparticles in drug delivery”. Adv Drug Deliver Rev 60:1225
Sharma A, Sharma US (1997) Liposomes in drug delivery: Progress and limitations. Int J Pharmaceut 154:123–140
Shi J, Kantoff PW, Wooster R et al (2017) Cancer nanomedicine: progress, challenges and opportunities. Nat Rev Cancer 17:20–37
Srinivasarao M, Galliford CV, Low PS (2015) Principles in the design of ligand-targeted cancer therapeutics and imaging agents. Nat Rev Drug Discov 14:203–219
Vandghanooni S, Eskandani M, Barar J et al (2018) Recent advances in aptamer-armed multimodal theranostic nanosystems for imaging and targeted therapy of cancer. Eur J Pharm Sci 117:301–312
Vivero-Escoto JL, Slowing II, Trewyn BG et al (2010) Mesoporous silica nanoparticles for intracellular controlled drug delivery. Small 6:1952–1967
Wang L, Deng R, Li J (2015a) Target-fueled DNA walker for highly selective miRNA detection. Chem Sci 6:6777–6782
Wang S, Kong H, Gong X et al (2014) Multicolor imaging of cancer cells with fluorophore-tagged aptamers for single cell typing. Anal Chem 86:8261–8266
Wang YM, Wu Z, Liu SJ et al (2015b) Structure-switching aptamer triggering hybridization chain reaction on the cell surface for activatable theranostics. Anal Chem 87:6470–6474
Weeks JC, Catalano PJ, Cronin A et al (2012) Patients’ expectations about effects of chemotherapy for advanced cancer. N Engl J Med 367:1616–1625
Wilhelm S, Tavares AJ, Dai Q et al (2016) Analysis of nanoparticle delivery to tumours. Nat Rev Mater 1:16014
Xiao B, Ma L, Merlin D (2017) Nanoparticle-mediated co-delivery of chemotherapeutic agent and siRNA for combination cancer therapy. Expert Opin Drug Deliv 14:65–73

Yano S, Takeuchi S, Nakagawa T et al (2012) Ligand-triggered resistance to molecular targeted drugs in lung cancer: roles of hepatocyte growth factor and epidermal growth factor receptor ligands. Cancer Sci 103:1189–1194

Zhang Z, Jiao Y, Zhu M et al (2017) Nuclear-shell biopolymers initiated by telomere elongation for individual cancer cell imaging and drug delivery. Anal Chem 89:4320–4327

Zhi PX, Zeng QH, Gao QL et al (2006) Inorganic nanoparticles as carriers for efficient cellular delivery. Chem Eng Sci 61:1027–1040

Zhu L, Wang T, Perche F et al (2013) Enhanced anticancer activity of nanopreparation containing an MMP2-sensitive PEG-drug conjugate and cell-penetrating moiety. Proc Natl Acad Sci U S A 110:17047–17052

Chapter 15
Microdroplet Array for Nucleic Acid Amplification Strategies

Yingnan Sun

Abstract Nucleic acid amplification strategies are often integrated with miniaturized devices including digital microfluidics, microfluidic chips, paper-based fluidic chips, and other open chip without microstructures. In contrast to microdroplet generation on chips with microchannels or on microchambers, recently developed techniques for the generation of droplet arrays (ranging from femtoliter to microliter volumes) on planar substrates have set the stage for the direct manipulation of individual droplets and for image acquisition and quantification. A droplet array on a planar substrate has some advantages over the previous picoliter or nanoliter chambers with solid walls. The integration of nucleic acid amplification into microdroplet array has facilitated the development of nucleic acid-based detection and diagnosis with high assay sensitivity. In this section, we highlight recent progress made on the characterization of open-access microdroplet array, focusing particularly on design, fabrication, and clinical application.

15.1 Introduction

In recent years, enormous efforts have been dedicated to develop droplet manipulation technology since isolated microdroplets in an oil phase have great potential for use in biochemical research and clinical diagnostics (Han et al. 2018). Compared to conventional microfluidics with fluidic channels, droplet-based microfluidic devices provide greater flexibility and versatility, and reaction in microdroplet has some unique advantages (Ma 2016). Firstly, the volume of reaction in droplet is as small as picoliters or nanoliters, the consumption of reagents can be decreased by more than three orders of magnitudes. Secondly, droplet segregated by immiscible phase can perform parallel high-throughput analysis for multiple targets. Thirdly, microdroplet can realize fast biochemical reactions due to rapid blend of reactant and high efficiency of heat and mass transfer, which dramatically reduces the reaction time.

Y. Sun (✉)
Shandong Provincial Key Laboratory of Detection Technology for Tumour Markers, College of Chemistry and Chemical Engineering, Linyi University, Linyi 276005, People's Republic of China
e-mail: syingnan@163.com

S. Zhang et al. (eds.), *Nucleic Acid Amplification Strategies for Biosensing, Bioimaging and Biomedicine*, https://doi.org/10.1007/978-981-13-7044-1_15

Fourthly, the size of microdroplet comparable to that of a cell enables analysis for single cell. Lastly, miniaturized reactors contribute to the combination of a series of operations including purification, mix, amplification, and detection of samples, which makes automation and portability of system more likely to come true. Currently, droplet technology has been widely used in biological detection technology such as protein detection, kinetics of enzyme reaction, polymerase chain reactions (PCR), and single-cell analysis. Many biochemical reactions have been successfully executed in single droplet (Huebner et al. 2008; Taly et al. 2007). Notably, parallel PCR in nanoliter- to picoliter-sized microdroplets (Takinoue and Takeuchi 2011; Teh et al. 2008; Theberge et al. 2010; Lorber et al. 2011) have garnered intense research interesting in the past few years (Sun et al. 2014).

The microdroplet chip can be further classified into the enclosed and open models. The former system requires designing and fabricating droplet-based microfluidics including microchannels and microchambers, using specialized facilities and complex procedures, which are not widely available. In contrast, the open-access microdroplet array has unique advantages in multistep operation of droplets and subsequent detection. Droplet arrays are emerging as an open platform which are totally different from the conventional, flow-based, lab-on-a-chip philosophy and compete with microplates, in terms of versatility and simplicity of operation (Garcia-Cordero and Fan 2017). A planar monolayer droplet array (PMDA) (Xu et al. 2016a, b) in flat substrate, offering exceptional convenience that can not only complete microscopically one-time imaging, but also perform droplet addressing and real-time in situ monitoring of the target droplets. Although this kind of microdroplet chip still has limitations in analyzing throughput compared with the emulsion microdroplet system, it is extremely suitable for the development of disposable POC diagnosis equipment. Therefore, microdroplet array is one of the focused researches of droplet methodology in recent years.

In this section, we highlight recent progress made on the characterization of open-access PDMA, focusing particularly on design, fabrication, and clinical application. What needs to be emphasized is that the here shown methodologies are important prototype as general and powerful tools not only for nucleic acid amplification strategies, but also for other important fields such as single-cell assays, molecular biology, immunology, and proteomics catalysis and so on.

15.2 Open-Access Microdroplet Array

In contrast to microdroplets generation under constant flow in microchannels or on microwell chips, recently developed methods for droplet arrays generation (ranging from femtoliter to microliter volumes) on planar substrates have set the stage for the direct manipulation of individual droplets, as well as images acquisition and quantification. A droplet array on a planar substrate has several advantages over the previous picoliter or nanoliter droplets in solid-walled chambers (Sakakihara et al. 2010). Because each droplet is isolated by immiscible phase, an individual droplet

with its biological or chemical contents is directly accessible from outside. Another important aspect of this feature is the ability to recover the droplet contents, which may be useful for further downstream analysis or processing. Most of the studies have used micropipettes to obtain regular droplet arrays with volumes in hundreds of nanoliters under an oil layer in a petri dish (Kim et al. 2009) or on a hydrophilic-in-hydrophobic-patterned chemically modified substrate (Sakakihara et al. 2010; Kantlehner et al. 2011; Schmidt et al. 2006; Zhang et al. 2011). Contact printing and inkjet printing (Arrabito et al. 2013) have also been developed and applied to high-throughput nucleic acid amplification assays through the precise generation and control of droplet volumes (Sun et al. 2014). In this section, we divide the microdroplet array into several categories for respective elaboration according to the droplet generation means and methods: (1) printing-based microdroplet array; (2) microallocation-based microdroplet array; (3) surface-pattern-based microdroplet array; (4) novel approaches for microdroplet array.

15.2.1 Printing-Based Microdroplet Array

Inkjet printing technology, as an alternative to microfluidic technology, can be utilized to directly generate large-scale droplet arrays on a two-dimensional plane and has the advantages of both high throughput and precise control of small volumes, which satisfy the critical demands for biomedical assays and clinic diagnostics, especially in field of POC detection. This technique, which can be precisely manipulated and applied with temporal and spatial control, does not require a complicated fabricating process and has been employed in many areas, thus making it one of the most widely used methods for efficient microarray fabrication (Zhang et al. 2016a, b). In addition, droplet volume can also be precisely controlled through adjusting the applied pulse amplitude and waveform on the piezo actuator of the inkjet system (Chen et al. 2013a, b; Luo et al. 2013; Zeng et al. 2016; Zhang et al. 2017). Nowadays droplet array formation based on printing approach is encountered with such intractable challenges as (1) evaporation of droplets during array fabrication. Evaporation effects typically hinder the extreme scale reduction of droplet reactions to picoliter volumes, even femtoliter levels; (2) multistep droplet manipulation based on inkjet printing approach. Since printing technology has the advantage of open operation, allowing easy access to the contents, it is also necessary to realize multistep droplet manipulation.

Conventional microarray biochips, such as gene chips, usually use microjet technology to prepare an array of one reactant and fix it on the surface of the array (Fodor et al. 1991) and then the sample solution to be tested interacts with the microarray to complete the screening assay. However, this detection scheme is not suitable for most biological/chemical reactions, since most of the biochemical reactions need to be completed in solution environment. Moreover, more and more studies require the reaction volume to be within the range of picoliter to nanoliter. Therefore, microjet technology has been adopted to prepare biochips of high-throughput and solution-

phase droplets array over the past decades. As early as 2003, Gosalia and Diamond from University of Pennsylvania have created discrete nanoliter reaction volumes in the liquid phase via contact printing combining with the low volatility of glycerol droplets on glass. Using aerosol deposition, this method has the capability to rapidly assemble multi-component reactions with minimal sample usage in a microarray format (Gosalia and Diamond 2003). The kinetic and specificity profiling of serine and cysteine proteases were performed on a 16 × 24 array of 200 μm diameter spots with 500 μm center-to-center spacing (Gosalia et al. 2005).

The addition of organic solvents, such as glycerin or DMSO, can alleviate the volatilization issue of nanoliter volume or even smaller droplets (Berthier et al. 2008), but the limitation of this method is that organic solvents are not compatible with many biochemical systems, and fluid droplets without fixation are not suitable for complex multistep operations. Mugherli et al. proposed an approach that combined piezoelectric printing and surface-tension microarrays to optimally suit for both the synthesis and the profiling of enzyme inhibitors. The microarray utilized a hydrophobic surface patterned with hydrophilic spots to maintain the position of the arrayed droplets in order to facilitate the handling of bigger (30–150 nL) droplets and thus alleviates the evaporation problem (Mugherli et al. 2009).

In order to further improve assay sensitivity, binding capacity and mass transport, 3D microarray substrates have been developed to achieve higher protein loading capacity, higher fluorescent signals, and better spot morphology compared to a 2D surface (Li et al. 2011). However, they often rely on photopolymers which have a complex manufacture process and small pore size that limits mass transport and demand long incubation time. To overcome some of these limitations, Juncker's group (Li et al. 2011) presented a novel 3D beads-in-gel droplet microarray (BiGDM) based on the entrapment of modified microbeads that were printed onto a glass slide using an inkjet printing technology. The hydrogels were highly porous and together with the 3D architecture which could help enhance mass transport during the assays. The printing parameters were also optimized for the attachment of the alginate to the substrate. BiGDM was applied for multiplexed sandwich immunoassays for the detection of six proteins including cytokines and breast cancer biomarkers in buffer solutions and 10% serum. The results illustrate the potential of 3D droplet microarrays for highly sensitive and multiplexed biochemical assay.

It is an important issue that multiplexed multistep operations based on printing technology are able to be realized on microdroplet array in sub-nanoliter to picoliter. This is also one of the keys to promote the applicability of printing technology in the field of clinical diagnosis, since this linkage is typically challenging for biomolecules since they might lose their function after covalent immobilization. In order to address this problem, in 2013, Arrabito et al. first showed a low-cost and rapid multistep/sequential picoliter droplets assembly on solid surfaces through non-immobilized molecules interacting dispensed by piezoelectric inkjet printer and for delivering multiple biomolecular systems. Biochemical reactions are conducted in such picoliter spots, which were stable during both the multilayer-assembling and the execution of the assay thanks to the high hygroscopicity of 30% glycerol in droplets. Since it can be extended to molecular and biomolecular systems, the here

shown methodology is an important prototype as a general approach not only for high-throughput screening of compound libraries, but also for other important fields such as PCR, genomics, catalysis, and single-cell assays (Arrabito et al. 2013).

It is the primary objective that employing the printing technology to develop a non-contact and sequential picoliter droplet printing model without evaporation in order to further improve the universality of printing applications in biochemical analysis. In our previous work (Sun et al. 2014, 2015), two novel printing methods based on droplet-in-oil structure were first developed and characterized. Droplet-in-oil array with picoliter volumes was first fabricated and characterized generated with a double-inkjet printing model on a hydrophobic substrate, which was successfully applied for quantitative polymerase chain reaction (qPCR) analysis (Sun et al. 2014). Double-inkjet printing was developed to address the picoliter droplets evaporation during large-scale array generation on a planar substrate without the assistance of a humidifier or glycerol. The method adopts piezoelectric inkjet printing to precisely eject a reagent droplet into an oil droplet on a hydrophobic and oleophobic substrate. There is no evaporation and random movement during array fabrication and thermal cycling. Besides, this method can also be adopted to fabricate multivolume droplet-in-oil arrays. This feature is useful for multivolume assays aimed at wide and tunable dynamic ranges. On the basis of the double-inkjet printing, sequential-inkjet printing method was further presented to describe the multiple injection procedures implemented by the inkjet printing approach (Sun et al. 2015). The multiple injection models demonstrate a novel sequential-inkjet printing method was proposed to generate picoliter-scale multi-component droplet-in-oil arrays via multistep printing. Based on the previous work, this technique utilizes the inkjet printing technology to fabricate an oil droplet array and print secondary droplets with different compositions and volumes into the oil array, which simultaneously addressing the evaporation issues associated with printing picoliter droplets without external assistance. Besides, a three-phase model was also developed based on the general numerical framework of the Gerris Flow Solver in order to perform a numerical simulation of the droplet-in-oil formation based on sequential-inkjet printing. We believe that applying the double-inkjet printing and sequential-inkjet printing methodology to the existing inkjet printing devices will enhance their use as general diagnostic tools as well as accelerate the application of inkjet printing in multistep screening experiments (Fig. 15.1).

Different kind of droplet array for different applications can be realized by flexible combination of the printing technique and other auxiliary strategies. Lin and co-worker reported that inkjet technology was used for continuously generating monodisperse droplets in the oil phase and droplets were then introduced into the capillary in the form of linear array (Zhang et al. 2018). The linear array of monodisperse droplets was detected by a fluorescence detector located at the downstream of the capillary for positive droplet counting. This combined system was able to achieve online amplification and detection without any liquid transfer steps, thus avoiding cross-contamination and sample loss. In our latest work, we combined inkjet printing technology with a sticky superhydrophobic surface (SH) to prepare high-resolution patterns with controllable diameters and large throughput (Sun et al.

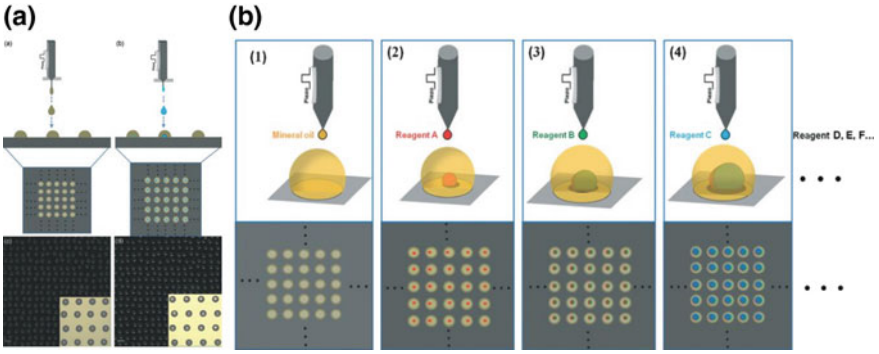

Fig. 15.1 **a** Schematic representation and bright-field images of picoliter droplet-in-oil array fabrication by double-inkjet printing on a solid support. Reproduced from Sun et al. (2014) by permission of The Royal Society of Chemistry. **b** Schematic representation of picoliter droplet-in-oil array fabrication by sequential inkjet printing on a silicon dioxide solid support. Reproduced from Sun et al. (2015) by permission of The Royal Society of Chemistry

2018). The SH surface with both high contact angle and high contact angle hysteresis (CAH) can not only obtain high-resolution spots with dewetting principle, but also avoid droplet bouncing and scattering behaviors. It is the first time that applying a transparent sticky SH surface to solve the bouncing issue during inkjet printing for fabricating high-resolution patterns. Based on an inkjet printer with ordinary precision, the minimum feature size was obtained with this method was as small as 4 μm. Although inkjet printing-based droplet generation procedure is set forth in detail in this section, other high-resolution jet printing can also be used to produce multiple submicroliter-sized droplets through piezoelectric or electrohydrodynamic-based droplet generation (Ferraro et al. 2010; Park et al. 2007).

15.2.2 Microallocation-Based Microdroplet Array

In addition to the printing technology, microallocation method is an alternative to be utilized to fabricate the microdroplets chip. This microallocation-based droplet manipulation method is different from previous microfluidic droplet systems based on continuous flow mode or digital microfluidics. Flexible droplet manipulations can be automatically achieved including droplet generation, indexing, sampling, transferring, splitting, and fusion in picoliter-scale precision, even femoliter scale. In the early stage of this field, Fang's group has carried out many related researches during the past dedicate. Back in 2006, the group reported a slotted-vial array sample injection system which was combined with a short fused-silica capillary to produce a highly efficient and simple μSIA system (Du et al. 2006). Even though the approach provides a useful means for online process monitoring and high-throughput screening, there is still a limitation of the present system that the bioanalysis was performed

in the capillary tubes. In their further study, they successfully extracted the droplets from the capillary and formed microdroplets array on substrates, which was covered by oil layer. On this basis, Du et al. (2010) developed a so-called DropLab microfluidic platform, to deposit the generated droplets in the capillary into a multiwell plate or an oil-immersed nanowell plate. A novel droplet generation approach based on the droplet assembling strategy was developed to produce multi-component droplets in the nanoliter to picoliter range (25 pL–25 nL) with high controllability on the size and composition of each droplet. Without the need of complex microchannel structures, various droplets with different parameters were automatically assembled and dispensed, aiming to multiple screening targets by simply adjusting the aspirated liquids on demand. In 2013, Zhu et al. (2013a, b, 2014) improved the droplet-based microfluidic system, named SODA, for forming a 2D picoliter-droplet array based on "aspirating-depositing-moving" (ADM) method. The ability of performing complicated and multistep droplet manipulation with SODA system was demonstrated in the serial dilution of inhibitor droplets which includes droplet generation, indexing, splitting, transferring, and fusion with picoliter precision. Du et al. (2018) constructed a 6×9 coculture droplet array by using the automated SODA system, and this array allows concurrent mimicking of angiogenic sprouting and analysis of multiple samples and multiple factors. This microallocation system is particularly suitable for screening of multiple samples and ultralow-consumption analysis and applications in other analysis and screening for multiple samples, such as nuclear acid screening, combinatorial chemistry, and clinical diagnosis. The tiny droplet array with volumes down to 179 fL was achieved by combining the pin-based contact printing and the oil-covered hydrophilic pillar microchip (Guo et al. 2018). To overcome the scale phenomenon appeared in picoliter-scale droplets, a water moat was designed to protect the femtoliter to picoliter droplets from volume loss through the cover oil during the droplet manipulation.

The uniformity and size of droplets produced by these methods are affected by many factors, such as the fluid properties of viscosity and surface tension, precision of the micro-fabrication, piezoelectric pulse parameters and so forth. Therefore, it is always challenging to precisely and robustly control droplet generation on demand in a wide volume range. Du et al. developed a simple active droplet generation method (Xu et al. 2016a, b; Liao et al. 2016; Hu et al. 2017), named as cross-interface emulsification (XiE), for the high-throughput generation of monodisperse droplets with controllable volumes from picoliter to nanoliter. Droplets were fabricated via the dynamic interfacial shearing driven by a mechanical vibration of a capillary at the interface of the continuous phase. The droplet volume can be precisely controlled on demand since it's governed by flow rate and vibrating frequency. What's more, monodroplet emulsions can automatically assemble into a planar monolayer microdroplet array on flat bottom, offering convenience for imaging thousands of droplets simultaneously. However, the technique could only support one premixed solution that severely restricts the fitness for use. The same group further developed a new method for multi-component active droplet generation, named as multichannel dynamic interfacial printing (MC-DIP) (Liao et al. 2017). This method converged multiple liquid components on the nozzle and generates droplets via the XiE mech-

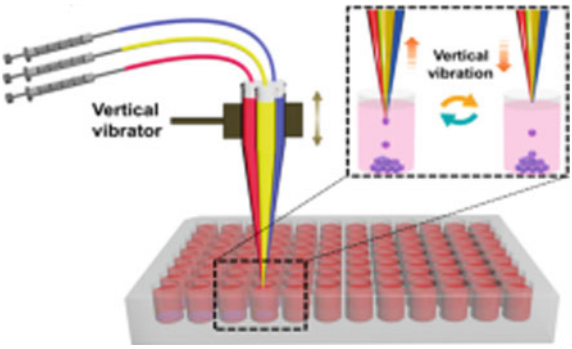

Fig. 15.2 Schematic illustration of multichannel dynamic interfacial printing (MC-DIP). Reprinted with the permission from Liao et al. (2017). Copyright 2017 American Chemical Society

anism. Compared with droplet microfluidic or printing technique, the XiE-based device was composed of simple parts without any complicated microfabrication. Therefore, the MC-DIP technique could perfectly offer opportunities for common laboratories, even without microfabrication or printing facilities, to carry out a widely accessible droplet generation and perform biochemical assays with high-throughput microdroplet array (Fig. 15.2).

15.2.3 Surface-Pattern-Based Microdroplet Array

Although plenty of methods have been employed to generate microdroplets array, most current methods require excellent prepared or sophisticated equipment (Li et al. 2015a, b), which restricts its versatility for various biochemical applications. Therefore, the development of a simple method to generate tiny microdroplets with controllable and uniform volume is urgently needed. Another kind of microdroplet arrays is sessile droplets that are confined within affinitive domains with non-movable droplets (Garcia-Cordero and Fan 2017). Sessile droplets are emerging as a platform capable of competing with microplates in terms of versatility and simplicity of operation. Such arrays usually require to prepare hydrophilic patterns on hydrophobic surfaces and rely less heavily on complicated techniques (Liang et al. 2017; Jin et al. 2014; Xu et al. 2016a, b). The extreme wettability contrast of the superhydrophobic-superhydrophilic (SH-SL) patterns allows the spontaneous separation of an aqueous solution into high-throughput arrays of microdroplets based on the effect of discontinuous dewetting. This efficient droplet formation does not require multiple pipetting or a liquid-handling device. The handling of small volumes of droplets requires fewer reagents than with conventional microplates. Recently, superwettable microchips with superhydrophobic-superhydrophilic patterns exhibit excellent ability of patterning microdroplets (Gu et al. 2002; Zhang et al. 2007; Nishimoto et al. 2009; Oliveira et al. 2013; Neto et al. 2016a, b) and have a profound impact upon diverse applications such as ultratrace detection of DNA (Xu et al. 2015) and cell microarray (Ueda et al. 2013; Feng et al. 2014; Oliveira et al. 2014).

Levkin's group (Efremov et al. 2013) recently demonstrated a versatile platform for generating thousands of isolated microdroplets array (DA) with specific geometry and volume, based on the utilization of precise SH-SL micropatterns on films. Due to the extreme difference in wettability between SH and SL areas and the phenomenon of discontinuous dewetting, aqueous solutions applied onto such surfaces spontaneously form an array of separated microdroplets array (Ueda et al. 2012). These droplet arrays can not only serve as a miniaturized platform for cell-based high-throughput assays, but also achieve the simultaneous gelation of the prehydrogel droplets array of defined sizes and shapes combined with the sandwiching method. The similar work of droplet-splitting strategy was also conducted by Song's group (Li et al. 2015a, b). A facile method for microdroplet array preparation was realized by sliding a droplet on a patterned SL/SH substrate. Tiny microdroplets with volume ranging from 83.5 pL to 9.7 fL were successfully fabricated on SH square patterns with lateral lengths ranging from 5 to 100 μm. The volume of microdroplets can be controlled precisely by adjusting the SL pattern size, the contact force and the relative sliding speed between the droplet and the substrate. This strategy was validated for fluorescent spheres and cancer cells separation in designated array. This method is facile, sample-effective, and low-cost for the development of microdroplet arrays for biochemical analysis (Fig. 15.3).

Since the volume of microdroplets can even be minimized to picoliters or femtoliters, free-standing and tiny aqueous droplets suffer an intractable issue with droplet evaporation in a few milliseconds in air (Sun et al. 2014, 2015). Therefore, microdroplet arrays should be covered with immiscible oil as soon as they are generated, to prevent evaporation for long-term analysis or high-temperature operation (Gorris and Walt 2010). Iino and Noji et al. (Sakakihara et al. 2010; Kim et al. 2012; Iino et al. 2012) prepared a femtoliter droplet array by using a hydrophilic-in-hydrophobic micropatterned surface. Since fluorinated oil has a higher density than water, the hydrophilic micropatterns retain the dome-shaped aqueous solution when the aqueous solution on the surface is exchanged with fluorinated oil, and more than 106 directly accessible femtoliter droplets were prepared simultaneously. In this paper, the author also proposes two important features of this method: One is accessible femtoliter and high-throughput droplet assay, which can be applied to the digital

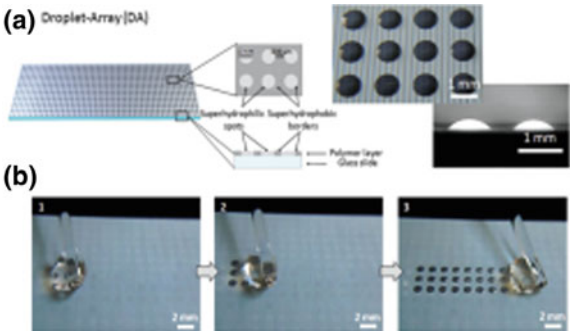

Fig. 15.3 Schematic representation and snapshots of the process of discontinuous dewetting leading to the formation of an array of microdroplets. Reproduced from Popova et al. (2015) by permission of John Wiley & Sons Ltd.

PCR and the digital ELISA, which detect very low amounts of DNA and diagnostic biomarkers down to the single-molecule level. Another important feature is the capability to recover the droplet content, which is useful for further applications of the accessible product in droplet array. The Iino group has reported a variety of successful applications based on the large-scale and directly accessible femtoliter droplet array, including measuring the kinetic parameters of the single-molecule enzyme and protein (Sakakihara et al. 2010), accessing a single-cell drug efflux assay in bacteria (Iino et al. 2012), and digital counting of extremely low concentrations of biomolecules (Kim et al. 2012). It is believed that the large-scale femtoliter droplet array immobilized on a substrate would have great potential as a highly sensitive, portable biochemical screening device that could be used to diagnose diseases.

Different from the Iino's work that the liquid exchange was induced by density differences on a hybrid surface, Wu et al. (2018a, b) generated the oil-covered uniformly picoliter droplet arrays by exploiting the capillarity principles to guide liquids sliding along a hydrophilic-in-hydrophobic patterned surface. The entire droplet array preparation process can be completed within a few minutes, and more than ten thousand microdroplets can be generated in 5 s, with more than 80% coverage and less than 10% variation in volume. In this paper, the separation experiments of single microspheres and cells were carried out to verify that this new method enables high-throughput generation. In addition, it is facile, efficient, and low-cost (Fig. 15.4).

SH-SL patterned surfaces are also adopted to accomplish biosensing in a microgravity environment. Xu and coworkers (Xu et al. 2017) jointly developed an superwettable microchip to meet stringent requirements solve the problem of droplet floating in a microgravity condition, providing a new scheme for the visual detection of routine biomarkers in astronauts, such as calcium, protein, and glucose. SL micropores have a great ability to trap droplets while the anti-droplet adsorption ability of the SH substrate can limit the movement of droplets. Deserved to be mentioned, the

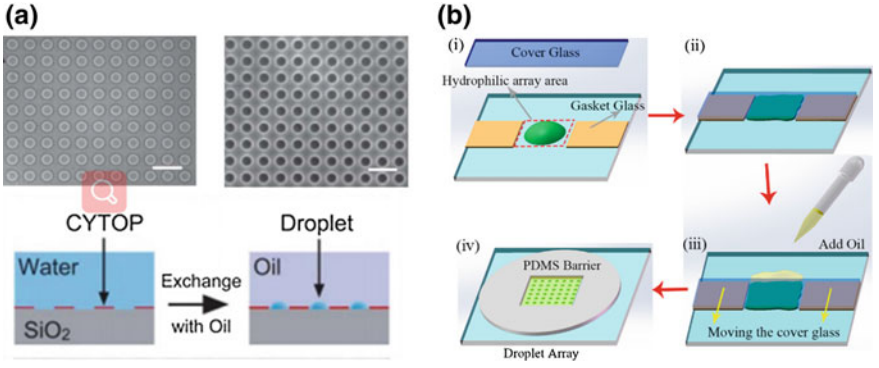

Fig. 15.4 **a** Droplet array preparation procedure. Water on the micropatterned surface is exchanged with oil. Reproduced from Sakakihara et al. (2010) by permission of The Royal Society of Chemistry. **b** Schematic drawing of the oil-covered droplet array preparation procedure. Reprinted with the permission from Wu et al. (2018a, b). Copyright 2018 American Chemical Society

silica nanodendritic structure in SH microwells could generate capillary force which was explained with capillary theoretical model on porous solid surfaces. This chip could capture different volumes of microdroplets against the gravity by designing the diameters of SH microwells, making the detection process easier in weightlessness or zero gravity.

15.2.4 Novel Approaches for Microdroplet Array

There are few reports about droplet-based microfluidic system allowing effective manipulation of biofluidic droplets with low surface tension and high viscosity, which limits the applications of related multiplex bioassays and point-of-care diagnostics. In 2018, Han and co-workers (Seo et al. 2015; Han et al. 2018) developed a single-droplet manipulation system with a superamphiphobic-superamphiphilic (SPO-SPI) pattern on a disposable cartridge PDMS substrate applied for a multiplex bioassay from single-droplet samples. A vacuum pressure was applied beneath the substrate through a vacuum tip to manipulate the single-droplets including transporting, mixing, and dispensing. The developed system could have broad applications in the biomedical field because of its simple fabrication process and great potential in combination with conventional biosensing methods.

Zhu et al. (2018) combined the evaporation and the deformability to control directed self-assembly of microdroplets in an evaporating liquid to fabricate large-scale ordered films. Firstly, they used the microfluidic chip to robustly produce uniform emulsions with silicone oil droplets in aqueous poly(vinyl alcohol) (PVA) solution. After emulsification, a dilute emulsion of oil droplets was deposited onto a glass substrate. Because oil droplets are lighter than aqueous PVA solutions in density, initially disordered droplets quickly self-assemble near the upper liquid–air interface driven by buoyancy within several minutes. Since the droplet assembly-based fabrication is compatible with tunable properties, this novel approach paves a new way for precisely engineering ordered and microstructured material networks over multiple length scales (Fig. 15.5).

Real-time observation of droplet digital detection is extremely beneficial for understanding phenomena of reaction kinetics and accurate quantification of nucleic acid in various samples. Because the dispersion of monodisperse droplets into continuous phase violates the thermodynamic equilibrium, the microdroplets dispersed in oil phase tend to move and merge into big ones, especially during droplet PCR process and long-term cell culture (Baret 2012). To solve this problem, droplets are usually injected into narrow capillaries or microchannels (Beer et al. 2008), where the droplets are sequentially spaced by oil or are fixed with wetting patterns of surface (Liu et al. 2017). However, these approaches will cause either low-throughput production or difficult real-time fluorescence measurements. As of now, high-throughput real-time monitoring systems based on droplets are rarely reported due to droplet coalescence and motion. Wu et al. (2018a, b) provided a straightforward method for real-time monitoring of individual droplets in droplet digital PCR (ddPCR) by

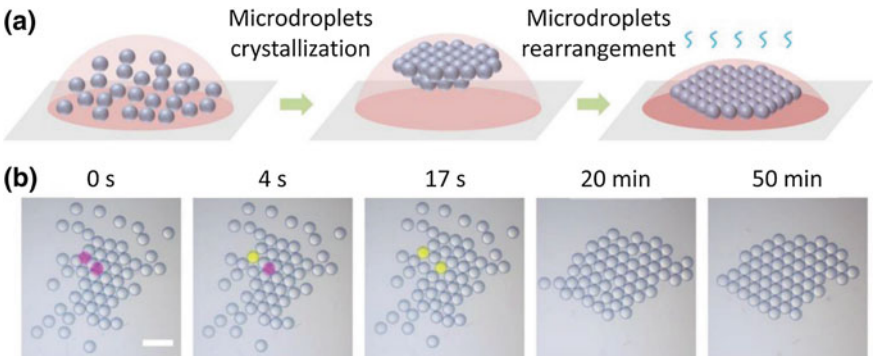

Fig. 15.5 Schematic showing the process of ordered microdroplet rearrangement in an evaporating emulsion. Reproduced from Zhu et al. (2018) by permission of John Wiley & Sons Ltd.

developing a novel thermosetting oil as a continuous phase to eliminate droplets coalescence through transforming into elastic solid after droplet generation. The oil is harmless to biomaterials in droplets because the hydrosilation-based polymerization of the curable material occurs spontaneously without inducers. More importantly, the PCR products can be recovered from microcapsules for downstream analysis, which is crucial for a wide application in molecular diagnosis and cell researches.

15.3 Nucleic Acid Amplification Strategies in Microdroplet Array for Clinical Diagnostics

Analysis of biological analytes in droplets containing multiple biological analytes is required for the clinical diagnosis and management of chronic diseases (Martinez et al. 2007; Kuan et al. 2016; Rice et al. 2010). Various biosensing techniques have been developed to analyze biological analytes. Among these methods, droplet-based bioassays have attracted particular attentions because of their straightforward, addressable, open-access, and easy fabrication with no need of expensive or sophisticated instruments (Han et al. 2018). The open microdroplet arrays have exhibited strong functionality in biological and chemical analysis fields (You et al. 2013; Mongersun et al. 2016; Du et al. 2013). The combination of nucleic acid amplification strategies and microdroplet arrays would be greatly beneficial to the development of point-of-care devices that enable multiplex bioassays using a single droplet (Kuan et al. 2016; Martinez et al. 2010; Gonzalez et al. 2016; Wu and Zhang 2015). Nucleic acid amplification is traditionally performed in tubes or in microwell plates. Although ideal for applications with an initial high amount of DNA material, they have several limitations when working with low-volume samples, including large dead volumes and template adsorption to the walls (Jose et al. 2017). For example, performing single-cell methylation analysis in tubes is prone to a partial recovery of cell nucleus,

decreased amplification efficiency, loss of DNA during various steps, among other causes (Kantlehner et al. 2011). While some microfluidic devices can perform genetic analysis on single cells, they are operated with specialized instrumentation and access to individual chambers for manipulation is difficult. In addition, these devices are fabricated in state-of-the-art clean rooms at a high cost with time-demanding techniques (Sun et al. 2014). Droplet arrays offer a very simple and inexpensive alternative to implement different nucleic acid amplification methods with less demanding instrumentation for thermal cycling and for the fluorescent readers (in the case of real-time monitoring), which makes them ideal for point-of-care applications or for resource-limited settings.

15.3.1 Multiplex Real-Time PCR System on Microdroplet Array

It has been shown that nucleic acid amplification in low volumes is a suitable way to enhance the sensitivity and efficiency of amplification. As early as in 2006, Mann et al. (Schmidt et al. 2006) implemented PCR in 1 μL droplets using as little as 32 pg of template DNA. A glass slide was patterned with 60 circular patches of hydrophobic and hydrophilic regions, each capable of holding volumes from 0.5 to 1.65 μL. The template was pipetted first on the slide, followed by the addition of the PCR mix on the inner circle, and finally overlaid with 5 μL of oil on the outside circle; forming a 2D droplet array on a flat, chemically structured glass slide. The chip was amplified on a regular thermocycle and the results can be detected by electrophoresis or sequencing. Schumacher et al. further applied this droplets slide to make pre-implantation genetic diagnosis (PGD) (May et al. 2009) and profile high-throughput DNA methylation (Kantlehner et al. 2011) in single cells deposited on the circular regions. At present, this slide of droplet array has been commercialized by Ampligrid (Beckman Coulter) due to its flexible operation and broad application prospect in the field of single-cell analysis. In our previous work, Sun et al. (Sun et al. 2014) successfully demonstrated quantitative real-time PCR on droplet-in-oil array with a picoliter volume, fabricated by the double-inkjet method on a uniform hydrophobic substrate. We employed human Raji cDNA of 18S rRNA to demonstrate the performance of real-time qPCR with serial dilutions of over five orders of magnitude from 500 to 0.05 pg/μL. Deserved to be mentioned, the reagent consumption here was at least 120 times lower than that in a conventional real-time PCR assay. Compared with microchannels and microwells at picoliter level, this method greatly reduces the reagent consumption since it does not require the use of extra reagent fluid for flushing. The further research would focus on optimizing the double-inkjet procedure for large-scale pico-droplet array preparations which has great potential applications for digital PCR technique.

15.3.2 Real-Time Reverse Transcription PCR

Real-time reverse transcription polymerase chain reaction (RT-PCR), as a laboratory technique based on the traditional PCR, is one of the most commonly used tools for quantitative measurement of gene transcription and nucleic acids (DNA and RNA) owing to its accuracy, high sensitivity and large dynamic range (Heid et al. 1996). In the past decade, more and more effort has been put into the development of microfabricated platforms for miniature qPCR and qRT-PCR technique, because it is no doubt a powerful tool for biomedical diagnosis and quantitative biology. There are numerous researches have been reported on miniaturized qPCR technique (Sanchez-Freire et al. 2012; Dalerba et al. 2011), especially, droplet array on microchip platforms could be an alternative to perform multistep and parallel assay with different samples. Fang and colleagues used a 6 × 6 nanoliter droplet array on silicon wafer to perform parallel two-step qRT-PCR assay for microRNAs quantification across five cultured cell lines. The micro-122 is a small non-coding RNAs with 18–25 nucleotides in length and is aberrantly expressed during disease development (Lagos-Quintana et al. 2001). The minimum total RNA input was as low as 1 pg per assay, which showed great potential for gene quantification at single-cell level. Single-cell RT-PCR is a powerful tool for the measurement of gene expression variation among individual cells, which has successfully applied in the study of cell heterogeneity of human, and gene expression signatures that are relevant to patient survival and clinical outcome in colon cancer patients. In a recent work, the same group (Zhu et al. 2015) successfully applied the 10 × 10 uniform array of 2-nL droplets for single-cell reverse transcription quantitative PCR assay (RT-qPCR). As shown in Fig. 15.6, such a droplet array can be accessed for multistep droplet manipulations required in single-cell RT-qPCR assay including droplet generation, single-cell encapsulation, cell lysis (thermally lysing), reagent addition (reverse transcription mix), reverse transcription (convert RNA to cDNA), PCR mix and quantitative PCR (real-time fluorescence) by printing a two-dimensional droplet array on an patterned microchip under the cover oil. In this study, the expression level of mir-122 in single Huh-7 cells was quantitative measured ranging from 3061 copies/cell to 79998 copies/cell.

15.3.3 Isothermal Amplification Assay on Microdroplet Array

Without requiring thermal cycling, isothermal microsystems, including LAMP, NASBA, RCA, HAD and SDA can be designed to be simple and portable with low-energy consumption for process automation and integration in a single device, which is superior to PCR. Hence, isothermal amplification methods are of great advantage in simplifying both the microchip design and the instrument requirement. Rolling circle amplification (RCA) is a commonly used research tool for medical biosensors and biomedical applications (Li et al. 2012). RCA is a simple and efficient isothermal enzymatic process that utilizes nuclease to generate long single-stranded DNA

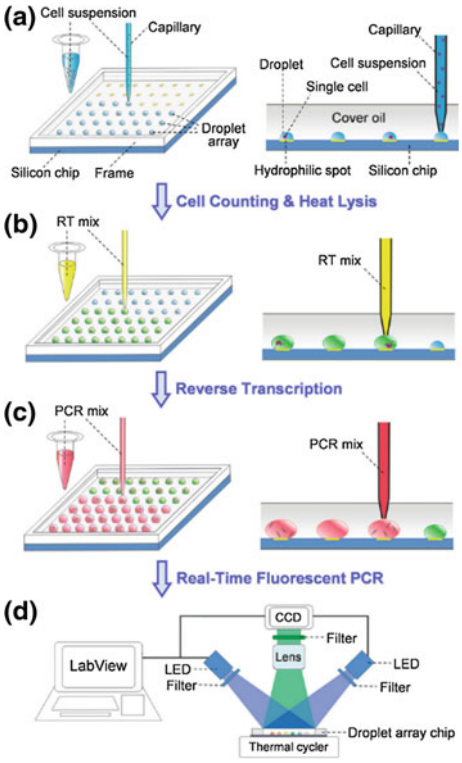

Fig. 15.6 Nucleic acid amplification based on RT-PCR in sessile droplet. Reproduced from Zhu et al. (2015) Open Acess

or RNA. The aptamer or DNAzyme could be replicated hundreds of times in a short period, and a lower LOD could be achieved if those units are combined with miniaturized devices. Various RCA-based platforms including droplet array have been developed to detect a variety of targets including nucleic acid, proteins, pathogens, cytokines, and diseased cells. As one means of isothermal nucleic acid amplification, the hyperbranched rolling circle amplification (HRCA) can be performed under isothermal conditions (Lizardi et al. 1998; Baner et al. 1998), which removed the requirement of stringent temperature control to cycle through the steps of denaturation, annealing, and elongation. Due to its simplicity and high efficiency, HRCA has also gained considerable attention in the detection of DNA (Cao and Zhang 2012), RNA (Zhang et al. 2014), as well as proteins (Zhu et al. 2013a, b). Ma et al. (Zhao et al. 2011; Ma et al. 2015) reported a HRCA reaction on a nanoliter droplet array with 0.5 μL per droplet on the hydrophilic-hydrophobic patterned chip. To further prove the performance of the nanoliter droplet array for real biological samples, the chip was applied to measure the OLR1 gene from human genomic DNA extracted from the A549 cell line. The results showed that the practicability of the nanoliter droplet array for amplifying and detecting nucleic acids in the genomic DNA sample and the ability of multiplex target detection. Obviously, this method,in conjunction with the isothermal amplification of nucleic acid, does not need a precise thermal

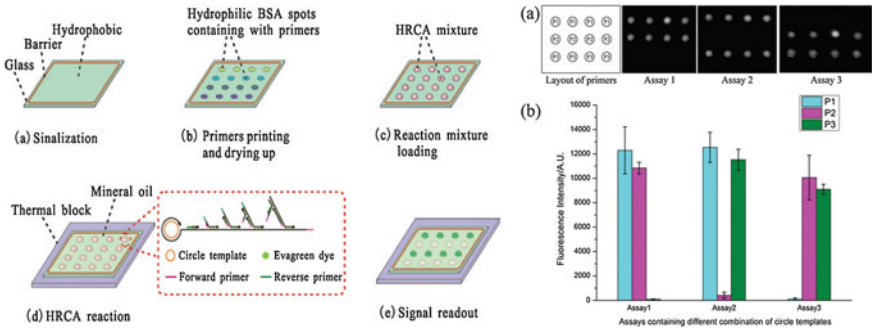

Fig. 15.7 Schematic illustration of the manufacture procedures for microfabrication-free nanoliter droplet array. Reproduced from Ma et al. (2015) by permission of The Royal Society of Chemistry

cycler, which would facilitate its use as a universal platform in ordinary biological laboratories. All the features provide the droplet array RCA a promising diagnostic approach for disease detection and prevention (Fig. 15.7).

15.3.4 Digital PCR on Microdroplet Array for Clinical Diagnosis

The best way to cure cancer is early diagnosis and early treatment, therefore, research efforts for the management of cancer are focused on developing new strategies for its early detection. There is a growing interest in techniques that allow an absolute quantification of nucleic acid which could be useful for early diagnosis. Recently, digital polymerase chain reaction (digital PCR, dPCR) emerges as a hopeful technology for precise and absolute quantification of nucleic acids. The dPCR concept was conceived in 1992 (Sykes et al. 1992) and was used to quantify KRAS mutations in DNA from colorectal cancer patients (Vogelstein and Kinzler 1999). As the "third generation" of PCR technology, the dPCR is a advanced nucleic acid detection method for absolute quantification of target templates without calibration (Kreutz et al. 2011). In dPCR, samples with target nucleic acids are seperated into tens of thousands of droplets, and each contains a few or no copies of target templates. After amplification, the droplets are classified into "positive" or "negative" according to fluorescence intensity, and the original concentrations of the templates can be calculated based on the Poisson distribution (Kreutz et al. 2011). Therefore, dPCR technology can complete accurate quantification of nucleic acid and provide the absolute quantitative results of target sequence. Compared with conventional quantitative PCR (qPCR), dPCR is independent of standards, more tolerant to inhibitors and provides the ability to detect target nucleic acids at low concentration (Kantlehner et al. 2011). With its outstanding performance, dPCR has been widely applied in nucleic acid-related tests, including the detection and quantification of low-level pathogens, rare genetic

sequences (Oliveira et al. 2014), copy number variations (CNVs) (Qin et al. 2008; Marques et al. 2014), gene expression in single cells (White et al. 2013; Ludlow et al. 2014), quantification of circulating miRNAs expression (Li et al. 2014) and noninvasive prenatal testing (NIPT) (Lo et al. 2007).

15.3.4.1 Digital PCR in Monodisperse Droplets

Printing technology, especially inkjet printing, represents an alternate method for producing monodisperse microdroplets for digital PCR assays, since the technique has the advantages of both high throughput and small volumes (Zhang et al. 2016a, b; Yang et al. 2016; Zeng et al. 2015; Chen et al. 2012, 2013a, b). In 2018, Lin et al. (Zhang et al. 2018) reported a work that aimed to utilize inkjet printing technology to fabricate high-throughput monodisperse droplets into the helical capillary for online digital PCR amplification, which subsequently applied to absolute detection of the HPV sequence in Caski cells with dynamic ranges spanning four orders of magnitude. Compared with previous reports, this system was stable, flexible, and inexpensive, without liquid transfer steps eliminating sample loss or cross-contamination what is worth mentioning, this is the first report of the application of inkjet system in digital PCR.

In recent years, Du and his associates have done much work in studying digital PCR in droplets and obtained fruitful results. The recent works are mainly focused on the open-access and microstructure-free droplet array for dPCR, as well as the fabrication methodology of low-cost and user-friendly device. In 2016, Du et al. (Hu et al. 2017) performed absolute quantification of H5-subtype influenza viruses by digital loop-mediated isothermal amplification (dLAMP) based on XiE method. The results show that dLAMP was not only highly specific and sensitive with a detection limit of less than 10 copies per reaction, but also highly tolerant to inhibitory substances. With regard to, viral loads from real samples, dLAMP and qPCR showed comparable detection efficiency. The study of H5N1 quantification in real samples validates that XiE could perform both dLAMP and dPCR for digital amplification of nucleic acids and can be readily extended to the analysis of human specimens, which will have more clinical applications. As mentioned in the article, the dLAMP in droplets would have broad applications in the early diagnosis of highly infectious viruses as well as other bacterial and fungal pathogens, enabling treatment evaluation. In order to solve several existing major issues associated with digital PCR, including reduction of cost, integration of the instrumental platform, and simplification of operations promote, and promote the wider use and clinical application of droplet dPCR, their latest work in 2019 (Nie et al. 2019) describes another novel method that conducts the on-chip multiplex digital PCR of eight samples simultaneously in nanoliter droplet arrays generated with step emulsification. The device was able to detect template DNA at concentrations as low as 10 copies/μL with a dynamic range of approximately four logs. They also employed this device in the quantitative assessment of human epidermal growth factor receptor 2 (HER2) copy number variation (CNV) for 16 clinical samples of breast cancer, which was important for targeted therapy and prognosis

of breast cancer. Since the results are comparable to commercial dPCR system, this low-cost, reusable, and user-friendly device has great potential in used in broad and various applications.

15.3.4.2 Multivolume Digital PCR

Typical droplet digital PCR platforms use droplets of only a single volume and, therefore, require a large number of droplets to achieve a large dynamic range. In single-volume digital PCR, the upper limit of quantification (ULQ) is determined predominantly by the volume and number of individual droplets; thus, a large dynamic range requires tens of thousands to millions of microdroplets. In addition, resolution and dynamic range cannot be adjusted independently in single volume platform. Especially for point-of-care application, it favors fewer droplets to make chip design, fabrication, and readout more manageable. Multivolume digital PCR (MV digital PCR) is able to overcome these limitations of single volume platform by minimizing the total number of droplets required for "digital" (single molecule) measurements and allow the user to quantify nucleic acid though adjusting dynamic range and resolution separately. MV digital PCR was first developed for quantification of HIV and hepatitis C virus load with the SlipChip technique (Shen et al. 2011). For complicated multistep, lithography and etching procedures were employed to produce microchambers with large volume range on one glass substrate. In a separate publication by Ismagilov et al. (Kreutz et al. 2011), a protocol using MPN theory methods and SlipChip device was presented to design and analyze MV digital PCR devices. Integrated pneumatic micropumps were also developed for generating droplets with multiple sizes from 73 to 265 μm for multivolume digital PCR (Warren et al. 2006). Liu et al. (2017) applied a dispensing approach to produce a droplet array with four different volumes used for multivolume digital PCR assay with a dynamic range spanning four orders of magnitude. Based on this multivolume design, the system provides a dynamic range of 4.6 orders of magnitude. To generate thousands of droplets, fluid flowing through a capillary is dragged onto an array of hydrophilic micropillars, which adheres to the top of the pillar, forming droplets of different volumes (from 1.2 to 150 nL). The present digital PCR system was also applied to quantify HER2 expression levels in different breast cancer cell lines to demonstrate its feasibility in clinical diagnosis and targeted therapy. The cDNA solution was prepared by reverse transcription from total RNA extracted from two different types of breast cancer cells, SKBR-3 and MCF-7 cells. In comparison with the previous system based on fixed-volume chambers, this approach is able to change droplet volume with no need of redesigning a new pattern, which facilitating to adjust the detection range of digital PCR assay according to the actual requirements of different samples with the same chip (Fig. 15.8).

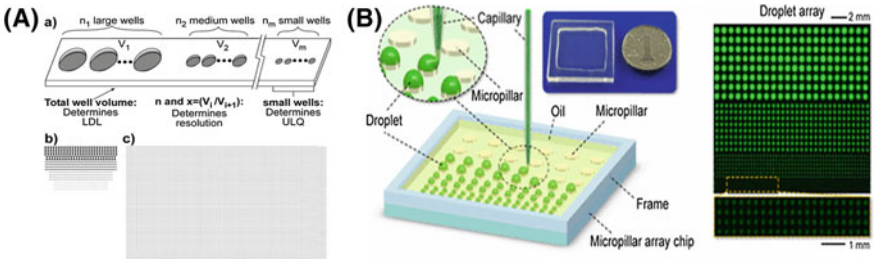

Fig. 15.8 **a** General schematic of multivolume system used for digital PCR (MV digital PCR), with relationship between device features and performance abilities. Reprinted with the permission from Kreutz et al. (2011). Copyright 2011 American Chemical Society. **b** Schematic diagram of the micropillar array chip. The insets show an enlarged image of the droplet during the generation process. Reprinted with the permission from Liu et al. (2017). Copyright 2017 American Chemical Society

15.3.4.3 Real-Time Digital PCR

In comparison with end point detection, achieving real-time optical interrogation of droplet digital detection will be more advantageous for accurate quantification of nucleic acid in various samples, since it can provide the temporal information to differentiate between individual reactors with gradual increasing signal from cycle to cycle and background noise from evaporation of reactors (Hatch et al. 2011). As of now, real-time monitoring of digital detection is rarely reported in droplet-based system because of the droplets motion during PCR process, which results from thermal expansion and compression during thermocycling. To obtain temporary information at the single droplet level, individual droplets are monitored over time by introducing them in a capillary, which greatly limits the number of analyzed droplets, as well as the functional combination with other microfluidic devices (Clausell-Tormos et al. 2008). Alternatively, trapping droplets in array by flow-dependent or independent manners is commonly adopted to fix them in position (Shim et al. 2007). This strategy compromises the flexibility of microfluidic droplet technology because any downstream areas must be compatible to the initial droplet generation parameters. Mu et al. (Wu et al. 2018a, b) successfully achieved real-time monitoring of dPCR process in droplets by applying the thermosetting oil to generate the droplet-in-oil emulsion droplet and eliminate droplet motion and coalescence after oil solidification. This ddPCR chip is integrated with the configuration of flow-focusing droplet generator and droplet array chamber fabricated using PDMS by soft lithography techniques. Certainly, it also can be applied to other types of digital detection which possesses great promise in molecular diagnosis. What's more, this oil can be used to generate hybrid emulsion to recover ddPCR products from the microcapsules with the aid of vacuum container for further downstream bioanalytical methods (Fig. 15.9).

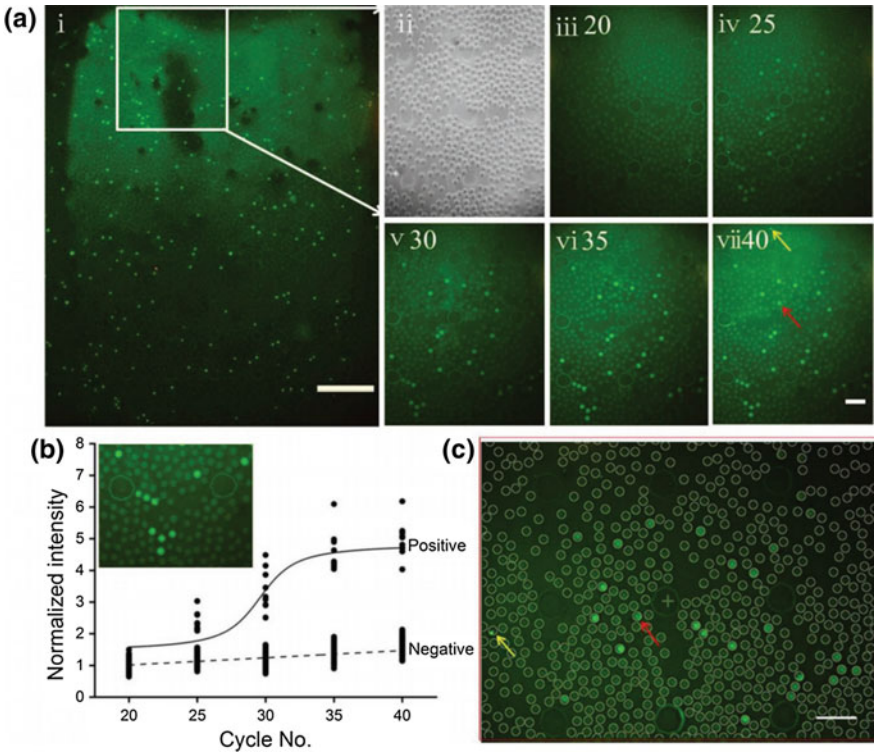

Fig. 15.9 Real-time fluorescence monitoring of droplets in solidified material. Reproduced from Wu et al. (2018a, b) by permission of John Wiley & Sons Ltd.

15.4 Conclusions and Outlooks

Open-access microdroplet array on 2D substrate has several advantages over previous microchambers with solid walls. (1) Because each droplet is isolated by oil and open-access, the droplets can be accessed from outside. (2) Precise control of the droplet volume, initiation and termination of the reaction, and exchange of the droplet content are attainable. (3) High-throughput quantitative assays of biological and chemical reactions with addressing of individual droplets can be realized under different conditions. This droplet array can be applied to the digital PCR, which detects very low amounts of DNA and diagnostic biomarkers down to the single-molecule level. (4) Droplets contents can be easily retrieved for further downstream analysis. (5) The equipment for real-time monitoring is considerably simplified in the sessile droplets platform, which makes them ideal for POC diagnosis. In this chapter, we summarize the state of the art in preparation methodology of microdroplet array and nucleic acid amplification strategies in microdroplet array for clinical diagnostics. The integration of nucleic acid amplification into droplet-based devices has great potential in

facilitating the development of nucleic acid-based POC and clinical diagnosis with high assay sensitivity.

References

Arrabito G, Galati C, Castellano S et al (2013) Luminometric sub-nanoliter droplet-to-droplet array (LUMDA) and its application to drug screening by phase I metabolism enzymes. Lab Chip 13:68–72

Baner J, Nilsson M, Mendel-Hartvig M et al (1998) Signal amplification of padlock probes by rolling circle replication. Nucleic Acids Res 26:5073–5078

Baret JC (2012) Surfactants in droplet-based microfluidics. Lab chip 12:422–433

Beer NR, Wheeler EK, Lee-Houghton L et al (2008) On-chip single-copy real-time reverse-transcription PCR in isolated picolater droplets. Anal Chem 80:1854–1858

Berthier E, Warrick J, Yu H et al (2008) Managing evaporation for more robust microscale assays Part 1. volume loss in high throughput assays. Lab Chip 8:852–859

Cao A, Zhang CY (2012) Sensitive and label-free DNA methylation detection by ligation-mediated hyperbranched rolling circle amplification. Anal Chem 84:6199–6205

Chen F, Lin Z, Zheng Y et al (2012) Development of an automatic multi-channel ink-jet ejection chemiluminescence system and its application to the determination of horseradish peroxidase. Anal Chim Acta 739:77–82

Chen F, Mao S, Zeng H et al (2013a) Inkjet nanoinjection for high-thoughput chemiluminescence immunoassay on multicapillary glass plate. Anal Chem 85:7413–7418

Chen F, Zhang Y, Nakagawa Y et al (2013b) A piezoelectric drop-on-demand generator for accurate samples in capillary electrophoresis. Talanta 107:111–117

Clausell-Tormos J, Lieber D, Baret JC (2008) Droplet-based microfluidic platforms for the encapsulation and screening of mammalian cells and multicellular organisms. Chem Biol 15:427–437

Dalerba P, Kalisky T, Sahoo D et al (2011) Single-cell dissection of transcriptional heterogeneity in human colon tumors. Nat Biotechnol 29:1111–1112

Du WB, Fang Q, Fang ZL (2006) Microfluidic sequential injection analysis in a short capillary. Anal Chem 78:6404–6410

Du WB, Sun M, Gu SQ et al (2010) Automated microfluidic screening assay platform based on DropLab. Anal Chem 82:9941–9947

Du GS, Pan JZ, Zhao SP et al (2013) Cell-based drug combination screening with a microfluidic droplet array system. Anal Chem 85:6740–6747

Du XH, Li WM, Du GS et al (2018) Droplet array-based 3D coculture system for high-throughput tumor angiogenesis assay. Anal Chem 90:3253–3261

Efremov AN, Stanganello E, Welle A et al (2013) Micropatterned superhydrophobic structures for the simultaneous culture of multiple cell types and the study of cell-cell communication. Biomaterials 34:1757–1763

Feng W, Li L, Ueda E et al (2014) Surface patterning via thiol-yne click chemistry: an extremely fast and versatile approach to superhydrophilic-super-hydrophobic micropatterns. Adv Mater Interfaces 1:1400269

Ferraro P, Coppola S, Grilli S et al (2010) Dispensing nano-pico droplets and liquid patterning by pyro-electrodynamic shooting. Nat Nanotechnol 5:429–435

Fodor SP, Read JL, Pirrung MC et al (1991) Light-directed, spatially addressable parallel chemical synthesis. Science 251:767–773

Garcia-Cordero JL, Fan ZH (2017) Sessile droplets for chemical and biological assays. Lab Chip 17:2150–2166

Gonzalez A, Estala L, Gaines M et al (2016) Mixed thread/paper-based microfluidic chips as a platform for glucose assays. Electrophoresis 37:1685–1690

Gorris HH, Walt DR (2010) Analytical chemistry on the femtoliter scale. Angew Chem Int Ed 49: 3880–3895
Gosalia DN, Diamond SL (2003) Printing chemical libraries on microarrays for fluid phase nanoliter reactions. PNAS 100:8721–8726
Gosalia DN, Salisbury CM, Ellman JA et al (2005) High throughput substrate specificity profiling of serine and cysteine proteases using solution-phase fluorogenic peptide microarrays. Mol Cell Proteomics 4:626–636
Gu ZZ, Fujishima A, Sato O (2002) Patterning of a colloidal crystal film on a modified hydrophilic and hydrophobic surface. Angew Chem Int Ed 41:2067–2070
Guo XL, Wei Y, Lou Q et al (2018) Manipulating femtoliter to picoliter droplets by pins for single cell analysis and quantitative biological assay. Anal Chem 90:5810–5817
Han H, Lee JS, Kim H et al (2018) Single-droplet multiplex bioassay on a robust and stretchable extreme wetting substrate through vacuum-based droplet manipulation. ACS Nano 12:932–941
Hatch AC, Fisher JS, Tovar AR et al (2011) 1-Million droplet array with wide-field fluorescence imaging for digital PCR. Lab Chip 11:3838–3845
Heid CA, Stevens J, Livak KJ et al (1996) Real time quantitative PCR. Genome Res 6:986–994
Hu Y, Xu P, Luo J et al (2017) Absolute quantification of H5-subtype avian influenza viruses using droplet digital loop-mediated isothermal amplification. Anal Chem 89:745–750
Huebner A, Sharma S, Demello AJ et al (2008) Microdroplets: a sea of applications. Lab Chip 8:1244–1254
Iino R, Hayama K, Amezawa H et al (2012) A single-cell drug efflux assay in bacteria by using a directly accessible femtoliter droplet array. Lab Chip 12:3923–3929
Jin DQ, Zhu Y, Fang Q (2014) Swan Probe: a nanoliter-scale and high-throughput sampling interface for coupling electrospray ionization mass spectrometry with microfluidic droplet array and multiwell plate. Anal Chem 86:10796–10803
Jose L, Garcia C, Fan ZH (2017) Sessile droplets for chemical and biological assays. Lab Chip 17:2150–2166
Kantlehner M, Kirchner R, Hartmann P et al (2011) Identification of rare DNA variants in mitochondrial disorders with improved array-based sequencing. Nucleic Acids Res 39:44–68
Kim H, Vishniakou S, Faris GW (2009) Petri dish PCR: laser-heated reactions in nanoliter droplet arrays. Lab Chip 9:1230–1235
Kim SH, Iwai S, Araki S et al (2012) Large-scale femtoliter droplet array for digital counting of single biomolecules. Lab Chip 12:4986–4991
Kreutz JE, Munson T, Huynh T et al (2011) Theoretical design and analysis of multivolume digital assays with wide dynamic range validated experimentally with microfluidic digital PCR. Anal Chem 83:8158–8168
Kuan CM, York RL, Cheng CM (2016) Lignocellulose-based analytical devices: bamboo as an analytical platform for chemical detection. Sci Rep 5:18570–18580
Lagos-Quintana M, Rauhut R, Lendeckel W et al (2001) Identification of novel genes coding for small expressed RNAs. Science 294:853–858
Li H, Leulmiab RF, Juncker D (2011) Hydrogel droplet microarrays with trapped antibody-functionalized beads for multiplexed protein analysis. Lab Chip 11:528–534
Li Y, Zeng Y, Ji X et al (2012) Cascade signal amplification for sensitive detection of cancer cell based on self-assembly of DNA scaffold and rolling circle amplification. Sens Actuators B Chem 361–366
Li N, Ma J, Guarnera MA et al (2014) Digital PCR quantification of miRNAs in sputum for diagnosis of lung cancer. J Cancer Res Clin Oncol 140145–140150
Li G, Li MZ, Wang ST et al (2015a) Splitting a droplet for femtoliter liquid patterns and single cell isolation. ACS Appl Mater Interfaces 7:9060–9065
Li H, Yang Q, Li G et al (2015b) Splitting a droplet for femtoliter liquid patterns and single cell isolation. ACS Appl Mater Interfaces 7:9060–9065

Liang YR, Zhu LN, Gao J et al (2017) 3D-printed high-density droplet array chip for miniaturized protein crystallization screening under vapor diffusion mode. ACS Appl Mater Interfaces 9:11837–11845

Liao S, He Y, Wang D et al (2016) Dynamic interfacial printing for monodisperse droplets and polymeric microparticles. Adv Mater Technol 1:1600021

Liao SL, Tao XL, Ju YJ et al (2017) Multichannel dynamic interfacial printing: an alternative multicomponent droplet generation technique for lab in a drop. ACS Appl Mater Interfaces 9:43545–43552

Liu W, Zhu Y, Feng Y et al (2017) Droplet-based multivolume digital polymerase chain reaction by a surface-assisted multifactor fluid segmentation approach. Anal Chem 89:822–829

Lizardi PM, Huang X, Zhu Z et al (1998) Mutation detection single molecule counting using isothermal rolling circle amplification. Nat Genet 19:225–232

Lo YM, Lun FM, Chan KC et al (2007) Digital PCR for the molecular detection of fetal chromosomal aneuploidy. Proc Natl Acad Sci USA 104:13116–13121

Lorber N, Sarrazin F, Guillot P et al (2011) High-throughput single-cell quantification using simple microwell-based cell docking and programmable time-course live-cell imaging. Lab Chip 11:779–787

Ludlow AT, Robin JD, Sayed M et al (2014) Quantitative telomerase enzyme activity determination using droplet digital PCR with single cell resolution. Nucleic Acids Res 42:e104–e115

Luo C, Ma Y, Li H et al (2013) Generation of picoliter droplets of liquid for electrospray ionization with piezoelectric inkjet. J Mass Spectrom 48:321–328

Ma XD (2016) Development of hydrophilic-hydrophobic-pattern-based microdroplet array and its application in multiplex nucleic acid detection. Southeast University

Ma XD, Xu WW, Chen C et al (2015) A microfabrication-free nanoliter droplet array for nucleic acid detection combined with isothermal amplification. Analyst 140:4370–4373

Marques FZ, Prestes PR, Pinheiro LB et al (2014) Measurement of absolute copy number variation reveals association with essential hypertension. BMC Med Genomics 7:44

Martinez AW, Phillips ST et al (2007) Patterned paper as a platform for inexpensive, low-volume, portable bioassays. Angew Chem Int Ed 46:1318–1320

Martinez AW, Phillips ST, Whitesides GM et al (2010) Diagnostics for the developing world: microfluidic paper-based analytical devices. Anal Chem 82:3–10

May A, May A, Kirchner R et al (2009) Multiplex RT-PCR expression analysis of developmentally important genesin individual mouse preimplantation embryos and blastomeres. Biol Reprod 80:194–202

Mongersun A, Smeenk I, Pratx G et al (2016) Droplet microfluidic platform for the determination of single-cell lactate release. Anal Chem 88:3257–3263

Mugherli L, Burchak ON, Balakireva LA et al (2009) In-situ assembly and screening of enzyme inhibitors with surface tension microarrays. Angew Chem Int Ed 48:7639–7644

Neto AI, Demir K, Popova AA et al (2016a) Fabrication of hydrogel particles of defined shapes using superhydrophobic-hydrophilic micropatterns. Adv Mater 28(35):7613–7619

Neto AI, Demir K, Popova AA et al (2016b) Fabrication of hydrogel particles of defined shapes using superhydrophobic-hydrophilic micropatterns. Adv Mater 28:7613–7619

Nie MY, Zheng M, Li CM et al (2019) Assembled step emulsification device for multiplex droplet digital polymerase chain reaction. Anal Chem 91:1779–1784

Nishimoto S, Sekine H, Zhang X et al (2009) Assembly of self-assembled monolayer-coated Al_2O_3 on TiO_2 thin films for the fabrication of renewable superhydrophobic-superhydrophilic structures. Langmuir 25:7226–7228

Oliveira NM, Reis RL, Mano JF (2013) Superhydrophobic surfaces engineered using diatomaceous earth. ACS Appl Mater Interfaces 5:4202–4208

Oliveira MB, Neto AI, Correia CR et al (2014) Superhydrophobic chips for cell spheroids high-throughput generation and drug screening. ACS Appl Mater Interfaces 6:9488–9495

Park JU, Hardy M, Kang SJ et al (2007) High-resolution electrohydrodynamic jet printing. Nat Mater 6:782–789

Popova AA, Schillo SM, Demir K et al (2015) Droplet-array (DA) sandwich chip: a versatile platform for high-throughput cell screening based on superhydrophobic-superhydrophilic micropatterning. Adv Mater 27:5217–5222
Qin J, Jones RC, Ramakrishnan R (2008) Studying copy number variations using a nanofluidic platform. Nucleic Acids Res 36:e116
Rice D, Kocurek B, Snead CA (2010) Chronic disease management for diabetes: baylor health care system' s coordinated efforts and the opening of the diabetes health and wellness institute. Proc Bayl Univ Med Cent 23:230–234
Sakakihara S, Araki S, Iinoand R et al (2010) A single-molecule enzymatic assay in a directly accessible femtoliter droplet array. Lab Chip 10:3355–3362
Sanchez-Freire V, Ebert AD, Kalisky T et al (2012) Microfluidic single-cell real-time PCR for comparative analysis of gene expression patterns. Nat Protoc 7:829–838
Schmidt U, Lutz-Bonengel S, Weisser HJ et al (2006) Low-volume amplification on chemically structured chips using the PowerPlex16 DNA amplification kit. Int J Legal Med 120:42–48
Seo J, Lee SK, Lee J et al (2015) Path-programmable water droplet manipulations on an adhesion controlled superhydrophobic surface. Sci Rep 5:12326–12335
Shen F, Sun B, Kreut JE et al (2011) Multiplexed quantification of nucleic acids with large dynamic range using multivolume digital RT-PCR on a rotational slipchip tested with hiv and hepatitis c viral load. J Am Chem Soc 133:17705–17712
Shim J, Cristobal G, Link DR et al (2007) Control and measurement of the phase behavior of aqueous solutions using microfluidics. J Am Chem Soc 129:8825
Sun YN, Zhou XG, Yu YD (2014) A novel picoliter droplet array for parallel real-time polymerase chain reaction based on double-inkjet printing. Lab Chip 14:3603–3610
Sun YN, Chen XD, Zhou XG et al (2015) Droplet-in-oil array for picoliter-scale analysis based on sequential-inkjet printing. Lab Chip 15:2429–2436
Sun YN, Song WH, Sun XH et al (2018) Inkjet-printing patterned chip on sticky superhydrophobic surface for high-efficiency single-cell array trapping and real-time observation of cellular apoptosis. ACS Appl Mater Interfaces 10:31054–31060
Sykes PJ, Neoh SH, Brisco MJ et al (1992) Quantitation of targets for PCR by use of limiting dilution. Biotechniques 13:444–449
Takinoue M, Takeuchi S (2011) Droplet microfluidics for the study of artificial cells. Anal Bioanal Chem 400:1705–1716
Taly V, Kelly BT, Griffiths AD (2007) Droplets as microreactors for high-throughput biology. ChemBioChem 8:263–272
Teh SY, Lin R, Lee AP et al (2008) Droplet microfluidics. Lab Chip 8(2):198–220
Theberge AB, Courtois F, Schaerli Y et al (2010) Microdroplets in microfluidics: an evolving platform for discoveries in chemistry and biology. Angew Chem Int Ed 49:5846–5868
Ueda E, Levkin PA (2013) Emerging applications of superhydrophilic-superhydrophobic micropatterns. Adv Mater 25:1234–1247
Ueda E, Geyer FL, Nedashkivska V et al (2012) Droplet microarray: facile formation of arrays of microdroplets and hydrogel micropads for cell screening applications. Lab Chip 12:5218
Vogelstein B, Kinzler KW (1999) Digital PCR. Proc Natl Acad Sci USA 96:9236–9241
Warren L, Bryder D, Weissman IL et al (2006) Transcription factor profiling in individual hematopoietic progenitors by digital RT-PCR. Proc Natl Acad Sci USA 103:17807–17812
White AK, Heyries KA, Doolin C et al (2013) High-throughput microfluidic single-cell digital polymerase chain reaction. Anal Chem 85:7182–7190
Wu P, Zhang C (2015) Low-cost, high-throughput fabrication of cloth-based microfluidic devices using a photolithographical patterning technique. Lab Chip 15:1598–1608
Wu H, Chen XL, Gao XH et al (2018a) High-throughput generation of durable droplet arrays for single-cell encapsulation, culture, and monitoring. Anal Chem 90:4303–4309
Wu WS, Zhou SF, Hu JM et al (2018) A thermosetting oil for droplet-based real-time monitoring of digital PCR and cell culture. Adv Funct Mater 1803559–1803569

Xu LP, Chen Y, Yang G et al (2015) Ultratrace DNA detection based on the condensing-enrichment effect of superwettable microchips. Adv Mater 27:6878–6884
Xu K, Wang X, Ford RM et al (2016a) Self-partitioned droplet array on laser-patterned superhydrophilic glass surface for wall-less cell arrays. Anal Chem 88:2652–2658
Xu P, Zheng X, Tao Y et al (2016b) Cross-interface emulsification for generating size-tunable droplets. Anal Chem 88:3171–3177
Xu TL, Shi WX, Huang JR et al (2017) Superwettable microchips as a platform toward microgravity biosensing. ACS Nano 11:621–626
Yang J, Katagiri D, Mao S et al (2016) Inkjet printing based assembly of thermoresponsive core–shell polymer microcapsules for controlled drug release. Mater Chem B 4:4156–4163
You I, Yun N, Lee H (2013) Surface-tension-confined microfluidics and their applications. ChemPhysChem 14:471–481
Zeng H, Yang J, Katagiri D et al (2015) Investigation of monodisperse droplet generation in liquids by inkjet. Sens Actuators, B 220:958–961
Zeng H, Katagiri D, Ogino T et al (2016) Droplet enhanced fluorescence for ultrasensitive detection using inkjet. Anal Chem 88:6135–6139
Zhang X, Jin M, Liu Z et al (2007) Superhydrophobic TiO_2 surfaces: preparation, photocatalytic wettability conversion, and superhydrophobic-superhydrophilic patterning. J Phys Chem C 111:14521–14529
Zhang Y, Zhu Y, Yao B et al (2011) Nanolitre droplet array for real time reverse transcription polymerase chain reaction. Lab Chip 11:1545–1549
Zhang L, Zhu G, Zhang C (2014) Homogeneous and label-free detection of microRNAs using bifunctional strand displacement amplification-mediated hyperbranched rolling circle amplification. Anal Chem 86:6703–6709
Zhang J, Chen F, He Z et al (2016a) A novel approach for precisely controlled multiple cell patterning in microfluidic chip by inkjet printing and the detection of drug metabolism and diffusion. Analyst 141:2940–2947
Zhang W, Mao S, Yang J et al (2016b) The use of an inkjet injection technique in immunoassays by quantitative on-line electrophoretically mediated microanalysis. Chromatogr A 1477:127–131
Zhang W, Li N, Zeng H et al (2017) Inkjet printing based separation of mammalian cells by capillary electrophoresis. Anal Chem 89:8674–8677
Zhang WF, Li N, Koga D et al (2018) Inkjet printing based droplet generation for integrated online digital polymerase chain reaction. Anal Chem 90:5329–5334
Zhao H, Ma XD, Li ML et al (2011) Analysis of CpG island methylation using rolling circle amplification (RCA) product microarry. J Biomed Nanoteclmol 7:292
Zhu Y, Zhang YX, Cai LF et al (2013a) Sequential operation droplet array: an automated microfluidic platform for picoliter-scale liquid handling, analysis and screening. Anal Chem 85:6723–6731
Zhu X, Xu H, Zheng H et al (2013b) An ultrasensitive aptameric sensor for proteins based on hyperbranched rolling circle amplification. Chem Comm 49:10115–10117
Zhu Y, Zhu LN, Guo R et al (2014) Nanoliter-scale protein crystallization and screening with a microfluidic droplet robot. Scientific Report 4:5046
Zhu Y, Zhang YX, Liu WW et al (2015) Printing 2-dimentional droplet array for single-cell reverse transcription quantitative PCR assay with a microfluidic robot. Sci Rep 5:9551
Zhu P, Kong T, Zhou C et al (2018) Engineering microstructure with evaporation-induced self-assembly of microdroplets. Small Methods 2:1800017

Index

S. Zhang et al. (eds.), *Nucleic Acid Amplification Strategies for Biosensing, Bioimaging and Biomedicine*, https://doi.org/10.1007/978-981-13-7044-1